TWO DIMENSIONAL DIFFUSERS WITH PLENUM AND TAILPIPE DISCHARGE.

A Dissertation Submitted to the C.N.A.A.

as Fulfilment for the Degree of Master of Philosophy.

by

BRIAN W. CHILTON.

Dept. of Mechanical and Production Engineering, Sheffield Polytechnic.

SUMMARY

Two dimensional diffusers, both with and without tailpipes, have been tested with different inlet boundary layer conditions and various diffuser geometries.

The effect on the developing boundary layer parameters within the diffuser and tailpipe are investigated for the various conditions. The interaction of all these various parameters are investigated and their effects on the diffuser performance determined.

A theoretical prediction technique based on the momentum integral equation and Head's entrainment function is developed and the prediction method tested against the experimental results. This prediction technique was shown to accurately predict the boundary layer and performance parameters for thin inlet boundary layers and low area ratios.

ACKNOWLEDGEMENTS.

I would like to express particular gratitude to Dr. E. F. C. Ferrett for his guidance and encouragement throughout the project.

Also to my wife Jenny for typing and re-typing this thesis.

I also thank the following for their assistance with this research project:-

G. Artingstall.

D. Lampard.

O. Bardsley.

D. Croft.

The technicians and staff of the Dept. of Mechanical/Production Engineering, Sheffield Polytechnic.

LIST OF CONTENTS.

APPENDICES.

LIST OF FIGURES.

Figure No.

Figure No.

Figure No.

Figure No.

80 Element considered for entrainment function.

LIST OF TABLES.

LIST OF PLATES.

NOMENCLATURE.

Symbol	Description	Units.
b	Breadth of diffuser.	m
l	Length of tailpipe.	m
L	Length of diffuser wall.	m
N	Length of diffuser.	m
u	Fluid velocity.	m/s
U or u_o	Freestream velocity (generally taken as centreline value)	m/s
$\bar{u}$	Mean velocity. (mass averaged velocity)	m/s
w_1	Inlet width. (Diffuser)	m
w_2	Outlet width.	m
w	Local width of duct.	m
α	Kinetic energy correction factor.	
β	Momentum correction factor	
2ϕ	Divergence angle.	
x	Distance from inlet of diffuser.	m
θ	Momentum thickness.	m
δ^*	Displacement thickness.	m
H	Shape factor.	
AR	Area ratio. (w_1/w_2)	
AS	Inlet aspect ratio. b/w_1	
Cp	Pressure recovery coefficient.	
η	Effectiveness.	
ρ	Density of fluid.	kg/m^3
$Re(N_R)$	Reynolds no. based on inlet width and mean velocity.	
p	Local static pressure.	N/m^2, mm H_2O
p_1	Inlet static pressure.	N/m^2, mm H_2O
$\dot{M}$	Mass flow.	kg/s
Cp_L	Pressure recovery coefficient based on a tailpipe pressure.	
Cp_E	Energy corrected Cp.	

		Units.
η_E	Energy corrected η.	
μ	Viscostiy of fluid.	kg/ms
ν	Kinematic viscosity of fluid.	m/s
Re_x	Re based on length.	
L/w_2	Length of tailpipe expressed in diffuser exit widths.	
δ	Distance to edge of boundary layer from wall i.e. thickness of boundary layer.	m
R.M.S.	Root mean square value.	
M	Mach number	

INTRODUCTION.

In many fluid flow systems it is required to increase the static pressure in the system by means of decelerating the flow and reducing the kinetic energy of the fluid. Provided that the flow everywhere is subsonic this may be achieved with a diverging duct. These are used extensively in such systems as gas turbine intakes, venturimeters, wind tunnels and air conditioning systems.

This particular work is confined to two dimensional diffusers, although conical diffuser performance is included in the review of relevant work.

A two dimensional diffuser is one which has two components of velocity, one along and the other perpendicular to the longitudinal axis. This implies an infinite diffuser breadth which is not possible in practice. However, it has been shown that for ratio of breadth to width, known as the Aspect Ratio (AS), of greater than six, the sidewall effects are minimal (this is discussed in further detail in the following section). It is interesting to note that many large annular diffusers may be likened to a two dimensional diffuser having a large aspect ratio.

(i) Diffuser Geometry.

A two dimensional diffuser geometry (shown in figure 1) may be described by a combination of various parameters.

The ones favoured in the present investigation are:-

Area Ratio (AR) = w_2/w_1

Divergence Angle = 2ϕ

Inlet Aspect Ratio (AS) = b/w_1

Distance from Inlet = x/w_1

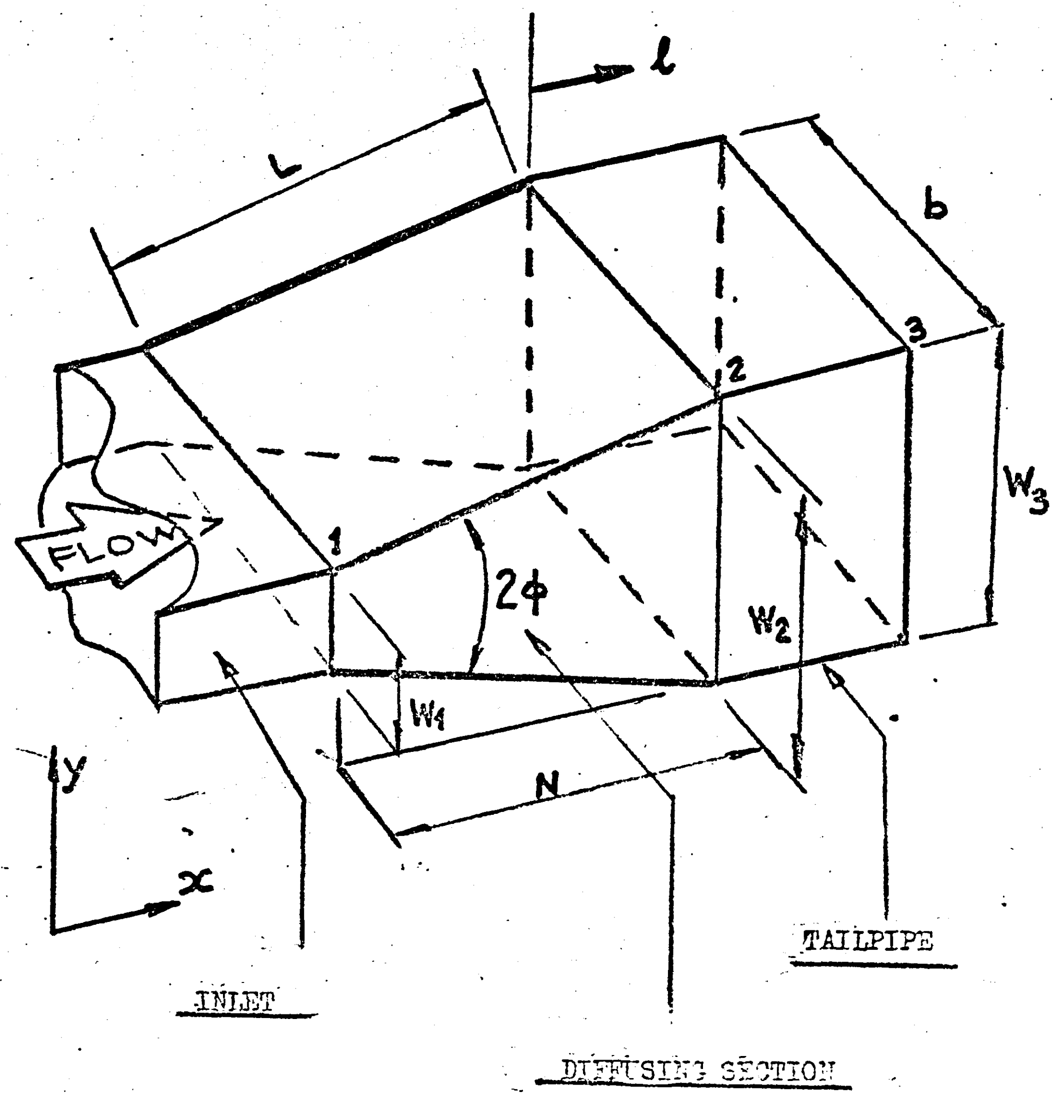

Diffuser geometry.

FIGURE.......1

Two other possible parameters are:-

Diffuser Wall Length Ratio L/w_1

Diffuser Axial Length Ratio N/w_1

If a diffuser is followed by a tailpipe then an extra parameter:-

Tailpipe Length = n

(where n = length of tailpipe/tailpipe width).

In diffusers a corner radius is normally provided at the diffuser inlet and exit. These radii prevent the diffuser wall length and the axial length from being determined accurately. Therefore, in this work the ratios L/w_1 and N/w_1 have not been used. However, several earlier workers have expressed performance data in terms of L/w_1 and N/w_1 in addition to either area ratio (AR) or divergence angle (2ϕ).

Diffuser Performance and Flow Parameters.

(ii) Inlet boundary layer thickness.

The inlet boundary layer thickness is usually described by the ratio of displacement thickness to half the inlet width ($2\delta^*/w_1$). The inlet boundary layer may also be described by a ratio of the momentum thickness to half the inlet width ($2\theta/w_1$). The shape of the velocity profile may be illustrated by the ratio of δ^*/θ, known as the shape factor (H). Fuller definitions of those boundary layer parameters will be included in chapter III.

(iii) Flow regimes.

There are three basic regimes of flow within a diffuser:-

(a) Unseparated flow; This occurs when the boundary layer remains attached to the diffuser wall at all times.

(b) Separated flow; It is generally accepted that this occurs when the boundary layer becomes detached from the wall (although it may re-attach at a later stage).

(c) Stall; This occurs when a stagnant, recirculatory flow is present.

The fluid near the wall tends to move upstream. Stall is an advanced stage of flow separation.

There are various degrees of stall and separation in a diffuser, but the two preceding definitions are generally used to discriminate between separation and stall.

(iv) Performance parameters.

Several parameters are needed to assess diffuser performance, but the two most commonly used are:-

(a) The pressure recovery coefficient (Cp) which is defined as the ratio of the static pressure rise between any station downstream of the diffuser inlet (p) and the station at the diffuser inlet (p_1), to the inlet dynamic pressure, $\frac{1}{2}\rho\bar{u}_1^2$, where $\bar{u}_1$, is the mass averaged inlet velocity.

$$\text{Hence } Cp = (p - p_1)/\tfrac{1}{2}\rho\bar{u}_1^2,$$

(b) The diffuser effectiveness which is defined as the ratio of the static pressure rise between the station at inlet and a station downstream ($p - p_1$), and the dynamic pressure decrease between the two positions, which is $\frac{1}{2}(\rho\bar{u}_1^2 - \rho\bar{u}_2^2)$ therefore effectiveness (η) for incompressible flow reduces to:-

$$\eta = (p - p_1)/\tfrac{1}{2}\rho_1\bar{u}^2\,(1 - 1/AR^2)$$

This is not an energy efficiency since it uses the mass averaged velocity $\bar{u}$ in the calculation of the dynamic pressure.

A true energy efficiency may be obtained by taking into account the discrepancy incurred by using the value of mean velocity determined from the mass flow, (i.e. $\bar{u} = 1/\rho w\int_0^w \rho\, u\,dw.$).

Hence the kinetic energy using $\bar{u}$ will be; $\frac{1}{2}\rho\bar{u}^3 w$ or $\frac{1}{2}\int_0^w \rho\ \bar{u}^3\,dw$ ---- (1)

The true kinetic energy is $\frac{1}{2}\int_0^w \rho u^3\,dw$ ------(2)

Therefore to convert the mass averaged velocity value of kinetic energy to the true value of kinetic energy a kinetic energy correction factor α can be used. Thus from equations 1 and 2, α may be defined as:-

$$\alpha = \frac{1}{2}\int_0^w \rho u^3 dw \Big/ \frac{1}{2}\int_0^w \rho\bar{u}^3 dw \quad \text{--------------(3a)}$$

which reduces to:-

$$\alpha = 1/w \int_0^W \left(\frac{u}{\bar{u}}\right)^3 \, dw \quad \text{-----} \quad (3b)$$

$$\text{or} \quad \alpha = 1/W \int_0^W \left(\frac{u}{\bar{u}}\right)^3 \, dy$$

Cp may be corrected to a true energy recovery.

$$Cp_E = (p - p_1)/\tfrac{1}{2}\rho\bar{u}_1^2\alpha_1$$

and similarly for effectiveness

$$\eta_E = (p - p_1)/\tfrac{1}{2}\rho(\alpha_1\bar{u}_1^2 - \alpha\bar{u}^2)$$

Other parameters used include:

The total pressure loss coefficient λ which is given by the expression;-

$$\lambda = 1 - (p - p_1)/\tfrac{1}{2}\rho\bar{u}_1^2(1 - 1/AR^2)$$

Therefore $\lambda = 1 - \eta$

Livesey[38] however, points out that since the kinetic energy is uncorrected λ is not strictly a total pressure loss coefficient.

Another form of total pressure loss coefficient is used by Idel Chik :-

$$\zeta = \frac{p - p_1}{\tfrac{1}{2}\rho\bar{u}_1^2} \quad \text{or} \quad \lambda\left(1 - \frac{1}{AR^2}\right)$$

(v) Inlet parameters.

An important parameter used in describing the inlet flow condition is the Inlet Reynolds number (Re). This is usually based on the inlet width w, as the characteristic dimension. Hence the inlet Re. is

$$\frac{\rho\bar{u}_1 w_1}{\mu} \quad \text{or} \quad \frac{\bar{u}_1 w_1}{\nu}$$

(vi) Summary

The various flow parameters used in this work are:-

Re number (based on inlet width) $= \dfrac{\rho\bar{u}_1 w_1}{\mu}$

δ^* = displacement thickness (m)

θ = Momentum thickness (m)

H = δ^*/θ = shape factor.

2ϕ = Divergence angle of diffuser. (degrees)

AR = Area Ratio of diffuser = w_2/w_1

C_p = Pressure recovery coefficient $= (p - p_1)/\frac{1}{2}\rho(\bar{u}_1^2)$

η = Effectiveness $= (p - p_1)/\frac{1}{2}\rho(\bar{u}_1^2 - \bar{u}^2)$

α = Kinetic energy correction factor $= \frac{1}{W}\int_0^W \left(\frac{u}{\bar{u}}\right)^3 \, dy$

REVIEW OF PREVIOUS WORK.

Certain early work was done on diffusers by various workers such as BORDA[33] and VENTURI[34] in the 18th century, but the first really comprehensive study was carried out by GIBSON[1]. He published many papers on his work between 1910 and 1913. In his experiments he tested over 90 different diffusers, both plane walled and conical, with angles of divergence varying from 3^o to 180^o and area ratios from 2.25 to 10.96. His general conclusions on the effect of divergence angle and area ratio on pressure recovery have been borne out by subsequent workers in this field. An example of Gibsons introduc~~ing~~tory work is shown in figure 2.

I.1 Effects of Geometry.

I.1.1 Area Ratio (AR) and Divergence Angle (2ϕ)

The effects of geometry of the diffuser has undergone extensive work and the optimum divergence angle has been found to be in the region of 7^o, the exact angle varying with inlet and stream conditions.

KLINE[2] et al conclude that the optimum divergence angle lies between 6^o and 8^o. At these angles of divergence the optimum effectiveness occurs at low area ratios (approximately 2 in unstalled diffusers). However, the optimum pressure recovery coefficient occurs at high area ratios with slight separation in the diffuser. These trends are shown in figures 3c and 3d. DERRICK[5] and KELNHOFFER[6] draw similar conclusions in their work, shown in figures 3d and 4.

Gibson, however, found the optimum pressure recovery coefficient to be dependent on diffuser type. His optimum divergence angles were 5^o for conical, 6^o for square and 10^o for a two dimensional diffuser of AR = 4. This can be seen in figure 2. These values, however, are suspect since he used a tailpipe pressure tapping approximately two diffuser exit diameters downstream. More recent workers have shown that when a diffuser is credited with the pressure rise in the tailpipe, then the divergence

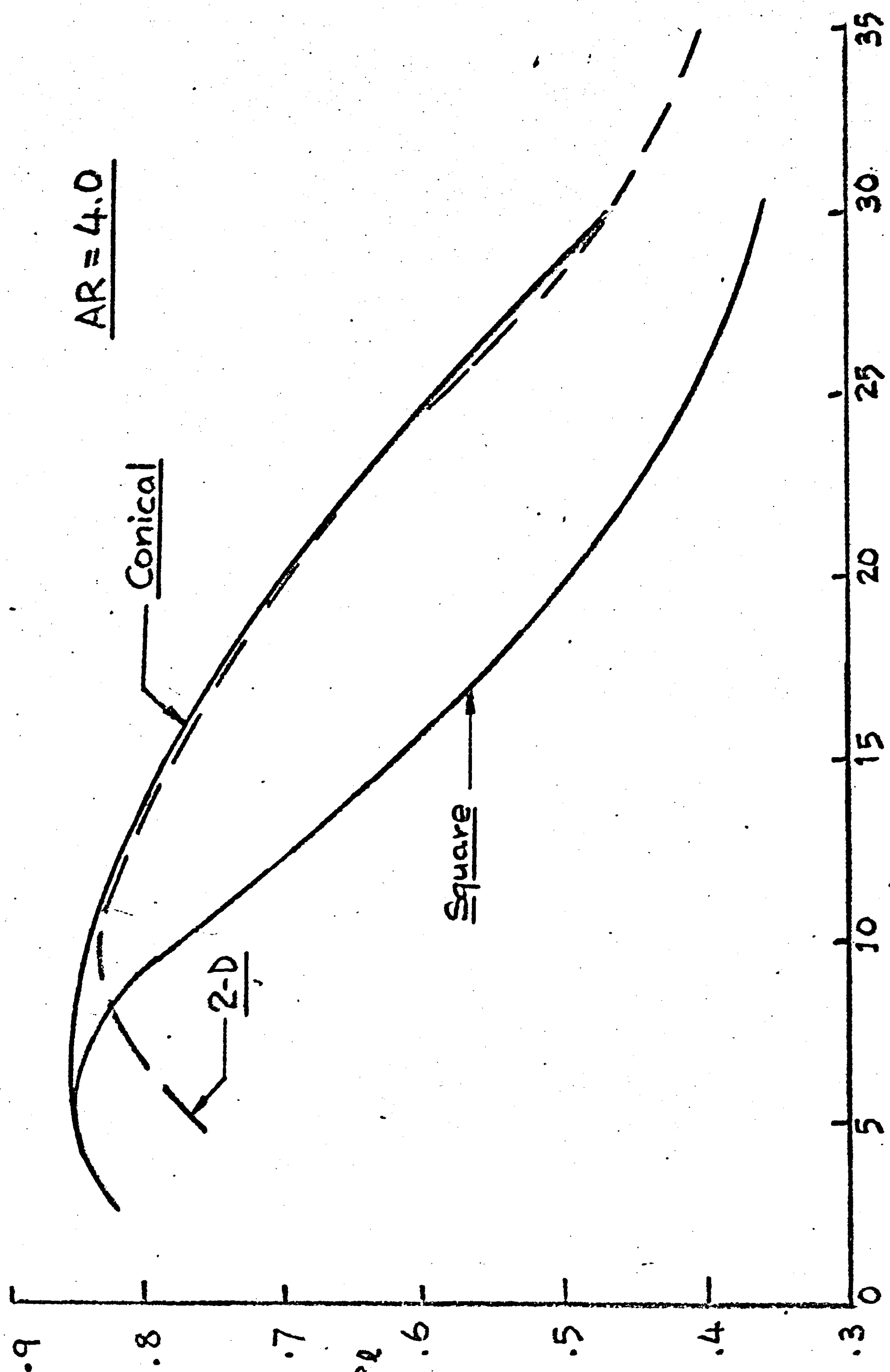

COMPARISON OF STRAIGHT WALLED DIFFUSER PERFORMANCE
(From GIBSON [1])

FIGURE....2

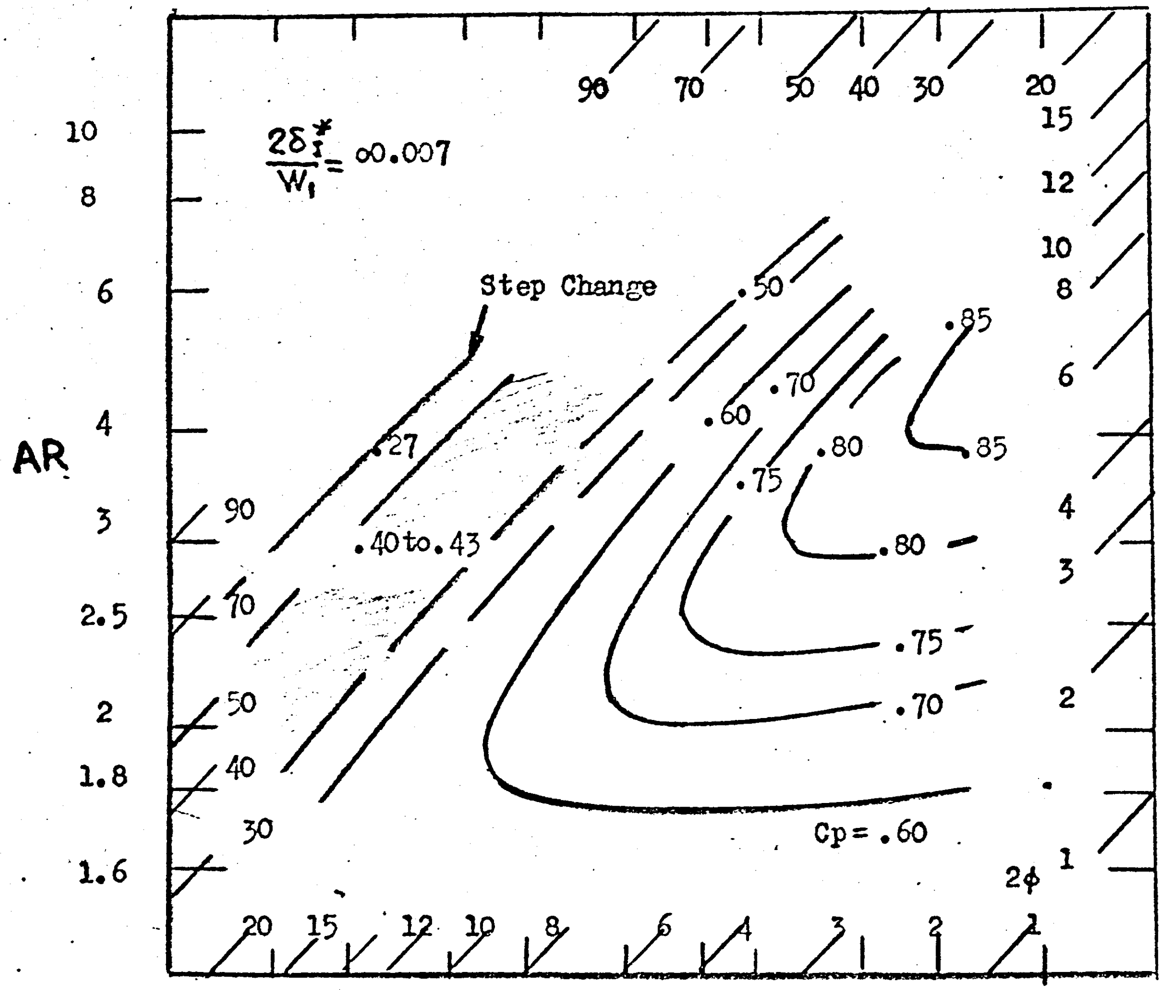

PRESSURE RECOVERY (From KLINE[2])

FIGURE....3(a)

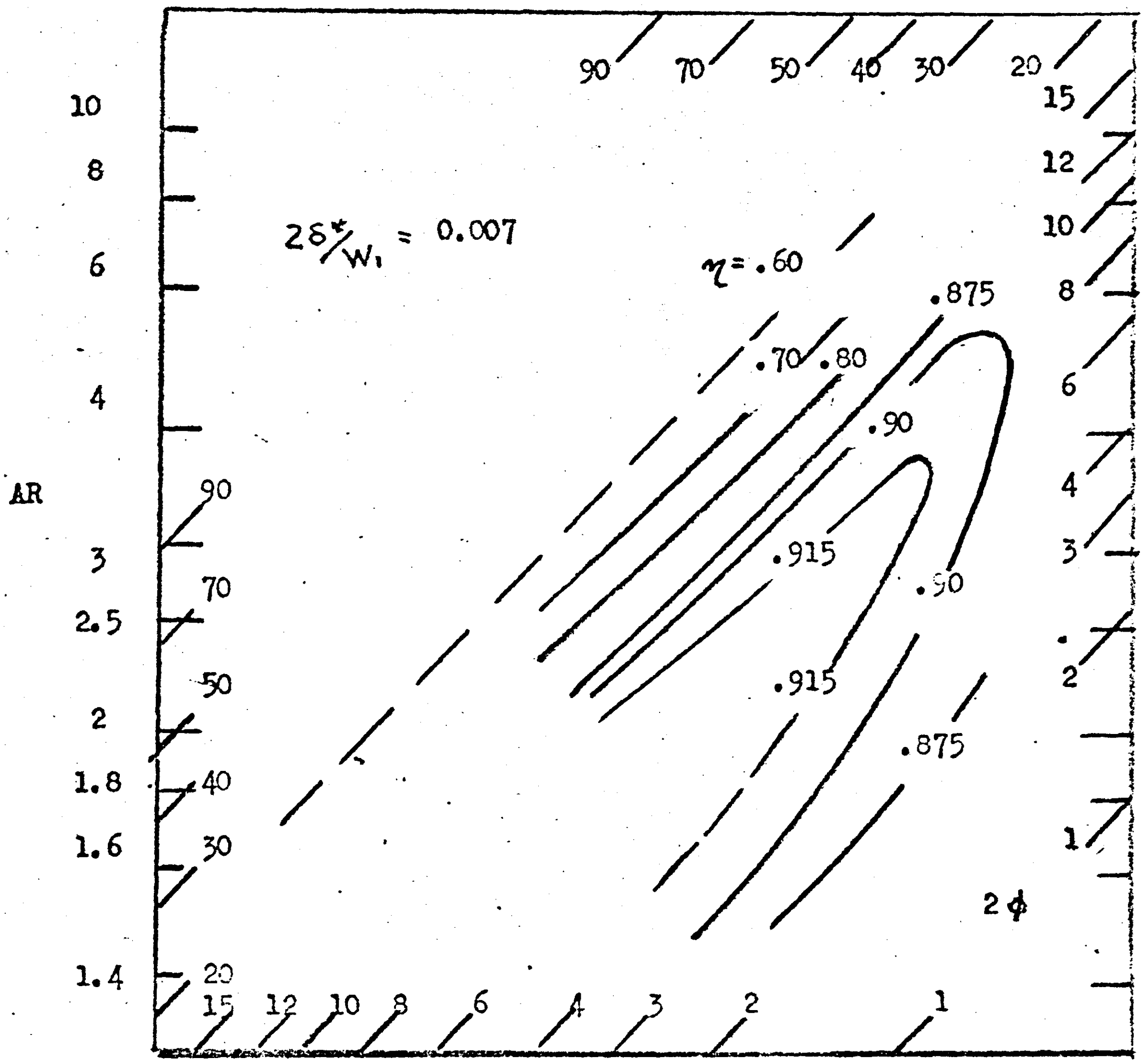

EFFECTIVENESS (From !LINE[2])

FIGURE...3(b)

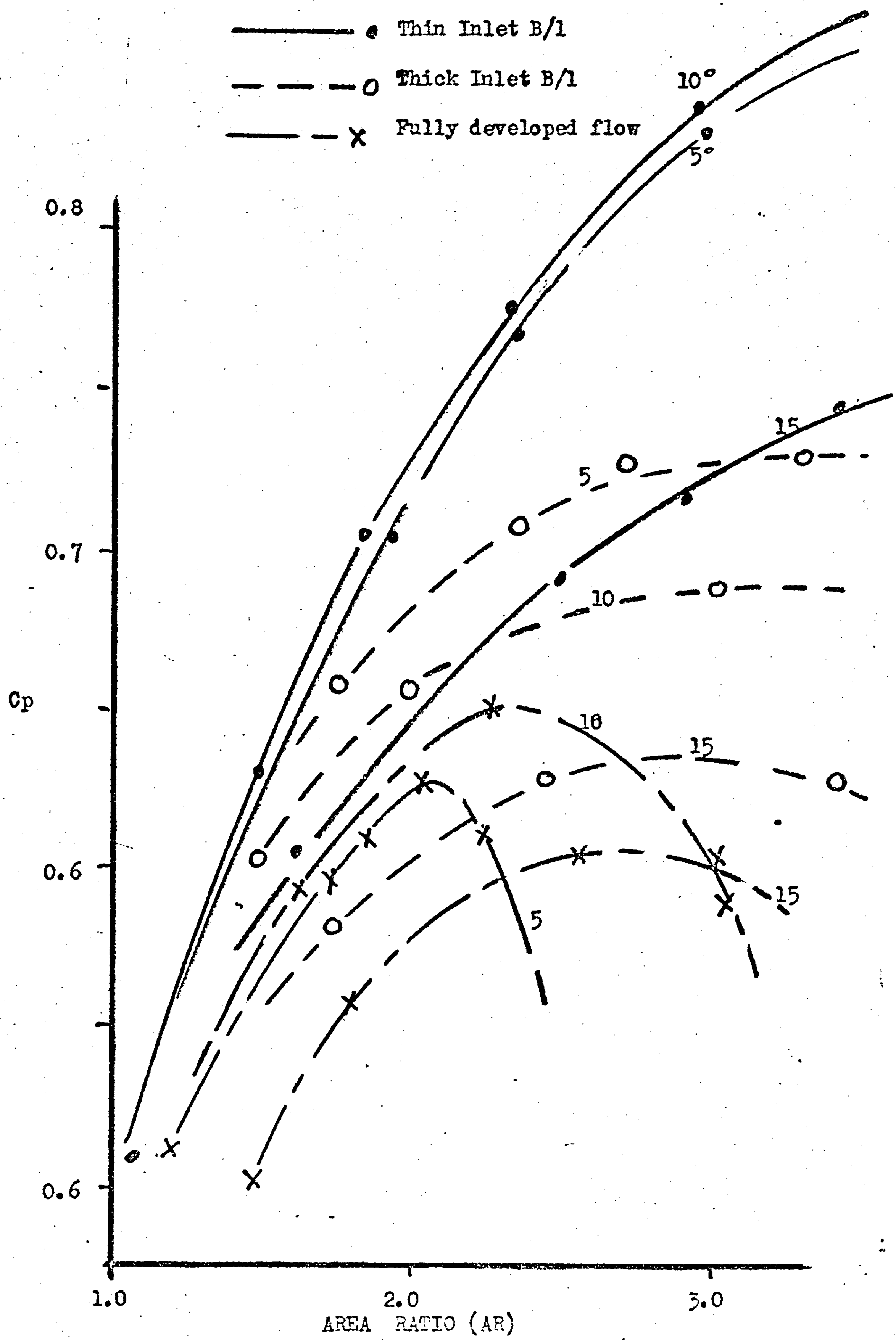

PRESSURE RECOVERY / AR (From KLINE[2])

FIGURE...3(c)

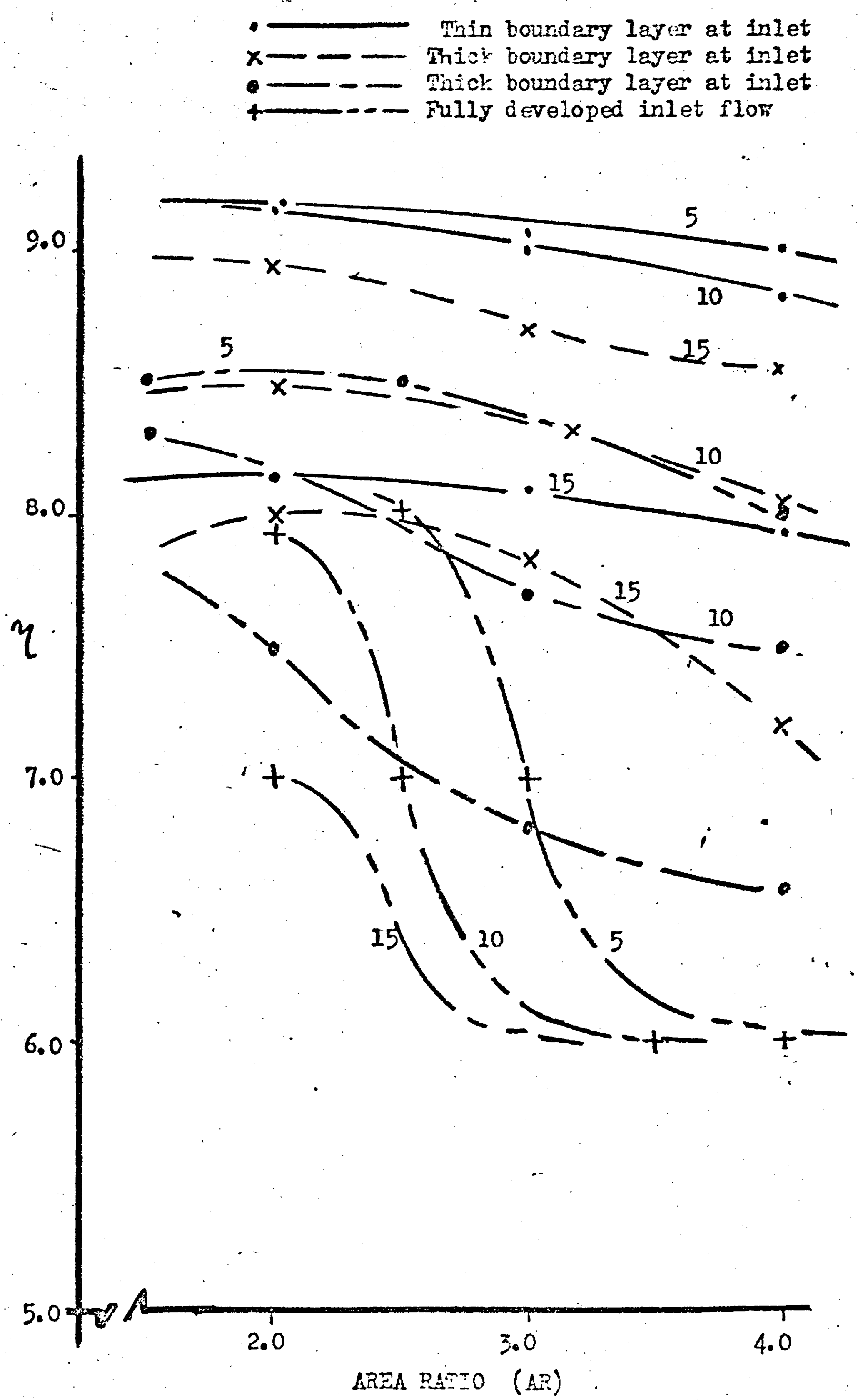

EFFECTIVENESS / AR (From KLINE[2])

FIGURE....3(d)

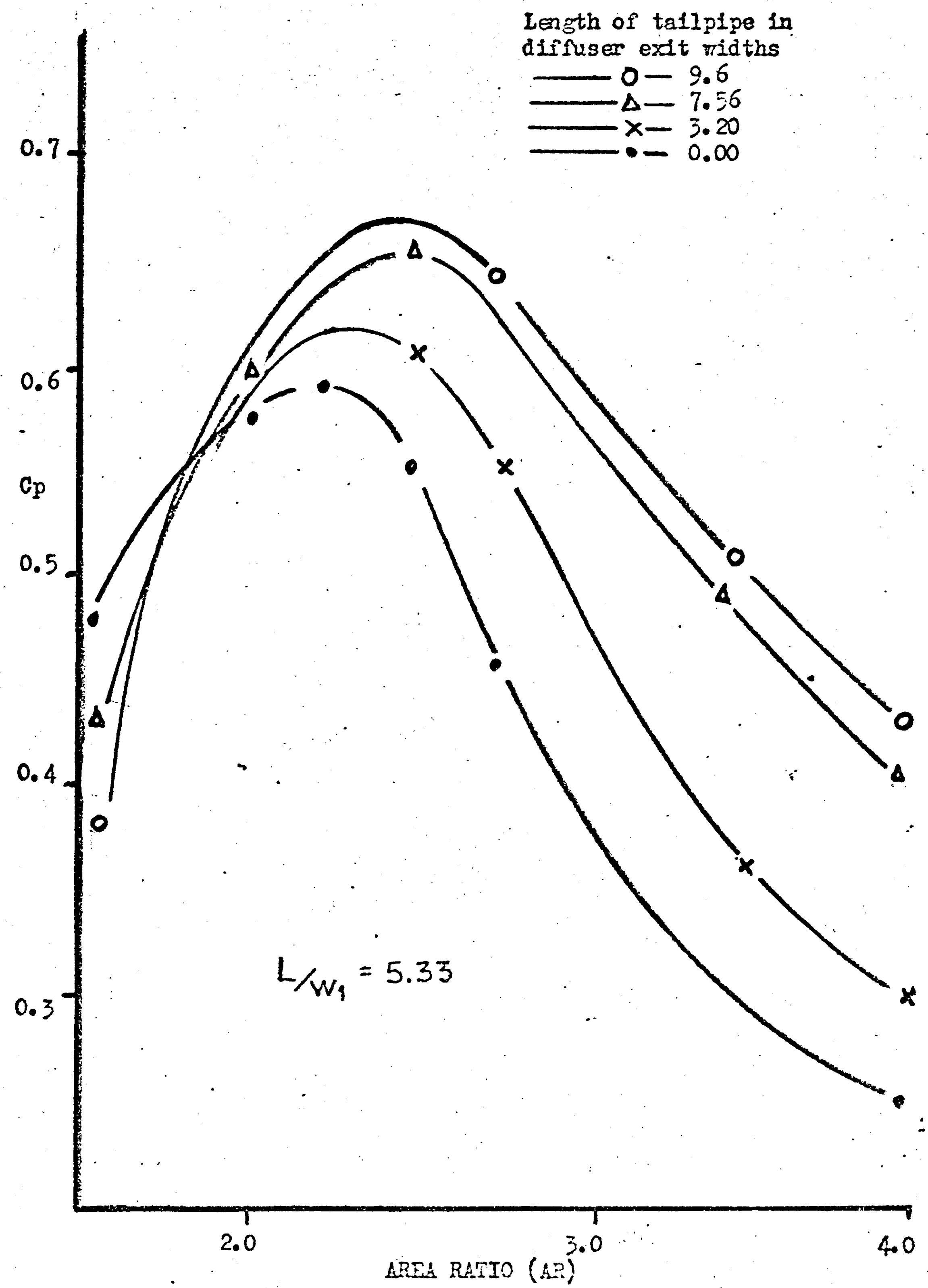

RESULTS OF THE INVESTIGATION OF DERRICK AND FELDHOFFER

FIGURE....4

THE EFFECT OF INCLUDING THE TAILPIPE PRESSURE RISE IN THE PERFORMANCE OF CONSTANT AREA RATIO TWO DIMENSIONAL DIFFUSERS (From HUDIMITO 1952)

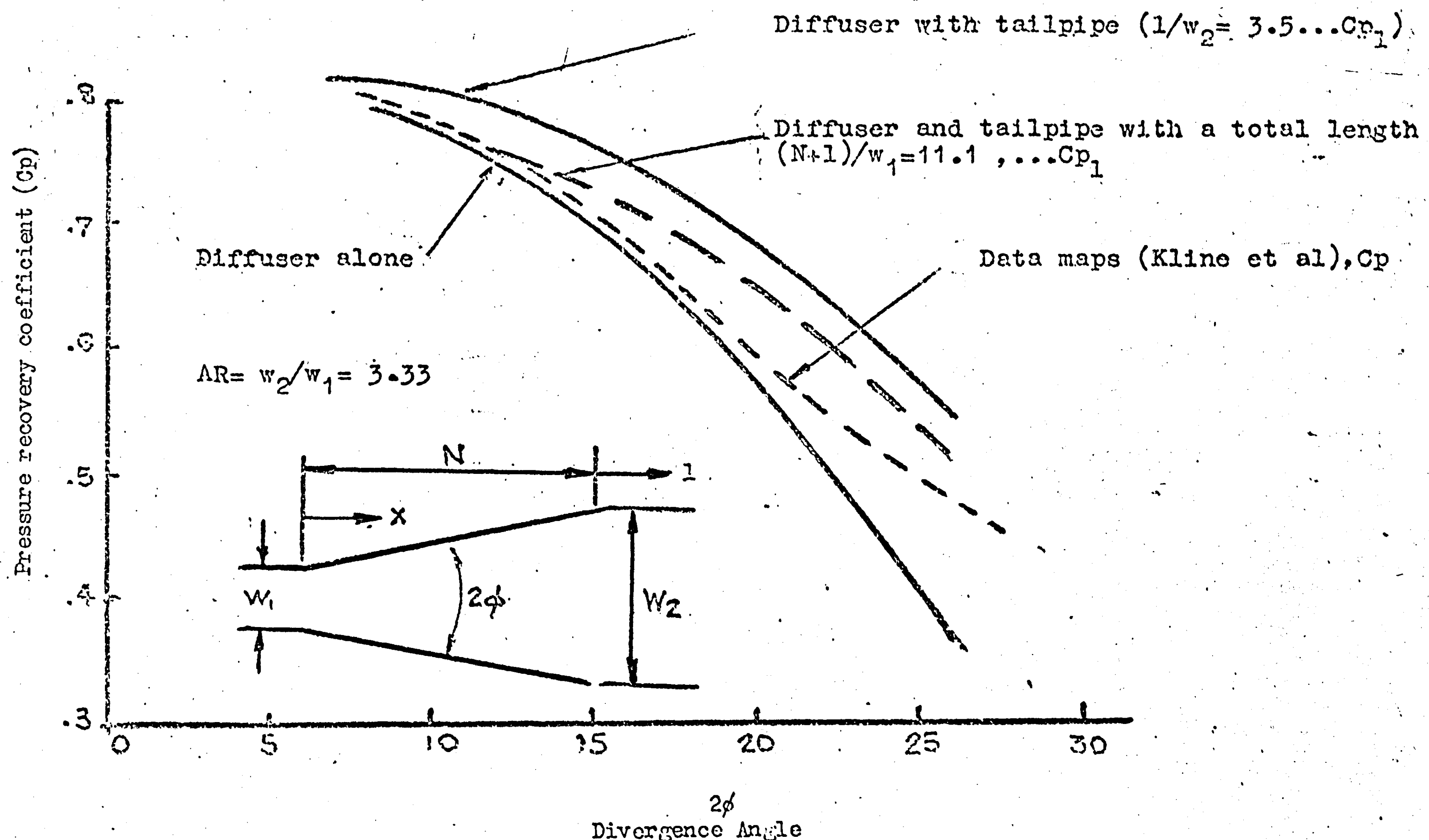

FIGURE.....5

angle at optimum performance is increased by 2 to 3 degrees. Thus Kline postulates that the reason Gibson's work varies from the generally accepted values is due to this small tailpipe addition.

A later worker in this field VULLERS[3] carried out an investigation into the performance of diffusers with plenum discharge. He situated the diffuser just downstream of the fan discharge. There was no flow straightening of any kind between the fan and diffuser inlet. Since inlet flow symmetry and turbulence have a large effect on performance, and no inlet conditions were stated, his results have not been included in the review. More important work was done by HUDIMITO[4] in 1952. His diffuser performance (Cp_L) was based on the maximum pressure in the tailpipe. He published data for area ratios of 1.5, 2.0 and 3.33 (shown in figure 5).

His results are consistent with those of GIBSON[1] and shows the optimum tailpipe recovery to occur with a diffuser of AR = 3.33 and divergence angle 10° at a position 3.5 exit diameters downstream. The optimum value of Cp in the tailpipe was 0.82.

This value agrees with Kline's optimum of 0.82 for $2\phi = 7^\circ$ with an AR= = 3.33 and a plenum discharge. However, Hudimito's value should be slightly higher due to the addition of the tailpipe. However, at optimum divergence angles, (7° for plenum discharge and 10° for tailpipe discharge) the difference between Cp and Cp_L is so slight that it may be obscured by experimental error.

The following general conclusions on optimum area ratios and divergence angles may be drawn from previous workers.

1. The maximum diffuser performance occurs between 6° and 8°.
2. Optimum effectiveness occurs at area ratios of approximately 2.
3. Maximum values of Cp occurs at area ratios of approximately 3 or slightly greater.
4. The actual values of maxium pressure recovery coefficient increases from 0.65 and 0.85 as the inlet boundary layer decreases.
   This effect is shown in figures 3c and 3d.

1.1.2 Aspect Ratio (AS)

Little work has been conducted solely into the effect of Aspect Ratio (AS) on two dimensional diffuser performance. However, Kline et al state that experimental evidence leads to the conclusion that aspect ratios greater than six will make sidewall effects insignificant (shown in figure 6). Even on small aspect ratio diffusers (AS = 1), it appears that aspect ratio is a much less important factor than Area Ratio in governing the performance of the Unstalled diffuser. However aspect ratio must be taken into account when results such as those of DERRICK [5] and KELNHOFFER, are assessed. (Derrick and Kelnhoffer investigated a diffuser having an aspect ratio less than unity).

1.2 Effect of Inlet Boundary Layer Conditions.

1.2.1 Boundary Layer Thickness.

The effect of boundary layer thickness appears to be one of the most significant factors governing diffuser performance. Therefore work which does not state the inlet boundary layer condition is of little practical value.

The inlet boundary layer thickness is described by the ratio of the displacement thickness to half the inlet width i.e. $2\delta^*/W_1$. DERRICK [5] who uses fully developed flow conditions ($2\delta^*/W_1 = 0.11$), states that the inlet boundary layer thickness for a fixed geometry diffuser establishes the absolute maximum Cp for that diffuser. Further, the inlet conditions affect the performance more than flow regime. He states that generally as the inlet boundary layer thickness increases, then Cp and η decrease (this is shown in figure 3c and 3d).

KLINE [2] has done extensive work on the effect of the inlet boundary layer thickness, from $2\delta^*/W_1 = 0.007$ (which he uses to define a thin boundary layer) to $2\delta^*/W_1 = 0.05$. It may be noted that fully developed flow at the inlet would have a value of $2\delta^*/W_1$ of around 0.11. (This has been found during preliminary investigations in the present work).

Kline has 'mapped' these inlet conditions for various divergence angles and area ratios, (Examples of these can be seen in figures 3a, 3b).

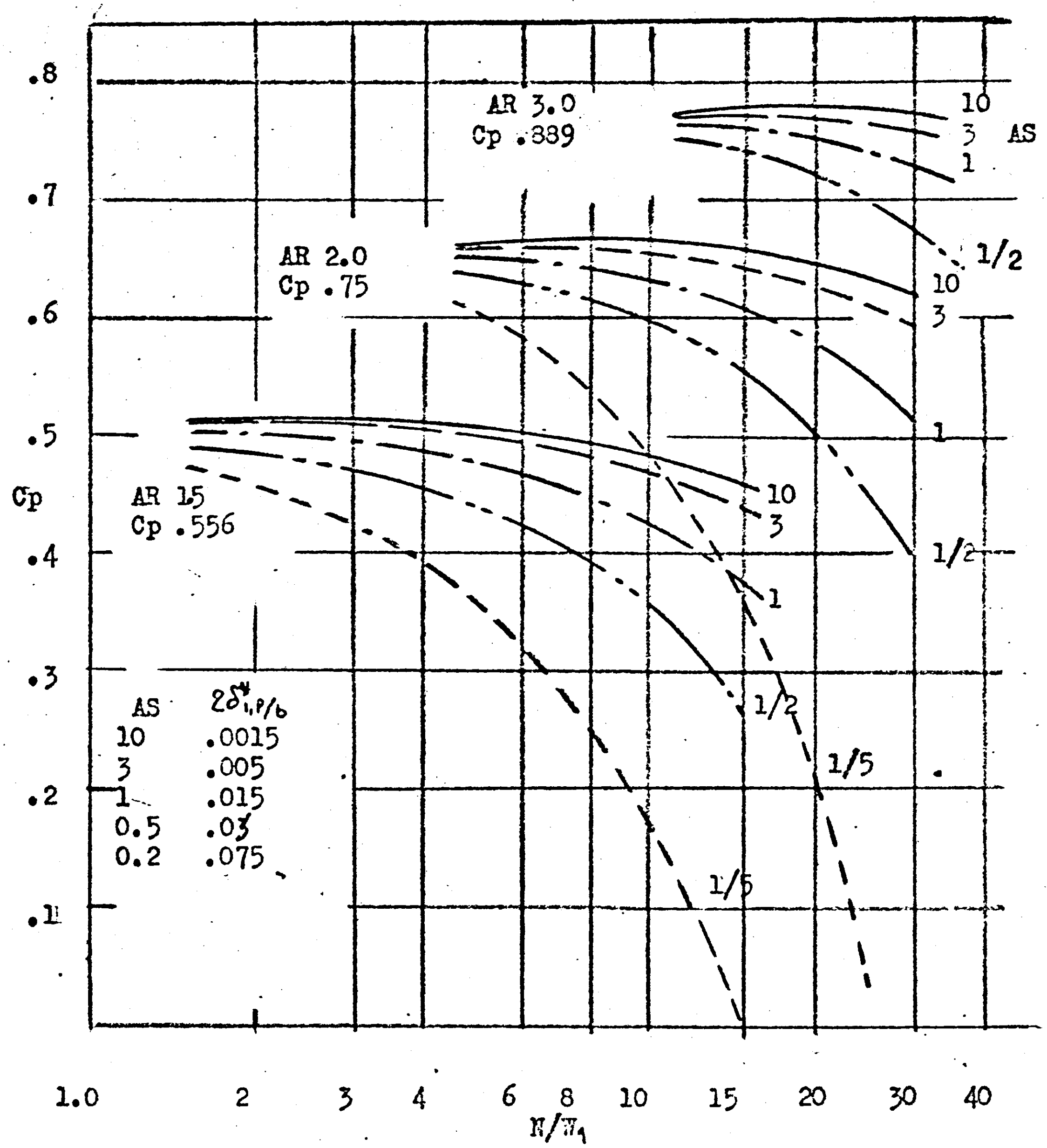

Effects of aspect ratio on performance for constant inlet boundary layer thickness on all four walls

$2\delta^{*}/W_1 = 0.015$,

FIGURE...6

Using this data, figures 3c, and 3d were plotted. These show that for optimum geometric conditions ($AR = 3.0$, $2\phi = 7^\circ$), the variation of inlet boundary layer thickness from $2\delta^*/W_1 = 0.007$ to 0.05 reduces the maximum Cp from 0.85 to 0.65. Kline et al also note that increases in boundary layer thickness are usually generated by an increased inlet pipe length. This increase may, however, have the effect of increasing the turbulence intensity, (to be discussed later) which also has an effect on performance.

There is a limited amount of data for fully developed flow at inlet. WAITMAN[6] for this inlet condition shows that peak recovery occurs at divergence angles between 10° and 20°.

Another inlet parameter which has an effect on performance is the boundary layer shape factor H. MOORE and KLINE[7] note that shape factor H and $2\delta^*/W_1$ together probably have an effect on performance but did not investigate it.

1.2.2 Turbulence Intensity $\left(\sqrt{\overline{u'^2}}/\bar{U}\right)$

The level of turbulence intensity affects the performance of the diffuser. Turbulence intensity being defined as the ratio root mean square value of the flow velocity fluctuations, $\sqrt{\overline{u'^2}}$ to the mean velocity of the flow $\bar{U}$, $\left(\sqrt{\overline{u'^2}}/\bar{U}\right)$.

WAITMAN, RENEAU and KLINE[6] observed that the level of turbulence affected the angle at which stall inception occurred. They noted that, generally, in small diffusers with divergence angles of less than 20°, low turbulence levels delay stall inception. However, at higher divergence angles and larger diffuser wall lengths, higher inlet turbulence levels delay stall inception. They conclude that pressure recovery is a function of both inlet turbulence intensity and the boundary layer thickness. These results are shown in figure 7.

Kline et al conclude that with a turbulence intensity of less than 3% the flow will be unaffected. If turbulence levels exceed 7% then a large transitory stall regime will only occur at higher area ratios.

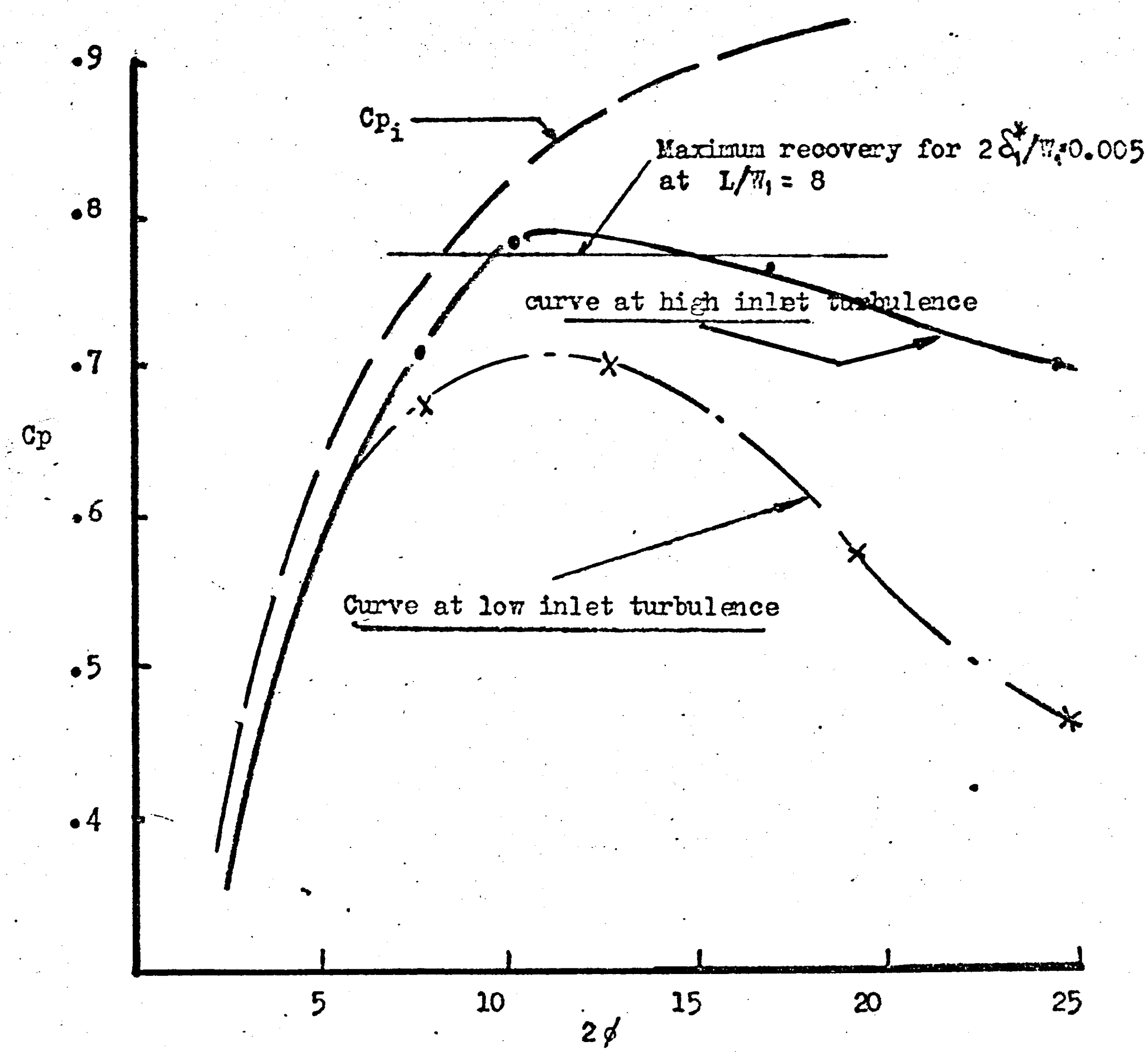

Effects on performance of high free stream turbulence

(from WAITMAN and RENAU)

FIGURE....7

In general most workers agree that low turbulence intensities (< 2%) will have little effect but with high inlet turbulence intensities ($\geqslant$ 5%) the onset of stall is delayed and therefore pressure recovery may be slightly increased.

I.3 Diffuser Performance.

Kline et al show conclusively that optimum performance occurs at low area ratios, (2 to 3), divergence angles between 6^0 to 10^0 and a thin inlet boundary layer. They also conclude that the optimum pressure recovery occurs in a large area ratio diffuser, (approximately 3), at the onset of slight flow separation. If, however, flow separation increases pressure pressure recovery will fall. Kline et al postulate a criterion for the detachment of the boundary layer which correlates the peak recovery geometry. Their criterion is that the flow will leave the diffuser wall when the local momentum thickness gradient reaches 0.012 i.e. $\frac{\partial\theta}{\partial x} = 0.012$. This they call their detachment criterion and is derived in ref. 2 chapter 5.

I.4 Reynolds Number Effects (Re)

Reynolds number for a diffuser is generally based on the inlet width or diameter. Kline in his extensive work on two dimensional diffusers assumed that Reynolds Number (based on inlet width) had no significant effect over the range of his tests. Although the Reynolds Number did vary, Kline carried out no tests to substantiate this view. COCKRELL and MARKLAND[29] conclude that Reynolds Number is only important in its effect on the size of the boundary layer thickness.

Similarly FERRETT[21] notes that in theory for a given diffuser geometry and upstream conditions then a variation in Reynolds Number will vary the inlet boundary layer thickness, and therefore performance. Secondly he points out that for a given inlet boundary layer thickness the Reynolds Number will affect the rate of growth of the boundary layer within the diffuser and hence performance. He goes on to point out that if one considers a simple power law velocity profile then it is evident that as Reynolds Number increases then $2\delta^*/W_1$ will be reduced. This trend is shown in his experimental work where he found η and Cp to increase until Reynolds Number reaches 2×10^5

after which he notes that further increases in Reynolds Number produce no detectable increases in Cp or η.

RIPPL[11], found that Cp was essentially constant in both conical and two dimensional diffusers for a variation in Reynolds Number from 8×10^4 to 6×10^5. GIBSON[1] in 1910 also stated that he found no change in performance with Reynolds Number over the range used in his work, (4×10^4 to 2×10^5) but gives no further information about his tests. YOUNG and GREEN[12] did tests from Reynolds Numbers of 1×10^5 to 1×10^6 and their data shows that up to the transonic region the Reynolds number effects were negligible. MOORE and KLINE[7], and FOX and KLINE[13] did not find any variation in performance with Reynolds Number, although the tests were confined to Reynolds Numbers of 5×10^3 to 2×10^4.

Kline, however, suggests three possible effects on performance of Reynolds Number variation.

(i) If the Reynolds Number is below 2×10^4, then an increase in Reynolds Number will produce an increase in performance parameters.

(ii) If Reynolds Number is above 2×10^4 and either a jet flow regime exists or the performance charateristics have not reached their optimum values, then there is still a slight Reynolds Number dependence.

(iii) Optimum performance is independent of Reynolds Number.

HUDIMITO[4] did publish some data on Reynolds Number effects, (shown in figure 8). He showed that for a particular diffuser ($AR = 3.33$, $N/w_1 = 16.67$, $2\phi = 7^\circ 42'$) the maximum pressure coefficient, Cp_L, increased by 30% as the Reynolds Number increased from 3×10^3 to 3×10^4. As the Reynolds Number was increased above 3×10^4, the increase in Cp_L was much reduced. The maximum Reynolds Number was 5×10^4. This value corresponds to the lower limit used by most workers in the field.

It is important to note that for many of these reported tests, particularly those at low Reynolds Number, the apparent effect of performance was not simply due to the transition of laminar to turbulent flow.

I.5 Tailpipe Addition.

The effect of tailpipe addition has been investigated by numerous workers.

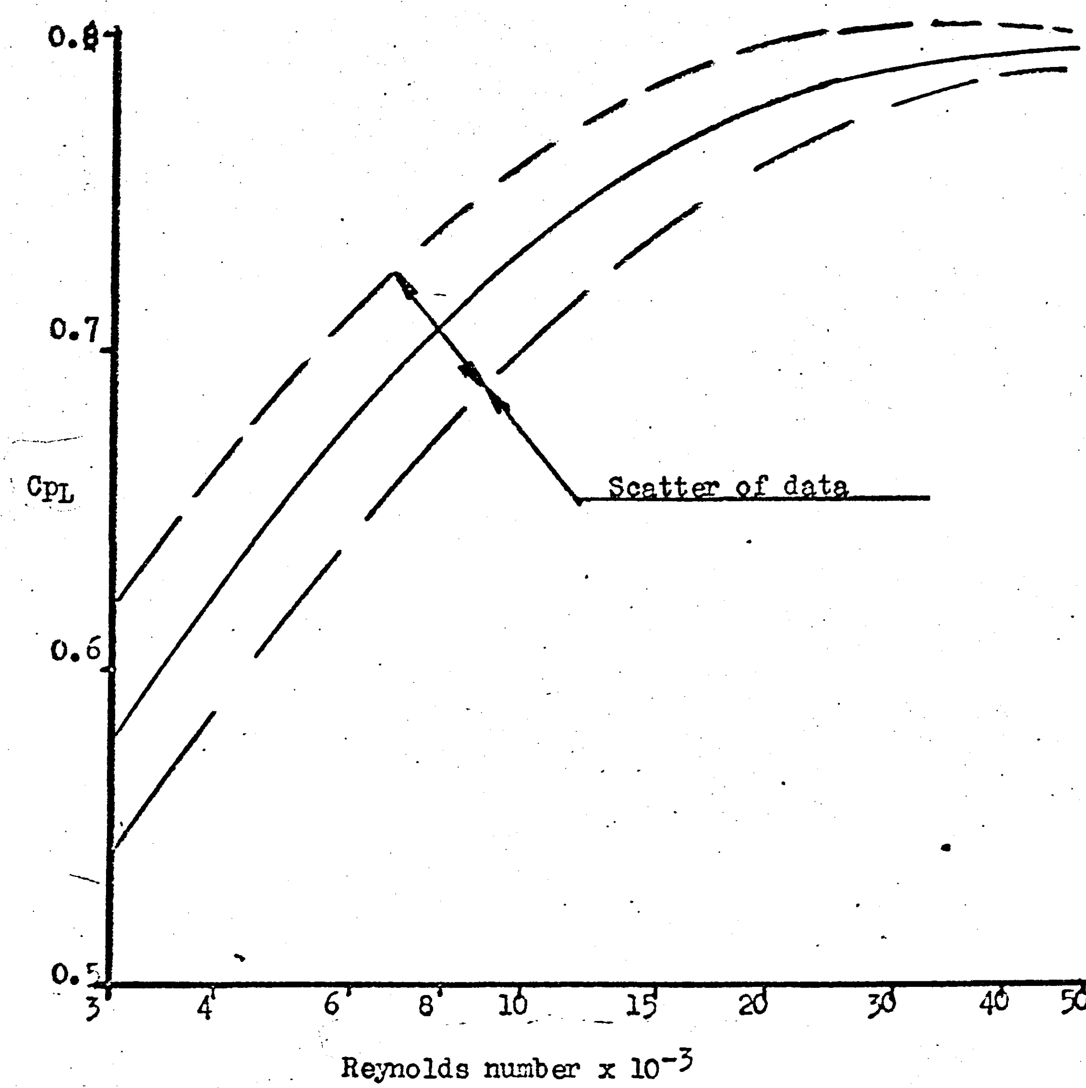

Cp_L(tailpipe recovery) / Reynolds number (From HUDIMITO)

FIGURE.....8

The first being that of GIBSON[1], who used the tailpipe pressure to compute the performance of his diffusers.

From his data it can be estimated that his tailpipe had a length of approximately two outlet diameters ($L/W_2 = 2$), and his optimum tailpipe pressure recovery (Cp_L) occurred with a divergence angle of 11^o (with two dimensional diffusers). KLINE[2] et al also did work on the effect of constant area ducts following the diffuser. He postulates that the pressure rise in the first part of the tailpipe is due to the increased uniformity of the velocity profile. However he concluded that the value of pressure recovery (Cp) at the exit plane of the diffuser was independent of the tailpipe to within the uncertainty of the data.

The fraction of pressure recovery which occurred in the tailpipe (Δ Cp) was small (up to 7%) for diffusers operating without flow separation. However it increased as the amount of separation increased until transitory stall was established, when it was about 30%. REID[16] showed that the addition of a tailpipe improved the performance of the diffuser and increased the divergence angle required for optimum performance. HUDIMITO[4] also found that the pressure recovery (Cp) increases when a tailpipe was added to the diffuser (shown in figure 9 and also figure 5). For a diffuser of $L/W_1 = 16.67$, $2\phi = 7^o42'$, and an area ratio 3.33, then the maximum Cp_L occurred in the tail-pipe at 3.5 exit widths dowstream (L/W_2).

COCKRELL and MARKLAND[29] also found that for a configuration of 15^o divergence angle, AR = 2.25 with a fully developed flow, the addition of a tailpipe increases the overall recovery increases dramatically by about 60%.

KELNHOFFER and DERRICK[5] state that performance increased by the addition of a tailpipe of 6 hydraulic diameters long. Kline in discussing Derricks paper suggests that complete velocity transverses of tailpipe and diffuser could be taken and would be a worth while topic of research.

MACDONALD and FOX[31] observed that such large variations occurred between plenum discharge and tailpipe that the use of plenum dishcarge data to predict tailpipe discharge performance could lead to serious errors being incurred.

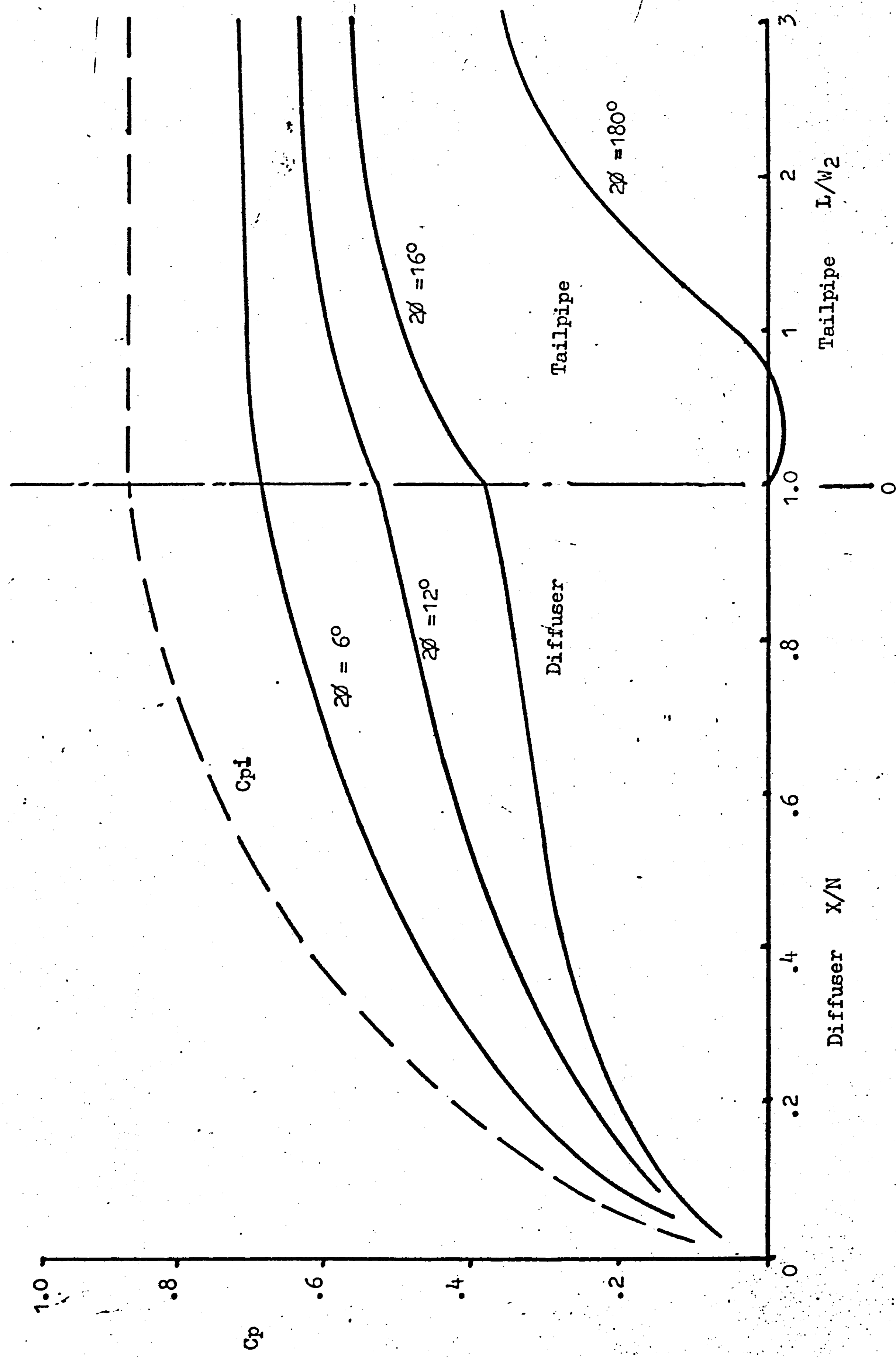

Comparison of actual and ideal static pressure distribution in square diffuser-tailpipe combinations with AR=2.98 (From Kline etal)

FIGURE 9

In conclusion it seems generally agreed that the addition of a tailpipe will increase performance, (except at very low divergence angles) due to the improvement in the velocity profiles in the tailpipe and the subsequent momentum recovery.

Chapter Two.

THE PRESENT INVESTIGATION.

II.1 Main Indications of the Review.

II.1.1 The Diffuser Geometry.

Most of the work reviewed in chapter I was concerned with either two dimensional or axisymetric diffusers having plenum or tailpipe discharge. The various divergence angles and area ratios have been covered comprehensively.

II.1.2 Diffuser performance

The previous chapter indicates that the optimum performance occurs when the divergence angle occurs between 7^{o} and 10^{o} and the area ratio lies between two and three for a two dimensional diffuser. The actual angle and area ratio is dependent on the inlet and outlet conditions, effectiveness decreases for area ratios above two and pressure recovery coefficient (Cp) decreases for area ratios above three, also an increase in area ratio appears to promote separation. The effect of the diffuser inlet boundary layer thickness is reasonably conclusive. As the boundary layer thickens, it adversely affects the diffusers overall performance, however, it must be noted that the method of boundary layer generation could be of some importance due to flow turbulence effects.

The presence of a downstream tailpipe appears to increase performance in high area ratios, high divergence angle diffusers. However the developing velocity profile within the diffuser (and tailpipe if fitted) appears to have been largely ignored.

The effect of Reynolds Number (Re) (based on inlet width) appears a little uncertain, since many workers have assumed its effects to be negligible but not carried out tests to verify their assumptions. It would however, appear that most workers have assumed that for Reynolds Numbers (Re) above 5×10^{4} the effect of Reynolds Number (Re) is small. Though the inlet boundary layer thickness would appear to significantly affect this point of independence.

The effect of turbulence intensity has not received much attention, however, the work done on this seemed to be in agreement as to its effect.

For values of turbulence intensity less than 3% the performance will be unaffected, above 6%, however, the boundary layer stability is improved and the onset of a transitory stall regime will tend to only occur at high area ratios.

II.2 The Present Investigation

It has been shown by the literature survey that a diffuser with plenum discharge has an optimum geometrical configuration (for maximum pressure recovery (Cp)) of approximately 7° divergence angle and an area ratio (AR) of 3. A diffuser with a tailpipe fitted (i.e. a parallel duct mounted downstream of the diffuser exit) has an optimum congiguration of 10° divergence angle and an area ratio(AR) of approximately 3. It has however been noted that the developing velocity profile within the diffuser and tailpipe has been largely ignored, although some workers comment on the usefulness of such information. This is surprising since it is the improvement on the velocity profile of the tailpipe which yields a better performance for the overall diffuser tailpipe combination. It was therefore decided to investigate, both theoretically and experimentally the developing boundary layer parameters within the diffuser and tailpipe and their effect on the performance parameters. Also the effect on the overall performance by the addition of a tailpipe was investigated.

For the theoretical investigation the Integral method used by Ferrett[21] was further developed for application to two dimensional diffusers, both with and without tailpipes. This method is based on the Momentum integral equation and uses the concept of entrainment as postulated by Head for the "auxiliary" equation. However the assumptions of the Head method are only valid if a substantial potential core flow exists at all points in the system. Therefore recordings of the developing velocity profile enabled the potential core to be measured at various stations along the diffuser and tailpipe. A preliminary investigation was carried out on an axisymetric parallel walled rig, to determine the length of inlet pipe required upstream of the diffuser to produce the required inlet boundary layer conditions. With this data a rig was designed and constructed to give three different diffuser inlet boundary layer thicknesses from $\frac{2\delta^*}{W_1} = 0.01$ to fully developed ($2\delta^*/W_1 = 0.11$); three divergence angles of 5°, 10° and 15°; two area ratios for each divergence angle and either plenum or tailpipe discharge. The rig was also constructed so that velocity traverses could be taken at various stations along both the diffuser and tailpipe to facilitate investigation of the developing velocity profile.

With this rig all thirty six different configurations were tested and the developing velocity profiles measured. Also a test to determine the effect of terminating the tailpipe at the maximum pressure position was performed.

Tests were also carried out on one configuration to determine the effects of increasing Reynolds Number on performance for the three different inlet boundary layer thicknesses.

Chapter Three.

FLOW DEFINITIONS AND PERFORMANCE PARAMETERS.

III.1 Boundary Layer Definitions.

These boundary layer definitions are true for two dimensional flow only (i.e. flow parallel to and perpendicular to the flow direction in one plane only). Fuller derivations can be found in appendix 8.

III.1.1 Displacement Thickness (δ^*)

This is defined as the distance by which the wall would be required to move towards the centreline of the diffuser if there were no boundary layer present (i.e. flow velocity was at the free steam or centre line value at all points, uniform flow velocity) to maintain the same mass flow. This is denoted by the symbol δ^* and has the value $\delta^* = \int_0^\delta (1 - \frac{u}{u_0})dw$.

III.1.2 Momentum Thickness (θ)

The Momentum Thickness has no strict physical meaning as in the case of δ^*, though for the two dimensional case it can however be defined as the distance by which the wall would have to be moved to maintain a constant flow of momentum flux past the position if the flow velocity was uniformly at the mainstream velocity. Though this does not hold for the axisymetric case. For two dimensional flow $\theta = \int_0^\delta \frac{u}{u_0}(1 - \frac{u}{u_0})dw$, Momentum Thickness ($\theta$) is strictly the distance the wall would have to be moved to pass the deficiency in momentum flux through that space at the mainstream velocity but for two dimensional case the distances are the same, but they are not for the axisymetric case.

III.1.3 Shape Factor (H)

This is the ratio of displacement thickness (δ^*) to momentum thickness (θ) and is denoted by the symbol H. This is an important flow parameter since it partially defines the shape of a velocity profile and can be used to give an indication of the onset of separation. This is generally accepted to occur when H exceeds 1.8 for non diverging flows. For diverging flows values of H in the region of 2.5 to 3 may be obtained before separation occurs.

It can also indicate flow irregularities and asymmetry.

III.2 Flow Properties.

III.2.1 Mean Velocity.

For the purpose of this work the mass averaged velocity $\bar{u}$ was used which can be defined as the velocity required to give the same mass flow along the duct and therefore must have a value of $\bar{u} = 1/\rho w \int_0^w \rho u \, dw$, therefore for incompressible flow would have a value of $\bar{u} = 1/w \int_0^w u \, dw$. Since this value is obtained from mass flow equivalence, a kinetic energy correction factor α must be used for kinetic energy equivalence $\left(\alpha = 1/w \int_0^w \left(\frac{u}{\bar{u}}\right)^3 dw\right)$ and similarly for momentum flux equivalence a momentum correction factor β would be required $\left(\beta = 1/w \int_0^w \left(\frac{u}{\bar{u}}\right)^2 dw\right)$.

III.2.2 Flow Steadiness (or Unsteadiness).

The unsteadiness is usually quoted as the ratio of the maximum fluctuation in the static pressure to the mean static pressure i.e. unsteadiness $= (p_{max} - p_{min}) / p$

III.2.3 Reynolds Number (Re).

The Reynolds Number for the present investigation is determined using the mass averaged flow velocity at the inlet to the diffuser and the viscosity, density and the width at the diffuser inlet station. $(Re = \rho_1 u_1 w_1 / \mu_1)$

III.2.4 Fluid Properties.

Since the flow velocities are low, any local Mach number will be less than 0.25 and the flow may be assumed incompressible. This implies that temperatures are constant along the duct and thus density and viscosity variations may be ignored. In addition static pressure and temperature may be assumed to remain constant across any cross section.

It may be noted that errors will be incurred here particularly in the case of density since static pressure is not constant along the duct, however, the error is less than 3%. This error could be eliminated for certain parameters using the static pressure at the point in question for the calculation of the density instead of using the inlet station values.

III.3 Flow Regimes.

There are three basic regimes of flow, these are;-

(a) Unseparated flow, this occurs when the boundary layer remains attached to the diffuser wall at all times.

(b) Separated flow; It is generally accepted that this occurs when the boundary layer becomes detached from the wall (though it may re-attach at a later stage).

(c) Stall; This occurs when a stagnant, recirculating flow is present and the fluid near the wall tends to move upstream. Stall is an advanced stage of flow separation.

There are various degrees of stall and separation within a diffuser, but the two preceding definitions are generally used to discriminate between stall and separation.

III.4 Turbulence Intensity.

The level of turbulence present in the flow is expressed as the R.M.S value of the flow velocity fluctuations, $\sqrt{u'^2}$ to the mean velocity of the flow $\bar{U}$, i.e. $\sqrt{u'^2}/\bar{U}$ this can be seen in figure 10.

III.5 Performance Parameters.

The performance parameters chosen to be of interest in this investigation were:-

(a) The Pressure Recovery Coefficient (Cp).

This is defined as the ratio of the static pressure rise between the diffuser inlet and another station downstream, and the inlet value of $\frac{1}{2}\rho\bar{u}_1^2$ of the fluid, where $\bar{u}$ is the mass averaged velocity and therefore $\frac{1}{2}\rho\bar{u}_1^2$ is not the true inlet kinetic energy of the fluid.

Therefore $Cp = (p - p_1)/\frac{1}{2}\rho\bar{u}_1^2$.

This is the parameter of general interest to the designer since diffusers are included to increase the static pressure at the expense of the flow kinetic energy. Cp therefore gives a guide to the relationship between the two parameters.

INSTANTANEOUS VELOCITY / TIME

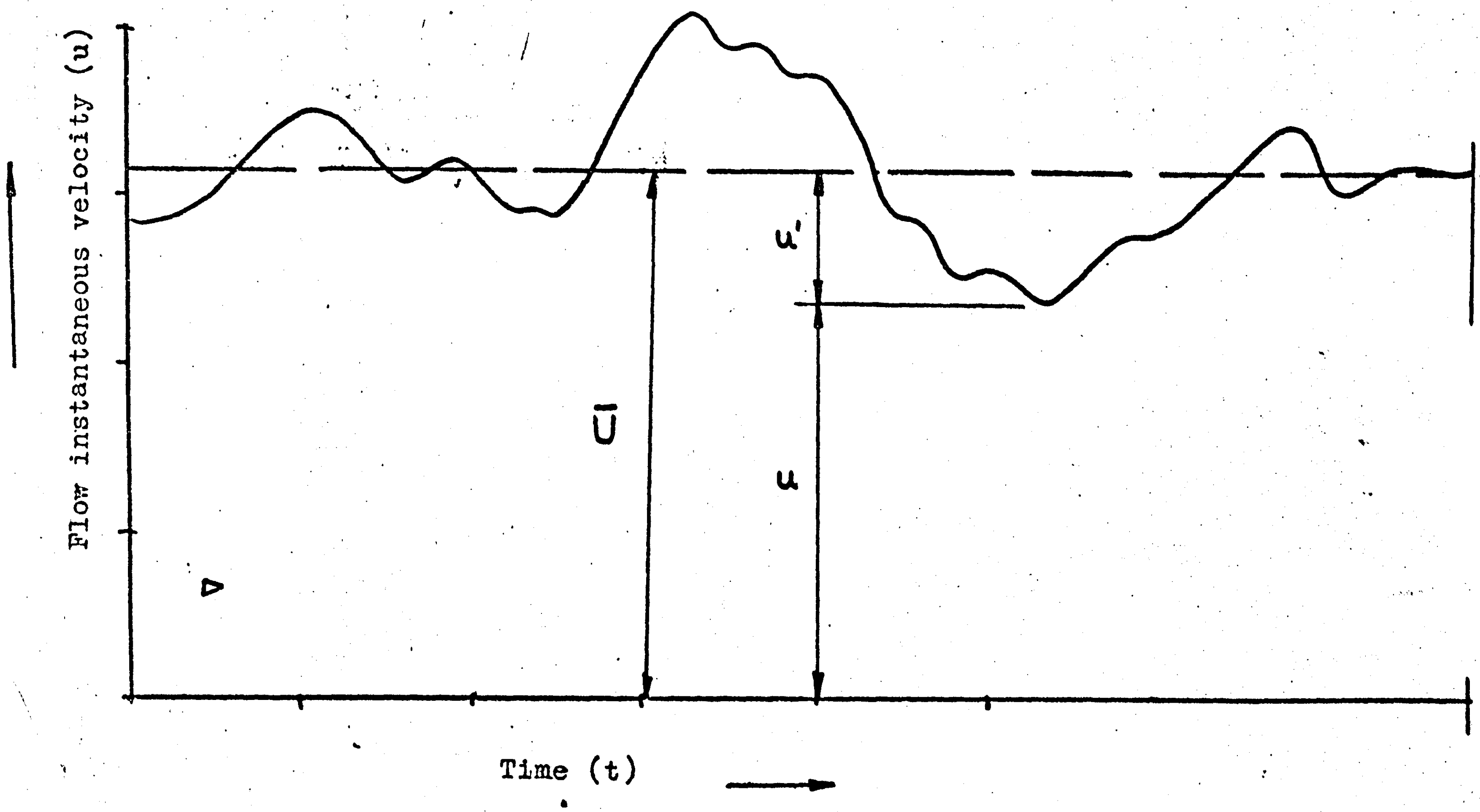

FIGURE....10

(b) Energy Corrected Cp. (Cp_E).

This is the value of Cp previously defined but corrected for the error incurred by calculating the inlet kinetic energy with the mass averaged velocity. This is achieved by including the kinetic energy correction factor (α), defined earlier as $\frac{1}{W}\int_c^W \left(\frac{u}{\bar{u}}\right)^3 dw$.

Therefore Cp_E can be expressed as:- $Cp_E = Cp/\alpha = (p - p_1)/\frac{1}{2}\alpha_1 \rho_1 \bar{u}_1^2$.

(c) Effectiveness of the Diffuser. (η).

Effectiveness is defined as the ratio of the pressure change between the inlet and a downstream station and the change in the "Kinetic Energy" between the two stations (Again based on mass averaged velocities, therefore, the effectiveness is not a true energy efficiency).

$$\eta = (p - p_1) \quad \tfrac{1}{2}(\rho_1\bar{u}_1^2 - \rho\bar{u}^2)$$

for incompressible flow can be expressed as

$$\eta = (p - p_1) \quad \tfrac{1}{2}\rho_1(\bar{u}_1^2 - \bar{u}^2) \text{ or } (p - p_1) \quad \tfrac{1}{2}\rho_1\bar{u}_1^2(1 - 1/AR^2).$$

The effectiveness, as its name implies gives a rough guide to the effectiveness of the diffuser in converting kinetic energy to a static pressure rise. This is not however an energy efficiency due to the error incurred in using the mass averaged velocities.

(d) Energy Corrected Effectiveness (η_E).

The energy corrected effectiveness of a diffuser has the same definition as the effectiveness except that the kinetic energies based on mass averaged velocities are corrected by the inclusion of a kinetic energy correction factor α for each station, therefore, η_E can be expressed as:-

$$\eta_E = (p - p_1)/\tfrac{1}{2}(\rho_1\bar{u}_1^2\alpha_1 - \rho\bar{u}^2\alpha)$$

or for incompressible flow

$$\eta_E = (p - p_1)/\tfrac{1}{2}\rho(\bar{u}_1^2\alpha_1 - \bar{u}^2\alpha)$$

or

$$\eta_E = Cp/(\alpha_1 - \alpha/AR^2)$$

(e) Loss coefficients.

The most general loss coefficient used (λ) is expressed as:-

$$\lambda = 1 - (p - p_1)/\tfrac{1}{2}\rho\bar{u}_1^2(1 - 1/AR^2) = 1 - \eta$$

This expresses the loss as a total pressure loss through the diffuser, but as with effectiveness (η) does not give the true energy loss since it employs the mass averaged velocity and would therefore have to have a uniform flow velocity at both stations to give an energy loss coefficient. An energy corrected total loss coefficient is given by the expression:

$$K_t = \alpha_1 - Cp - \alpha (A_1/A)^2$$

Chapter Four.

EXPERIMENTAL FACILITIES.

IV.1 Choice of the Experimental Rig.

The work of Kline et al and Kelnhoffer and Derick described in chapter I, indicated that areas of interest for optimum diffuser performance were, angles of divergence from 5^{o} to 15^{o} and area ratios in the range of 2 to 3. It was therefore decided to construct a variable geometry diffuser having three possible divergence angles, 5^{o}, 10^{o} and 15^{o} and two area ratios, 2 and 3. To this was added a detachable tailpipe which could be varied in length to a maximum of 12 diffuser exit widths for AR = 3, and 18 diffuser exit widths for AR = 2. It was also required that the boundary layer could be interchanged at the inlet to the diffuser between thin, thick and fully developed.

The method used to vary the inlet boundary layer thickness was to make the duct length variable. This particular method was chosen because the duct could be constructed easily and significant variations in turbulence intensity and velocity profile distortion were unlikely. In addition the use of a duct enabled a series of static pressure tappings to be positioned at various stations upstream of the diffuser inlet. Hence the effect of streamline curvature on the diffuser inlet static pressure could be examined and the static pressure reading corrected by extrapolating results taken along the duct upstream of the zone affected by streamline curvature. For the three inlet boundary layer thicknesses, the inlet duct was required to be three different lengths. The values of boundary layer thickness chosen (based on the displacement thickness/half the duct width) were 0.01, and 0.06 for the thin and thick boundary layers respectively, and from a simple power law analysis a fully developed inlet flow was found to be in the region of 0.11.

To determine the actual duct lengths required for these boundary layer conditions a preliminary investigation was carried out on a 3" diameter brass tube. Since these results were for an axisymmetric case the values of $2\delta^{*}/D$ were therefore smaller than required values of $2\delta^{*}/W_{1}$, but since this effect reduces with the boundary layer thickness a fair comparison can be made if suitable allowance is made.

IV.2 Preliminary Investigation

A brass tube shown schematically in figures 11a and 11b, was used to carry out a preliminary investigation into the growth of a turbulent boundary layer. A pitot traverse (shown in figure 22) was located in tappings and traverses of the developing boundary layer made, (the tappings are shown in figure 12). The results obtained (figure 13), clearly show that for a fully developed flow, $2\delta^*/D = 0.084$ for axisymmetric case, an inlet pipe length of x/D in the region of 32 to 36 is required. Therefore, a value of x/w_1 of 37 was chosen for the two dimensional case giving a $2\delta^*/w_1$ value of 0.11 at the diffuser inlet. For a value of $2\delta^*/w_1$ of 0.06 the relationship shows that x/D values in the range of 11 to 12 for the axisymmetric case, give the required boundary layer thickness, but since the two dimensional boundary layer has a larger $2\delta^*/w_1$ than for the axisymetric case and the boundary layer growth is slower, a value of 13 was chosen, i.e. 1 metre. For the thin inlet boundary layer a value of x/w_1 of 1 was chosen this being the smallest value allowable to avoid the effects of the boundary layer trip wire. (The trip wire is described later in this chapter). The values of x/w_1 = 37, 13 and 1 gave diffuser rig inlet boundary layer values of $2\delta^*/w_1$ of; 0.11, 0.06 and 0.01 respectively, (The full results of the preliminary investigation are shown in appendix 2.). These values of inlet duct length, determined from the preliminary investigation, were all substantiated by early tests on the main diffuser experimental rig.

IV.3 Diffuser Rig Design.

The experimental diffuser rig, shown schematically in figure 14, consisted of a radial flow fan, settling chamber contraction and experimental diffuser rig. From the previous work of other researchers, summarised in chapter one, it has been shown that for sidewall effects to be minimal, the aspect ratio (AS) should be at least six. Therefore, an inlet aspect ratio of eight was chosen. The width of the duct was determined from consideration of the

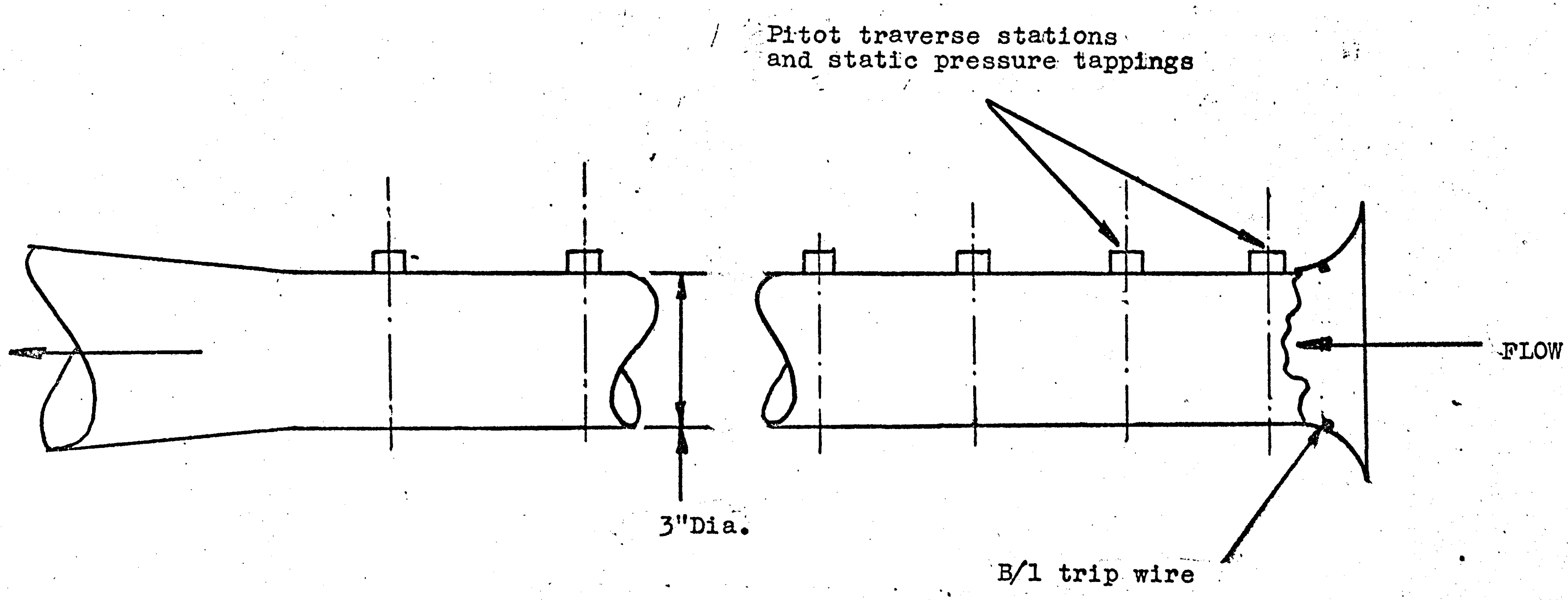

EXPERIMENTAL RIG USED FOR PRELIMINARY BOUNDARY LAYER INVESTIGATION

FIGURE....11(a)

PRELIMINARY RIG STATIC PRESSURE TAPPING POSITIONS

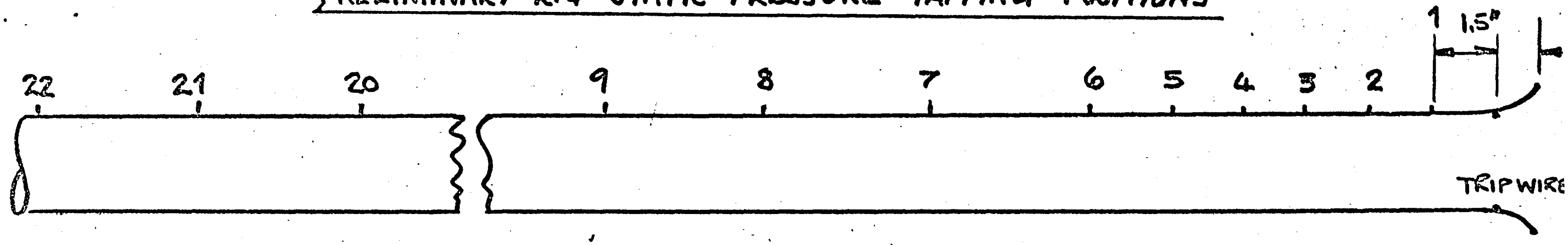

ALL DISTANCES MEASURED FROM TRIP WIRE IN INCHES (TRIP WIRE DIA = 0.012")

1	2	3	4	5	6	7	8	9	10	11	12	13	14	15	16	17	18
1.5"	7.5	16.5	25.5	34.5	43.5	55.5	67.5	79.5	91.5	103.5	115.5	127.5	139.5	151.5	163.5	175.5	187.5

19	20	21	22
199.5	211.5	223.5	235.5

FIGURE....11(b)

PRESSURE TAPPINGS

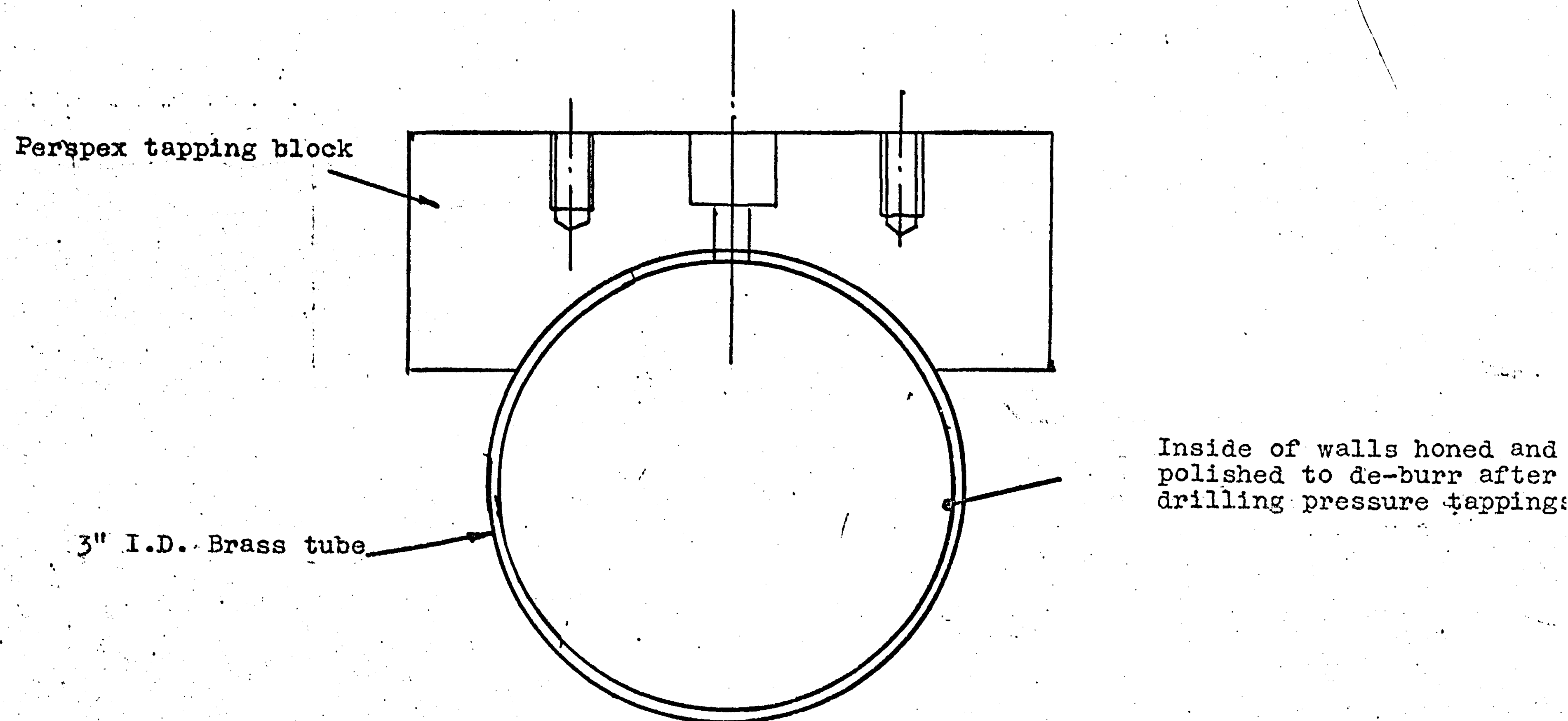

FIGURE....12

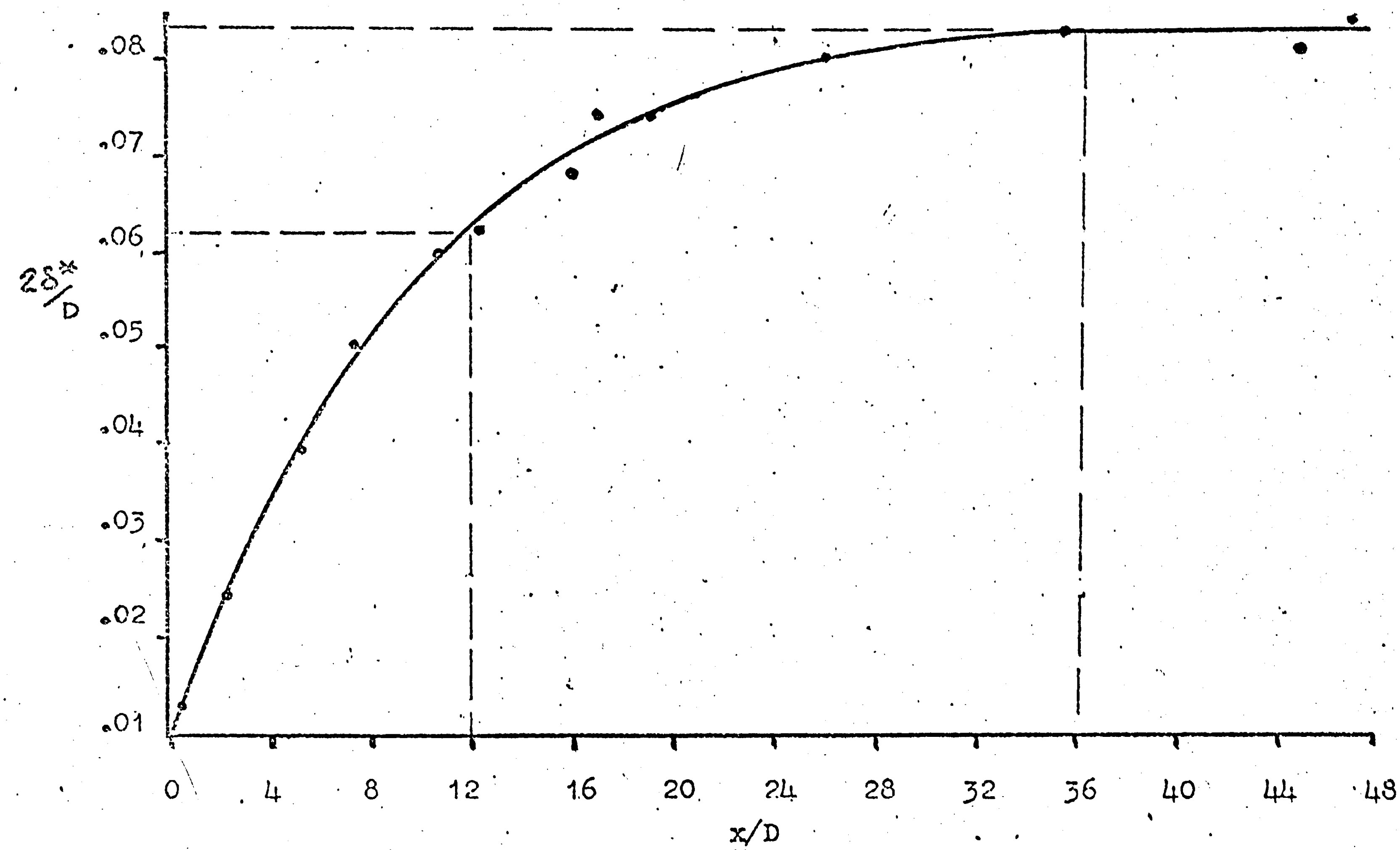

BOUNDARY LAYER GROWTH FOR THE AXISYMETRIC RIG WITH DISTANCE FROM INLET (X/D)

FIGURE 13

minimum dimension which could be accurately traversed by a pitot tube in the boundary layer. To satisfy this objective it was decided that the width of the duct would have to be at least 80 mm., thus giving a duct breadth of 640mm.

The investigation was only concerned with incompressible flow (the mach number being less than 0.25). This required a volumetric flow in the region of 7,600 cubic ft/min. at delivery pressures from 50 mm. to 250 mm water gauge (the preliminary calculations made to estimate these quantities are shown in appendix 1). It was decided that the best means of acheiving this large variation in delivery pressure, without resorting to a variable speed fan, was by using a 24 inch, backward curved aerofoil section radial flow fan running at 2100 rpm , powered by a 25 h.p. motor, with a radially feathering damper at the inlet to the fan. However it was found during preliminary investigations that with a small back pressure (50 mm w.g.), the fan needed to be damped to a very low inlet area. This caused the fan discharge to become very unstable, producing both a flow which pulsated severely and excessive vibration of the fan and the experimental rig. Thus it was found necessary to slow the fan speed down to 1800 rpm. for the thin and thick inlet boundary layer conditions. This measure produced a steady and non pulsating flow.

IV.3.2 Settling Chamber and Contractions.

The fan discharged through a flexible coupling into a 0.6 metre x 1 metre x 2 metres long settling chamber. The settling chamber (shown in figure 15) consisted of five sets of 28 s.w.g. x 16 mesh wire gauzes and two $\frac{3}{8}$" cell by 75 mm long aluminium honeycomb flow straighteners ($\frac{3}{8}$" x 75 mm gives a cell diameter to cell length ratio of $\frac{1}{8}$ as recommended by the National Physical Laboratory in their publication N.P.L. 1218.[26]).

This settling chamber discharged into a perspex contraction, constructed to N.P.L 1218 specification (The co-ordinates of the contraction profile are given in appendix 1) to give a thin boundary layer and uniform profile (shown in figure 16a) at the exit. In order to ensure that the boundary layer was turbulent on exit from the contraction the boundary layer was 'tripped'. From Pankhurst and Holders text "Wind Tunnel Technique" it was calculated that

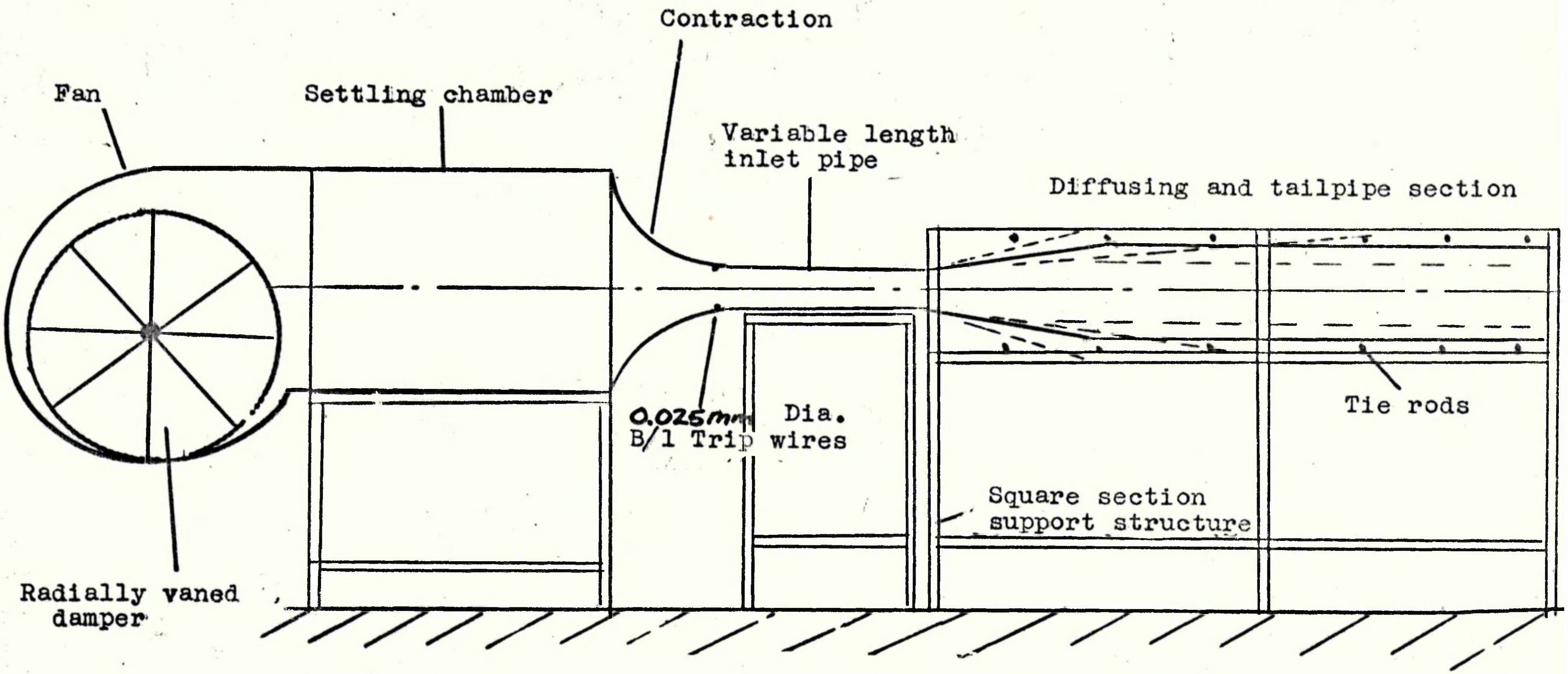

SCHEMATIC DIAGRAM OF THE MAIN EXPERIMENTAL RIG (DIFFUSER)

FIGURE.....14

SETTLING CHAMBER

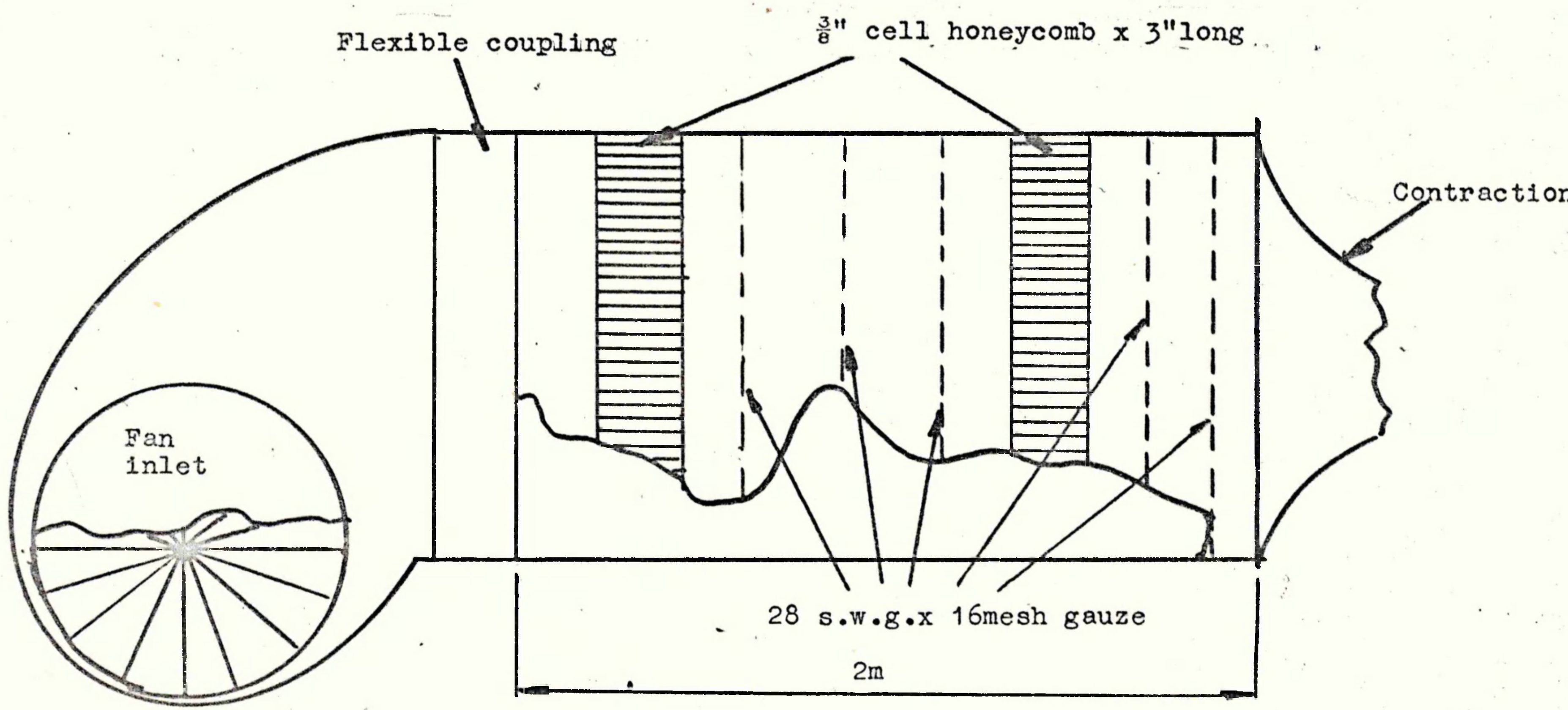

FIGURE........15

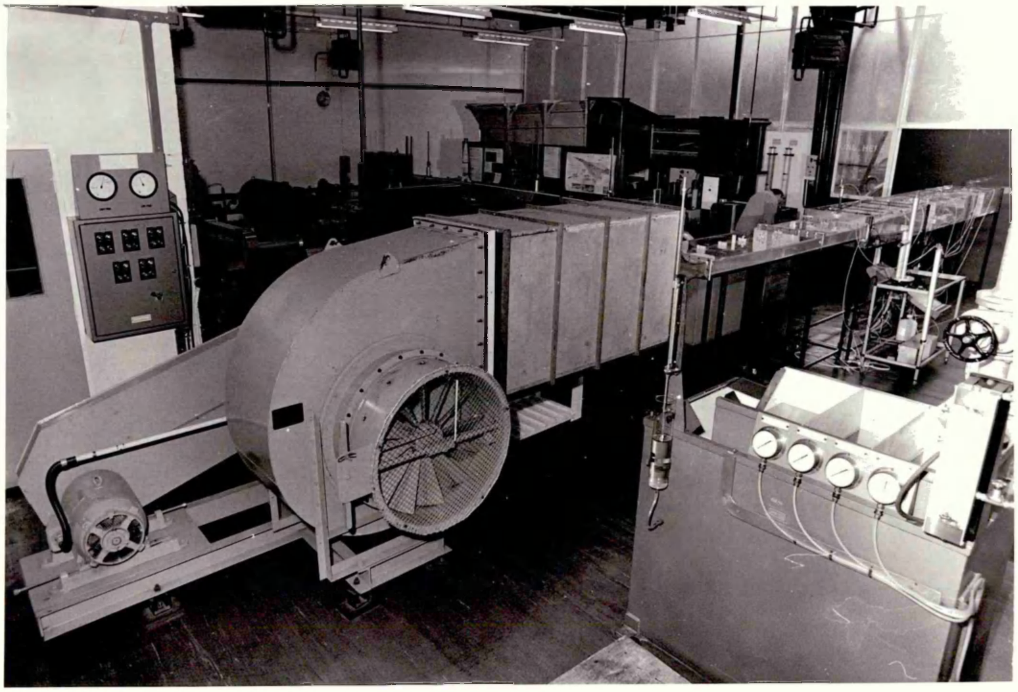

The Main Diffuser Experimental Facilities.

PLATE........1

a boundary layer trip wire of diameter 0.25 mm at the contraction exit plane would be required to effect this, thus ensuring a turbulent boundary layer on entry to the diffusing section. (calculation shown in appendix 1).

IV.3.3 Diffuser and Tailpipe.

The flow from the contraction passed into the inlet duct, whose dimensions (mentioned previously in this chapter) were determined by the boundary layer thickness required at the inlet plane of the diffuser. Then the flow entered the experimental diffuser and tailpipe.

The inlet of the diffuser was given a 12mm blending radius on the corner, as shown in figure 17. This was to reduce the probability of the boundary separating from the wall on entering the diffuser. A blending radius was also given to the diffuser/tailpipe joint though the effects on the boundary layer here would not be as serious as they could be at the inlet since a sharp corner would not tend to separate the boundary layer from the wall at this point.

The diffuser/tailpipe rig was constructed from 1" thick perspex sidewalls with slots milled along them. These slots enabled the diffuser and tailpipe walls, which were both constructed of ½" perspex sheet, to be located in position. This enabled the various configurations of the diffuser and tailpipe (12 in all) to be changed quickly. The walls were sealed in the slots by slicone grease and the joints taped to prevent air leakage. The complete assembly was secured to the inlet section by a flange at the inlet of the diffusing section. Tie bars were used to clamp the sidewalls and thus secure the whole assembly rigidly together. This can be seen in figures 18 and 19.

IV.3.4 Static and Pitot Tappings.

The velocity of flow was measured by a pitot traverse which was located in tappings as shown in figure 20. Initially it was envisaged to use these tappings for both the pitot and the static pressure tappings, by incorporating a 0.6mm diameter hole in the locating head for the pitot traverse, and therefore to obtain the dynamic head directly. Unfortunately a certain amount

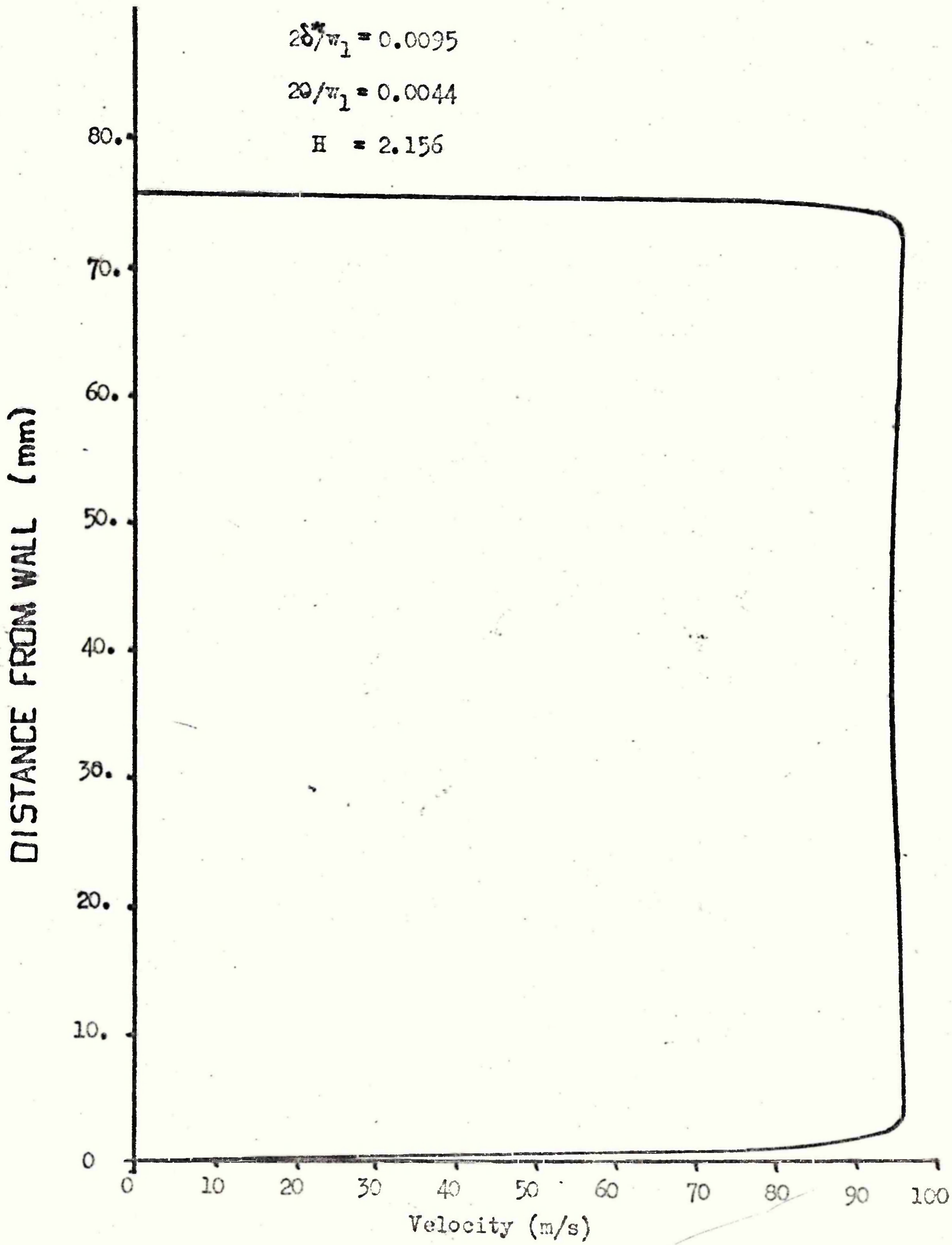

INLET PROFILE AT EXIT FROM CONTRACTION (Thin boundary layer)

FIGURE....16(a)

$2\delta^*/w_1 = 0.109$

$2\theta/w_1 = 0.083$

$H = 1.312$

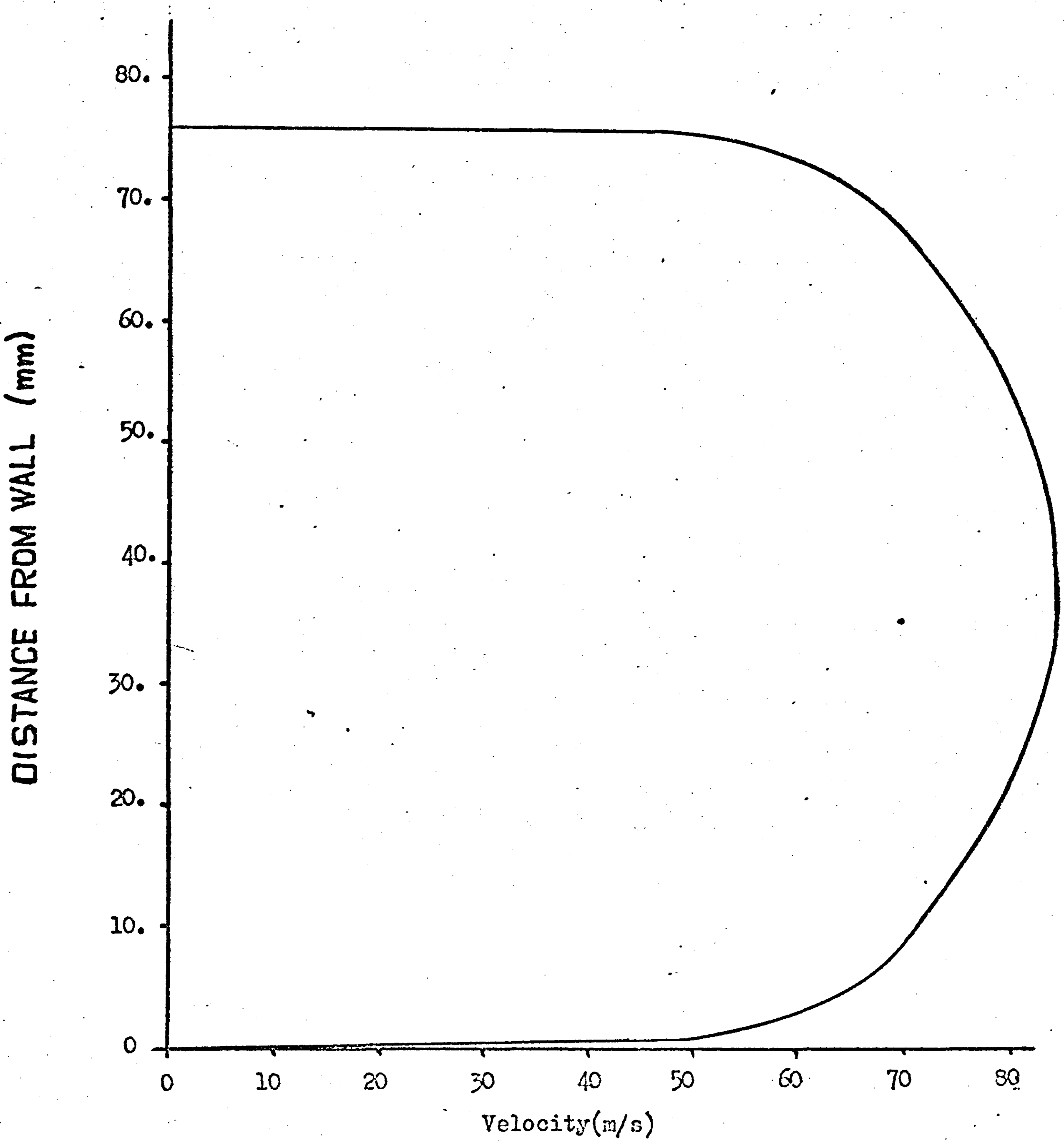

FULLY DEVELOPED FLOW INLET VELOCITY PROFILE

FIGURE.....16(b)

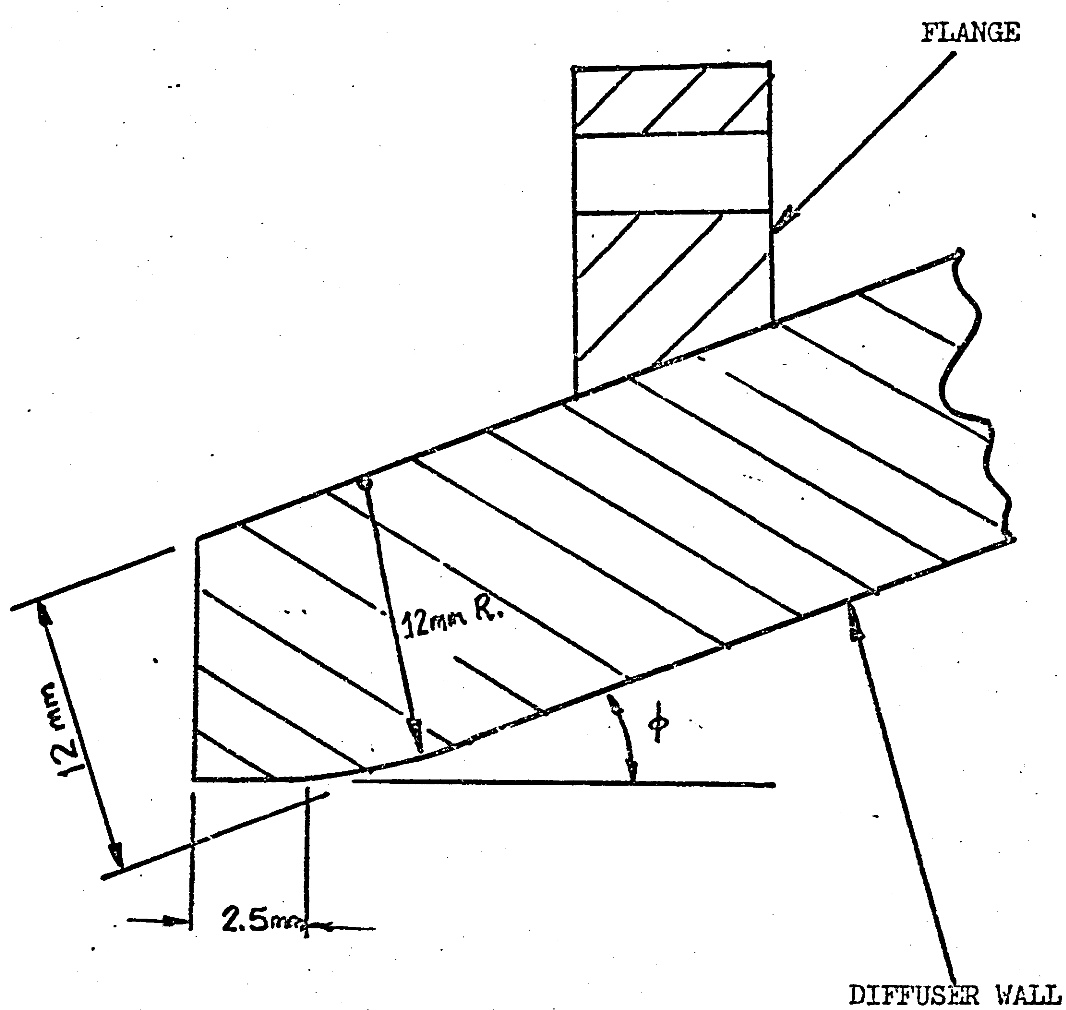

INLET BLENDING RADIUS

FIGURE.....17

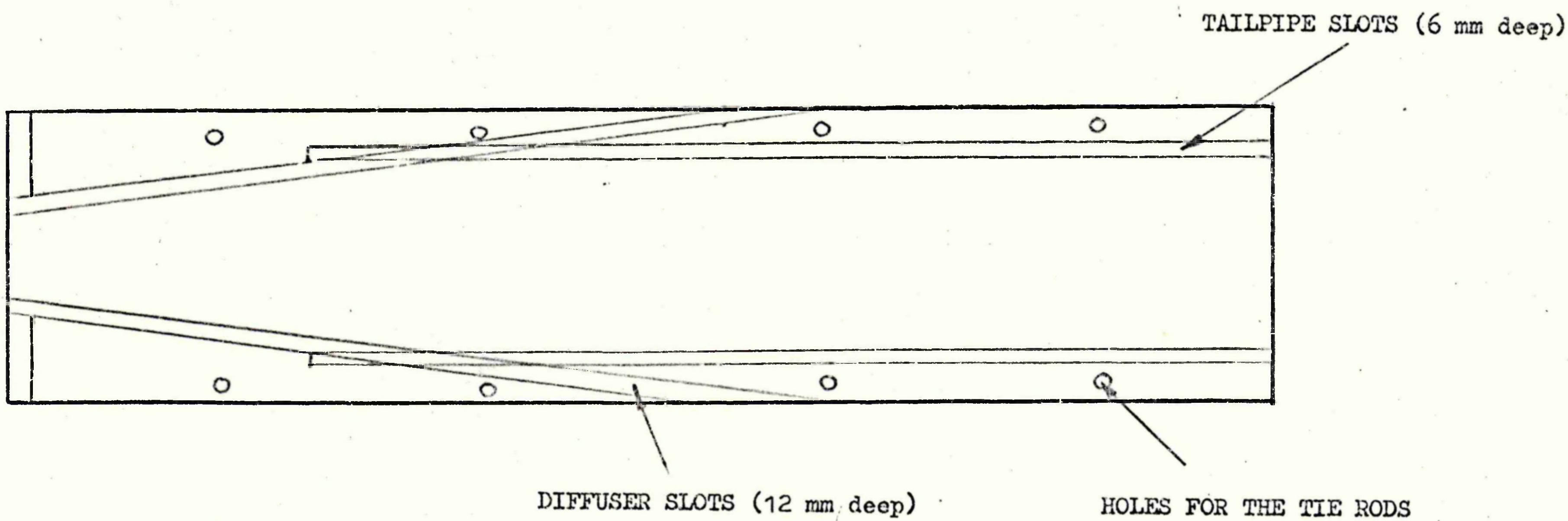

PARALLEL WALLS SHOWING ONE SET OF SET OF LOCATION SLOTS FOR DIFFUSER AND TAILPIPE

FIGURE....18

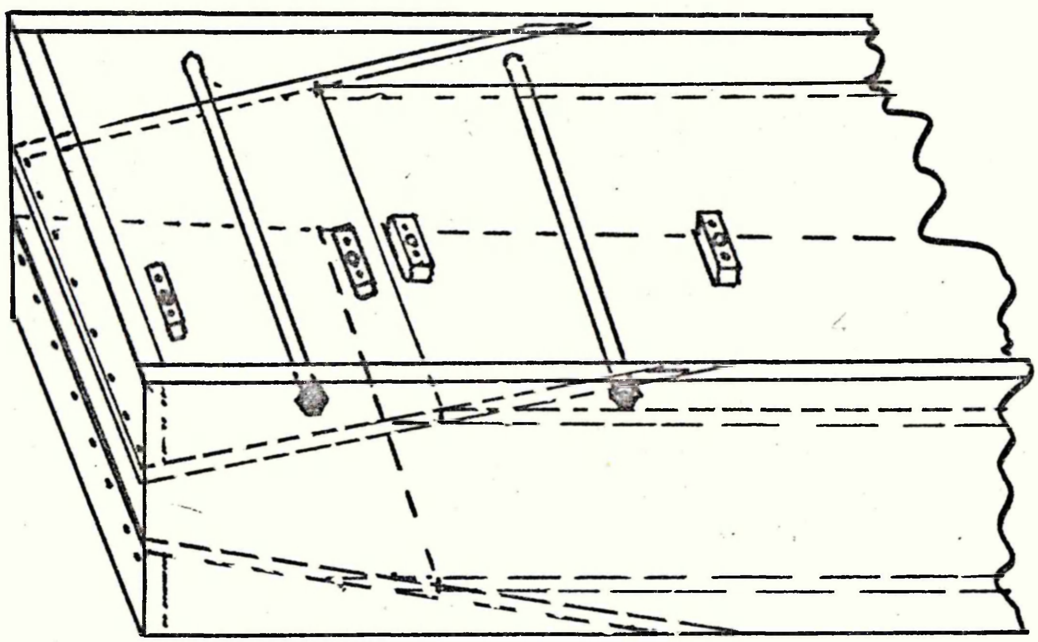

THE DIFFUSER AND TAILPIPE ASSEMBLY.

FIGURE....19

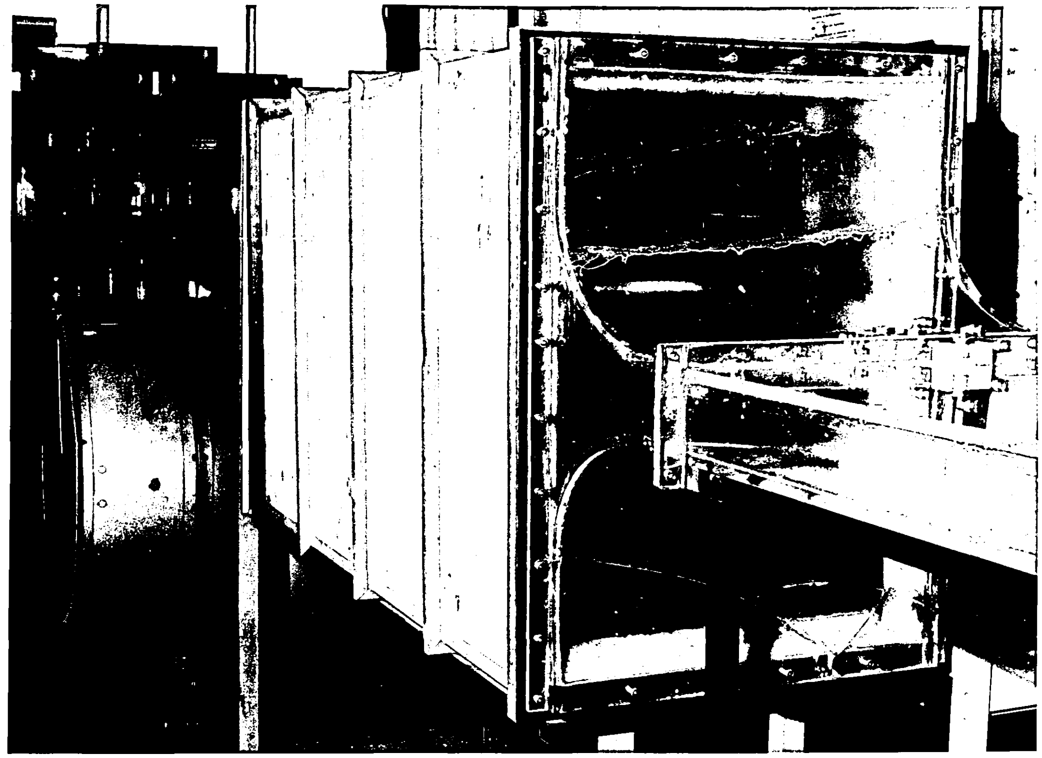

The Inlet Contraction

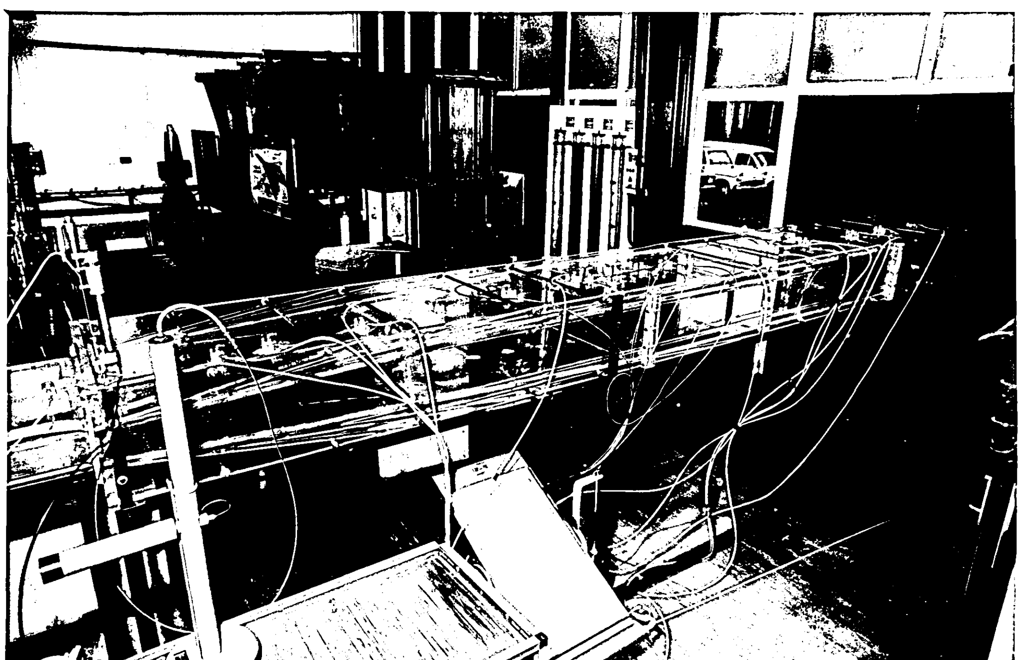

The Diffusing and Tailpipe sections

PLATE......2

of interaction was experienced between the pitot head and the static tapping when the pitot head was traversing close to the wall which caused inaccuracies in the dynamic head (shown by an apparent distortion of the velocity profile, figure 21). Finally an independent static tapping of 0.8mm diameter was incorporated as shown in figure 20.

IV.4 Instrumentation.

IV.4.1 Pitot Probe.

The actual pitot traverse was taken from a design used by Ferrett[21] in his investigation into truncated conical diffusers.

The actual pitot locating head was larger and the pitot probe was of a larger diameter, 0.6mm diameter with a bore of 0.15 mm diameter. This was done to reduce the response time of the instrument and thus remove the necessity for balancing manometers or other arrangements. Also a spring was incorporated in the micrometer screw movement to remove any backlash. The instrument is shown in figure 22.

The pitot was traversed perpendicular to the diffuser wall since it was the boundary layer which was of major interest, and the cosine error at the centreline was at a mxiumum less than 1%. Due to the thickness of the pitot probe tubing (0.8mm) some rotation of the end was experienced due to drag. This was calculated, (shown in appendix 1) and found to be never more than $2^{o}20'$ which gave an error of 0.08% and was neglected.

IV.4.2 Manometers.

The pitot probe, which was described previously was connected to an "Airflow Developments" manometer graduated in 1.0mm's water gauge intervals from - 10mm to 600mm. Due to the distance between the graduations, approximately 1.5mm, it is unlikely that the readings taken are of a greater accuracy than ± 0.5mm of water gauge. The static pressure side of the manometer was also connected to a T.E.M micromanometer. This micromanometer was graduated in 0.2mm of water gauge which was magnified by an optical system and had a range of 0.0 to 600.0 mm of water gauge. The probable accuracy of this instrument was in the region of ±0.1mm of water. The

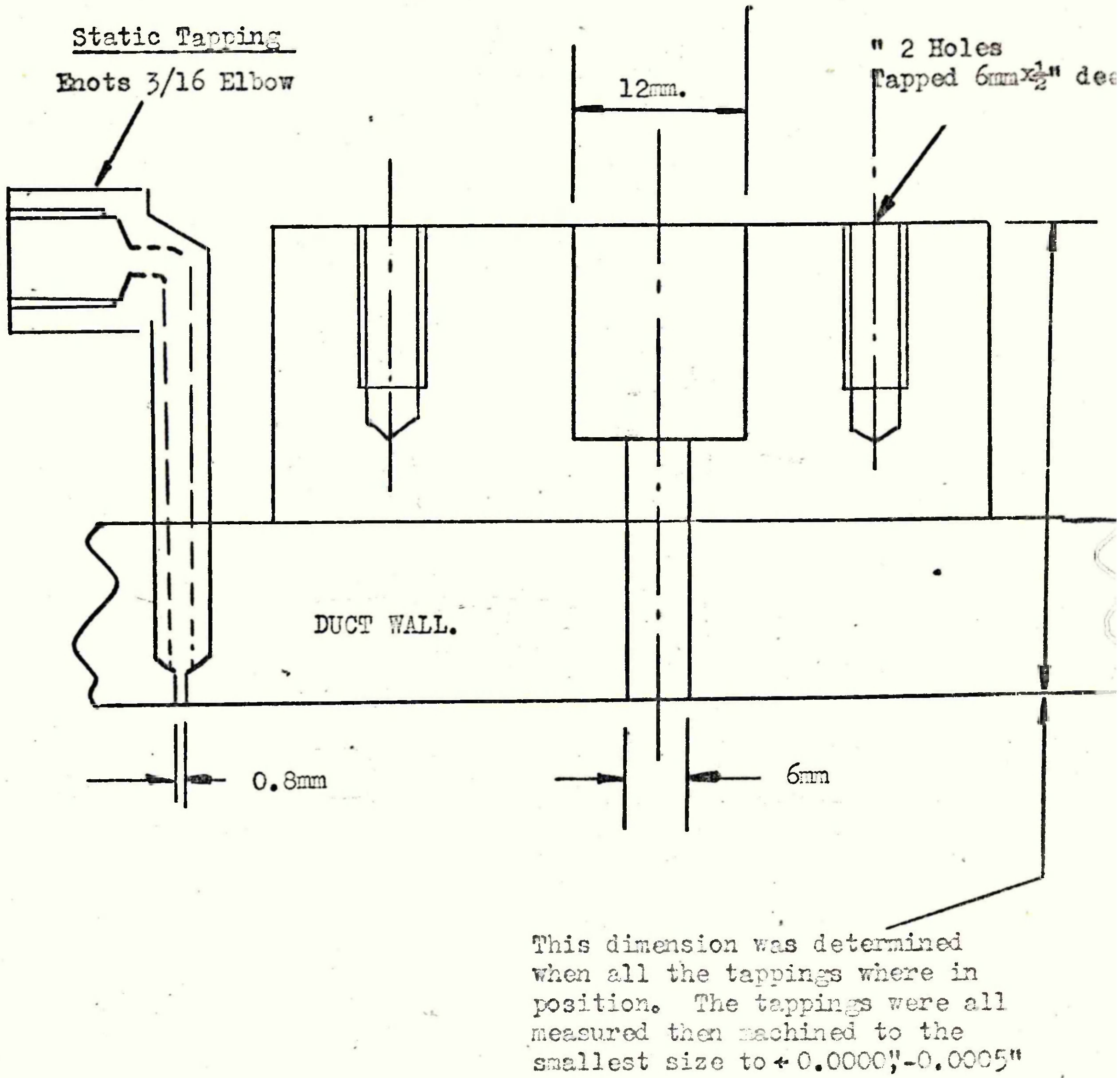

PITOT TRAVERSE STATIONS AND STATIC PRESSURE TAPPINGS

FIGURE.....20

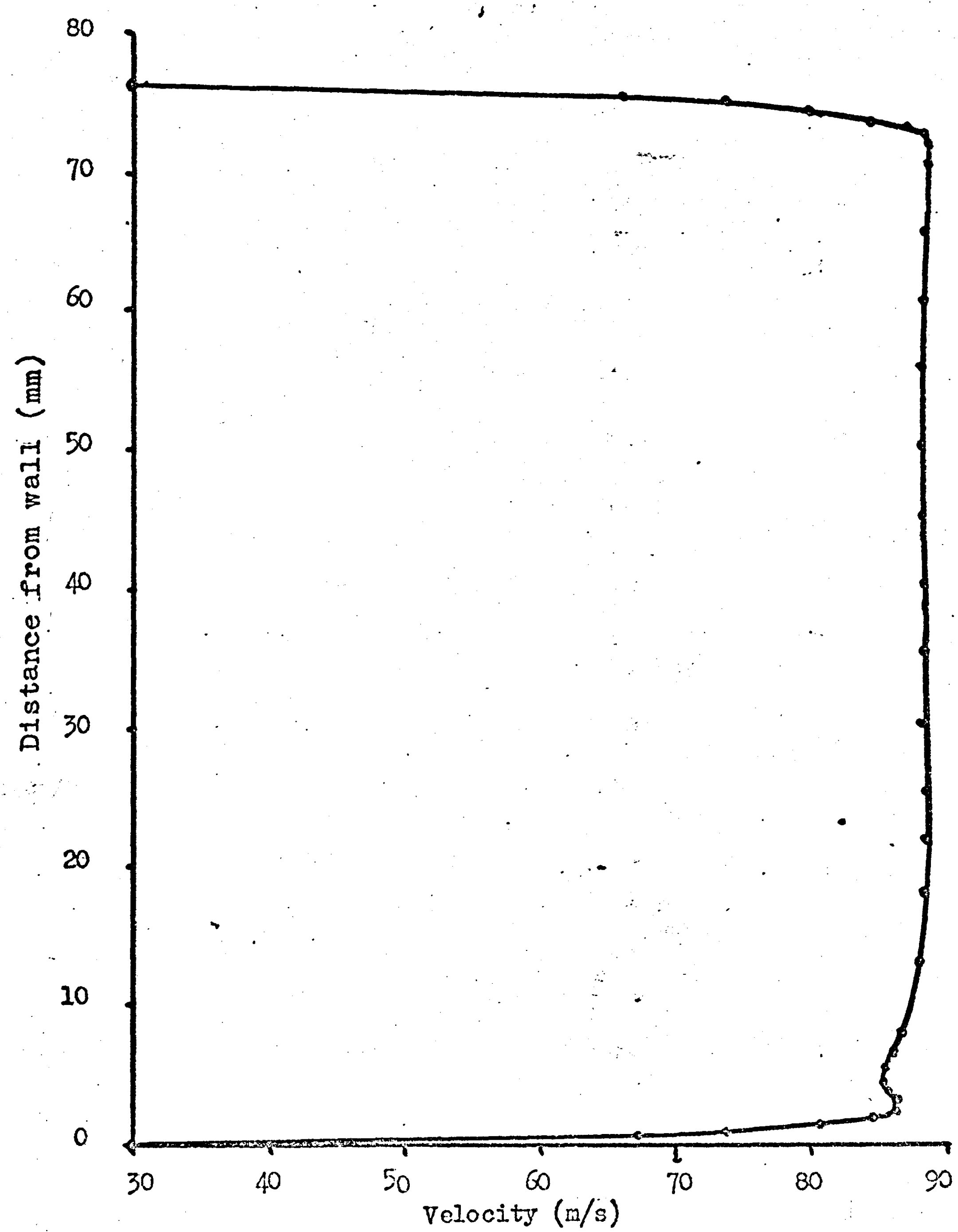

VELOCITY PROFILE AT INLET USING THE COMBINED PITOT STATIC TRAVERSE HEAD.

FIGURE...21

small inaccuracy was caused by friction in the sliding glass graduated suspended measure and float system.

It was found that a considerable time lag was inherent in the system due to the small size of the static pressure tapping (0.8mm) and the volume within the micromanometer. This had the effect of damping out small pressure fluctuations in the system. This damping could be increased if necessary by increasing the restriction in the static pressure line by the use of a valve. Due to the small size of the pitot probe bore, there was also a considerable time lag on this side of the differential system which could also be increased further by the use of a flow restriction valve if necessary, thus giving the effect of damping out small pressure fluctuations. It was therefore found unnecessary to additionally damp the instruments by the use of reservoirs. In addition to these two manometers a 36 tube multitube manometer was used and attached to the static pressure tappings. This was employed to determine the most important positions at which to make velocity traverses.

The layout of the pressure measuring systems which were used are shown schematically in figure 23.

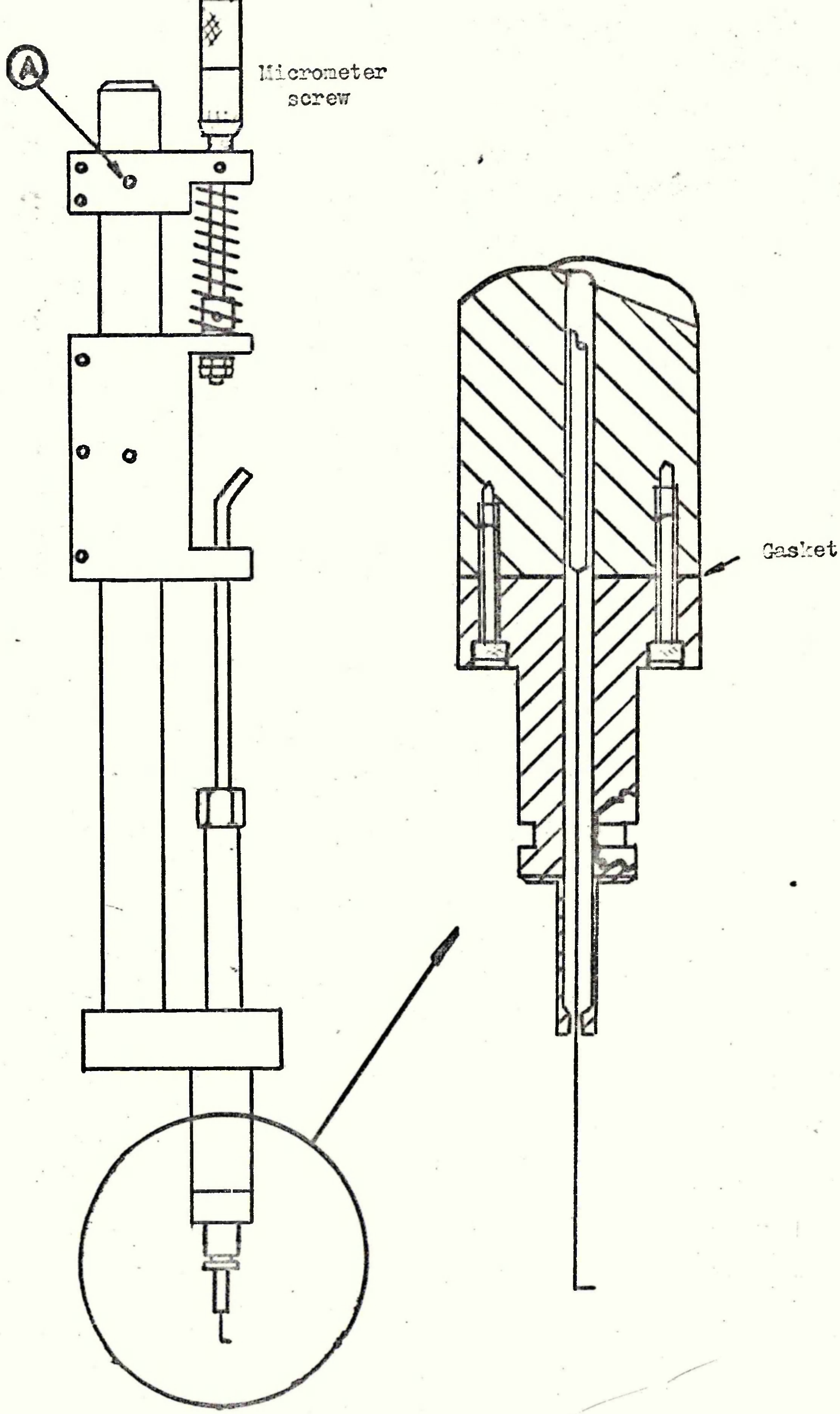

PITOT TRAVERSE

FIGURE....22

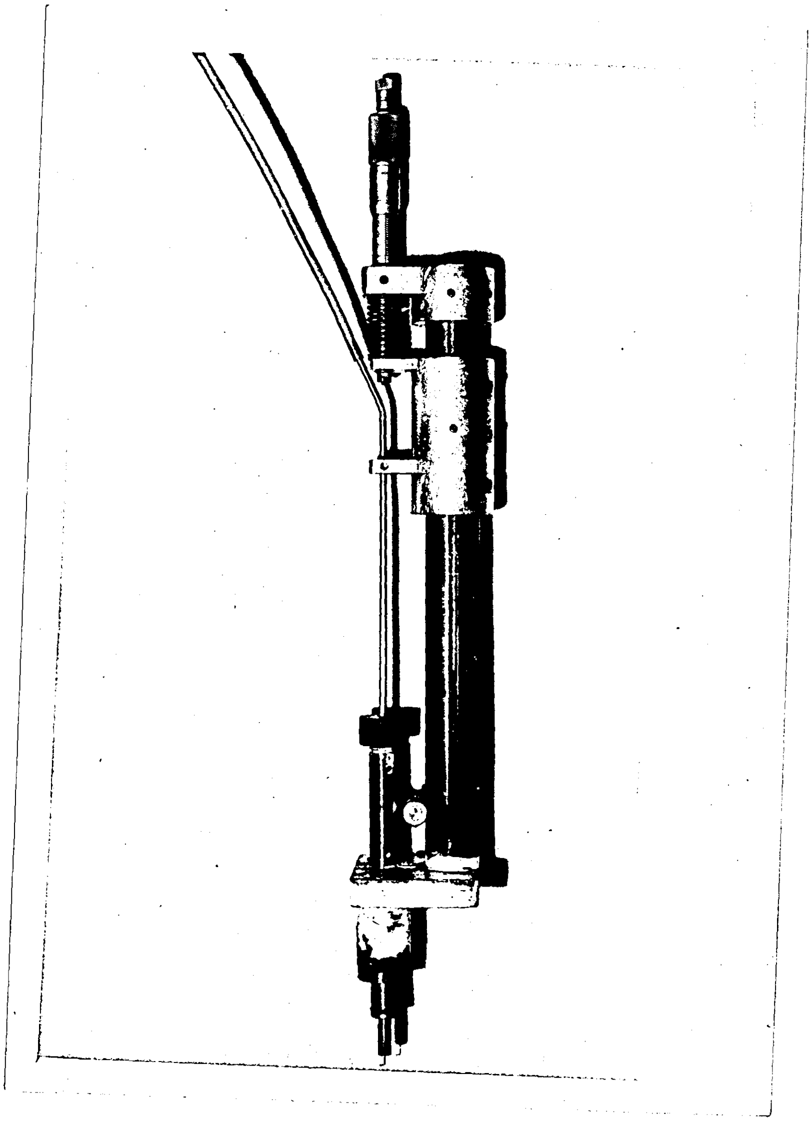

The Pitot Traverse

PLATE......3

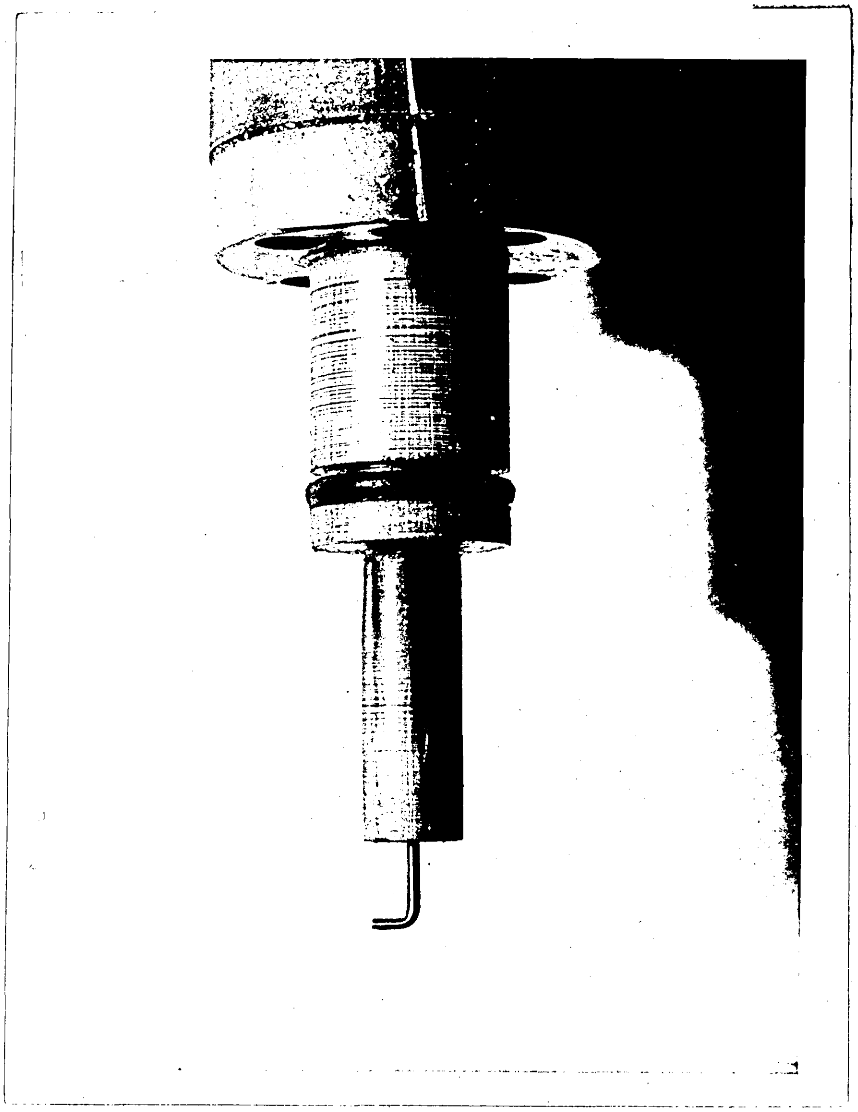

The Pitot Probe Head

PLATE..4

SCHEMATIC DIAGRAM OF INSTRUMENTATION

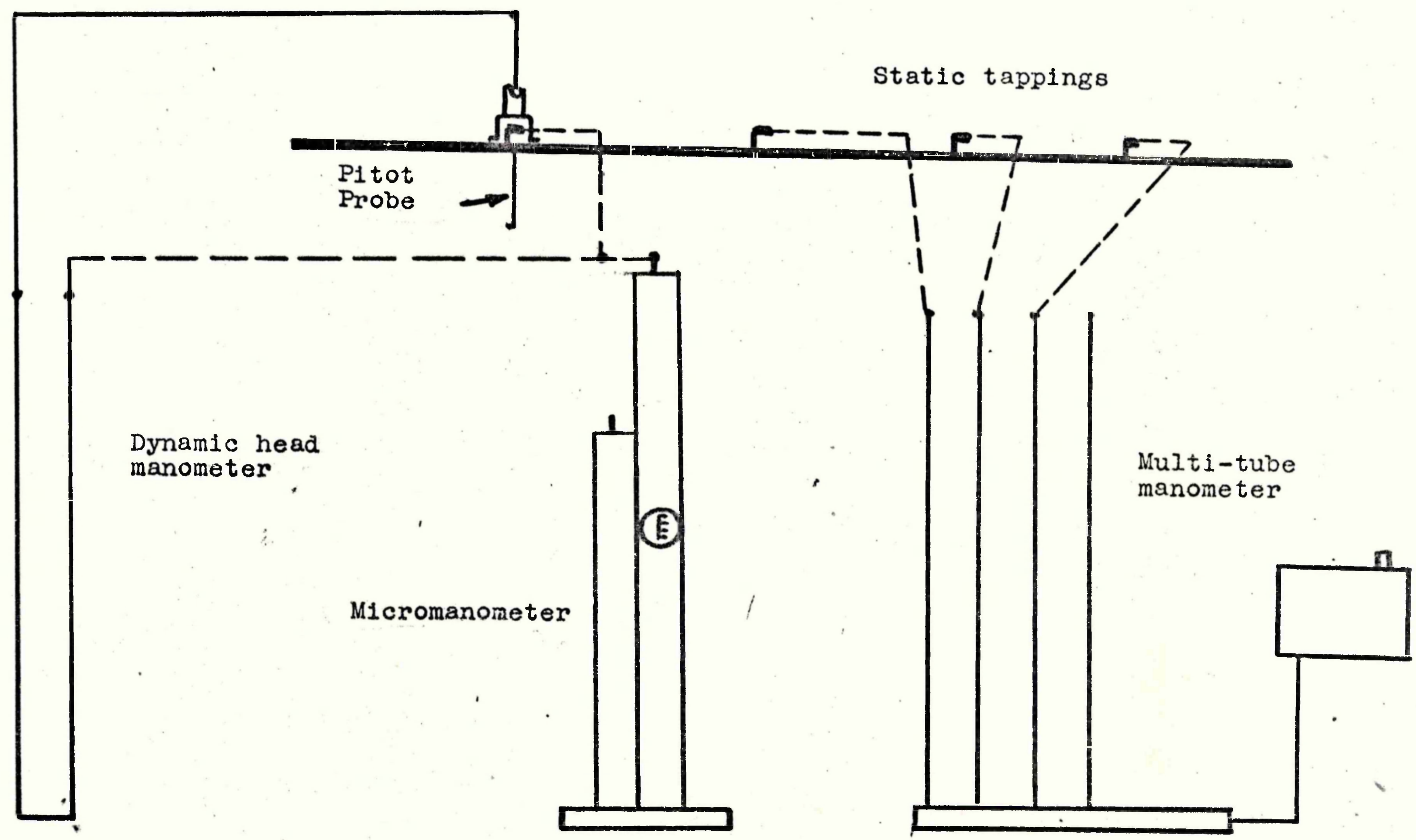

FIGURE....23

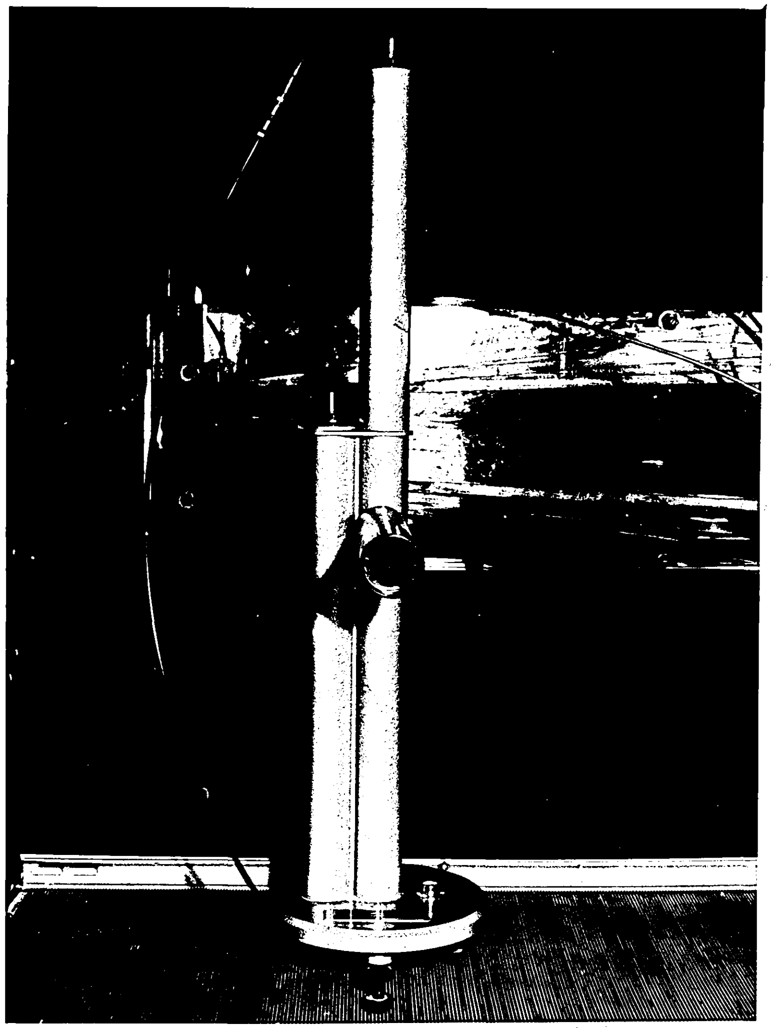

The Micromanometer

PLATE.....5

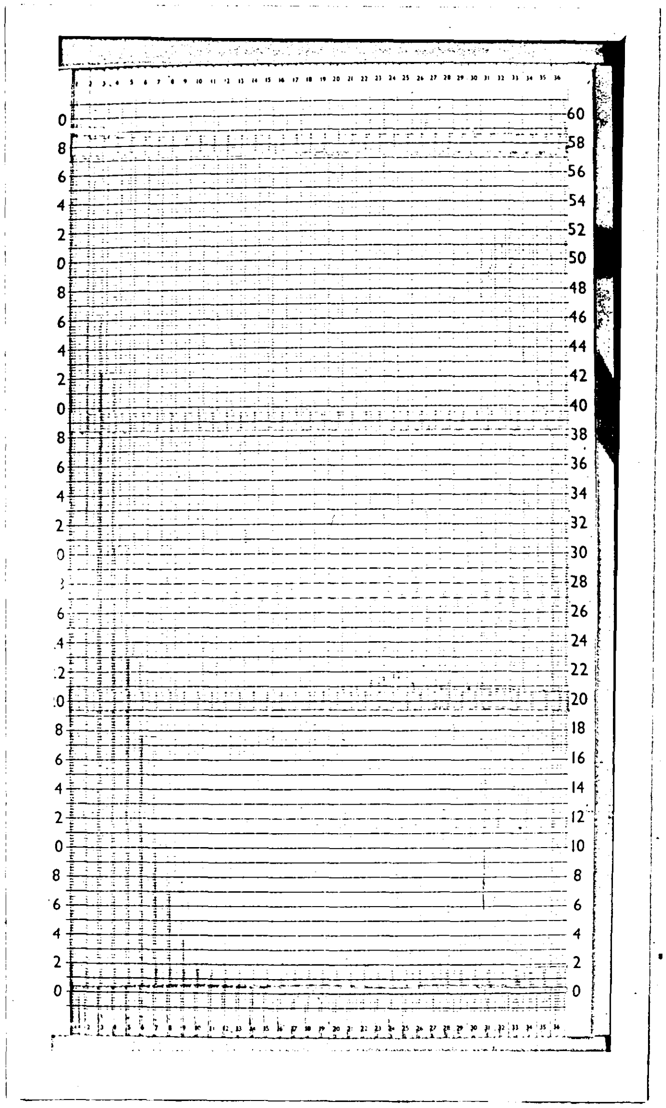

The Multi-tube Manometer (36 tube)

PLATE...6

Chapter Five.

GENERAL TEST PROCEDURE AND RANGE OF TESTS.

V.1 Preliminary Investigation Procedure.

During the preliminary investigation, the pressure measurement circuit was connected initially as indicated by the schematic layout shown in figure 24 (i). The procedure followed using this layout was as follows:

Any flow in the pitot dynamic pressure side caused a pressure differential across the restriction 'C' which was indicated on the balancing manometer. The balancing valve 'A' was then opened and air bled into the system through the restriction 'B'. When the balancing manometer showed no differential it could be assumed that the value of pressure 'P' had been reached in the micromanometer. Unfortunately this system was so sensitive to small variations in flow that it was difficult to obtain a balance and any slight drift gave the impression of balance not being acheived. It was therefore decided to use the simpler system shown in figure 24 (ii) together with a larger pitot head diameter. Thus the response time and the effect of drift were reduced.

Using this system, tests were performed at 22 stations along the brass tube which has been described earlier. The experimental procedure was the same as that used for the main diffuser work to be described later in the chapter. The only difference between the preliminary investigation and the main one was that, during the former, velocity traverses were taken at every station.

V.2 Experimental Procedure for Diffuser Investigation.

The rig was assembled to the required configuration, (inlet duct length divergence angle, area ratio and tailpipe length).

The pitot probe was then adjusted so that the centre line of the probe head would be 0.5mm. from the wall when in position. The reason for the pitot probe not being positioned at the wall was to reduce the effect of the local pressure gradient caused between the pitot head and the wall thus causing the streamlines near the wall to be deflected towards the wall.

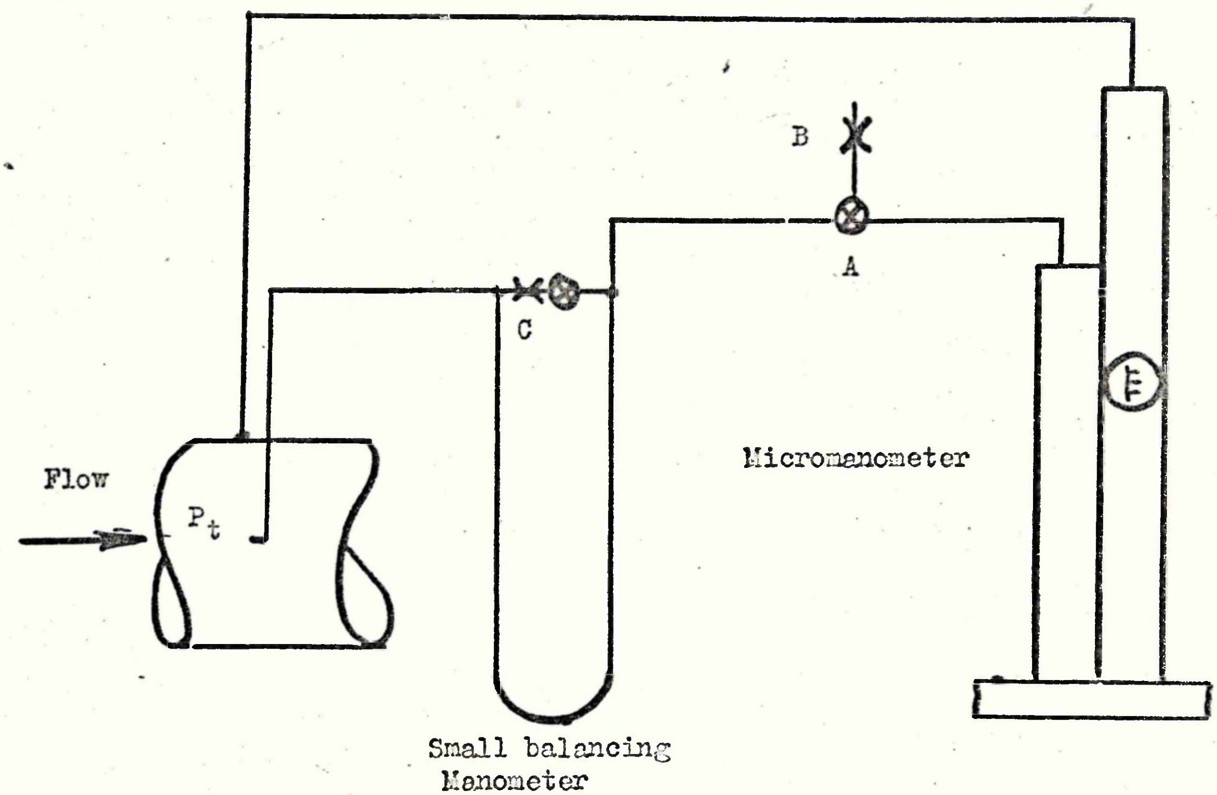

ARRANGEMENT (i)

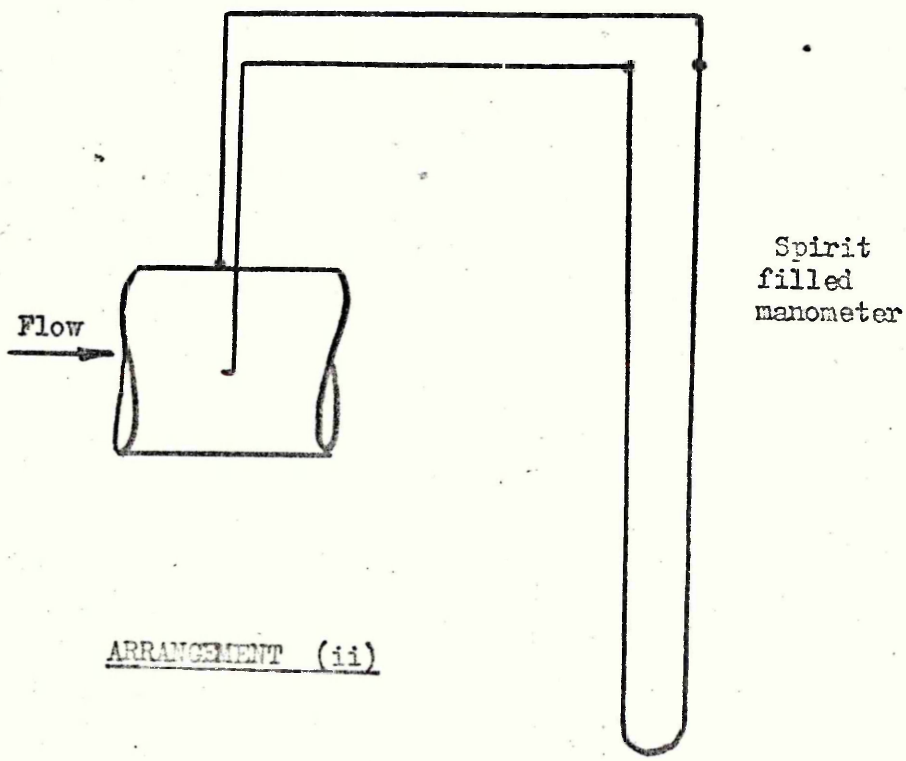

ARRANGEMENT (ii)

ALTERNATIVE INSTRUMENTATION USED DURING PRELIMINARY INVESTIGATION.

FIGURE...24

The positioning of the probe head was accomplished by the use of a feeler gauge (figure 25) being placed under the head and then adjusting the zero by means of a grub screw at the very top of the pitot traverse, marked 'A' on figure 22.

The probe was then placed in the first position upstream of the diffuser inlet and traversed to the duct centre line. The fan was started and the damper opened slowly until the centreline velocity head was in the region of 350 mm. w.g. (77m/s) or 400 mm for fully developed flow conditions. The pitot probe head was then returned to its original positon at 0.5mm. from the wall and the rig left for a few minutes to allow the fan and flow to stabilise.

The position was traversed initially at 0.5mm. intervals followed by larger increments (depending on the boundary layer thickness) to the centreline of the duct. Whilst traversing the duct, the readings were plotted to ensure the elimination of erroneous results (these only tended to occur when the flow in the boundary layer was becoming unstable.). A time of between 15 to 30 seconds was allowed between each reading to allow the manometers to reach a steady state condition.

The traverse was then returned to zero, removed from the duct, re-set to its initial 0.5mm condition, and placed in the next station of interest, which was determined from the multitube manometer (mentioned in the previous chapter). Another traverse to the duct centreline was then carried out. This procedure was reapeated until all the stations of interest had been traversed. If, however, the flow had separated or stalled only a static pressure measurement was taken at the station.

This data was placed on computer punch cards and processed into the requisite form and the required parameters calculated by the data reduction program described in the following chapter (chapter V1).

V.3 Range of Tests.

Test were carried out for three diffuser inlet boundary layer thicknesses

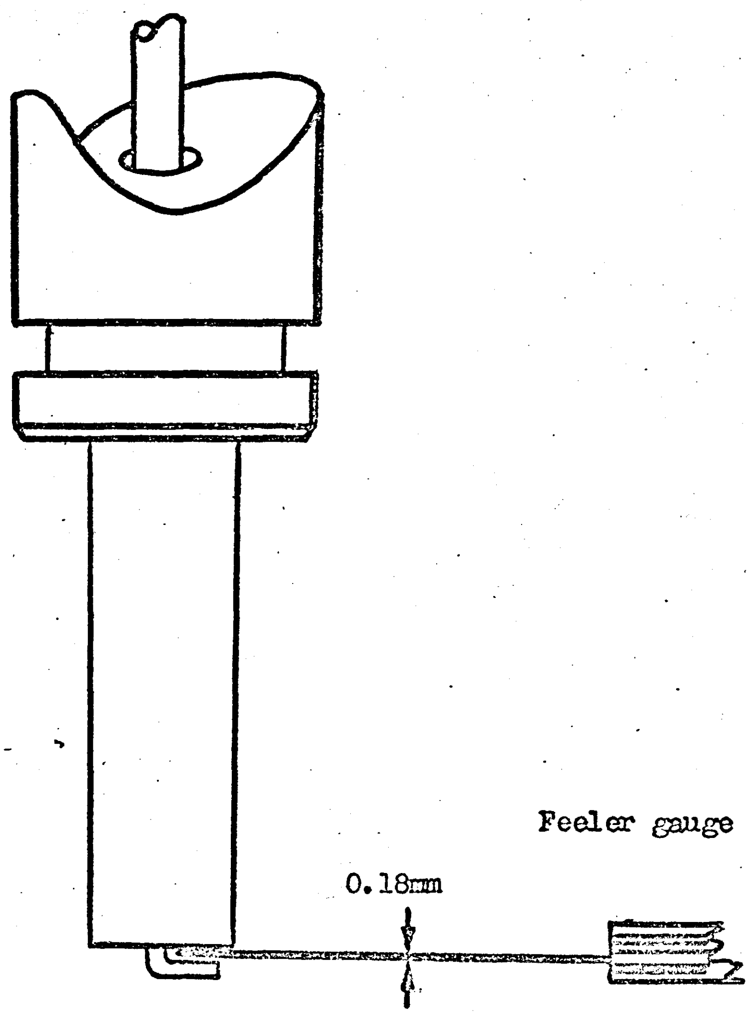

INITIAL POSITIONING OF PITOT HEAD

FIGURE.....25

of $2\delta^*/w_1$ of 0.01, 0.06 and 0.11 which were described as thin, thick and fully developed respectively. For these three inlet conditions a series of Reynolds Number tests were carried out at Reynolds at Numbers ranging from 6×10^4 to 4×10^5. These tests are listed in Table I (the full results can be seen in appendices 5 and 6). These tests established where the limits of Reynolds Number dependence lay and thereby indicated the limiting values of Reynolds Number for subsequent tests.

The next series of tests were comprehensive velocity traverses for the three inlet boundary layer thicknesses at the stations of interest both in the diffuser and tailpipe (where fitted). These tests were carried out for three angles of diffuser divergence (5°, 10° and 15°), and for each angle two area ratios were tested (2 and 3). All these geometric and flow conditions were tested both under plenum discharge and tailpipe discharge conditions. This produced a total of 36 different configurations, the results of which are shown in appendix 6.

A test was also made with a thick boundary layer and a divergence angle of 10° with the tailpipe terminated at the maximum pressure position (as deter mined from the multitube manometer) to determine the effect of this measure. All these tests are listed in Table I.

Additional tests were also carried out on the test rig. One of these tests was to take static pressure readings in the inlet for each configuration in order to determine the actual static pressure at the inlet to the diffusing section (as mentioned in chapter IV). Another test was to carry out full velocity traverses of the duct at various stations, and in particular at the inlet, to determine the symmetry of the flow. (This particular test helped to resolve the pitot and static interaction which caused distortion at the wall and thus very much accentuated the slight distortion caused by the trip wire). Also tests were carried out to verify the assumptions of inlet duct length required to obtain the required inlet condition to the diffuser which were based on the preliminary investigations with the brass pipe. As mentioned in the previous chapter a good agreement was acheived between the required and actual values of $2\,\mathcal{E}^*/w_1$.

TEST No.	CONDITION OF RIG.
	Thin Inlet B/L $(2\delta^*/W_1 = 0.01)$
109	5° AR2 plenum discharge.
112	5° AR2 tailpipe discharge.
110	5° AR3 plenum discharge.
111	5° AR3 tailpipe discharge.
103	10° AR2 plenum discharge.
104	10° AR2 tailpipe discharge.
102	10° AR3 Plenum discharge.
101	10° Tailpipe discharge.
105	15° AR2 plenum discharge.
108	15° AR2 tailpipe discharge.
106	15° AR3 plenum discharge.
107	15° AR3 tailpipe discharge.
	Thick Inlet B/L $(2\delta^*/W_1 = 0.06)$.
202	5° AR2 plenum discharge.
201	5° AR2 tailpipe discharge.
203	5° AR3 plenum discharge.
204	5° AR3 tailpipe discharge.
205	10° AR2 plenum discharge.
206	10° AR2 tailpipe discharge.
207	10° AR2 optimum tailpipe length.
210	10° AR3 plenum discharge.
208	10° AR3 tailpipe discharge.
209	10° AR3 tailpipe discharge.
211	15° AR2 plenum discharge.
214	15° AR2 tailpipe discharge.
212	15° AR3 plenum discharge.
213	15° AR3 tailpipe discharge.

TEST No.	CONDITION OF RIG.
	Fully Developed Inlet Flow = 0.11
302	15° AR2 plenum discharge.
301	15° AR2 tailpipe discharge.
303	15° AR3 plenum discharge.
304	15° AR3 tailpipe discharge.
305	10° AR3 tailpipe discharge.
306	10° AR3 plenum dishcarge.
307	10° AR2 plenumdischarge.
308	10° AR2 tailpipe discharge.
309	5° AR2 plenum discharge.
310	5° AR2 tailpipe discharge.
311	5° AR3 plenum discharge.
312	5° tailpipe discharge.
000	Thin inlet boundary layer inlet profile.
350	Fully developed velocity profile. (inlet).

REYNOLDS No. TESTS

Test No.	Re. No.	Configuration.
1	4.68×10^5	10° AR3 tailpipe thin boundary layer.
2	4.44×10^5	
3	4.25×10^5	
4	2.25×10^5	
5	1.44×10^5	
6	1.07×10^5	
7	2.61×10^5	
8	3.02×10^5	
9	0.61×10^5	

Test No.	Reynolds No.	Configuration.
10	4.08×10^5	10° AR 3 Tailpipe thin boundary layer.
20	3.5×10^5	5° AR 2 Tailpipe thick boundary layer
21	2.9×10^5	
22	2.0×10^5	
23	1.4×10^5	
24	0.57×10^5	
30	4.0×10^5	10° AR 3 tailpipe thick boundary layer.
31	3.6×10^5	
32	2.9×10^5	
33	2.3×10^5	
34	1.7×10^5	
35	0.6×10^5	
40	4.0×10^5	15° AR 2 tailpipe fully developed
41	3.9×10^5	
42	3.5×10^5	
43	3.2×10^5	
44	2.6×10^5	
45	2.2×10^5	
46	1.5×10^5	
50	4.3×10^5	10° AR 3 tailpipe fully developed.
51	3.8×10^5	
52	3.4×10^5	
53	2.4×10^5	
54	1.8×10^5	
55	1.4×10^5	

VI.1 DATA REDUCTION.

The data reduction was carried out by a program on an I.B.M. 1130 computer. The data obtained during the experimental run was punched onto data cards in the following sequence:-

(a) The divergence angle, area ratio, tailpipe length and the designated number for the run.

(b) The atmospheric pressure temperature.

(c) The static pressure at the position, being traversed, width at the position. The number of the position, distance of the position from the diffuser inlet, the centre line dynamic pressure.

(d) The pitot dynamic pressure measured in mm. water, the distance between the readings and the number of readings at that particular spacing, less one, were then read in and repeated until all the data for that position had been read in.

The program produced the parameters listed below (numerical integration was performed using a modified Simpson's rule subroutine, as outlined in appendix 4.).

Mean Velocity, $\bar{u} = 2/w \int_0^{w/2} u\,dw$

Re. Number, $(Re) = \rho \bar{u} w / \mu$

Non-dimensionalised displacement thickness, $2\delta^*/w = \frac{2}{w}\int_0^{w/2} (1 - u/u_o)\,dw$

Non-dimensional Momentum thickness, $2\theta/w = \frac{2}{w}\int_0^{w/2} u/u_c\,(1 - u/u_o)\,dw$

Shape factor, $H = \delta^*/\theta$

Kinetic Energy Correction factor, $= 2/w \int_0^{w/2} \left(\frac{u}{\bar{u}}\right)^3 dw.$

Pressure Recovery Coefficient, $Cp = (p - p_1)/\frac{1}{2}\rho\bar{u}_1^2$

Effectiveness, $\eta = (p - p_1)/\frac{1}{2}\rho(\bar{u}_1^2 - \bar{u}^2)$

or in the case of stalled or separated flow, $= \dfrac{(p - p_1)}{\frac{1}{2}\rho\bar{u}_1^2(1 - 1/AR^2)}$

Energy Corrected Effectiveness, $= \frac{(p - p_1)}{\frac{1}{2}\rho(\alpha_1 \bar{u}_1^2 - \alpha \bar{u}^2)}$

Energy corrected Cp, Cp $= \frac{(p - p_1)}{\frac{1}{2}\rho\alpha_1 \bar{u}_1^2}$

Momentum Correction Coefficient, $\beta = 2/w \int_0^{w/2} (u/\bar{u})^2 \, dw$

Non-dimensional distance from diffuser inlet,

$x/w_1 = \frac{\text{Distance from diffuser inlet.}}{\text{Width at diffuser inlet.}}$

An example of these parameters is tabulated in Table II Graphs showing velocity profiles and variations in Cp, Cp_E, and η along the duct from the diffuser inlet are illustrated in figures 26a and 26b similar graphs were plotted for each diffuser configuration tested.

A flow diagram of the program is shown in figure 27 and the actual program is included in appendix 4.

INLET B/L THICKNESS = 0.0624 DIV. ANGLE = 15DEG., AREA RATIO = 2, TAILPIPE LENGTH = 2.740M , RUN NO.

PCSN	WIDTH M/M	DIST FRCM INLET	STATIC PRESS. M/M H2O	MEAN VEL. M/S	LOCAL REYNOLDS NUMBER	2DELTA* ------- WIDTH	2THETA ------ WIDTH	SHAPE FACTOR	K.E.CORR. FACTOR	PRESS. RECOV. COEFF.	EFFECT-IVENESS	ENERGY CORR. EFFECT.	ENE COR C
1	76.2	-0.070	-184.	68.4	350445.	0.0624	0.0448	1.392	1.045	0.000	1.000	0.000	0.C
2	89.4	0.050	-137.	62.6	376452.	0.0827	0.0546	1.513	1.051	0.161	1.001	0.984	0.1
3	128.6	0.201	-47.	44.5	384627.	0.2076	0.0890	2.333	1.306	0.472	0.818	0.957	0.4
4	152.4	0.468	-15.	39.1	400561.	0.2276	0.1128	2.017	1.301	0.582	0.864	0.938	0.5
5	152.4	0.923	-1.	39.5	404860.	0.1787	0.1224	1.459	1.109	0.630	0.946	0.933	0.6
6	152.4	1.839	4.	39.0	399942.	0.0869	0.0706	1.230	1.033	0.647	0.960	0.913	0.6
7	152.4	2.734	1.	38.5	394327.	0.0620	0.0509	1.217	1.026	0.639	0.935	0.886	0.6

PCSN.	BETA	C/L VEL.	TEMP.	ATM.PRESS.	X/W1
1	1.018	73.2	19.0	764.5	-0.918
2	1.018	67.8	19.0	764.5	0.656
3	1.116	55.9	19.0	764.5	2.637
4	1.108	50.8	19.0	764.5	6.141
5	1.038	48.3	19.0	764.5	12.112
6	1.013	42.9	19.0	764.5	24.133
7	1.010	41.1	19.0	764.5	35.879

TABLE II

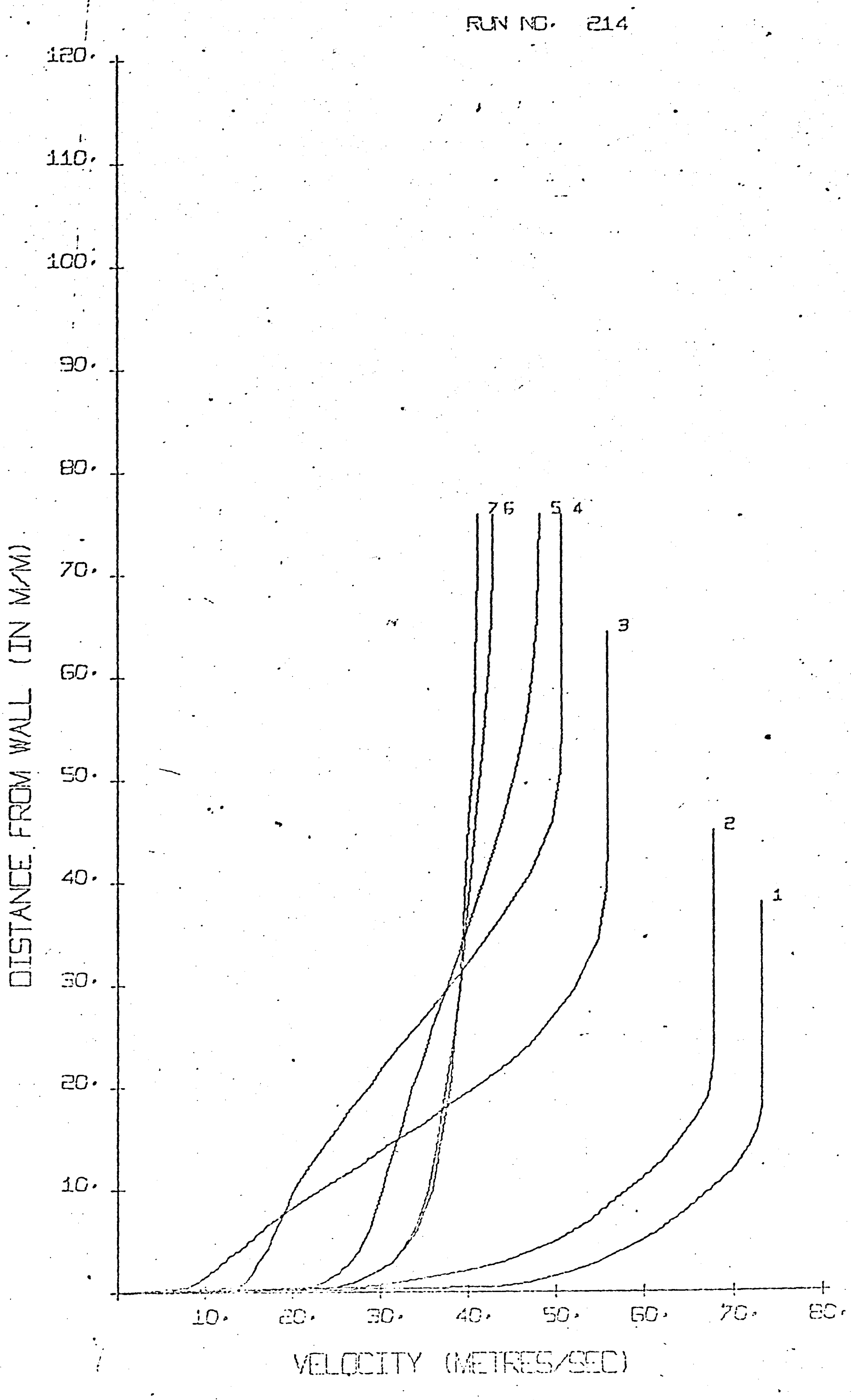
RUN NO. 214
DISTANCE FROM WALL (IN M/M)
120.
110.
100.
90.
80.
70.
60.
50.
40.
30.
20.
10.
10.
20.
30.
40.
50.
60.
70.
80.
VELOCITY (METRES/SEC)
1
2
3
4
5
6
7

FIGURE...26(a)

RUN NO. 214

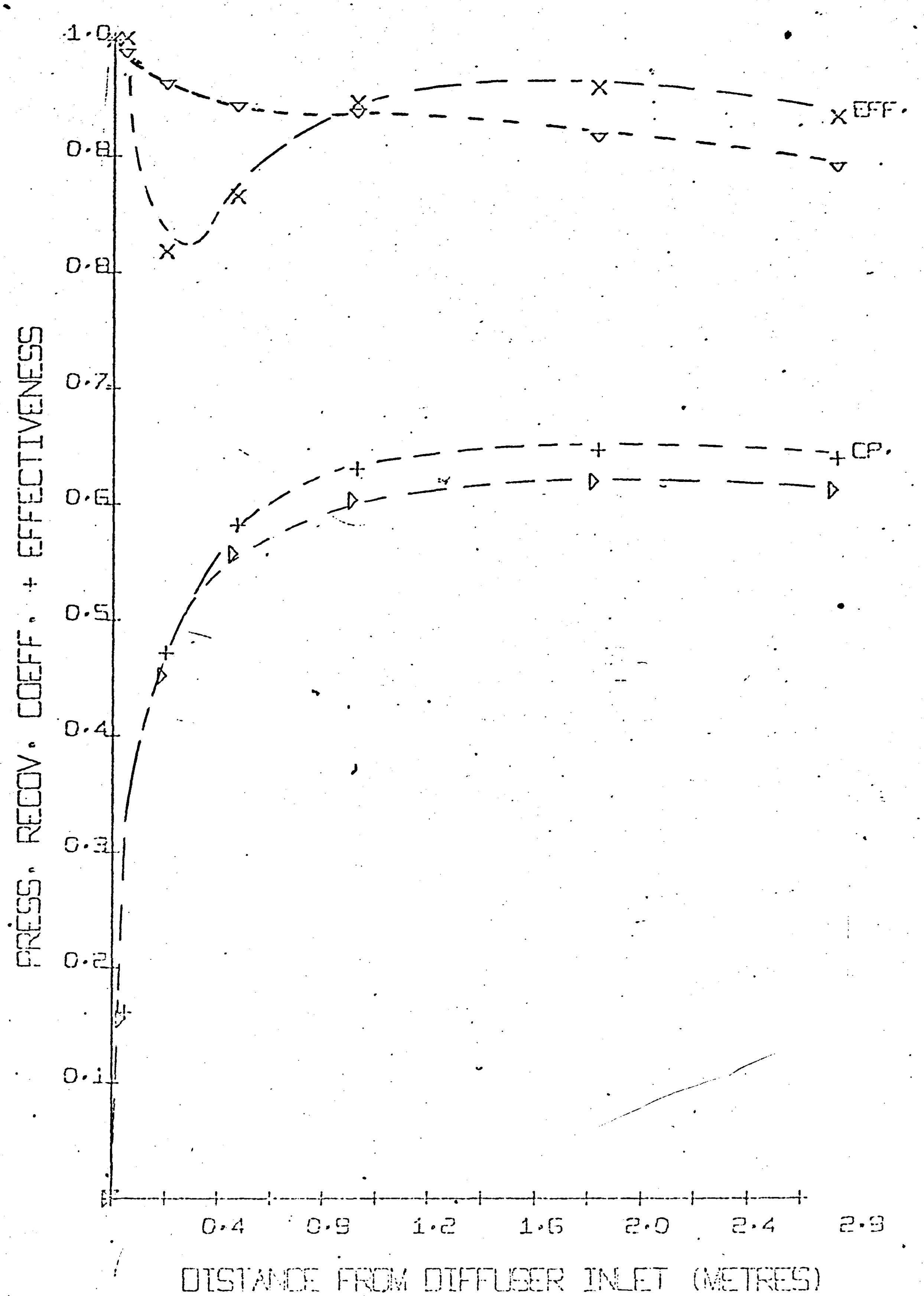

FIGURE....26(b)

DATA REDUCTION PROGRAM.

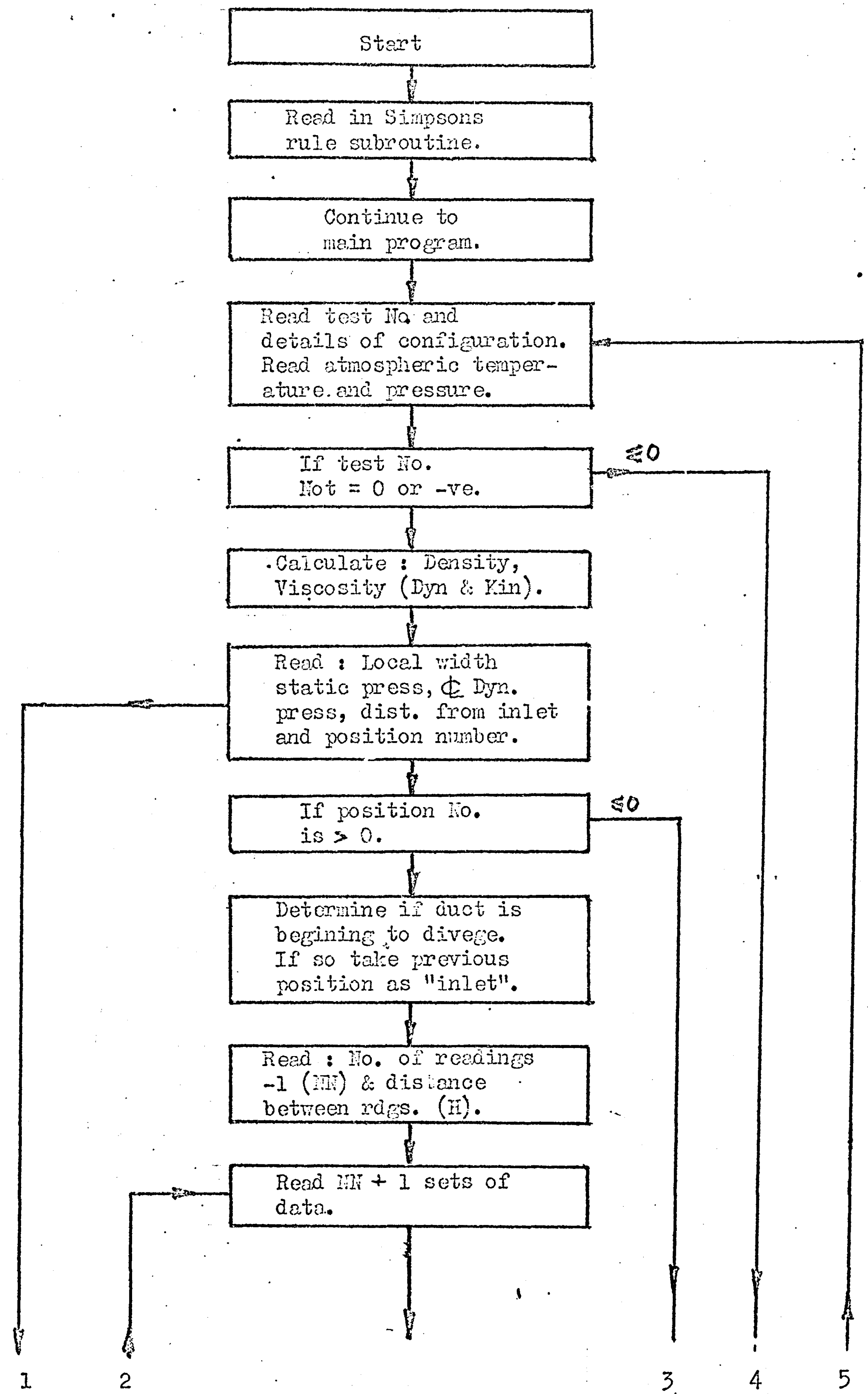

FIGURE...27

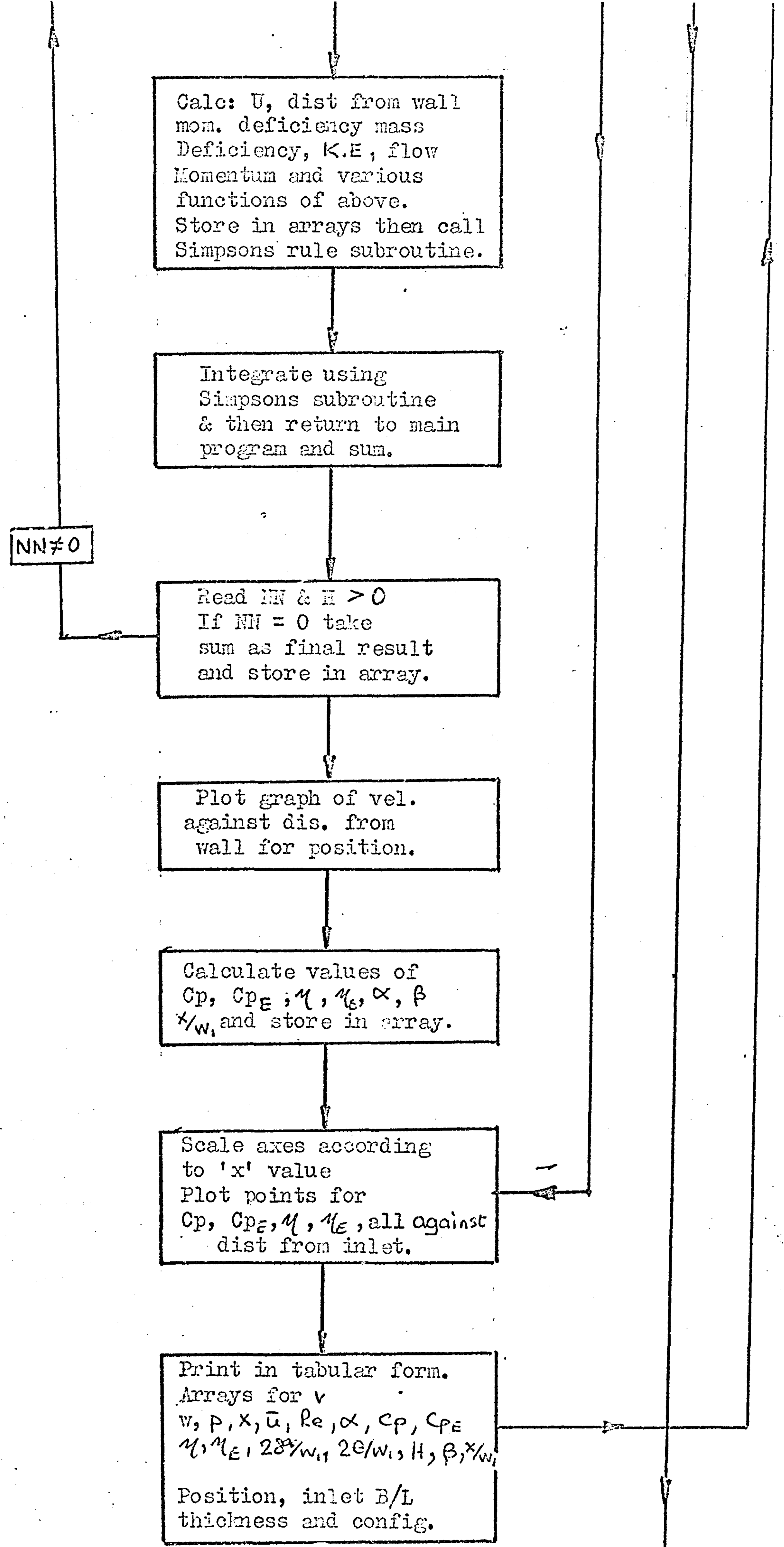
Calc: U, dist from wall mom. deficiency mass Deficiency, K.E, flow Momentum and various functions of above. Store in arrays then call Simpsons rule subroutine.
Integrate using Simpsons subroutine & then return to main program and sum.
NN≠0
Read NN & H > 0 If NN = 0 take sum as final result and store in array.
Plot graph of vel. against dis. from wall for position.
Calculate values of Cp, Cp$_E$; η, η$_E$, α, β x/w$_1$ and store in array.
Scale axes according to 'x' value Plot points for Cp, Cp$_E$, η, η$_E$, all against dist from inlet.
Print in tabular form. Arrays for v w, p, x, ū, Re, α, Cp, Cp$_E$ η, η$_E$, 2δ*/w$_1$, 2θ/w$_1$, H, β, x/w$_1$
Position, inlet B/L thickness and config.

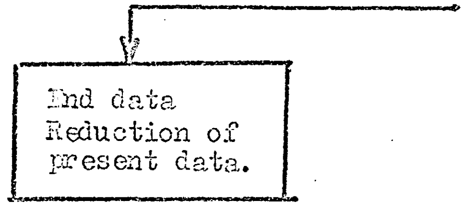

Figure 27 cont...

Chapter Seven.

REYNOLDS NO. TESTS.

VII.1 The Test Conditions.

As mentioned in Chapter V the Reynolds Number dependence tests were mainly carried out for one diffuser geometry ($2\phi = 10^{\circ}$, AR = 3, with a tailpipe fitted), and the Cp measured between the inlet and exit planes of the diffuser. (For the exit plane a position 0.25 mm upstream of the exit was used). Tests on this configuration were carried out for three inlet boundary thicknesses with Reynolds Numbers varying from approximately 6×10^{4} to 4×10^{5}. Two additional tests on the other geometries were carried out subsequently. These were:-

(a) The first additional configuration tested was for a fully developed flow into a 15° divergence angle diffuser of area ratio 3. In this test the Cp was measured at a position 0.025m into the tailpipe i.e. $x_t/w_2 = 0.1$ (where x_t is the distance measured from the diffuser exit plane into the tailpipe).

(b) The second was a thick inlet boundary layer with a diffuser configuration of $2\phi = 5^{\circ}$ and AR = 2 with the Cp taken between the diffuser inlet and the diffuser exit plane. (as for the 10° case).

VII.2 Reynolds No. Tests Results.

VII.2.1 Thin Inlet Boundary Layer.

For the thin inlet boundary layer ($2\delta^{*}/w_1 = 0.01$) it can be seen that Cp is largely independent of Reynolds number in the region of 2×10^{5} upwards, but below this the dependence would appear to increase slightly, though the Cp remains within 2% from Re's of 1×10^{5} upwards (figure 28). Below this value it is difficult to determine the effects due to the difficulties in measuring the low flow velocities with a pitot static probe.

VII.2.2 Thick Inlet Boundary Layer.

With a thicker inlet boundary layer ($2\delta^{*}/w_1$ = 0.06, this value increases as the Re. No. decreases), the Cp falls sharply and also there is a noticeable

PRESSURE RECOVERY / REYNOLDS NUMBER

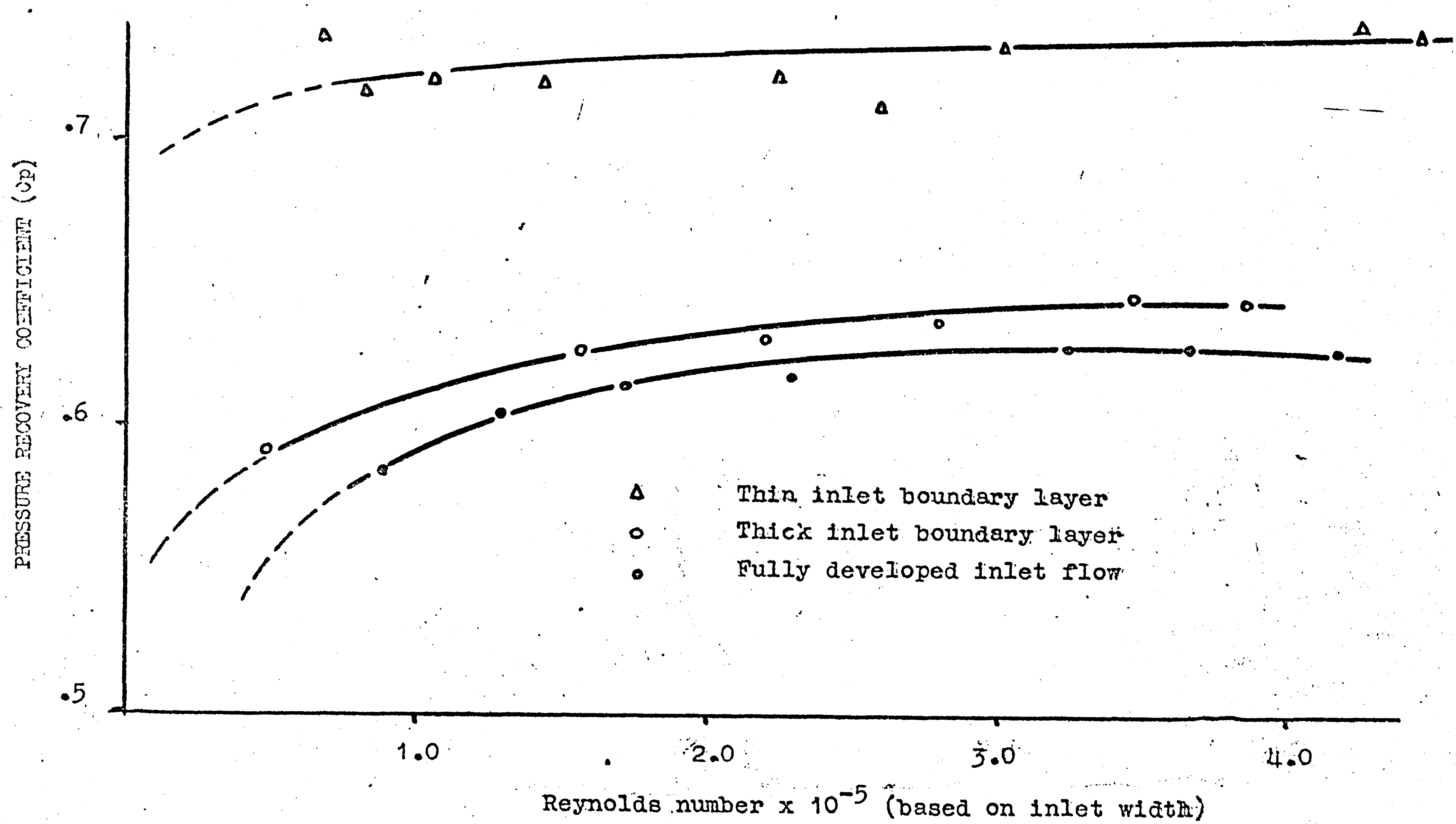

FIGURE.....28

increase in the Reynolds Number (Re) dependence for this particular flow condition. The Reynolds number dependence would appear to become significant in the region of Reynolds numbers of 2.5×10^5 and lower (i.e. greater than 1%). Below Re. = 2.5×10^5 Reynolds number dependence increases sharply and at a Reynolds number of 1×10^5 the Cp has fallen by 5%, this can be seen on figure 28.

VII.2.3 Fully Developed Flow.

For the fully developed flow case a similar trend can be seen but even more markedly than for the two previous inlet conditions, in that by Reynolds numbers around 1.0×10^5 the Cp has fallen by as much as 7%.

VII.2.4 Further Reynolds Number Tests.

This effect is shown even more in the test on the 15° diffuser with the fully developed inlet flow. In this test the Cp was 12% lower at a Reynolds number of 1×10^5 than at a Reynolds number of 4.0×10^5. An opposite effect can be seen for the 5°, AR = 2 test with the thick inlet boundary layer, in that the Cp falls off less quickly at low Reynolds numbers than for the 10°, AR = 3 configuration. (Shown in figure 29).

VII.3.1. General Conclusions from the Reynolds Number Tests.

For convenience a critical Reynolds number will be defined such that all flows with Reynolds numbers above this are independent (to within 2%) and conversely all flows with Reynolds Numbers below this are dependent on Re. This critical Reynolds Number should not be confused with the general meaning of critical Reynolds Number.

It can be seen from the graphs of pressure recovery coefficient (Cp) against Reynolds Number for the three different inlet boundary layer conditions (for a 10° divergence angle diffuser), shown in figure 28, that the point of Reynolds Number (Re) independence occurs at a higher Reynolds Number as the boundary layer thickens and it would seem reasonable to assume that the effect will be as shown extrapolated in figure 28. The results also shown a similar trend to those shown by FERRETT[21] in his water tests.

The tests carried out on other divergence angles would seem to indicate

PRESSURE RECOVERY / REYNOLDS NUMBER

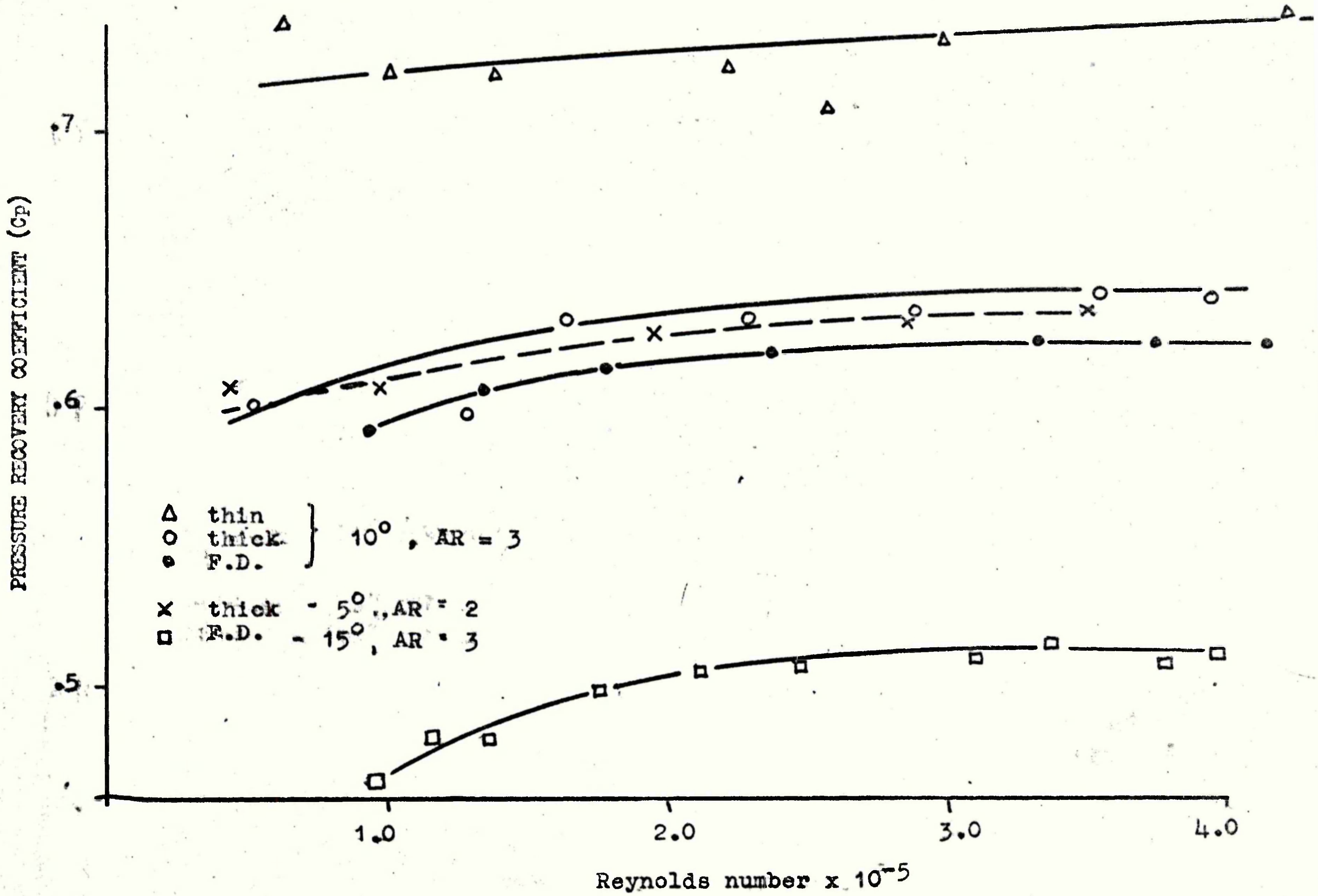

FIGURE.....29

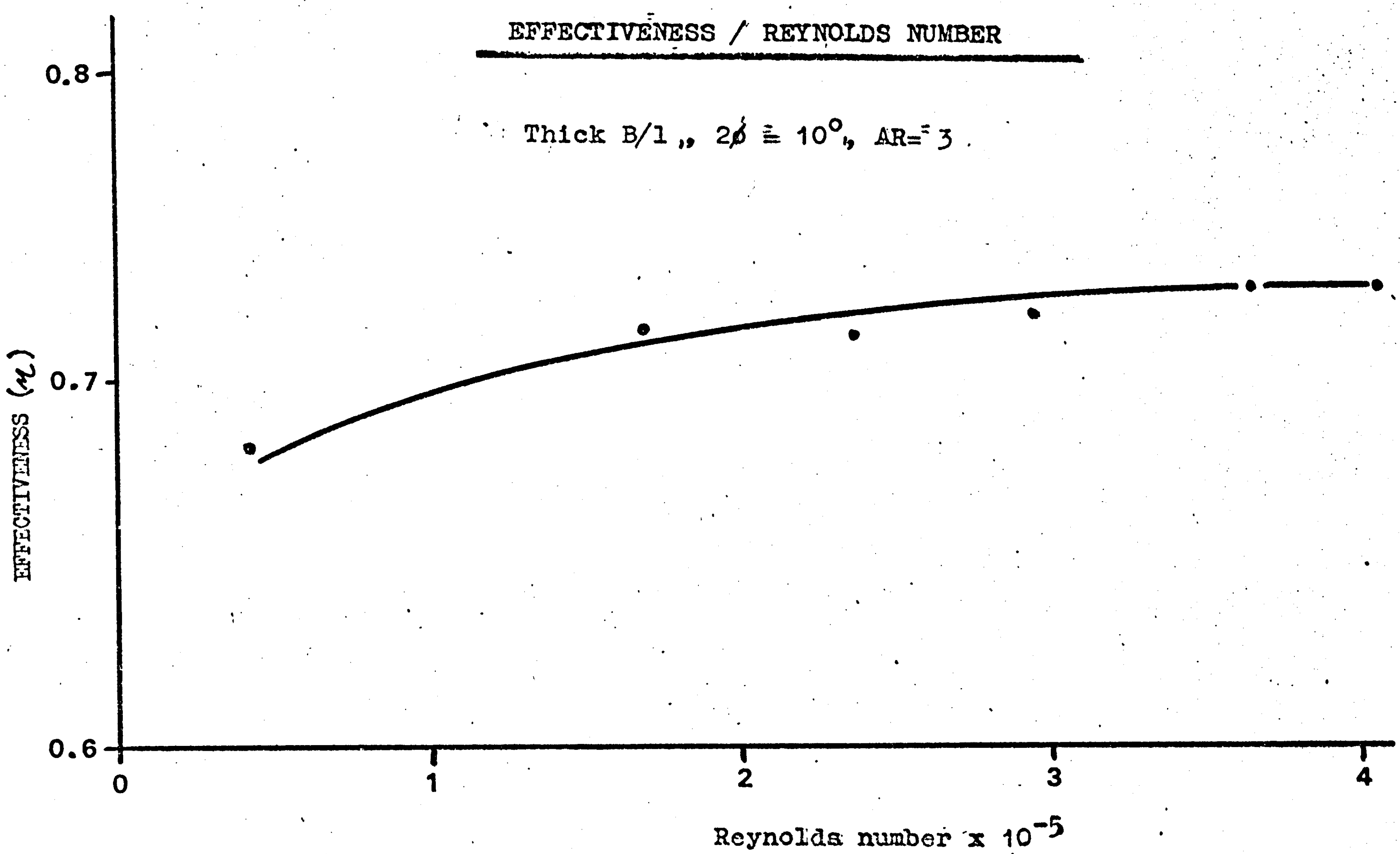

EFFECTIVENESS / REYNOLDS NUMBER
Thick B/1 ,, 2ϕ = 10°, AR= 3
0.8
0.7
0.6
EFFECTIVENESS (μ)
0
1
2
3
4
Reynolds number x 10^-5

FIGURE....30

$2\delta^*/W_1$ and H / REYNOLDS NUMBER : (for fully developed flow)

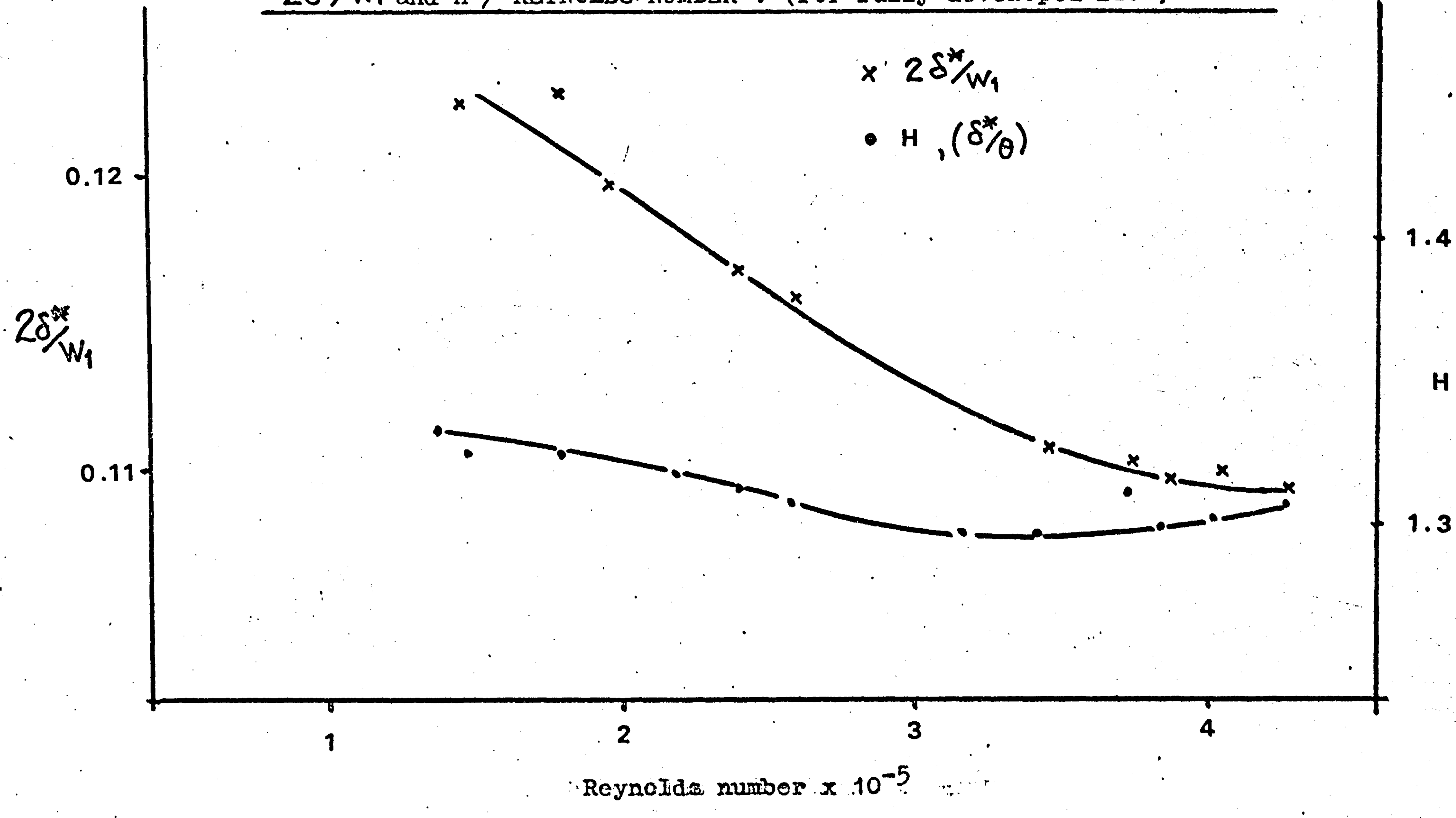

FIGURE.....31

that for a given boundary layer condition Reynolds number independence decreases away from the optimum geometrical configuration.

VII.4 Discussion of the Results.

From the experimental results it can be seen that the probable reason for the increase in Reynolds number dependence as the Reynolds number decreases below the critical value, is due to an increase in the boundary layer thickness ($2\delta^*/w_1$). The boundary layer will grow as the Reynolds number is reduced, shown in figure 31. A similar effect can be seen for the momentum thickness ($2\theta/w_1$) and to a much lesser extent for the shape factor (H), (shown in figure 31). It is therefore apparent that as Reynolds number decreases the boundary layer thickens and Cp falls.

This is due to the reduction in the momentum of the boundary layer which decreases its ability to flow against the adverse pressure gradient in the diffuser, therefore causing increased distortion of the boundary layer velocity profile and a reduction in the Cp of the diffuser (shown in figures 28 and 29). The distortion of the velocity profile will also reduce the effectiveness of the diffuser, (shown in figure 30).

These tests show that performance is never independent of Reynolds number although the dependency is markedly less significant as the Reynolds number increases.

It also shows that the inlet boundary layer thickness, and the geometrical configuration of the diffuser affect the extent of the Reynolds number dependence. Therefore it can be concluded that for Reynolds numbers 3.0×10^5 the effect of Reynolds number dependence on any of the tested configurations is less than 1%. However the tests would seem to indicate that a more adverse condition, such as a very high divergence angle, may increase the Reynolds number dependence to even higher values of Reynolds number.

It was therefore assumed for the general diffuser testing, discussed in chapter VIII, that if the inlet Reynolds numbers were kept above 3.0×10^5 the Reynolds number effects would be negligible. However the work did show that Reynolds number effects above 2.0×10^4 are not as negligible as many workers in this field have assumed.

Chapter Eight.

DISCUSSION OF THE EXPERIMENTAL RESULTS.

VIII.1 General Observations from the Plenum Discharge Work.

Chapter I shows that previous workers seem to show that the pressure recovery coefficient (Cp) should be at a maximum for an area ratio of approximately 3.0 and a divergence angle of 7°. Whereas the optimum effectiveness (η) occurs at a divergence angle of 7° also, but an area ratio of 2.0. The results obtained during this investigation indicate that the optimum diffuser geometry for pressure recovery coefficient (Cp) and effectiveness (η) occur with a divergence angle of 5° and area ratio of 3.0 for both parameters. However it must be borne in mind that this investigation was carried out at around the optimum geometries for both Cp and η and figure 33 shows that the optimum pressure recovery (Cp) probably occurs in the region of 6° to 7° depending upon the thickness of the inlet boundary layer.

VIII.2 Plenum Discharge Pressure Recovery Coefficient. (Cp).

VIII.2.1 Thin Inlet Boundary Layer.

Closer examination of the results indicate that though distortion of the boundary layer is low for the 5° divergence angle diffuser of AR = 3.0, the boundary layer thickness is becoming very large, caused by the long wall length and the adverse pressure gradient $\partial p/\partial x$. Therefore any further increase in area ratio (AR) will be unlikely to have any effect for the case of a thin inlet boundary layer at inlet to the diffuser. The pressure recovery coefficient (Cp) for a 5° included angle diffuser can be seen to be at its optimum for an area ratio of 3.0.

Examination of the 10° divergence angle, AR = 3.0 diffuser results show that the distortion of the boundary layer, shown by the shape factor (H), is not sufficiently large to cause separation of the boundary layer from the wall and the boundary layer thickness at the exit plane of the diffuser ($2\,\delta^{*}/w_2$) indicates that further diffusion may be possible without inducing separation

$2\phi = 10$, AR = 2, Thick Inlet Boundary layer

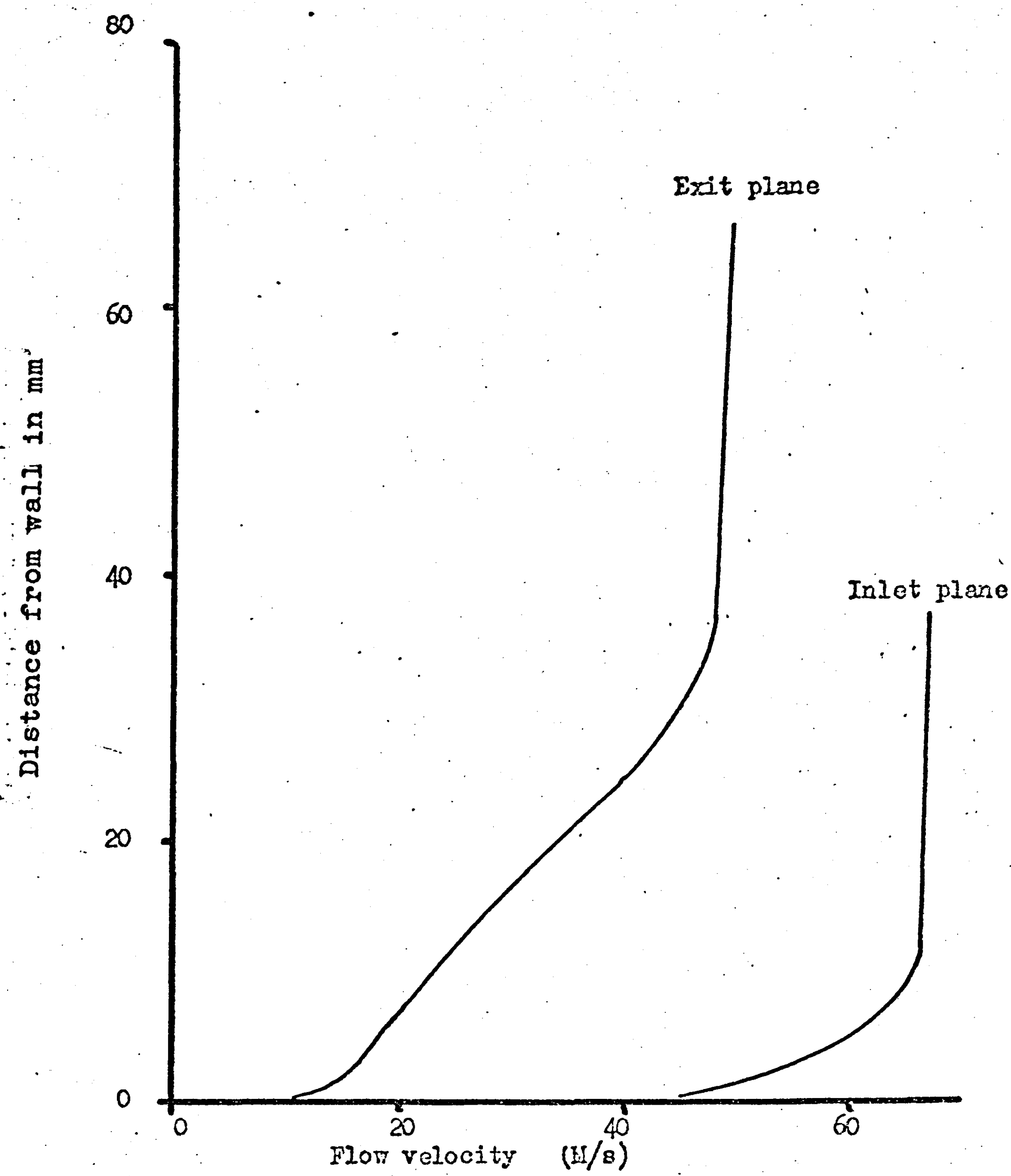

TYPICAL BOUNDARY LAYER VELOCITY PROFILES

FIGURE.....32

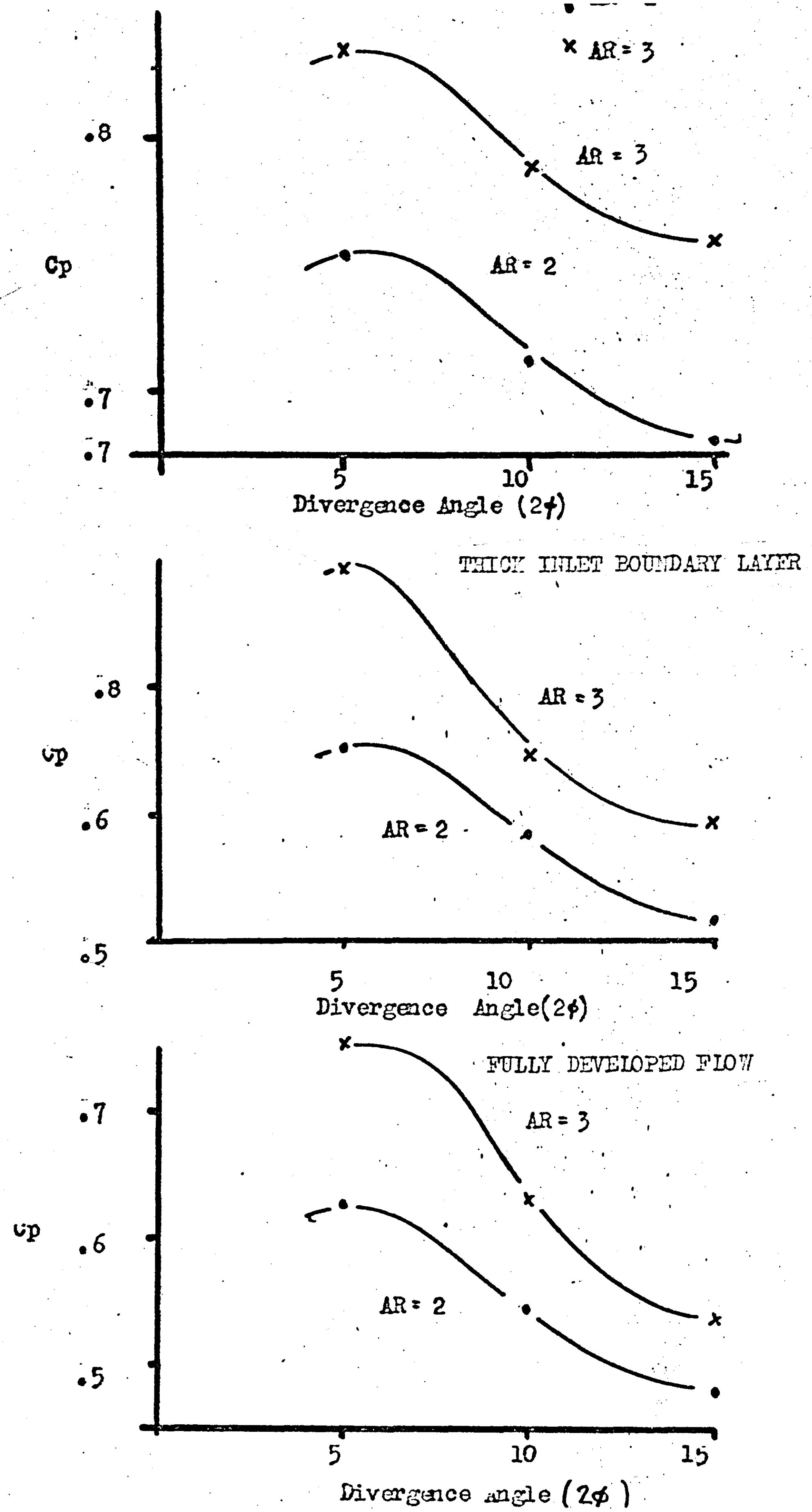

PLENUM DISCHARGE PRESSURE RECOVERY(Cp)

FIGURE.....33

or increasing the boundary layer thickness to such a value that it would either promote separation or reduce the recovery (shown in figure 35). Therefore a higher pressure recovery coefficient could probably be attained by using an area ratio of 4.0.

For the 15^{o} divergence angle diffuser it can be seen that a further increase in the area ratio (AR) should also increase the pressure recovery coefficient, though probably less than for the 10^{o} diffuser since the adverse pressure gradient $\partial p/\partial x$ is very severe and slight thickening of the boundary layer together with increased distortion may induce separation of the boundary layer. Thus it can be concluded that the results are probably misleading, in that the optimum area ratio for peak pressure recovery (Cp) for a 5^{o} divergence angle diffuser is 3.0. Any further increase in AR would cause the boundary layer thickness to become so large that it would make further improvement unlikely. However, in the cases of the 10^{o} and 15^{o} divergence angle diffusers, the boundary layer thickness is sufficiently small to allow a further increase in the area ratio (AR). Also since the shape factor (H) is fairly small the boundary layer could still withstand a further loss of momentum. Therefore the optimum geometry probably lies between 7^{o} and 10^{o} divergence angle with an area ratio (AR) of between 3.0 and 4.0, which is in agreement with many previous workers.

VIII.2.2 Thickening of the Inlet Boundary Layer.

Any increase in the inlet boundary layer thickness has a severe effect on the pressure recovery of the diffuser (Cp), shown in figure 33 (though it is less marked with the 5^{o} diffuser). This is because there is less forward momentum in the boundary layer and also the rate of entrainment of momentum into the boundary layer is lower with the thicker inlet boundary layer. Thus the distortion of the boundary layer when flowing against an adverse pressure gradient ($\partial p/\partial x$) is more severe, and therefore smaller pressure gradients give better pressure recovery in the diffuser. Figure 35 shows that for flow with a "thick" inlet boundary layer ($2\delta^{*}/w_{1}$ = .06) flowing in a diffuser with an area ratio (AR) of 3.0 the boundary layer will separate from the diffuser

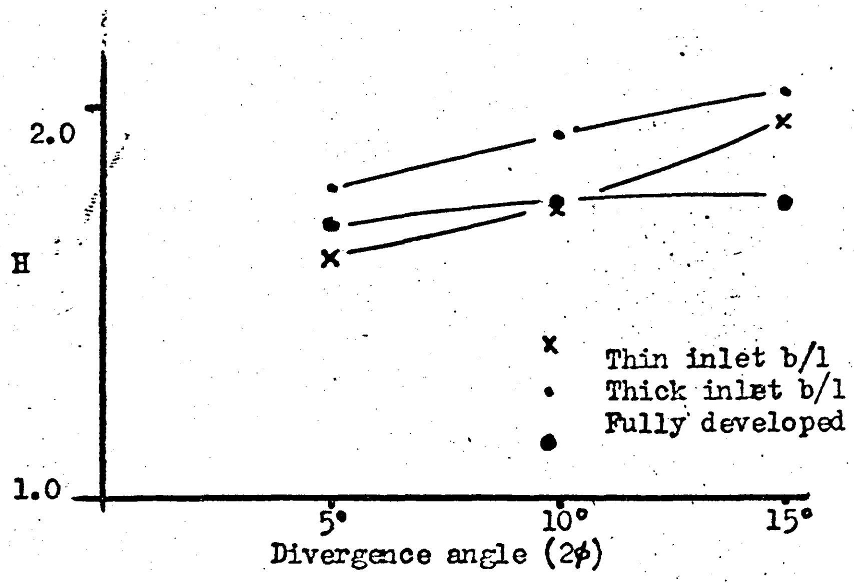

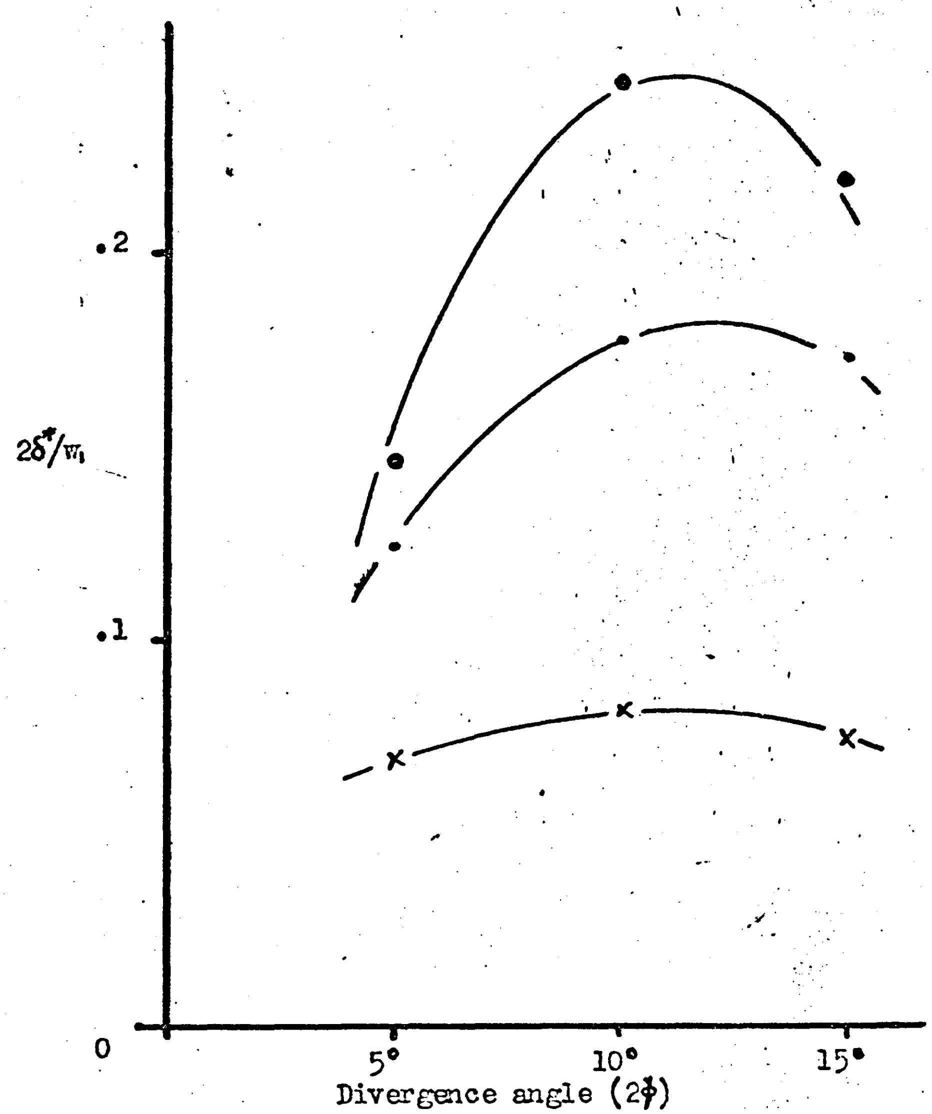

FIGURE 34

Boundary layer thickness and shape factor at the diffuser exit plane for plenum discharge AR = 2.

PLENUM DISCHARGE, AR = 3

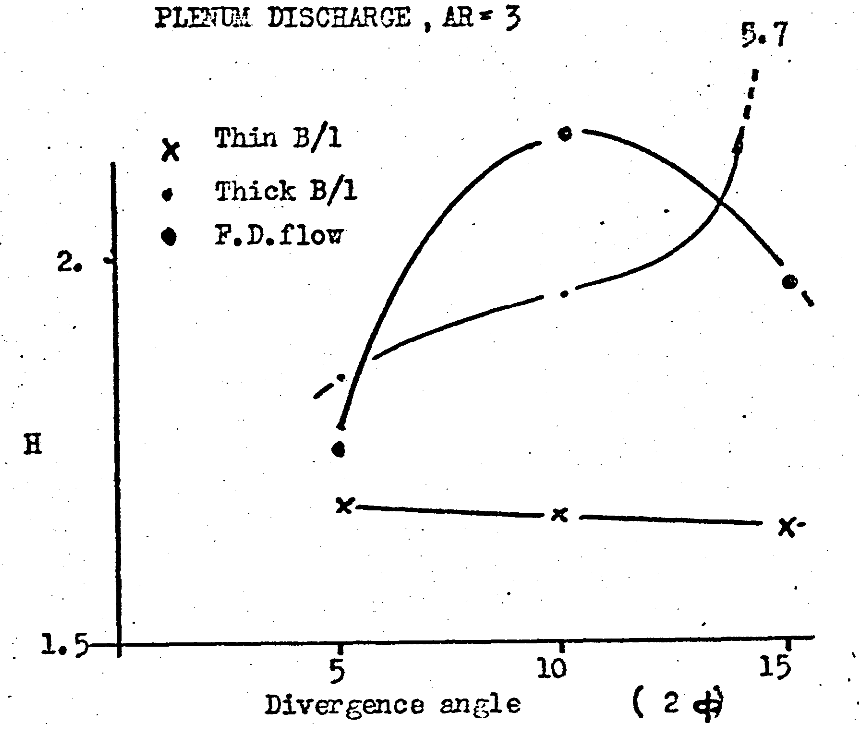

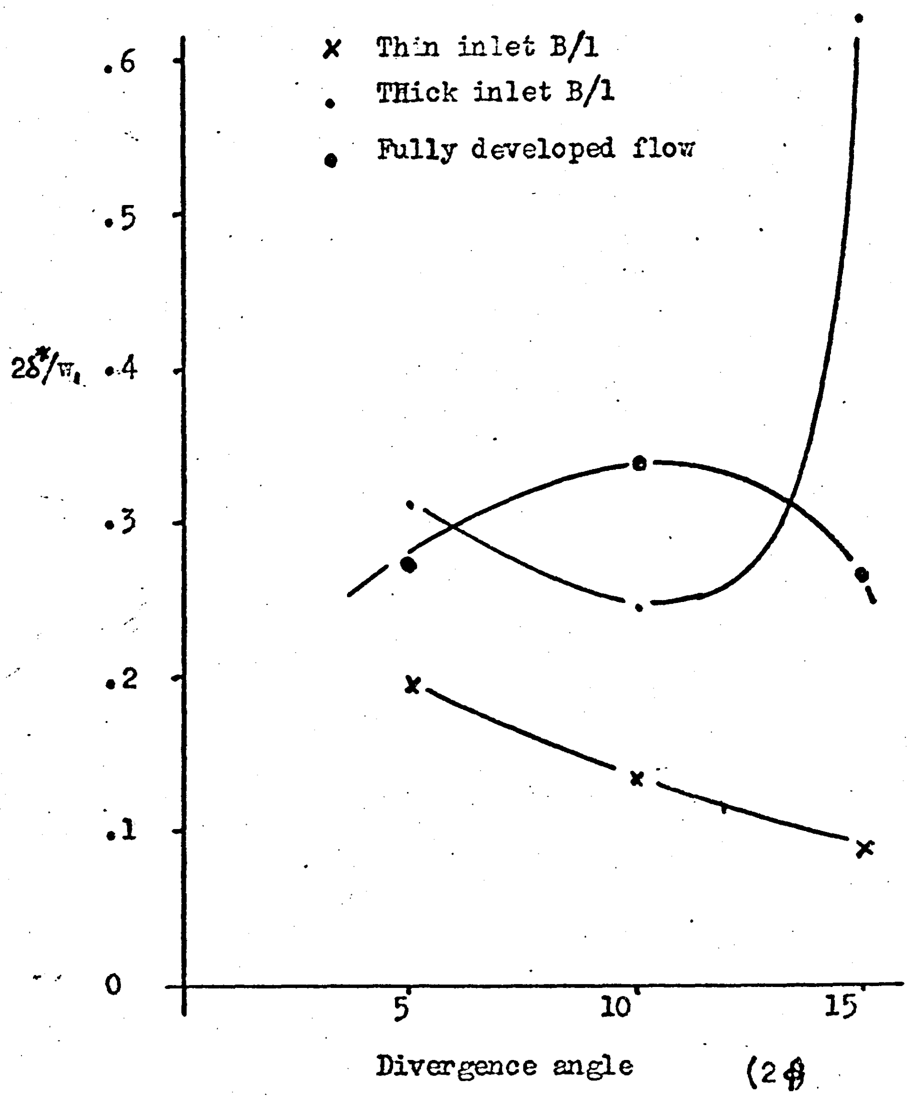

FIGURE 35

Boundary layer thickness and shape factor at the diffuser exit plane for plenum dishcarge AR = 3.

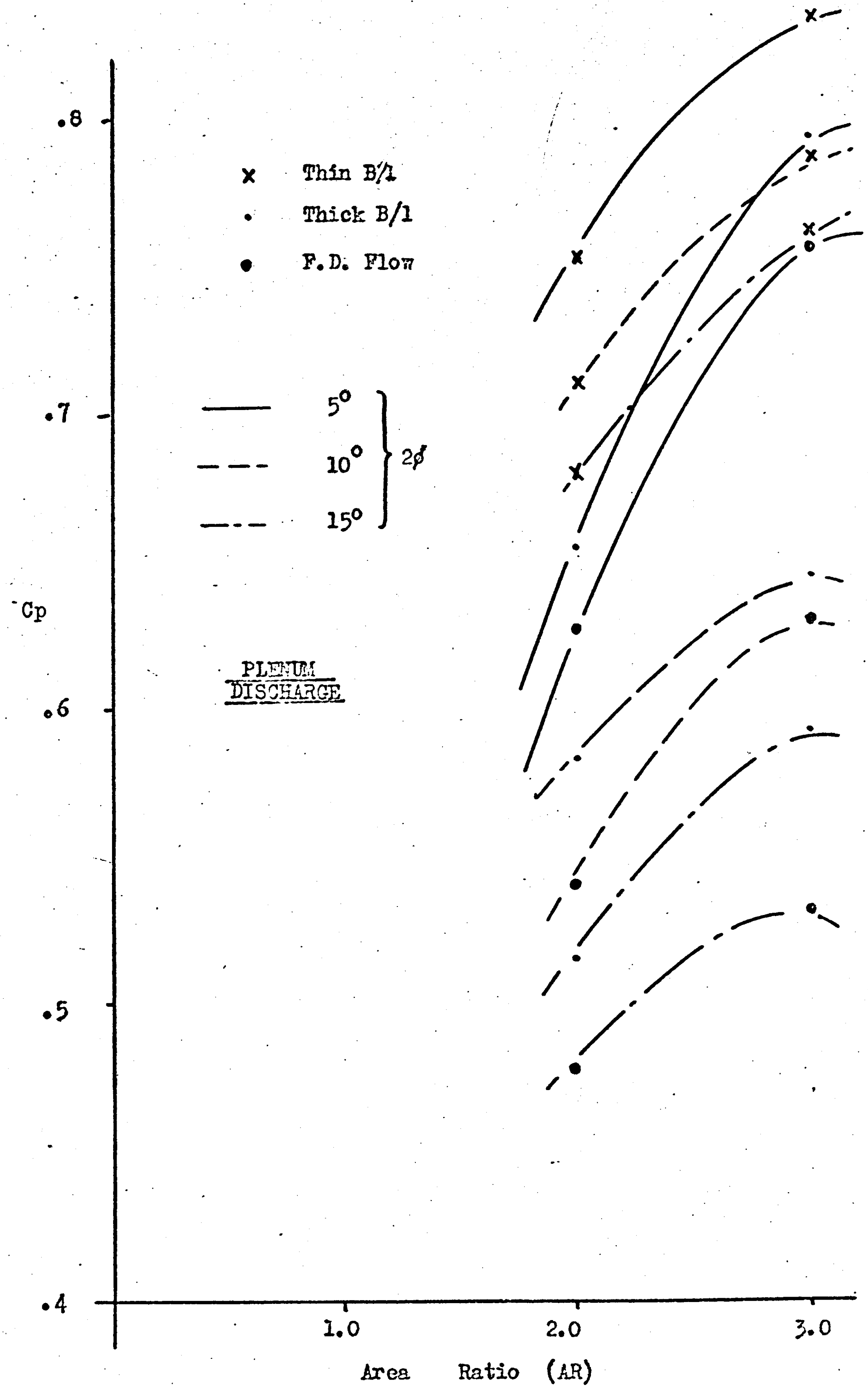

FIGURE......36

Cp/AR for various divergence angles from experimental results.

wall when the divergence angle is between 10^{o} and 15^{o}. However, fully developed flow at the inlet ($2\,\delta^{*}/w_1 = 0.11$) is more stable within the diffuser than the thick boundary layer. Figure 35 also shows that for this fully developed inlet flow case there is a reduction in the distortion of the boundary layer as the divergence angle is increased above 10^{o}, (as defined by the shape factor (H)). This is due to the lower pressure recovery and therefore a smaller adverse pressure gradient. This phenomenon is discussed more fully in paragraph VIII.5.

Therefore it can be generally concluded that any increase in the diffuser inlet boundary layer thickness will reduce the pressure recovery coefficient (Cp) and reduces the ability of the boundary layer to flow against an adverse pressure gradient ($\partial p/\partial x$) due to its lack of momentum, thus increasing the distortion and the likelihood of separation or stall within the diffuser. This reduction in 'Cp' with the boundary layer thickness can be seen in figure 36.

VIII.3 Plenum Discharge Effectiveness (η).

VIII.3.1 Thin Inlet Boundary Layer.

It must be noted that effectiveness is usually only of secondary importance, the important parameter being generally the pressure recovery coefficient (Cp); which gives an indication of the efficiency of the diffuser in converting the inlet kinetic energy into a pressure rise at the diffuser exit. The effectiveness (η) is used to give a measure of the proportion of the kinetic energy reduction occurring within the diffuser which can be accounted for by the static pressure increase. However a term such as efficiency for this parameter, even when corrected for energy deficiencies, would be misleading therefore effectiveness is used to denote this parameter. This prevents problems occuring from the use of a highly effective diffuser ("efficient") with low pressure recovery when a high pressure recovery is required.

For a thin inlet boundary layer the effectiveness of the diffuser can be seen in figure 37 to be at a maximum with a diffuser divergence angle of 15^{o}, and an AR = 3.0. This again is contrary to the findings of Gibson[1] .

However Gibson used a tailpipe pressure tapping to measure his pressure recovery, this alone would give quite a large discrepancy against plenum discharge work. The reason for this is in the use of the expression for effectiveness based on mass continuity within the diffuser ($\eta = Cp/(1 - 1/AR^2)$). The use of this expression only gives a true estimation of the 'energy effectiveness' of a diffuser if the inlet and outlet velocity profiles are identical. Therefore as the distortion at the diffuser exit plane increases, the kinetic energy based on the mass contiuity ($\frac{1}{2}\rho\bar{u}_2^2$) increasingly underestimates the actual exit kinetic energy ($\frac{1}{2}\int_c^W u^2 \; dw$) and for certain conditions the error can be in excess of 10%, (shown in figure 37). The addition of a tailpipe will recover some of this energy 'deficiency' incurred from the use of the continuity expression by reducing the distortion of the velocity profile (discussed in paragraph VIII.4), thus as in Gibson's case overestimating the plenum discharge effectiveness. When the effectiveness is corrected for this energy deficiency by using the kinetic energy correction factor α, the effectiveness (η_E) will increase considerably. The use of this corrected value of effectiveness (η_E) is shown in figure 37 and it can be seen that this 'true' effectiveness (η_E) is higher than the normally used effectiveness (η). The effect is most marked for the highly distorted profiles i.e. AR = 3.0, $2\phi = 10^\circ, 15^\circ$. The 15° divergence angle diffuser with an area ratio of 3.0 increases in effectiveness from 0.95 for η to 0.97 for η_E an increase of approximately 2%. However the optimum area ratio remains at 3.0, and not 2.0 as found by many previous workers, also the divergence angle of 15° can be seen to be the optimum geometry for peak effectiveness.

VIII.3.2. Thickening of the Inlet Boundary Layer.

If a thicker boundary layer is present at the inlet to the diffuser distortion of the boundary layer increases, shown by an increase in the shape factor (H). The figure 37 shows the peak effectiveness (η) to occur with a diffuser area ratio (AR) of 3.0, similar to the thin inlet boundary layer condition. The divergence angle of the diffuser for this optimum value of effectiveness (η) is reduced to a value of 5° and figure 37 indicates that

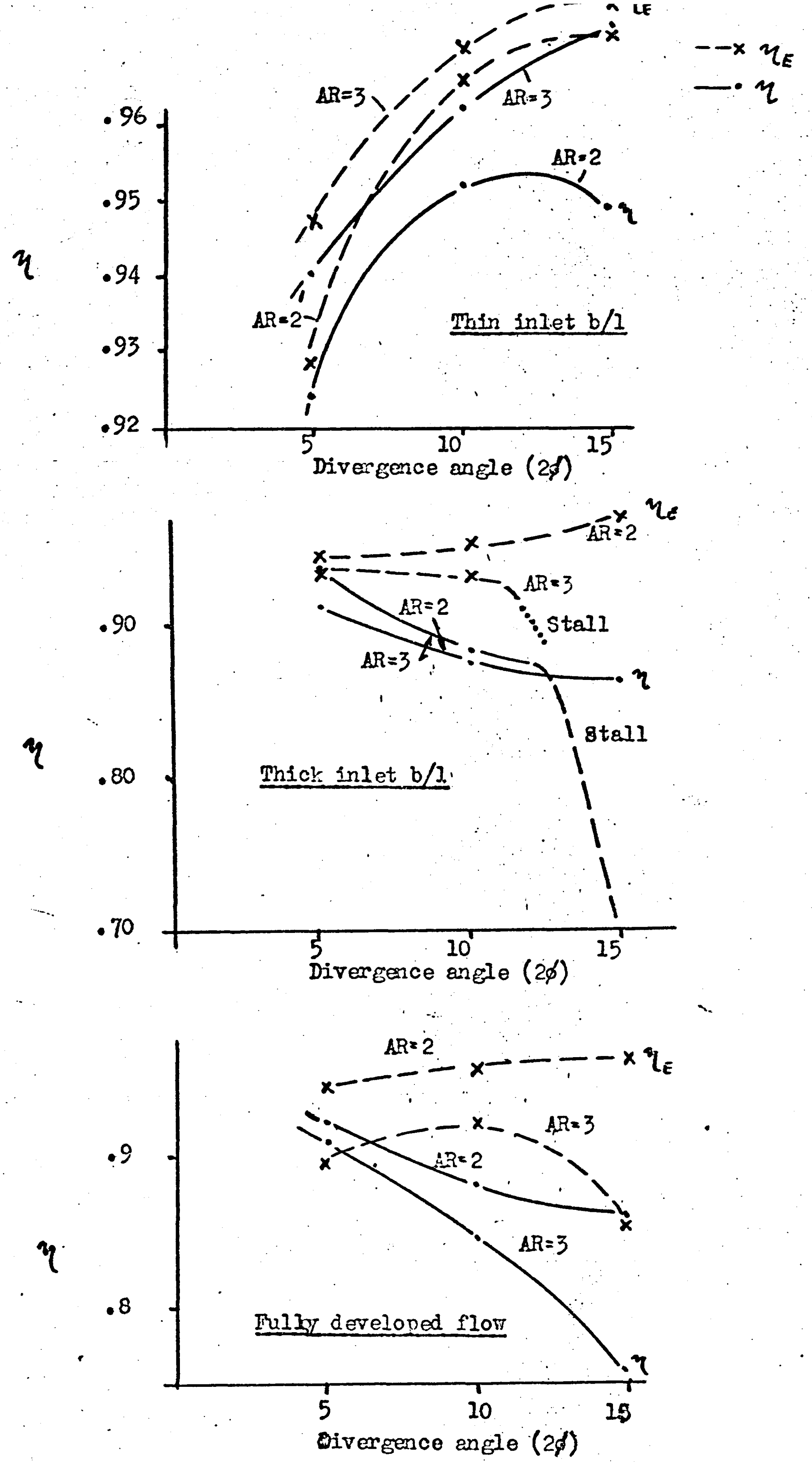

η and η_E /Divergence angle for plenum discharge.

FIGURE 37

the divergence angle for peak effectiveness may be even smaller.

The use of the energy corrected effectivness (η_E) changes this situation entirely and the optimum geometry of the diffuser is changed to 15° divergence angle and area ratio of 2.0. This is important since it can be seen that if a tailpipe is to be included in the system, as in Gibson's work, then some of this energy may be recovered in the tailpipe as a static pressure rise and thus the Cp_L and η_E (tailpipe values) would be likely to increase above the diffuser plenum dishcarge values. The use of the energy corrected effectiveness gives the same optimum geometries for both thin and thick inlet boundary layer thicknesses. The effect of a further increase of the inlet boundary layer thickness to a fully developed flow condition at the inlet can be seen in figure 37, to give optimum values of η and η_E at the same area ratio i.e. 2.0. Also, the divergence angle required for the peak effectiveness (η) is similar to that for a thick inlet boundary layer, that is 5° or less. However for the optimum η_E the divergence angle is again 15°.

These are important design points since the use of optimum plenum discharge effectiveness to design a diffuser/tailpipe system would indicate the use of the wrong divergence angle for the system.

VIII.4 Discussion of Tailpipe Addition.

VIII.4.1 Comparison with Plenum Discharge.

Figure 38 shows that with a thin boundary layer at the inlet ($2\delta^*/w_1$ = .001) there is a reduction in pressure recovery coefficient (Cp) at the diffuser exit plane for the diffuser/tailpipe combination when compared with the plenum discharge case. However, for thick inlet boundary layers and fully developed inlet flows the values of pressure recovery coefficient (Cp) for plenum dis- and for tailpipe discharge at the diffuser exit plane are the same, within experimental error, for all except the 15° divergence angle. This error, however, can be explained. In both these cases the diffusers have stalled, but in the plenum discharge case the flow stalled much earlier within the diffuser than it did in the diffuser/tailpipe configuration. Thus indicating that for non-

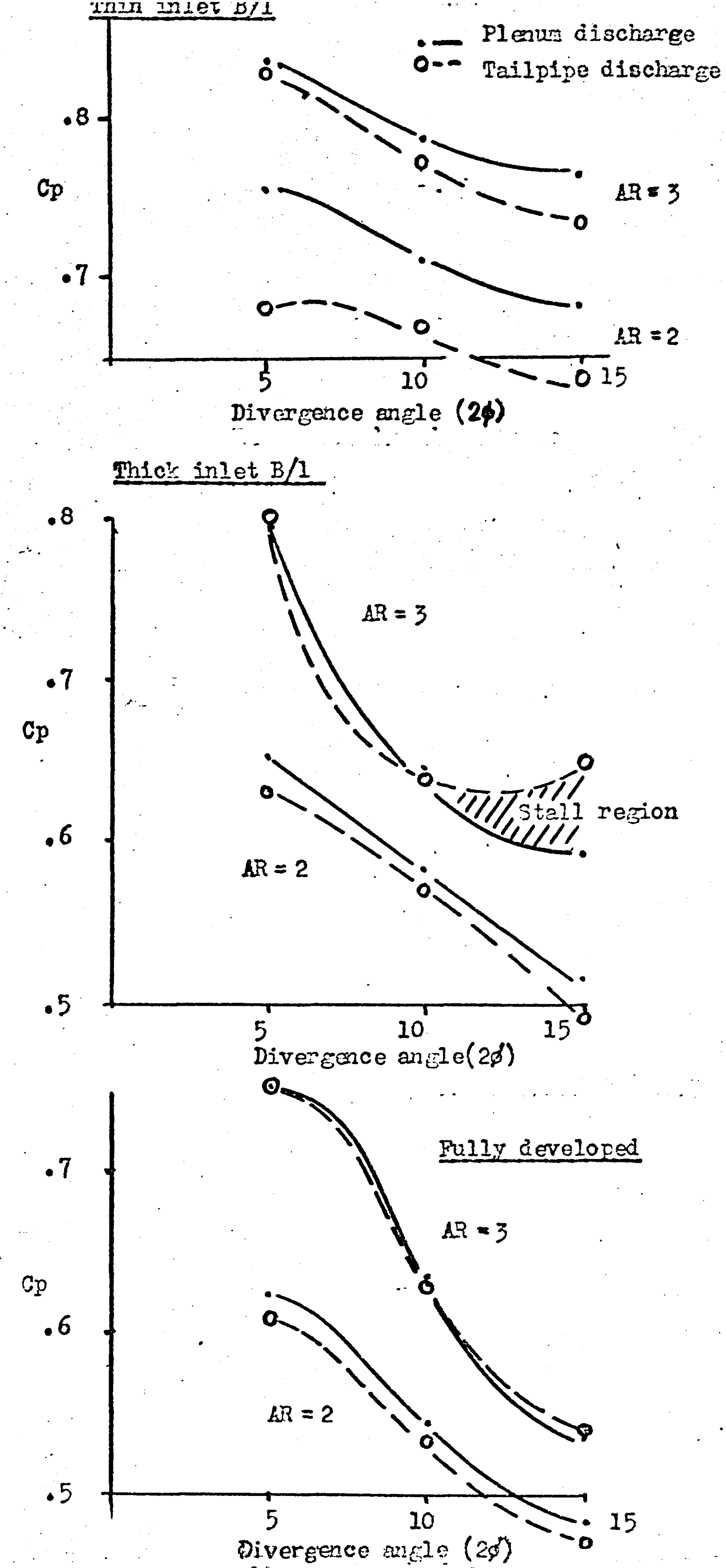

PRESSURE RECOVERY COEFFICIENT AT THE DIFFUSER EXIT PLANE FOR PLENUM AND TAILPIPE DISCHARGE.

FIGURE....38

optimum conditions there is an effect transmitted into the diffuser from the tailpipe addition. Comparison of the figures 34, 35, 39 and 40 show that the shape factor 'H' at the diffuser exit plane for both tailpipe discharge and plenum discharge are the same, within experimental error, and that the boundary layer thicknesses ($2\delta^*/w_1$) at the exit plane have a high degree of similarity for the two discharge cases. This indicates that the tailpipe has an almost negligible effect on the flow within the diffuser (except at the limit of the flow stability i.e. separation or stall). However figure 38 would seem to contradict this statement for the case of a thin inlet boundary layer. Indicated by a fall in pressure recovery within the diffusing section when a tailpipe is fitted.

Results taken just inside the diffuser (that is, at a position 25mm upstream of the diffuser exit plane) with a thin inlet boundary layer (shown in figure 41) show that for an area ratio of 3 there is a very good agreement between the plenum and tailpipe discharge values of pressure recovery coefficient(Cp) within 1% and for an area ratio of 2.0 the agreement is within 2% except for the 5° divergence angle diffuser. This shows that the tailpipe has a negligable effect on the flow within the diffuser even for a thin inlet boundary layer at the inlet to the diffuser. It is only with a thin inlet boundary layer and low area ratios that there is any appreciable pressure recovery 'on' or shortly after the diffuser exit plane for a plenum discharge (shown in figure 42). This indicates that the sudden expansion occuring at the exit plane diffuses upstream affecting the flow within the diffuser slightly, therefore the inclusion of a tailpipe will degrade the performance for this condition.

For tailpipe discharge, figure 43 shows that within the tailpipe there is a considerable pressure recovery for all boundary layer thicknesses at the inlet, and all geometries except for the small divergence angles with a low area ratio (AR = 2.0). This is due to the very small distortion of the boundary layer and therefore wall frictional losses in the tailpipe offset any slight increase in pressure recovery. It can also be seen that for

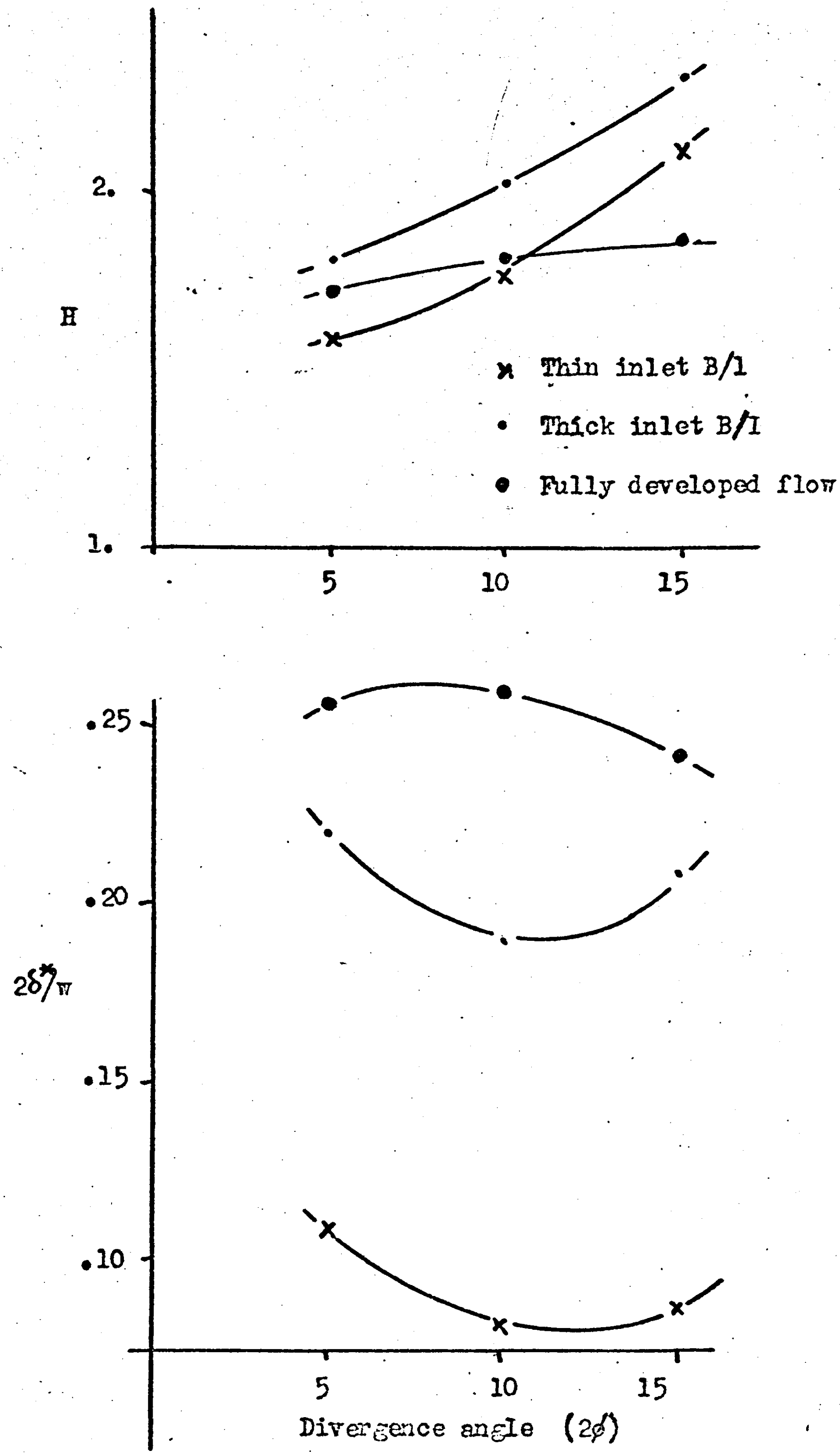

SHAPE FACTOR AND BOUNDARY LAYER THICKNESS AT DIFFUSER EXIT TO TAILPIPE (AREA RATIO 2.0)

FIGURE.....39

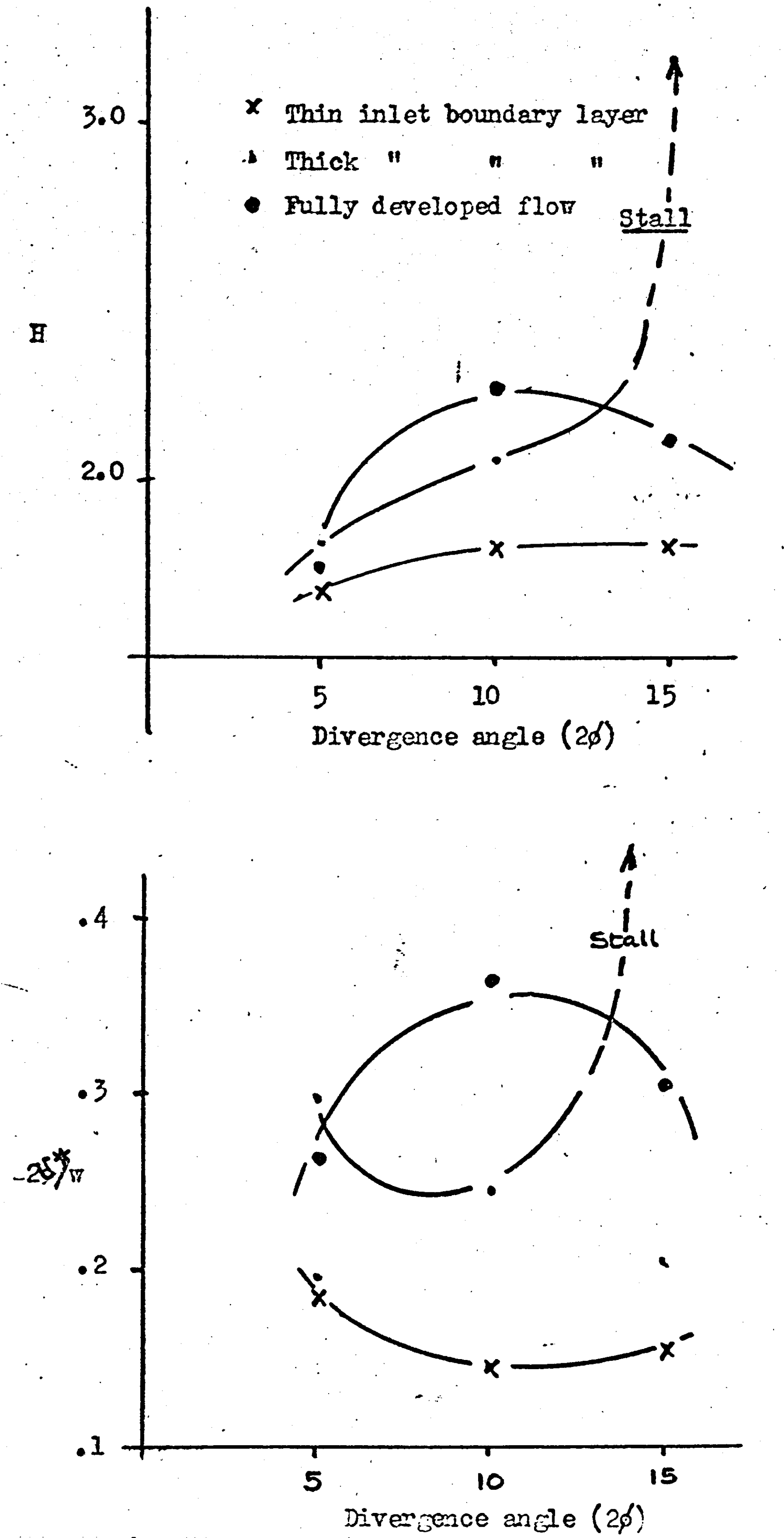

SHAPE FACTOR AND BOUNDARY LAYER THICKNESS AT DIFFUSER EXIT INTO TAILPIPE (AREA RATIO 3.0)

FIGURE....40

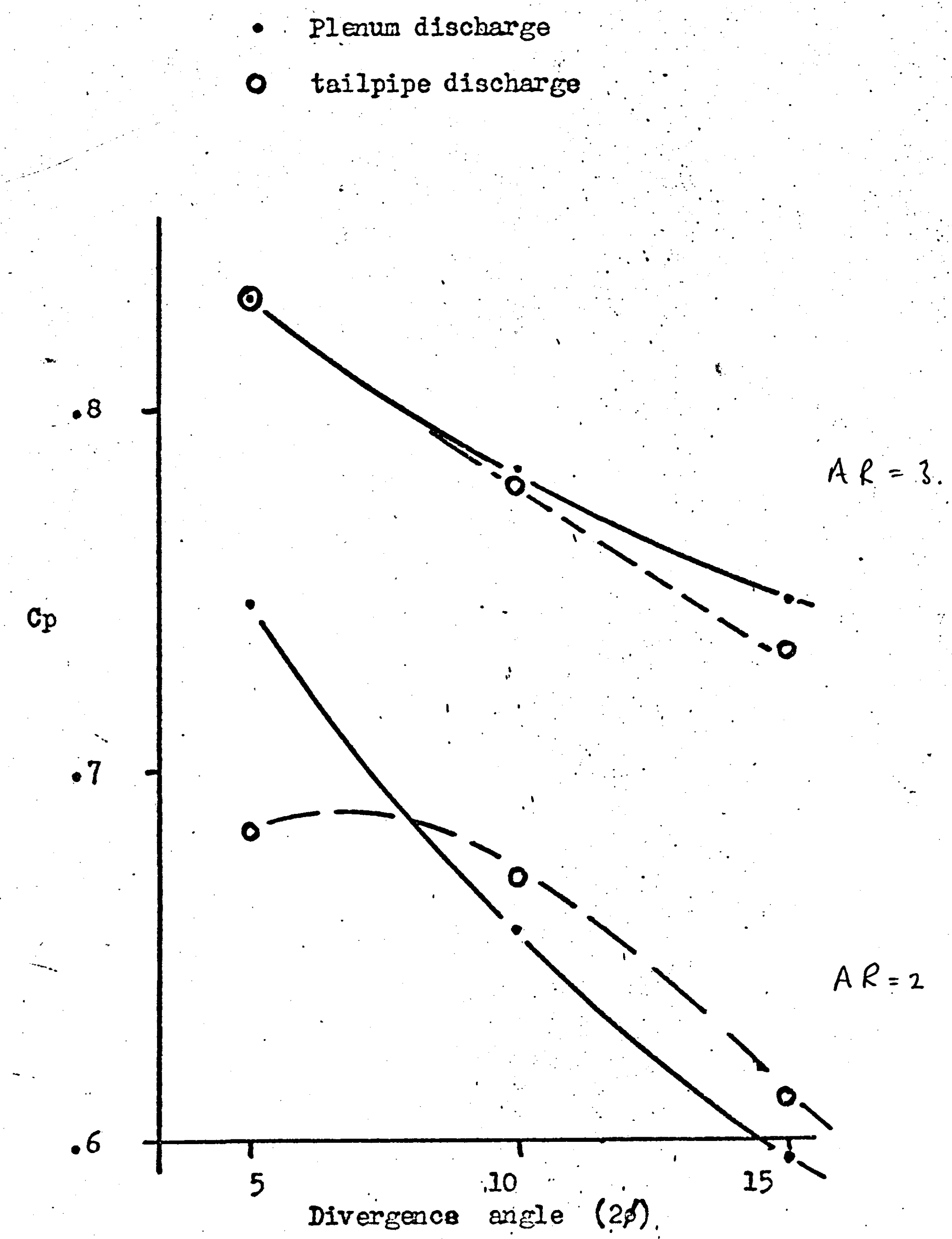

RESULTS TAKEN AT A POSITION 25mm UPSTREAM OF THE DIFFUSER EXIT PLANE...(FOR BOTH PLENUM AND TAILPIPE DISCHARGE.)..WITH A THIN INLET BOUNDARY LAYER.

FIGURE....41

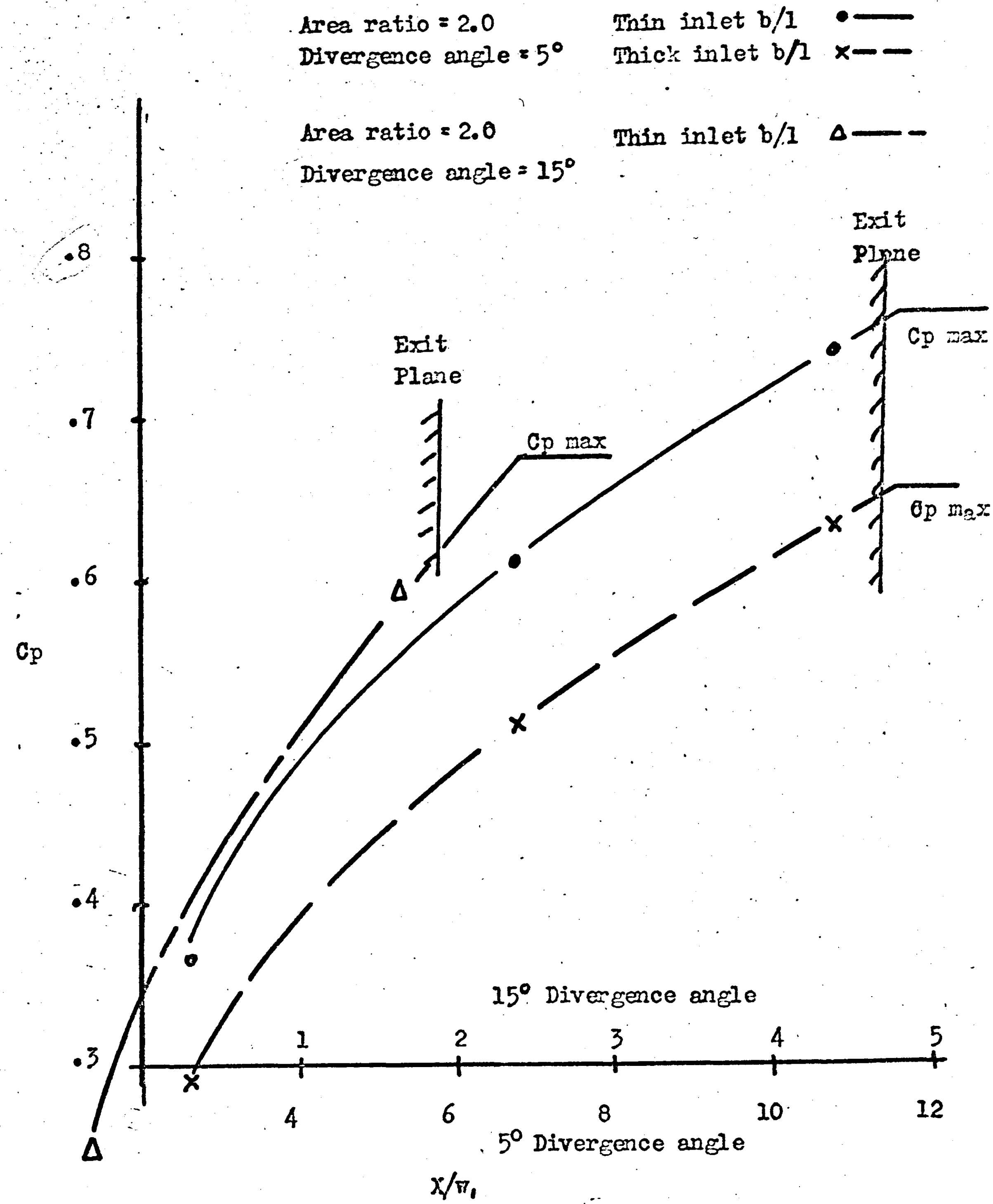

PRESURE RECOVERY AFTER DIFFUSER EXIT PLANE FOR PLENUM DISCHARGE WITH LOW AREA RATIO.

FIGURE....42

the thick and fully developed flows an improvement in the pressure recovery coefficient (Cp) is of the order of 5% for a 5^{o} divergence angle diffuser, 8% for a 10^{o} diffuser and 10% for a 15^{o} diffuser. This could, however, increase up to 20% for a 15^{o} divergence angle diffuser with an area ratio of 3.0 and a fully developed flow at the inlet.

VIII.4.2 Pressure Recovery Coefficient (Cp).

It has been shown that only in the case of a thin inlet boundary layer flowing into a small area ratio (AR = 2.0) and a small divergence angle ($2\phi = 5^{o}$) diffuser is there no increase in the pressure recovery coefficient by including a tailpipe. This is due to the very low distortion of the velocity profile within the diffuser, shown by the low shape factor (H = 1.6) coupled with the thin boundary layer at the diffuser exit ($2\delta^{*}/w_2 = .11$). However for all the other configurations tested there is an increase in the pressure recovery coefficient (Cp) by using a tailpipe. The increase in Cp_L (Cp_L = tailpipe recovery) to the plenum discharge figure can be seen to be very marked for thick and fully developed inlet boundary layers, especially with high area ratios and with divergence angles above 10^{o}; for example figure 44 shows that there is a 30% increase for a 15^{o} divergence angle diffuser, with an area ratio of 3.0 and a thick inlet boundary layer. This reduces to a 15% increase for a 10^{o} divergence angle diffuser and an area ratio of 3.0 with a thick or fully developed flow at the inlet.

VIII.4.3 Position of the Maximum Recovery.

As the boundary layer at the inlet thickens then the position of the maximum pressure recovery in the tailpipe moves downstream (this is shown in figure 45). Also as the distortion of the boundary layer within the diffuser increases then the position of the peak recovery also moves downstream. This is as expected since as the distortion increases the deficiency of momentum within the boundary layer increases therefore it will take longer for the transfer of momentum into the boundary layer from the core flow to occur.

Another factor affecting the transfer of momentum from the core flow to the boundary layer is the thickness of the boundary layer at the inlet to the

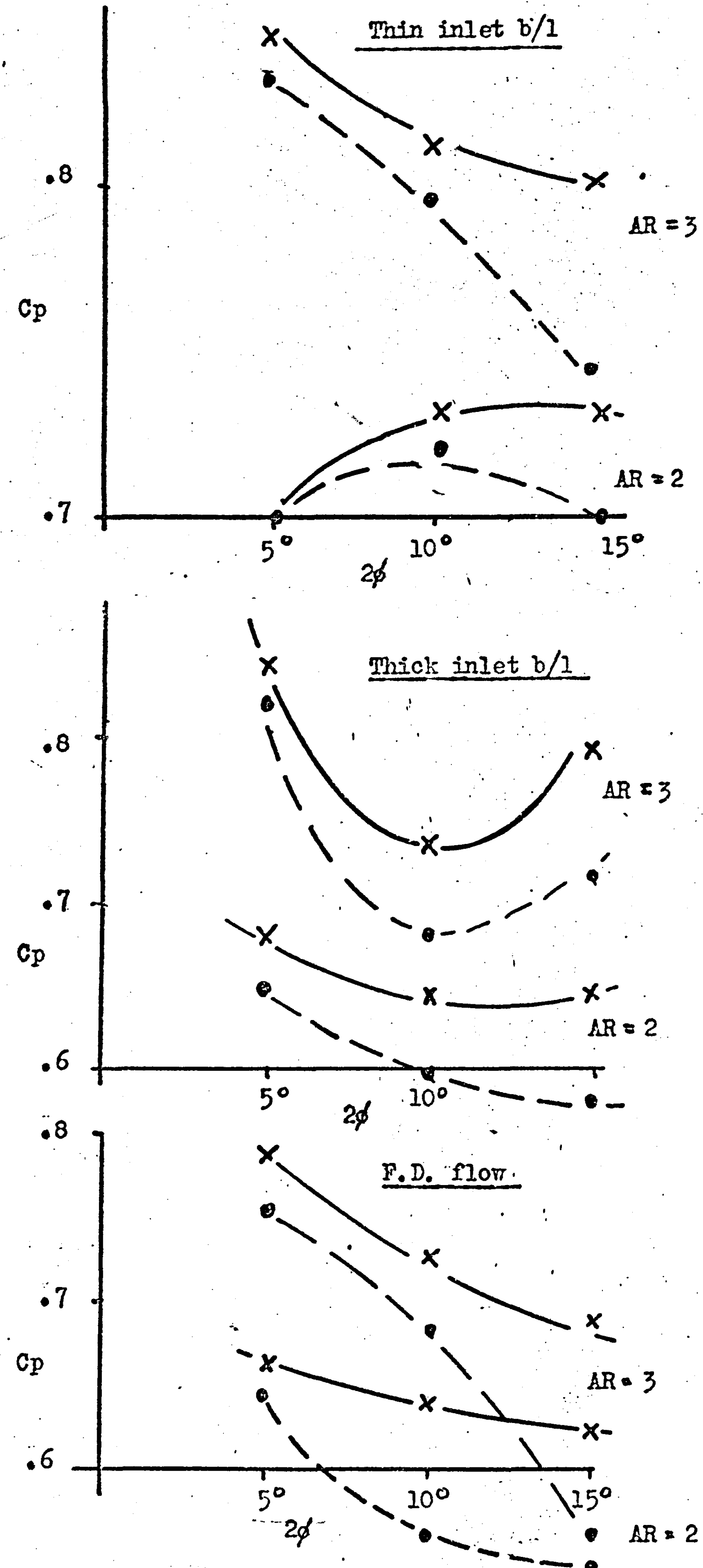

Cp MAXIMUM IN THE TAILPIPE AND Cp AT THE DIFFUSER EXIT PLANE FOR TAILPIPE DISCHARGE.

FIGURE.....43

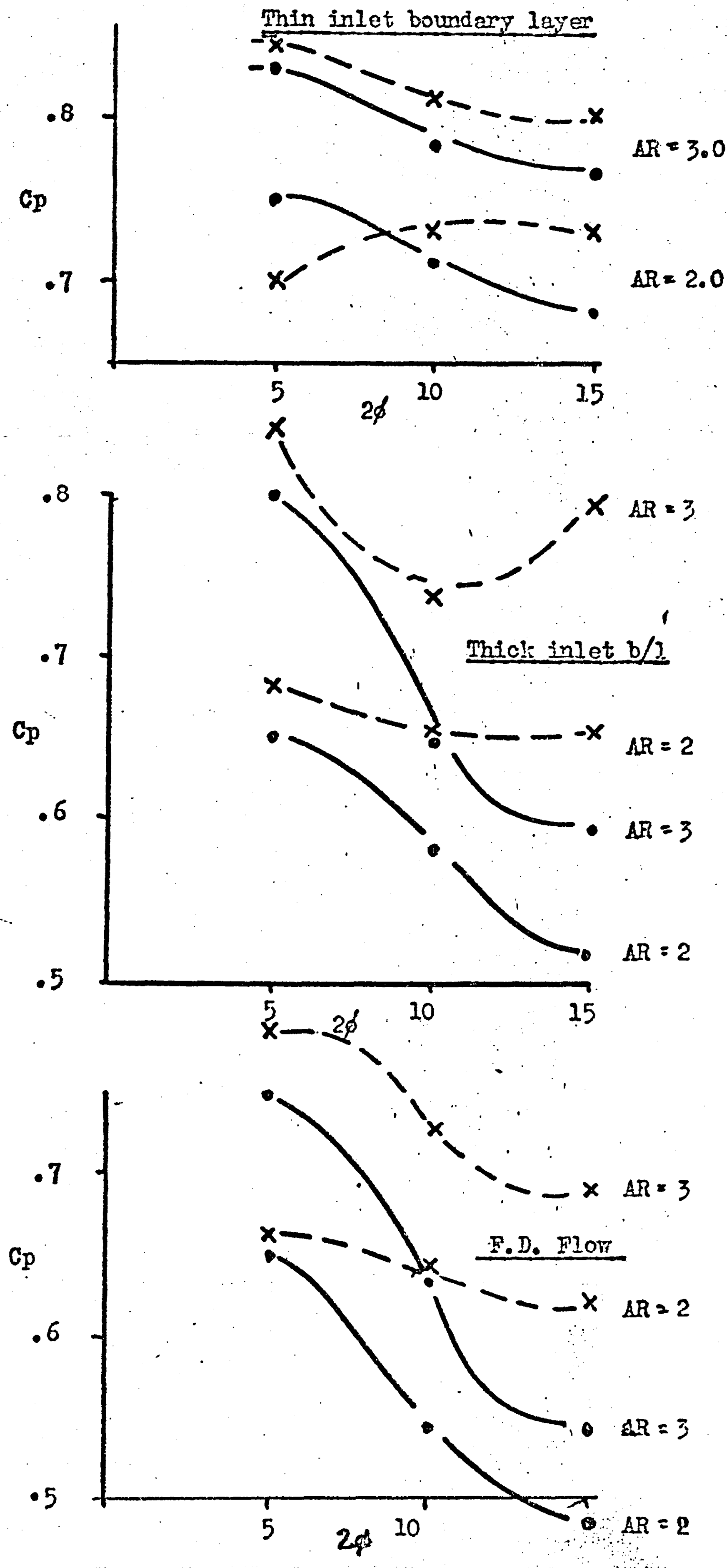

Maximum Cp for plenum and tailpipe discharge.

FIGURE.......44

tailpipe, therefore as the inlet boundary layer thickens for a given geometry diffuser then the position of Cp_L maximum moves downstream. With a low divergence angle diffuser ($2\phi = 5^{\circ}$), a low area ratio (2.0) and a thin inlet boundary layer the position of themaxiumum recovery in the tailpipe moves so far upstream that it coincides with the diffuser exit plane. Therefore, with a smaller area ratio the 10° and 15° divergence angle diffuser peak recoveries will move upstream until at some small area ratio they will be coincident with the diffusing section exit plane. At this condition there is obviously no advantage in having a tailpipe; in fact a slight improvement will probably be attained by using a plenum discharge. An interesting point worth noting is the effect of terminating the tailpipe at the position of maximum recovery. This was done for a 10° divergence angle diffuser of an area ratio 2.0 with a thick inlet boundary layer. The values of Cp_L maximum for the whole tailpipe and the 'truncated' tailpipe are 0.645, and 0.644 respectively which indicates that terminating the tailpipe at the peak recovery position has no measurable effect upon the pressure recovery of the diffuser/tailpipe configuration. This is as expected since the results have shown that the tailpipe has little or no effect on the conditions within the diffuser, except at the limit of flow stability, therefore it would seem reasonable to expect a further length of parallel duct downstream of the termination point to have little effect on the conditions at the point of termination.

VIII.4.4 Optimum Pressure Recovery.

It has been shown by the results that the maximum pressure recovery occurs for a particular divergence angle and boundary layer thickness when the area ratio is such that the flow at the diffuser exit plane is distorted to the limit of flow stability within the diffuser, (onset of separation). This flow condition will exist at the geometry for optimum pressure recovery for both plenum and tailpipe discharge. The results shown in figure 44 indicate that the optimum geometries for both discharge conditions are coincident. However figure 44 may not be sufficiently comprehensive to give a true indication of the diffuser/tailpipe optimum geometry.

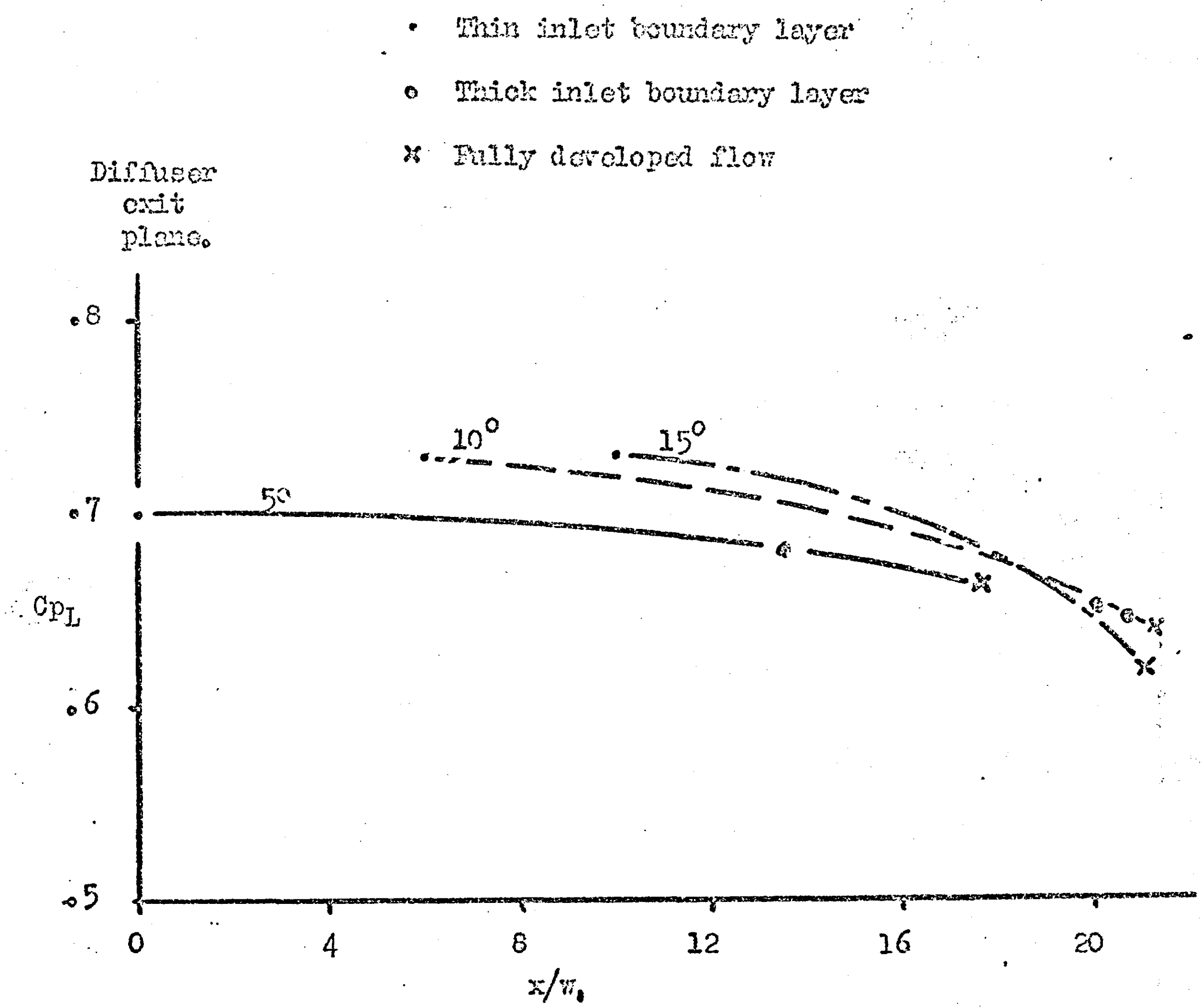

POSITION OF Cp_L MAX. IN THE TAILPIPE FOR AREA RATIO 2.0
(DOWNSTREAM OF DIFFUSER EXIT PLANE)

FIGURE....45

A....Profile at diffuser exit plane

B....Profile in tailpipe

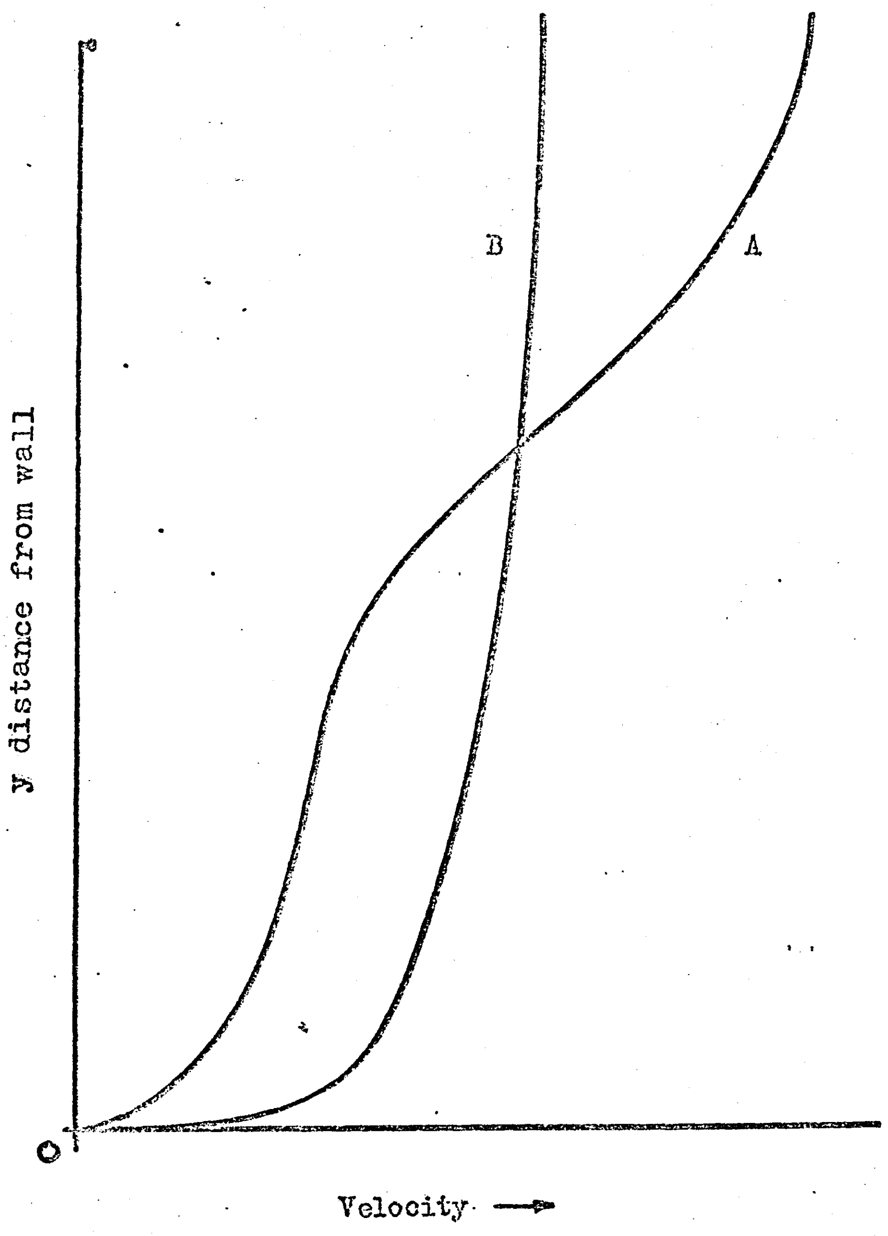

Typical velocity profiles at diffuser exit and in tailpipe.

FIGURE....46

It has been shown previously that the inclusion of a tailpipe has the effect of extending the limit of flow stability to higher divergence angles than would be expected with plenum discharge. Therefore the optimum divergence angle for a diffuser/tailpipe combination will be higher than that for the optimum pressure recovery for plenum discharge. The optimum geometry for a system fitted with a tailpipe is likely to be in the region of 10^{o} divergence angle with an area ratio of 4.0 to 5.0. In contrast with 7^{o} for plenum discharge with an area ratio of approximately 4.0; Both these geometries are for thin inlet boundary layer conditions. This area ratio for the optimum pressure recovery will reduce as the inlet boundary layer thickens, there may also be a slight reduction in the diveregence angle required.

VIII.4.5 Effectiveness. (η_L)

It has been mentioned several times during this chapter that the addition of a tailpipe does not affect the performance of the diffusing section significantly, therefore the effectiveness (η) at the diffuser exit plane will be lower than the energy corrected effectiveness (η_E) due to the distortion of the boundary layer, this can be seen in the expressions.

$$\eta = Cp/(1 - 1/AR^2) \quad \text{-----------} \quad 1$$

$$\eta_E = Cp/(\alpha_1 - \alpha_2 /AR^2) \quad \text{-------} \quad 2$$

Therefore since α_1 and α_2 are always greater than unity, with high distortion of the velocity profile within the diffuser α_2 will become large and will make the expression ($\alpha_1 - \alpha_2 /AR^2$) less than ($1 - 1/AR^2$) due to this very high value of α_2. Unlike the plenum discharge case there is a reduction in the distortion within tailpipe thus the α_2 value reduces making the expression ($\alpha_1 - \alpha_2 /AR^2$) greater than ($1 - 1/AR^2$). Thus η_E becomes less than the value of effectiveness (η) shown in figures 49g - 491. There is also a general improvement in the effectiveness (η) in the tailpipe due to the improvement in the velocity profile and pressure recovery. This was true for all the configurations tested. The reason for this quite appreciable increase in the pressure recovery coefficient and the effectiveness (η) is solely due

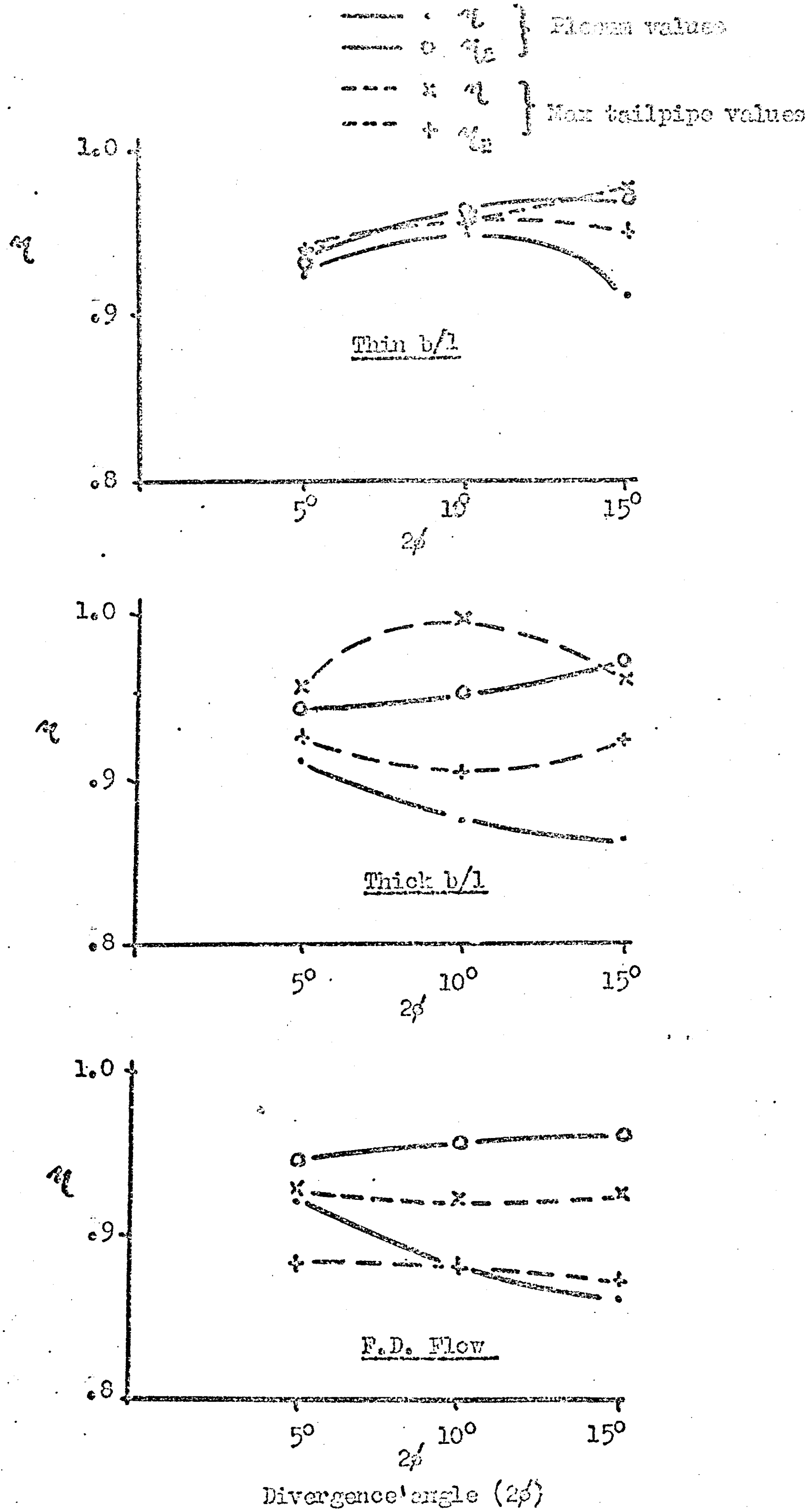

EFFECTIVENESS...TAILPIPE AND PLENUM DISCHARGE AR 2.0

FIGURE....47

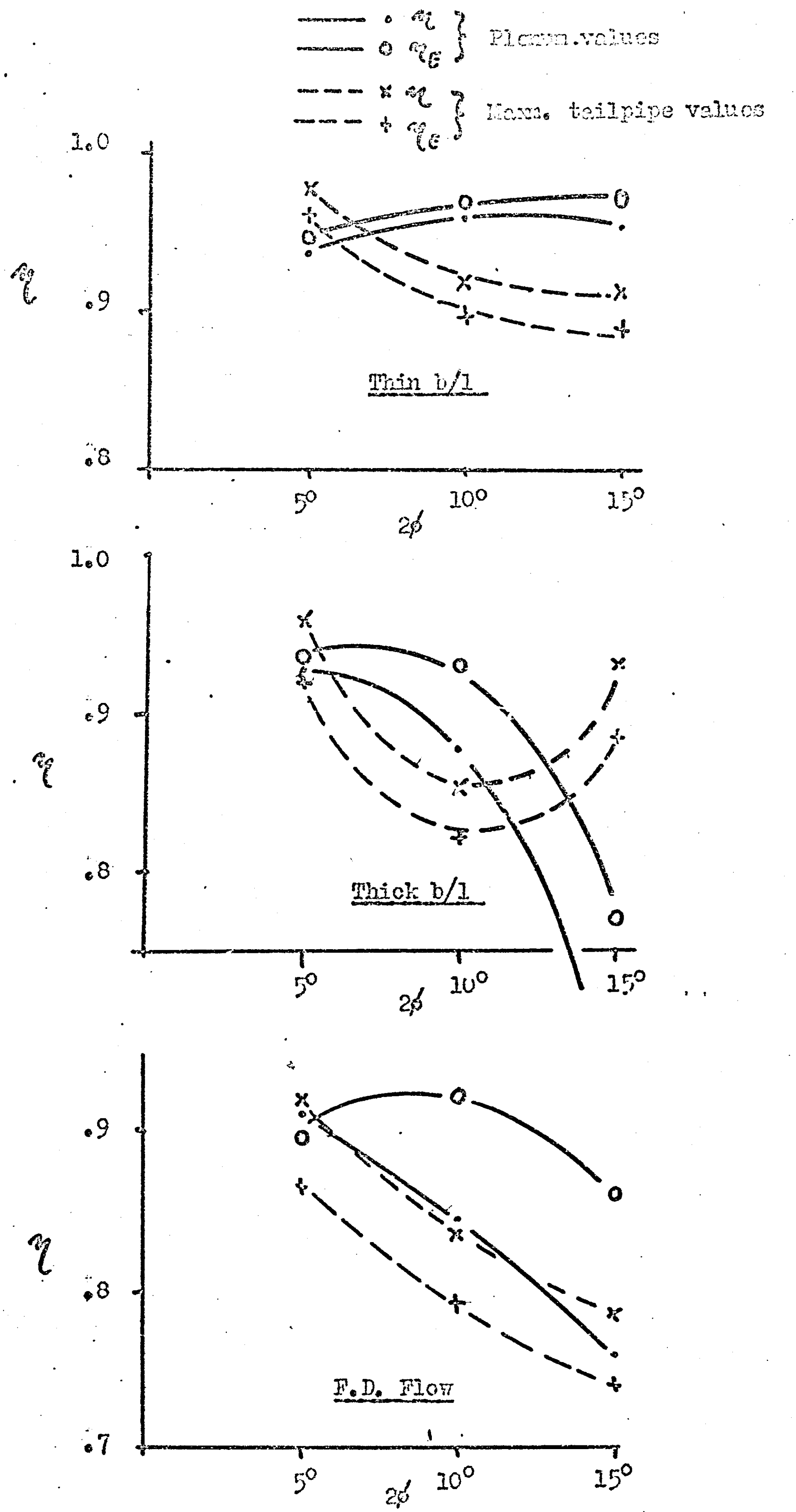

EFFECTIVENESS...TAILPIPE AND PLENUM DISCHARGE AR 3.0

FIGURE....48

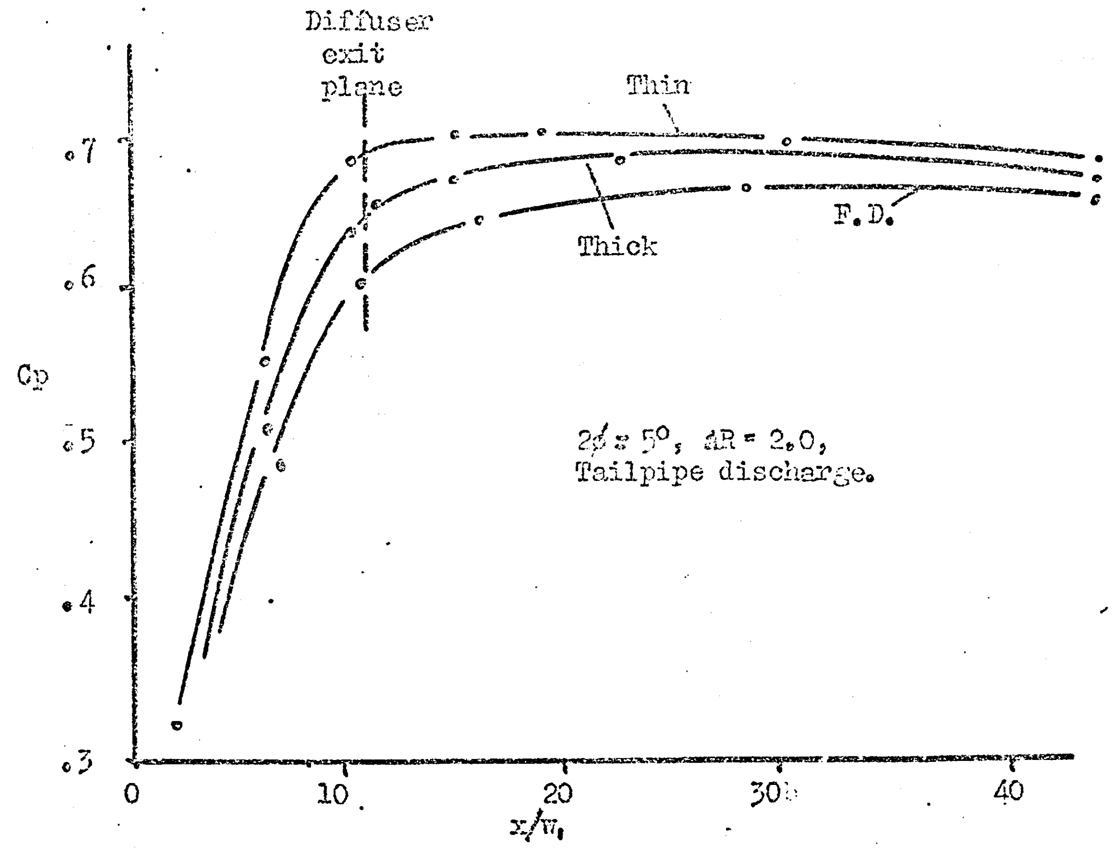

FIGURE ....49(a)

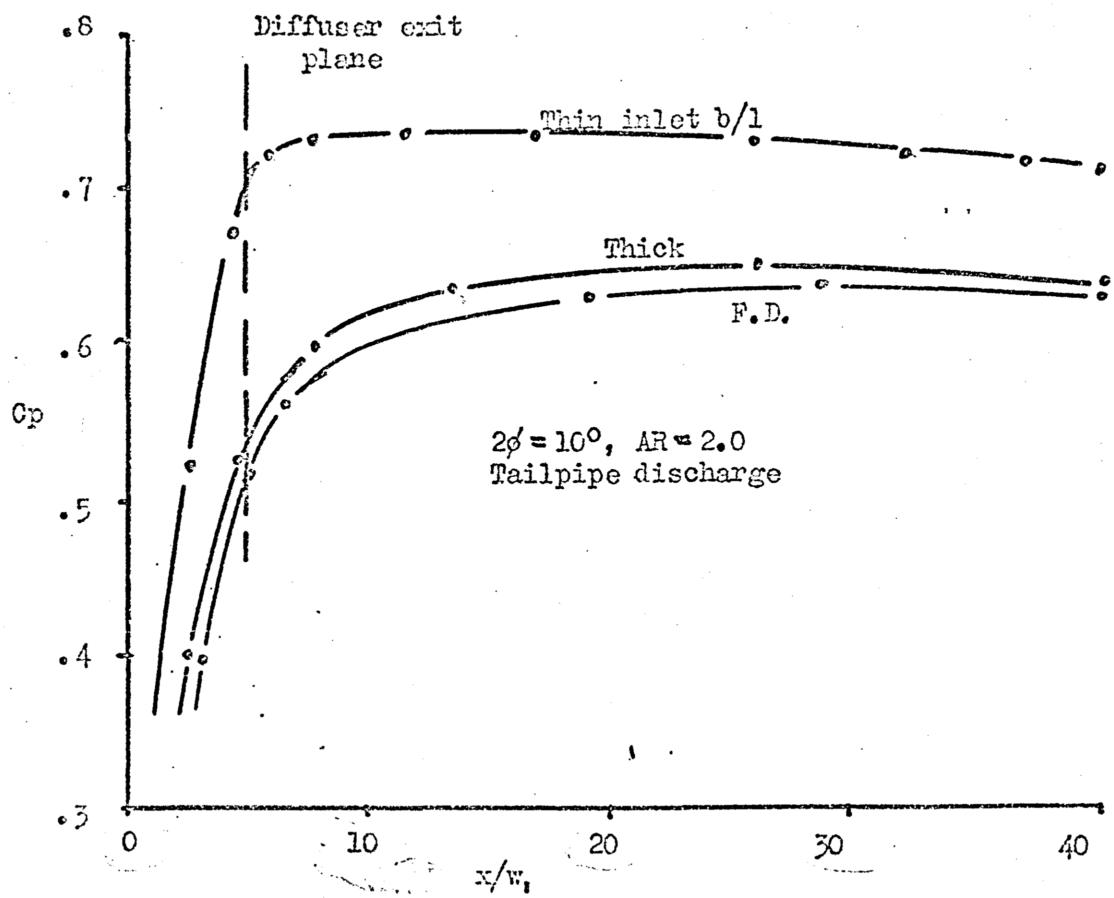

49(a - f) Cp/distance from inlet (x/w_1)

FIGURE....49(b)

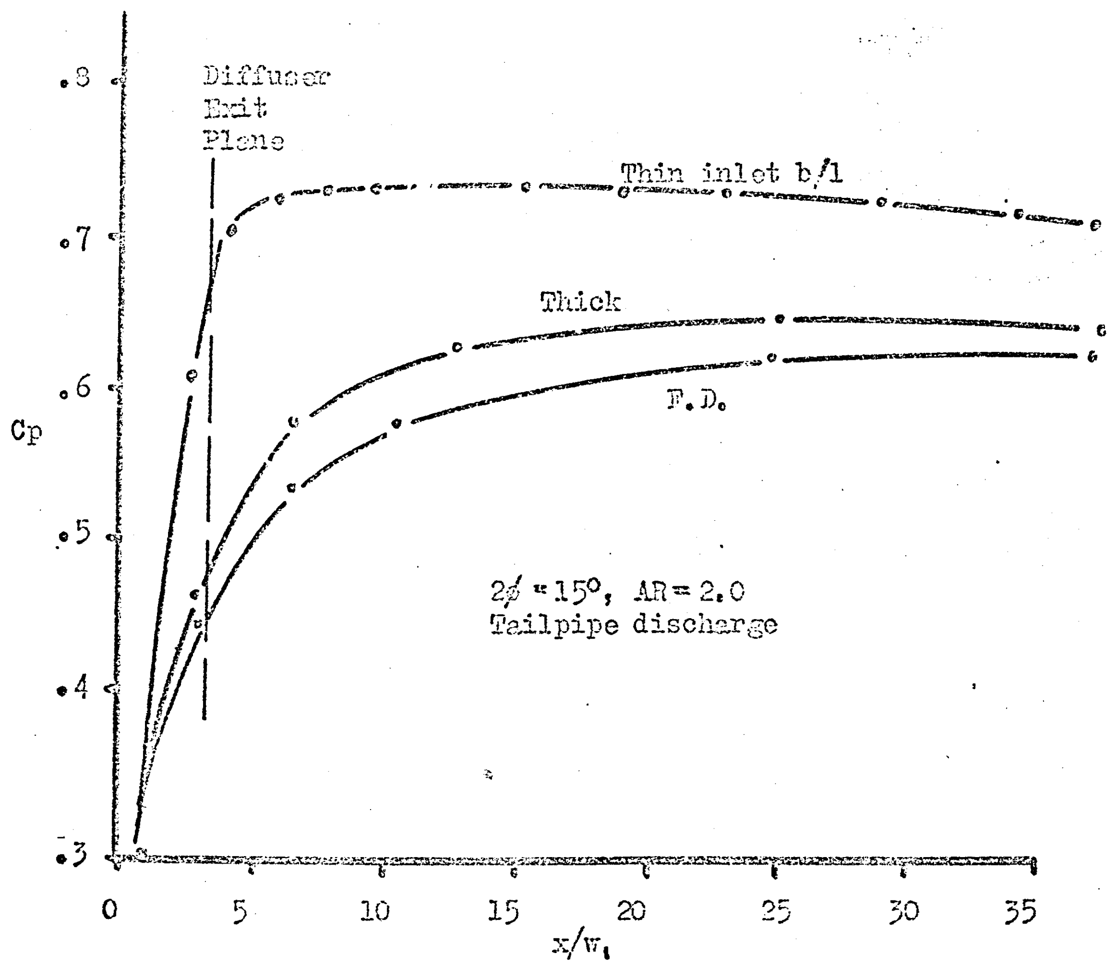
Diffuser
Exit
Plane
Thin inlet b/l
Thick
F.D.
$2\phi = 15^o$, AR = 2.0
Tailpipe discharge
Cp
.8
.7
.6
.5
.4
.3
0
5
10
15
20
25
30
35
x/w_1

FIGURE.....49(c)

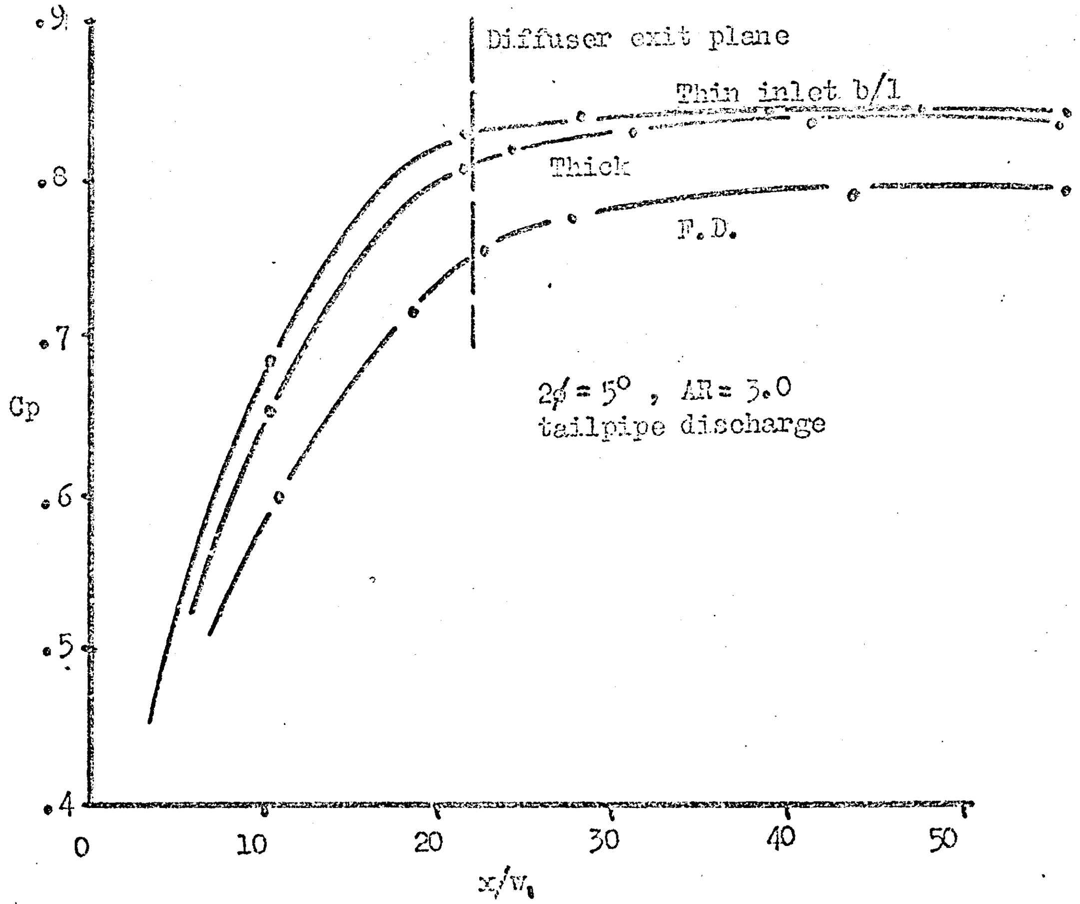

FIGURE..........49(d)

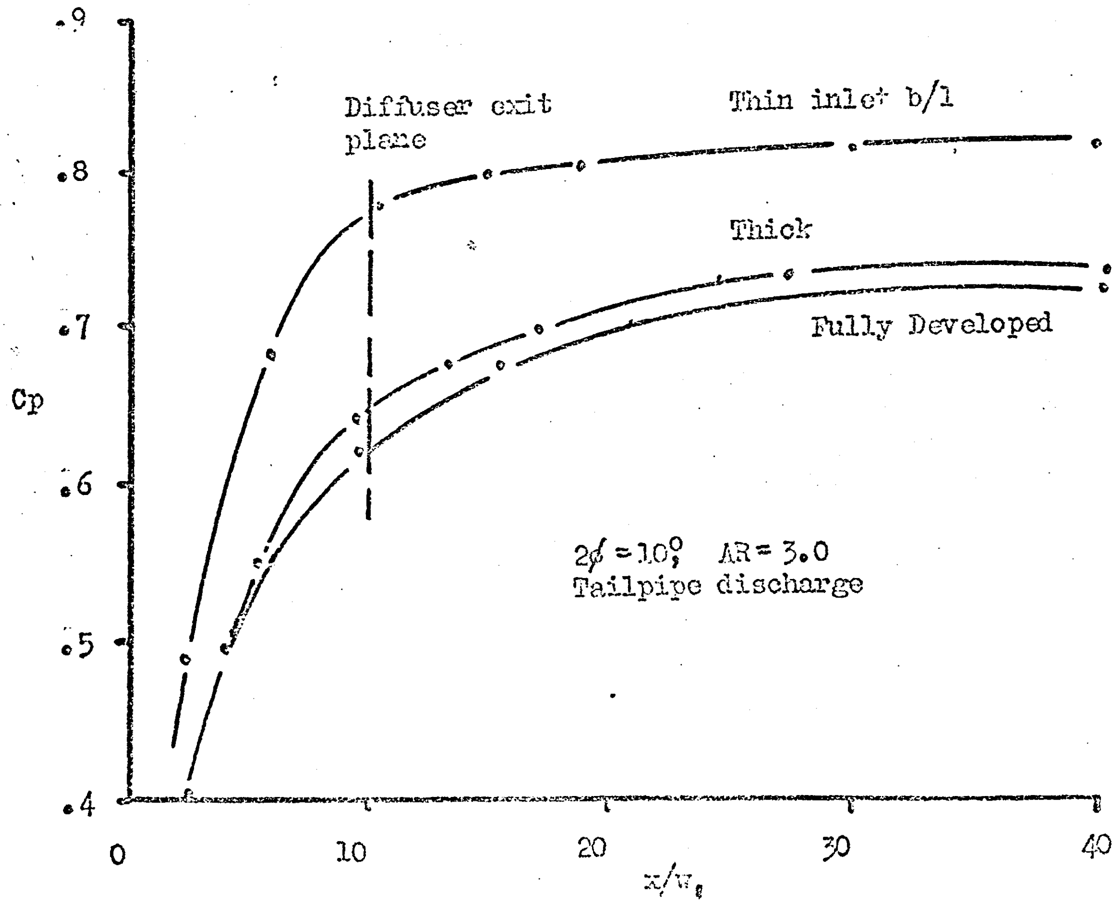

FIGURE....49(e)

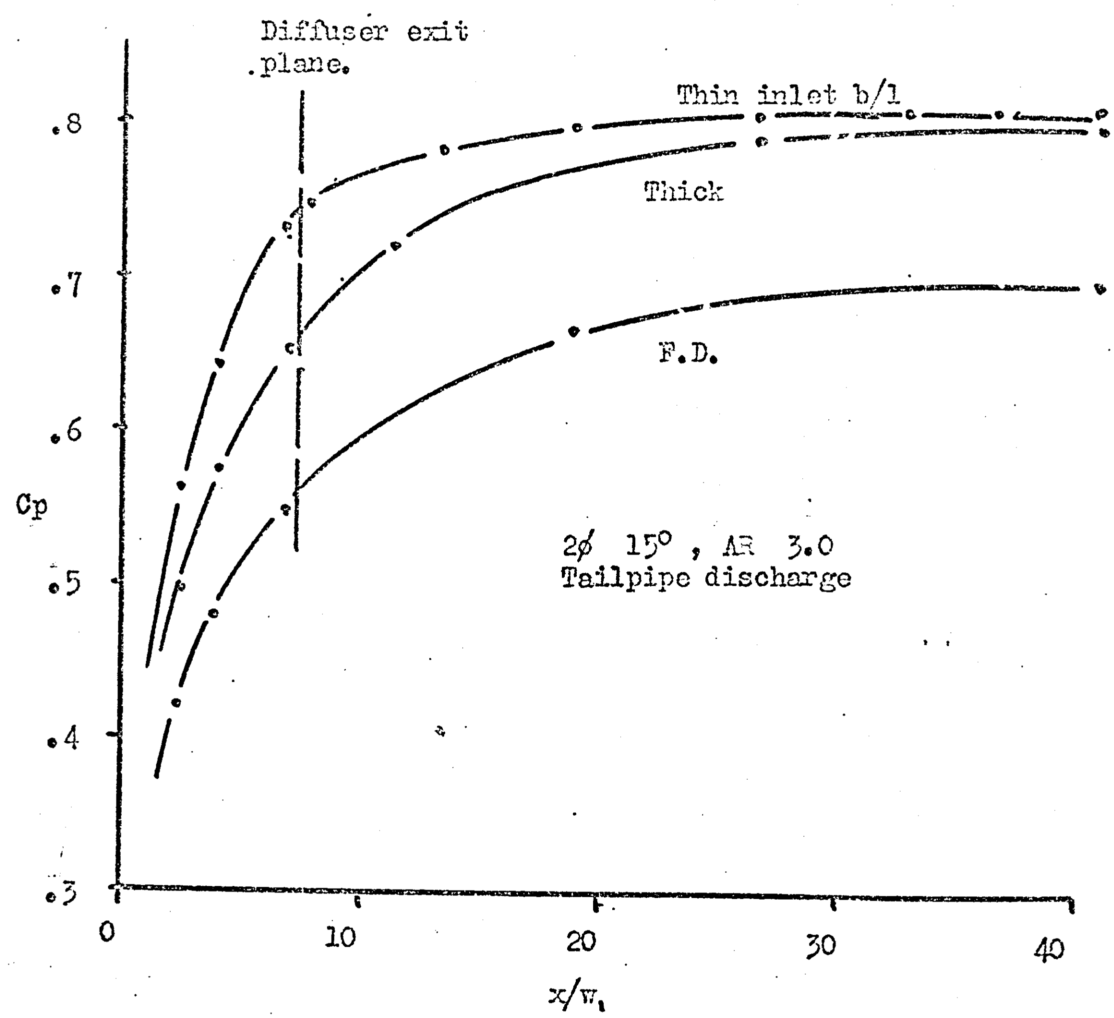

Diffuser exit
plane.
Thin inlet b/l
Thick
F.D.
2φ 15° , AR 3.0
Tailpipe discharge
Cp
.8
.7
.6
.5
.4
.3
0
10
20
30
40
x/w₁

FIGURE....49(f)

Divergence angle = 5°, AR = 2.0, Tailpipe discharge

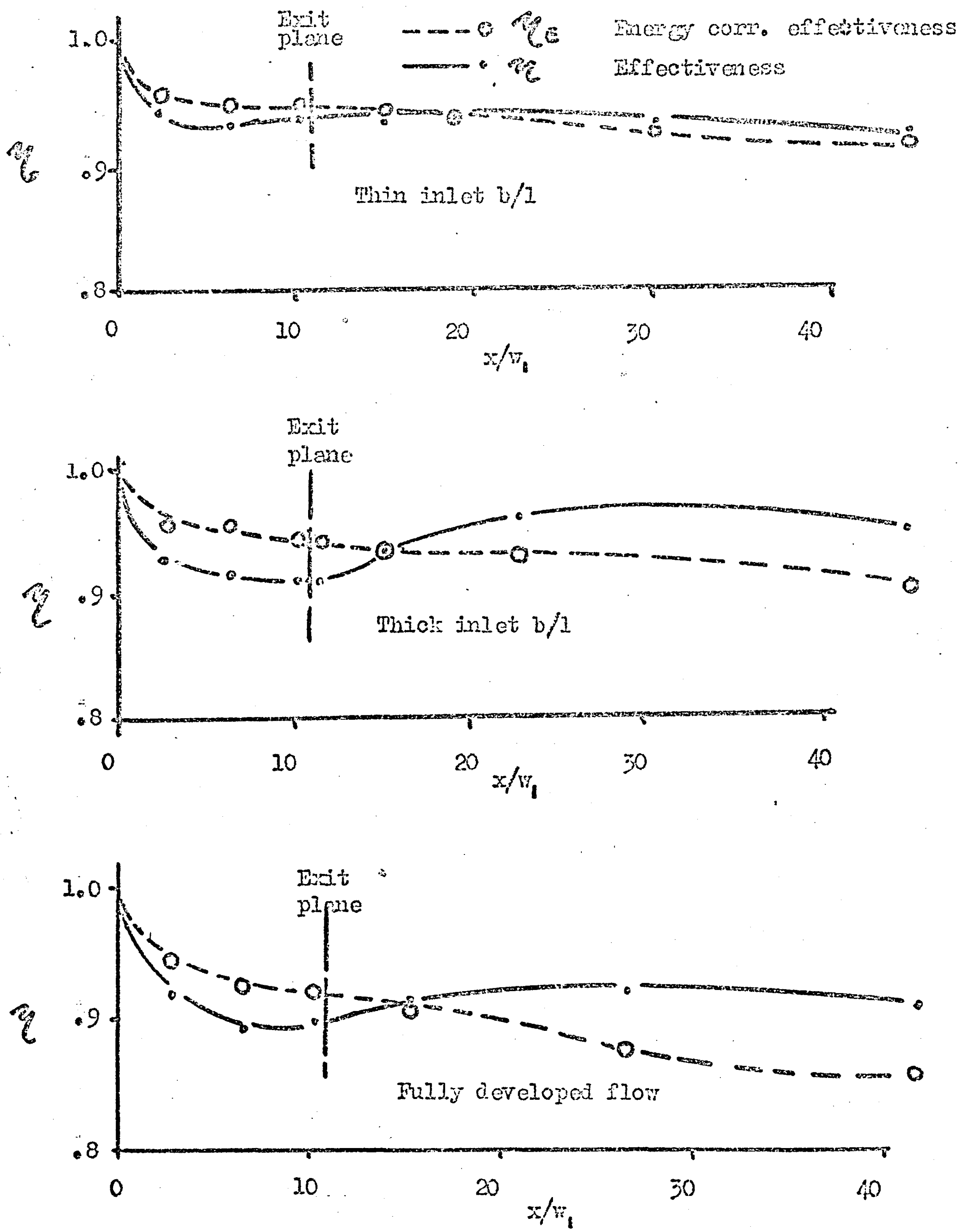

49(g - 1) η and η_E /distance from inlet (x/w_1)

FIGURE......49(g)

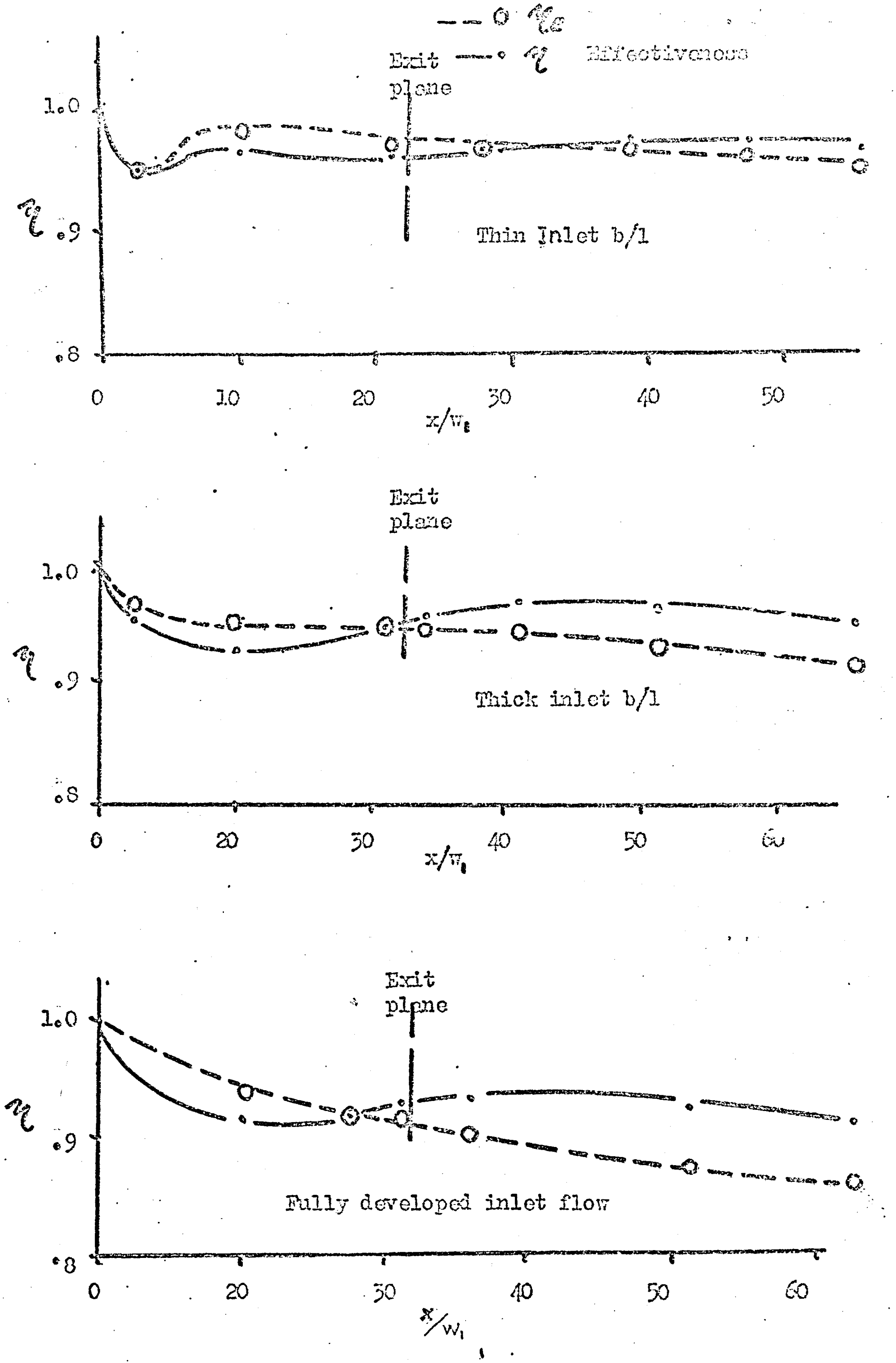

η_c
η Effectiveness
Exit plane
1.0
.9
.8
η
Thin Inlet b/l
0
10
20
30
40
50
x/w_1
Exit plane
1.0
.9
.8
η
Thick inlet b/l
0
20
30
40
50
60
x/w_1
Exit plane
1.0
.9
.8
η
Fully developed inlet flow
0
20
30
40
50
60
x/w_1

FIGURE.....49(h)

Divergence angle = 10°, AR = 2.0, Tailpipe discharge

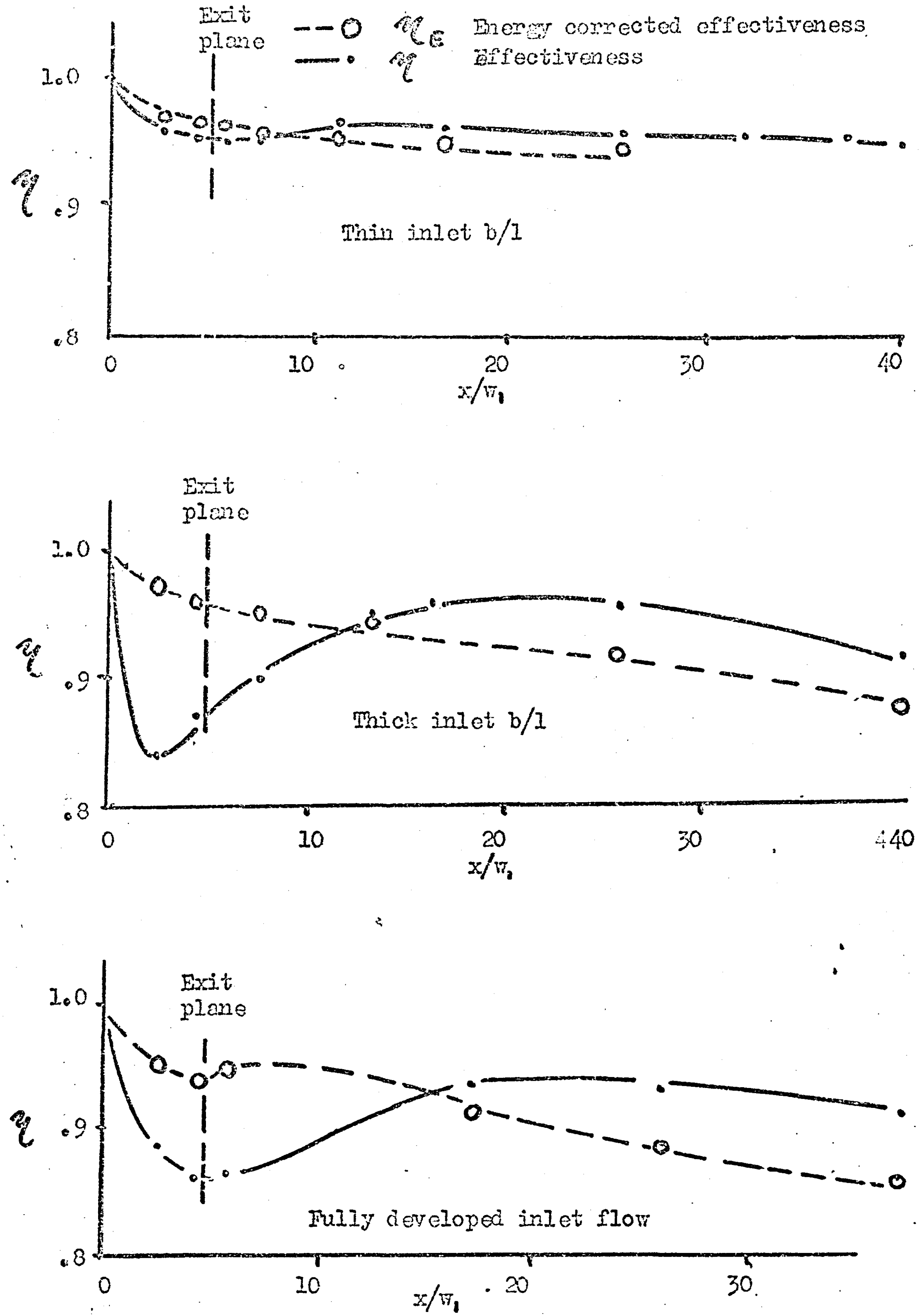

FIGURE......49(i)

Divergence angle = 10°, AR = 3.0, Tailpipe discharge

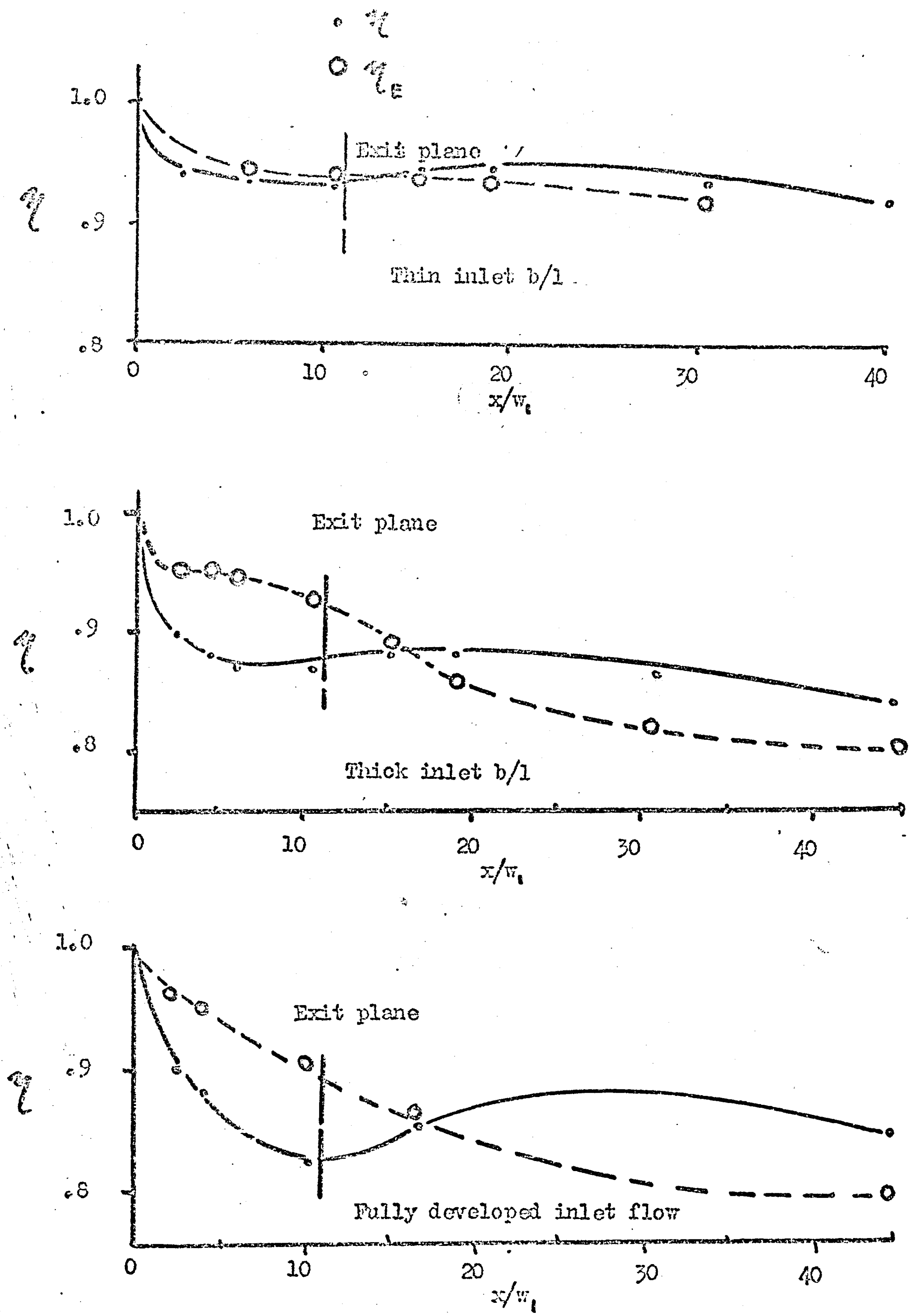

FIGURE.....49(j)

Divergence angle =15°, AR = 2.0, Tailpipe discharge

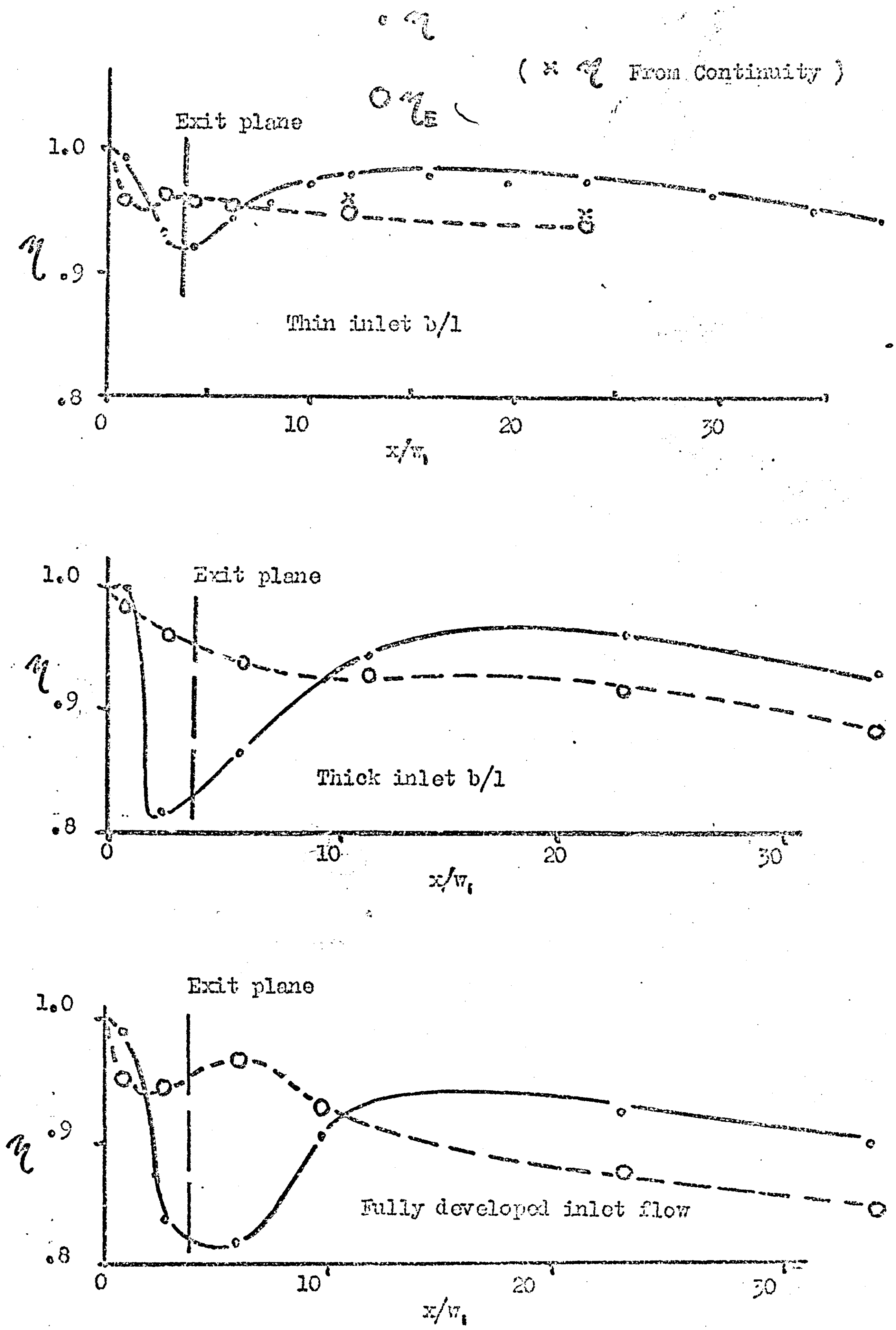

FIGURE.....49(b)

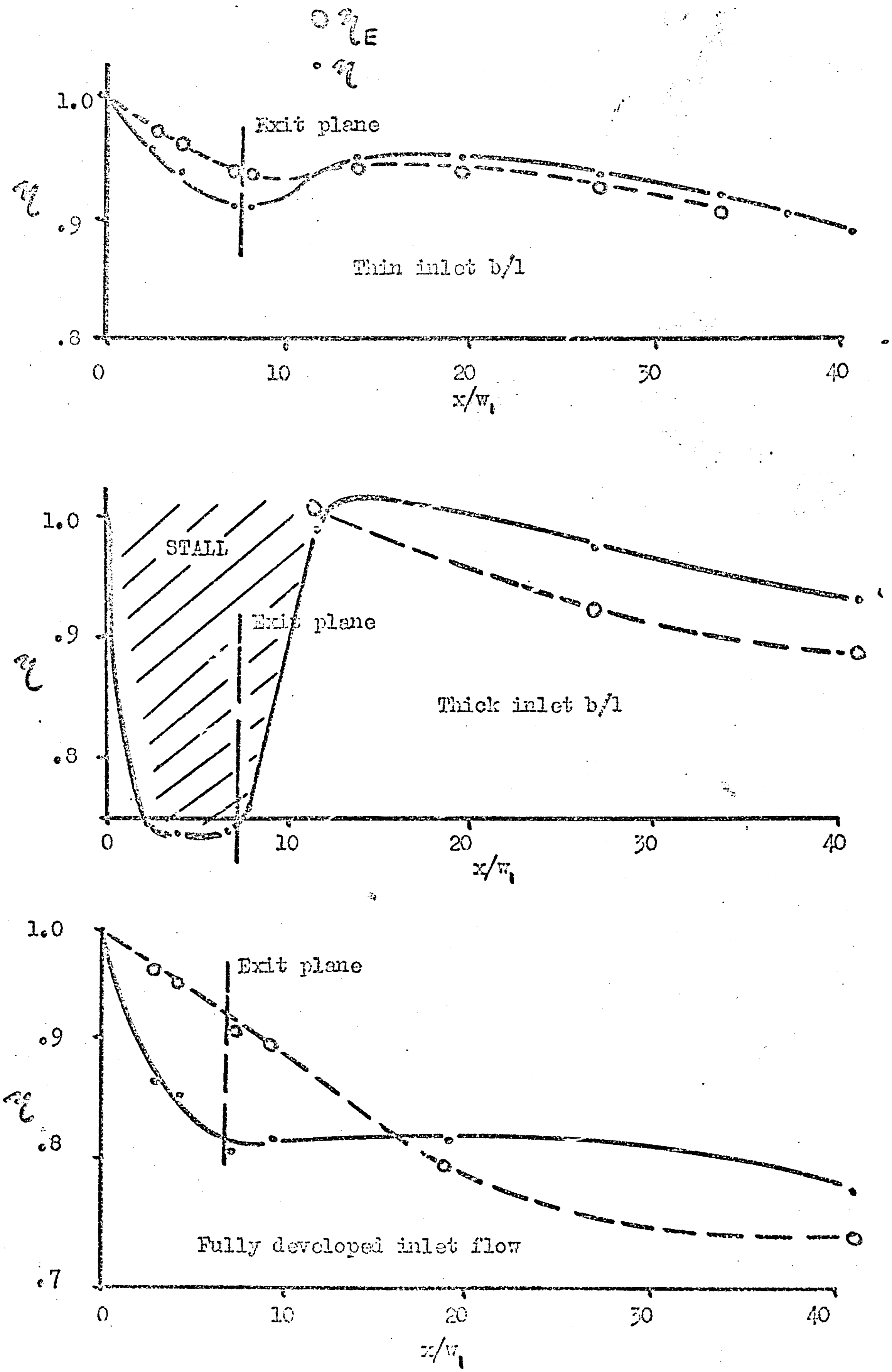

$\circ\ \eta_E$
$\cdot\ \eta$
Exit plane
Thin inlet b/l
STALL
Exit plane
Thick inlet b/l
Exit plane
Fully developed inlet flow
x/w_1
η

FIGURE.....49(1)

to the improvement of the velocity profile (shown in figure 46) caused by the re-energising of the boundary layer in the tailpipe therefore reducing the flow kinetic energy. This can also be seen in figures 51 and 52 by the abrupt fall in both boundary layer thickness ($2\delta^*/w$) and the shape factor (H) on entering the tailpipe. The effect, however, can be seen to be more marked with the greater distortion of the boundary layer within the diffuser, indicating that the maximum pressure recovery will occur when the flow is near to separation at the diffuser exit plane, (as previously mentioned). Also as the boundary layer thickens and as distortion increases then the crossover point of effectiveness (η) and the energy corrected effectiveness (η_E) moves downstream due to the greater momentum transfer required, and for the case of the thicker boundary layers the momentum transfer will be much slower. Another point of interest can be seen when high values of pressure gradient $\partial p / \partial x$ exist as in the 15^o divergence angle diffuser. In this case there is a secondary initial crossover of η and η_E presumably due to the very high initial diffusion without severely distorting the boundary layer, (shown in figure 49k). It can be also seen in figures 49g - 49l that as the boundary layer at the inlet to the diffuser thickens then the energy corrected effectiveness falls more rapidly in the tailpipe due to the increased wall friction for the thick boundary layers and fully developed flows. This effect is shown in figure 50.

VIII.5 Flow Stability in Plenum and Tailpipe Discharge.

The flow 'stability' seems to be very sensitive to the shape factor (H) and boundary layer thickness ($2\delta^*/w$) combination. For a thin inlet boundary layer thickness and a thin local boundary layer thickness ($2\delta^*/w$), the shape factor (H) can reach a value in the region of 3.0 before any separation of the boundary layer occurs. However for thick inlet boundary layer flows and fully developed inlet flows, shape factors in the region of 2.0 to 2.2 appear to be the limit for stable flow (This is shown in figure 53 and table V).

When for a particular configuration having optimum geometry, this point is reached, the boundary layer thickness continues to increase but the shape factor remains constant. This indicates an increase in the rate of growth in the momentum thickness, perhaps due to small amounts of 'transitory' or

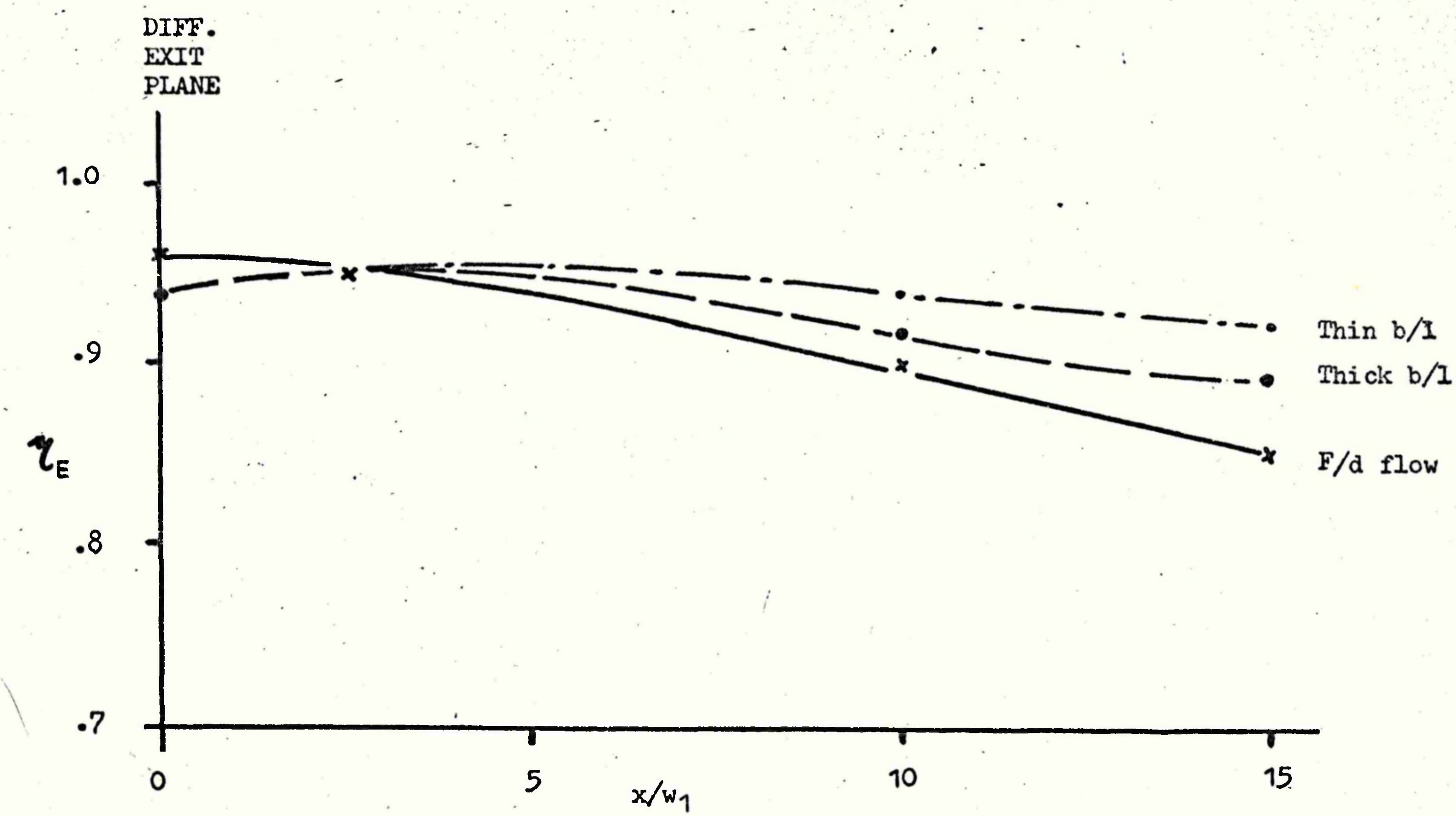

FIGURE.....50

η_E /tailpipe length for different inlet boundary layer thickness.

$2\delta^*/w$ and H/distance from inlet (x/w_1) AR = 2.

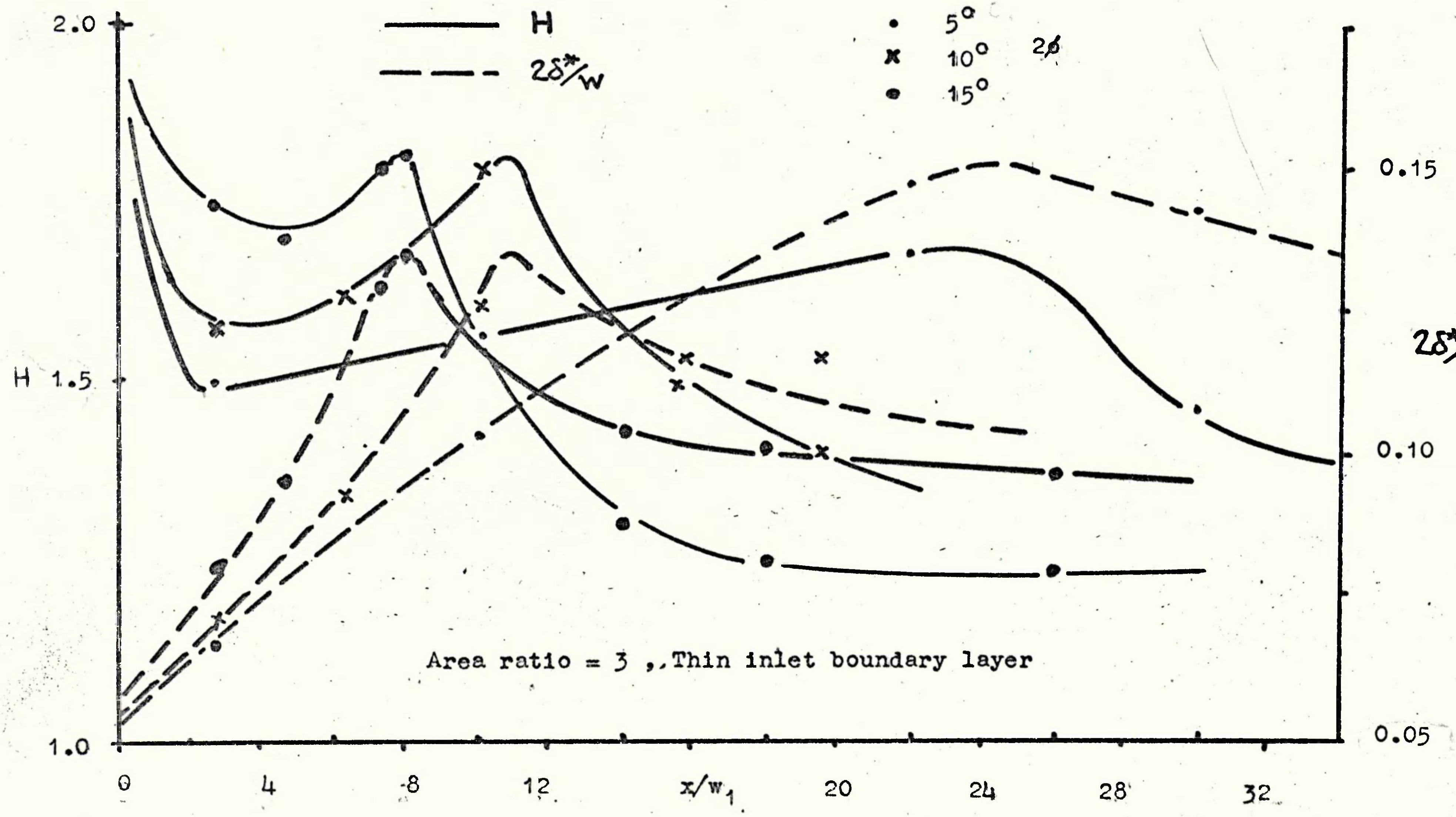

FIGURE.......51

$2\delta^*/w$ and H/distance from inlet (x/w_1) AR = 3.

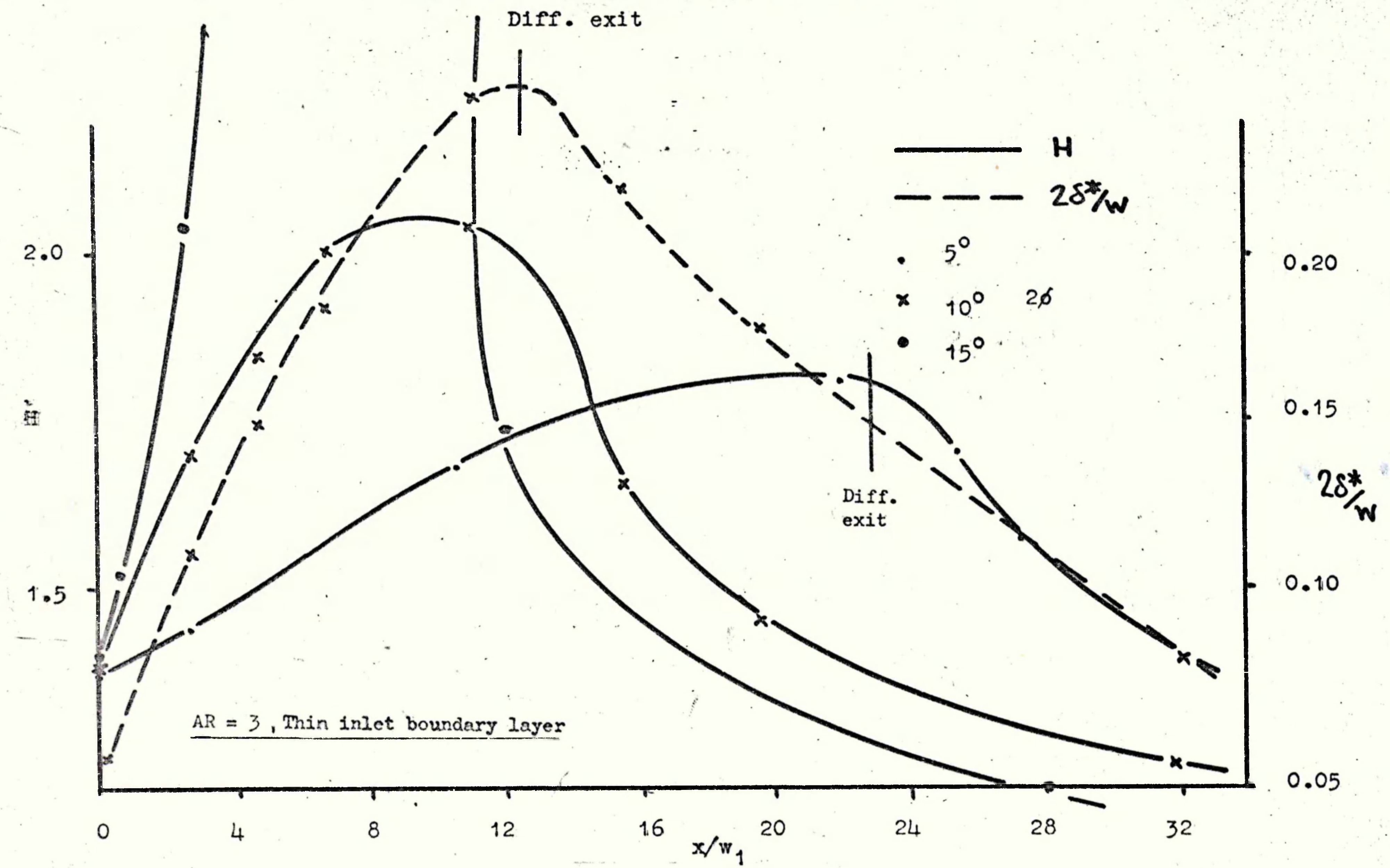

FIGURE.......52

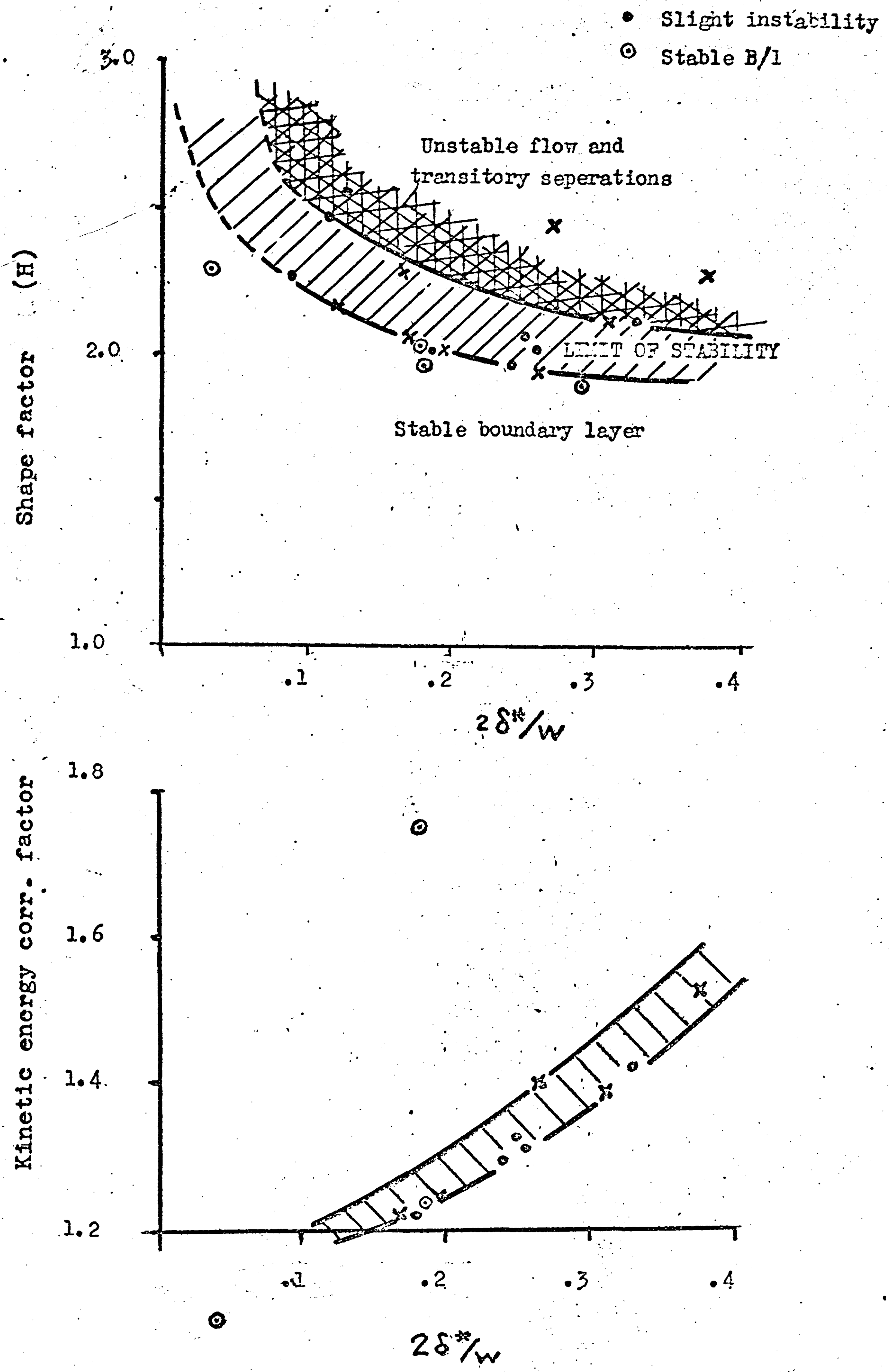

BOUNDARY LAYER STABILITY CRITERIA

FIGURE....53

'incipient' separation at the wall. This effect appears to be an indication of imminent separation of the boundary layer. Figure 54 shows a profile for a 10^{o} divergence angle diffuser of area ratio = 3.0 at a position where the shape factor (H) has reached a value of 2.26. The profile shows definite instability of the boundary layer probably due to slight transitiory separation occurring. Divergence angles above this can be seen to cause the diffuser to stall. However comparison of figures 34, 35, 39, 40 and table IV show that stall inception in a diffuser fitted with a tailpipe occurs further downstream in the diffuser (This can be seen in table IV which gives 'H' values at the same point for a plenum and tailpipe discharge). This indicates that there is a slight interaction between the tailpipe and diffuser when the flow is approaching the limit for stable flow due to a diffusion of the more stable tailpipe flow upstream. Also thick inlet boundary layers seem to be less stable than fully developed flows. This is a function of the lower pressure gradient associated with fully developed inlet flows, and can be seen reflected in the shape factor (H) in figure 39 and the lower values of pressure recovery (Cp) for fully developed flows.

Another interesting point observed during the tests was that when slight or transitory separations occurred, the flow separated from the diverging walls. However, when the diffuser "stalled" it tended to separate from the side wall and flow down one side of the diffuser only, (this phenomenon is illustrated in figure 55), the flow would then after several minutes change over to the other sidewall. The reason for the stall occurring on the sidewall is probably due to the large divergence angle (15^{o}) requiring quite a considerable momentum change when the flow stalls to follow the diverging wall whereas by stalling from the sidewall the abrupt direction and therefore momentum change can be reduced but a sufficient cross section change occurring to reduce the 'diffusion' of the flow.

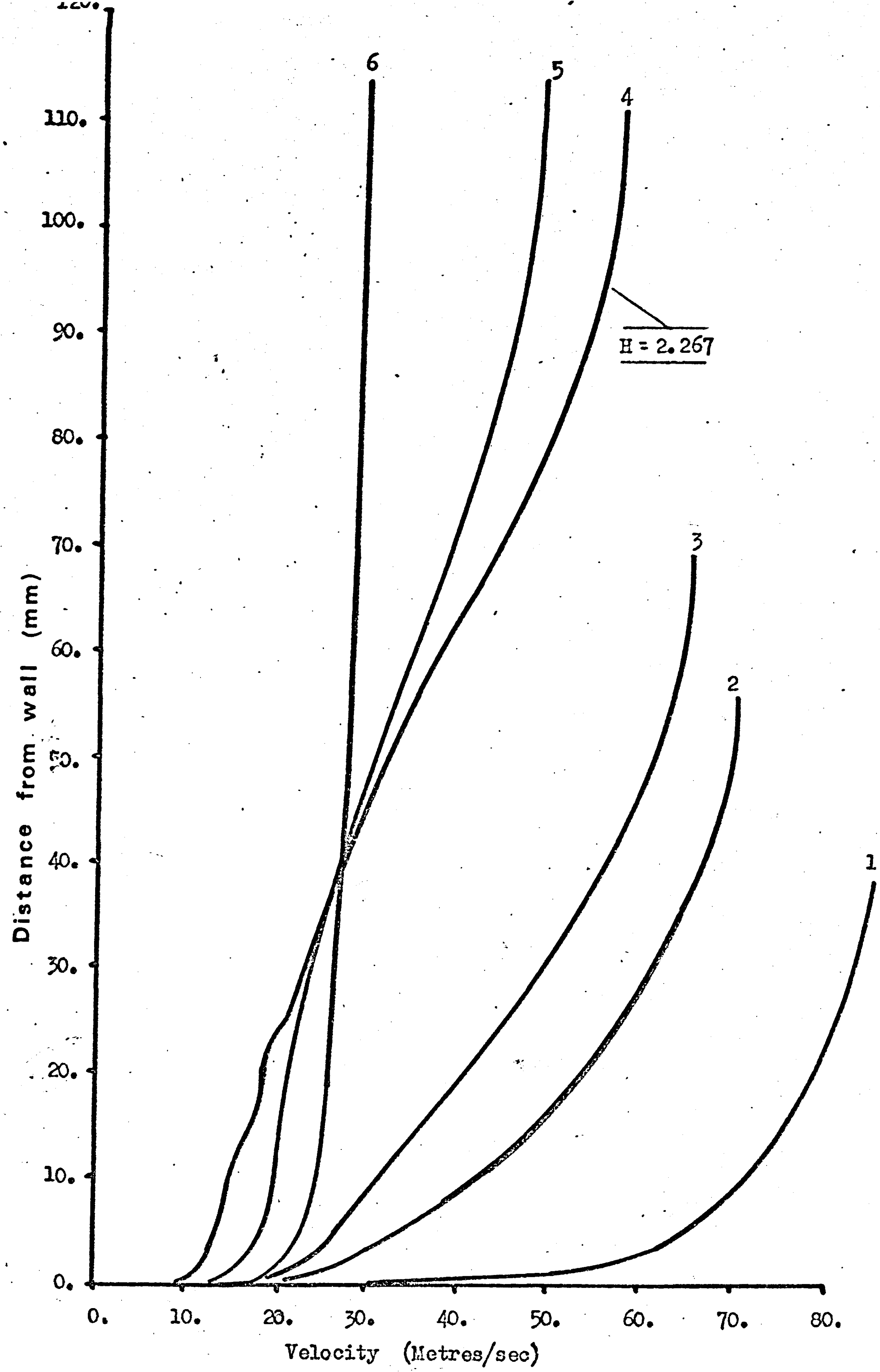

VELOCITY PROFILES IN DIFFUSER AND TAILPIPE AT THE LIMIT OF FLOW STABILITY

FIGURE. . 54

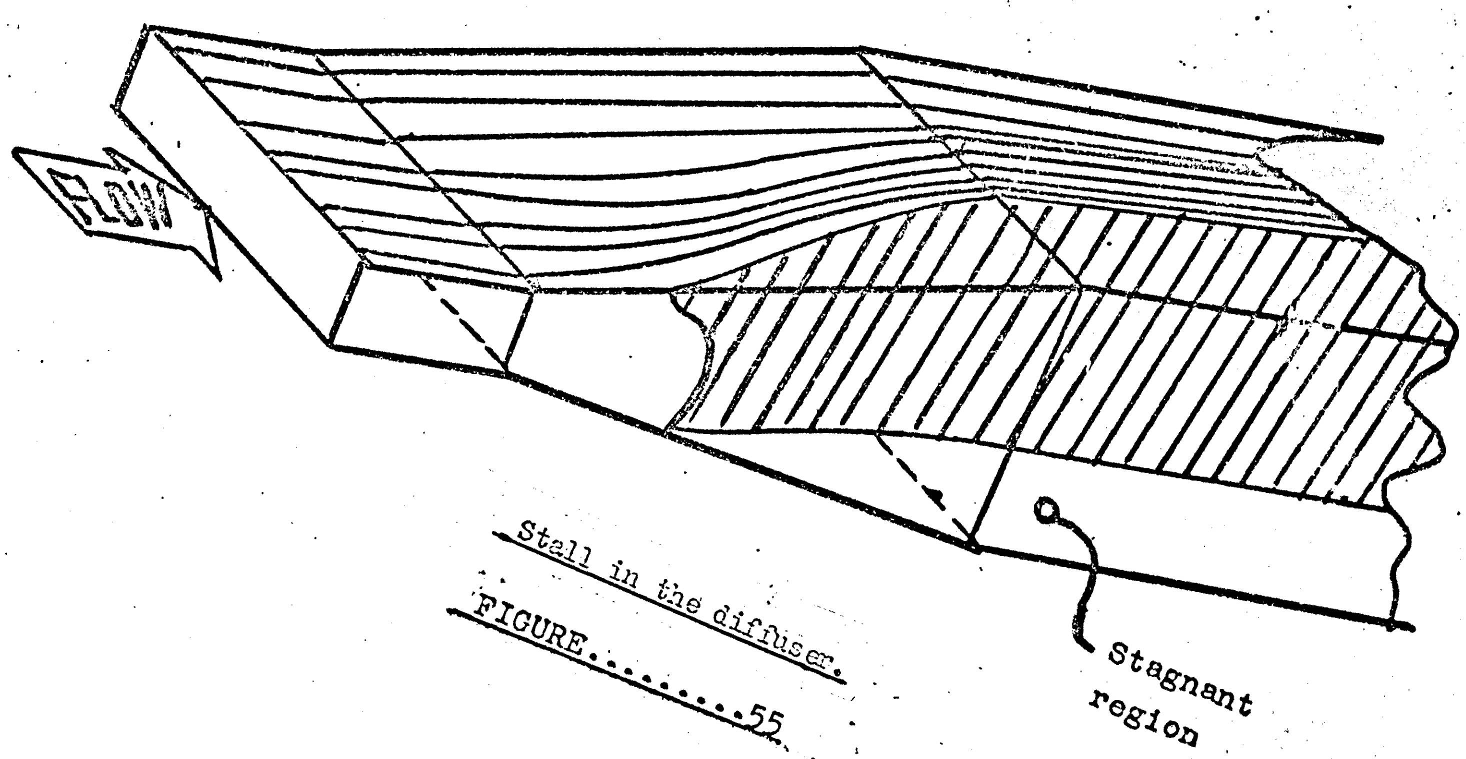

Stall in the diffuser.

FIGURE.........55

TABLE...III

Configuration Inlet b/l	AR	2ϕ	Cp max.	Position of cp max. x/w_1	x_t/w_2	Remarks
Thin	2	5°	.753			
Thick	2	5°	.656			
F.D.	2	5°	.627			
PLENUM DISCHARGE						
Thin	2	5°	.700	15.787	2.55	Position moves downstream as b/l thickens at inlet
Thick	2	5°	.681	23.792	6.55	
F.D.	2	5°	.664	27.79	8.55	
TAILPIPE DISCHARGE						
Thin	3	5°	.836			
Thick	3	5°	.795			
F.D.	3	5°	.756			
PLENUM DISCHARGE						
Thin	3	5°	.845	49.698	8.13	Position moves upstream as b/l thickens at inlet
Thick	3	5°	.842	43.26	6.99	
F.D.	3	5°	.790	43.26	6.99	
TAILPIPE DISCHARGE						
Thin	2	10°	.711			
Thick	2	10°	.583			
F.D.	2	10°	.541			
PLENUM DISCHARGE						
Thin	2	10°	.732	12.05	3.73	Position moves downstream with thickening b/l. Figures in ( ) for tailpipe truncated at max. press. posn.
Thick	2	10°	.645 (.644)	27.34	11.37	
F.D.	2	10°	.640			
TAILPIPE DISCHARGE						
Thin	3	10°	.788			
Thick	3	10°	.645			
F.D.	3	10°	.631			
PLENUM DISCHARGE						
Thin	3	10°	.812	42.257	10.40	Position moves downstream with thickening inlet b/l.
Thick	3	10°	.734	42.257	10.40	
F.D.	3	10°	.729	46.85	11.93	
TAILPIPE DISCHARGE						

TABLE.. III cont. ....

Configuration Inlet b/1 AR 2ø	Cp max.	Position of Cp max.		Remarks
		x/w1	x/w2	
Thin 2 15° Thick 2 15° F.D. 2 15° PLENUM DISCHARGE	.680 .515 .478			
Thin 2 15° Thick 2 15° F.D. 2 15° TAILPIPE DISCHARGE	.732 .647 .622	12.139 24.133 24.133	4.66 10.66 10.66	Cp max. moves upstream with thickening inlet b/1.
Thin 3 15° Thick 3 15° F.D. 3 15° PLENUM DISCHARGE	.761 .593 .532			
Thin 3 15° Thick 3 15° F.D. 3 15° TAILPIPE DISCHARGE	.882 .793 .689	42.950 43.018 43.018	11.91 11.94 11.94	Cp max. moves slightly upstream as b/1 thickens However longer tailpipe reqd. to accurately assess results.

TABLE.. III cont. ....

Configuration Inlet b/l AR 2ϕ			Cp max.	Position of Cp max. x/w_1	x/w_2	Remarks
Thin	2	15°	.680			
Thick	2	15°	.515			
F.D.	2	15°	.478			
PLENUM DISCHARGE						
Thin	2	15°	.732	12.139	4.66	Cp max. moves upstream with thickening inlet b/l.
Thick	2	15°	.647	24.133	10.66	
F.D.	2	15°	.622	24.133	10.66	
TAILPIPE DISCHARGE						
Thin	3	15°	.761			
Thick	3	15°	.593			
F.D.	3	15°	.532			
PLENUM DISCHARGE						
Thin	3	15°	.882	42.950	11.91	Cp max. moves slightly upstream as b/l thickens However longer tailpipe reqd. to accurately assess results.
Thick	3	15°	.793	43.018	11.94	
F.D.	3	15°	.689	43.018	11.94	
TAILPIPE DISCHARGE						

Comparison of parameters for plenum and tailpipe discharge.

x	α_p	α_t	Cp_p	Cp_t	η_p	η_t	η_{ep}	η_{et}	Remarks.
		Thin inlet boundary layer $2/w_1$ 0.01							
0.812	1.103	1.096	0.748	0.684	0.924	0.936	0.928	0.949	5°, AR 2 No effect
1.700	1.181	1.178	0.832	0.831	0.941	0.963	0.947	0.973	5°, AR 3 No effect
0.354	1.086	1.090	0.658	0.668	0.952	0.952	0.966	0.965	10°, AR 2 No effect
0.842	1.124	1.166	0.784	0.780	0.962	0.926	0.969	0.936	10°, AR 3 No effect
0.201	1.084	1.108	0.596	0.612	0.949	0.932	0.972	0.931	15°, AR 2 Slight improv.
0.554	1.081	1.174	0.749	0.728	0.973	0.910	0.976	0.931	15°, AR 3 No effect.
		Thick inlet boundary layer $2/w_1$ 0.06							
0.812	1.232	1.233	0.635	0.635	0.911	0.909	0.945	0.943	5°, AR 2 No effect
1.700	1.284	1.267	0.790	0.810	0.933	0.936	0.936	0.945	5°, AR 3 No effect
0.358	1.219	1.245	0.536	0.520	0.877	0.865	0.954	0.954	10°, AR 2 No effect
(H..	1.942	2.013)							
0.843	1.292	1.329	0.640	0.645	0.880	0.869	0.932	0.925	10°, AR 3 Slightly worse for tailp. dis
(H..	1.958	2.056)							
0.201	1.219	1.306	0.463	0.472	0.867	0.818	0.972	0.957	15°, AR 2 Better profile for tail. dis.
(H..	2.056	2.33)							
0.554	5.0	1.76	0.556	0.650	0.632	0.738	-	-	15°, AR 3 Noticable improvement for tailpipe discharge.
(H..	3.9	2.05)							

p Plenum discharge value

t Tailpipe discharge value

ep Energy corrected plenun value

et Energy corrected tailpipe value

TABLE V

HIGH SHAPE FACTOR STABILITY VALUES AT DIFFUSER EXIT OR STATION PRIOR TO STALL, FOR PLENUM AND TAILPIPE DISCHARGE

2ϕ	AR	$2\delta^*/w$	H	α	COMMENTS
15°	2	0.032	2.32	1.03	very stable
15°	2	0.173	2.05	1.22	slightly unstable
10°	2	0.190	2.01	1.25	slightly unstable
10°	3	0.182	1.96	1.22	stable
10°	3	0.24	1.96	1.29	stable
10°	3	0.33	2.12	1.426	stable
15	3	0.37	3.90	1.924	separation
15	3	.66	10	5.84	stall
15	3	0.266	1.93	1.40	unstable
10	3	.185	2.02	1.24	stable
10	3	.250	2.06	1.33	stable
10	3	.374	2.277	1.53	unstable
15	3	.174	2.05	1.763	stable (stall at next station)
15	3	.07	2.10	1.39	unstable
10	3	.251	2.01	1.31	stable

VIII.6. Mass Continuity Check

To check the accuracy of the results obtained a mass flow continuity check can be carried out along the diffusing and tailpipe sections. An example is shown in table V(a) for a 5^{o} divergence angle, AR = 2.0, diffuser and tailpipe with various inlet boundary layer thicknesses.

It can be seen for the thin inlet boundary layer condition that the error in the mass flow continuity is very low especially within the diffusing section (less than 0.3%), and it is not until approximately 10 diffuser outlet widths ($X/W_1 = 30$) that the error exceeds the experimental uncertainty. However, for the thicker inlet boundary layer conditions the error is greater than that which would be expected from experimental uncertainty within 3 inlet widths into the diffuser ($X/W_1 = 3$)

The reason for this error is the growth of the boundary layer on the sidewalls i.e. the non-diverging walls. This has the effect of increasing the centreline velocity due to the reduction in mass flow in this boundary layer. This can be seen in the thin inlet boundary layer case at the very end of the tailpipe, approximately 18 diffuser exit diameters downstream. However, for the thick inlet boundary layer the effect can be seen to be increasing in magnitude down the whole system, which would be consistent with a growing sidewall boundary layer. The fully developed flow exhibits even larger errors within the diffuser which again indicate that the error is due to the thickening sidewall boundary layer. However the sidewall boundary layer appears to be sufficiently large that distortion of this boundary layer occurs within the diffuser, which later recovers in the tailpipe which is indicated by a reduction in error in the tailpipe as the boundary layer recovers. This distortion can also be seen to a lesser extent for the thick inlet boundary layer case by the slight reduction in error early in the tailpipe.

MASS FLOW CONTINUITY CHECK

5^{o} divergence angle, AR = 2, tailpipe discharge.

	Mass Flow/metre breadth (kg/s)					
X/W_1	Thin inlet B/1	Mass Flow error %	Thick Inlet B/1	Mass Flow Error %	Fully Dev. Inlet Flow	Mass Flow Error %
	Diffusing Section					
0.0	7.715	0.0	6.848	0.0	6.830	0.0
2.66	7.684	-0.4	7.039	+2.80	7.083	+3.70
6.66	7.740	+0.27	7.219	+5.00	7.269	+6.40
10.66	7.250	+0.13	7.239	+5.70	7.496	+9.70
	Tailpipe Section					
11.78			7.220	+5.40		
15.78	7.734	+0.24	7.278	+6.30	7.430	+8.70
19.84	7.754	+0.5				
23.79			7.354	+7.40		
31.78	7.84	+1.7			7.278	+6.50
46.87	7.906	+2.5	7.391	+7.90	7.296	+6.80

Chapter Nine.

PREDICTION OF BOUNDARY LAYER AND PERFORMANCE PARAMETERS.

IX.1.1 The Theoretical Prediction.

The objective of the theoretical approach developed by Ferrett[21] was to predict the boundary growth within the diffuser and tailpipe and thus determine the flow parameters Cp, H, and θ along the diffuser/tailpipe system. This method of theoretical approach requires to be tested against extensive data on the growth of actual boundary layer parameters within such a system to determine the validity of the assumptions made in predicting the developing boundary layer.

During this investigation a fairly extensive study was made of the developing boundary layer parameters in a diffuser and a diffuser/tailpipe system, thus further analysis of the accuracy and the limitations of the prediction method developed by Ferrett can be usefully carried out using this experimental data.

IX.1.2 The Prediction Method.

The theoretical approach developed by Ferrett was an integral method to solve the boundary layer equations.

The momentum integral equation for a two dimensional compressible flow is used. Head's entrainment function (using the compressible form proposed by Green) is used as the auxiliary shape factor equation and continuity is used for the prediction of the centreline velocity. Greens skin friction law is employed for the calculation of the skin friction. Air viscosity is calculated from Sutherlands viscosity law and the static pressure rise calculated by application of the Euler equation along the centre line streamline of the diffuser/tailpipe and the pressure assumed constant across the cross section.

IX.1.3 The Boundary Layer Equations used and the Method of Solution.

The boundary layer equations used to describe the developing boundary layer are as follows:-

(1) The Momentum Integral Equation for a two dimensional compressible flow.

$$Cf\ /2 \quad = \frac{d\theta}{dx} + \theta\left[\frac{1}{M_o}\cdot\frac{dMo}{dx}\frac{(H+2-Mc^2)}{(1+0.2Mc^2)} + \frac{1}{W}\frac{dW}{dx}\right]$$

(2) Continuity.

$$\frac{(w - 2H\theta)(Mo^2 - 1)}{Mo\ (1 + 0.2\ Mo^2)} \quad = \quad \frac{dw}{dx} - 2\left[H\frac{d\theta}{dx} + \frac{dH}{dx}\right]$$

(3) Divergence.

$$\frac{dw}{dx} = 2\tan\phi$$

(4) Entrainment.

$$\frac{\theta\ H1}{dx} - H1\left(\frac{d\theta}{dx}\right) = F - \frac{H1\ \theta\ (Mo^2-1)}{(1-0.2Mo^2)}\cdot\frac{1}{Mo}\cdot\frac{dMo}{dx}$$

(5) Skin Friction.

$$\left(\frac{Cf}{Cf_{FP}} + 0.5\right)\left(\frac{\bar{H}}{\bar{H}_{FP}} - 0.4\right) = 0.9$$

Where $\bar{H}_{FP}$ and Cf_{FP} are flat plate values. Cf_{FP} is derived from the expressions

$$FcCf_{FP} = (0.012/\log_{10}(F_\delta R_\theta) - 0.04) - 0.00093.$$

Where $Fc = (1 - Mo^2/5)^{1/2}$ and $F_\delta = 1 + 0.056Mo^2$

And $\bar{H}_{FP}$ is defined as $\frac{1}{H_{FP}} = 1 - 6.8\sqrt{\frac{Cf_{FP}}{2}}$, and $R_\theta = \frac{\rho_o u_o \theta}{\mu_o}$

These five differential equations are then rearranged into the non-dimensional form of:-

$$\frac{d\theta'}{dx} = \theta'(\theta', Mo, w', H, H1)$$

$$\frac{dMo}{dx} = Mo(\theta', Mo, w', H, H1)$$

$$\frac{dw'}{dx} = w'(\theta', Mo, w', H, H1)$$

$$\frac{dH}{dx} = H(\theta', Mo, w', H, H1)$$

$$\frac{dH1}{dx} = H1(\theta', Mo, w', H, H1)$$

Thus giving:-

$Y(1) = \theta'$

$Y(2) = Mo$

$Y(3) = w'$

$Y(4) = H$

$Y(5) = H1$

These equations are then integrated simultaneously using the Runge - Kutta routine and values of Cp, Cp_{ε}, H, $H1$, $2\theta/_W$, $2\delta^*/_W$, α and Mo are calculated continuously down the diffuser tailpipe.

The solution of these equations requires the following diffuser inlet data to be specified in advance.

1. Centreline velocity. (u_o)
2. Total temperature (T_T)
3. Effective total pressure (P_{Te})
4. Effective static pressure (p_e)
5. Diffuser divergence ($\tan \phi /2$)
6. Shape factor (H)
7. Momentum thickness (θ)
8. Measured static pressure (p_o)
9. Area Ratio (AR)
10. Inlet width (w_1)

IX.1.4 Assumptions of the Method.

1. Since this method of prediction of the boundary layer parameters uses both the Momentum Integral Equation and an entrainment function 'F' the solution assumes that there is no interaction between the boundary layers on opposing walls and that a potential core exists at all points in the diffuser tailpipe system. Therefore, it would be expected that this approach would only be accurate for thin inlet boundary layers and small area ratios and would become increasingly inaccurate as the boundary layer grows in the diffuser/tailpipe system.

2. The method assumes that the static pressure is constant across the duct cross section, which would seem a reasonable assumption for the low mach no.'s tested. ($M < 0.25$)

3. That the velocity components perpendicular to the centreline are negligible.

4. The total temperature is constant at all longitudinal and transverse stations. Therefore the total temperature is always equal to the inlet value.

5. The flow in the boundary layer is steady, two dimensional and always turbulent.

6. The normal Reynolds stress term, in the equations of motion for the boundary layer, is negligible.

IX.2 Prediction of the Pressure Recovery Coefficient (Cp).

IX.2.1 The Thin Inlet Boundary Layer.

The theoretical and experimental values, of pressure recovery (Cp) are compared for a thin inlet boundary layer, an area ratio of 2.0 and plenum discharge in figure 56. There can be seen to be a very good correlation for the divergence angle of 5°, (within 2%). This figure increases slightly for the 10° and 15° divergence angle cases, (the error for the 15° divergence angle is 10%). When the area ratio (AR) is increased to 3.0 (shown in figure 57) the error increases to 15% to 20%.

The addition of a tailpipe to this system does appear to improve the situation slightly (shown in figure 58) and for an area ratio of 2.0 the difference between the predicted and experimental results is within 2%, for all divergence angles. However when the area ratio is increased to 3.0 (figure 59) the improvement is only slight, the error being between experimental and predicted pressure recovery falls to ± 15% the over/under estimation depending upon the divergence angle. This means that the theoretical, approach overestimates the high divergence angle cases and underestimates the low divergence angle cases.

IX.2.2 Thickening of the Inlet Boundary Layer.

As the inlet boundary layer thickens the error between predicted and experimental results for the plenum discharge increases for all cases. For the 5° divergence angle diffuser, of area ratio (AR) 2.0 and area ratio 3.0 with plenum discharge (shown in figure 60) the error, increases from -2% to -10%, though at the diffuser exit plane for the area ratio 3.0 case, the predicted and experimental values are within 2%. Figure 61 shows the 10° and

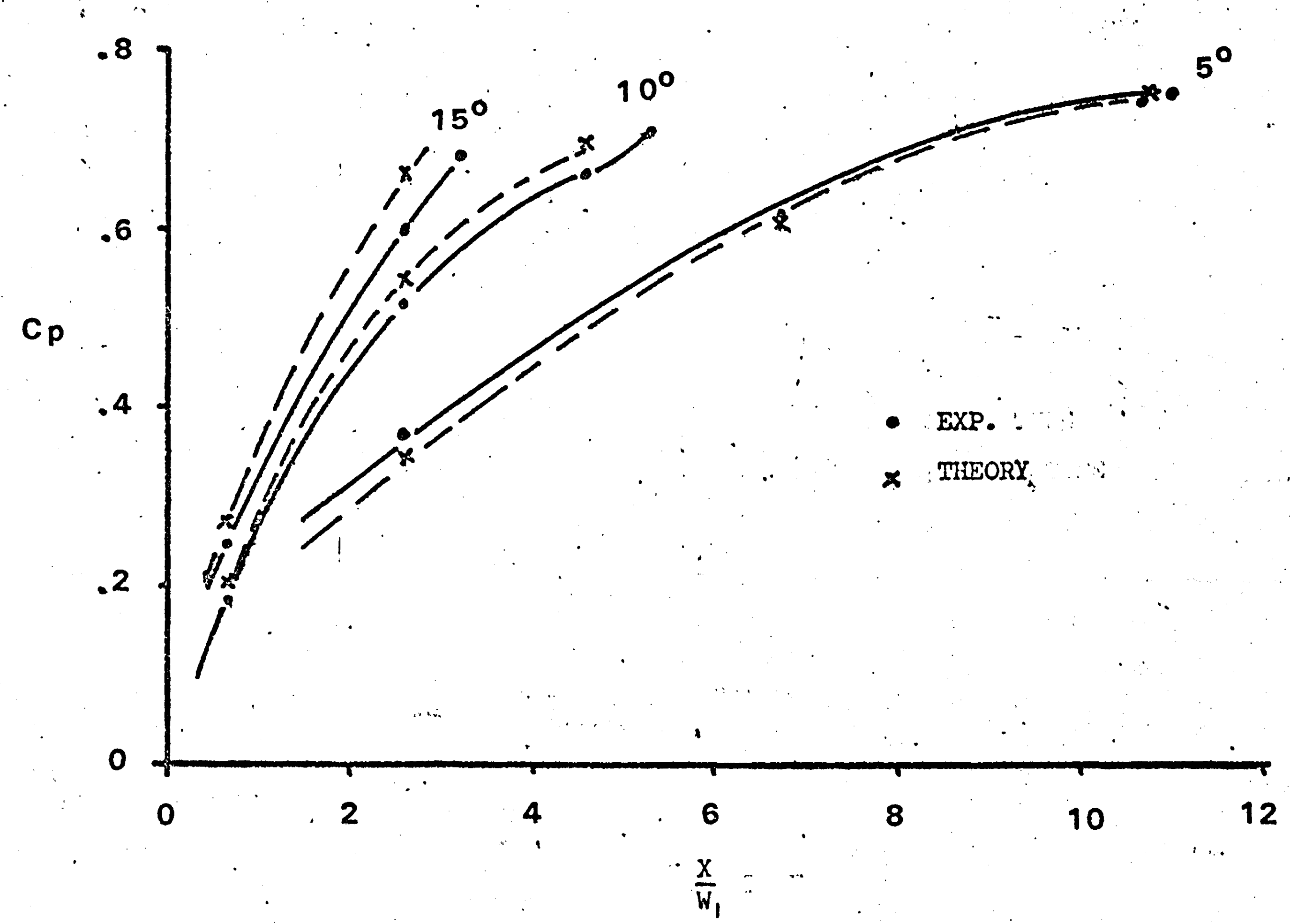

THIN INLET BOUNDARY LAYER, AR=2, PLENUM DISCHARGE

FIGURE 56

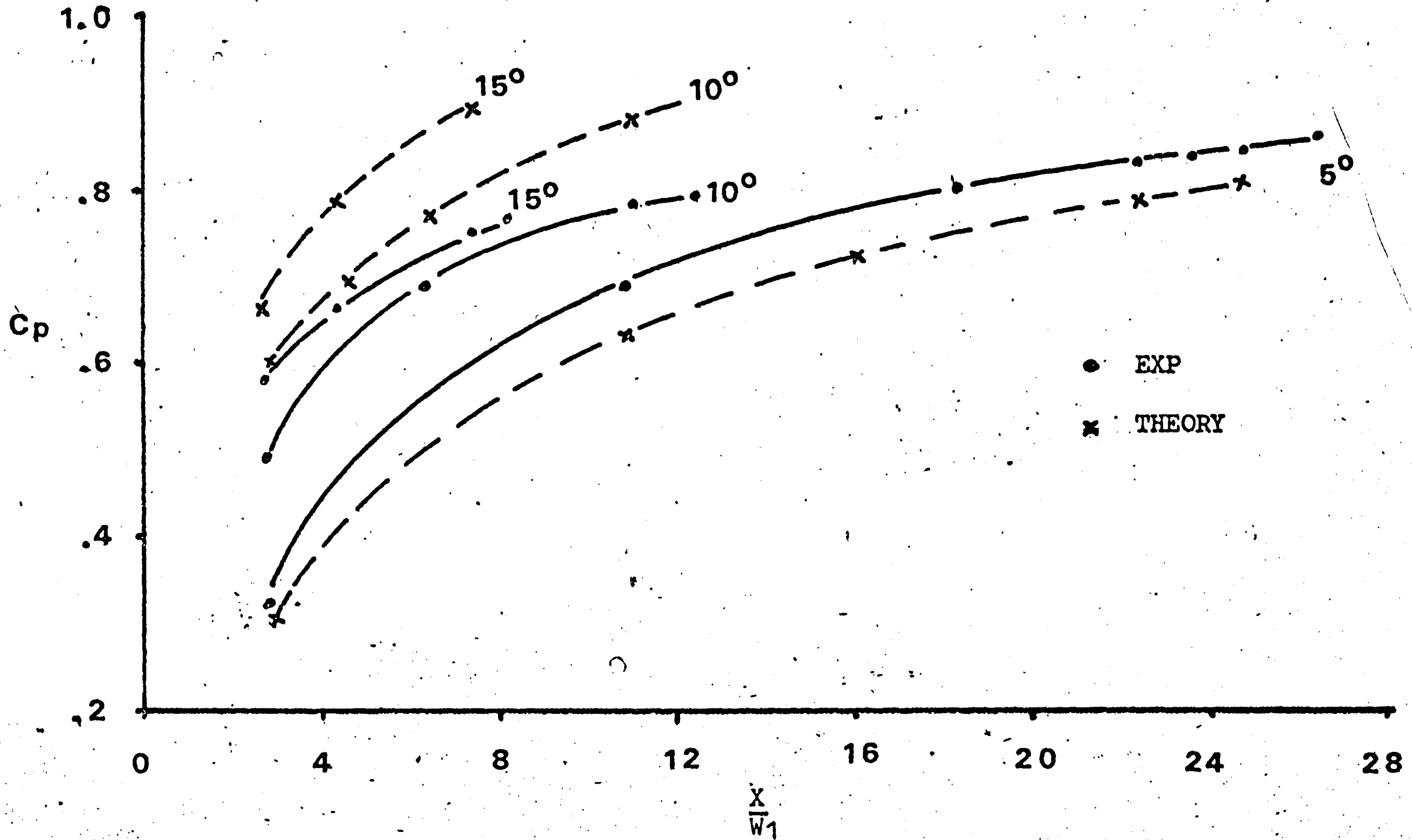

THIN INLET BOUNDARY LAYER, AR=3, PLENUM DISCHARGE

FIGURE 57

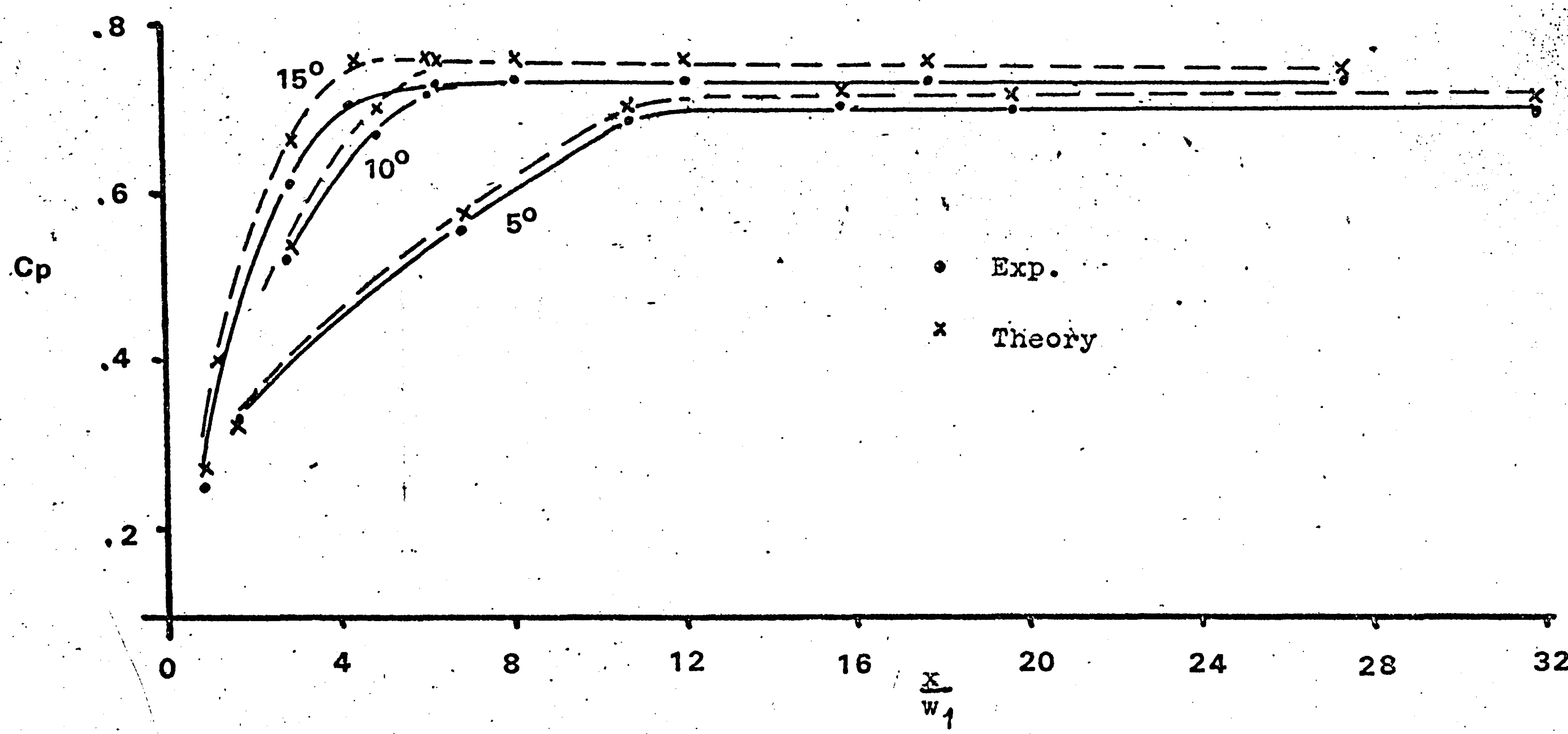

THIN INLET BOUNDARY LAYER , AR = 2 , TAILPIPE DISCHARGE

FIGURE......58

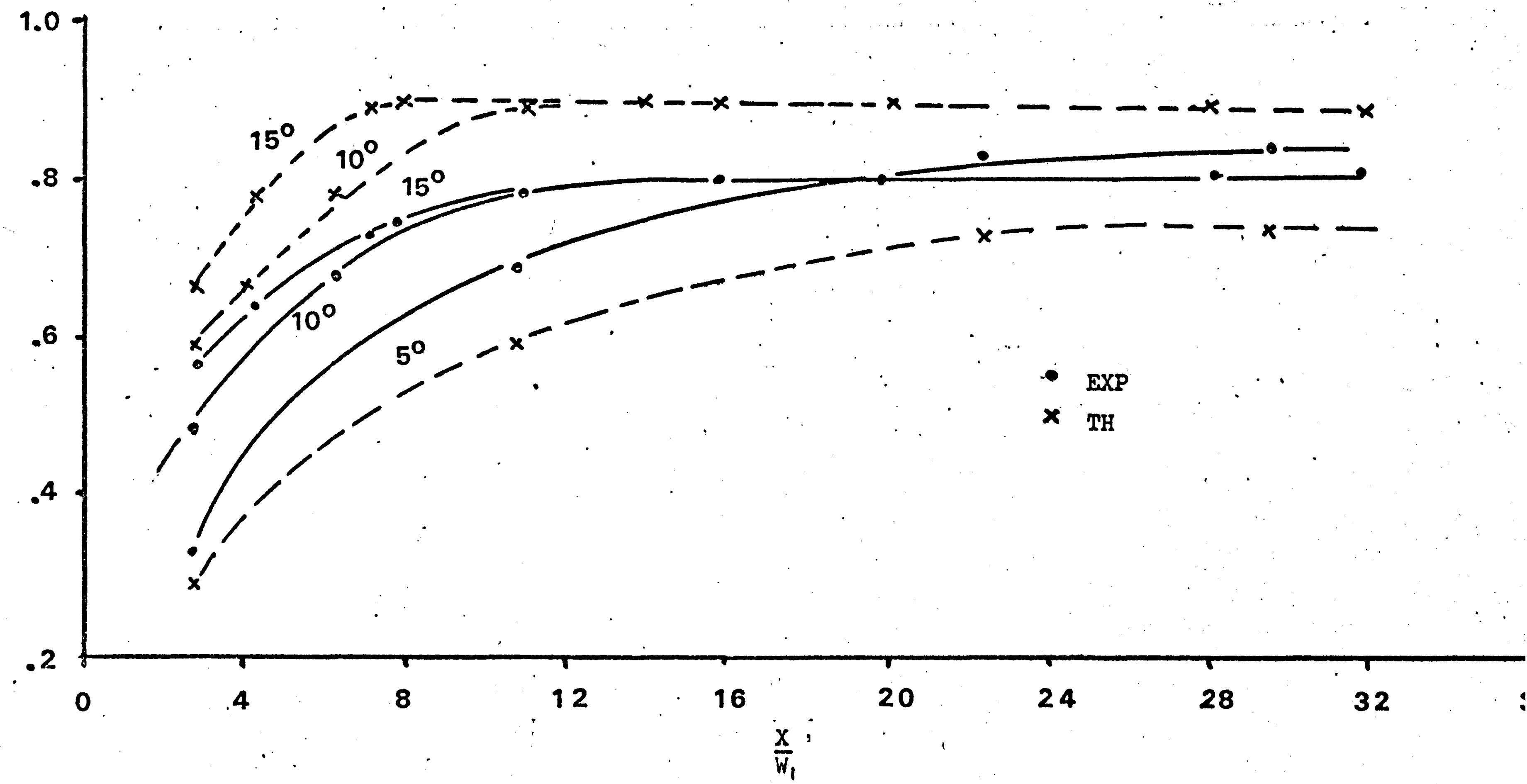

THIN INLET BOUNDARY LAYER, AR=3, TAILPIPE DISCHARGE

FIGURE 59

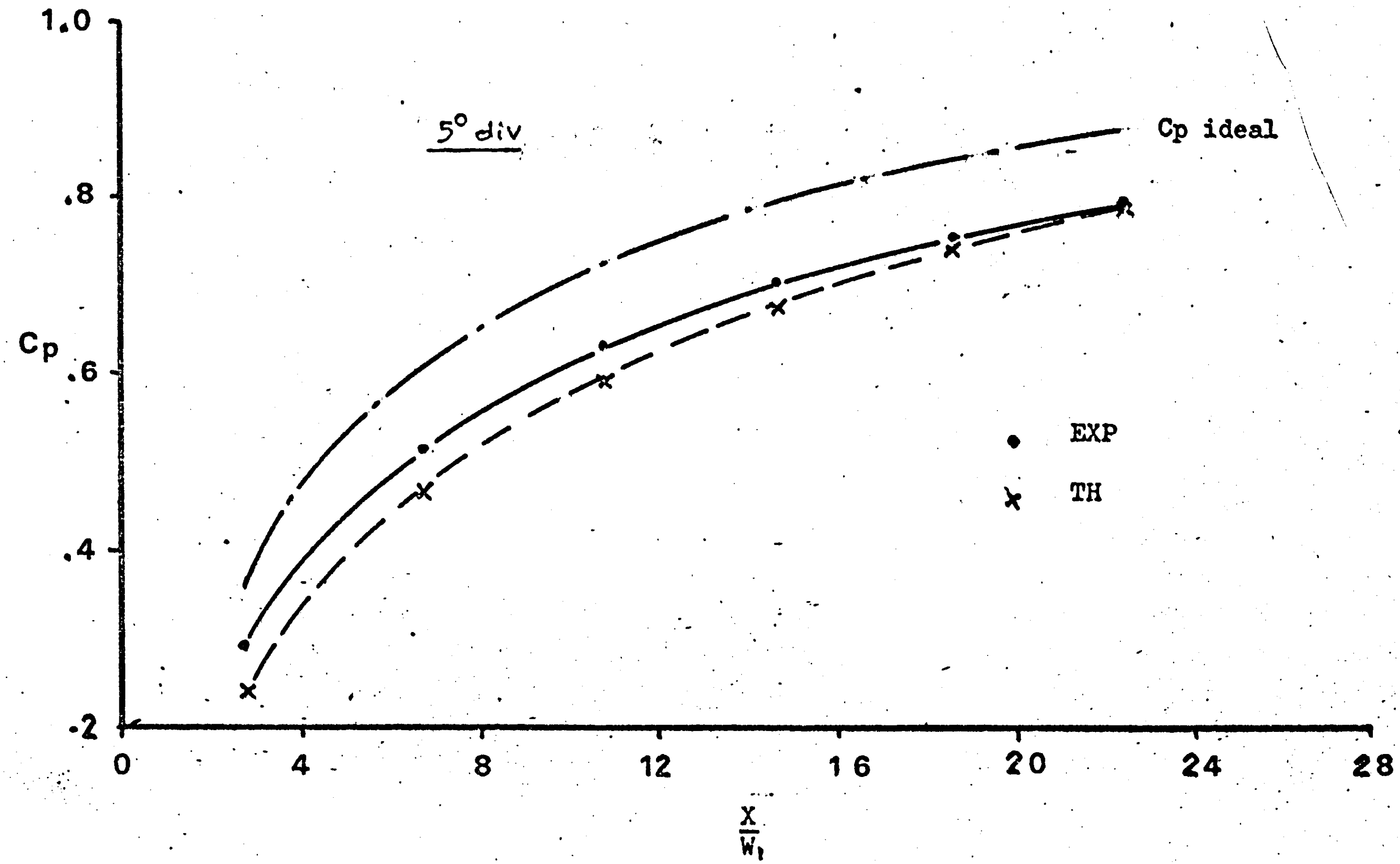

THICK INLET BOUNDARY LAYER, AR2 & 3, PLENUM DISCHARGE

FIGURE 60

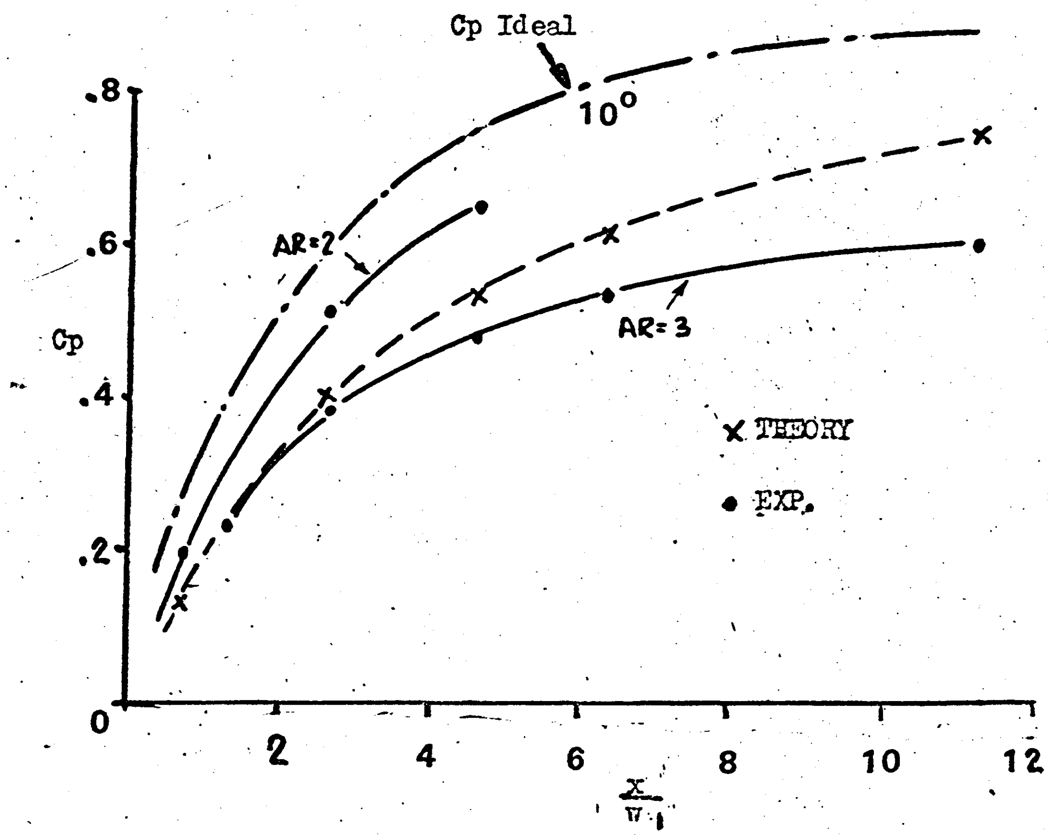

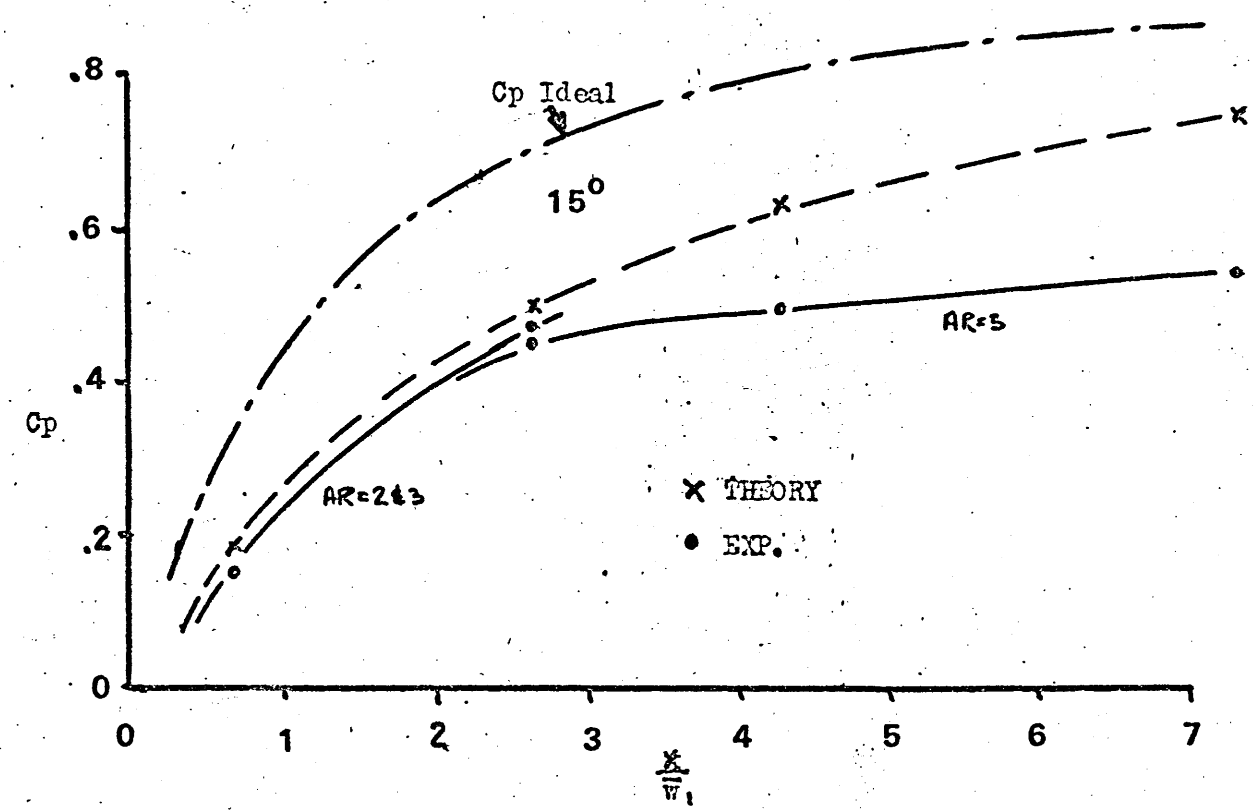

Thick inlet boundary layer , Area ratios 2 and 3

FIGURE...61

15^o divergence angle, area ratios 2 and 3 results compared with the theoretical results. For the 10^o divergence angle case the predicted values are in error by up to -15% for the area ratio 2.0 case, and up to +15% for the area ratio 3.0 case, for the 15^o divergence angle, area ratio = 3.0, case the theoretical prediction overestimates by 40%. The error in the 15^o divergence angles cases can be substantially explained by the failure of the theory to predict the separation of the boundary layer and infact stalling of the diffuser in the case of the area ratio 3 diffuser. Therefore, as can be seen, the error is much more reasonable for the area ratio (AR) = 2 diffuser (i.e. 8%). In the case of the 10^o divergence angle diffuser the theory appears to take a mean between the AR = 2 and the AR = 3 cases. However since the theory does not take into account the effect of the downstream conditions diffusing upstream and affecting the flow, which in the case of a very small divergence angle diffuser or a tailpipe would appear to be a valid assumption (as shown in chapter VIII). However this is not the case when a further highly diverging section is included. The effect of the downstream conditions affecting the local boundary layer is obviously greater for thick boundary layers and high area ratio and high divergence angle diffusers. In addition the interaction between the boundary layers on the opposing walls will increase as the boundary layer thickens further in the diffuser. This can be seen in figure 62 which shows a fully developed inlet flow case with a divergence angle of 5^o and an area ratio of 3. The experimental value of pressure recovery coefficient (Cp) is underestimated as usual for the 5^o divergence angle case but is within 5% for much of the diffuser, however after approximately the first 30% of the diffuser the theory fails to predict the rapid fall in the $\partial p/\partial x$ values and the error at the exit is an overestimation by the theory of approximately 10%. This trend to change from under estimation to over estimation as the inlet boundary layer thickens is shown in figure 63 for a 5^o divergence angle diffuser of AR = 3.0 with thin, thick and fully developed inlet boundary layers. This reduction

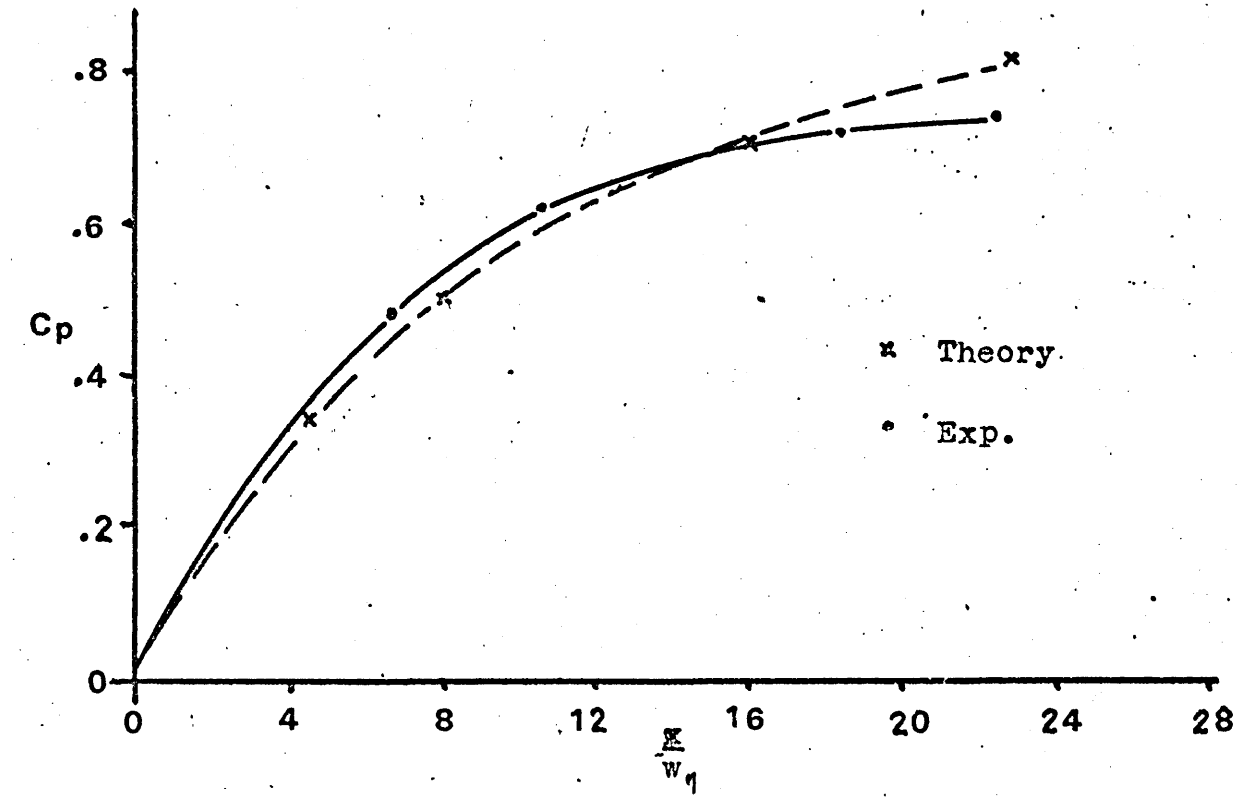

FULLY DEVELOPED FLOW , AR = 3 , 5^{o} DIV.

FIGURE.....62

C_p FOR VARIOUS INLET BOUNDARY LAYERS; DIVERGENCE ANGLE 5°, AREA RATIO = 3 -

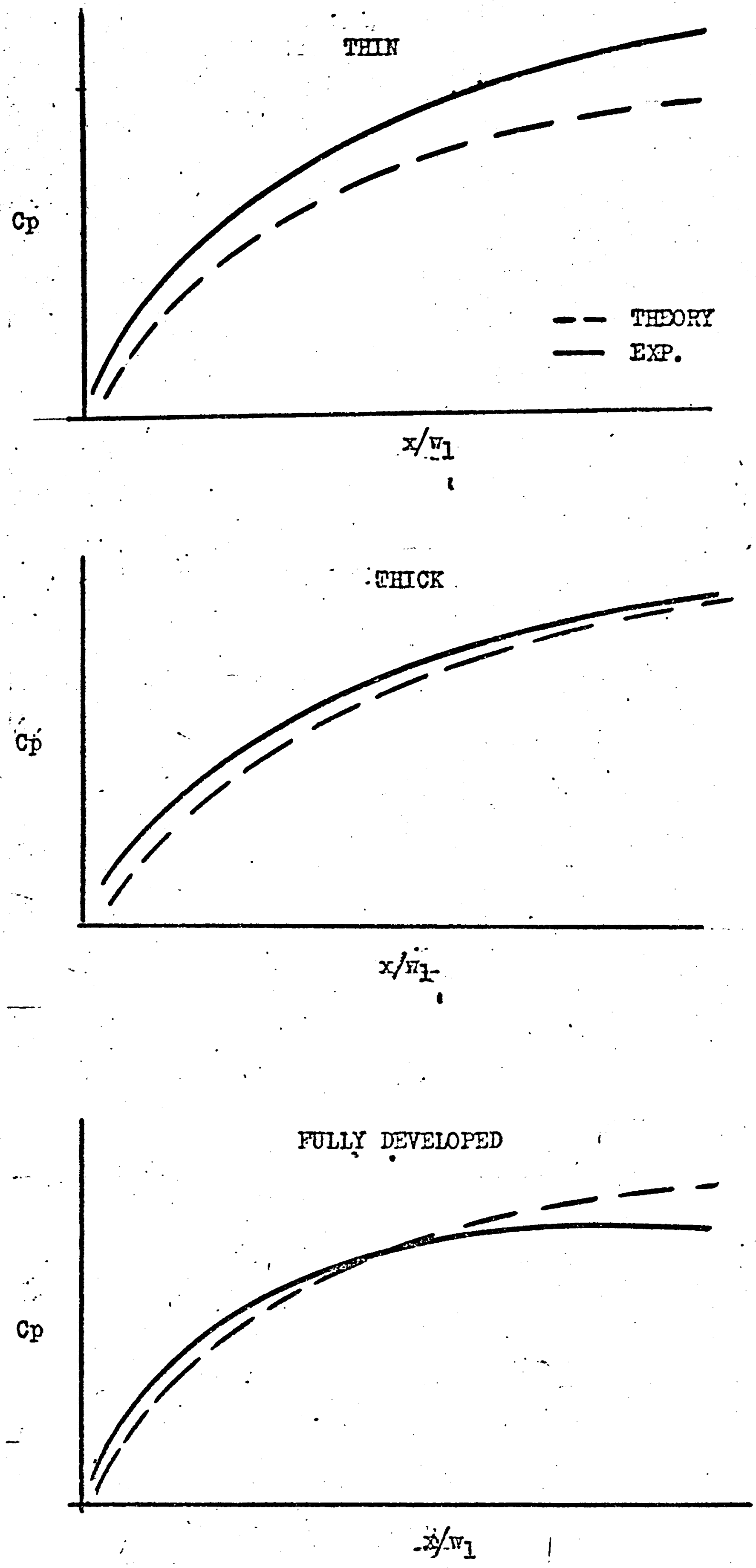

of the prediction accuracy as the inlet boundary layer thickens is to be expected since the basis of this theoretical approach is the assumption that the opposing boundary layers do not interact and that a potential core exists at all points in the system. Therefore any increase in the boundary layer thickness at the inlet must increase the error of the prediction method which will be seen as an overestimation of the pressure recovery.

IX.3 Shape Factor (H).

IX.3.1 Thin Boundary Layer at Inlet.

The prediction of the boundary layer shape factor for plenum discharge with a thin inlet boundary layer can be seen in figures 64 and 65. The theoretical approach can be seen to underestimate the distortion of the boundary layer for all except the 15^{o} diffuser of area ratio 3. However the general form of the prediction can be seen to be very similar to the experimental results and figure 64 shows how for small divergence angles the prediction becomes increasingly accurate. The sharp fall in shape factor (H) after the high inlet figure (caused by the boundary layer trip wire) is accurately predicted for the small divergence angle diffuser. As the divergence angle increases the prediction accuracy reduces especially when the area ratio also is increased. However, the prediction method fails to predict the later rapid increase in the shape factor, an error which increases with decreasing area ratios, the exception to this being shown in figure 65 for the 15^{o} divergence angle diffuser area ratio = 3.0.

It would therefore seem that the prediction method in the case of a thin inlet boundary layer either underestimates the growth of the displacement thickness therefore the boundary layer growth, or overestimates the growth of the momentum thickness, both of which would be seen as an overestimation of pressure recovery due to the incorrect centre line velocity calculated.. (This is discussed in paragraph IX.4); This can be seen in figure 56 for the 10^{o} and 15^{o} divergence angle diffusers.

IX.3.2 The Effect of Thickening the Inlet Boundary Layer.

As the inlet boundary layer thickens the prediction method can be seen

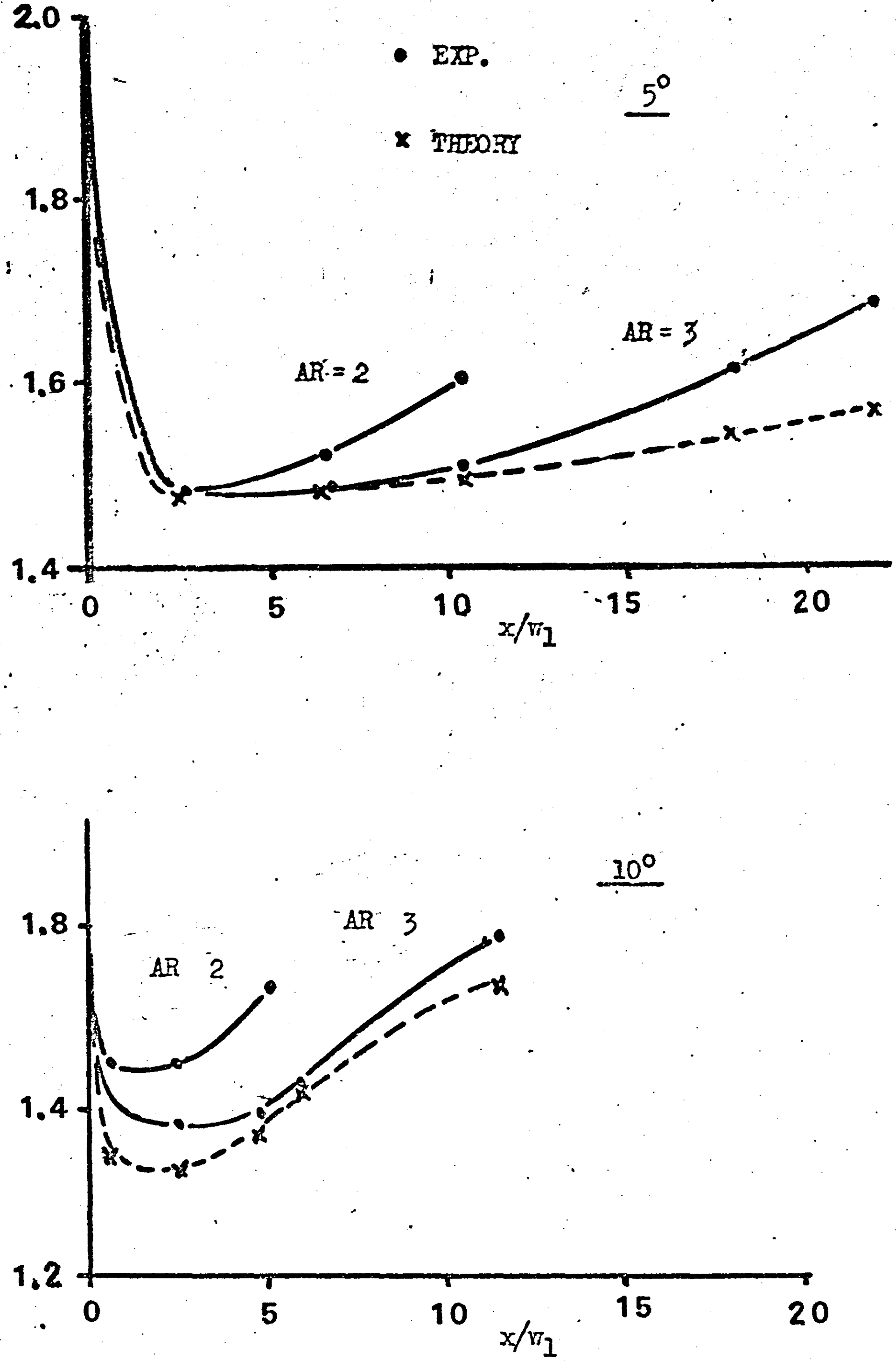

THIN INLET BOUNDARY LAYER SHAPE FACTOR (H)

FIGURE....64

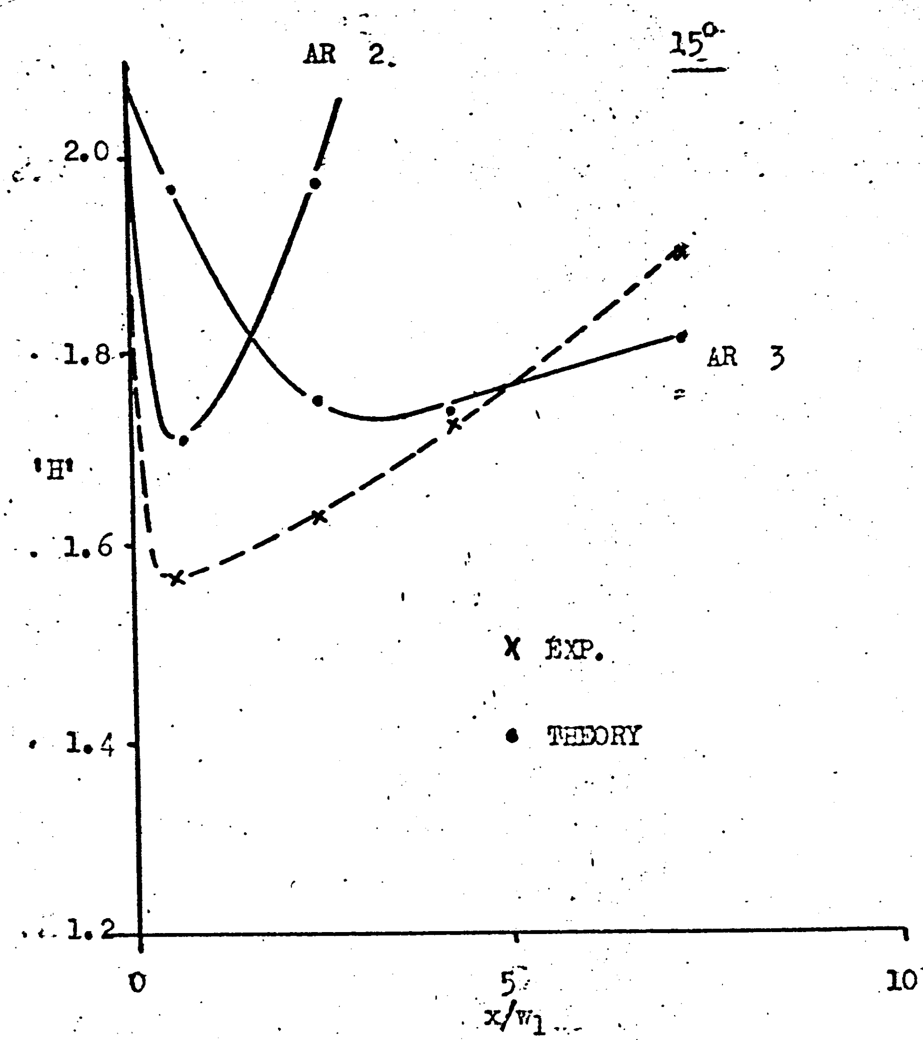

THIN INLET BOUNDARY LAYER SHAPE FACTOR(H)

FIGURE.......65

to again underestimate the shape factor (figures 66 and 67). This can be seen to be grossly underestimated in the 15^o divergence angle case shown in figure 67. This accounts for the very large errors in pressure recovery predicted for this case when compared to the actual results. For both plenum discharge and tailpipe discharge (shown in figure 67), $\frac{\partial H}{\partial x}$ is so high that within 3 to 4 inlet widths as the distortion of the boundary layer is so large causing the boundary layer to separate, and the diffuser to stall. The theoretical prediction however fails to predict this thus giving far higher pressure recoveries than were experienced (40% higher).

It can be seen that the prediction method generally underestimates the boundary layer distortion for all the inlet boundary layer conditions tested, and thus fails to predict separation of the boundary layer, which it would normally do when the shape factor 'H' reached 2.8.

IX.3.4 The Inclusion of a Tailpipe.

The effect of the inclusion of a tailpipe on the shape factor 'H' is predicted as can be seen in figures 66 and 67. However the very rapid recovery of the boundary layer is not accurately predicted, thus explaining why a more rapid pressure rise occurs in the tailpipe at the limit of flow stability than is predicted for the thick inlet boundary layer case. Therefore the prediction of the boundary layer shape factor (H) is closest for a thin inlet boundary layer, especially with a small divergence angle and area ratio. The prediction of the shape factor for this case is within 2%- 4% (shown in Table VI).

IX.4 Momentum Thickness Prediction.

As previously suggested in paragraph IX.3 the underestimation of the shape factor is due to an overestimation of momentum thickness. It can be seen in figure 69 that in the early part of the diffuser/tailpipe system the correlation between experimental and predicted results is good, however, as the area ratio enlarges the error in the theoretical result increases. However with low area ratio diffusers (AR = 2), shown in figure 70 with thin inlet boundary layer

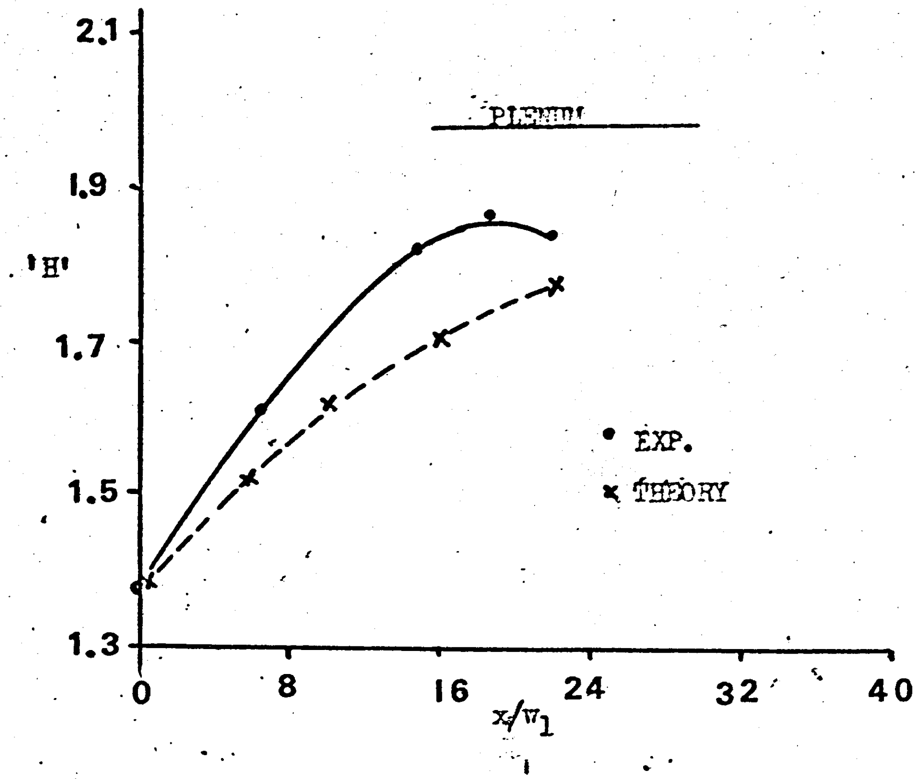

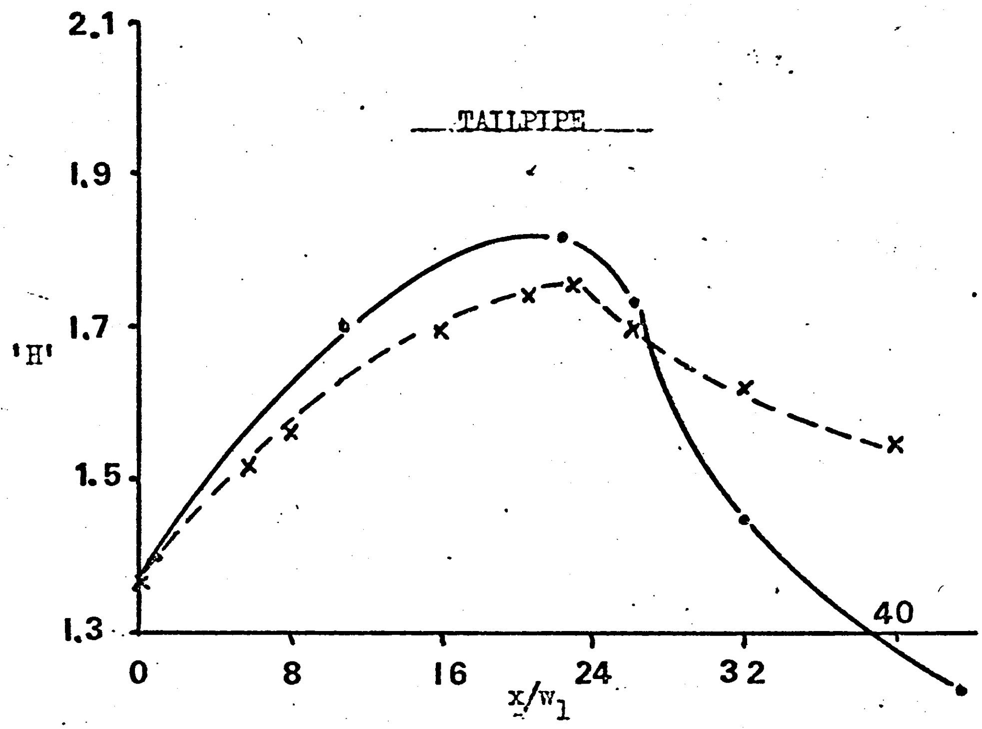

THICK INLET BOUNDARY LAYER , AR = 5 , 5° DIVERGENCE

FIGURE....66

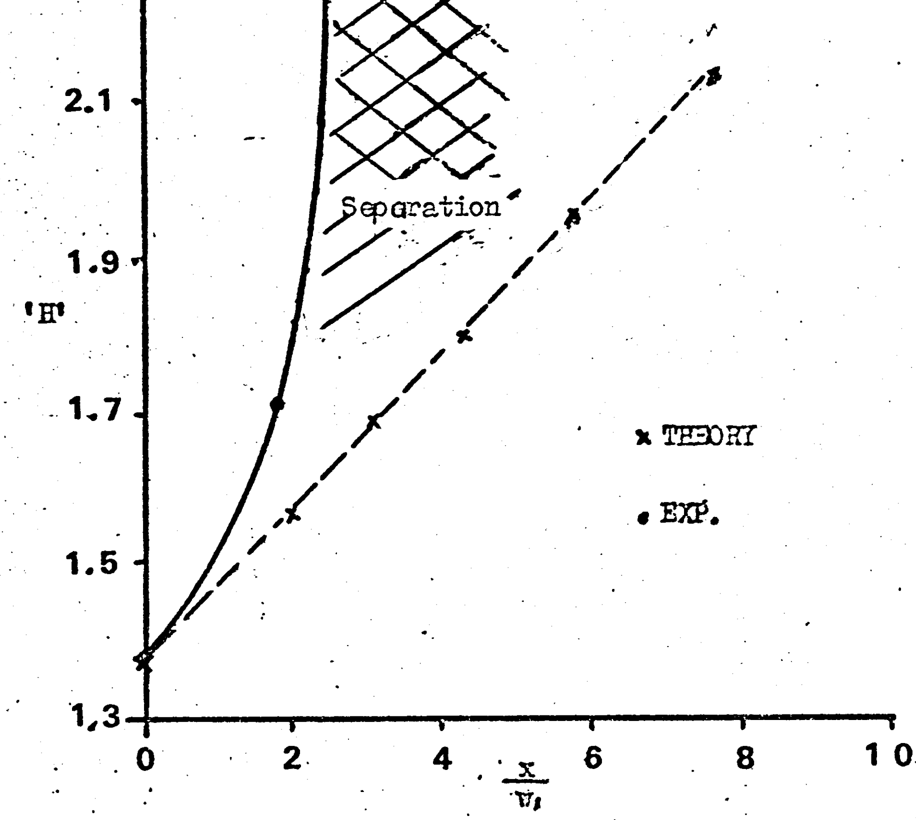

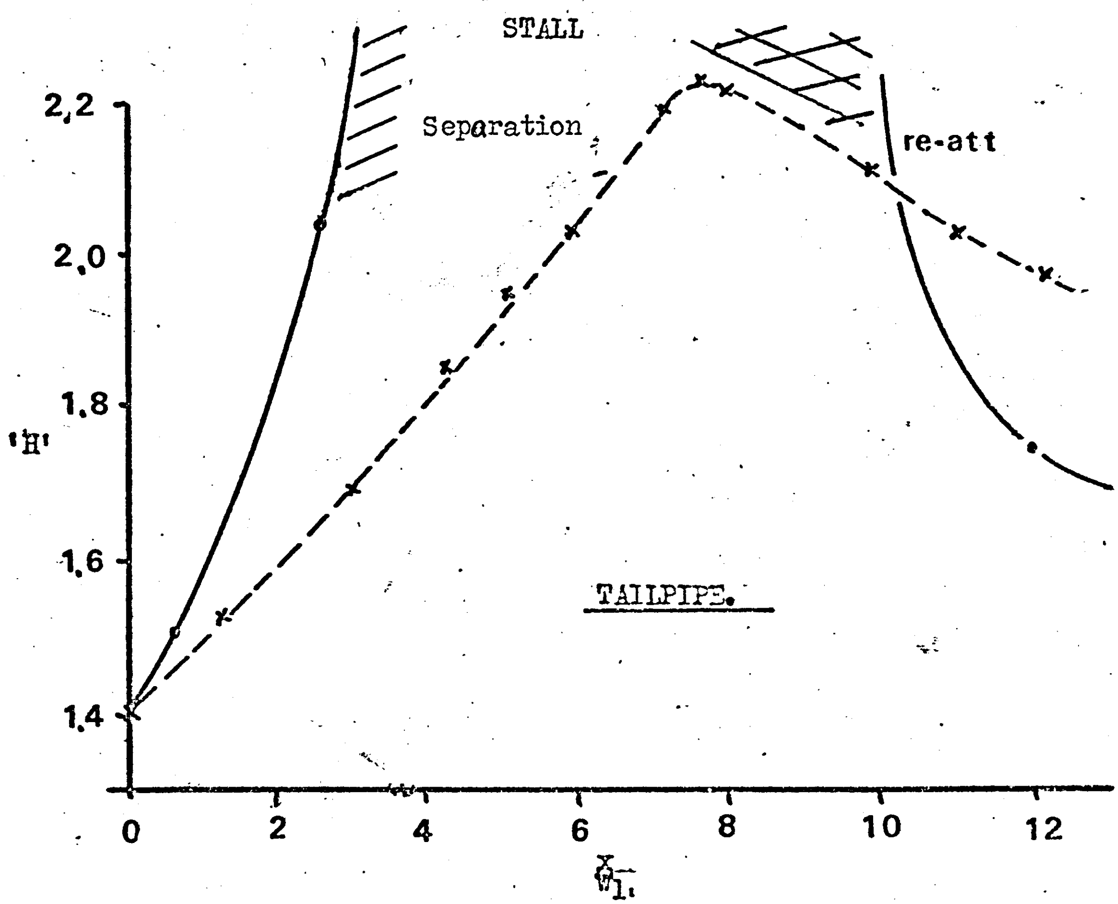

THICK INLET BOUNDARY LAYER , AR = 3 , 15^{o} DIVERGENCE

FIGURE....67

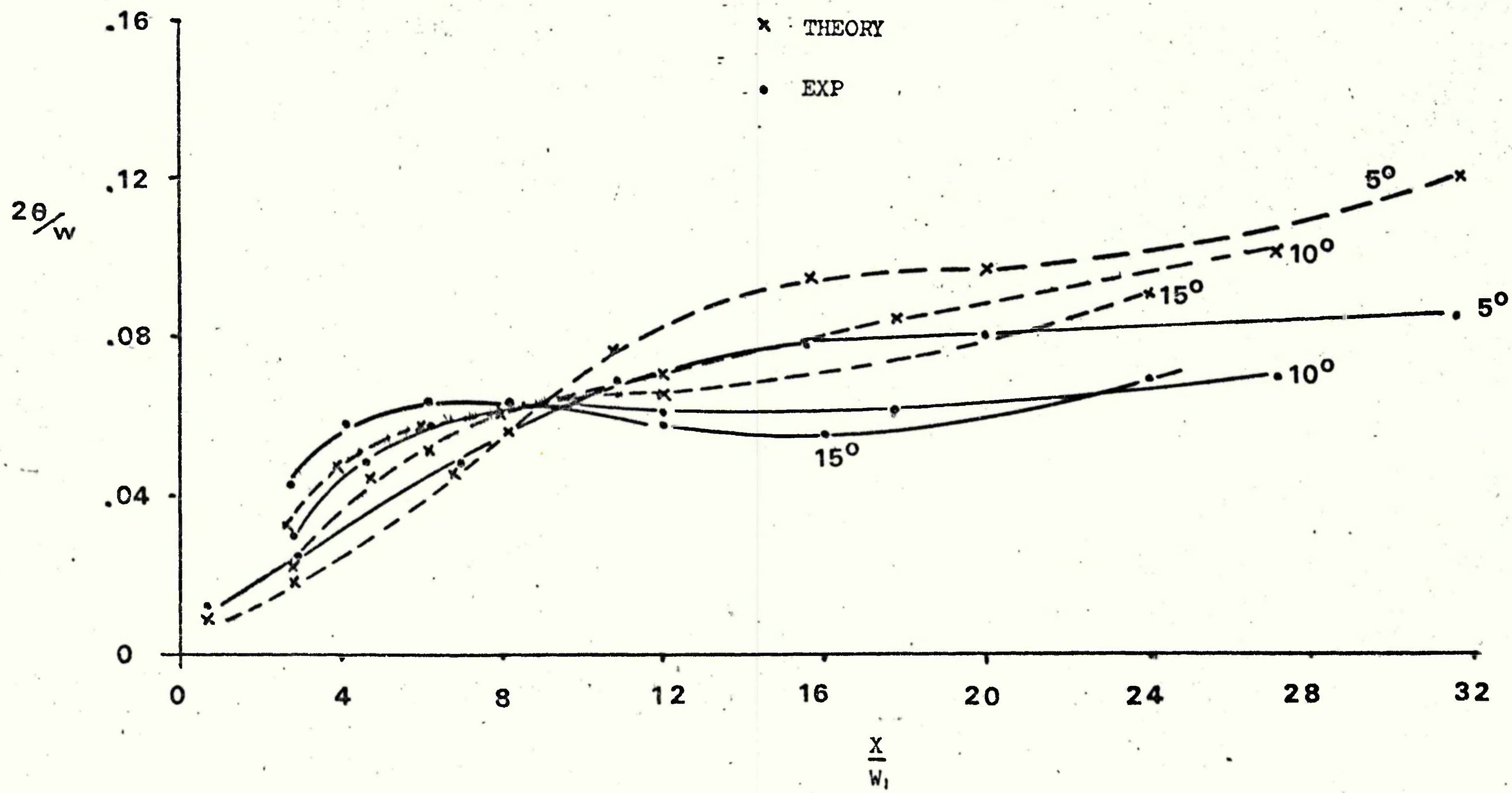

THIN INLET BOUNDARY LAYER, AR = 2, TAILPIPE DISCHARGE

FIGURE 68

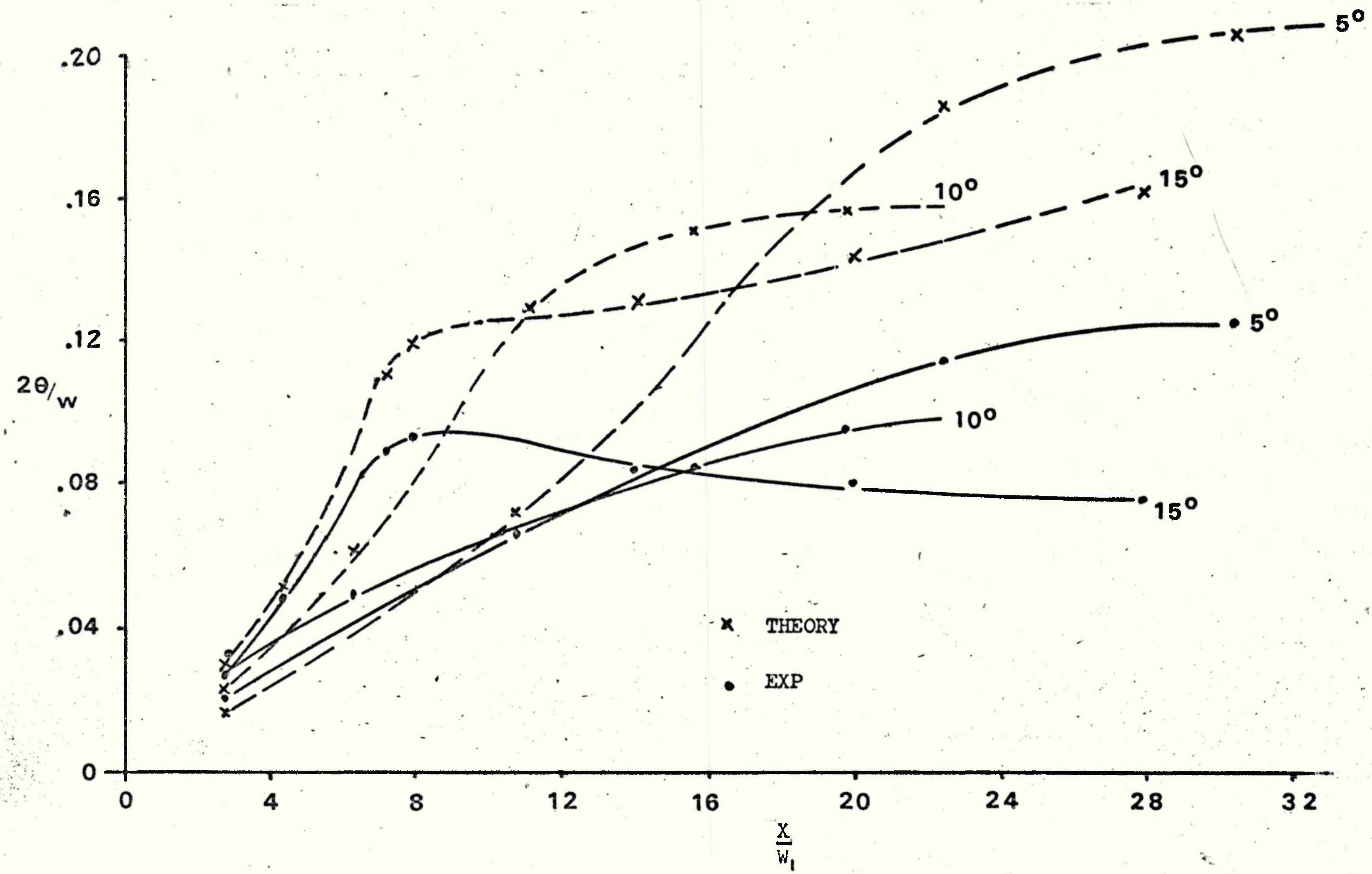

THIN INLET B/L, AR-3, TAILPIPE DISCHARGE

FIGURE 69

THIN INLET BOUNDARY LAYER , AR = 2 , PLENUM DISCHARGE

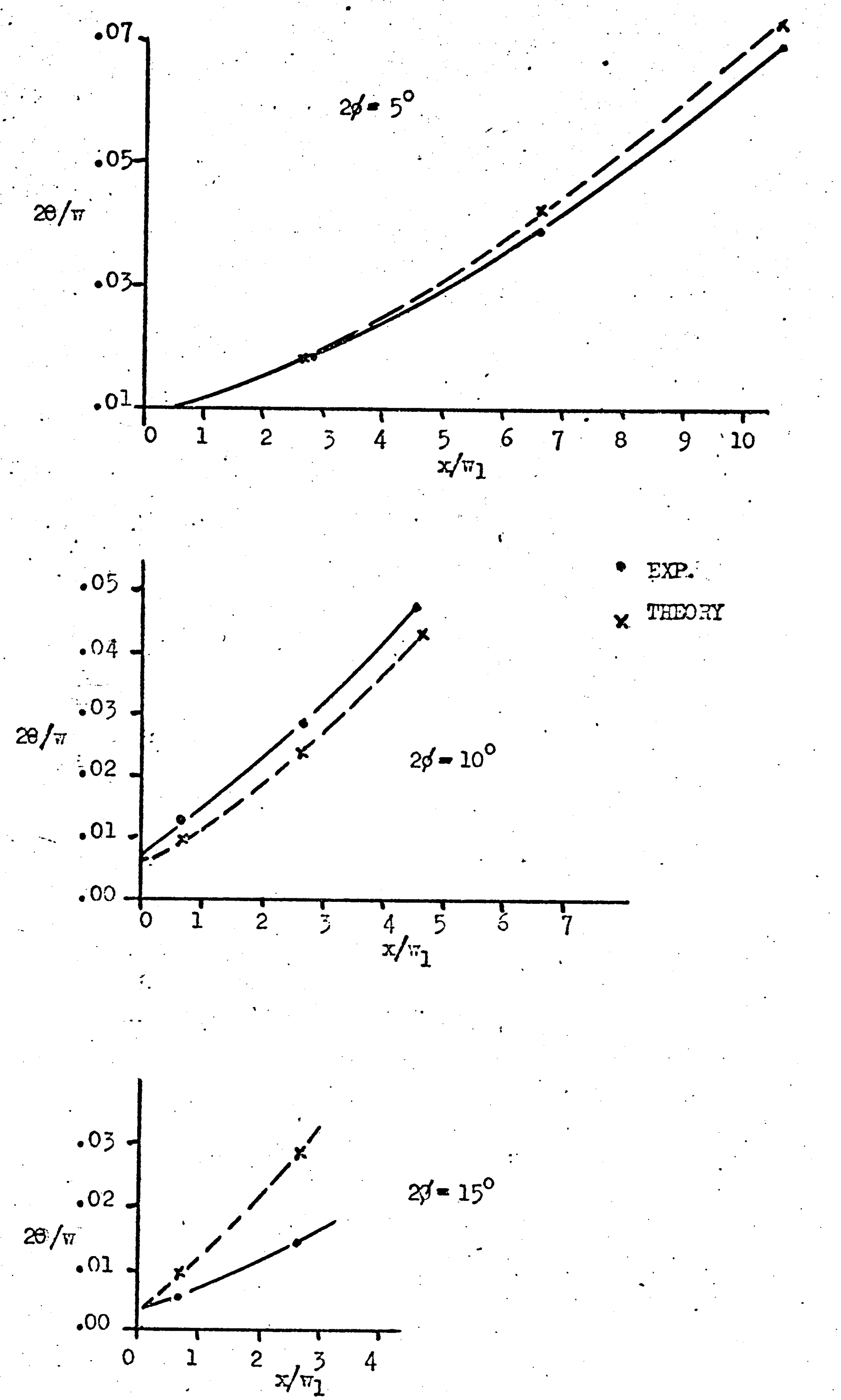

FIGURE.........70

conditions the correlation is good, especially for the 5^{o} divergence angle case and as described previously the shape factor correlation for this case is also in good agreement. Thus the boundary layer is accurately predicted for these cases, accounting for the close agreement between the experimental and theoretical prediction results of the performance parameters for these cases

IX.5 Limits for Accurate Prediction of Flow and Performance Parameters.

It can be seen from the results obtained that for low area ratios and low divergence angle diffusers, that is below 15^{o}., the correlation between the predicted boundary layer and the performance parameters is very good for a thin inlet boundary layer. For these particular geometrical configurations the agreement remains relatively close for a thick inlet boundary layer ($2\delta^*/w_1 = 0.06$) and even for the fully developed inlet flow case. Provided that the divergence angle is kept below 10^{o} the correlation is quite good for most boundary layer and performance parameters, even, without any correction for the interaction of the opposing boundary layers.

EXPERIMENTAL VS THEORETICAL PARAMETERS

$2\phi = 5^{\circ}$

PLENUM AR2	Cp			H			2θ/W1		
X/W1	EXP	2-D TH	AX1.TH	EXP	2D	AX1	EXP	2-D	AX1-THEORY
2.66	.367	.350	.571	1.47	1.47	1.60	0.019	.018	.026
6.67	.617	.615	.757	1.40	1.48	1.53	0.039	.042	.058
10.66	.748	.755	.754	1.61	1.50	1.41	0.069	.072	.066
ATMOS.	.753	-							
TAILPIPE AR2 X/W	EXP	2D	AX1	EXP	2D	AX1	EXP	2-D	AX1
2.66	.328	.325	.540	1.54	1.46	1.61	.024	.018	.026
6.67	.556	.571	.675	1.53	1.48	1.53	.046	.042	.058
10.66	.684	.699	.671	1.59	1.50	1.41	.068	.076	.066
15.79	.700	.717	.662	1.44	1.42	1.36	.078	.095	.076
19.84	.699	.715	.654	1.36	1.38	1.33	.079	.097	.085
31.78	.691	.708	-	1.27	1.33	-	.084	.121	-
46.88	.679	.698	-	1.25	1.30	-	.078	.152	-
PLENUM AR=3 X/W	EXP	2D	AX1	EXP	2D	AX1	EXP	2-D	AX1
2.66	.325	.29	.550	1.48	1.46	1.61	.021	.018	.026
10.66	.689	.59	.863	1.51	1.50	1.68	.064	.074	.120
18.32	.800	.69	.865	1.63	1.55	1.45	.102	.144	.138
22.31	.832	.724	.863	1.69	1.57	1.41	.117	.186	.144
ATMOS.	.836	-							
TAILPIPE AR=3 X/W	EXP	2D	AX1	EXP	2D	AX1	EXP	2-D	AX1
2.66	.329	.29	.490	1.49	1.46	1.60	.021	.018	.026
10.66	.687	.59	.783	1.56	1.50	1.73	.067	.074	.122
22.31	.831	.724	.783	1.68	1.57	1.41	.116	.186	.145
29.3	.841	.728	.780	1.47	1.47	1.36	.126	.206	.157
40.6	.844	.727	.770	1.33	1.39	1.32	.116	.225	.175
49.7	.845	.726	-	1.24	1.35	-	.092	.241	-
58.7	.843	.725	-	1.22	1.33	-	-074	.256	

10°

PLENUM AR2	Cp			H			2θ/W1		
X/W1	EXP	TH-2D	AXI	EXP	2D	AXI	EXP	2D	AXI
0.76	.188	.204	.320	1.647	1.55	1.72	.013	.009	.012
2.64	.513	.540	.674	1.654	1.53	1.92	.029	.024	.044
4.65	.658	.696	.681	1.739	1.57	1.56	.047	.044	.050
ATMOS	.711								
TAILP. AR=2									
X/W1	EXP	2D	AXI	EXP	2D	AXI	EXP	2D	AXI
2.65	.519	.535	.674	1.65	1.54	1.94	.029	.023	.045
4.64	.668	.697	.681	1.762	1.58	1.56	.047	.044	.050
6.04	.721	.753	.681	1.77	1.58	1.48	.058	.058	.054
8.04	.729	.753	.678	1.50	1.48	1.43	.061	.062	.058
12.05	.732	.751	.671	1.35	1.39	1.37	.059	.071	.066
17.72	.731	.747	-	1.29	1.35	-	.062	.084	-
27.35	.727	.739	-	1.28	1.32	-	.071	.105	-
33.78	.719	-							
39.03	.714	-							
42.38	.710								
PLENUM AR=3	EXP	2D	AXI	EXP	2D	AXI	EXP	2D	AXI
4.65	.426	.688	.764	1.592	1.62	2.43	0.021	.050	.106
6.31	.693	.768	.776	1.631	1.66	1.90	.050	.073	.120
11.06	.784	.879	.784	1.670	1.78	1.58	.076	.148	.136
ATMOS.	.788								
TAILPIPE AR=3	EXP	2D	AXI	EXP	2D	AXI	EXP	2D	AXI
2.64	.487	.587	.691	1.58	1.54	2.10	.027	.024	.052
6.31	.682	.796	.792	1.62	1.62	1.85	.051	.064	.107
11.06	.780	.886	.797	1.80	1.73	1.54	.083	.130	.120
15.76	.795	.897	.796	1.49	1.54	1.45	.086	.150	.128
19.76	.801	.897	.794	1.41	1.47	1.40	.097	.156	.136
31.76	.811	.896							
42.26	.812	.894							

TABLE VI (Contd.)

$2\phi = 15^{\circ}$

PLENUM AR 2	CP			H			2θ/W1		
X/W1	EXP	2D	AX1	EXP	2-D	AX1	EXP	2-D	AX1
0.66	.247	.270	.43	2.317	1.570	1.94	.005	.009	.014
2.64	.596	.662	.679	1.975	1.630	1.74	.014	.029	.044
ATMOS	.680								
TAILPIPE AR=2	EXP	2D	AX1	EXP	2-D	AX1	EXP	2-D	AX1
0.66	.249	.272	.44	1.704	1.59	1.92	.013	.009	.014
2.64	.612	.661	.685	2.124	1.64	1.73	.041	.031	.043
4.13	.703	.758	.687	2.282	1.65	1.54	.058	.046	.046
6.14	.724	.758	.686	1.531	1.49	1.45	.062	.052	.050
8.14	.730	.757	.683	1.381	1.43	1.405	.062	.057	.054
10.14	.731	.756	-	-	1.40	-	-	.060	-
12.14	.732	.755	-	1.287	1.38	-	.058	.066	-
16.14	.732	.752		-	1.38		-	.076	
24.13	.729	.747		1.243	1.34		.067	.090	
PLENUM AR-3	EXP	2D	AX1	EXP	2-D	AX1	EXP	2-D	AX1
2.64	.580	.661	SEP'N	1.827	1.64	(2.92) SEP'N	.036	.030	(.044) SEP'N
4.29	.663	.784		1.747	1.73		.045	.054	
7.27	.749	.894		1.650	1.90		.052	.118	
ATMOS	.761								
TAILPIPE AR=3	EXP	2D	AX1	EXP	2-D	AX1	EXP	2-D	AX1
2.64	.560	.664	SEP'N	1.75	1.65	(2.97) SEP'N	.034	.031	(.045) SEP'N
4.29	.639	.788		1.74	1.73		.051	.054	
7.27	.728	.889		1.81	1.91		.090	.112	
7.93	.744	.900		1.82	1.88		.094	.120	
13.94	.777	.900		1.30	1.52		.083	.134	
19.94	.792	.899		1.25	1.43		.082	.146	
27.93	.800	.898		1.24	1.35		.077	.162	
34.42	.801	.897							
38.29	.801	.896							
42.95	.802	.895							

Chapter Ten

POSSIBLE EXTENSIONS OF WORK.

X.1 Reynolds Number.

The present investigation has shown that diffuser performance is not as independent of inlet Re. as many workers assume. Therefore useful work could be carried out on the following:-

(i) The effect of Reynolds number on performance parameters for diffusers with both plenum and tailpipe discharge to determine the effect of tailpipe addition on Reynolds number dependance.

(ii) The effect of diffuser configuration (up to high divergence angles and area ratios) on Reynolds number effects.

(iii) The effect of Reynolds number on the inlet boundary layer parameters.

X.2 Boundary Layer Stability.

The present work indicates that there is a relationship between shape factor and displacement thickness which could be used to define the onset of boundary layer instability. Therefore if work was carried out with varying boundary layer thicknesses and shape factors by using more varied divergence angle diffusers than used in this work, with two area ratios to check the correlation. The relationship could then be accurately established, this would give a much better parameter than shape factor (H) for determining the onset of separation.

X.3 Theoretical Prediction.

The theoretical prediction method tested indicated that with large area ratios and thickening boundary layers the boundary layer prediction becomes increasingly inaccurate. Therefore the inclusion of some factor to allow for the reduction of entrainment with a thickening boundary layer could be usefully employed to increase the accuracy of this method at high area ratios and boundary layer thicknesses.

Chapter Eleven

MAIN CONCLUSIONS.

XI.1 The Reynolds Number Effects.

The Reynolds number investigation (chapter V11) shows conclusively that Cp is dependent on the inlet Reynolds number for all Reynolds numbers.
As the Reynolds number decreases the inlet boundary layer thickness, the momentum thickness, and the shape factor (H) increase. Also as the inlet boundary layer thickness is increased (by the addition of an inlet pipe) the Reynolds number dependance increases at the lower Reynolds numbers, indicating the sole reason for the increase in Cp with increasing Reynolds number is due to the reduction of the inlet boundary layer thickness, this is also shown by a reduction in momentum thickness and shape factor.

The Reynolds number dependence increases as the divergence angle increases and as the inlet boundary layer thickness and shape factor increase.
However the experimental results indicate that the results are within 1% for Reynolds numbers above 3×10^5, though there are indications that this error will increase for diffusers with divergence angles above 15^o. Therefore it can be concluded that the effects on performance of Reynolds number are as follows:-

1. For inlet Reynolds numbers above 3×10^5, the performance is independent of Reynolds number.
2. For very high divergence angle diffusers, stalled diffusers or diffusers in which a jet flow regime exists the Reynolds number dependence will increase and may be significant above 3×10^5.
3. That the optimum diffuser geometry is independent of Reynolds number (since as optimum configuration are approached then the Re dependence appears to reduce.)

Xl.2 Diffuser Investigation Conclusions

Xl.2.1 The Effect of the Boundary Layer Parameters.

Xl.2.1.1 Inlet Boundary Layer Thickness.

Increase of the inlet boundary layer thickness, defined in this work by the displacement thickness non-dimensionalised by dividing by the local duct width, has a severe effect on the perfomance of the diffuser causing a fall in pressure recovery and effectiveness. This effect is particularly noticeable in the case of the higher divergence angle diffusers (due to the higher dp/dx values), and there is a generally increased growth of the boundary layer parameters with the thicker inlet boundary layers thus indicating a slower rate of momentum transfer.

It can therefore be concluded from the results of this work that the smaller the inlet boundary layer thickness the higher will be the pressure recovery and the effectiveness of the diffuser.

Xl.2.1.2 Effects of Thickening the Boundary Layer

As the boundary layer thickens there is an increased tendency for the boundary layer to separate, (due to the lower rate of momentum transfer), however when the boundary layer is approaching a fully developed condition at inlet the pressure recovery falls by up to 40 - 50% of that of the thin inlet boundary layer case thus giving the appearance of an increased stability of the boundary layer as the inlet flow approaches a fully developed condition.

Xl.2.1.3 Shape Factor (H)

The inlet shape factor for the thin inlet boundary layer was particularly high (due mainly to the boundary layer trip wire). It can be seen from the profile figure 16a that there is a slight velocity deficiency on the centre-line, however, this would not affect the performance severely. The distortion due to the trip wire, however, would reduce the performance, due to the momentum deficiency of the boundary layer, this was most noticeable with the case of the high divergence angle diffusers in which high pressure gradients occur, and any deficiency of momentum in the inlet boundary layer is less likely to recover for these cases. Therefore the performance values for the high divergence angle diffusers may be lower than that which would normally expected.

As the boundary layer thickens in the diffuser the ability of the diffuser to withstand further diffusion is a function of both the boundary layer thickness and the shape factor. That is, with a small boundary layer thickness the flow is able to withstand highly distorted flows (i.e. high shape factor) whereas with a large boundary layer thickness a much smaller shape factor can be withstood before separation occurs. Thus it can be seen that there is an important link between the stability of the boundary layer, the displacement thickness and the shape factor, this is discussed more fully in paragraph X1.2.1.6

X1.2.1.4 Flow Unsteadiness.

The flow unsteadiness, that is the fluctuation of the static pressure with respect to the mean static pressure was at a low level for all this work. However it was noticable that the unsteadiness increased with the area ratio and divergence angle and was at a maximum at separation or onset of stall, indicating that the separations were neither symmetric or stable conditions.

X1.2.1.5 Kinetic Energy Correction Factor (α)

This parameter was calculated for the experimental results and the values of pressure recovery and effectiveness were corrected by the inclusion of this factor.

For the pressure recovery coefficient (Cp) the corrected value was always lower, since α_1 (inlet value) must always be less than 1.0. Though the error between Cp and Cp_E was never very large, due to the small inlet kinetic energy correction factor (largest for fully developed inlet flow conditions).

The effect on effectiveness is somewhat different, since the kinetic energy correction factor (α) of the developing boundary layer is taken into account. It was seen that for moderately high divergence angle diffusers ($2\phi = 15^{o}$) the effectiveness underestimated the energy corrected value severely therefore indicating that when a tailpipe is fitted the effectiveness will increase as the distortion, and therefore the α, of the boundary layer decreases. This effect becomes more marked as the divergence angle and the AR increase.

Generally it can be concluded that the distortion of the velocity profile causing the discrepancy between η and η_E, is an important consideration when designing a fluid flow system where a tailpipe is fitted, especially if plenum discharge data is used. The use of non energy corrected effectiveness would not only give a pessimistic assessment of the effectiveness but may also indicate a totally incorrect geometry for the optimum effectiveness of the system being designed.

XI.2.1.6 Flow Stability Criteria.

The use of a relationship between the kinetic energy correction factor ($\propto$) and the displacement thickness $2\delta^*/w$ is shown to be unreliable in predicting instability of the boundary layer, and similar displacement thicknesses and kinetic energy correction factors can have totally different flow stability.

Shape factor (H) which has often been postulated as a criterion for flow stability also does not define the area of instability adequately.

However, a relationship between shape factor (H) and the boundary layer stability, and could usefully be used in prediction techniques, such as the one tested using this work, to predict flow seperation. For very small boundary layer thicknesses, high shape factors of the order of 3.0 can be sustained without instability, whereas at higher boundary layer thicknesses above $2\delta^*/w = 0.2$, the limit of stability is constant at a value of shape factor of 2.0

XI.2.2 The Effect of Diffuser Geometry.

XI.2.2.1 Divergence Angle and Area Ratio.

The divergence angle and area ratio have similar effects on the performance of the diffuser. As the divergence angle increases the value of dp/dx and therefore distortion of the boundary layer increases, whereas with increasing AR the boundary layer thickness for a given divergence angle increases.

Therefore these two parameters are interdependent in determining the performance of a diffuser since a low divergence angle will give a high boundary layer thickness but a low $\frac{dp}{dx}$ value, and a high divergence angle, a high pressure gradient in conjunction with a thin boundary layer. Since the interdependence of distortion and boundary layer thicknesses has been mentioned previously, it must follow that for a particular inlet boundary layer conditions there must be optimum geometries for both pressure recovery and effectiveness.

X1.2.2.2. The Optimum Geometry

The optimum configuration for pressure recovery is between 7° and 10° at an area ratio of approximately 4, (for a thin inlet boundary layer). This will reduce both in area ratio and divergence angle as the inlet boundary layer thickens. The effect of these geometric parameters on diffuser effectiveness is similar except that the optimum diffuser effectiveness occurs at a lower area ratio, (approximately AR = 2.0).

An exception to this occurs with the inclusion of a tailpipe in the system. This increases the optimum area ratio, due to the reduction in the distortion of the boundary layer.

X1.3 The Addition of a Tailpipe

X1.3.1 The Effects with the Diffuser Geometry.

The inclusion of a tailpipe can be detrimental at low area ratios due to the diffusion which occurs outside the diffuser exit plane. However at higher area ratios and high divergence angles there is a marked improvement in all performance parameters, and infact the addition of a tailpipe has the effect of increasing the divergence angle at which the optimum performance occurs since the increased distortion of the boundary layer recovers inside the tailpipe and the inclusion of a tailpipe to a stalled diffuser results in a large performance increase.

X1.3.2 The Effect of the Tailpipe on the Diffuser Parameters.

There is a slight stabilising effect on the boundary layer within the diffuser transmitted from the tailpipe, thus increasing the divergence angle at which separation will occur. This effect however, is limited to cases of high boundary layer distortion, and at other conditions the effect of the tailpipe on the diffuser parameters is not measureable. This is also true within the tailpipe itself and if truncated at the maximum pressure position the parameters at that point remain the same, (within experimental error).

XI.3.3 Position of Peak Recovery in the Tailpipe.

As the boundary layer at the inlet thickens the advantage of the inclusion of a tailpipe increases. However the momentum transfer required to improve the boundary layer profile is slower and thus a longer tailpipe is required for the optimum pressure recovery. This is seen as a movement of the peak pressure position downstream as the inlet boundary layer thickens.

XI.3.4 The General Effects of Tailpipe Addition

It can be generally concluded that:

1. The inclusion of a tailpipe is only detrimental for a very low area ratio and for moderate divergence angles probably ~~20~~$^{\circ}$. $\leq 10^{\circ}$

2. For large area ratios, particularly with high divergence angles, the addition of a tailpipe always improves the performance.

3. There is no effect on the conditions within the diffuser transmitted upstream by the addition of a tailpipe. The exception to this is at the limit of flow stability where some stabilisation of the diffuser boundary layer is introduced by the addition of a tailpipe.

4. When a diffuser has stalled large increases in Cp can be obtained (up to 50%) by the inclusion of a tailpipe.

XI.4 Theoretical Prediction of Performance and Boundary Layer Parameters

XI.4.1 Pressure Recovery Coefficient (Cp) and Effectiveness (η)

The theoretical prediction technique tested gave very good correlation between theoretical and experimental performance parameters for the divergence angles tested, that is up to 15°, and providing the area ratio was not greater than 2.0. Above this area ratio the prediction technique becomes increasingly inaccurate. Increase in the inlet boundary layer thickness reduces the accuracy of the prediction though not markedly for the low area ratio cases (AR = 2).

XI.4.2 Prediction of Boundary Layer Parameters.

The prediction of the boundary layer thickness is accurate for small area ratio diffusers. Similarly the prediction of the momentum thickness is quite accurate for a small area ratio diffuser and a small divergence angle, but as the divergence angle or area ratio increase the prediction of the momentum thickness becomes increasingly inaccurate. However the momentum thickness is very small numerically and therefore accurate prediction of this parameter is very difficult. The prediction of shape factor (H) is quite accurate, for all the diffuser geometries tested except where flow instability or stall occurs. However even in the case of flow instability or stall the shape factor prediction can be seen to follow a similar trend to the actual results, though underestimating the actual value.

XI.4.3 Prediction of Separation of the Boundary Layer.

The prediction of separation of the boundary layer by the program is attempted by the use of a critical shape factor to define when separation will occur. The value of 2.8 used in this analysis is somewhat high and a value of 2.2 would seem to be a more suitable value, this would increase the accuracy of the prediction of separated flows. However it has been shown in chapter VIII that there is a definite relationship between the displacement thickness and shape factor at separation. Therefore the inclusion of a function of $2\delta^*/w$ and H to define separation could be included into the prediction program to give a more accurate prediction of separation.

XI.4.4 Error due to the Boundary Layer Interaction.

The error increase with thickening inlet boundary layers occurs not only with a thickening inlet boundary layer, but also with low divergence angle large area ratios. This is due to an interaction between the boundary layers on the opposing walls and since the basis of the prediction technique is that of a potential core existing at all times then this will obviously reduce the accuracy of the technique. The inclusion of some form of blockage factor depending upon the displacement thickness to allow for the interaction of the opposing boundary layers could be included to increase the accuracy with increasing boundary layer thickness.

REFERENCES.

1. GIBSON.

   Flow of water through pipes or passages having diverging boundaries.

   Trans. R. Soc. (Edinb.) 1913. Volume 48.

2. RENEAU, JOHNSTONE & KLINE.

   Performance of two dimensional diffusers.

   Report PD 8 Sept. 1964.

   Thermosciences Div., Dept. Mech. Eng. Stamford Univ. California.

3. VULLERS.

   Utilisation of outlet K.E. of blowers by means of diffusers.

   ZVDI Vo. 77, No. 31. 1933.

4. HUDIMITO B.

   The experimental results of diverging flows.

   Bulletin of Eng. Research Institute, Kyoto Univ. Vol 2 Sept. 1952.

5. KELNHOFFER & DERICK C.T.

   Tailpipe effects on gas turbine diffuser performance, with fully developed inlet conditions.

   A.S.M.E. Journal Eng. for Power. January 1971.

6. KLINE, WAITMAN & RENEAU.

   Effect of inlet conditions on performance of two dimensional diffusers.

   A.S.M.E. Journal Basic Eng. Sept. 1961.

7. MOORE & KLINE.

   Some effects of vanes and turbulence in two dimensional wide angled subsonic diffusers.

   N.A.C.A. TN 4080.

8. COCKRELL D. J. & KING A.L.

   A review of the literature on subsonic flow through diffusers.

   B.H.R.A. TN 902 1967.

9. SANDBORNE V.A.

   An equation for the mean velocity distribution of boundary layers.

N.A.S.A Memo. 2-5-59E.

10. KLINE S. J. & SANDBORNE V. A.

Flow models in boundary layer stall inception.

A.S.M.E. Journal Basic Eng. Sept. 1961.

11. RIPPL.

Experimental investigation on efficiency of slim conical diffusers and their behaviour with regards to flow separation.

Monthly Tech. Review. Vol. 2. No. 3 March 1958

12. BRADLEY O. C. & COCKRELL D. J.

Boundary layer methods applied to integral fluid problems.

Proc. of the 1970 Heat Transfer and Fluid Mech. Institute.

Stamford Univ. press. Stamford, California.

13. FOX & KLINE.

Flow regime data and design methods for curved subsonic diffusers.

A.S.M.E. Journal Basic Eng. Vol. 84. ser. D. Sept. 1963. pp 303 - 312.

14. COCHRAN D. L.

Use of short flat vanes in two dimensional diffusers.

N.A.C.A. Tech. Note 4309.

15. FERRETT E.F.C. & LAMPARD D.

Calculation method for the pressure recovery produced by diffusers fitted with tailpipes.

Paper 2, 1971, Dept. Mech. Eng. University of Nottingham.

16. REID.

Performance characteristics of plane walled two dimensional diffusers.

N.A.C.A. TN 2888

17. BRADSHAW P.

Performance of a diffuser with fully developed pipe flow at entry.

Journal Royal Aero Soc. Nov. 1963. Vol. 67.

18. BRADSHAW P.

Simple wind tunnel design.

N.P.L Aero Report 1258.

19. BRADSHAW P. & PANKHURST R. C.

Design of low speed wind tunnels.

N.P.L. Report 1039. June 1963

20. BROWN BOVERI REVIEW .

Calculation of rotationally symmetrical turbulent flow trough diffusers.
Brown Boveri Review . Vol.51, No.12 Dec.1964

21. FERRETT E. F. C.

Truncated conical diffusers.

Phd. thesis. Nottingham University, 1970

22. WALLACE F.J. .
Pressure pulsations in reciprocating compressor delivery systems.
J.Mech.Eng.Sc. Vol.8 No.2, 1966

23. KLINE S. J. & McCLINTOCK F. A.

Uncertainties of single sample experiments.

A.S.M.E. Journal of Basic Eng. 1971.

24. KUCHEMANN D.

Inviscid flow near the trailing edge of an aerofoil.
Z.Flugwiss 15, (1967), Heft 8/9

25. NICOLL W. B. & RAMARIAN B. R.

Modified entrainment theory for prediction of turbulent boundary layer growth in adverse press. gradients.

A.S.M.E. paper FE16 1969.

26. SALTER C.

Low speed wind tunnels for specific purposes.

N.P.L. Report 1218. Dec. 1966

27. YANG TAH - TEA.

Splitter effects in conical diffusers.

Bulletin 103 Eng. Exp. Station. College of Engineering Clemson Univ.

28. GREEN J. E.

Application of Heads entrainment method to prediction of turbulent boundary layer and wakes in compressible flow.

R.A.E. Technical Report 72079. April 1972

A review of incompressible diffuser flows.

Aircraft eng. Oct. 1963.

30. PANKHURST & HOLDER.

Wind tunnel technique.

Pitman text.

31. McDONALD A. T. & FOX R. W.

Incompressible flow in concial diffusers.

Purdue Technology report 1. Sept. 1964.

32. DUGGINS R. K.

The performance of conical diffusers discharging through tailpipes.

Aircraft Engineering. August 1970.

33. BORDA J.C.

Memoir on the flow of fluids through orifices of vessels.

Memoirs de l'Academic Royale Des Sciences.

34. VENTURI G. B.

Recherches experimentales sur le principe de communication lateral

dams les fluides. Paris 1797.

(Transl. in Nicholson's Journal of natural philosophy 3, London 1802)

35. LIVESEY J. L. & TURNER J.T.

The dependence of performance upon inlet flow conditions.

J. Roy. Aero. Soc. vol 69. November 1965

36. IDELCHIK I.E.

Handbook of hydraulic resistance; coefficient of local resistance

and friction.

Gosud. Energ. Izd. Moskva-Leningrad (1960) Translated by Israel

program for scientific translations for the U.S.A.E.C. and Nat.

Sci. Foundation U.S.A (Jan 1966).

37. COCKRELL D. J. & MARKLAND E.

Effects of inlet conditions on incompressible flow through conical

diffusers.

J. Royal Aeron. Soc. vol.66,613 , Jan. 1962

38. LIVESEY J.L. & HUGH T.

Suitable mean values in one dimensional gas dynamics.

J. Mech. Eng. Sci 8 No. 4, P374 (Dec. 1966).

39. DERRICK C.T.

Effect of the addition of a straight walled duct on diffuser performance with fully developed inlet conditions.

M.Sc. Thesis , School of Engineering and Architecture, Catholic University of America, Washington D.C. 1965

40. DUNCAN W.J., THOM A.S. & YOUNG A.D.

Mechanics of fluids, second edition.

Edward Arnold, Text, 1970

41. SCHLICHTING H.

Boundary layer theory (Translated by J. Kestin)

McGraw Hill, Text, 1963.

Other useful references not referred to in text:

Engineering Sciences Data Unit

Item 74015.

Performance in incompressible flow of plane walled diffusers with single-plane expansion.

MILLER D.S.

Performance of straight walled diffusers.

British Hydromechanics Research Association 1971

Two Dimensional diffusers with plenum and tail pipe discharge.
Vol. 2. Appendices.

B. W. Chilton.

PhD.

APPENDIX 1.

EXPERIMENTAL RIG DESIGN CALCULATIONS.

1.1 Experimental Rig Static Pressure Drop.

For the maximum flow required, that is $M = 0.2$, the mean flow velocity required would be 224 ft/s which corresponds to a flowrate (Q) of 112 cu ft/sec or 6850 cuft/min. This corresponds to an inlet Reynolds number of 3.5×10^5 (based on a 3" inlet width).

1.1.1 Settling Chamber Pressure Drop.

From N.P.L 1218 for a 2'0" x 2'0" settling chamber, with a flow velocity $\bar{u}_1$ o 28 ft/s would have the following loss coefficients.

'K' for honeycomb flow straighteners (2) = 0.5.

'K' for wire gauzes (5) = 0.2

Therefore $K_1 = 11$

Therefore $\Delta h_1 = -1.99$ inches w.g.

(Dynamic Head = 0.18 inches w.g.)

1.1.2 The Contraction.

The loss factor for the contraction 'K_2' = 0.05

Therefore $\Delta h_2 = 0.58$ inches w.g. (Dynamic head = 11.4 ins. w.g.)

1.1.3 The Inlet Duct.

From OLSON effective dia of the inlet duct = 4 x AREA/PERIMETER = hydraulic diameter.

Hydraulic diameter = 0.44ft. = Dh

Therefore effective Reynolds number = 6.16×10^5

Giving ; $f = 0.013$

The loss coefficient $K_3 = fL/Dh$

Therefore $\Delta h_3 = 0$ to 3.5 inches of w.g. depending on inlet boundary layer conditions required, that is the length of the inlet duct.

1.1.4 Diffuser.

For AR = 3, divergence angle 5^o.

$\Delta h_4 = 0.77$ inches w.g. (Dynamic head = + 10.29 inches w.g.)

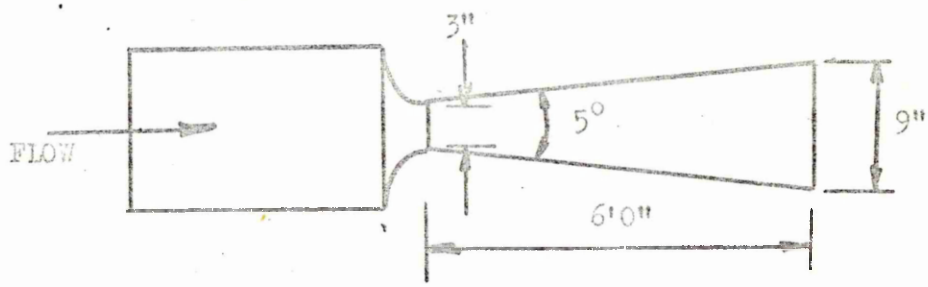

Case...1

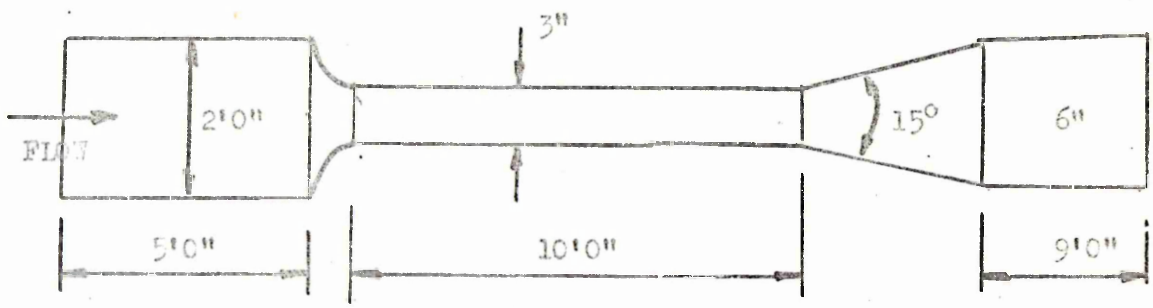

Case..2

REYNOLDS NO. $x10^{-5}$	CASE 1 "w. g.	CASE 2 "w. g.	APPROX. FLOW RATE Cu ft/min.
3.5	4.46	10.07	7000.
3.0	3.0	7.16	6000.
2.5	2.0	4.98	5000.
2.0	1.21	3.22	4000.

Reynolds no. based on 3" diffuser inlet width

71 Diffuser rig design conditions.

FIGURE.....71

For AR = 2, divergence angle 15°

Δh_4 = 0.86 inches w.g. (Dynamic head = + 8.68 inches w.g.)

1.1.5 Tailpipe.

For AR = 2, L = 9 exit diameters.

Δh_5 = 0.42 inches w.g.

For AR = 3, L = 9 exit diameters

Δh_5 = 0.28 inches w.g.

1.1.6 Plenum Discharge.

Loss coefficient 'K' = 1.0

AR = 2; Δh_6 = 2.89 inches w.g.

AR = 3; Δh_6 = 1.29 inches w.g.

1.1.6 The Cases Considered.

The two extreme cases considered were:-

(1) AR = 3, $2\phi = 5^{\circ}$, thin inlet boundary layer and plenum discharge.

(2) AR = 2, $2\phi = 15^{\circ}$, fully developed inlet flow and tailpipe discharge.

The maximum and minimum values of static pressure drop for the rig were calcualted using the above two configurations.

For case 1; 4.46 inches w.g. being the minimum pressure drop.

For case 2; 10.07 inches of water gauge for the maximum pressure drop.

This shown for other inlet Reynolds numbers in figure 71.

Therefore a pump of 12" water gauge minimum delivery pressure at a flow of 7000 cuft/min. Also to allow the flow to be varied to the lower flow conditions a radial damper is required, this would increase the flow resistance slightly, but would be easily catered for in the 12 inches water gauge pressure fan requirement.

1.1.7 Power Requirements.

Therefore the minimum fan requirement is 10.07 static pressure drop plus the dynamic head at the fan outlet this gives a power requirement of $Q \times \Delta h_T \times \rho_w$. which for the design case is 15 H.P.

If the fan is assumed to be 80% efficient a power requirement of 20H.P input would be required. Therefore a motor size of 25 H.P. was decided upon.

1.2 Rotation of Pitot Traverse due to Air Flow.

1.2.1 Basic Data used for Calculation.

Diameter of traverse = 0.032 inches.

Maximum extensions = 4.5 inches

= 3.0 inches.

Calculations based on an inlet Reynolds number of 3.5×10^5, mean velocity $\bar{U}$ = 224 ft/s, $\bar{U}$ in tailpipe ≈ 112 ft/s (AR = 2)

Re_p (based on pitot in tailpipe) = 1.89 x 10

Drag coefficient from PAO Cd ≈ 0.95

Though due to turbulence of flow, drag may be considerably reduced.

Fd (Drag force)/unit length - (foot) =

$Cd \frac{1}{2} \rho u^2 A$

Assuming flat velocity profile of 112 ft/s

Fd ≈ 0.04215 lbf/ft or 0.00351 lbf/in.

For an area ratio of 3, $\bar{U}$ = 74.6 ft/s

$Re_p = 1.26 \times 10^3$, Cd = 1.00.

Therefore Fd = 0.00156 lbf/in.

1.2.2 Rotation of End of Pitot Traverse subjected to Flow with a Flat Velocity Profile.

Figure 72 shows the assumptions made for this analysis.

$M = Rx - M_R - \frac{Fdx^2}{2}$ = bending moment at x.

Therefore $EI \frac{d^2y}{dx^2} = Rx - M_R - \frac{Fdx^2}{2}$

Therefore $\frac{dy}{dx} EI = Rx^2/2 - M_R x - Fdx^3/6 + A$ -----(1)

When x = 0, dy/dx = 0, therefore A = 0

Moments about wall

$= M_R - FdL^2/2 - 0$, therefore $M_R = FdL^2/2$ -------(2)

Moments about end.

$RL - M_R - FdL^2/2 = 0$

Therefore substituting (2)

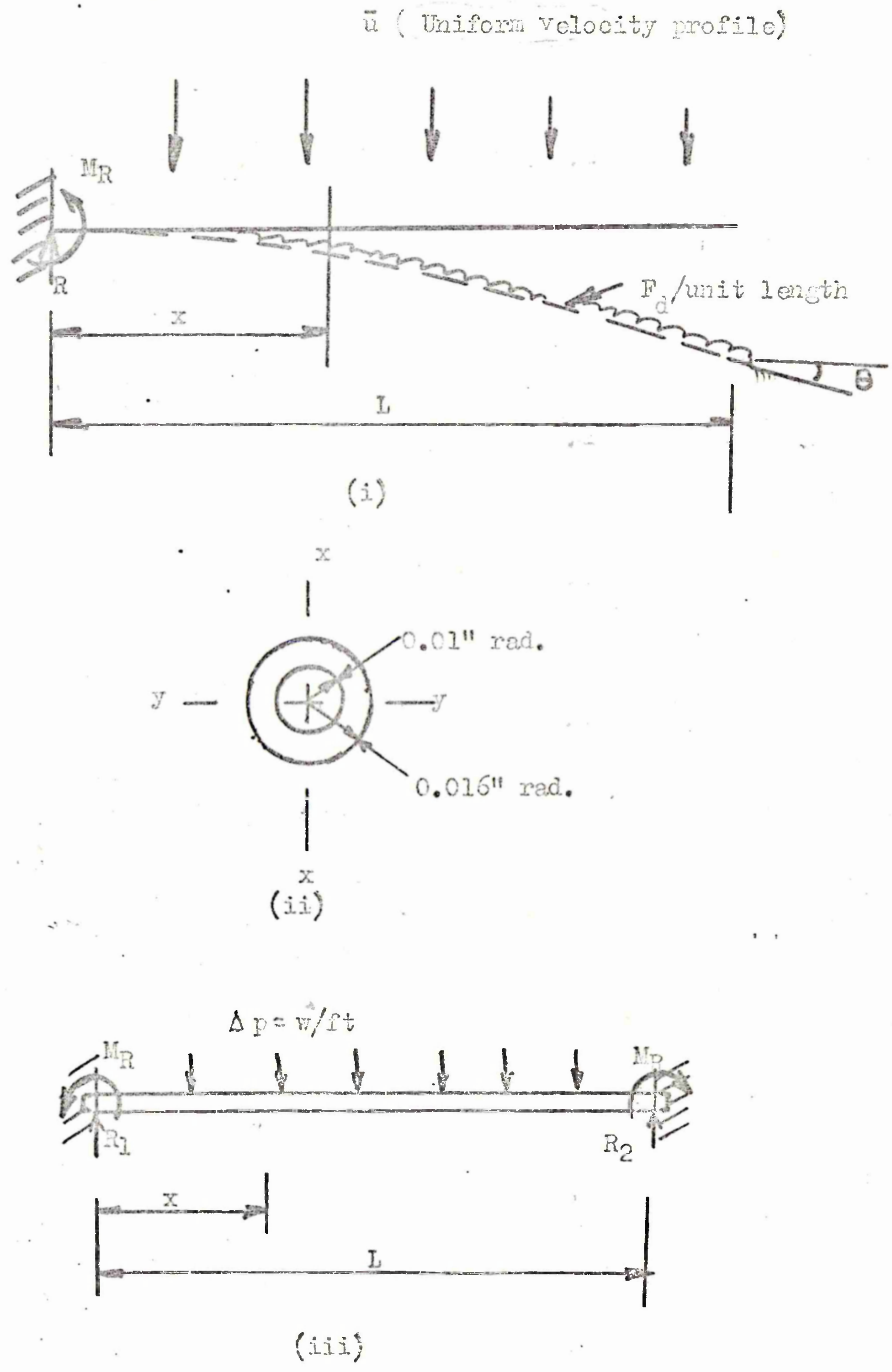

72 Pitot probe and sidewall models.

FIGURE....72

$RL - FdL^2/2 - FdL^2/2 = 0$

Therefore $R = FdL$ ---- - -----(3)

Substitute (2) and (3) in (1)

$$\frac{dy}{dx} EI = FdLx^2/2 - FdL^2x/2 - Fdx^3/6 \quad \text{-- -- ---} \quad \text{-(1a)}$$

Therefore subsitute in (1a) for $x = L$ i.e. pitot end.

$$\frac{dy}{dx} EI = -FdL^3/6$$

From figure 72 (ii) the polar second moment of area $= \pi/2 \, (R^4 - r^4)$

Therefore $Ixx = \pi/4 \, (R^4 - r^4)$

$= 4.362 \times 10^{-8}$ in^4

Therefore $\frac{dy}{dx}$ at end of pitot traverse in tailpipe if traversed $4\frac{1}{2}$" (in 6" duct)

$$dy/dx = \frac{1}{EI} \times \frac{FdL^3}{6} = 0.04073$$

Therefore $\theta = 2^{o}20'$ for AR of 3 with a $4\frac{1}{2}$" traverse.

$dy/dx = 0.0181$

$\theta = 1^{o}2'$

Thus the maximum cosine error will be given for the $2^{o}20'$ rotation case. The error for this rotation will be 0.08% i.e. less than 0.1% therefore was considered insignificant.

1.3 Maximum Deflection of the Duct Wall.

Figure 72(iii) shows how this anlysis was carried out with the assumption of a uniform pressure at a section producing a uniformly distributed load of w/ft. The wall has been likened to a built in beam since the end positions are not free to rotate. The analysis is not strictly correct since it assumes the wall to be made up of strips not connected to their neighbouring strips. This will incur a slight error which will tend to overestimate the deflection. However for the thicknesses and lengths being considered this will be insignificant.

Bending moment at x.

$= Rx - wx^2/2 - M_{\ell} = M$

also $R_1 = wL/2$

$M = wLx/2 - wx^2/2 - M_R$

Therefore $M = wLx/2 - wx^2/2 - M_R$ -------------(1)

since $\frac{d^2yEI}{dx^2} = M$ ----(2), at $x = 0, L/2, dy/dx = 0$ equating (2) and (1) and integrating. Then substituting for the above conditions in the expressions for dy/dx and y, we obtain the solution:

$$yEI = \frac{wL^4}{4.96}$$

Since the maximum static pressure on the rig is of the region of -7.5" w.g. The maximum deflection will occur at the duct centreline and will be 0.035". However it may be noted that pressures of this order will only be experienced in the inlet pipe.

At the outlet from the contraction and inlet to the diffuser and along the inlet pipe there are substantial flanges reinforced by 1" square steel stiffners to prevent this deflection being so severe and the maximum measured was 0.01" in the inlet pipe

1.4 Transition to Turbulent Boundary Layer using a Trip Wire.

PANKHURST and HOLDER give the following relationships:-

$Uod/\nu \;\; 600$ -----------(1)

$Uod/\nu \;\; 36\,(Uox/\nu)^{\frac{1}{2}}$ ----------(2)

where d = diameter of trip wire

x = distance from leading edge.

using $\nu = 1.6 \times 10$

$Uo = \bar{U} = 200$ft/s

from (1)

$d > 0.575 \times 10^{-2}$ inches.

However for low Reynolds number where $\bar{U}$ may be substantially lower a more realistic value of $d > 1.00 \times 10^{-2}$ inches.

Similarly from (2) with a value of x = 1.0 inches.

$d > 5.0 \times 10^{-3}$ inches.

Similarly this may be substantially higher for the lower Reynolds number tests therefore a trip wire diameter of 0.01" at 1" from the end of the contraction was used for the experimental rig. That is 0.25mm. diameter, 25mm.

APPENDIX 2.

PRELIMINARY INVESTIGATION ON AXI SYMMETRIC RIG.

This rig consisted of a 3 inch internal diameter brass tube 20ft long, consisting of two 10 ft. long tube s connected by a flanged coupling in the centre and with a bellmouth at the inlet.

The original rig was checked for alignment of the two pipes shown by figure 73 and re-aligned as shown to reduce the effect of a step as much as possible, especially in the areas where measurements were to be taken. The 'perspex' traverse positions were then manufactured to the form shown in figure 12.

To determine the best method of securing the tapping blocks to the tube a tensile test with two brass strips connected by a piece of perspex was carried out. Two tests for each adhesive were carried out (Araldite and Tensol No. 7). The results of this test were that for Araldite the joint broke at a mean force of 0.55 kN whereas the mean for the tensol cement case was 0.98 kN. However, the joint did not break in shear on the adhesive/perspex joint as in the Araldite case but fractured the perspex stips therefore the stength of the joint would be considerably higher than this value. (The area of the joints were 200 sq. mm). This test showed conclusively that the adhesive to use for a brass/perspex joint was Tensol No. 7 cement.

The tube was then marked out as shown in figure 11 (a) and drilled. The tapping blocks were than cemented in position (using dummy tappings to accurately position the blocks). After this the actual static pressure tappings to be used were inserted and the whole pipe interior honed to de-burr the tappings and to polish the interior. A boundary layer trip wire was then attached (similar to in the main rig) 1 inch in from the bell mouth intake and then the whole rig levelled by means of adjusting the support points to remove any significant deflections of the pipe assembly which might influence the flow.

A data reduction program was then written to analyse the experimental work on the boundary layer growth with distance can be seen in figure 13. Typical

ERRORS IN WALL THICKNESS LOOKING IN
FLOW DIRECTION

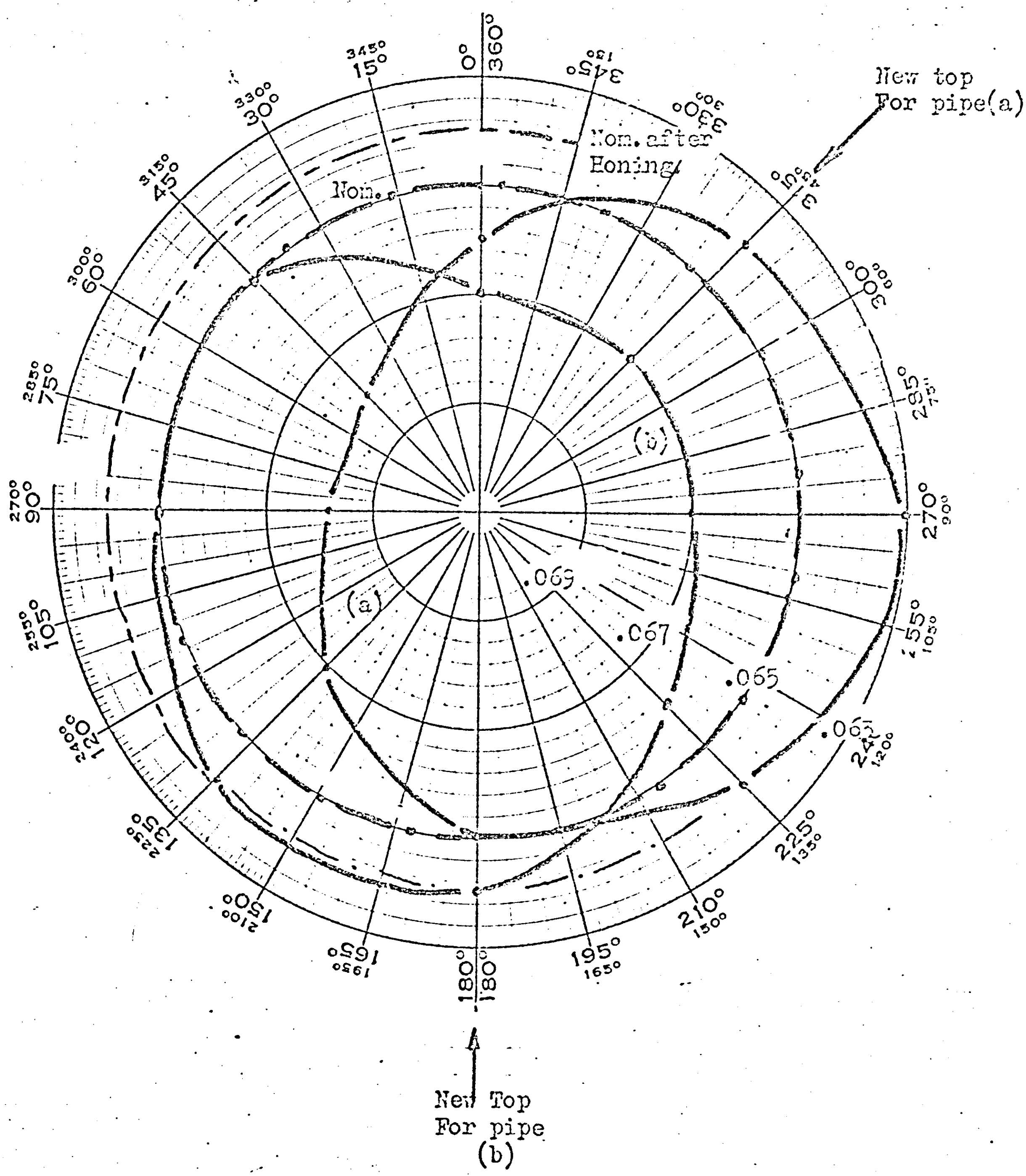

FIGURE.....73

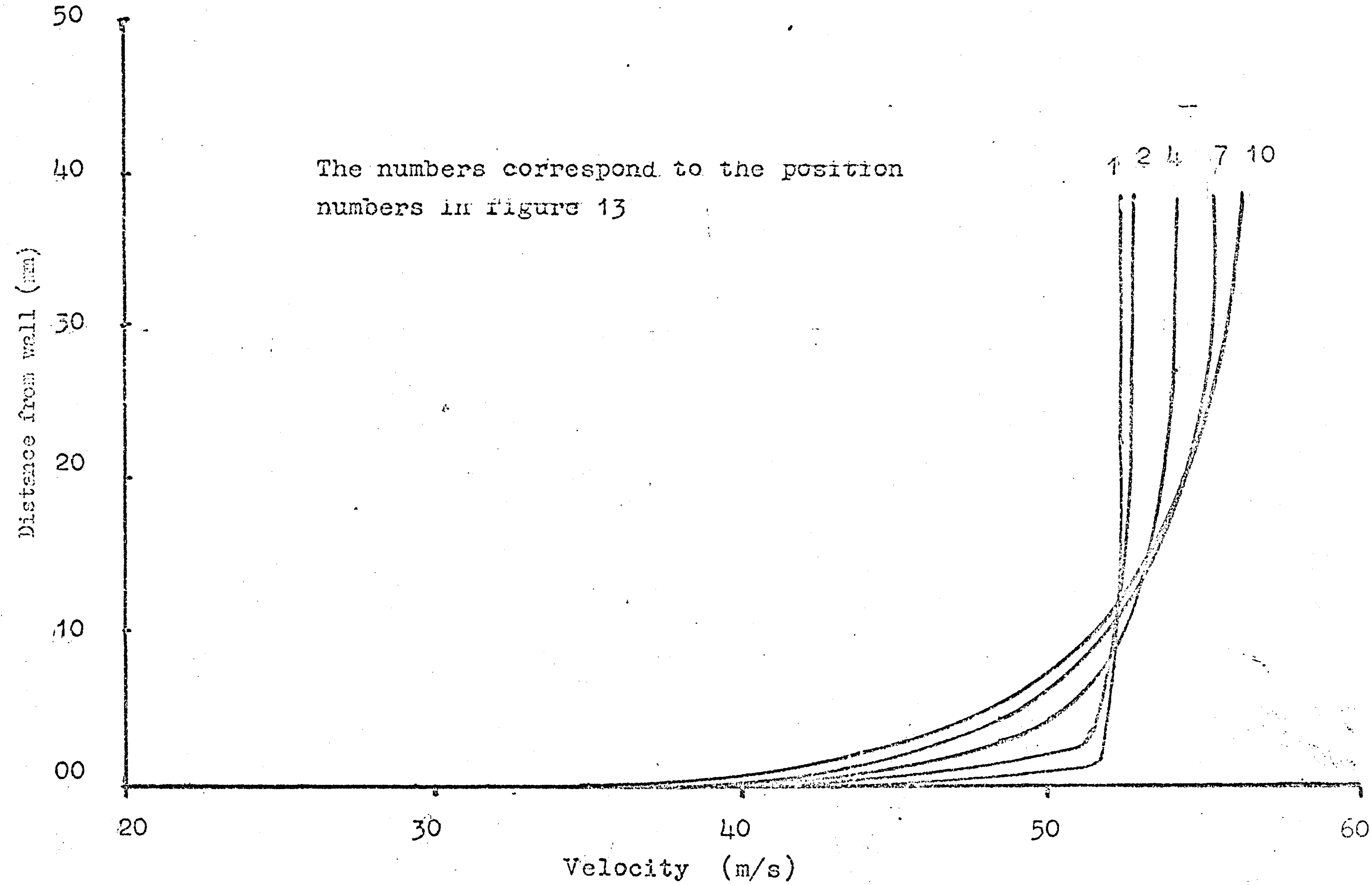

The developing axisymmetric velocity profile

FIGURE...74

profiles obtained from the rig are shown in Figure 74.

APPENDIX 3.

THE INLET PIPE/DIFFUSER INTERFACE STREAMLINE CURVATURE.

To determine the effect of streamline curvature at the inlet pipe/diffuser interface on the static pressure, the static pressure was measured along the inlet pipe; A typical set of results is shown in table VII and table VIII. The results were plotted against the distance from the diffuser inlet plane (shown in figure 75). This clearly shows the effect of distortion of the streamlines at inlet to the diffuser. However the magnitude is small, approximately 2% lower than the unaffected or 'effective' value.

The 'effective' value of the diffuser inlet static pressure was obtained by extrapolating the results taken sufficiently upstream of the diffuser not to be affected by the streamline curvature at the inlet plane.

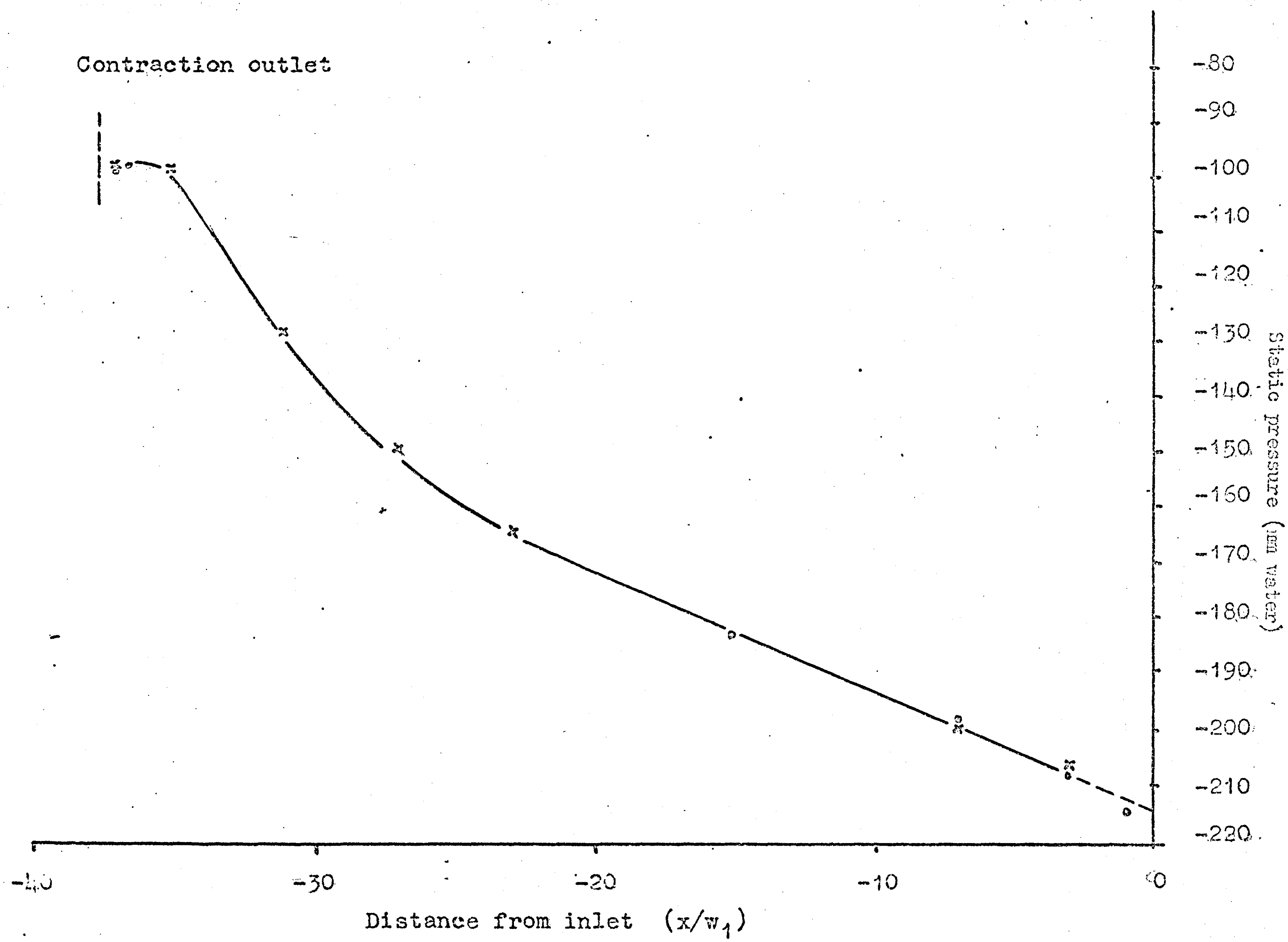
Contraction outlet
-80
-90
-100
-110
-120
-130
-140
-150
-160
-170
-180
-190
-200
-210
-220
Static pressure (mm water)
-30
-20
-10
0
Distance from inlet (x/w1)

FIGURE....75

INLET B/L THICKNESS = 0.0000 DIV. ANGLE = 10DEG.. AREA RATIO = 3, TAILPIPE LENGTH = 2.740M . RUN NO.

POSN	WIDTH M/M	DIST FROM INLET	STATIC PRESS. M/M H2O	MEAN VEL. M/S	LOCAL REYNOLDS NUMBER	2DELTA* ------- WIDTH	2THETA ------ WIDTH	SHAPE FACTOR	K.E.CORR. FACTOR	PRESS. RECOV. COEFF.	EFFECT-IVENESS	ENERGY CORR. EFFECT.	E C
1	76.2	36.500	-154.	76.9	390361.	0.0132	0.0063	2.078	1.020	0.000	1.000	0.000	0
2	76.2	35.000	-154.	0.0	0.	0.0000	0.0000	0.000	0.000	0.000	1.000	0.000	0
3	76.2	31.000	-198.	0.0	0.	0.0000	0.0000	0.000	0.000	0.000	1.000	0.000	0
4	76.2	27.000	-222.	0.0	0.	0.0000	0.0000	0.000	0.000	0.000	1.000	0.000	0
5	76.2	23.000	-226.	0.0	0.	0.0000	0.0000	0.000	0.000	0.000	1.000	0.000	0
6	76.2	19.000	-250.	0.0	0.	0.0000	0.0000	0.000	0.000	0.000	1.000	0.000	0
7	76.2	15.000	-249.	0.0	0.	0.0000	0.0000	0.000	0.000	0.000	1.000	0.000	0
8	76.2	7.000	-269.	0.0	0.	0.0000	0.0000	0.000	0.000	0.000	1.000	0.000	0
9	76.2	3.000	-275.	0.0	0.	0.0000	0.0000	0.000	0.000	0.000	1.000	0.000	0
10	76.2	1.000	-280.	0.0	0.	0.0000	0.0000	0.000	0.000	0.000	1.000	0.000	0

POSN.	BETA	C/L VEL.	TEMP.	ATM.PRESS.	X/W1	
1	1.009	78.1	18.0	753.4	36.500	36.5
2	0.000	0.0	18.0	753.4	******	35.0
3	0.000	0.0	18.0	753.4	******	31.0
4	0.000	0.0	18.0	753.4	******	27.0
5	0.000	0.0	18.0	753.4	******	23.0
6	0.000	0.0	18.0	753.4	******	19.0
7	0.000	0.0	18.0	753.4	******	15.0
8	0.000	0.0	18.0	753.4	51.863	7.0
9	0.000	0.0	18.0	753.4	39.370	3.0
10	0.000	0.0	18.0	753.4	13.123	1.0

TABLE VII

Distance from trip wire in cont.		Undimensionalised dist. from inlet.	Static pressure tappings.	Pitot stations.	Comments.
Inches	mm	x/w	mm H O	mm H O	$2\phi = 15^{\circ}$, AR = 2
112.5	-	0	-	-	
109.5	2781	-1.0	-215	-210	3" from inlet
103.5	2629	-3.0	-208	-206	
91.5	2324	-7.0	-198	-199	
79.5	2019	-11.0	-184	-176	2" after flange
67.5	1715	-15.0	-183	-177	
55.5	1410	-19.0	-187	-175	
43.5	1105	-23.0	-96	-164	checked (96)
31.5	800	-27.0	-161	-149	
19.5	495	-31.0	-150	-128	
7.5	190	-35.0	-156	-98.5	Flange
3.0	76	-36.5	-98	-98	exit from
1.5	38	-37.0	-99	-98	contraction.

Table VIII.

THE DATA REDUCTION PROGRAM.

4.1 Input of Data.

The experimental data is analysed as shown in figure 27 (The flow diagram) by a computer program on an 1130 IBM computer.

The data was input as follows:

1. Divergence angle, area ratio, tailpipe length and the number of the run.
2. The atmospheric pressure and temperature.
3. The width of the duct at the first position, the static pressure at the position, the centreline at dynamic pressure at that position, and the position number.
4. The number of readings taken at a particular spacing - 1, and the distance a between the readings (mm).
5. The data was then read in. Cards 4 and 5 were then repeated until all the readings at that station had been input.
6. The next station data was then input as in 3 to 5 this was repeated until all the data for the stations had been run, then any additional runs were analysed by starting from card 1 again until all the data required to be analysed had been input.

4.2 The Analysis of the Experimental Data.

The density was calculated from the static pressure, the viscosity was also calculated from the expression:-

$$(4.84 \times 10^{-3} \times (T + 273.2)) + 0.394) \times 10^{-5} \quad \text{-----------------(1)}$$

When T = ambient temperature in ^{o}c.

The velocity was then calculated for each experimental point taken for the relationship $V(I) = 2p\,(I)/\rho$ -----------(2)

where (I) is the array used for that set of data a value of flow deficiency was then calculated (Used to calculate δ^{*})

$DEL(I) = 1 - V(I)/Uo$ --------------(3)

and also a momentum deficiency term

DF MOM(I) - (1 - V(I)/Uo) × V(I)/Uo ------- - ---(4)

Then the kinetic energy and momentum at that particular point were calculated and stored in an array (I).

AKE(I) $= \frac{1}{2} \times V(I)^3 \times \rho$ --- --(5)

AMOM(I) = $V(I)^2 \times \rho$ -------(6)

These parameters were then integrated for the set of data in the array using a Simpson's rule subroutine which included a routine for the $\frac{3}{8}$'ths rule for use on the last four values if an odd number of values was read in. Using this subroutine the parameters were calculated by integrating the data for each block input and then summing the results to find the value for the particular station being analysed. The parameters calculated using this technique were:

(a) Flow (m^3/s)

(b) Mass Flow (kg/s)

(c) Displacement Thickness.

(d) Momentum Thickness.

(e) Flow Kinetic Energy.

(f) Flow Momentum.

From these values and the previously calculated values the following parameters were calculated.

(g) Reynolds Number.

(h) α

(i) β

(k) $\tilde{u}$

(l) H

(m) Cp

(n) Cp_E

(o) η

(p) η_E

(q) λ

The values of velocity for each point was stored in an array together with its corresponding value of distance from the wall, for each station Cp, Cp_E η and η_E were also stored in an array with its corresponding value of x/w_1. After the run had been analysed these values, that is, vel/distance from the wall, and Cp, Cp_E, η, and $\eta_E/x/w_1$, were plotted by the computer. This had the advantage of showing any obvious erronious results or even punching errors which had not been detected.

The data reduction program used can be seen in figure 76 and typical outputs in appendix 5 and 6.

DATA REDUCTION PROGRAM.

FIGURE...76

...... F O R T R A N   S O U R C E   S T A T E M E N T S

```
SUBROUTINE SIMSN(FN,A,N)
DIMENSION FN(50)
COMMON H
L=0
A=0.0
MM=N
M=N/2
B=N/2.0
C=B-M
```

```
...STNO.C.....  F O R T R A N   S O U R C E   S T A T E M E N T S  ........

         IF(C-0.4)1,2,2
   2     L=1
   6     N=N-3
         IF(N)1,5,1
   1     A=FN(1)+FN(N+1)
         J=2
         K=2
         DO3I=2,N
         J=J+K
         A=A+J*FN(I)
   3     K=-K
         A=A*H/3.0
         IF(L-1)4,5,5
   5     N=MM
         A=A+0.375*H*(FN(N-2)+3.0*FN(N-1)+3.0*FN(N)+FN(N+1))
   4     RETURN
         END

RENCED STATEMENTS


ES SUPPORTED
ORD INTEGERS
ARD PRECISION

EQUIREMENTS FOR - SIMSN
N-      2,   VARIABLES AND TEMPORARIES-      18,    CONSTANTS AND PROGRAM-    234

VE ENTRY POINT ADDRESS IS 0020 (HEX)

 SUCCESSFUL COMPILATION



      WS   UA   SIMSN              1111
  1111    DB ADDR   5AF7    DB CNT    0011


   *IOCS(CARD,1403PRINTER,DISK,PLOTTER,TYPEWRITER,KEYBOARD)
   *LIST SOURCE PROGRAM
   *ONE WORD INTEGERS

 ..STNO.C.....  F O R T R A N   S O U R C E   S T A T E M E N T S  ........

         INTEGER AR
         INTEGER DIV
         INTEGER RUN
         EXTERNAL SIMSN
          DIMENSION AMOM(30)
         DIMENSION V(30),DELP(30),DEL(30),DFMOM(30),AKE(30),VMEAN(30),
        1W(30),P(30),DELTA(30),THETA(30),UTHET(30),UDEL(30),SHAPE(30)
        1,AK(30),ALP(30),CP(30),ETA(30),ENETA(30),LAMDA(30),WM(30),DI(30),
        1RENC(30) ,CVEL(30),ATMPR(30) ,ATEM(30)
```

```
'O.C..... F O R T R A N   S O U R C E   S T A T E M E N T S ........ IDEN

   DIMENSION CPE(30) ,BETA(30)
    DIMENSION VEL(100),Y(100)
   DIMENSION XW(30)
   COMMON H
   NOTE    PLACE BLANK CARD BETWEEN EACH SET  OF DATA
   DATA IN THE FOLLOWIING UNITS &
   DI = DISTANCE FROM INLET TO RIG  I.E. AFTER CONTRACTION
   WM = WIDTH IN M/M
   AWM(WIDTH) IN M/M, NTOT = TOTAL NUMBER OF READINGS AT A PARTICULAR
   POSITION, SPRES = STATIC PRESSURE, TEMP IN DEGREES CENTIGRADE
   ATMP = ATMOSPHERIC PRESSURE IN M/M MERCURY
   DELPC = CENTRELINE TOTAL PRESSURE IN M/M WATER,
   POSN = THE NUMBER GIVEN TO THE PARTICULAR LOCATION
   ADI = THE DISTANCE FROM THE INLET (I.E. AFTER CONTRACTION) TO THE POSIT
   IN METRES
    WRITE(1,65)
   FORMAT(1X,'PLEASE READY PLOTTER , PLACE PEN **EXACTLY** 1.0 INCH
  1FROM RIGHT HAND EDGE , THEN PRESS START ')
    PAUSE
   READ(2,81)DIV,AR,TL,RUN
   READ(2,291)ATMP,TEMP
    IF(RUN)42,42,64
   CONTINUE
    ********NORMAL PLOTTING SCALES  ********************
    CALL SCALF(0.065,0.074,0.0,0.0)
    CALL FPLOT(1,160.0,0.0)
    CALL SCALF(0.065,0.074,0.0,0.0)
    CALL FGRID(0,0.0,0.0,10.0,8)
    CALL FGRID(1,0.0,0.0,10.0,12)
    CALL FCHAR(-10.0,30.0,0.12,0.15,1.57)
    WRITE(7,651)
    FORMAT('DISTANCE FROM WALL (IN M/M)')
   CALL FCHAR(20.0,-8.0,0.12,0.15,0.0)
    WRITE(7,652)
    FORMAT('VELOCITY (METRES/SEC)')
    DO 660 I=1,12
    YI=I*10.0
   CALL FCHAR(-8.0,YI,0.1,0.1,0.0)
    WRITE(7,661)YI
    FORMAT(F4.0)
    CONTINUE
    DO 662 I=1,8
    X=I*10.0
   XI=I*10.0-3.0
    CALL FCHAR(XI,-3.0,0.1,0.1,0.0)
    WRITE(7,663)X
    FORMAT(F4.0)
    CONTINUE
   CALL FCHAR(40.0,123.0,0.1,0.1,0.)
    WRITE(7,670)RUN
    FORMAT('RUN NO. ',I4)
    CALL FPLOT(1,0.0,0.0)
    CALL FPLOT(2,0.0,0.0)
    *********END OF NORMAL PLOTTING SCALES ************
```

```
300    CONTINUE
       GOTO1
3      INLET=POSN
        ETA(INLET)=1.0
1      CONTINUE
       READ(2,290)AWM,SPRES,DELPC,ADI,POSN
100    CONTINUE
       IF(AWM)40,40,2
2      CONTINUE
       J=POSN+0.01
        ABET=0.0
        AMCM(J)=0.0
        BET=0.0
        BETA(J)=0.0
        AAK=0.0
       FLOW=0.0
       FLOWM=0.0
       DELTS=0.0
       DEFM=0.0
       AKEN=0.0
       NT=0.0
       VMEAN(J)=0.0
        UDEL(J)=0.0
        UTHET(J)=0.0
        SHAPE(J)=0.0
        RENC(J)=0.0
        ALP(J)=C.0
        CP(J)=0.0
       CPE(J)=0.0
        ENETA(J)=0.0
C      WM IN M/M
       W(J)=AWM*0.001
         P(J)=SPRES
C        AWM=VALUE OF WIDTH READ IN IN M/M FOR POSN. TO BE CALCULATE
         DI(J)=ADI
         WM(J)=AWM
       XW(J)=DI(J)/W(INLET)
       WRITE(5,9)AWM,POSN,RUN
       WRITE(5,31)ATMP,TEMP
       WRITE(5,34)DELPC
       DENSY=ATMP*13.6*9.81/(287.4*(TEMP+273.2))
       AMU=((4.84*0.001*(TEMP+273.2))+0.394)*0.00001
       ANU=AMU/DENSY
       WRITE(5,10)DENSY,AMU,ANU
       U=SQRT(2.0*DELPC*9.81/DENSY)
        ATMPR(J)=ATMP
       ATEM(J)=TEMP
       CVEL(J)=U
        AY=0.0
        L=1
C       READS H IN M/M
       READ(2,33)NN,H
       WRITE(5,13)NN,H
```

```
      H=H*0.001
       VEL(L)=C.0
      IF(NN)401,401,6
6     NNN=NN+1
C     DELP IN M/M WATER
      READ(2,32)(DELP(K),K=1,NNN)
      DO7I=1,NNN
      IF(DELP(I))605,606,606
605   DELP(I)=-DELP(I)
      V(I)=SQRT(2*DELP(I)*9.81/DENSY)
      V(I)=-V(I)
      GO TO 607
606   V(I)=SQRT(2*DELP(I)*9.81/DENSY)
607   CONTINUE
       Y(L)=AY
       VEL(L)=V(I)
       L=L+1
       AY=AY+1000.0*H
      DEL(I)=1-V(I)/U
      DFMOM(I)=(1-V(I)/U)*V(I)/U
      AKE(I)=V(I)**3*DENSY
        AMOM(I)=V(I)**2*DENSY
7     CONTINUE
       AY=AY-1000.0*H
      L=L-1
      WRITE(5,35)
      WRITE(5,12)(DELP(K),K=1,NNN)
      WRITE(5,36)
      WRITE(5,12)(V(I),I=1,NN)
        CALL SIMSN(V,Q,NN)
      FLOW=FLOW+Q*2.0
      CALL SIMSN(DEL,DELS,NN)
      DELTS=DELTS+DELS
      CALL SIMSN(DFMOM,DMOMS,NN)
      DEFM=DEFM+DMOMS
      CALL SIMSN(AKE,AKEN,NN)
       AAK=AAK+AKEN
       CALL SIMSN(AMOM,ABET,NN)
      BET=BET+ABET
      READ(2,33)NN,H
      WRITE(5,13)NN,H
        H=H*0.001
71    CONTINUE
      IF(NN)6,8,6
8     VMEAN(J)=FLOW/W(J)
        FLOWM=FLOW*DENSY
      RENO(J)=VMEAN(J)*W(J)/ANU
        DELTA(J)=DELTS
        THETA(J)=DEFM
        SHAPE(J)=DELTA(J)/THETA(J)
       AK(J)=AAK
        ALP(J)=2*AK(J)/(FLOWM*VMEAN(J)**2)
      UDEL(J)=2*DELTA(J)/W(J)
       BETA(J)=2.*BET/(FLOWM*VMEAN(J))
```

```
      UTHET(J)=2*THETA(J)/W(J)
        WRITE(5,15)VMEAN(J)
        WRITE(5,14)FLOW
        WRITE(5,16)FLOWM
      WRITE(5,17)RENO(J)
        WRITE(5,18)DELTA(J)
        WRITE(5,19)THETA(J)
        WRITE(5,37)UDEL(J),UTHET(J)
        WRITE(5,20)SHAPE(J)
        WRITE(5,21)AK(J)
        WRITE(5,22)ALP(J)
      DO802I=1,L
      CALL FPLOT(0,VEL(I),Y(I))
802   CONTINUE
      CALL FCHAR(VEL(L),Y(L),0.08,0.08,0.0)
      WRITE(7,655)J
655   FORMAT(I2)
       CALL FPLOT(1,0.0,0.0)
      CALL FPLOT(2,0.0,0.0)
9     FORMAT(' WIDTH = ',F5.1,' POSITION = ',F3.0,' RUN NO. ',I4)
10    FORMAT(11H DENSITY = ,F9.7,17H DYN VISCOSITY = ,F9.7,23H KINEMATI
     1 VISCOSITY  = ,F9.7)
12    FORMAT(1H ,15F7.2)
13    FORMAT(1X,I3,1X,F8.5)
14    FORMAT(8H, FLOW = ,F9.6)
15    FORMAT(17H MEAN VELOCITY = ,F9.2)
16    FORMAT(13H MASS FLOW = ,F9.6)
17    FORMAT(16H REYNOLDS NO. = ,F9.2)
18    FORMAT(10H DELTA* = ,F7.5)
19    FORMAT(9H THETA = ,F7.5)
20    FORMAT(16H SHAPE FACTOR = ,F5.3)
21     FORMAT(16H KINETIC ENERGY = ,F11.1)
22    FORMAT(32H K.E.CORRECTION FACTOR(ALPHA) = ,F6.4 ,/// )
290   FORMAT(F5.1,1X,F6.1,F6.2,F6.3,F3.0)
291   FORMAT(F5.1,F5.1)
30    FORMAT(3F6.2,1X,F3.0)
31    FORMAT(20H ATMOSPHERIC PRESS. ,F6.2,19H ATMOSPHERIC TEMP. ,F6.2)
32    FORMAT(16F5.1)
33    FORMAT(I3,1X,F6.2)
34    FORMAT(35H CENTRELINE DYN HEAD (M/M WATER) = ,F6.2)
35    FORMAT(26H DYN HEAD IN M/M WATER =     )
36    FORMAT(24H VELOCITY IN METRES/SEC.,)
37    FORMAT(13H 2DELTA*/W = ,F6.4,3X,12H 2THETA/W = ,F6.4)
401   CONTINUE
       IF(W(J)-W(1))3,3,41
41    CP(J)=9.81*(P(J)-P(INLET))/(0.5*DENSY*VMEAN(INLET)**2)
      IF(VMEAN(J))412,411,412
411   ETA(J)=9.81*(P(J)-P(INLET))/(0.5*DENSY*VMEAN(INLET)**2*(1.0-W(INLE
     1T)**2/W(J)**2))
      GO TO 50
412   ETA(J)=9.81*(P(J)-P(INLET))/(0.5*DENSY*(VMEAN(INLET)**2-VMEAN(J)**
     12))
      ENETA(J)=9.81*(P(J)-P(INLET))/(0.5*DENSY*(VMEAN(INLET)**2*ALP(INLE
```

S...STNO.C...... F O R T R A N   S O U R C E   S T A T E M E N T S ....

```
      1T)-ALP(J)*VMEAN(J)**2))
       LAMDA(J)=1-ETA(J)
 50    CONTINUE
       CPE(J)=CP(J)/ALP(INLET)
       GO TO 1
 40    CONTINUE
       WRITE(5,80)UDEL(INLET),DIV,AR,TL,RUN
       WRITE(5,60)
       WRITE(5,61)
       WRITE(5,62)
 59    FORMAT(1H1)
 60    FORMAT(120H POSN  WIDTH  DIST  STATIC  MEAN  LOCAL  2DELTA*  2TH
      1ETA  SHAPE  K.E.CORR.  PRESS.  EFFECT-  ENERGY  ENERGY        ;
      1)
 61    FORMAT(120H               FROM  PRESS.  VEL.  REYNOLDS -------  ---
      1---  FACTOR  FACTOR   RECOV.  IVENESS  CORR.   CORR.          ;
      1)
 62    FORMAT(120H          M/M    INLET M/M H2O M/S    NUMBER   WIDTH   WID
      1TH                   COEFF.            EFFECT.   CP.          ;
      1)
 63    FORMAT(I3,2X,F5.1,2X,F6.3,2X,F5.0,2X,F4.1,2X,F8.0,2X,F7.4,2X,F6.4,
      12X,F5.3,3X,F5.3,6X,F5.3,3X,F5.3,3X,F5.3,3X,F5.3)
       DO70I=1,J
 70    WRITE(5,63)I,WM(I),DI(I),P(I),VMEAN(I),RENO(I),UDEL(I),UTHET(I),SH
      1APE(I),ALP(I),CP(I),ETA(I),ENETA(I),CPE(I)
 600   FORMAT('  POSN.  BETA  C/L VEL.  TEMP.  ATM.PRESS.  X/W1 '/)
       WRITE(5,604)
 604   FORMAT(1X,//)
         WRITE(5,600)
        DO 601 I=1,J
 601   WRITE(5,602)I,BETA(I),CVEL(I),ATEM(I),ATMPR(I),XW(I)
 602   FORMAT(4X,I2,5X,F5.3,2X,F5.1,5X,F4.1,4X,4X,F5.1,4X,F6.3)
C*************PLOTTING ROUTINE FOR CP +ETA  VS DISTANCE FROM INLET ****
       CALL SCALF(0.065,0.074,0.0,0.0)
        CALL FPLOT(1,160.0,0.0)
        DI(INLET)=0.0
        ADI=DI(J)
        XA=ADI/0.2
        NS=XA
        XS=5/ADI
        CALL SCALF(XS,7.8,0.0,0.0)
        CALL FGRID(0,0.0,0.0,0.2,NS)
        CALL FGRID(1,0.0,0.0,0.1,10)
        XSC=ADI/10.
        XSN=XSC/1.5
       CALL FCHAR(-XSC,0.2,0.12,0.15,1.57)
        WRITE(7,700)
 700    FORMAT('PRESS. RECOV. COEFF. + EFFECTIVENESS')
        DO 711 I=1,10
        YCP=I*0.1
        CALL FCHAR(-XSN,YCP,0.1,0.1,0.0)
 711    WRITE(7,701)YCP
 701    FORMAT(F3.1)
        XCH=XSC
```

```
      CALL FCHAR(XCH,-0.08,0.12,0.15,0.0)
       WRITE(7,702)
702    FORMAT('DISTANCE FROM DIFFUSER INLET (METRES)')
       DO 709 I=1,NS
       IF(ADI-2.0)712,712,7111
7111  I=I+1
712   XL=I*0.2
       XLL=XL-ADI*.02
       CALL FCHAR(XLL,-0.03,0.1,0.1,0.0)
709    WRITE(7,703)XL
703    FORMAT(F3.1)
       CALL FPLOT(1,0.0,0.0)
       CALL FPLOT(2,0.0,0.0)
       DO 704 I=INLET,J
       CALL FPLOT(1,DI(I),CP(I))
       CALL FPLOT(2,DI(I),CP(I))
       CALL POINT(0)
      CALL FPLOT(1,DI(I),CPE(I))
      CALL FPLOT(2,DI(I),CPE(I))
      CALL POINT(2)
704    CONTINUE
       CALL FCHAR(DI(J),CP(J),0.1,0.1,0.0)
       WRITE(7,705)
705    FORMAT(' CP.')
       CALL FPLOT(1,0.0,0.0)
       CALL FPLOT(2,0.0,0.0)
       DO 706I=INLET,J
       CALL FPLOT(1,DI(I),ETA(I))
       CALL FPLOT(2,DI(I),ETA(I))
       CALL POINT(1)
      CALL FPLOT(1,DI(I),ENETA(I))
      CALL FPLOT(2,DI(I),ENETA(I))
      CALL POINT(3)
706    CONTINUE
       CALL FCHAR(DI(J),ETA(J),0.1,0.1,0.0)
       WRITE(7,707)
707    FORMAT(' EFF.')
708    CONTINUE
       CALL FCHAR(0.2,1.2,0.1,0.1,0.0)
       WRITE(7,710)RUN
710    FORMAT('    RUN NO. ',I4)
       CALL FPLOT(1,0.0,0.0)
C      *********END OF PLOTTING ROUTINE **************
80    FORMAT(1H1,'INLET B/L THICKNESS = ',F6.4,'  DIV. ANGLE = ',I2,'DEG
     1.,  AREA RATIO = ',I1,', TAILPIPE LENGTH = ',F5.3,'M  , RUN NO. ',
     1I4,////)
81    FORMAT(I2,1X,I2,1X,F5.3,1X,I4)
      WRITE(5,59)
      READ(2,81)DIV,AR,TL,RUN
810   READ(2,291)ATMP,TEMP
      IF(RUN)42,42,64
42    CALL EXIT
      END
```

APPENDIX 5

Reynolds number test results.

Test No.	Reynolds No.	Configuration
1	4.68×10^5	10° AR 3 Tailpipe thin boundary
2	4.44×10^5	
3	4.25×10^5	
4	2.25×10^5	
5	1.44×10^5	
6	1.07×10^5	
7	2.61×10^5	
8	3.02×10^5	
9	0.61×10^5	
10	4.08×10^5	
20	3.5×10^5	5° AR 2 Tailpipe thick boundary layer
21	2.9×10^5	
22	2.0×10^5	
23	1.4×10^5	
24	0.57×10^5	
30	4.0×10^5	10° AR 3 tailpipe thick boundary layer.
31	3.6×10^5	
32	2.9×10^5	
33	2.3×10^5	
34	1.7×10^5	
35	0.6×10^5	

Test No.	Reynolds No.	Configuration.
40	4.0×10^5	15° AR 2 tailpipe fully developed
41	3.9×10^5	
42	3.5×10^5	
43	3.2×10^5	
44	2.6×10^5	
45	2.2×10^5	
46	1.5×10^5	
50	4.3×10^5	10° AR 3 tailpipe fully developed.
51	3.8×10^5	
52	3.4×10^5	
53	2.4×10^5	
54	1.8×10^5	
55	1.4×10^5	

**** INLET B/L THICKNESS = 0.014,DIV. ANGLE = 10DEG., AREA RATIO = 3,TAILPIPE LENGTH = 1.830M , RUN NO.

POSN	WIDTH M/M	DIST FROM INLET	STATIC PRESS. M/M H2O	MEAN VEL. M/S	LOCAL REYNOLDS NUMBER	2DELTA* ------- WIDTH	2THETA ------ WIDTH	SHAPE FACTOR	K.E.CORR. FACTOR	PRESS. RECOV. COEFF.	EFFECT-IVENESS	ENERGY CORR. EFFECT.	ENER CCRR CI
1	0.1	******	0.	-0.0	********	0.0000	0.0000	0.000	0.000	0.000	0.000	*****	***
2	76.0	-0.038	-420.	93.9	468363.	0.0149	0.0095	1.567	1.011	0.000	0.000	0.000	0.0C
3	0.2	******	*****	-0.0	0.	0.0000	0.0000	*****	*****	*****	*****	0.000	***
4	7.7	-0.000	0.	-0.0	0.	0.0000	0.0000	0.000	*****	*****	*****	0.000	***
5	0.7	******	0.	-0.0	0.	0.0000	0.1503	0.000	*****	*****	*****	0.000	0.0C
6	0.2	-0.000	*****	-0.0	-0.	0.0000	0.0000	0.000	*****	*****	0.000	0.000	***
7	213.0	0.784	-29.	45.0	629496.	0.1101	0.0692	1.590	1.098	0.732	0.951	0.965	0.72
8	4.9	******	0.	-0.0	********	0.4980	0.0000	0.000	*****	*****	0.000	0.000	***
9	0.0	******	580.	-0.0	********	0.4980	0.0000	0.000	0.000	0.000	*****	0.000	***
10	10.8	******	580.	****	-0.	0.4980	0.4966	0.000	0.000	0.418	*****	0.000	0.0C
11	*****	******	*****	0.0	********	0.4980	0.0000	0.000	0.000	0.000	0.000	*****	***
12	0.0	******	*****	0.0	********	0.4980	0.0000	0.000	*****	0.000	*****	0.000	***
13	*****	******	*****	-0.0	-0.	0.4980	0.0000	0.000	*****	0.000	0.000	0.000	***
14	*****	******	*****	0.0	********	0.4980	0.0000	0.000	*****	0.000	*****	*****	***
15	229.0	2.116	-5.	36.3	546310.	0.1394	0.1028	1.356	1.065	0.777	0.914	0.912	0.76

**** INLET B/L THICKNESS = 0.014,DIV. ANGLE = 10DEG., AREA RATIO = 3,TAILPIPE LENGTH = 1.830M , RUN NC.

POSN	WIDTH M/M	DIST FRCM INLET	STATIC PRESS. M/M H2O	MEAN VEL. M/S	LOCAL REYNOLDS NUMBER	2DELTA* ------- WIDTH	2THETA ------ WIDTH	SHAPE FACTOR	K.E.CORR. FACTOR	PRESS. RECOV. COEFF.	EFFECT-IVENESS	ENERGY CORR. EFFECT.	ENER CORR CP
1	0.1	******	0.	-0.0	********	0.0000	0.0000	0.000	0.000	0.000	0.000	*****	****
2	76.0	-0.038	-375.	87.9	444899.	0.0146	0.0091	1.606	1.011	0.000	0.000	0.000	0.00
3	0.2	******	*****	-0.0	0.	0.0000	0.0000	*****	*****	*****	*****	0.000	****
4	7.7	-0.000	0.	-0.0	0.	0.0000	0.0000	0.000	*****	*****	*****	0.000	****
5	0.7	******	0.	-0.0	0.	0.0000	0.1503	0.000	*****	*****	*****	0.000	0.00
6	0.2	-0.000	*****	-0.0	-0.	0.0000	0.0000	0.000	*****	*****	0.000	0.000	****
7	113.0	0.784	-26.	79.9	601817.	0.2147	0.1389	1.546	0.307	0.739	4.293 ?	0.977	0.73
8	4.9	******	0.	-0.0	********	0.4980	0.0000	0.000	*****	*****	0.000	0.000	****
9	0.0	******	580.	-0.0	********	0.4980	0.0000	0.000	0.000	0.000	*****	0.000	****
10	10.8	******	580.	****	-0.	0.4980	0.4966	0.000	0.000	0.418	*****	0.000	0.00
11	*****	******	*****	0.0	********	0.4980	0.0000	0.000	0.000	0.000	0.000	*****	****
12	0.0	******	*****	0.0	********	0.4980	0.0000	0.000	*****	0.000	*****	0.000	****
13	*****	******	*****	-0.0	-0.	0.4980	0.0000	0.000	*****	0.000	0.000	0.000	****
14	*****	******	*****	0.0	********	0.4980	0.0000	0.000	*****	0.000	*****	*****	****
15	129.0	2.116	-3.	61.4	527669.	0.2419	0.1791	1.350	0.337	0.788	1.540	0.930	0.77

**** INLET B/L THICKNESS = 0.015,DIV. ANGLE = 10DEG., AREA RATIO = 3,TAILPIPE LENGTH = 1.830M , RUN NC

PCSN	WIDTH M/M	DIST FRCM INLET	STATIC PRESS. M/M H2O	MEAN VEL. M/S	LOCAL REYNOLDS NUMBER	2DELTA* ------- WIDTH	2THETA ------ WIDTH	SHAPE FACTOR	K.E.CORR. FACTOR	PRESS. RECOV. COEFF.	EFFECT-IVENESS	ENERGY CORR. EFFECT.	ENE CCR C
1	0.1	******	0.	-0.0	********	0.0000	0.0000	0.000	0.000	0.000	0.000	*****	***
2	76.0	-0.038	-345.	84.1	425566.	0.0150	0.0094	1.586	1.011	0.000	0.000	0.000	0.C
3	0.2	******	*****	-0.0	0.	0.0000	0.0000	*****	*****	*****	*****	0.000	***
4	7.7	-0.000	0.	-0.0	0.	0.0000	0.0000	0.000	*****	*****	*****	0.000	***
5	0.7	******	0.	-0.0	0.	0.0000	0.1503	0.000	*****	*****	*****	0.000	0.C
6	0.2	-0.000	*****	-0.0	-0.	0.0000	0.0000	0.000	*****	*****	0.000	0.000	***
7	213.0	0.784	-24.	40.8	579202.	0.1150	0.0730	1.574	1.099	0.742	0.971	0.986	0.7
8	4.9	******	0.	-0.0	********	0.4980	0.0000	0.000	*****	*****	0.000	0.000	***
9	0.0	******	580.	-0.0	********	0.4980	0.0000	0.000	0.000	0.000	*****	0.000	***
10	10.8	******	580.	****	-0.	0.4980	0.4966	0.000	0.000	0.418	*****	0.000	0.C
11	*****	******	*****	0.0	********	0.4980	0.0000	0.000	0.000	0.000	0.000	*****	***
12	0.0	******	*****	0.0	********	0.4980	0.0000	0.000	*****	0.000	*****	0.000	***
13	*****	******	*****	-0.0	-0.	0.4980	0.0000	0.000	*****	0.000	0.000	0.000	***
14	*****	******	*****	0.0	********	0.4980	0.0000	0.000	*****	0.000	*****	*****	***
15	229.0	2.116	-3.	33.5	510914.	0.1321	0.0978	1.350	1.062	0.792	0.941	0.939	0.7

**** INLET B/L THICKNESS = 0.015,DIV. ANGLE = 10DEG., AREA RATIO = 3,TAILPIPE LENGTH = 1.830M , RUN

POSN	WIDTH M/M	DIST FROM INLET	STATIC PRESS. M/M H2O	MEAN VEL. M/S	LOCAL REYNOLDS NUMBER	2DELTA* ------- WIDTH	2THETA ------ WIDTH	SHAPE FACTOR	K.E.CORR. FACTOR	PRESS. RECOV. COEFF.	EFFECT-IVENESS	ENERGY CORR. EFFECT.	E C
1	0.1	******	0.	-0.0	********	0.0000	0.0000	0.000	0.000	0.000	0.000	*****	*
2	76.0	-0.038	-93.	43.9	224827.	0.0154	0.0100	1.541	1.011	0.000	0.000	0.000	0
3	0.2	******	*****	-0.0	0.	0.0000	0.0000	*****	*****	*****	*****	0.000	*
4	7.7	-0.000	0.	-0.0	0.	0.0000	0.0000	0.000	*****	*****	*****	0.000	*
5	0.7	******	0.	-0.0	0.	0.0000	0.1503	0.000	*****	*****	*****	0.000	0
6	0.2	-0.000	*****	-0.0	-0.	0.0000	0.0000	0.000	*****	*****	0.000	0.000	*
7	212.8	0.784	-6.	32.4	460162.	0.1147	0.0700	1.639	1.108	0.723	1.589	1.775	0
8	4.9	******	0.	-0.0	********	0.4980	0.0000	0.000	*****	*****	0.000	0.000	*
9	0.0	******	580.	-0.0	********	0.4980	0.0000	0.000	0.000	0.000	*****	0.000	*
10	10.8	******	580.	****	-0.	0.4980	0.4966	0.000	0.000	0.418	*****	0.000	0
11	*****	******	*****	0.0	********	0.4980	0.0000	0.000	0.000	0.000	0.000	*****	*
12	0.0	******	*****	0.0	********	0.4980	0.0000	0.000	*****	0.000	*****	0.000	*
13	*****	******	*****	-0.0	-0.	0.4980	0.0000	0.000	*****	0.000	0.000	0.000	*
14	*****	******	*****	0.0	********	0.4980	0.0000	0.000	*****	0.000	*****	*****	*
15	228.6	2.116	-0.	33.5	510914.	0.1321	0.0978	1.350	1.062	0.769	1.836	1.952	0

**** INLET B/L THICKNESS = 0.008,DIV. ANGLE = 10DEG., AREA RATIO = 3,TAILPIPE LENGTH = 1.830M , RUN

POSN	WIDTH M/M	DIST FRCM INLET	STATIC PRESS. M/M H2O	MEAN VEL. M/S	LOCAL REYNOLDS NUMBER	2DELTA* ------- WIDTH	2THETA ------ WIDTH	SHAPE FACTOR	K.E.CORR. FACTOR	PRESS. RECOV. COEFF.	EFFECT-IVENESS	ENERGY CORR. EFFECT.	E C
1	0.1	******	0.	-0.0	********	0.0000	0.CCCO	0.CCO	0.000	0.C00	0.00C	*****	*
2	76.0	-0.038	-38.	28.1	143741.	0.0087	0.0035	2.470	1.011	0.C00	0.000	0.000	0
3	0.2	******	*****	-0.0	0.	0.0000	0.C000	*****	*****	*****	*****	0.000	*
4	7.7	-0.000	0.	-0.0	0.	0.0000	0.0000	0.000	*****	*****	*****	0.000	*
5	0.7	******	0.	-0.0	0.	0.0000	0.1503	C.000	*****	*****	*****	0.000	0
6	0.2	-0.C00	*****	-0.0	-0.	0.0000	0.CCCO	0.C00	*****	*****	0.00C	0.000	*
7	212.8	0.784	-2.	32.4	460162.	0.1147	0.0700	1.639	1.108	0.722	*****	*****	0
8	4.9	******	0.	-0.0	********	0.4980	0.C000	0.000	*****	*****	0.00C	0.000	*
9	0.0	******	580.	-0.0	********	0.4980	0.CC00	0.CC0	0.000	0.C00	*****	0.000	*
10	10.8	******	580.	****	-0.	0.4980	0.4966	0.000	0.C00	0.418	*****	0.000	0
11	*****	******	*****	0.0	********	0.4980	0.CCC0	0.C00	0.000	0.C00	0.00C	*****	*
12	0.0	******	*****	0.0	********	0.4980	0.CCC0	0.CC0	*****	0.C00	*****	0.000	*
13	*****	******	*****	-0.0	-0.	0.4980	0.CC00	0.000	*****	0.C00	0.CCC	0.000	*
14	*****	******	*****	0.0	********	0.4980	0.0C00	0.C0C	*****	0.C00	*****	*****	*
15	228.6	2.116	-0.	33.5	510914.	0.1321	C.0978	1.350	1.062	0.769	*****	*****	0

**** INLET B/L THICKNESS = 0.010,DIV. ANGLE = 10DEG., AREA RATIO = 3,TAILPIPE LENGTH = 1.830M , RUN

POSN	WIDTH M/M	DIST FROM INLET	STATIC PRESS. M/M H2O	MEAN VEL. M/S	LOCAL REYNOLDS NUMBER	2DELTA* ------- WIDTH	2THETA ------- WIDTH	SHAPE FACTOR	K.E.CORR. FACTOR	PRESS. RECOV. COEFF.	EFFECT-IVENESS	ENERGY CORR. EFFECT.	E C
1	0.1	******	0.	-0.0	********	0.0000	0.0000	0.000	0.000	0.000	0.000	*****	*
2	76.0	-0.038	-21.	20.9	107351.	0.0107	0.0048	2.203	1.012	0.000	0.000	0.000	0
3	0.2	******	*****	-0.0	0.	0.0000	0.0000	*****	*****	*****	*****	0.000	*
4	7.7	-0.000	0.	-0.0	0.	0.0000	0.0000	0.000	*****	*****	*****	0.000	*
5	0.7	******	0.	-0.0	0.	0.0000	0.1503	0.000	*****	*****	*****	0.000	0
6	0.2	-0.000	*****	-0.0	-0.	0.0000	0.0000	0.000	*****	*****	0.000	0.000	*
7	212.8	0.784	-1.	32.4	460162.	0.1147	0.0700	1.639	1.108	0.722	*****	*****	0
8	4.9	******	0.	-0.0	********	0.4980	0.0000	0.000	*****	*****	0.000	0.000	*
9	0.0	******	580.	-0.0	********	0.4930	0.0000	0.000	0.000	0.000	*****	0.000	*
10	10.8	******	580.	****	-0.	0.4980	0.4966	0.000	0.000	0.418	*****	0.000	0
11	*****	******	*****	0.0	********	0.4980	0.0000	0.000	0.000	0.000	0.000	*****	*
12	0.0	******	*****	0.0	********	0.4980	0.0000	0.000	*****	0.000	*****	0.000	*
13	*****	******	*****	-0.0	-0.	0.4980	0.0000	0.000	*****	0.000	0.000	0.000	*
14	*****	******	*****	0.0	********	0.4980	0.0000	0.000	*****	0.000	*****	*****	*
15	228.6	2.116	-0.	33.5	510914.	0.1321	0.0978	1.350	1.062	0.762	*****	*****	0

**** INLET B/L THICKNESS = 0.010,DIV. ANGLE = 10DEG., AREA RATIO = 3,TAILPIPE LENGTH = 1.830M , RUN N

POSN	WIDTH M/M	DIST FROM INLET	STATIC PRESS. M/M H2O	MEAN VEL. M/S	LOCAL REYNOLDS NUMBER	2DELTA* ------- WIDTH	2THETA ------ WIDTH	SHAPE FACTOR	K.E.CORR. FACTOR	PRESS. RECOV. COEFF.	EFFECT- IVENESS	ENERGY CORR. EFFECT.	EN CO
1	0.1	******	0.	-0.0	********	0.0000	0.0000	0.000	0.000	0.000	0.000	*****	**
2	76.0	-0.038	-122.	50.9	260619.	0.0106	0.0052	2.033	1.011	0.000	0.000	0.000	0.
3	0.2	******	*****	-0.0	0.	0.0000	0.0000	*****	*****	*****	*****	0.000	**
4	7.7	-0.000	0.	-0.0	0.	0.0000	0.0000	0.000	*****	*****	*****	0.000	**
5	0.7	******	0.	-0.0	0.	0.0000	0.1503	0.000	*****	*****	*****	0.000	0.
6	0.2	-0.000	*****	-0.0	-0.	0.0000	0.0000	0.000	*****	*****	0.000	0.000	**
7	212.8	0.784	-8.	32.4	460162.	0.1147	0.0700	1.639	1.108	0.708	1.192	1.260	0.
8	4.9	******	0.	-0.0	********	0.4980	0.0000	0.000	*****	*****	0.000	0.000	**
9	0.0	******	580.	-0.0	********	0.4980	0.0000	0.000	0.000	0.000	*****	0.000	**
10	10.8	******	580.	****	-0.	0.4980	0.4966	0.000	0.000	0.418	*****	0.000	0.
11	*****	******	*****	0.0	********	0.4980	0.0000	0.000	0.000	0.000	0.000	*****	**
12	0.0	******	*****	0.0	********	0.4980	0.0000	0.000	*****	0.000	*****	0.000	**
13	*****	******	*****	-0.0	-0.	0.4980	0.0000	0.000	*****	0.000	0.000	0.000	**
14	*****	******	*****	0.0	********	0.4980	0.0000	0.000	*****	0.000	*****	*****	**
15	228.6	2.116	-0.	33.5	510914.	0.1321	0.0978	1.350	1.062	0.754	1.329	1.366	0.

**** INLET B/L THICKNESS = 0.014,DIV. ANGLE = 10DEG., AREA RATIO = 3,TAILPIPE LENGTH = 1.830M , RUN N

POSN	WIDTH M/M	DIST FROM INLET	STATIC PRESS. M/M H2O	MEAN VEL. M/S	LOCAL REYNOLDS NUMBER	2DELTA* ------- WIDTH	2THETA ------ WIDTH	SHAPE FACTOR	K.E.CORR. FACTOR	PRESS. RECOV. COEFF.	EFFECT-IVENESS	ENERGY CORR. EFFECT.	EN CO
1	0.1	******	0.	-0.0	********	0.0000	0.0000	0.000	0.000	0.000	0.00C	*****	**
2	76.0	0.038	-171.	59.1	302454.	0.0145	0.0091	1.593	1.011	0.000	0.00C	0.000	0.
3	0.2	******	*****	-0.0	0.	0.0000	0.C000	*****	*****	*****	*****	0.000	**
4	7.7	-0.000	0.	-0.0	0.	0.0000	0.CC00	0.030	*****	*****	*****	0.000	**
5	0.7	******	0.	-0.0	0.	0.0000	0.1503	0.000	*****	*****	*****	0.000	0.
6	0.2	-0.000	*****	-0.0	-0.	0.0000	0.C000	0.000	*****	*****	0.000	0.000	**
7	212.8	0.784	-11.	32.4	460162.	0.1147	0.0700	1.639	1.108	0.733	1.048	1.081	0.
8	4.9	******	0.	-0.0	********	C.4980	C.C000	0.000	*****	*****	0.00C	0.000	**
9	0.0	******	580.	-0.0	********	0.4980	0.0000	0.000	0.000	0.000	*****	0.000	**
10	10.8	******	580.	****	-0.	0.4980	0.4966	0.000	0.000	0.418	*****	0.000	0.
11	*****	******	*****	0.0	********	0.4980	0.C000	0.000	0.000	0.000	0.00C	*****	**
12	0.0	******	*****	0.0	********	0.4980	0.C000	0.000	*****	0.000	*****	0.000	**
13	*****	******	*****	-0.0	-0.	0.4980	0.C000	0.000	*****	0.000	0.000	0.000	**
14	*****	******	*****	0.0	********	0.4980	0.0000	0.000	*****	0.C00	*****	*****	**
15	228.6	2.116	-1.	33.5	510914.	0.1321	0.0978	1.350	1.062	0.781	1.15C	1.165	0.

**** INLET B/L THICKNESS = 0.013,DIV. ANGLE = 10DEG., AREA RATIO = 3,TAILPIPE LENGTH = 1.830M , RUN

PCSN	WIDTH M/M	DIST FROM INLET	STATIC PRESS. M/M H2O	MEAN VEL. M/S	LOCAL REYNOLDS NUMBER	2DELTA* ------- WIDTH	2THETA ------ WIDTH	SHAPE FACTOR	K.E.CORR. FACTOR	PRESS. RECOV. COEFF.	EFFECT-IVENESS	ENERGY CORR. EFFECT.	E C
1	0.1	******	0.	-0.0	********	0.0000	0.0000	0.000	0.000	0.000	0.000	*****	*
2	76.0	-0.038	-7.	11.8	60680.	0.0130	0.0061	2.113	1.015	0.000	0.000	0.000	C
3	0.2	******	*****	-0.0	0.	0.0000	0.0000	*****	*****	*****	*****	0.000	*
4	7.7	-0.000	0.	-0.0	0.	0.0000	0.0000	0.000	*****	*****	*****	0.000	*
5	0.7	******	0.	-0.0	0.	0.0000	0.1503	0.000	*****	*****	*****	0.000	C
6	0.2	-0.000	*****	-0.0	-0.	0.0000	0.0000	0.000	*****	*****	0.000	0.000	*
7	212.8	0.784	-0.	32.4	460162.	0.1147	0.0700	1.639	1.108	0.752	*****	*****	C

INLET B/L THICKNESS = C.0525 DIV. ANGLE = 10DEG., AREA RATIC = 3, TAILPIPE LENGTH = 2.74CM , RUN NC.

PCSN	WIDTH M/M	DIST FRCM INLET	STATIC PRESS. M/M H2O	MEAN VEL. M/S	LCCAL REYNOLDS NUMBER	2DELTA* / WIDTH	2THETA / WIDTH	SHAPE FACTOR	K.E.CORR. FACTOR	PRESS. RECOV. COEFF.	EFFECT-IVENESS	ENERGY CORR. EFFECT.	ENE CORI C
1	76.2	-0.070	-269.	76.6	398378.	0.0525	C.C376	1.395	1.C40	C.C00	1.000	0.000	0.C
2	223.0	0.843	-32.	C.0	0.	C.CC00	0.CC00	C.CCC	C.C00	0.644	0.729	0.CCC	0.6

PCSN.	BETA	C/L VEL.	TEMP.	ATM.PRESS.	X/W1
1	1.016	81.1	16.5	764.5	-C.140
2	C.CCO	C.0	16.5	764.5	11.C62

INLET B/L THICKNESS = C.0528 DIV. ANGLE = 10DEG., AREA RATIO = 3, TAILPIPE LENGTH = 2.74CM , RUN NO.

PCSN	WIDTH M/M	DIST FROM INLET	STATIC PRESS. M/M H2O	MEAN VEL. M/S	LOCAL REYNOLDS NUMBER	2DELTA* / WIDTH	2THETA / WIDTH	SHAPE FACTOR	K.E.CORR. FACTOR	PRESS. RECOV. COEFF.	EFFECT-IVENESS	ENERGY CORR. EFFECT.	EN CC
1	76.2	-0.070	-218.	69.0	359013.	0.0528	0.0380	1.388	1.039	0.000	1.000	0.000	0.
2	223.C	0.843	-26.	C.0	C.	C.CCCO	C.CCCC	C.CCC	C.COO	C.646	C.731	0.0CC	C.

PCSN.	BETA	C/L VEL.	TEMP.	ATM.PRESS.	X/W1
1	1.016	73.1	16.5	764.5	-C.918
2	C.CCC	C.0	16.5	764.5	11.C62

INLET B/L THICKNESS = 0.0529 DIV. ANGLE = 10DEG., AREA RATIO = 3, TAILPIPE LENGTH = 2.74CM , RUN NO.

POSN	WIDTH M/M	DIST FROM INLET	STATIC PRESS. M/M H2O	MEAN VEL. M/S	LOCAL REYNOLDS NUMBER	2DELTA* ------- WIDTH	2THETA ------ WIDTH	SHAPE FACTOR	K.E.CORR. FACTOR	PRESS. RECOV. COEFF.	EFFECT- IVENESS	ENERGY CORR. EFFECT.	ENE CCF
1	76.2	-0.070	-144.	56.4	292690.	0.0529	0.0383	1.381	1.039	0.000	1.000	0.000	0.0
2	223.0	0.843	-17.	0.0	0.	0.0000	0.0000	0.000	0.000	0.638	0.722	0.000	0.4

POSN.	BETA	C/L VEL.	TEMP.	ATM.PRESS.	X/W1
1	1.015	59.8	17.0	764.5	-0.918
2	0.000	0.0	17.0	764.5	11.062

INLET B/L THICKNESS = 0.0540 DIV. ANGLE = 10DEG., AREA RATIO = 3, TAILPIPE LENGTH = 2.74CM , RUN NO.

POSN	WIDTH M/M	DIST FROM INLET	STATIC PRESS. M/M H2O	MEAN VEL. M/S	LOCAL REYNOLDS NUMBER	2DELTA* ------- WIDTH	2THETA ------ WIDTH	SHAPE FACTOR	K.E.CORR. FACTOR	PRESS. RECOV. COEFF.	EFFECT-IVENESS	ENERGY CORR. EFFECT.	EN CO
1	76.2	-0.070	-91.	45.0	233291.	0.0540	0.0390	1.383	1.039	0.000	1.000	0.000	0.
2	223.0	0.843	-11.	0.0	0.	0.0000	0.0000	0.000	0.000	0.633	0.716	0.000	0.

POSN.	BETA	C/L VEL.	TEMP.	ATM.PRESS.	X/W1
1	1.016	47.7	17.0	764.5	-0.918
2	0.000	0.0	17.0	764.5	11.062

INLET B/L THICKNESS = 0.0560 DIV. ANGLE = 10DEG., AREA RATIO = 3, TAILPIPE LENGTH = 2.74CM , RUN NO.

PCSN	WIDTH M/M	DIST FRCM INLET	STATIC PRESS. M/M H2O	MEAN VEL. M/S	LOCAL REYNOLDS NUMBER	2DELTA* / WIDTH	2THETA / WIDTH	SHAPE FACTOR	K.E.CORR. FACTOR	PRESS. RECOV. COEFF.	EFFECT-IVENESS	ENERGY CORR. EFFECT.	EN CC
1	76.2	-0.070	-47.	32.6	169179.	0.0560	0.0407	1.374	1.040	0.000	1.000	0.000	0.
2	223.0	0.843	-5.	0.0	0.	0.0000	0.0000	0.000	0.000	0.631	0.715	0.000	0.

PCSN.	BETA	C/L VEL.	TEMP.	ATM.PRESS.	X/W1
1	1.016	34.6	17.0	764.5	-0.918
2	0.000	0.0	17.0	764.5	11.062

INLET B/L THICKNESS = C.C337 DIV. ANGLE = 10DEG., AREA RATIC = 3, TAILPIPE LENGTH = 2.74CM ; RUN NC.

PCSN	WIDTH M/M	DIST FRCM INLET	STATIC PRESS. M/M H2O	MEAN VEL. M/S	LCCAL REYNCLDS NUMBER	2CELTA* ------- WIDTH	2THETA ------ WIDTH	SHAPE FACTCR	K.E.CCRR. FACTCR	PRESS. RECCV. CCEFF.	EFFECT-IVENESS	ENERGY CCRR. EFFECT.	EN CC(
1	76.2	-C.C7C	-5.	11.5	59995.	C.C337	0.C231	1.453	1.029	C.C00	1.CCC	C.CCC	0.(
2	223.0	0.843	-0.	C.C	0.	C.CCC0	C.CCCC	0.C00	0.000	0.598	0.677	0.000	0.!

PCSN.	BETA	C/L VEL.	TEMP.	ATM.PRESS.	X/W1
1	1.012	12.0	17.0	764.5	-C.918
2	C.CC0	C.0	17.0	764.5	11.062

INLET B/L THICKNESS = 0.1103 DIV. ANGLE = 15DEG., AREA RATIO = 2, TAILPIPE LENGTH = 2.740M , RUN NO

POSN	WIDTH M/M	DIST FROM INLET	STATIC PRESS. M/M H2O	MEAN VEL. M/S	LOCAL REYNOLDS NUMBER	2DELTA* ------- WIDTH	2THETA ------ WIDTH	SHAPE FACTOR	K.E.CORR. FACTOR	PRESS. RECOV. COEFF.	EFFECT-IVENESS	ENERGY CORR. EFFECT.
1	76.2	-0.070	-236.	78.4	404392.	0.1103	0.0846	1.303	1.050	0.000	1.000	0.000
2	152.4	0.315	-37.	0.0	0.	0.0000	0.0000	0.000	0.000	0.522	0.696	0.000

POSN.	BETA	C/L VEL.	TEMP.	ATM.PRESS.	X/W1
1	1.019	88.4	16.0	755.5	******
2	0.000	0.0	16.0	755.5	4.133

INLET B/L THICKNESS = 0.1098 DIV. ANGLE = 15DEG., AREA RATIO = 2, TAILPIPE LENGTH = 2.740M , RUN NO.

POSN	WIDTH M/M	DIST FROM INLET	STATIC PRESS. M/M H2O	MEAN VEL. M/S	LOCAL REYNOLDS NUMBER	2DELTA* / WIDTH	2THETA / WIDTH	SHAPE FACTOR	K.E.CORR. FACTOR	PRESS. RECOV. COEFF.	EFFECT-IVENESS	ENERGY CORR. EFFECT.	E C
1	76.2	-0.070	-212.	74.8	385763.	0.1098	0.0841	1.305	1.051	0.000	1.000	0.000	0
2	152.4	0.315	-33.	0.0	0.	0.0000	0.0000	0.000	0.000	0.516	0.688	0.000	0

POSN.	BETA	C/L VEL.	TEMP.	ATM.PRESS.	X/W1
1	1.019	84.3	16.0	755.5	-0.918
2	0.000	0.0	16.0	755.5	4.133

INLET B/L THICKNESS = 0.1108 DIV. ANGLE = 15DEG., AREA RATIO = 2, TAILPIPE LENGTH = 2.740M , RUN NO.

POSN	WIDTH M/M	DIST FROM INLET	STATIC PRESS. M/M H2O	MEAN VEL. M/S	LOCAL REYNOLDS NUMBER	2DELTA* ------- WIDTH	2THETA ------ WIDTH	SHAPE FACTOR	K.E.CORR. FACTOR	PRESS. RECOV. COEFF.	EFFECT-IVENESS	ENERGY CORR. EFFECT.	E C
1	76.2	-0.070	-171.	66.6	345688.	0.1108	0.0853	1.299	1.049	0.000	1.000	0.000	C
2	152.4	0.315	-26.	0.0	0.	0.0000	0.0000	0.000	0.000	0.523	0.698	0.000	C

POSN.	BETA	C/L VEL.	TEMP.	ATM.PRESS.	X/W1
1	1.019	75.2	15.0	755.5	-0.918
2	0.000	0.0	15.0	755.5	4.133

INLET B/L THICKNESS = 0.1088 DIV. ANGLE = 15DEG., AREA RATIO = 2, TAILPIPE LENGTH = 2.740M , RUN NO.

POSN	WIDTH M/M	DIST FROM INLET	STATIC PRESS. M/M H2O	MEAN VEL. M/S	LOCAL REYNOLDS NUMBER	2DELTA* ------- WIDTH	2THETA ------ WIDTH	SHAPE FACTOR	K.E.CORR. FACTOR	PRESS. RECOV. COEFF.	EFFECT-IVENESS	ENERGY CORR. EFFECT.	EN CO
1	76.2	-0.070	-144.	61.7	320330.	0.1088	0.0837	1.299	1.049	0.000	1.000	0.000	0.
2	152.4	-0.312	-22.	0.0	0.	0.0000	0.0000	0.000	0.000	0.515	0.686	0.000	0.

POSN.	BETA	C/L VEL.	TEMP.	ATM.PRESS.	X/W1
1	1.019	69.5	15.0	755.5	-0.918
2	0.000	0.0	15.0	755.5	-4.094

INLET B/L THICKNESS = 0.1160 DIV. ANGLE = 15DEG., AREA RATIO = 2, TAILPIPE LENGTH = 2.740M , RUN NO

POSN	WIDTH M/M	DIST FROM INLET	STATIC PRESS. M/M H2O	MEAN VEL. M/S	LOCAL REYNOLDS NUMBER	2DELTA* / WIDTH	2THETA / WIDTH	SHAPE FACTOR	K.E.CORR. FACTOR	PRESS. RECOV. COEFF.	EFFECT-IVENESS	ENERGY CORR. EFFECT.
1	76.2	0.312	-94.	50.0	259412.	0.1160	0.0886	1.309	1.053	0.000	1.000	0.000
2	152.4	0.312	-14.	0.0	0.	0.0000	0.0000	0.000	0.000	0.515	0.686	0.000

POSN.	BETA	C/L VEL.	TEMP.	ATM.PRESS.	X/W1
1	1.020	56.7	15.0	755.5	4.094
2	0.000	0.0	15.0	755.5	4.094

INLET B/L THICKNESS = 0.1139 DIV. ANGLE = 15DEG., AREA RATIO = 2, TAILPIPE LENGTH = 2.740M , RUN NO.

POSN	WIDTH M/M	DIST FROM INLET	STATIC PRESS. M/M H2O	MEAN VEL. M/S	LOCAL REYNOLDS NUMBER	2DELTA* / WIDTH	2THETA / WIDTH	SHAPE FACTOR	K.E.CORR. FACTOR	PRESS. RECOV. COEFF.	EFFECT-IVENESS	ENERGY CORR. EFFECT.	E C
1	76.2	-0.070	-68.	42.7	221417.	0.1139	0.0867	1.313	1.053	0.000	1.000	0.000	0.
2	152.4	0.312	-10.	0.0	0.	0.0000	0.0000	0.000	0.000	0.508	0.677	0.000	0.

POSN.	BETA	C/L VEL.	TEMP.	ATM.PRESS.	X/W1
1	1.020	48.3	15.0	755.5	-0.918
2	0.000	48.3	15.0	755.5	4.094

INLET B/L THICKNESS = 0.1226 DIV. ANGLE = 15DEG., AREA RATIO = 2. TAILPIPE LENGTH = 2.740M , RUN N(

POSN	WIDTH M/M	DIST FROM INLET	STATIC PRESS. M/M H2O	MEAN VEL. M/S	LOCAL REYNOLDS NUMBER	2DELTA* / WIDTH	2THETA / WIDTH	SHAPE FACTOR	K.E.CORR. FACTOR	PRESS. RECOV. COEFF.	EFFECT-IVENESS	ENERGY CORR. EFFECT.
1	76.2	-0.070	-28.	28.4	148561.	0.1226	0.0926	1.324	1.058	0.000	1.000	0.000
2	152.4	0.312	-4.	0.0	0.	0.0000	0.0000	0.000	0.000	0.479	0.639	0.000

POSN.	BETA	C/L VEL.	TEMP.	ATM.PRESS.	X/W1
1	1.022	32.5	14.0	755.5	-0.918
2	0.000	0.0	14.0	755.5	4.094

INLET B/L THICKNESS = 0.1094 DIV. ANGLE = 10DEG., AREA RATIO = 3, TAILPIPE LENGTH = 2.740M , RUN NO.

POSN	WIDTH M/M	DIST FROM INLET	STATIC PRESS. M/M H2O	MEAN VEL. M/S	LOCAL REYNOLDS NUMBER	2DELTA* / WIDTH	2THETA / WIDTH	SHAPE FACTOR	K.E.CORR. FACTOR	PRESS. RECOV. COEFF.	EFFECT-IVENESS	ENERGY CORR. EFFECT.	EN CO
1	76.2	-0.070	-319.	84.3	427888.	0.1094	0.0834	1.311	1.052	0.000	1.000	0.000	0.
2	228.6	0.896	-42.	0.0	0.	0.0000	0.0000	0.000	0.000	0.636	0.716	0.000	0.

POSN.	BETA	C/L VEL.	TEMP.	ATM.PRESS.	X/W1
1	1.020	94.9	18.0	753.4	******
2	0.000	0.0	18.0	753.4	11.758

INLET B/L THICKNESS = 0.1106 DIV. ANGLE = 10DEG., AREA RATIO = 3, TAILPIPE LENGTH = 2.740M , RUN NO.

POSN	WIDTH M/M	DIST FROM INLET	STATIC PRESS. M/M H2O	MEAN VEL. M/S	LOCAL REYNOLDS NUMBER	2DELTA* ------- WIDTH	2THETA ------- WIDTH	SHAPE FACTOR	K.E.CORR. FACTOR	PRESS. RECOV. COEFF.	EFFECT-IVENESS	ENERGY CORR. EFFECT.	EN CO
1	76.2	-0.070	-248.	74.3	377126.	0.1106	0.0842	1.314	1.053	0.000	1.000	0.000	0.[illegible]
2	228.6	0.896	-32.	0.0	0.	0.0000	0.0000	0.000	0.000	0.638	0.718	0.000	0.[illegible]

POSN.	BETA	C/L VEL.	TEMP.	ATM.PRESS.	X/W1
1	1.020	83.8	18.0	753.4	-0.918
2	0.000	0.0	18.0	753.4	11.758

INLET B/L THICKNESS = 0.1169 DIV. ANGLE = 10DEG., AREA RATIO = 3, TAILPIPE LENGTH = 2.740M , RUN NO.

POSN	WIDTH M/M	DIST FROM INLET	STATIC PRESS. M/M H2O	MEAN VEL. M/S	LOCAL REYNOLDS NUMBER	2DELTA* / WIDTH	2THETA / WIDTH	SHAPE FACTOR	K.E.CORR. FACTOR	PRESS. RECOV. COEFF.	EFFECT-IVENESS	ENERGY CORR. EFFECT.	E[illegible] C[illegible]
1	76.2	-0.070	-103.	48.4	240011.	0.1169	0.0886	1.319	1.055	0.000	1.000	0.000	0.[illegible]
2	228.6	0.896	-13.	0.0	0.	0.0000	0.0000	0.000	0.000	0.630	0.709	0.000	0.[illegible]

POSN.	BETA	C/L VEL.	TEMP.	ATM.PRESS.	X/W1
1	1.021	55.0	22.0	753.1	-0.918
2	0.000	0.0	22.0	753.1	11.758

INLET B/L THICKNESS = 0.1263 DIV. ANGLE = 10DEG., AREA RATIO = 3, TAILPIPE LENGTH = 2.740M , RUN NO.

POSN	WIDTH M/M	DIST FROM INLET	STATIC PRESS. M/M H2O	MEAN VEL. M/S	LOCAL REYNOLDS NUMBER	2DELTA* / WIDTH	2THETA / WIDTH	SHAPE FACTOR	K.E.CORR. FACTOR	PRESS. RECOV. COEFF.	EFFECT-IVENESS	ENERGY CORR. EFFECT.	ENE COR C
1	76.2	-0.070	-59.	36.8	182406.	0.1263	0.0953	1.325	1.058	0.000	1.000	0.000	0.0
2	228.6	0.896	-8.	0.0	0.	0.0000	0.0000	0.000	0.000	0.628	0.707	0.000	0.5

POSN.	BETA	C/L VEL.	TEMP.	ATM.PRESS.	X/W1
1	1.022	42.2	22.0	753.1	-0.918
2	0.000	0.0	22.0	753.1	11.758

INLET B/L THICKNESS = 0.1214 DIV. ANGLE = 10DEG., AREA RATIO = 3. TAILPIPE LENGTH = 2.740M . RUN NO

POSN	WIDTH M/M.	DIST FROM INLET	STATIC PRESS. M/M H2O	MEAN VEL. M/S	LOCAL REYNOLDS NUMBER	2DELTA* ------- WIDTH	2THETA ------ WIDTH	SHAPE FACTOR	K.E.CORR. FACTOR	PRESS. RECOV. COEFF.	EFFECT- IVENESS	ENERGY CORR. EFFECT.
1	76.2	-0.070	-35.	28.2	140094.	0.1214	0.0911	1.332	1.059	0.000	1.000	0.000
2	228.6	0.896	-5.	0.0	0.	0.0000	0.0000	0.000	0.000	0.620	0.698	0.000

POSN.	BETA	C/L VEL.	TEMP.	ATM.PRESS.	X/W1
1	1.022	32.3	22.0	753.1	-0.918
2	0.000	0.0	22.0	753.1	11.758

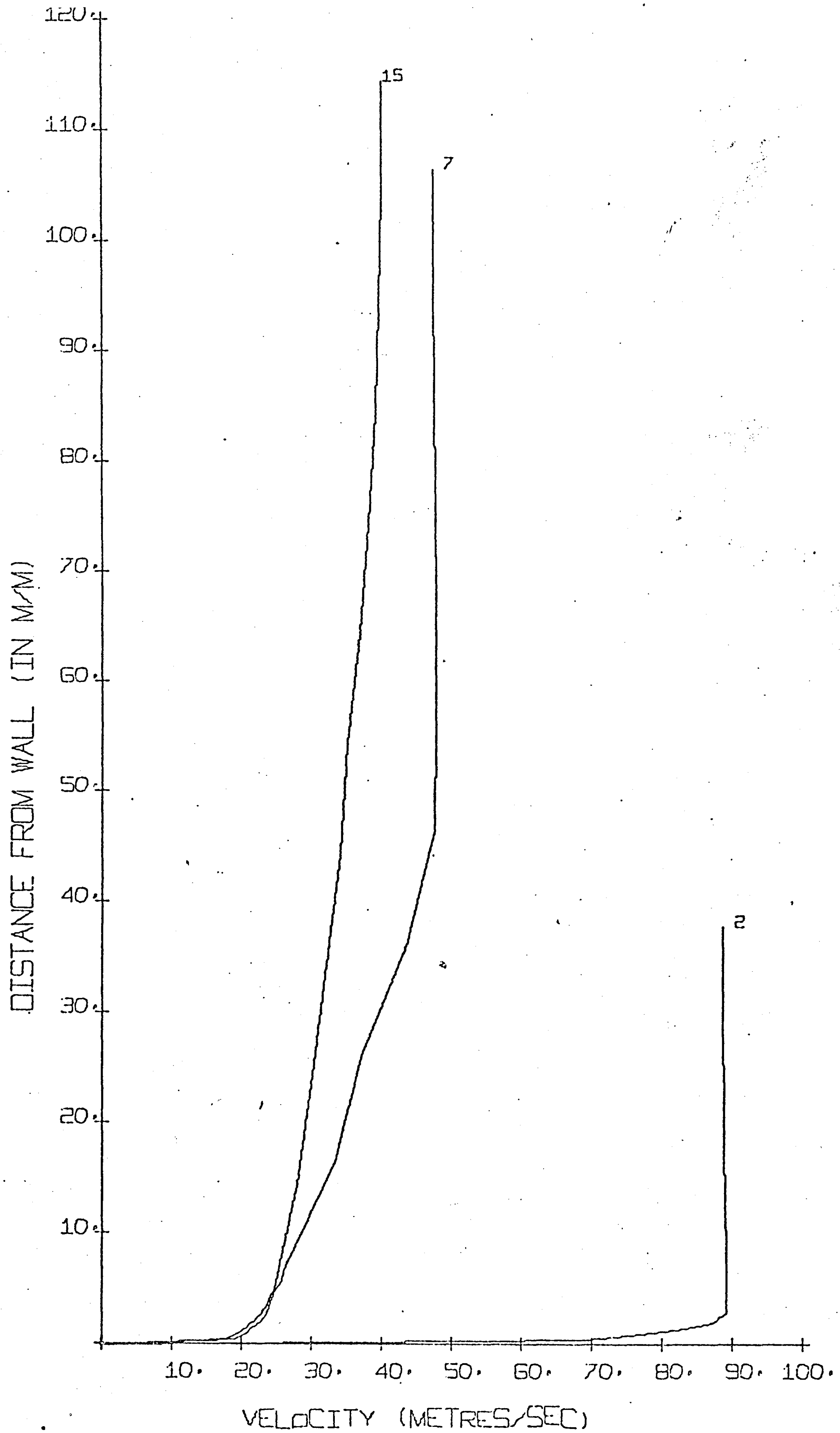

120.
110.
100.
90.
80.
70.
60.
50.
40.
30.
20.
10.
DISTANCE FROM WALL (IN M/M)
15
7
2
10. 20. 30. 40. 50. 60. 70. 80. 90. 100.
VELOCITY (METRES/SEC)

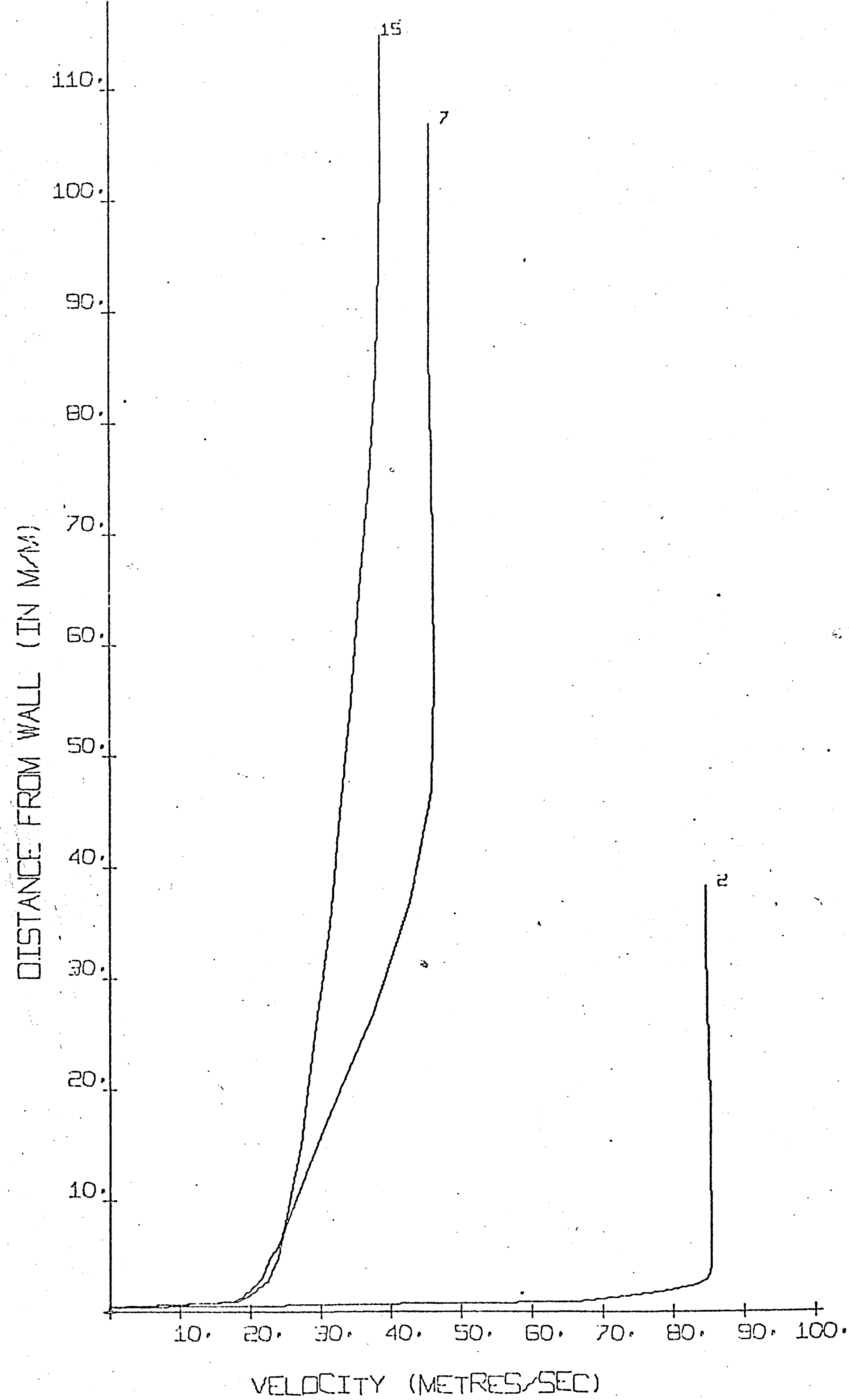

DISTANCE FROM WALL (IN M/M)
VELOCITY (METRES/SEC)
15
7
2
110.
100.
90.
80.
70.
60.
50.
40.
30.
20.
10.
10.
20.
30.
40.
50.
60.
70.
80.
90.
100.

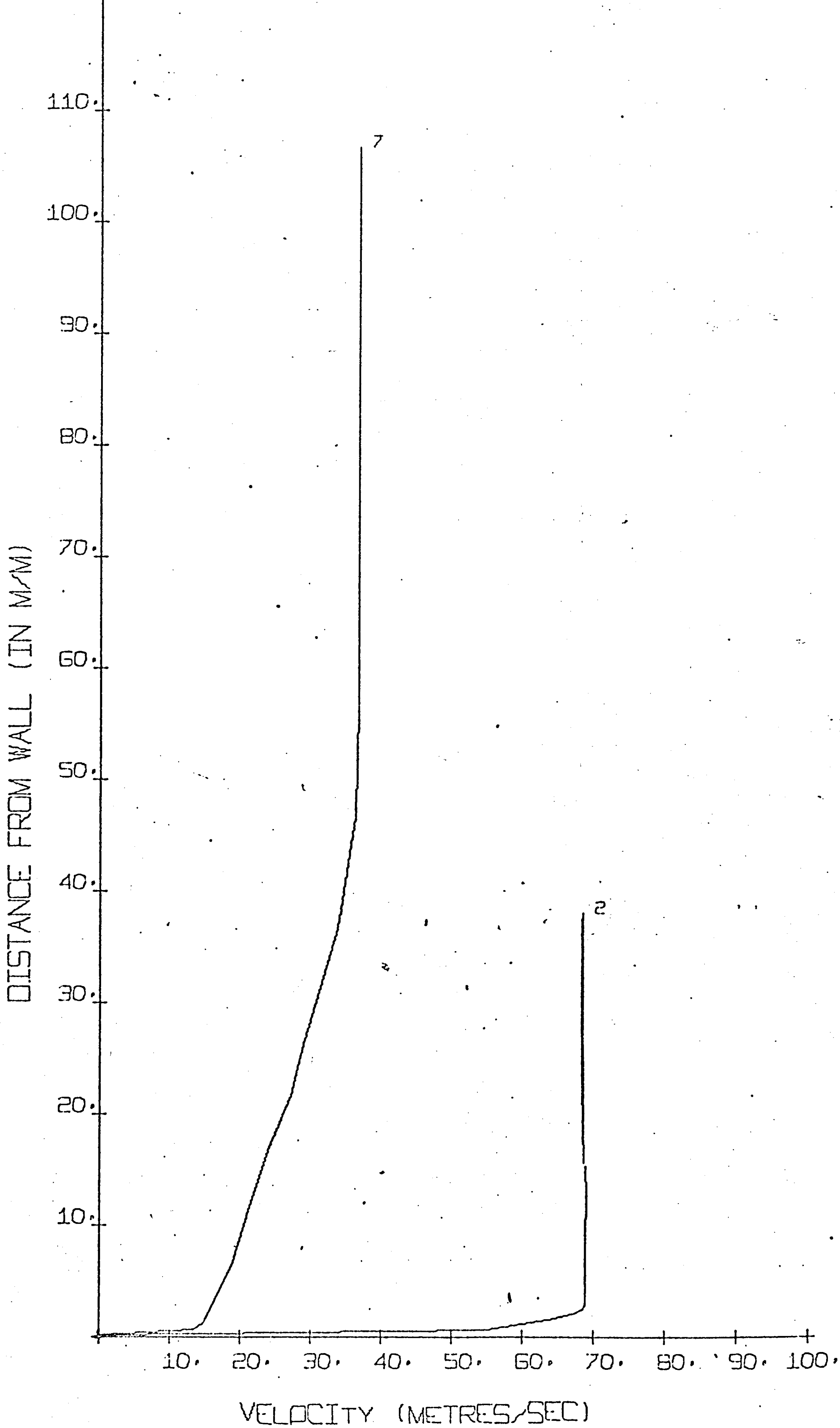

110.
100.
90.
80.
70.
60.
50.
40.
30.
20.
10.
DISTANCE FROM WALL (IN M/M)
7
2
10. 20. 30. 40. 50. 60. 70. 80. 90. 100.
VELOCITY (METRES/SEC)

RUN NO. 5

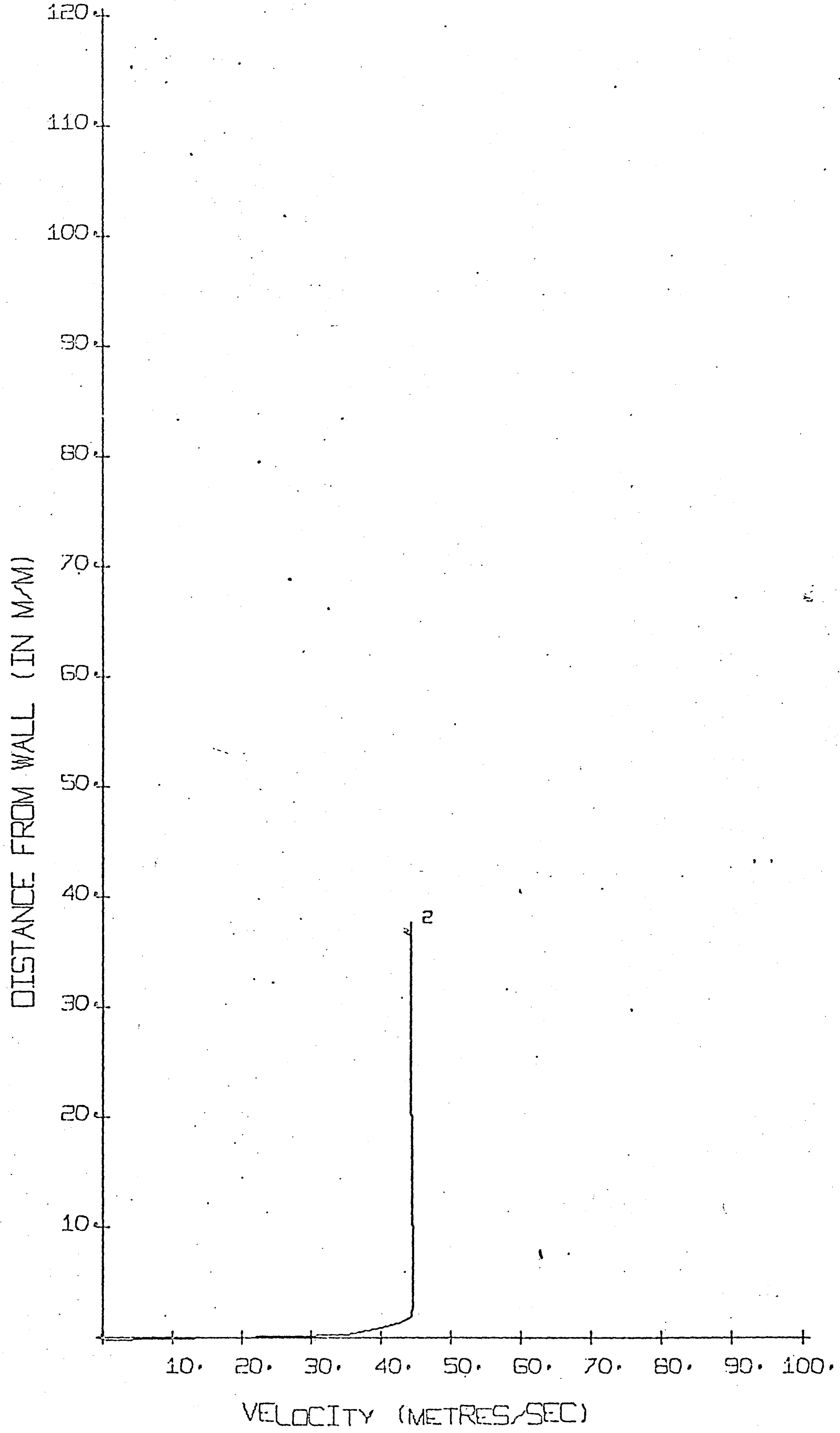

120
110
100
90
80
70
60
50
40
30
20
10
DISTANCE FROM WALL (IN M/M)
2
10.
20.
30.
40.
50.
60.
70.
80.
90.
100.
VELOCITY (METRES/SEC)

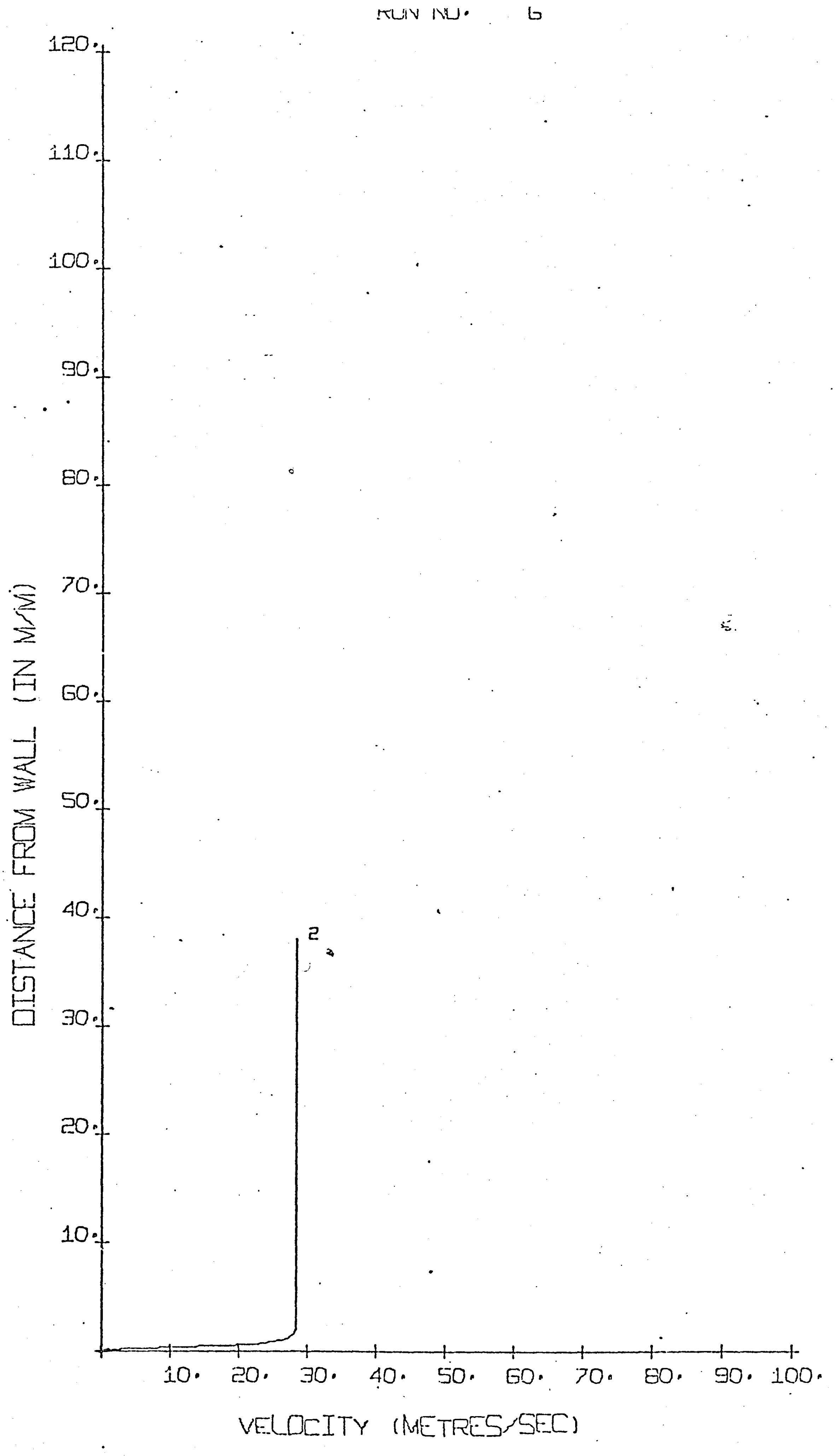
RUN NO. 6
DISTANCE FROM WALL (IN M/M)
120.
110.
100.
90.
80.
70.
60.
50.
40.
30.
20.
10.
2
10.
20.
30.
40.
50.
60.
70.
80.
90.
100.
VELOCITY (METRES/SEC)

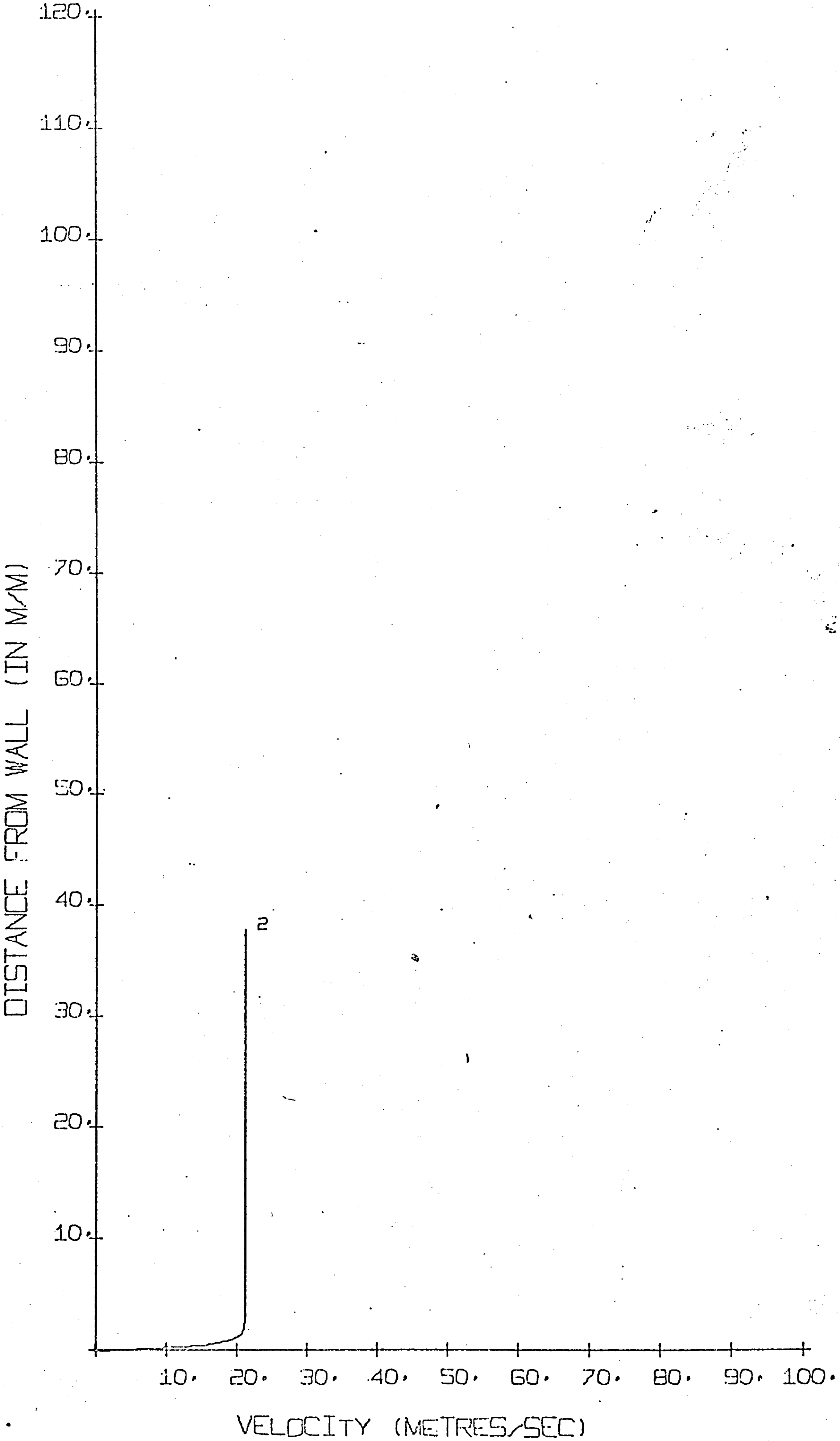

120.
110.
100.
90.
80.
70.
60.
50.
40.
30.
20.
10.
DISTANCE FROM WALL (IN M/M)
2
10. 20. 30. 40. 50. 60. 70. 80. 90. 100.
VELOCITY (METRES/SEC)

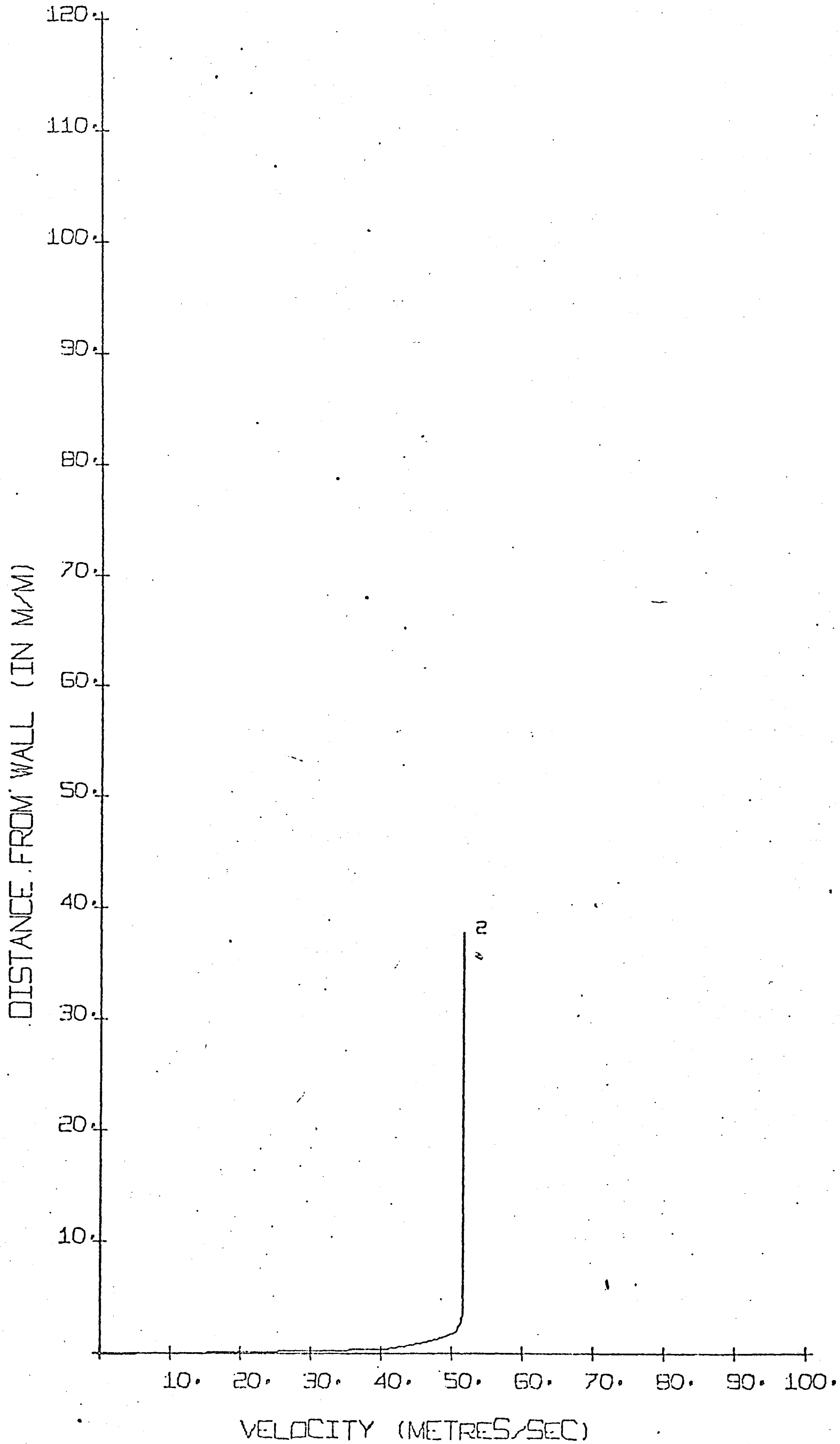

DISTANCE FROM WALL (IN M/M)
120.
110.
100.
90.
80.
70.
60.
50.
40.
30.
20.
10.
2
10. 20. 30. 40. 50. 60. 70. 80. 90. 100.
VELOCITY (METRES/SEC)

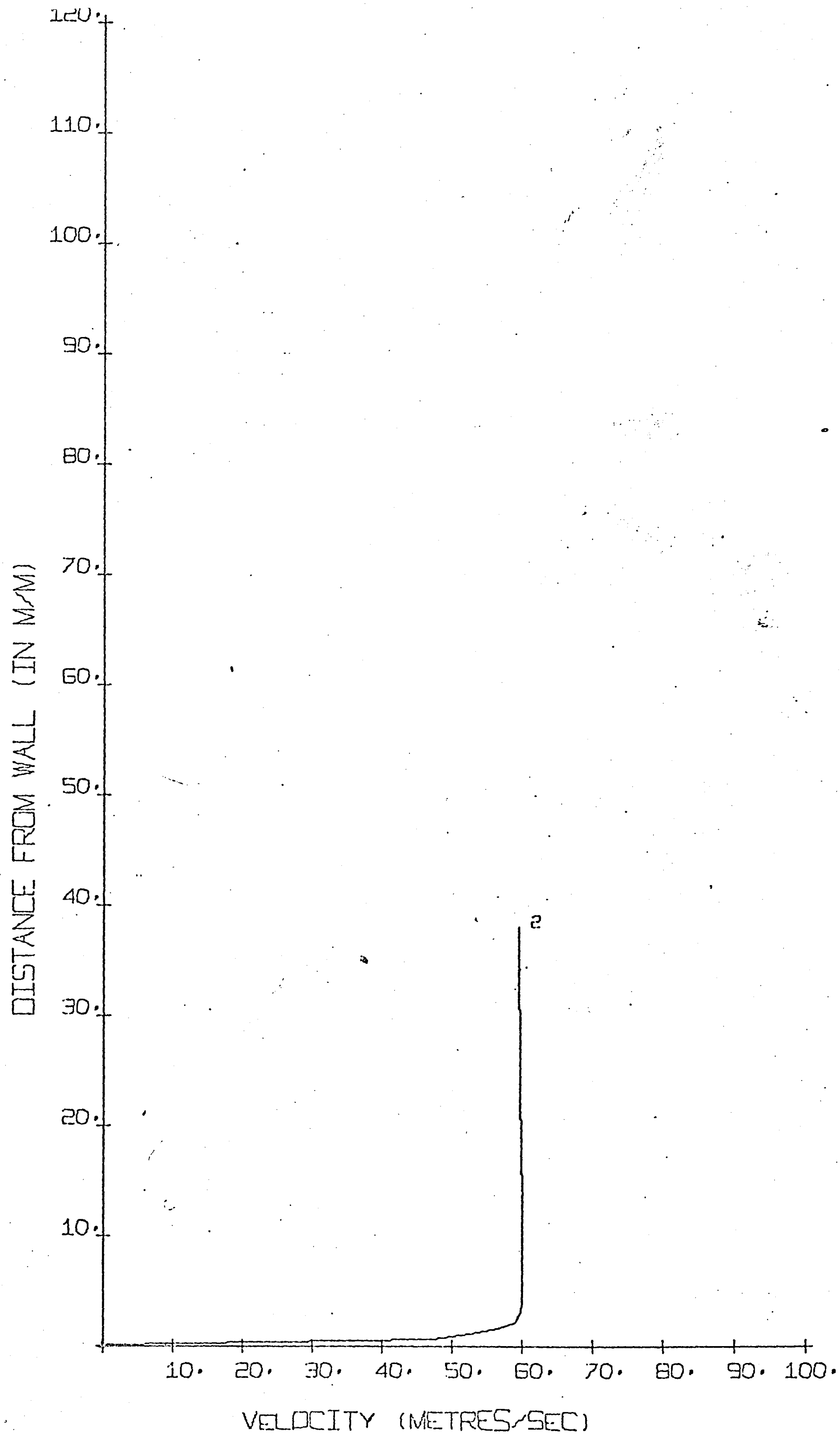

120.
110.
100.
90.
80.
70.
60.
50.
40.
30.
20.
10.
DISTANCE FROM WALL (IN M/M)
2
10. 20. 30. 40. 50. 60. 70. 80. 90. 100.
VELOCITY (METRES/SEC)

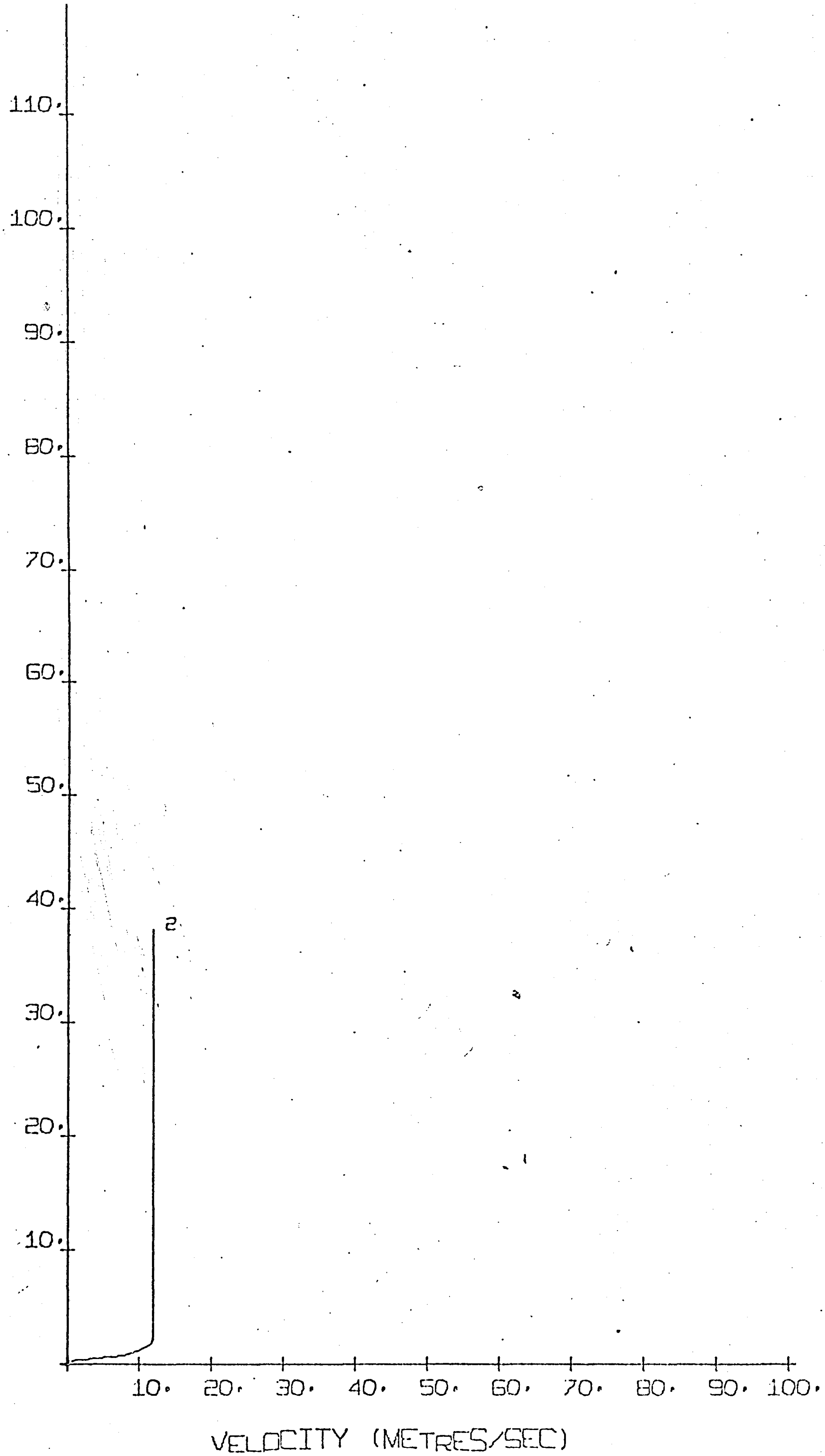
110.
100.
90.
80.
70.
60.
50.
40.
30.
20.
10.
2
10. 20. 30. 40. 50. 60. 70. 80. 90. 100.
VELOCITY (METRES/SEC)

APPENDIX 6.

DIFFUSER EXPERIMENTAL RESULTS.

Table IX is included here as an Index to the results. These are the tabulated results of the experimental performance and flow parameters. The graph plots are of the velocity traverses and of; Cp, Cp_E, η, and η_E against x/w_1 for each test.

SYMBOLS.

x η

∇ η_E

+ Cp

$\triangleright$ Cp_E

TABLE IX.

Test No.	Condition of Rig.
	Thin Inlet B/L $(2\delta^*/w = 0.01)$
109	5° AR2 plenum discharge.
112	5° AR2 tailpipe discharge.
110	5° AR3 plenum discharge.
111	5° AR3 tailpipe discharge.
103	10° AR2 plenum discharge.
104	10° AR2 tailpipe discharge.
102	10° AR3 plenum discharge.
101	10° tailpipe discharge.
105	15° AR2 plenum discharge.
108	15° AR2 tailpipe discharge.
106	15° AR3 plenum discharge.
107	15° AR3 tailpipe discharge.
	Thick Inlet B/L $(2\delta^*/w = 0.06)$
202	5° AR2 plenum discharge.
201	5° AR2 tailpipe discharge.
203	5° AR3 plenum discharge.
204	5° AR3 tailpipe discharge.
205	10° AR2 plenum discharge.
206	10° AR2 tailpipe discharge.
207	10° AR2 optimum tailpipe length.
210	10° AR3 plenum discharge.
208	10° AR3 tailpipe discharge.
209	10° AR3 tailpipe discharge.

Table IX contd.

211	15^{o} AR2 plenum discharge.
214	15^{o} AR2 tailpipe discharge.
212	15^{o} AR3 plenum discharge.
213	15^{o} AR3 tailpipe discharge.
	Fully Developed Inlet Flow ($2\delta^{*}/w = 0.11$)
302	15^{o} AR2 plenum discharge.
301	15^{o} AR2 tailpipe discharge.
303	15^{o} AR3 plenum discharge.
304	15^{o} AR3 tailpipe discharge.
305	10^{o} AR3 tailpipe discharge.
306	10^{o} AR3 plenum discharge.
307	10^{o} AR2 plenum discharge.
308	10^{o} AR2 tailpipe discharge.
309	5^{o} AR2 plenum discharge.
310	5^{o} AR2 tailpipe discharge.
311	5^{o} AR3 plenum discharge.
312	5^{o} tailpipe discharge.
000	Thin inlet boundary layer inlet profile.
350	Fully developed velocity profile. (inlet).

INLET B/L THICKNESS = 0.0106 DIV. ANGLE = 10DEG., AREA RATIO = 3, TAILPIPE LENGTH = 2.74CM , RUN NC.

PCSN	WIDTH M/M	DIST FRCM INLET	STATIC PRESS. M/M H2O	MEAN VEL. M/S	LOCAL REYNOLDS NUMBER	2DELTA* ------- WIDTH	2THETA ------ WIDTH	SHAPE FACTOR	K.E.CORR. FACTOR	PRESS. RECOV. COEFF.	EFFECT-IVENESS	ENERGY CORR. EFFECT.	EN CC
1	76.2	-0.038	-375.	87.2	431682.	0.0106	0.0052	2.031	1.017	0.000	1.000	0.000	0.
2	111.6	0.201	-150.	60.4	437987.	0.0429	0.0271	1.580	1.031	0.487	0.937	0.933	0.
3	160.0	0.481	-60.	45.4	472138.	0.0833	0.0513	1.622	1.079	0.682	0.936	0.942	0.
4	223.0	0.843	-15.	34.6	501922.	0.1507	0.0837	1.800	1.166	0.780	0.926	0.936	0.
5	228.6	1.201	-8.	34.1	507686.	0.1284	0.0859	1.494	1.091	0.795	0.939	0.936	0.
6	228.6	1.506	-5.	33.9	504463.	0.1366	0.0966	1.413	1.030	0.801	0.945	0.931	0.
7	228.6	2.420	-0.	0.0	0.	0.0000	0.0000	0.000	0.000	0.811	0.912	0.000	0.
8	228.6	3.220	-0.	0.0	0.	0.0000	0.0000	0.000	0.000	0.812	0.913	0.000	0.

PCSN.	BETA	C/L VEL.	TEMP.	ATM.PRESS.	X/W1
1	1.008	88.3	24.0	762.0	0.000
2	1.011	62.8	24.0	762.0	2.637
3	1.029	49.5	24.0	762.0	6.312
4	1.061	40.8	24.0	762.0	11.062
5	1.032	39.1	24.0	762.0	15.761
6	1.004	38.3	24.0	762.0	19.763
7	0.000	35.8	24.0	762.0	31.758
8	0.000	0.0	24.0	762.0	42.257

INLET B/L THICKNESS = 0.0133 DIV. ANGLE = 10DEG., AREA RATIO = 3, TAILPIPE LENGTH = 0.000M , RUN NO.

POSN	WIDTH	DIST FROM INLET	STATIC PRESS. M/M H2O	MEAN VEL. M/S	LOCAL REYNOLDS NUMBER	2DELTA* ------- WIDTH	2THETA ------ WIDTH	SHAPE FACTOR	K.E.CORR. FACTOR	PRESS. RECOV. COEFF.	EFFECT-IVENESS	ENERGY CORR. EFFECT.	E C
	M/M												
1	76.2	-0.038	-323.	81.6	414843.	0.0133	0.0079	1.683	1.017	0.000	1.000	0.000	0
2	138.0	0.354	-119.	57.5	529356.	0.0342	0.0214	1.592	1.031	0.496	0.986	0.984	0
3	160.0	0.481	-38.	43.5	464335.	0.0816	0.0500	1.631	1.078	0.693	0.969	0.976	0
4	223.0	0.843	-1.	35.0	520871.	0.1273	0.0764	1.666	1.124	0.784	0.962	0.969	0
5	999.9	1.100	0.	0.0	0.	0.0000	0.0000	0.000	0.000	0.788	0.793	0.000	0

POSN.	BETA	C/L VEL.	TEMP.	ATM.PRESS.	X/W1
1	1.008	82.9	19.0	759.1	-0.498
2	1.012	59.5	19.0	759.1	4.645
3	1.029	47.3	19.0	759.1	6.312
4	1.045	40.1	19.0	759.1	11.062
5	0.000	0.0	19.0	759.1	14.435

INLET B/L THICKNESS = 0.0105 DIV. ANGLE = 10DEG., AREA RATIO = 2, TAILPIPE LENGTH = 0.00CM , RUN NO.

PCSN	WIDTH	DIST FROM INLET	STATIC PRESS.	MEAN VEL.	LOCAL REYNOLDS NUMBER	2DELTA* / WIDTH	2THETA / WIDTH	SHAPE FACTOR	K.E.CORR. FACTOR	PRESS. RECOV. COEFF.	EFFECT-IVENESS	ENERGY CORR. EFFECT.	E C
	M/M		M/M H2O	M/S									
1	76.2	-0.038	-255.	76.6	385318.	0.0105	0.0051	2.046	1.016	0.000	1.000	0.000	0
2	85.0	0.051	-187.	68.8	385761.	0.0206	0.0125	1.647	1.019	0.188	0.968	0.960	0
3	112.0	0.201	-71.	52.1	385277.	0.0479	0.0289	1.654	1.047	0.513	0.955	0.964	0
4	138.0	0.354	-19.	42.6	387756.	0.0809	0.0465	1.739	1.086	0.658	0.952	0.966	0
5	152.0	0.500	0.	0.0	0.	0.0000	0.0000	0.000	0.000	0.711	0.950	0.000	0

PCSN.	BETA	C/L VEL.	TEMP.	ATM.PRESS.	X/W1
1	1.008	77.7	20.0	755.0	-0.498
2	1.008	70.2	20.0	755.0	0.669
3	1.018	54.8	20.0	755.0	2.637
4	1.032	46.3	20.0	755.0	4.645
5	0.000	0.0	20.0	755.0	6.551

INLET B/L THICKNESS = 0.0105 DIV. ANGLE = 10DEG., AREA RATIO = 2, TAILPIPE LENGTH = 2.74CM , RUN NC.

PCSN	WIDTH M/M	DIST FRCM INLET	STATIC PRESS. N/M H2C	MEAN VEL. M/S	LCCAL REYNOLDS NUMBER	2DELTA* ------- WIDTH	2THETA ------ WIDTH	SHAPE FACTCR	K.E.CCRR. FACTCR	PRESS. RECCV. CCEFF.	EFFECT-IVENESS	ENERGY CCRR. EFFECT.	E C
1	76.2	-0.038	-259.	76.7	394515.	0.0105	0.0052	2.015	1.016	0.000	1.000	0.000	0
2	111.6	0.202	-68.	52.0	392024.	0.0490	0.0297	1.652	1.040	0.519	0.962	0.965	0
3	138.0	0.345	-14.	41.9	390199.	0.0834	0.0473	1.762	1.090	0.668	0.952	0.965	0
4	152.4	0.460	5.	37.6	386868.	0.1028	0.0580	1.771	1.118	0.721	0.949	0.963	0
5	152.4	0.613	8.	37.4	384771.	0.0910	0.0606	1.502	1.078	0.729	0.956	0.959	0
6	152.0	0.918	9.	37.4	383802.	0.0804	0.0594	1.353	1.047	0.732	0.960	0.953	0
7	152.0	1.350	8.	37.3	383025.	0.0801	0.0622	1.287	1.036	0.731	0.958	0.948	0
8	152.0	2.084	7.	37.3	383230.	0.0906	0.0708	1.279	1.038	0.727	0.953	0.944	0
9	152.0	2.574	4.	0.0	0.	0.0000	0.0000	0.000	0.000	0.719	0.961	0.000	0
10	152.0	2.974	2.	0.0	0.	0.0000	0.0000	0.000	0.000	0.714	0.954	0.000	0
11	152.0	3.229	1.	0.0	0.	0.0000	0.0000	0.000	0.000	0.710	0.948	0.000	0

PCSN.	BETA	C/L VEL.	TEMP.	ATM.PRESS.	X/W1
1	1.007	77.7	19.0	768.0	-0.498
2	1.015	54.5	19.0	768.0	2.650
3	1.034	45.7	19.0	768.0	4.527
4	1.045	42.0	19.0	768.0	6.036
5	1.029	41.2	19.0	768.0	8.044
6	1.017	40.6	19.0	768.0	12.047
7	1.013	40.5	19.0	768.0	17.716
8	1.014	41.0	19.0	768.0	27.349
9	0.000	0.0	19.0	768.0	33.779
10	0.000	0.0	19.0	768.0	39.028
11	0.000	0.0	19.0	768.0	42.375

.NLET B/L THICKNESS = 0.0100 DIV. ANGLE = 15DEG.. AREA RATIO = 2. TAILPIPE LENGTH = 0.000M . RUN NO. 10

OSN	WIDTH M/M	DIST FROM INLET	STATIC PRESS. M/M H2O	MEAN VEL. M/S	LOCAL REYNOLDS NUMBER	2DELTA* ------- WIDTH	2THETA ------ WIDTH	SHAPE FACTOR	K.E.CORR. FACTOR	PRESS. RECOV. COEFF.	EFFECT-IVENESS	ENERGY CORR. EFFECT.	ENERGY CORR. CP
1	76.2	-0.038	-227.	74.2	369654.	0.0100	0.0048	2.087	1.016	0.000	1.000	0.000	0.000
2	89.4	0.050	-144.	64.3	375492.	0.0323	0.0139	2.317	1.027	0.247	0.987	1.003	0.243
3	128.6	0.201	-28.	45.2	380216.	0.0743	0.0376	1.975	1.084	0.596	0.949	0.972	0.586
4	152.4	0.300	0.	0.0	0.	0.0000	0.0000	0.000	0.000	0.680	0.907	0.000	0.669

POSN.	BETA	C/L VEL.	TEMP.	ATM.PRESS.	X/W1
1	1.007	75.2	21.5	754.6	-0.498
2	1.011	66.0	21.5	754.6	0.656
3	1.033	48.7	21.5	754.6	2.637
4	0.000	0.0	21.5	754.6	3.937

NLET B/L THICKNESS = 0.0101 DIV. ANGLE = 15DEG., AREA RATIO = 3, TAILPIPE LENGTH = 0.000M , RUN NO. 106

OSN	WIDTH M/M	DIST FROM INLET	STATIC PRESS. M/M H2O	MEAN VEL. M/S	LOCAL REYNOLDS NUMBER	2DELTA* / WIDTH	2THETA / WIDTH	SHAPE FACTOR	K.E.CORR. FACTOR	PRESS. RECOV. COEFF.	EFFECT-IVENESS	ENERGY CORR. EFFECT.	ENERGY CORR. CP
1	76.2	-0.038	-270.	76.0	386606.	0.0101	0.0049	2.066	1.016	0.000	1.000	0.000	0.000
2	128.6	0.201	-64.	47.9	410959.	0.0652	0.0356	1.827	1.067	0.580	0.962	0.978	0.571
3	161.4	0.327	-34.	42.7	460293.	0.0787	0.0450	1.747	1.076	0.663	0.970	0.981	0.653
4	220.6	0.554	-4.	36.4	536467.	0.0851	0.0516	1.650	1.081	0.749	0.973	0.976	0.737
5	228.6	0.700	0.	0.0	0.	0.0000	0.0000	C.000	0.000	0.761	0.856	0.000	0.748

POSN.	BETA	C/L VEL.	TEMP.	ATM.PRESS.	X/W1
1	1.007	77.0	18.0	754.5	-0.498
2	1.025	51.0	18.0	754.5	2.637
3	1.028	46.2	18.0	754.5	4.291
4	1.029	39.7	18.0	754.5	7.270
5	0.000	0.0	18.0	754.5	9.186

INLET B/L THICKNESS = 0.0103 DIV. ANGLE = 15DEG., AREA RATIO = 3, TAILPIPE LENGTH = 2.740M , RUN NO. 10

POSN	WIDTH M/M	DIST FROM INLET	STATIC PRESS. M/M H2O	MEAN VEL. M/S	LOCAL REYNOLDS NUMBER	2DELTA* ------- WIDTH	2THETA ------ WIDTH	SHAPE FACTOR	K.E.CORR. FACTOR	PRESS. RECOV. COEFF.	EFFECT-IVENESS	ENERGY CORR. EFFECT.	ENERG CORR. CP
1	76.2	-0.038	-322.	80.8	409115.	0.0103	0.0051	2.020	1.016	0.000	1.000	0.000	0.000
2	128.6	0.201	-97.	51.9	443646.	0.0592	0.0338	1.748	1.056	0.560	0.954	0.965	0.551
3	161.4	0.327	-65.	45.6	489466.	0.0888	0.0511	1.738	1.085	0.639	0.939	0.954	0.629
4	220.6	0.554	-29.	36.1	529414.	0.1630	0.0902	1.806	1.174	0.728	0.910	0.931	0.716
5	228.6	0.604	-23.	34.8	528415.	0.1717	0.0946	1.815	1.184	0.744	0.914	0.934	0.732
6	228.6	1.062	-10.	34.6	525570.	0.1073	0.0825	1.300	1.043	0.777	0.951	0.941	0.764
7	228.6	1.519	-4.	32.9	500133.	0.1029	0.0820	1.253	1.032	0.792	0.950	0.937	0.779
8	228.6	2.128	-0.	31.0	470989.	0.0956	0.0770	1.241	1.028	0.800	0.938	0.925	0.787
9	228.6	2.623	-0.	0.0	0.	0.0000	0.0000	0.000	0.000	0.801	0.901	0.000	0.788
10	228.6	2.918	-0.	0.0	0.	0.0000	0.0000	0.000	0.000	0.801	0.901	0.000	0.788
11	228.6	3.273	0.	0.0	0.	0.0000	0.0000	C.000	0.000	0.802	0.903	0.000	0.789

POSN.	BETA	C/L VEL.	TEMP.	ATM.PRESS.	X/W1
1	1.007	81.9	20.0	760.0	-0.498
2	1.021	55.0	20.0	760.0	2.637
3	1.031	49.9	20.0	760.0	4.291
4	1.063	43.1	20.0	760.0	7.270
5	1.067	41.9	20.0	760.0	7.926
6	1.014	38.7	20.0	760.0	13.937
7	1.010	36.6	20.0	760.0	19.934
8	1.009	34.2	20.0	760.0	27.926
9	0.000	0.0	20.0	760.0	34.422
10	0.000	0.0	20.0	760.0	38.293
11	0.000	0.0	20.0	760.0	42.952

INLET B/L THICKNESS = 0.0097 DIV. ANGLE = 15DEG., AREA RATIO = 2, TAILPIPE LENGTH = 2.740M , RUN NO. 10

POSN	WIDTH M/M	DIST FROM INLET	STATIC PRESS. M/M H2O	MEAN VEL. M/S	LOCAL REYNOLDS NUMBER	2DELTA* ------- WIDTH	2THETA ------ WIDTH	SHAPE FACTOR	K.E.CORR. FACTOR	PRESS. RECOV. COEFF.	EFFECT-IVENESS	ENERGY CORR. EFFECT.	ENERG CORR. CP
1	76.2	-0.038	-284.	81.3	403549.	0.0097	0.0045	2.130	1.016	0.000	1.000	0.000	0.000
2	89.4	0.050	-184.	70.4	409695.	0.0226	0.0133	1.704	1.008	0.249	0.993	0.955	0.245
3	128.6	0.201	-38.	47.6	399014.	0.0871	0.0410	2.124	1.108	0.612	0.932	0.963	0.602
4	152.4	0.315	-2.	39.4	391073.	0.1331	0.0583	2.282	1.200	0.703	0.919	0.957	0.692
5	152.4	0.468	6.	39.4	391682.	0.0952	0.0621	1.531	1.085	0.724	0.947	0.952	0.712
6	152.4	0.620	9.	39.5	392698.	0.0849	0.0615	1.381	1.058	0.730	0.957	0.954	0.719
7	152.4	0.773	9.	0.0	0.	0.0000	0.0000	0.000	0.000	0.731	0.975	0.000	0.720
8	152.4	0.925	9.	39.4	391665.	0.0751	0.0583	1.287	1.040	0.732	0.957	0.949	0.720
9	152.4	1.230	9.	0.0	0.	0.0000	0.0000	0.000	0.000	0.732	0.976	0.000	0.720
10	152.4	1.535	8.	0.0	0.	0.0000	0.0000	0.000	0.000	0.730	0.973	0.000	0.718
11	152.4	1.839	8.	39.1	388276.	0.0831	0.0668	1.243	1.035	0.729	0.949	0.939	0.717
12	152.4	2.329	5.	0.0	0.	0.0000	0.0000	0.000	0.000	0.722	0.963	0.000	0.710
13	152.4	2.734	2.	0.0	0.	0.0000	0.0000	0.000	0.000	0.714	0.952	0.000	0.702
14	152.4	2.989	0.	0.0	0.	0.0000	0.0000	0.000	0.000	0.710	0.947	0.000	0.698

POSN.	BETA	C/L VEL.	TEMP.	ATM.PRESS.	X/W1
1	1.007	82.3	22.5	756.7	-0.498
2	1.002	71.5	22.5	756.7	0.656
3	1.042	52.0	22.5	756.7	2.637
4	1.078	45.6	22.5	756.7	4.133
5	1.032	43.7	22.5	756.7	6.141
6	1.022	43.3	22.5	756.7	8.136
7	0.000	0.0	22.5	756.7	10.144
8	1.015	42.8	22.5	756.7	12.139
9	0.000	0.0	22.5	756.7	16.141
10	0.000	0.0	22.5	756.7	20.144
11	1.013	42.8	22.5	756.7	24.133
12	0.000	0.0	22.5	756.7	30.564
13	0.000	0.0	22.5	756.7	35.879
14	0.000	0.0	22.5	756.7	39.225

INLET B/L THICKNESS = 0.0091 DIV. ANGLE = 5DEG., AREA RATIO = 2, TAILPIPE LENGTH = 0.000M , RUN NO.

POSN	WIDTH M/M	DIST FROM INLET	STATIC PRESS. M/M H2O	MEAN VEL. M/S	LOCAL REYNOLDS NUMBER	2DELTA* ------- WIDTH	2THETA ------ WIDTH	SHAPE FACTOR	K.E.CORR. FACTOR	PRESS. RECOV. COEFF.	EFFECT-IVENESS	ENERGY CORR. EFFECT.	ENE COR C
1	76.2	-0.038	-296.	80.1	402853.	0.0091	0.0041	2.221	1.015	0.000	1.000	0.000	0.0
2	94.0	0.203	-151.	62.5	388010.	0.0293	0.0199	1.471	1.022	0.367	0.941	0.935	0.3
3	120.4	0.508	-53.	49.5	393330.	0.0548	0.0390	1.404	1.044	0.617	0.998	1.000	0.6
4	147.0	0.812	-2.	34.9	339322.	0.1124	0.0698	1.610	1.103	0.748	0.924	0.928	0.7
5	200.0	1.000	0.	0.0	0.	0.0000	0.0000	0.000	0.000	0.753	0.881	0.000	0.7

POSN.	BETA	C/L VEL.	TEMP.	ATM.PRESS.	X/W1
1	1.007	81.0	21.0	760.0	-0.498
2	1.009	64.4	21.0	760.0	2.664
3	1.017	52.5	21.0	760.0	6.666
4	1.038	39.4	21.0	760.0	10.656
5	0.000	0.0	21.0	760.0	13.123

INLET B/L THICKNESS = 0.0095 DIV. ANGLE = 5DEG., AREA RATIO = 3, TAILPIPE LENGTH = 0.000M , RUN NO.

POSN	WIDTH M/M	DIST FROM INLET	STATIC PRESS. M/M H2O	MEAN VEL. M/S	LOCAL REYNOLDS NUMBER	2DELTA* ------- WIDTH	2THETA ------ WIDTH	SHAPE FACTOR	K.E.CORR. FACTOR	PRESS. RECOV. COEFF.	EFFECT-IVENESS	ENERGY CORR. EFFECT.	E C
1	76.2	-0.038	-343.	81.6	415072.	0.0095	0.0044	2.156	1.016	0.000	1.000	0.000	0
2	94.0	0.203	-209.	66.0	414471.	0.0310	0.0206	1.484	1.024	0.325	0.944	0.943	0
3	147.0	0.812	-60.	42.3	415283.	0.0963	0.0639	1.507	1.077	0.689	0.943	0.949	0
4	200.2	1.396	-15.	31.5	420865.	0.1661	0.1020	1.628	1.149	0.800	0.940	0.947	0
5	226.8	1.700	-2.	27.8	421959.	0.1971	0.1166	1.689	1.181	0.832	0.941	0.947	0
6	400.0	1.800	0.	0.0	0.	0.0000	0.0000	0.000	0.000	0.836	0.868	0.000	0

POSN.	BETA	C/L VEL.	TEMP.	ATM.PRESS.	X/W1
1	1.007	82.6	19.0	759.5	-0.498
2	1.009	68.1	19.0	759.5	2.664
3	1.028	46.8	19.0	759.5	10.656
4	1.053	37.8	19.0	759.5	18.320
5	1.063	34.6	19.0	759.5	22.309
6	0.000	0.0	19.0	759.5	23.622

INLET B/L THICKNESS = 0.0095 DIV. ANGLE = 5DEG., AREA RATIO = 3, TAILPIPE LENGTH = 2.740M , RUN NC

POSN	WIDTH M/M	DIST FROM INLET	STATIC PRESS. M/M H2O	MEAN VEL. M/S	LOCAL REYNOLDS NUMBER	2DELTA* / WIDTH	2THETA / WIDTH	SHAPE FACTOR	K.E.CORR. FACTOR	PRESS. RECOV. COEFF.	EFFECT-IVENESS	ENERGY CORR. EFFECT.
1	76.2	-0.038	-361.	83.5	424714.	0.0095	0.0044	2.162	1.016	0.000	1.000	0.000
2	94.0	0.203	-220.	67.5	423207.	0.0320	0.0214	1.494	1.025	0.329	0.948	0.949
3	147.0	0.812	-66.	45.0	441618.	0.1057	0.0675	1.567	1.091	0.687	0.968	0.982
4	226.8	1.700	-4.	31.0	468927.	0.1951	0.1156	1.687	1.178	0.831	0.963	0.973
5	228.6	2.231	-0.	30.5	466156.	0.1866	0.1265	1.475	1.106	0.841	0.971	0.969
6	228.6	3.093	1.	30.9	471886.	0.1542	0.1159	1.330	1.054	0.844	0.978	0.968
7	228.6	3.787	1.	30.8	469570.	0.1140	0.0919	1.239	1.028	0.845	0.978	0.964
8	228.6	4.447	0.	30.4	463968.	0.0911	0.0745	1.222	1.015	0.843	0.972	0.956

POSN.	BETA	C/L VEL.	TEMP.	ATM.PRESS.	X/W1
1	1.007	84.6	19.0	759.0	-0.498
2	1.010	69.7	19.0	759.0	2.664
3	1.033	50.3	19.0	759.0	10.656
4	1.062	38.4	19.0	759.0	22.309
5	1.036	37.5	19.0	759.0	29.278
6	1.018	36.5	19.0	759.0	40.590
7	1.009	34.6	19.0	759.0	49.698
8	1.003	33.2	19.0	759.0	58.359

INLET B/L THICKNESS = 0.0101 DIV. ANGLE = 5DEG., AREA RATIO = 2, TAILPIPE LENGTH = 2.780M , RUN NO. 1

POSN	WIDTH M/M	DIST FROM INLET	STATIC PRESS. M/M H2O	MEAN VEL. M/S	LOCAL REYNOLDS NUMBER	2DELTA* ------- WIDTH	2THETA ------ WIDTH	SHAPE FACTOR	K.E.CORR. FACTOR	PRESS. RECOV. COEFF.	EFFECT-IVENESS	ENERGY CORR. EFFECT.	ENER CORR CP
1	76.2	-0.038	-270.	81.0	404252.	0.0101	0.0048	2.096	1.016	0.000	1.000	0.000	0.00
2	94.0	0.203	-139.	65.4	402578.	0.0367	0.0239	1.535	1.031	0.328	0.943	0.953	0.32
3	120.4	0.508	-48.	51.4	404891.	0.0711	0.0465	1.527	1.057	0.556	0.930	0.947	0.54
4	147.0	0.812	2.	42.1	404955.	0.1076	0.0677	1.590	1.096	0.684	0.936	0.949	0.67
5	152.4	1.203	9.	40.6	405325.	0.1126	0.0781	1.440	1.082	0.700	0.935	0.940	0.68
6	152.4	1.512	9.	40.7	406031.	0.1076	0.0788	1.364	1.065	0.699	0.935	0.935	0.68
7	152.4	2.422	5.	41.2	411138.	0.1069	0.0842	1.262	1.044	0.691	0.932	0.925	0.67
8	152.4	3.572	1.	41.5	413928.	0.0973	0.0780	1.247	1.038	0.679	0.921	0.913	0.66

POSN.	BETA	C/L VEL.	TEMP.	ATM.PRESS.	X/W1
1	1.007	82.1	21.0	753.7	******
2	1.012	67.9	21.0	753.7	2.664
3	1.026	55.5	21.0	753.7	6.666
4	1.035	47.1	21.0	753.7	10.656
5	1.030	45.9	21.0	753.7	15.787
6	1.024	45.7	21.0	753.7	19.842
7	1.016	46.3	21.0	753.7	31.784
8	1.014	46.1	21.0	753.7	46.876

INLET B/L THICKNESS = 0.0615 DIV. ANGLE = 5DEG., AREA RATIO = 2, TAILPIPE LENGTH = 2.74CM , RUN NC.

PCSN	WIDTH M/M	DIST FRCM INLET	STATIC PRESS. M/M H2O	MEAN VEL. M/S	LCCAL REYNCLDS NUMBER	2DELTA* / WIDTH	2THETA / WIDTH	SHAPE FACTCR	K.E.CCRR. FACTCR	PRESS. RECCV. COEFF.	EFFECT-IVENESS	ENERGY CORR. EFFECT.	EN CC
1	76.2	-C.C50	-213.	71.9	367562.	C.0615	C.C443	1.387	1.045	C.COO	1.CCC	C.COC	C.
2	94.C	0.203	-123.	59.9	377762.	C.0984	C.C652	1.5C9	1.077	0.283	0.925	0.953	0.
3	120.4	C.5C8	-5C.	47.8	386475.	0.1553	0.C955	1.626	1.146	0.511	C.917	C.952	C.
4	147.C	0.812	-1C.	39.4	389183.	C.2217	C.1225	1.809	1.233	0.635	0.909	0.943	C.
5	152.4	C.898	-4.	37.9	388107.	C.2342	0.1298	1.8C3	1.247	C.655	0.908	0.939	O.
6	152.4	1.203	1.	38.2	390568.	C.2138	C.1359	1.572	1.156	0.670	C.934	0.933	C.
7	152.4	1.813	4.	38.6	395070.	C.1641	C.1207	1.359	1.073	C.681	0.958	0.927	O.
8	152.4	3.572	C.	38.8	396891.	0.0663	0.0546	1.214	1.C27	0.669	C.944	0.897	C.

PCSN.	BETA	C/L VEL.	TEMP.	ATM.PRESS.	X/W1
1	1.C17	76.8	19.C	763.5	C.CCO
2	1.028	66.4	19.0	763.5	2.664
3	1.C53	56.8	19.0	763.5	6.666
4	1.C82	5C.7	19.C	763.5	1C.656
5	1.C87	49.7	19.C	763.5	11.784
6	1.C54	48.7	19.0	763.5	15.787
7	1.026	46.3	19.0	763.5	23.792
8	1.C11	41.6	19.C	763.5	46.876

INLET B/L THICKNESS = 0.0598 DIV. ANGLE = 5DEG., AREA RATIO = 2, TAILPIPE LENGTH = 0.00CM , RUN NO.

POSN	WIDTH M/M	DIST FROM INLET	STATIC PRESS. M/M H2O	MEAN VEL. M/S	LOCAL REYNOLDS NUMBER	2DELTA* ------- WIDTH	2THETA ------ WIDTH	SHAPE FACTOR	K.E.CORR. FACTOR	PRESS. RECOV. COEFF.	EFFECT-IVENESS	ENERGY CORR. EFFECT.	EN CO
1	76.2	-0.070	-203.	71.1	356410.	0.0598	0.0429	1.395	1.044	0.000	1.000	0.000	0.
2	94.0	0.203	-113.	58.9	364018.	0.1003	0.0664	1.508	1.078	0.290	0.924	0.953	0.
3	120.4	0.508	-44.	47.1	373306.	0.1574	0.0958	1.641	1.151	0.513	0.916	0.954	0.
4	147.0	0.812	-6.	39.1	378118.	0.2230	0.1238	1.801	1.232	0.635	0.911	0.945	0.
5	200.0	1.000	0.	0.0	0.	0.0000	0.0000	0.000	0.000	0.656	0.767	0.000	0.

POSN.	BETA	C/L VEL.	TEMP.	ATM.PRESS.	X/W1
1	1.017	75.9	22.0	761.5	-0.918
2	1.029	65.5	22.0	761.5	2.664
3	1.055	56.2	22.0	761.5	6.666
4	1.081	50.3	22.0	761.5	10.656
5	0.000	0.0	22.0	761.5	13.123

INLET B/L THICKNESS = 0.0572   DIV. ANGLE = 5DEG.,   AREA RATIO = 3, TAILPIPE LENGTH = 0.000M , RUN NO.

PCSN	WIDTH M/M	DIST FROM INLET	STATIC PRESS. M/M H2O	MEAN VEL. M/S	LOCAL REYNOLDS NUMBER	2DELTA* ------- WIDTH	2THETA ------ WIDTH	SHAPE FACTOR	K.E.CORR. FACTOR	PRESS. RECOV. COEFF.	EFFECT-IVENESS	ENERGY CORR. EFFECT.	EN CC
1	76.2	-0.070	-312.	80.0	402205.	0.0572	0.0415	1.376	1.041	0.000	1.000	0.000	0.
2	94.0	0.203	-198.	66.5	412781.	0.0941	0.0640	1.469	1.069	0.289	0.939	0.960	0.
3	120.4	0.508	-110.	53.5	425480.	0.1510	0.0943	1.600	1.138	0.514	0.931	0.968	0.
4	147.0	0.812	-62.	44.4	430519.	0.2168	0.1212	1.789	1.224	0.637	0.920	0.958	0.
5	173.8	1.091	-36.	39.4	452130.	0.2556	0.1399	1.826	1.259	0.703	0.928	0.956	0.
6	200.2	1.396	-16.	34.6	457292.	0.2919	0.1566	1.863	1.295	0.754	0.928	0.944	0.
7	226.8	1.700	-2.	31.4	470139.	0.3077	0.1665	1.848	1.284	0.789	0.933	0.936	0.
8	300.0	2.000	0.	0.0	0.	0.0000	0.0000	0.000	0.000	0.795	0.849	0.000	0.

PCSN.	BETA	C/L VEL.	TEMP.	ATM.PRESS.	X/W1
1	1.016	85.1	22.0	764.5	-0.918
2	1.025	73.4	22.0	764.5	2.664
3	1.050	63.3	22.0	764.5	6.666
4	1.079	56.7	22.0	764.5	10.656
5	1.089	52.9	22.0	764.5	14.317
6	1.100	48.9	22.0	764.5	18.320
7	1.096	45.3	22.0	764.5	22.309
8	0.000	0.0	22.0	764.5	26.246

INLET B/L THICKNESS = 0.0549 DIV. ANGLE = 5DEG., AREA RATIO = 3, TAILPIPE LENGTH = 2.74CM , RUN NO.

PCSN	WIDTH M/M	DIST FROM INLET	STATIC PRESS. M/M H2O	MEAN VEL. M/S	LOCAL REYNOLDS NUMBER	2DELTA* / WIDTH	2THETA / WIDTH	SHAPE FACTOR	K.E.CORR. FACTOR	PRESS. RECOV. COEFF.	EFFECT-IVENESS	ENERGY CORR. EFFECT.	EN CO
1	76.2	-0.070	-348.	81.2	427643.	0.0549	0.0400	1.369	1.039	0.000	1.000	0.000	0.
2	94.0	0.203	-227.	67.7	439647.	0.0865	0.0600	1.439	1.060	0.291	0.952	0.962	0.
3	147.0	0.812	-76.	44.2	448872.	0.1993	0.1179	1.690	1.184	0.653	0.928	0.949	0.
4	226.8	1.700	-11.	30.8	483246.	0.3000	0.1654	1.813	1.267	0.810	0.946	0.945	0.
5	228.6	1.926	-6.	30.4	480180.	0.2806	0.1646	1.704	1.208	0.821	0.955	0.944	0.
6	228.6	2.483	-1.	30.2	477306.	0.2021	0.1389	1.454	1.098	0.834	0.968	0.940	0.
7	228.6	3.297	2.	28.8	454937.	0.0979	0.0802	1.220	1.023	0.842	0.963	0.925	0.
8	228.6	4.447	0.	27.9	441645.	0.0720	0.0603	1.194	1.016	0.837	0.950	0.911	0.

PCSN.	BETA	C/L VEL.	TEMP.	ATM.PRESS.	X/W1
1	1.015	86.1	15.0	767.2	-0.918
2	1.022	74.1	15.0	767.2	2.654
3	1.065	55.2	15.0	767.2	10.656
4	1.089	44.0	15.0	767.2	22.309
5	1.070	42.1	15.0	767.2	25.275
6	1.033	37.8	15.0	767.2	32.585
7	1.008	31.8	15.0	767.2	43.267
8	1.005	30.0	15.0	767.2	58.359

INLET B/L THICKNESS = 0.0498 DIV. ANGLE = 10DEG., AREA RATIO = 2, TAILPIPE LENGTH = 0.000M , RUN NO.

POSN	WIDTH M/M	DIST FROM INLET	STATIC PRESS. M/M H2O	MEAN VEL. M/S	LOCAL REYNOLDS NUMBER	2DELTA* ------- WIDTH	2THETA ------ WIDTH	SHAPE FACTOR	K.E.CORR. FACTOR	PRESS. RECOV. COEFF.	EFFECT-IVENESS	ENERGY CORR. EFFECT.	ENE COR C
1	76.2	-0.070	-151.	64.8	331072.	0.0498	0.0364	1.367	1.036	0.000	1.000	0.000	0.0
2	111.6	0.202	-44.	47.9	358726.	0.1168	0.0711	1.641	1.101	0.411	0.909	0.950	0.3
3	138.0	0.358	-12.	40.4	373684.	0.1789	0.0921	1.942	1.219	0.536	0.877	0.954	0.5
4	200.0	0.500	0.	0.0	0.	0.0000	0.0000	0.000	0.000	0.583	0.683	0.000	0.5

POSN.	BETA	C/L VEL.	TEMP.	ATM.PRESS.	X/W1
1	1.014	68.4	17.5	755.8	******
2	1.037	54.0	17.5	755.8	2.650
3	1.081	49.2	17.5	755.8	4.698
4	0.000	0.0	17.5	755.8	6.561

INLET B/L THICKNESS = 0.0560 DIV. ANGLE = 10DEG., AREA RATIO = 2, TAILPIPE LENGTH = 2.740M , RUN NO.

PCSN	WIDTH M/M	DIST FRCM INLET	STATIC PRESS. M/M H2O	MEAN VEL. M/S	LOCAL REYNOLDS NUMBER	2DELTA* ------- WIDTH	2THETA ------ WIDTH	SHAPE FACTOR	K.E.CORR. FACTOR	PRESS. RECOV. COEFF.	EFFECT-IVENESS	ENERGY CORR. EFFECT.	ENE COR (
1	76.2	-0.070	-188.	69.9	353409.	0.0560	0.0403	1.388	1.041	0.000	1.000	0.000	0.(
2	116.0	0.202	-69.	50.6	389550.	0.1206	0.0710	1.698	1.206	0.395	0.831	0.966	0.3
3	138.0	0.354	-32.	44.1	403782.	0.1906	0.0947	2.013	1.245	0.520	0.865	0.954	0.5
4	152.4	0.613	-10.	40.5	409429.	0.2023	0.1091	1.853	1.235	0.594	0.894	0.947	0.5
5	152.4	1.070	1.	40.3	408063.	0.1760	0.1198	1.469	1.112	0.631	0.946	0.940	0.6
6	152.4	2.084	5.	42.2	426469.	0.1097	0.0883	1.242	0.913	0.645	1.014	0.909	0.6
7	152.4	3.234	0.	39.1	395300.	0.0572	0.0469	1.221	1.026	0.630	0.917	0.874	0.6

PCSN.	BETA	C/L VEL.	TEMP.	ATM.PRESS.	X/W1
1	1.016	74.3	19.5	756.7	-0.918
2	1.084	59.9	19.5	756.7	2.650
3	1.091	54.5	19.5	756.7	4.645
4	1.085	50.9	19.5	756.7	8.044
5	1.039	49.1	19.5	756.7	14.041
6	0.951	44.2	19.5	756.7	27.349
7	1.010	41.6	19.5	756.7	42.440

INLET B/L THICKNESS = 0.0572 DIV. ANGLE = 10DEG., AREA RATIO = 2, TAILPIPE LENGTH = 1.829M , RUN NO.

POSN	WIDTH M/M	DIST FROM INLET	STATIC PRESS. M/M H2O	MEAN VEL. M/S	LOCAL REYNOLDS NUMBER	2DELTA* / WIDTH	2THETA / WIDTH	SHAPE FACTOR	K.E.CORR. FACTOR	PRESS. RECOV. COEFF.	EFFECT-IVENESS	ENERGY CORR. EFFECT.	EN CC (
1	76.2	-0.070	-195.	70.6	355057.	0.0572	0.0412	1.389	1.042	0.000	1.000	0.000	0.0
2	152.4	2.084	1.	40.3	405940.	0.0986	0.0791	1.246	1.038	0.644	0.957	0.916	0.6

POSN.	BETA	C/L VEL.	TEMP.	ATM.PRESS.	X/W1
1	1.017	75.1	20.0	755.7	-0.918
2	1.014	44.9	20.0	755.7	27.349

INLET B/L THICKNESS = 0.0529 DIV. ANGLE = 10DEG., AREA RATIO = 3, TAILPIPE LENGTH = 2.740M , RUN NO.

PCSN	WIDTH M/M	DIST FROM INLET	STATIC PRESS. M/M H2O	MEAN VEL. M/S	LOCAL REYNOLDS NUMBER	2DELTA* ------- WIDTH	2THETA ------ WIDTH	SHAPE FACTOR	K.E.CORR. FACTOR	PRESS. RECOV. COEFF.	EFFECT-IVENESS	ENERGY CORR. EFFECT.	EN CC
1	76.2	-0.070	-281.	77.7	403334.	0.0529	0.0380	1.389	1.039	0.000	1.00C	0.000	0.
2	111.6	0.201	-131.	59.0	448317.	0.1225	0.0711	1.722	1.117	0.396	0.934	1.000	0.
3	138.0	0.354	-89.	52.0	488708.	0.1575	0.0848	1.856	1.181	0.508	0.921	0.996	0.
4	160.0	0.481	-66.	48.2	525621.	0.1777	0.0905	1.963	1.222	0.568	0.925	1.000	0.
5	223.0	0.843	-34.	39.9	605747.	0.2507	0.1246	2.011	1.317	0.654	0.888	0.944	0.
6	228.6	1.201	-22.	38.1	594086.	0.2230	0.1357	1.642	1.175	0.686	0.904	0.907	0.

POSN.	BETA	C/L VEL.	TEMP.	ATM.PRESS.	X/W1
1	1.016	82.3	17.0	765.3	-0.918
2	1.043	66.9	17.0	765.3	2.637
3	1.067	61.7	17.0	765.3	4.645
4	1.082	58.7	17.0	765.3	6.312
5	1.112	53.2	17.0	765.3	11.062
6	1.060	49.0	17.0	765.3	15.761

INLET B/L THICKNESS = 0.0522 DIV. ANGLE = 10DEG., AREA RATIO = 3, TAILPIPE LENGTH = 2.740M , RUN NO.

POSN	WIDTH M/M	DIST FROM INLET	STATIC PRESS. M/M H2O	MEAN VEL. M/S	LOCAL REYNOLDS NUMBER	2DELTA* / WIDTH	2THETA / WIDTH	SHAPE FACTOR	K.E.CORR. FACTOR	PRESS. RECOV. COEFF.	EFFECT-IVENESS	ENERGY CORR. EFFECT.	EN CC (
1	76.2	-0.070	-275.	77.5	402299.	0.0522	0.0376	1.387	1.039	0.000	1.000	0.000	0.[illegible]
2	111.6	0.201	-131.	58.5	445277.	0.1176	0.0690	1.703	1.110	0.384	0.896	0.949	0.[illegible]
3	138.0	0.354	-89.	51.3	482310.	0.1531	0.0854	1.851	1.181	0.496	0.883	0.951	0.[illegible]
4	160.0	0.431	-69.	47.1	513568.	0.1854	0.0914	2.026	1.239	0.549	0.871	0.945	0.[illegible]
5	223.0	0.843	-33.	39.3	597094.	0.2487	0.1209	2.056	1.329	0.645	0.869	0.925	0.[illegible]
6	228.6	1.201	-21.	37.4	583138.	0.2245	0.1349	1.663	1.183	0.677	0.883	0.888	0.[illegible]
7	228.6	1.506	-12.	34.8	543200.	0.1816	0.1243	1.460	1.100	0.700	0.878	0.857	0.[illegible]
8	228.6	2.420	0.	29.2	455254.	0.0884	0.0712	1.241	1.027	0.734	0.856	0.822	0.7
9	228.6	3.570	0.	27.4	427019.	0.0776	0.0640	1.212	1.020	0.734	0.839	0.805	0.7

POSN.	BETA	C/L VEL.	TEMP.	ATM.PRESS.	X/W1
1	1.015	82.0	17.0	765.7	-0.918
2	1.040	66.1	17.0	765.7	2.637
3	1.067	60.9	17.0	765.7	4.645
4	1.089	57.8	17.0	765.7	6.312
5	1.116	52.3	17.0	765.7	11.062
6	1.063	48.1	17.0	765.7	15.761
7	1.034	42.5	17.0	765.7	19.763
8	1.009	32.0	17.0	765.7	31.758
9	1.007	29.6	17.0	765.7	46.850

INLET B/L THICKNESS = 0.0542 DIV. ANGLE = 10DEG., AREA RATIO = 3, TAILPIPE LENGTH = 0.000M , RUN NO.

PCSN	WIDTH M/M	DIST FROM INLET	STATIC PRESS. M/M H2O	MEAN VEL. M/S	LOCAL REYNOLDS NUMBER	2DELTA* ------- WIDTH	2THETA ------ WIDTH	SHAPE FACTOR	K.E.CORR. FACTOR	PRESS. RECOV. COEFF.	EFFECT-IVENESS	ENERGY. CORR. EFFECT.	ENE COR C
1	76.2	-0.070	-197.	70.8	356160.	0.0542	0.0395	1.372	1.039	0.000	1.000	0.000	0.0
2	111.6	0.201	-79.	53.8	396605.	0.1221	0.0718	1.699	1.113	0.386	0.916	0.978	0.3
3	138.0	0.354	-46.	47.0	428498.	0.1604	0.0858	1.869	1.186	0.494	0.885	0.960	0.4
4	160.0	0.481	-30.	44.0	464772.	0.1817	0.0927	1.960	1.226	0.547	0.891	0.968	0.5
5	223.0	0.843	-1.	36.9	544266.	0.2399	0.1225	1.958	1.292	0.640	0.880	0.932	0.6
6	300.0	1.000	0.	0.0	0.	0.0000	0.0000	0.000	0.000	0.645	0.690	0.000	0.6

PCSN.	BETA	C/L VEL.	TEMP.	ATM.PRESS.	X/W1
1	1.015	75.0	19.0	751.2	-0.918
2	1.042	61.0	19.0	751.2	2.637
3	1.069	56.0	19.0	751.2	4.645
4	1.083	53.7	19.0	751.2	6.312
5	1.103	48.6	19.0	751.2	11.062
6	0.000	0.0	19.0	751.2	13.123

INLET B/L THICKNESS = 0.0609 DIV. ANGLE = 15DEG., AREA RATIO = 2, TAILPIPE LENGTH = 0.000M , RUN NO.

POSN	WIDTH M/M	DIST FROM INLET	STATIC PRESS. M/M H2O	MEAN VEL. M/S	LOCAL REYNOLDS NUMBER	2DELTA* ------- WIDTH	2THETA ------ WIDTH	SHAPE FACTOR	K.E.CORR. FACTOR	PRESS. RECOV. COEFF.	EFFECT-IVENESS	ENERGY CORR. EFFECT.	ENE COR C
1	76.2	-0.070	-128.	63.1	327657.	0.0609	0.0438	1.390	1.044	0.000	1.000	0.000	0.C
2	89.4	0.050	-90.	57.9	352745.	0.0813	0.0540	1.503	1.049	0.153	0.969	0.948	0.1
3	128.6	0.201	-13.	43.0	377395.	0.1736	0.0844	2.056	1.219	0.463	0.867	0.972	0.4
4	300.0	0.300	0.	0.0	0.	0.0000	0.0000	0.000	0.000	0.515	0.551	0.000	0.4

POSN.	BETA	C/L VEL.	TEMP.	ATM.PRESS.	X/W1
1	1.017	67.4	16.0	761.2	-0.918
2	1.017	62.5	16.0	761.2	0.656
3	1.082	51.9	16.0	761.2	2.637
4	0.000	0.0	16.0	761.2	3.937

INLET B/L THICKNESS = 0.0619 DIV. ANGLE = 15DEG., AREA RATIO = 3, TAILPIPE LENGTH = 0.000M , RUN NO.

POSN	WIDTH M/M	DIST FROM INLET	STATIC PRESS. M/M H2O	MEAN VEL. M/S	LOCAL REYNOLDS NUMBER	2DELTA* / WIDTH	2THETA / WIDTH	SHAPE FACTOR	K.E.CORR. FACTOR	PRESS. RECOV. COEFF.	EFFECT-IVENESS	ENERGY CORR. EFFECT.	ENE CCR C
1	76.2	-0.070	-162.	66.3	341833.	0.0619	0.0447	1.382	1.044	0.000	1.000	0.000	0.C
2	128.6	0.201	-34.	33.9	294654.	0.3740	0.0958	3.902	1.924	0.468	0.634	0.864	0.4
3	161.4	0.327	-27.	17.4	190565.	0.6599	0.0472	*****	5.837	0.494	0.531	0.772	0.4
4	220.6	0.554	-10.	0.0	0.	0.0000	0.0000	0.000	0.000	0.556	0.632	0.000	0.5
5	500.0	0.700	0.	0.0	0.	0.0000	0.0000	0.000	0.000	0.593	0.607	0.000	0.5

POSN.	BETA	C/L VEL.	TEMP.	ATM.PRESS.	X/W1
1	1.017	70.9	17.0	759.7	-0.918
2	1.347	53.9	17.0	759.7	2.637
3	2.509	50.8	17.0	759.7	4.291
4	0.000	0.0	17.0	759.7	7.270
5	0.000	0.0	17.0	759.7	9.186

INLET B/L THICKNESS = 0.0628 DIV. ANGLE = 15DEG., AREA RATIO = 3, TAILPIPE LENGTH = 2.740M , RUN NO.

POSN	WIDTH M/M	DIST FROM INLET	STATIC PRESS. N/M H2O	MEAN VEL. M/S	LOCAL REYNOLDS NUMBER	2DELTA* ------- WIDTH	2THETA ------ WIDTH	SHAPE FACTOR	K.E.CORR. FACTOR	PRESS. RECOV. COEFF.	EFFECT-IVENESS	ENERGY CORR. EFFECT.	ENE CORR C
1	76.2	-0.070	-255.	71.5	374417.	0.0628	0.0445	1.408	1.047	0.000	1.000	0.000	0.0
2	89.4	0.050	-199.	65.9	404712.	0.0833	0.0546	1.526	1.053	0.174	1.152	1.133	0.16
3	128.6	0.201	-95.	41.3	365461.	0.1740	0.0850	2.046	1.763	0.497	0.747	1.087	0.47
4	161.4	0.327	-71.	0.0	0.	0.0000	0.0000	0.000	0.000	0.572	0.736	0.000	0.54
5	220.6	0.554	-46.	0.0	0.	0.0000	0.0000	0.000	0.000	0.650	0.738	0.000	0.62
6	228.6	0.909	-24.	37.6	590874.	0.2317	0.1341	1.727	1.209	0.718	0.993	1.007	0.68
7	228.6	2.128	-1.	31.1	489364.	0.0614	0.0513	1.197	1.015	0.790	0.975	0.924	0.75
8	228.6	3.278	0.	27.7	436095.	0.0716	0.0597	1.198	1.017	0.793	0.934	0.887	0.75

POSN.	BETA	C/L VEL.	TEMP.	ATM.PRESS.	X/W1
1	1.018	76.5	16.0	767.4	-0.918
2	1.018	71.3	16.0	767.4	0.656
3	1.297	61.4	16.0	767.4	2.637
4	0.000	0.0	16.0	767.4	4.291
5	0.000	0.0	16.0	767.4	7.270
6	1.072	48.8	16.0	767.4	11.929
7	1.005	33.1	16.0	767.4	27.926
8	1.006	29.8	16.0	767.4	43.018

INLET B/L THICKNESS = 0.0624 DIV. ANGLE = 15DEG., AREA RATIO = 2, TAILPIPE LENGTH = 2.740M , RUN NO.

PCSN	WIDTH M/M	DIST FROM INLET	STATIC PRESS. M/M H2O	MEAN VEL. M/S	LOCAL REYNOLDS NUMBER	2DELTA* ------- WIDTH	2THETA ------ WIDTH	SHAPE FACTOR	K.E.CORR. FACTOR	PRESS. RECOV. COEFF.	EFFECT-IVENESS	ENERGY CORR. EFFECT.	ENE COR C
1	76.2	-0.070	-184.	68.4	350445.	0.0624	0.0448	1.392	1.045	0.000	1.000	0.000	0.0
2	89.4	0.050	-137.	62.6	376452.	0.0827	0.0546	1.513	1.051	0.161	1.001	0.984	0.1
3	128.6	0.201	-47.	44.5	384627.	0.2076	0.0890	2.333	1.366	0.472	0.818	0.957	0.4
4	152.4	0.468	-15.	39.1	400561.	0.2276	0.1128	2.017	1.301	0.582	0.864	0.938	0.5
5	152.4	0.923	-1.	39.5	404860.	0.1787	0.1224	1.459	1.109	0.630	0.946	0.933	0.6
6	152.4	1.839	4.	39.0	399942.	0.0869	0.0706	1.230	1.033	0.647	0.960	0.913	0.6
7	152.4	2.734	1.	38.5	394327.	0.0620	0.0509	1.217	1.026	0.639	0.935	0.886	0.6

PCSN.	BETA	C/L VEL.	TEMP.	ATM.PRESS.	X/W1
1	1.018	73.2	19.0	764.5	-0.918
2	1.018	67.8	19.0	764.5	0.656
3	1.116	55.9	19.0	764.5	2.637
4	1.108	50.8	19.0	764.5	6.141
5	1.038	48.3	19.0	764.5	12.112
6	1.013	42.9	19.0	764.5	24.133
7	1.010	41.1	19.0	764.5	35.879

INLET B/L THICKNESS = 0.1102 DIV. ANGLE = 15DEG., AREA RATIO = 2, TAILPIPE LENGTH = 2.740M , RUN NO.

POSN	WIDTH M/M	DIST FROM INLET	STATIC PRESS. M/M H2O	MEAN VEL. M/S	LOCAL REYNOLDS NUMBER	2DELTA* / WIDTH	2THETA / WIDTH	SHAPE FACTOR	K.E.CORR. FACTOR	PRESS. RECOV. COEFF.	EFFECT-IVENESS	ENERGY CORR. EFFECT.	ENE COF C
1	76.2	-0.070	-221.	75.7	392540.	0.1102	0.0845	1.304	1.051	0.000	1.000	0.000	0.C
2	89.4	0.050	-169.	70.0	425473.	0.1272	0.0921	1.380	1.052	0.144	0.989	0.947	0.1
3	128.6	0.201	-59.	51.3	448929.	0.2427	0.1314	1.846	1.241	0.451	0.834	0.938	0.4
4	152.4	0.468	-28.	44.2	458337.	0.2088	0.1238	1.686	1.456	0.537	0.815	0.969	0.5
5	152.4	0.773	-14.	45.5	472149.	0.2431	0.1509	1.631	1.184	0.576	0.903	0.926	0.5
6	152.4	1.839	2.	42.9	444952.	0.1148	0.0903	1.270	1.045	0.622	0.917	0.870	0.5
7	152.4	2.734	1.	41.7	432758.	0.0744	0.0612	1.214	1.028	0.619	0.889	0.838	0.5

POSN.	BETA	C/L VEL.	TEMP.	ATM.PRESS.	X/W1
1	1.019	85.4	18.0	769.0	******
2	1.017	79.6	18.0	769.0	0.656
3	1.087	67.5	18.0	769.0	2.637
4	1.180	63.5	18.0	769.0	6.141
5	1.063	60.6	18.0	769.0	10.144
6	1.017	48.6	18.0	769.0	24.133
7	1.011	45.2	18.0	769.0	35.879

INLET B/L THICKNESS = 0.1114 DIV. ANGLE = 15DEG., AREA RATIO = 2, TAILPIPE LENGTH = 0.000M , RUN NO.

POSN	WIDTH M/M	DIST FROM INLET	STATIC PRESS. M/M H2O	MEAN VEL. M/S	LOCAL REYNOLDS NUMBER	2DELTA* / WIDTH	2THETA / WIDTH	SHAPE FACTOR	K.E.CORR. FACTOR	PRESS. RECOV. COEFF.	EFFECT-IVENESS	ENERGY CORR. EFFECT.	ENE COR C
1	76.2	-0.070	-146.	70.3	359898.	0.1114	0.0857	1.299	1.050	0.000	1.000	0.000	0.0
2	89.4	0.050	-105.	65.2	391720.	0.1302	0.0934	1.393	1.055	0.134	0.963	0.949	0.1
3	128.6	0.201	-17.	50.1	433570.	0.2205	0.1248	1.766	1.201	0.422	0.861	0.964	0.4
4	500.0	0.300	0.	0.0	0.	0.0000	0.0000	0.000	0.000	0.478	0.489	0.000	0.4

POSN.	BETA	C/L VEL.	TEMP.	ATM.PRESS.	X/W1
1	1.019	79.3	18.0	759.8	-0.000
2	1.019	74.4	18.0	759.8	0.656
3	1.074	64.1	18.0	759.8	2.637
4	0.000	0.0	18.0	759.8	3.937

INLET B/L THICKNESS = 0.1082 DIV. ANGLE = 15DEG., AREA RATIO = 3, TAILPIPE LENGTH = 0.000M , RUN N

POSN	WIDTH M/M	DIST FROM INLET	STATIC PRESS. M/M H2O	MEAN VEL. M/S	LOCAL REYNOLDS NUMBER	2DELTA* / WIDTH	2THETA / WIDTH	SHAPE FACTOR	K.E.CORR. FACTOR	PRESS. RECOV. COEFF.	EFFECT-IVENESS	ENERGY CORR. EFFECT.
1	76.2	-0.070	-178.	73.1	380788.	0.1082	0.0826	1.309	1.052	0.000	1.000	0.000
2	128.6	0.201	-40.	52.6	461950.	0.2175	0.1265	1.720	1.188	0.412	0.853	0.942
3	161.4	0.327	-24.	48.6	536215.	0.2409	0.1315	1.831	1.239	0.460	0.825	0.913
4	220.6	0.554	-6.	41.5	625305.	0.2662	0.1380	1.928	1.405	0.514	0.758	0.857
5	500.0	0.700	0.	0.0	0.	0.0000	0.0000	0.000	0.000	0.532	0.545	0.000

POSN.	BETA	C/L VEL.	TEMP.	ATM.PRESS.	X/W1
1	1.020	82.3	16.0	763.0	-0.918
2	1.068	66.9	16.0	763.0	2.637
3	1.084	63.7	16.0	763.0	4.291
4	1.147	59.3	16.0	763.0	7.270
5	0.000	0.0	16.0	763.0	9.186

INLET B/L THICKNESS = 0.1095 DIV. ANGLE = 15DEG., AREA RATIO = 3, TAILPIPE LENGTH = 2.740M , RUN NO.

POSN	WIDTH M/M	DIST FROM INLET	STATIC PRESS. M/M H2O	MEAN VEL. M/S	LOCAL REYNOLDS NUMBER	2DELTA* ------- WIDTH	2THETA ------ WIDTH	SHAPE FACTOR	K.E.CORR. FACTOR	PRESS. RECOV. COEFF.	EFFECT- IVENESS	ENERGY CORR. EFFECT.	EN CO
1	76.2	-0.070	-253.	77.4	394419.	0.1095	0.0838	1.307	1.051	0.000	1.000	0.000	0.
2	128.6	0.201	-101.	55.9	481317.	0.2147	0.1253	1.712	1.185	0.413	0.867	0.958	0.
3	161.4	0.327	-79.	52.0	561584.	0.2337	0.1300	1.798	1.225	0.473	0.864	0.951	0.
4	220.6	0.554	-54.	43.9	647983.	0.3069	0.1461	2.100	1.395	0.541	0.799	0.899	0.
5	228.6	0.757	-48.	44.1	675587.	0.2879	0.1485	1.937	1.320	0.558	0.828	0.898	0.
6	228.6	1.519	-12.	35.2	539296.	0.1763	0.1188	1.483	1.108	0.656	0.828	0.798	0.
7	228.6	3.278	0.	26.9	412520.	0.0706	0.0594	1.188	1.015	0.689	0.785	0.742	0.

POSN.	BETA	C/L VEL.	TEMP.	ATM.PRESS.	X/W1
1	1.020	87.1	17.0	751.8	-0.918
2	1.066	71.0	17.0	751.8	2.637
3	1.079	67.5	17.0	751.8	4.291
4	1.136	63.2	17.0	751.8	7.270
5	1.109	61.9	17.0	751.8	9.934
6	1.037	42.7	17.0	751.8	19.934
7	1.005	28.9	17.0	751.8	43.018

INLET B/L THICKNESS = 0.1106 DIV. ANGLE = 10DEG., AREA RATIO = 3, TAILPIPE LENGTH = 2.740M , RUN N

POSN	WIDTH M/M	DIST FROM INLET	STATIC PRESS. M/M H2O	MEAN VEL. M/S	LOCAL REYNOLDS NUMBER	2DELTA* / WIDTH	2THETA / WIDTH	SHAPE FACTOR	K.E.CORR. FACTOR	PRESS. RECOV. COEFF.	EFFECT-IVENESS	ENERGY CORR. EFFECT.
1	76.2	-0.070	-262.	75.4	396670.	0.1106	0.0845	1.308	1.052	0.000	1.000	0.000
2	111.6	0.201	-121.	56.5	435113.	0.2011	0.1256	1.600	1.143	0.392	0.893	0.956
3	138.0	0.354	-81.	49.4	470719.	0.2427	0.1390	1.745	1.221	0.503	0.882	0.954
4	223.0	0.843	-36.	36.2	557971.	0.3742	0.1650	2.267	1.528	0.628	0.817	0.899
5	228.6	1.354	-16.	33.6	529791.	0.3080	0.1657	1.858	1.291	0.683	0.852	0.858
6	228.6	3.570	0.	26.9	424835.	0.0633	0.0531	1.190	1.014	0.729	0.836	0.790

POSN.	BETA	C/L VEL.	TEMP.	ATM.PRESS.	X/W1
1	1.020	85.1	16.0	770.5	0.000
2	1.050	70.4	16.0	770.5	2.637
3	1.078	65.3	16.0	770.5	4.645
4	1.176	57.9	16.0	770.5	11.062
5	1.097	48.4	16.0	770.5	17.769
6	1.005	28.7	16.0	770.5	46.850

INLET B/L THICKNESS = 0.1112 DIV. ANGLE = 10DEG., AREA RATIO = 5, TAILPIPE LENGTH = 0.000M , RUN NO.

POSN	WIDTH M/M	DIST FROM INLET	STATIC PRESS. M/M H2O	MEAN VEL. M/S	LOCAL REYNOLDS NUMBER	2DELTA* ------- WIDTH	2THETA ------ WIDTH	SHAPE FACTOR	K.F.CORR. FACTOR	PRESS. RECOV. COEFF.	EFFECT-IVENESS	ENERGY CORR. EFFECT.	E C
1	76.2	-0.070	-196.	71.1	356842.	0.1112	0.0851	1.306	1.051	0.000	1.000	0.000	0
2	111.6	0.201	-75.	53.2	391473.	0.2007	0.1251	1.603	1.144	0.388	0.885	0.948	0
3	138.0	0.354	-43.	47.4	431618.	0.2359	0.1385	1.702	1.202	0.493	0.890	0.956	0
4	223.0	0.843	-2.	36.4	535529.	0.3305	0.1561	2.117	1.426	0.625	0.848	0.924	0
5	500.0	1.000	0.	0.0	0.	0.0000	0.0000	0.000	0.000	0.631	0.645	0.000	0

POSN.	BETA	C/L VEL.	TEMP.	ATM.PRESS.	X/W1
1	1.020	80.2	23.0	768.0	0.000
2	1.051	66.3	23.0	768.0	2.637
3	1.071	62.1	23.0	768.0	4.645
4	1.145	54.4	23.0	768.0	11.062
5	0.000	0.0	23.0	768.0	13.123

INLET B/L THICKNESS = 0.1122 DIV. ANGLE = 10DEG., AREA RATIO = 2, TAILPIPE LENGTH = 0.000M , RUN N

POSN	WIDTH M/M	DIST FROM INLET	STATIC PRESS. M/M H2O	MEAN VEL. M/S	LOCAL REYNOLDS NUMBER	2DELTA* / WIDTH	2THETA / WIDTH	SHAPE FACTOR	K.E.CORR. FACTOR	PRESS. RECOV. COEFF.	EFFECT-IVENESS	ENERGY CORR. EFFECT.
1	76.2	-0.070	-179.	73.1	371615.	0.1122	0.0856	1.311	1.053	0.000	1.000	0.000
2	111.6	0.202	-48.	54.5	406150.	0.2040	0.1257	1.622	1.152	0.396	0.894	0.963
3	138.0	0.354	-13.	48.0	441876.	0.2449	0.1395	1.755	1.226	0.502	0.882	0.957
4	200.0	0.500	0.	0.0	0.	0.0000	0.0000	0.000	0.000	0.541	0.633	0.000

POSN.	BETA	C/L VEL.	TEMP.	ATM.PRESS.	X/W1
1	1.020	82.6	21.0	768.0	-0.918
2	1.054	68.2	21.0	768.0	2.650
3	1.079	63.6	21.0	768.0	4.645
4	0.000	0.0	21.0	768.0	6.561

INLET B/L THICKNESS = 0.1089 DIV. ANGLE = 10DEG., AREA RATIO = 2, TAILPIPE LENGTH = 2.740M , RUN NO. 3

POSN	WIDTH M/M	DIST FROM INLET	STATIC PRESS. M/M H2O	MEAN VEL. M/S	LOCAL REYNOLDS NUMBER	2DELTA* / WIDTH	2THETA / WIDTH	SHAPE FACTOR	K.E.CORR. FACTOR	PRESS. RECOV. COEFF.	EFFECT-IVENESS	ENERGY CORR. EFFECT.	ENER CORR CP
1	76.2	-0.070	-203.	71.4	379391.	0.1089	0.0833	1.306	1.051	0.000	1.000	0.000	0.00
2	111.6	0.202	-74.	52.9	411761.	0.2035	0.1253	1.624	1.152	0.398	0.882	0.950	0.37
3	138.0	0.354	-36.	45.0	433914.	0.2597	0.1426	1.820	1.256	0.515	0.857	0.937	0.49
4	152.4	0.460	-22.	42.3	450298.	0.2768	0.1462	1.892	1.302	0.560	0.865	0.945	0.53
5	152.4	1.375	0.	40.8	433718.	0.1879	0.1313	1.431	1.099	0.630	0.935	0.909	0.59
6	152.4	2.084	3.	39.7	422829.	0.1123	0.0883	1.271	1.045	0.640	0.928	0.880	0.60
7	152.4	2.979	1.	39.2	417517.	0.0652	0.0534	1.221	1.028	0.632	0.907	0.854	0.60

POSN.	BETA	C/L VEL.	TEMP.	ATM.PRESS.	X/W1
1	1.019	80.3	13.5	767.2	-0.918
2	1.054	66.1	13.5	767.2	2.650
3	1.090	60.9	13.5	767.2	4.645
4	1.106	58.8	13.5	767.2	6.036
5	1.034	50.4	13.5	767.2	18.044
6	1.017	44.9	13.5	767.2	27.349
7	1.011	42.1	13.5	767.2	39.094

INLET B/L THICKNESS = 0.1089 DIV. ANGLE = 5DEG., AREA RATIO = 2, TAILPIPE LENGTH = 2.740M , RUN

POSN	WIDTH M/M	DIST FROM INLET	STATIC PRESS. M/M H2O	MEAN VEL. M/S	LOCAL REYNOLDS NUMBER	2DELTA* ------- WIDTH	2THETA ------ WIDTH	SHAPE FACTOR	K.E.CORR. FACTOR	PRESS. RECOV. COEFF.	EFFECT-IVENESS	ENERGY CORR. EFFECT.
1	76.2	-0.070	-207.	71.7	371162.	0.1089	0.0830	1.310	1.052	0.000	1.000	0.000
2	94.0	0.203	-121.	60.3	385331.	0.1505	0.1057	1.422	1.084	0.269	0.924	0.948
3	120.4	0.508	-51.	48.3	395212.	0.2082	0.1318	1.579	1.158	0.489	0.896	0.929
4	147.0	0.812	-13.	40.8	407476.	0.2568	0.1491	1.721	1.219	0.608	0.899	0.925
5	152.4	1.203	-1.	39.0	404278.	0.2308	0.1477	1.562	1.153	0.645	0.917	0.908
6	152.4	2.118	5.	38.2	395640.	0.1211	0.0940	1.288	1.050	0.664	0.928	0.881
7	152.4	3.317	1.	38.3	397373.	0.0688	0.0566	1.216	1.028	0.653	0.916	0.862

POSN.	BETA	C/L VEL.	TEMP.	ATM.PRESS.	X/W1
1	1.020	80.7	15.5	756.7	-0.918
2	1.030	71.0	15.5	756.7	2.664
3	1.056	61.2	15.5	756.7	6.666
4	1.075	54.9	15.5	756.7	10.656
5	1.053	50.9	15.5	756.7	15.787
6	1.018	43.6	15.5	756.7	27.795
7	1.011	41.3	15.5	756.7	43.530

INLET B/L THICKNESS = 0.1090 DIV. ANGLE = 5DEG., AREA RATIO = 2, TAILPIPE LENGTH = 0.000M , RUN NO.

POSN	WIDTH M/M	DIST FROM INLET	STATIC PRESS. M/M H2O	MEAN VEL. M/S	LOCAL REYNOLDS NUMBER	2DELTA* / WIDTH	2THETA / WIDTH	SHAPE FACTOR	K.E.CORR. FACTOR	PRESS. RECOV. COEFF.	EFFECT-IVENESS	ENERGY CORR. EFFECT.	EN CO
1	76.2	-0.070	-212.	74.1	376426.	0.1090	0.0830	1.313	1.053	0.000	1.000	0.000	0.
2	94.0	0.203	-110.	62.4	390666.	0.1501	0.1052	1.426	1.085	0.302	1.033	1.060	0.
3	120.4	0.508	-39.	50.0	401576.	0.2103	0.1325	1.586	1.161	0.512	0.941	0.978	0.
4	147.0	0.812	-5.	42.9	420817.	0.2450	0.1431	1.712	1.213	0.612	0.921	0.948	0.
5	200.0	1.000	0.	0.0	0.	0.0000	0.0000	0.000	0.000	0.627	0.734	0.000	0.

POSN.	BETA	C/L VEL.	TEMP.	ATM.PRESS.	X/W1
1	1.020	83.5	19.0	758.0	-0.918
2	1.030	73.4	19.0	758.0	2.664
3	1.057	63.6	19.0	758.0	6.666
4	1.073	56.9	19.0	758.0	10.656
5	0.000	0.0	19.0	758.0	13.123

LFT B/L THICKNESS = 0.1095 DIV. ANGLE = 5DEG.. AREA RATIO = 3. TAILPIPE LENGTH = 0.000M . RUN NO. 311

SN WIDTH M/M	DIST FROM INLET	STATIC PRESS. M/M H2O	MEAN VEL. M/S	LOCAL REYNOLDS NUMBER	2DELTA* / WIDTH	2THETA / WIDTH	SHAPE FACTOR	K.E.CORR. FACTOR	PRESS. RECOV. COEFF.	EFFECT-IVENESS	ENERGY CORR. EFFECT.	ENERGY CORR. CP
76.2	-0.070	-264.	75.4	382761.	0.1095	0.0834	1.313	1.053	0.000	1.000	0.000	0.000
120.4	0.508	-91.	51.3	411917.	0.2073	0.1308	1.584	1.159	0.494	0.921	0.959	0.459
147.0	0.812	-50.	43.7	428417.	0.2482	0.1468	1.690	1.203	0.612	0.923	0.946	0.581
200.2	1.396	-14.	35.1	468173.	0.2740	0.1562	1.753	1.240	0.714	0.912	0.911	0.678
226.8	1.700	-2.	31.8	481093.	0.2682	0.1536	1.745	1.232	0.748	0.911	0.898	0.711
400.0	2.000	0.	0.0	0.	0.0000	0.0000	0.000	0.000	0.756	0.784	0.000	0.717

POSN.	BETA	C/L VEL.	TEMP.	ATM.PRESS.	X/W1
1	1.020	84.9	19.0	758.0	-0.918
2	1.056	65.0	19.0	758.0	6.666
3	1.070	58.2	19.0	758.0	10.656
4	1.082	48.4	19.0	758.0	18.320
5	1.078	43.4	19.0	758.0	22.309
6	0.000	0.0	19.0	758.0	26.246

NLET B/L THICKNESS = 0.1108 DIV. ANGLE = 5DEG., AREA RATIO = 3, TAILPIPE LENGTH = 2.740M , RUN NO. 312

OSN	WIDTH M/M	DIST FROM INLET	STATIC PRESS. M/M H2O	MEAN VEL. M/S	LOCAL REYNOLDS NUMBER	2DELTA* / WIDTH	2THETA / WIDTH	SHAPE FACTOR	K.E.CORR. FACTOR	PRESS. RECOV. COEFF.	EFFECT-IVENESS	ENERGY CORR. EFFECT.	ENERGY CORR. CP
	76.2	-0.070	-288.	76.9	399019.	0.1108	0.0843	1.313	1.053	0.000	1.000	0.000	0.000
	80.6	0.051	-254.	73.8	405491.	0.1203	0.0889	1.353	1.048	0.092	1.206	1.083	0.088
	147.0	0.812	-69.	45.1	451444.	0.2450	0.1460	1.677	1.199	0.598	0.911	0.932	0.567
	200.2	1.396	-26.	35.8	489298.	0.2721	0.1555	1.751	1.241	0.715	0.914	0.913	0.679
	228.6	1.700	-11.	32.9	512776.	0.2508	0.1504	1.667	1.213	0.756	0.926	0.910	0.718
	228.6	2.078	-4.	31.2	485933.	0.2306	0.1455	1.584	1.153	0.775	0.928	0.898	0.736
	228.6	3.297	1.	28.7	447601.	0.0779	0.0651	1.196	1.017	0.790	0.918	0.867	0.750
	228.6	4.192	0.	27.7	432477.	0.0520	0.0442	1.177	1.0[illegible]1	0.788	0.906	0.855	0.748

POSN.	BETA	C/L VEL.	TEMP.	ATM.PRESS.	X/W1
1	1.020	86.7	14.0	751.5	-0.918
2	1.016	83.5	14.0	751.5	0.669
3	1.068	59.7	14.0	751.5	10.656
4	1.081	49.3	14.0	751.5	18.320
5	1.074	44.3	14.0	751.5	22.309
6	1.052	40.4	14.0	751.5	27.270
7	1.006	31.1	14.0	751.5	43.267
8	1.003	29.2	14.0	751.5	55.013

INLET B/L THICKNESS = 0.1084 DIV. ANGLE = 5DEG., AREA RATIO = 3, TAILPIPE LENGTH = 0.000M , RU

POSN	WIDTH M/M	DIST FROM INLET	STATIC PRESS. M/M H2O	MEAN VEL. M/S	LOCAL REYNOLDS NUMBER	2DELTA* ------- WIDTH	2THETA ------ WIDTH	SHAPE FACTOR	K.E.CORR. FACTOR	PRESS. RECOV. COEFF.	EFFECT-IVENESS	ENE CORR EFFE
1	152.4	-0.070	-264.	75.5	766488.	0.1084	0.0826	1.312	1.052	0.000	1.000	0.00

POSN.	BETA	C/L VEL.	TEMP.	ATM.PRESS.	X/W1
1	1.020	84.9	19.0	758.0	-0.459

INLET B/L THICKNESS = 0.0000 DIV. ANGLE = 10DEG., AREA RATIO = 3, TAILPIPE LENGTH = 2.740M , RUN NO.

POSN	WIDTH M/M	DIST FROM INLET	STATIC PRESS. M/M H2O	MEAN VEL. M/S	LOCAL REYNOLDS NUMBER	2DELTA* ------- WIDTH	2THETA ------ WIDTH	SHAPE FACTOR	K.E.CORR. FACTOR	PRESS. RECOV. COEFF.	EFFECT-IVENESS	ENERGY CORR. EFFECT.	ENE COR C
1	76.2	36.500	-154.	76.9	390361.	0.0132	0.0063	2.078	1.020	0.000	1.000	0.000	0.0
2	76.2	35.000	-164.	0.0	0.	0.0000	0.0000	0.000	0.000	0.000	1.000	0.000	0.0
3	76.2	31.000	-198.	0.0	0.	0.0000	0.0000	0.000	0.000	0.000	1.000	0.000	0.0
4	76.2	27.000	-222.	0.0	0.	0.0000	0.0000	0.000	0.000	0.000	1.000	0.000	0.0
5	76.2	23.000	-226.	0.0	0.	0.0000	0.0000	0.000	0.000	0.000	1.000	0.000	0.0
6	76.2	19.000	-250.	0.0	0.	0.0000	0.0000	0.000	0.000	0.000	1.000	0.000	0.0
7	76.2	15.000	-249.	0.0	0.	0.0000	0.0000	0.000	0.000	0.000	1.000	0.000	0.0
8	76.2	7.000	-269.	0.0	0.	0.0000	0.0000	0.000	0.000	0.000	1.000	0.000	0.0
9	76.2	3.000	-275.	0.0	0.	0.0000	0.0000	0.000	0.000	0.000	1.000	0.000	0.0
10	76.2	1.000	-280.	0.0	0.	0.0000	0.0000	0.000	0.000	0.000	1.000	0.000	0.0

POSN.	BETA	C/L VEL.	TEMP.	ATM.PRESS.	X/W1	
1	1.009	78.1	18.0	753.4	36.500	36.5
2	0.000	0.0	18.0	753.4	******	35.0
3	0.000	0.0	18.0	753.4	******	31.0
4	0.000	0.0	18.0	753.4	******	27.0
5	0.000	0.0	18.0	753.4	******	23.0
6	0.000	0.0	18.0	753.4	******	19.0
7	0.000	0.0	18.0	753.4	******	15.0
8	0.000	0.0	18.0	753.4	91.863	7.0
9	0.000	0.0	18.0	753.4	39.370	3.0
10	0.000	0.0	18.0	753.4	13.123	1.0

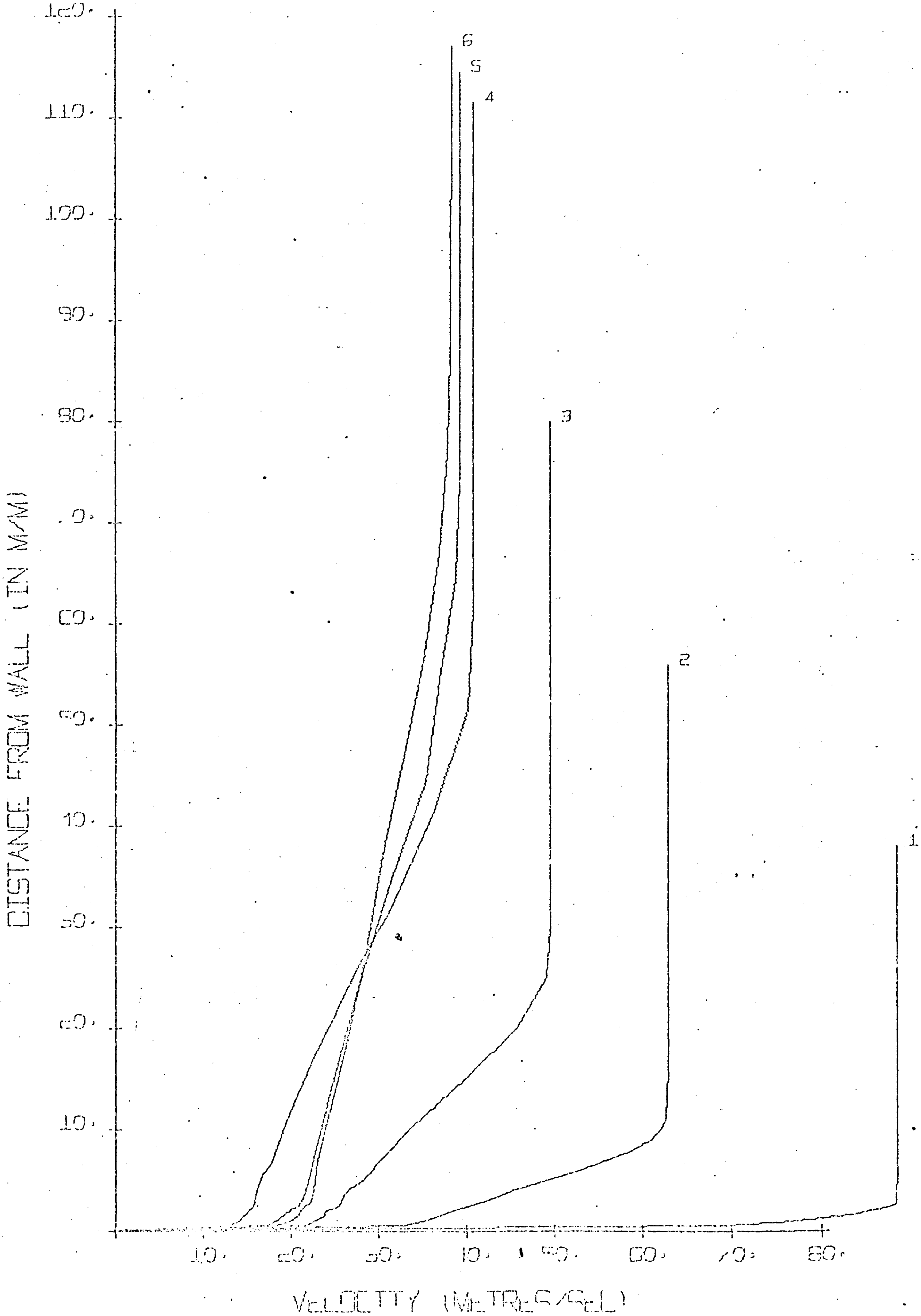
DISTANCE FROM WALL (IN M/M)
VELOCITY (METRES/SEC)
6
5
4
3
2
1

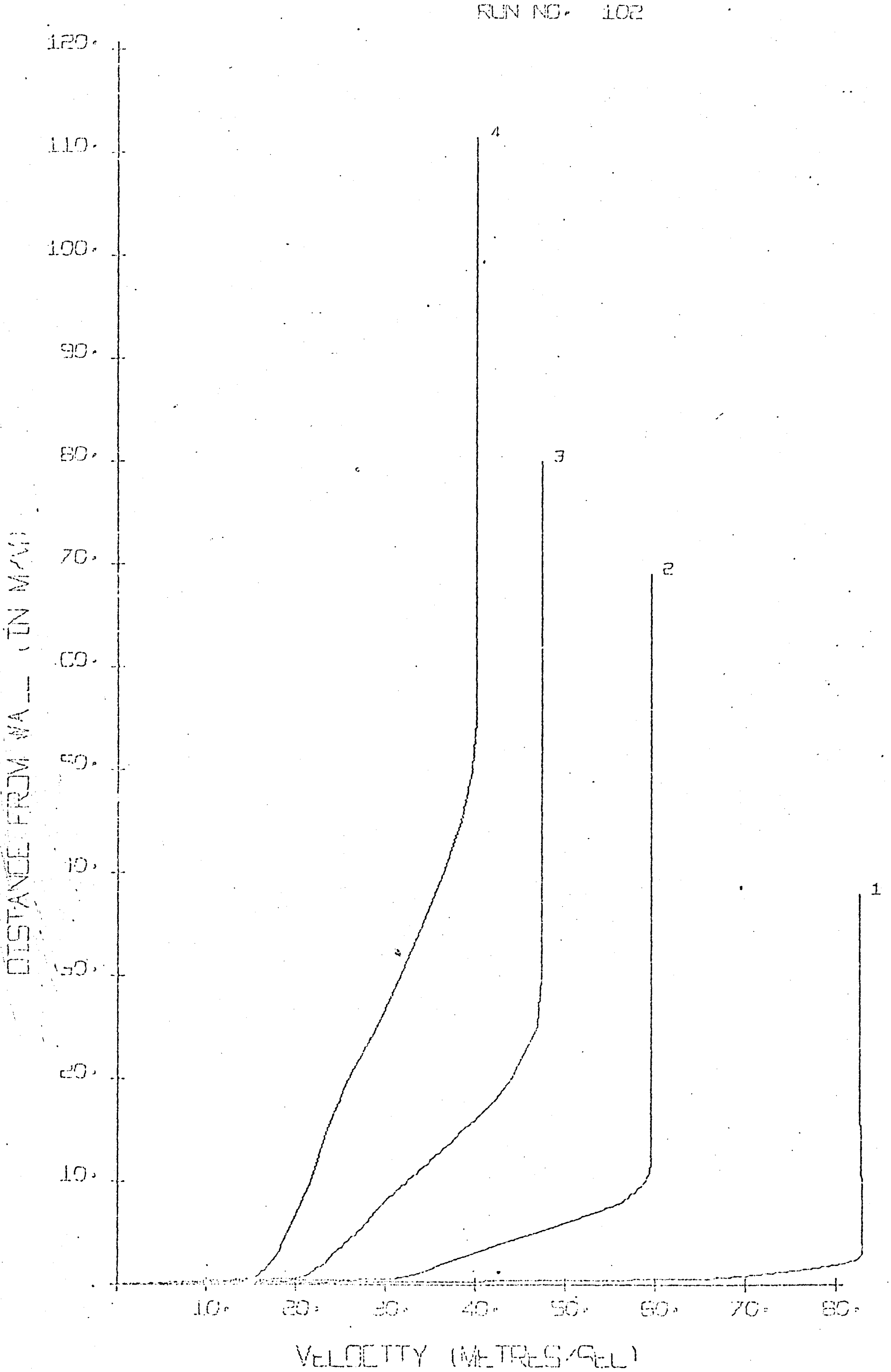
RUN NO. 102
DISTANCE FROM WALL (IN MM)
VELOCITY (METRES/SEC)
120.
110.
100.
90.
80.
70.
60.
50.
40.
30.
20.
10.
10.
20.
30.
40.
50.
60.
70.
80.
1
2
3
4

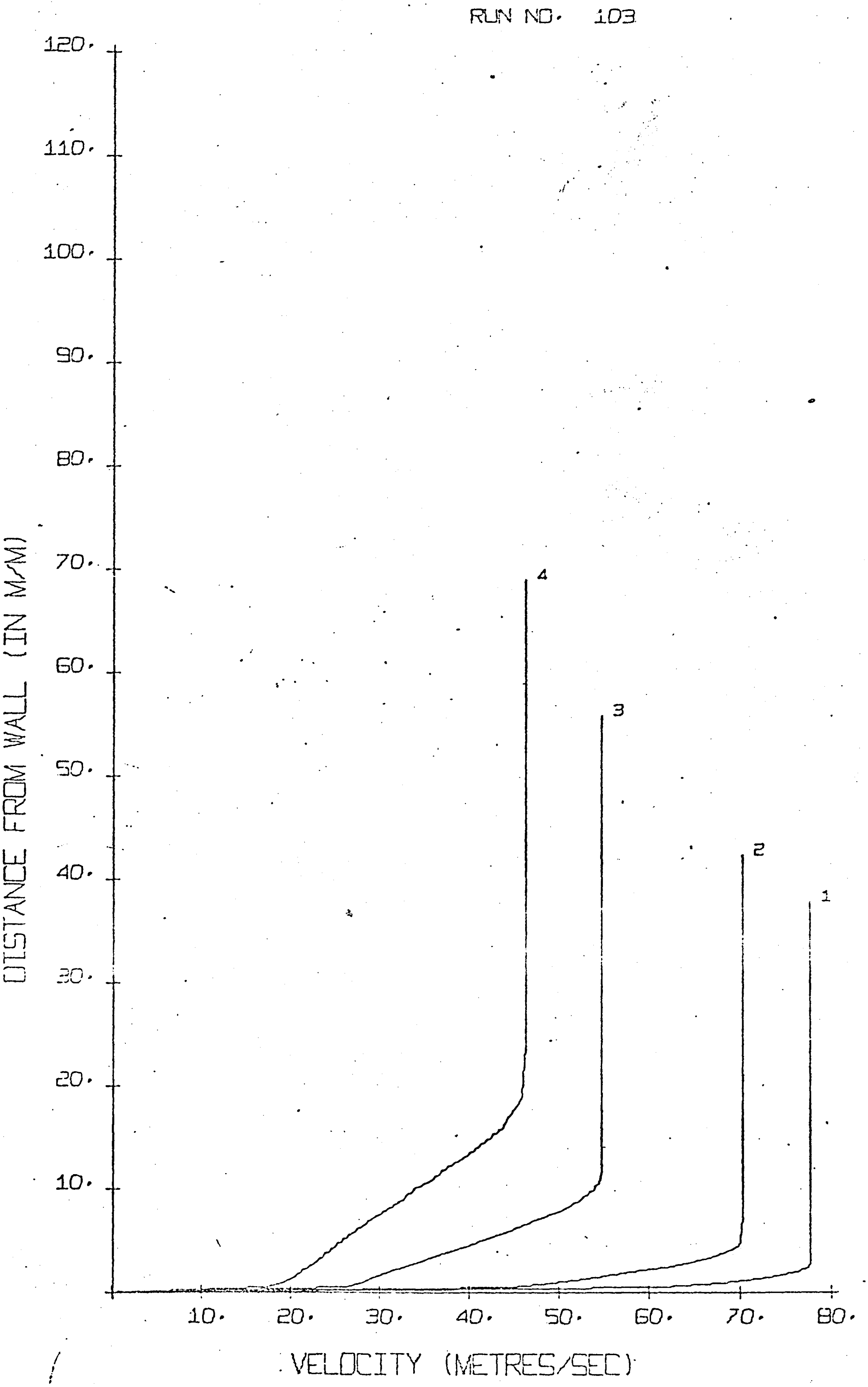
RUN NO. 103
DISTANCE FROM WALL (IN M/M)
VELOCITY (METRES/SEC)
120.
110.
100.
90.
80.
70.
60.
50.
40.
30.
20.
10.
10.
20.
30.
40.
50.
60.
70.
80.
4
3
2
1

RUN NO. 104

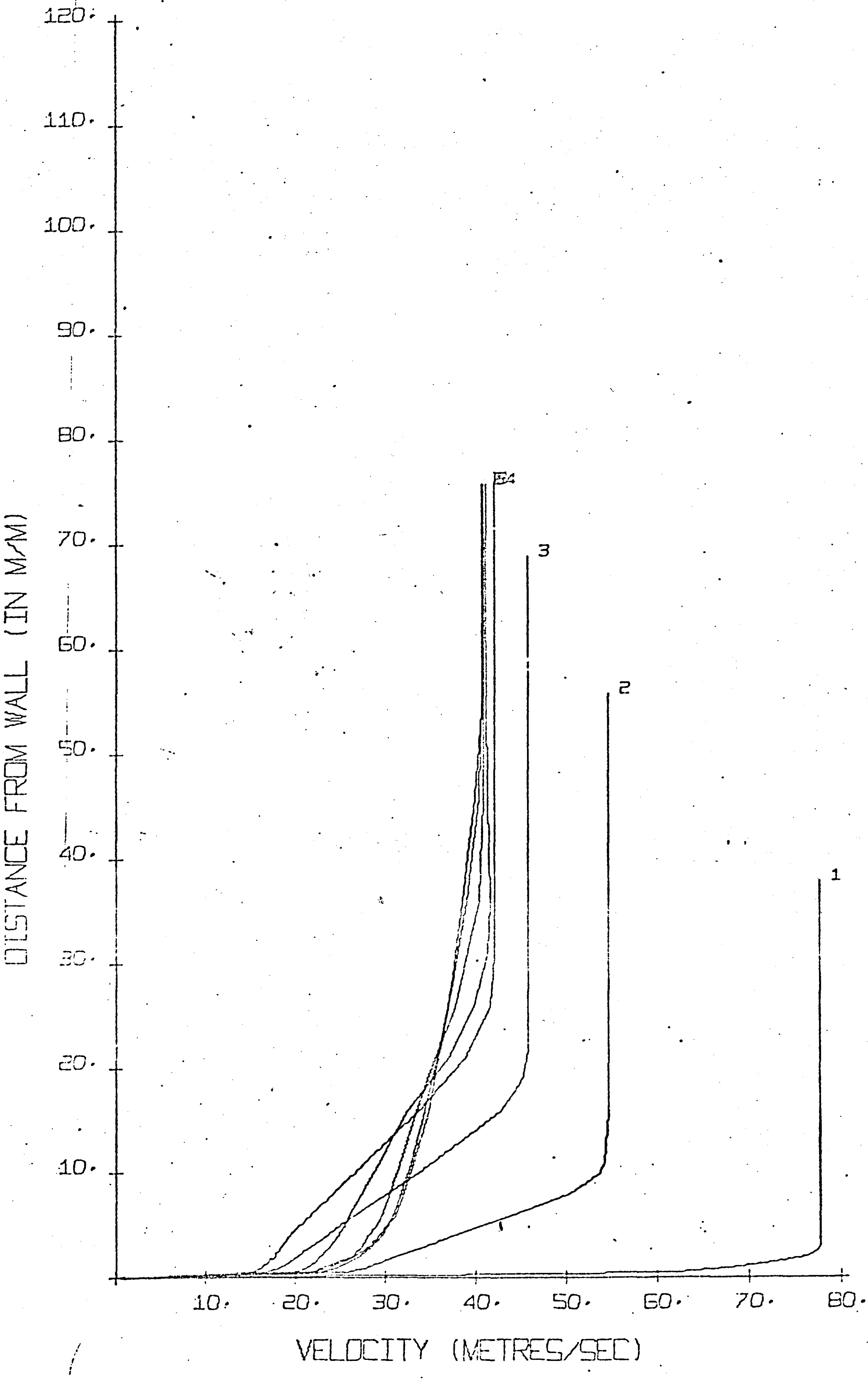

120.
110.
100.
90.
80.
70.
60.
50.
40.
30.
20.
10.
DISTANCE FROM WALL (IN M/M)
10.
20.
30.
40.
50.
60.
70.
80.
VELOCITY (METRES/SEC)
1
2
3
4

RUN NO. 105

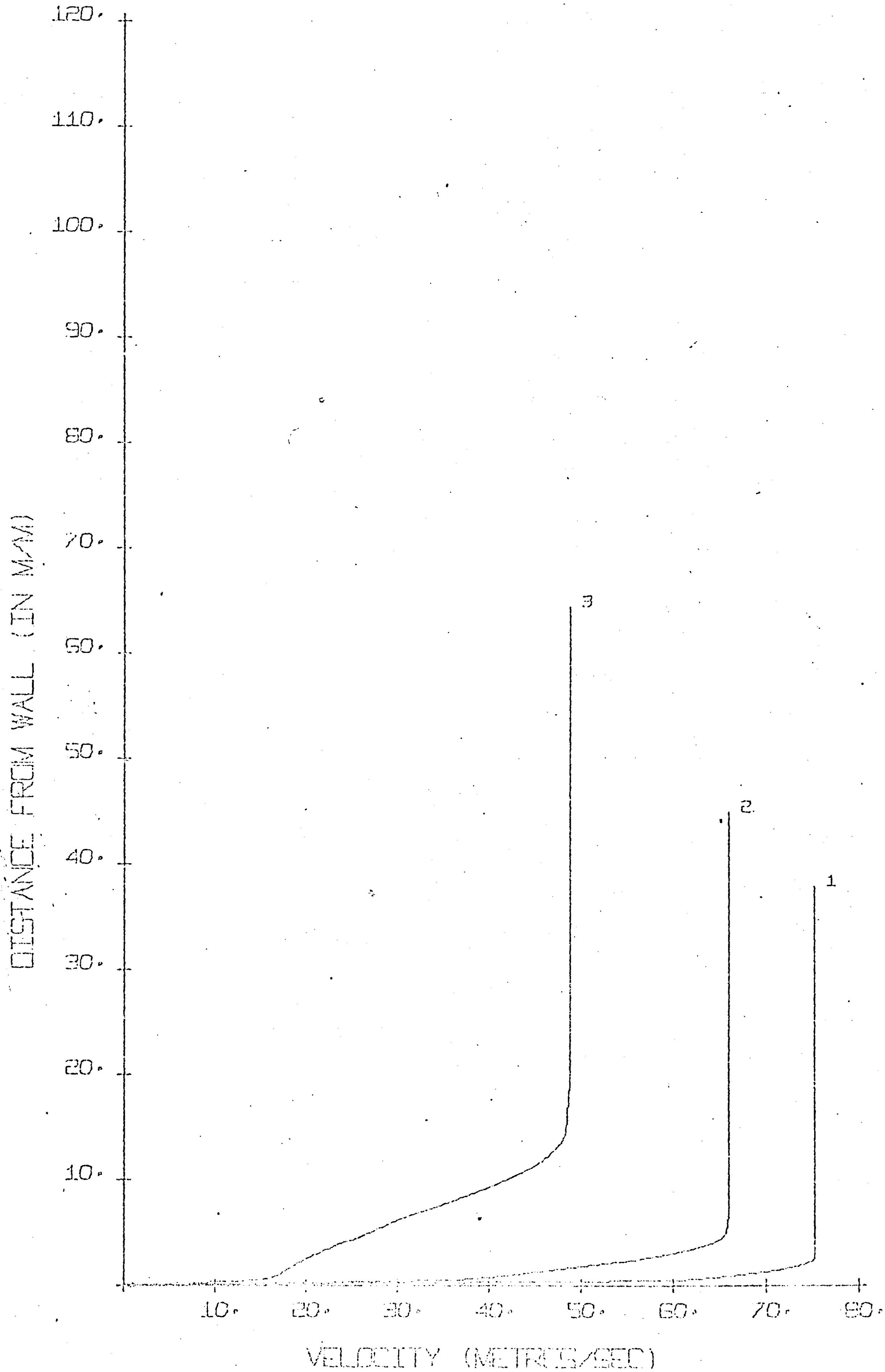

120.
110.
100.
90.
80.
70.
60.
50.
40.
30.
20.
10.
DISTANCE FROM WALL (IN M/M)
3
2.
1
10.
20.
30.
40.
50.
60.
70.
80.
VELOCITY (METRES/SEC)

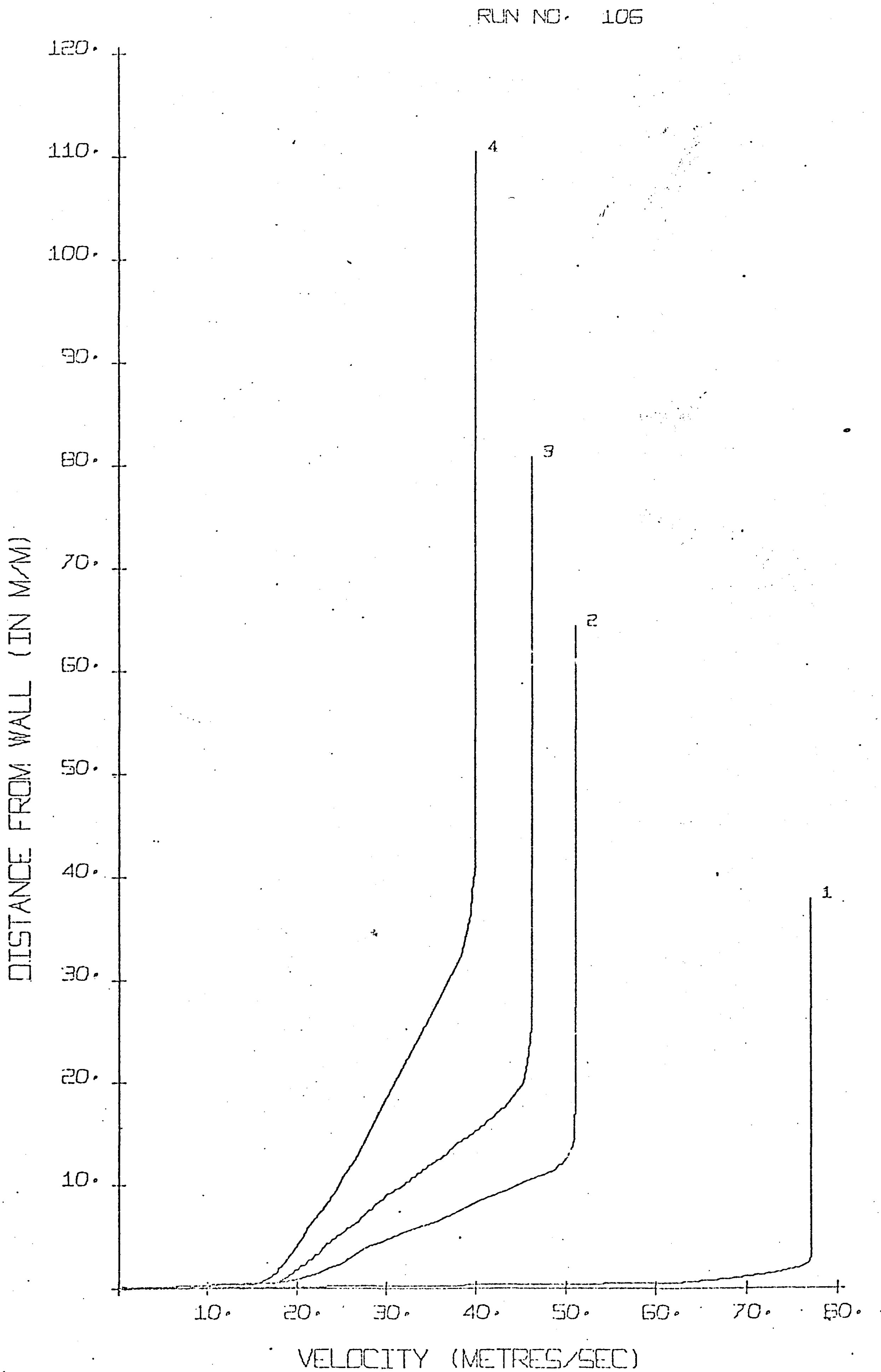

RUN NO. 106
DISTANCE FROM WALL (IN M/M)
VELOCITY (METRES/SEC)
120.
110.
100.
90.
80.
70.
60.
50.
40.
30.
20.
10.
10.
20.
30.
40.
50.
60.
70.
80.
1
2
3
4

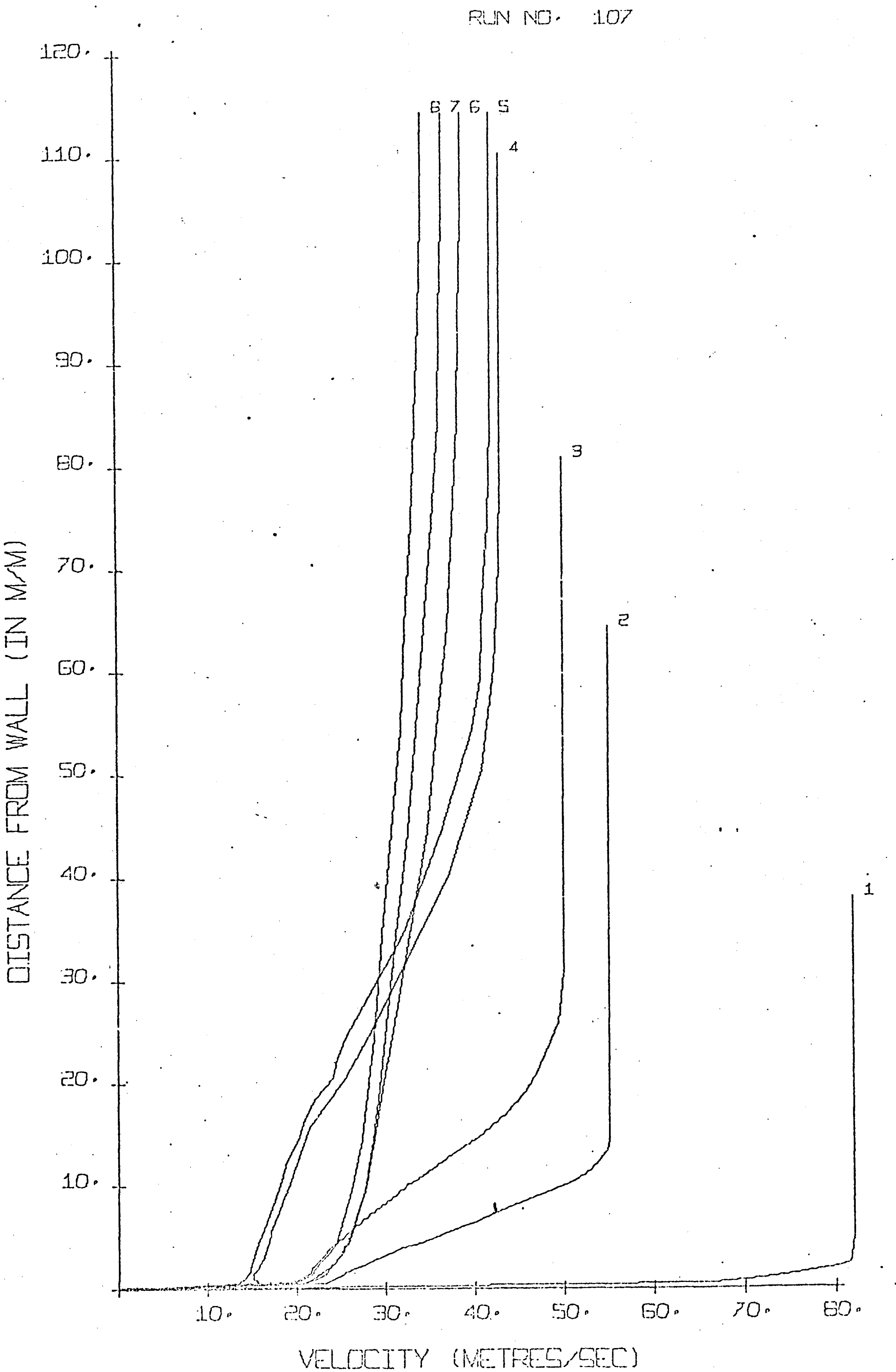

RUN NO. 107
DISTANCE FROM WALL (IN M/M)
VELOCITY (METRES/SEC)
120.
110.
100.
90.
80.
70.
60.
50.
40.
30.
20.
10.
10.
20.
30.
40.
50.
60.
70.
80.
8
7
6
5
4
3
2
1

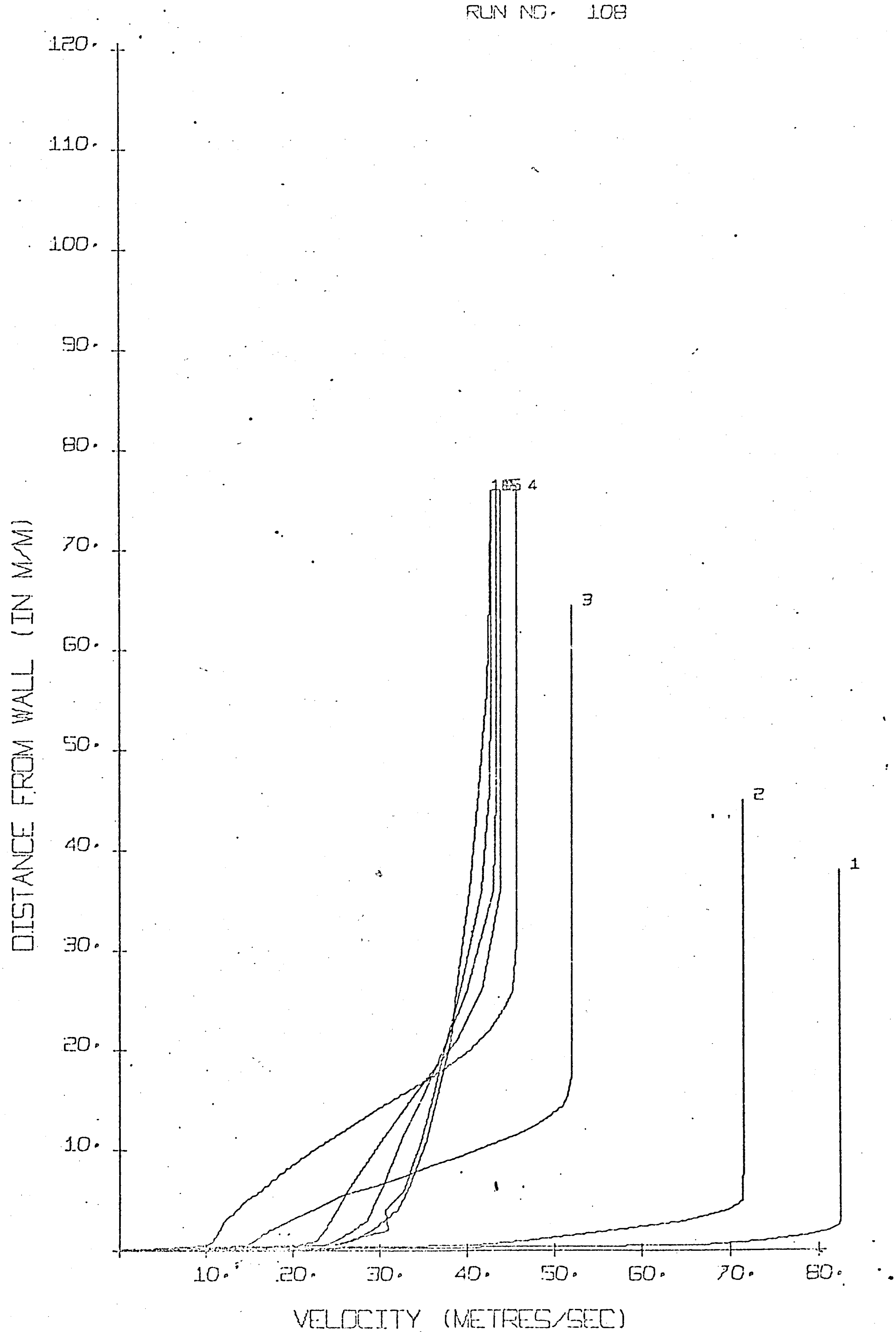

RUN NO. 108
DISTANCE FROM WALL (IN M/M)
VELOCITY (METRES/SEC)
120.
110.
100.
90.
80.
70.
60.
50.
40.
30.
20.
10.
10.
20.
30.
40.
50.
60.
70.
80.
1
2
3
4

RUN NO. 109

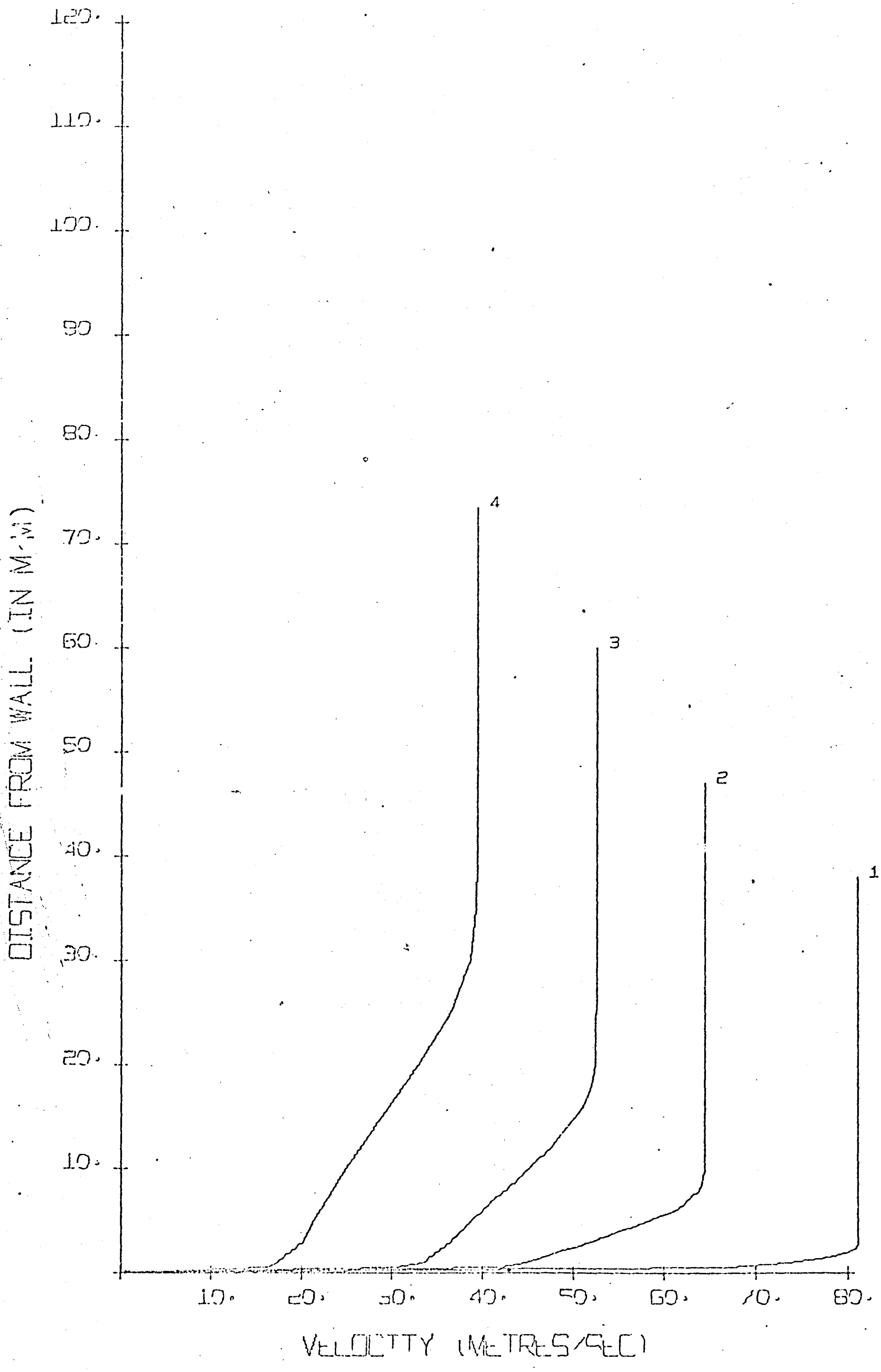

DISTANCE FROM WALL (IN M.M)
120.
110.
100.
90
80.
70.
60.
50
40.
30.
20.
10.
4
3
2
1
10.
20.
30.
40.
50.
60.
70.
80.
VELOCITY (METRES/SEC)

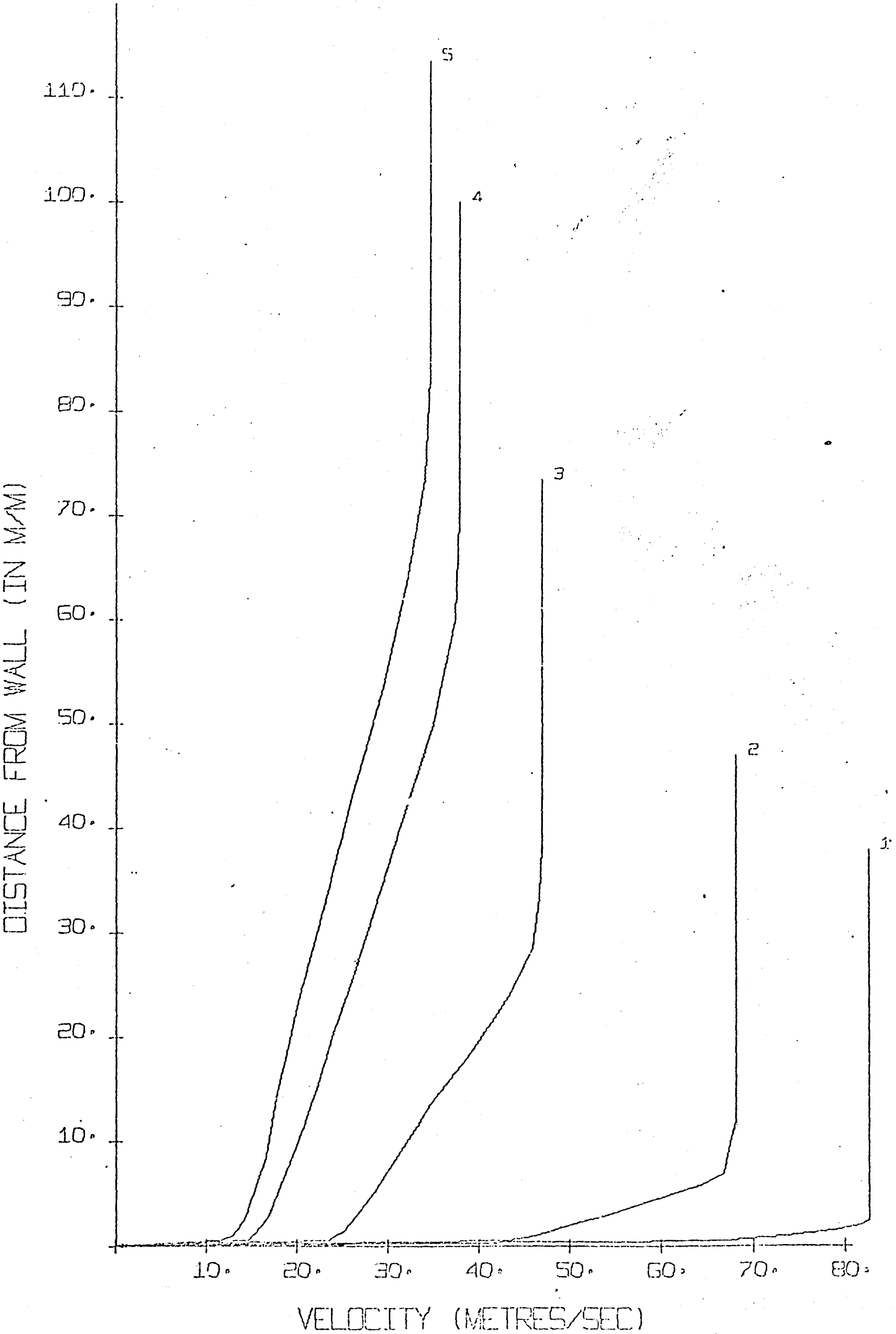
DISTANCE FROM WALL (IN M/M)
110.
100.
90.
80.
70.
60.
50.
40.
30.
20.
10.
5
4
3
2
1
10.
20.
30.
40.
50.
60.
70.
80.
VELOCITY (METRES/SEC)

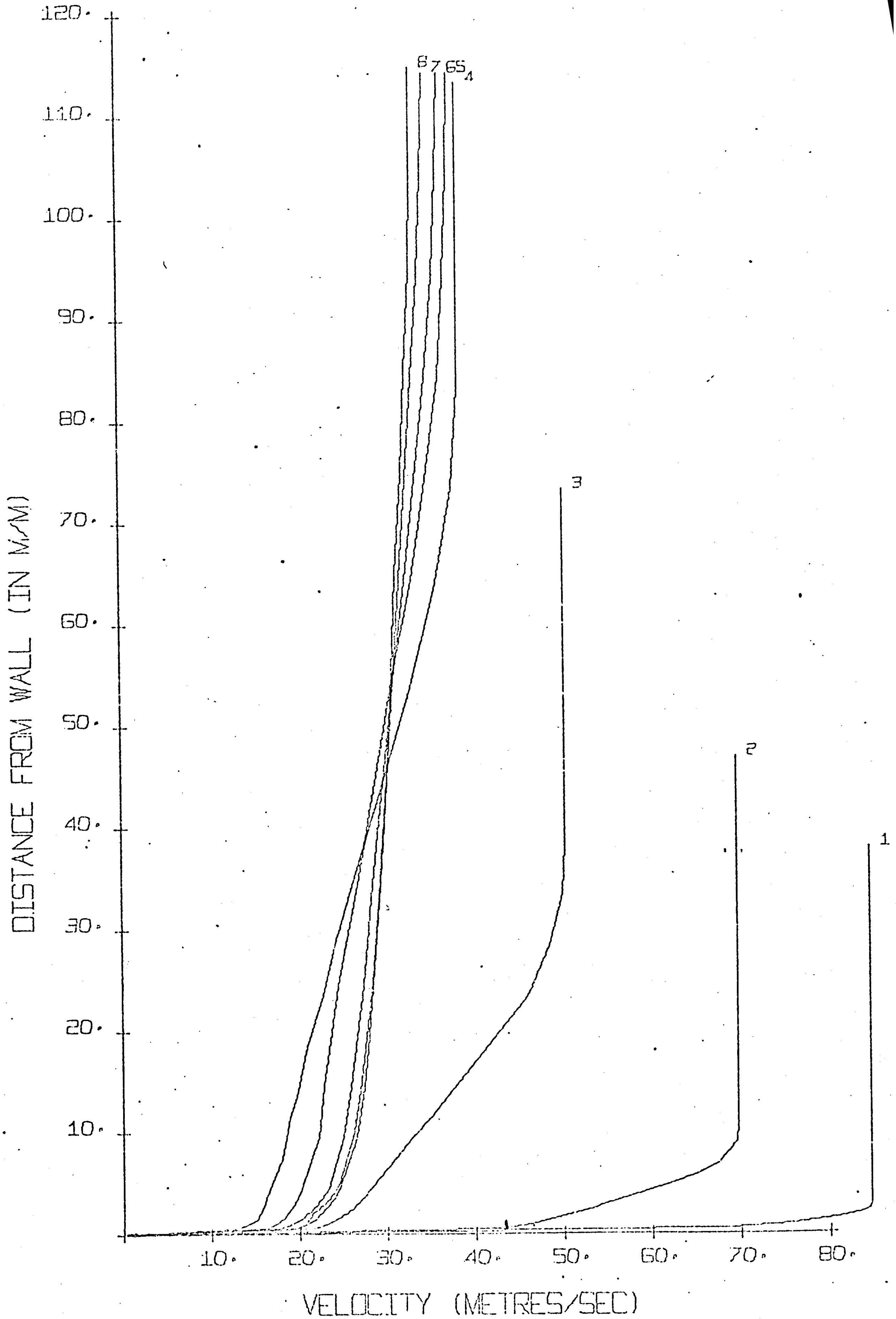
120
110
100
90
80
70
60
50
40
30
20
10
DISTANCE FROM WALL (IN M/M)
10
20
30
40
50
60
70
80
VELOCITY (METRES/SEC)
8
7
6
5
4
3
2
1

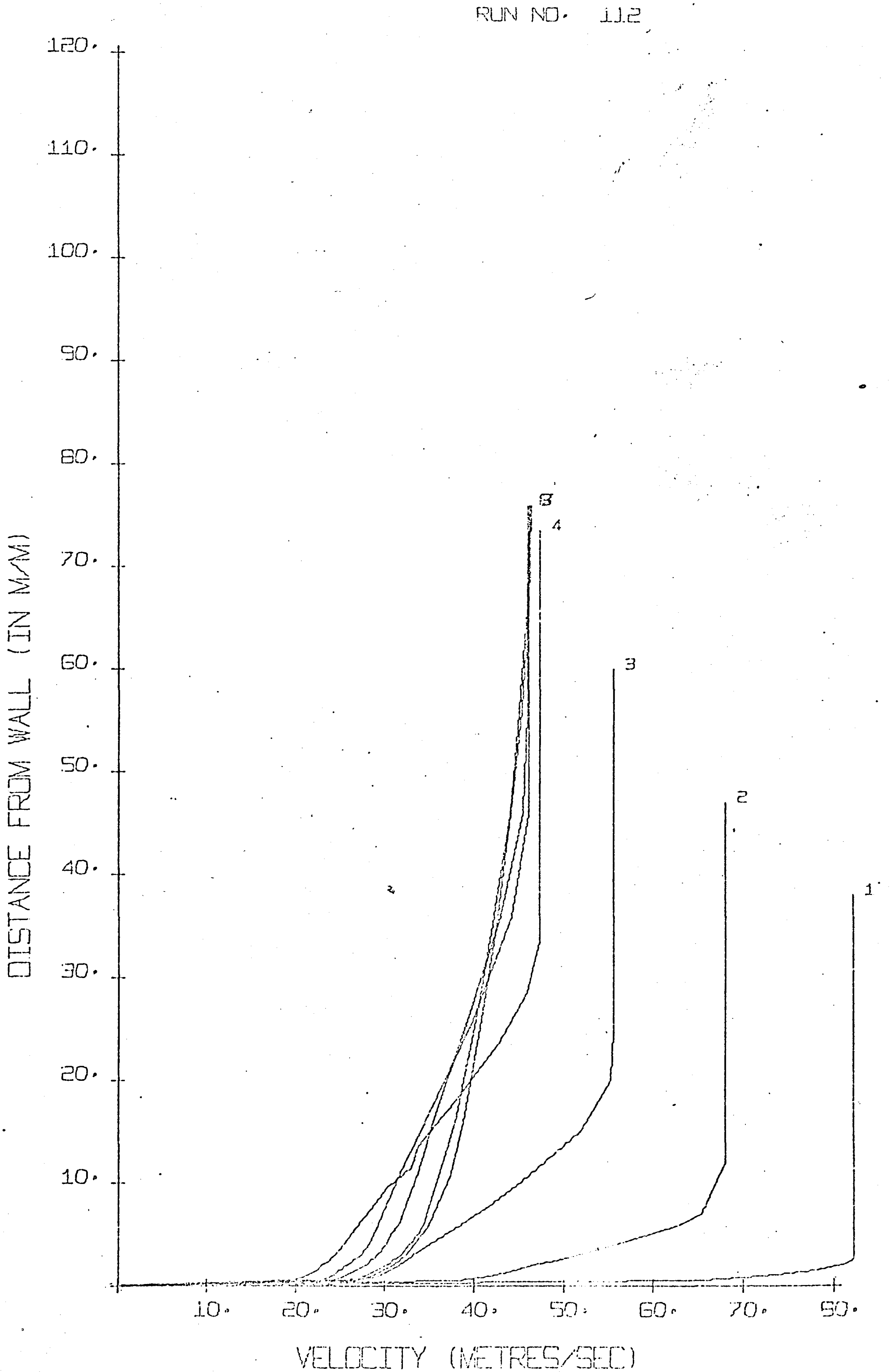
RUN NO. 112
120.
110.
100.
90.
80.
70.
60.
50.
40.
30.
20.
10.
DISTANCE FROM WALL (IN M/M)
10.
20.
30.
40.
50.
60.
70.
80.
VELOCITY (METRES/SEC)
1
2
3
4
8

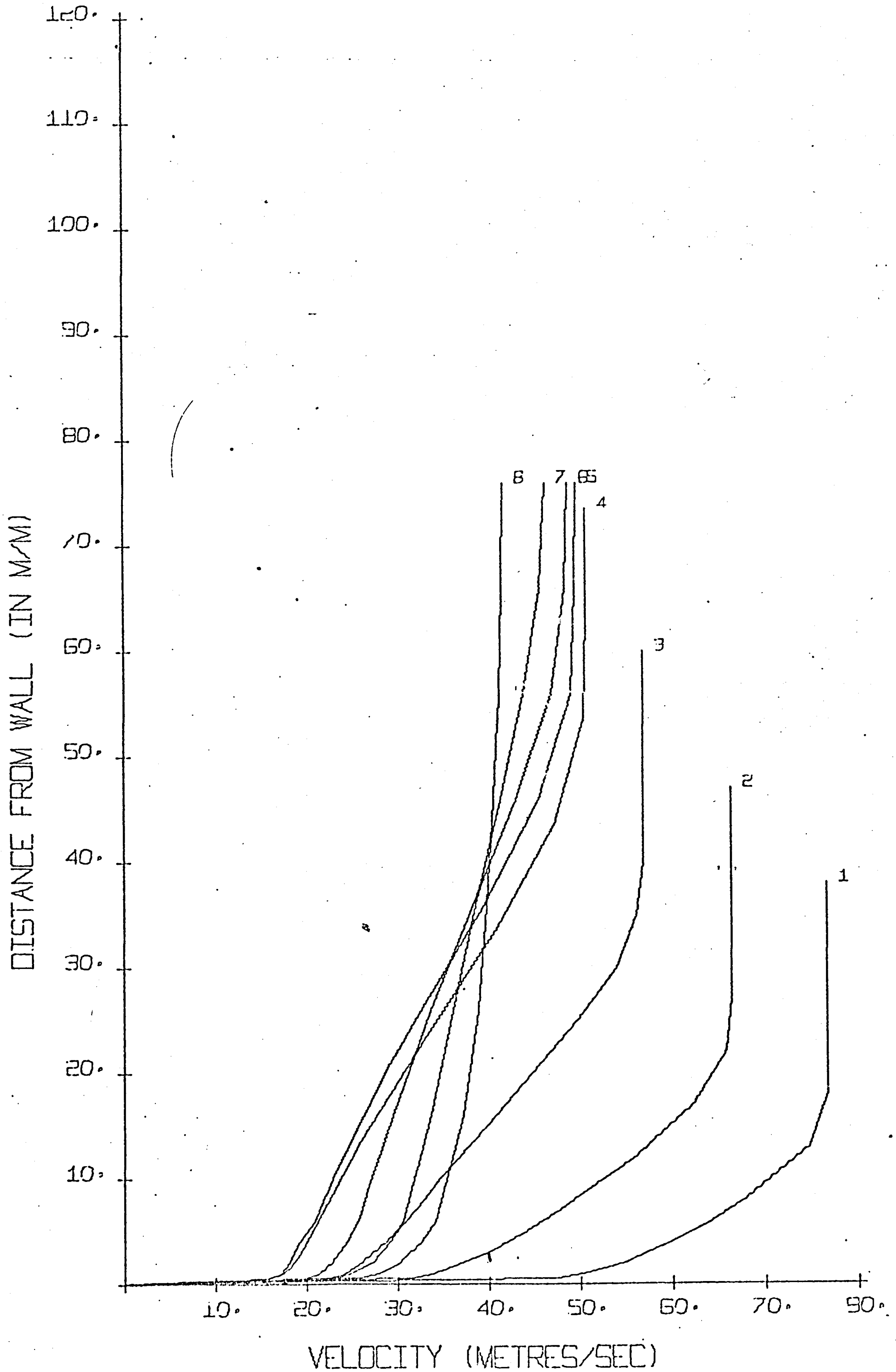

120.
110.
100.
90.
80.
70.
60.
50.
40.
30.
20.
10.
DISTANCE FROM WALL (IN M/M)
10.
20.
30.
40.
50.
60.
70.
80.
VELOCITY (METRES/SEC)
8
7
6
5
4
3
2
1

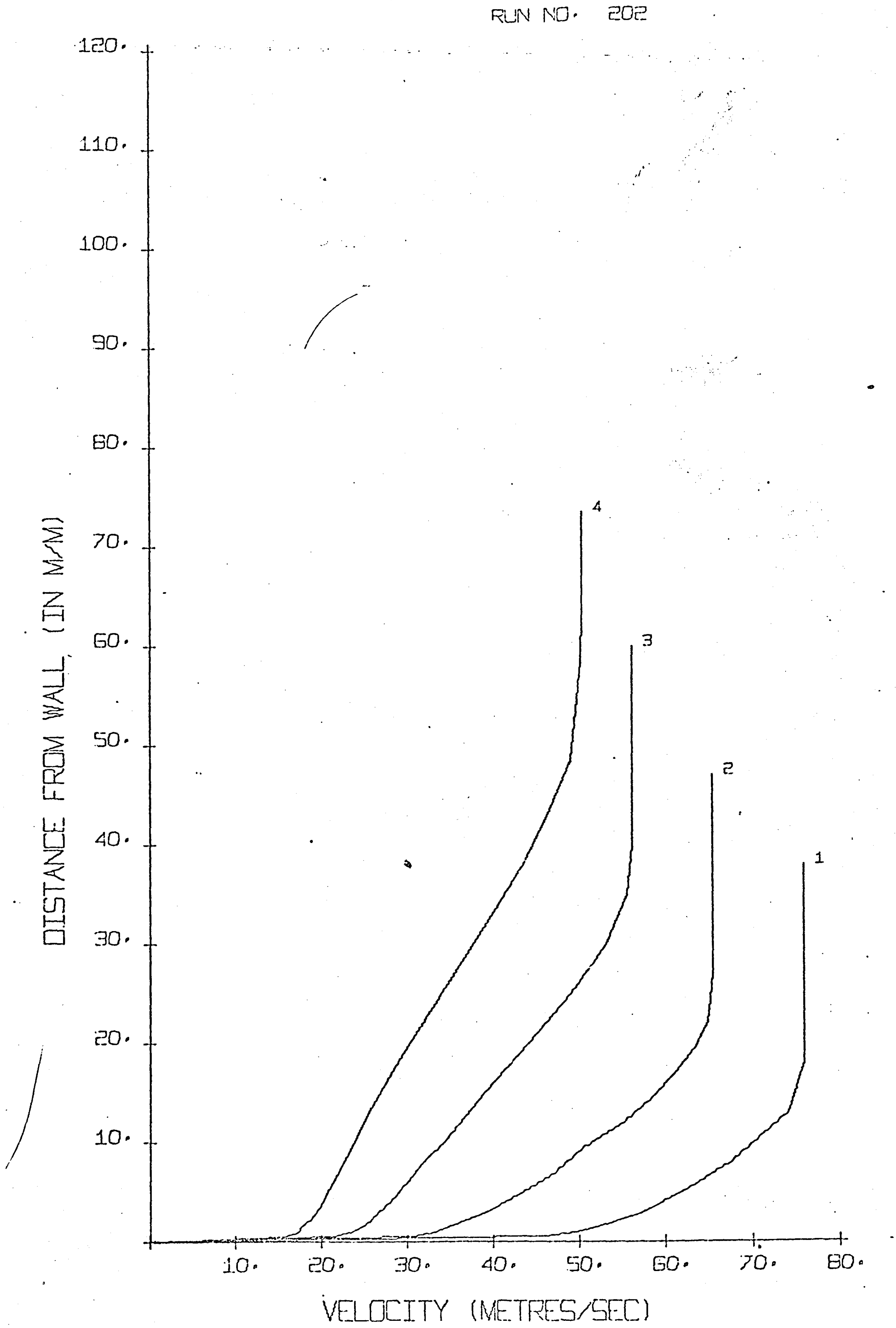
RUN NO. 202
DISTANCE FROM WALL (IN M/M)
120.
110.
100.
90.
80.
70.
60.
50.
40.
30.
20.
10.
10.
20.
30.
40.
50.
60.
70.
80.
VELOCITY (METRES/SEC)
1
2
3
4

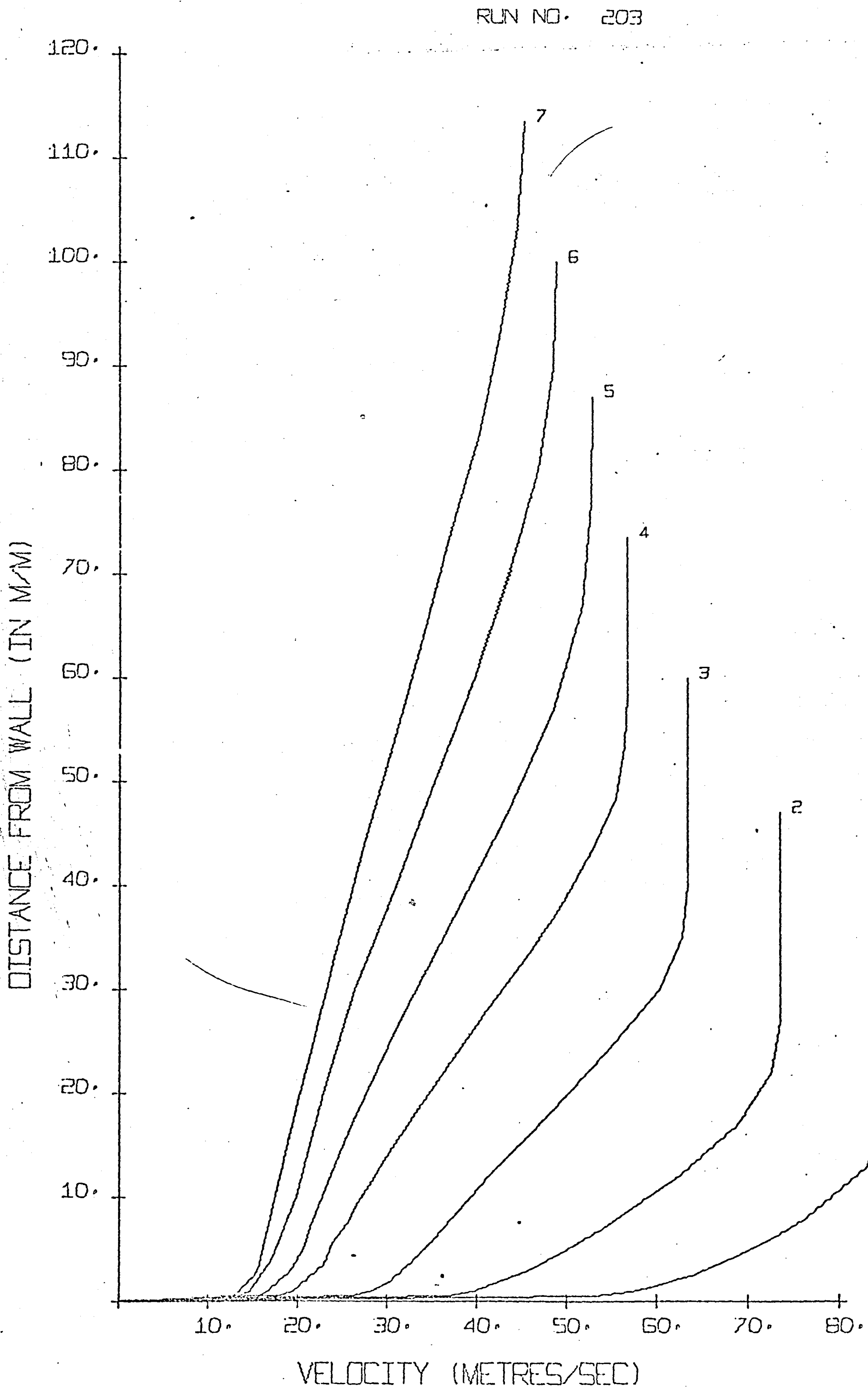

RUN NO. 203
120.
110.
100.
90.
80.
70.
60.
50.
40.
30.
20.
10.
DISTANCE FROM WALL (IN M/M)
7
6
5
4
3
2
1
10.
20.
30.
40.
50.
60.
70.
80.
VELOCITY (METRES/SEC)

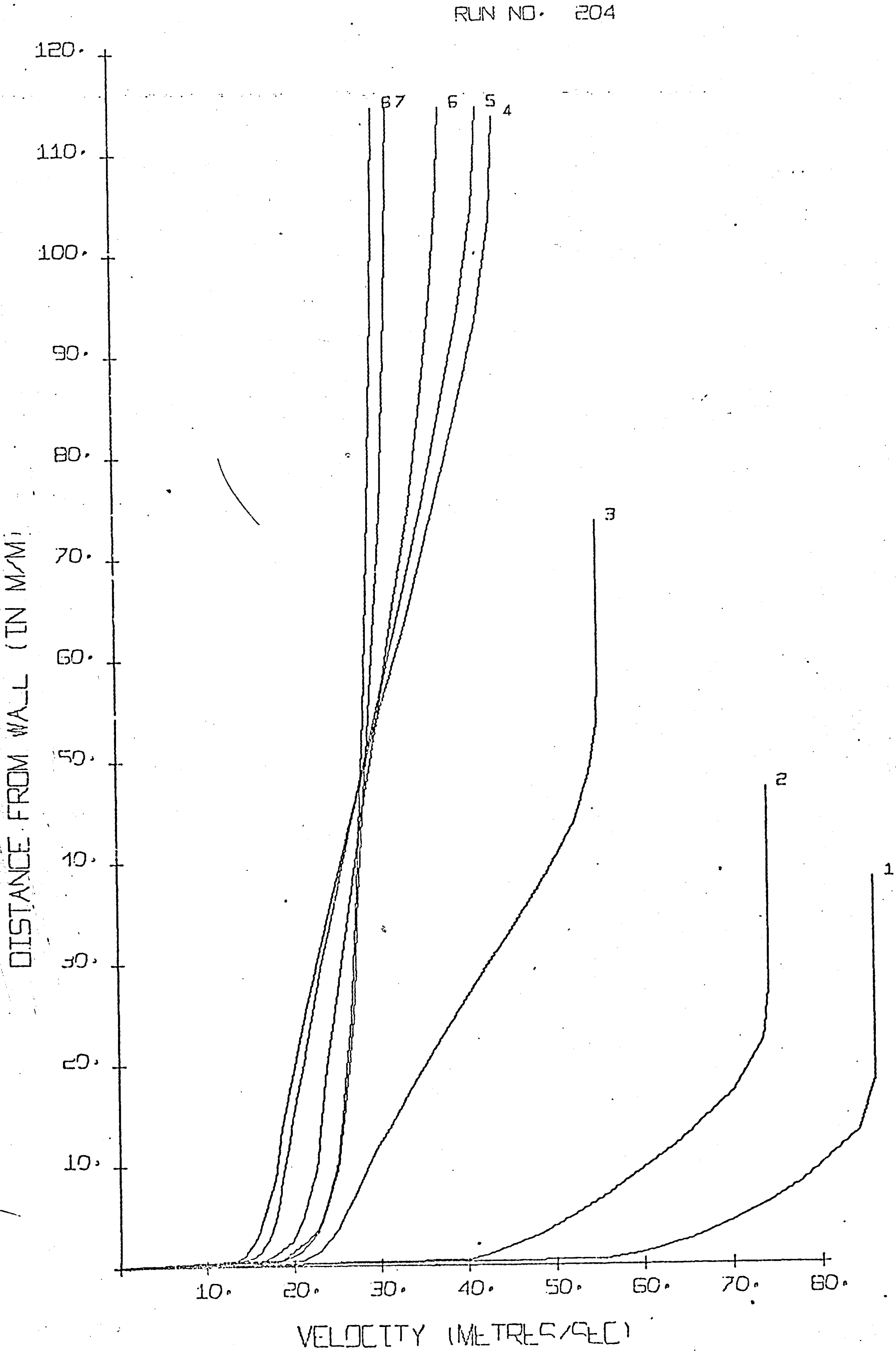
RUN NO. 204
DISTANCE FROM WALL (IN M/M)
VELOCITY (METRES/SEC)
120.
110.
100.
90.
80.
70.
60.
50.
40.
30.
20.
10.
10.
20.
30.
40.
50.
60.
70.
80.
8
7
6
5
4
3
2
1

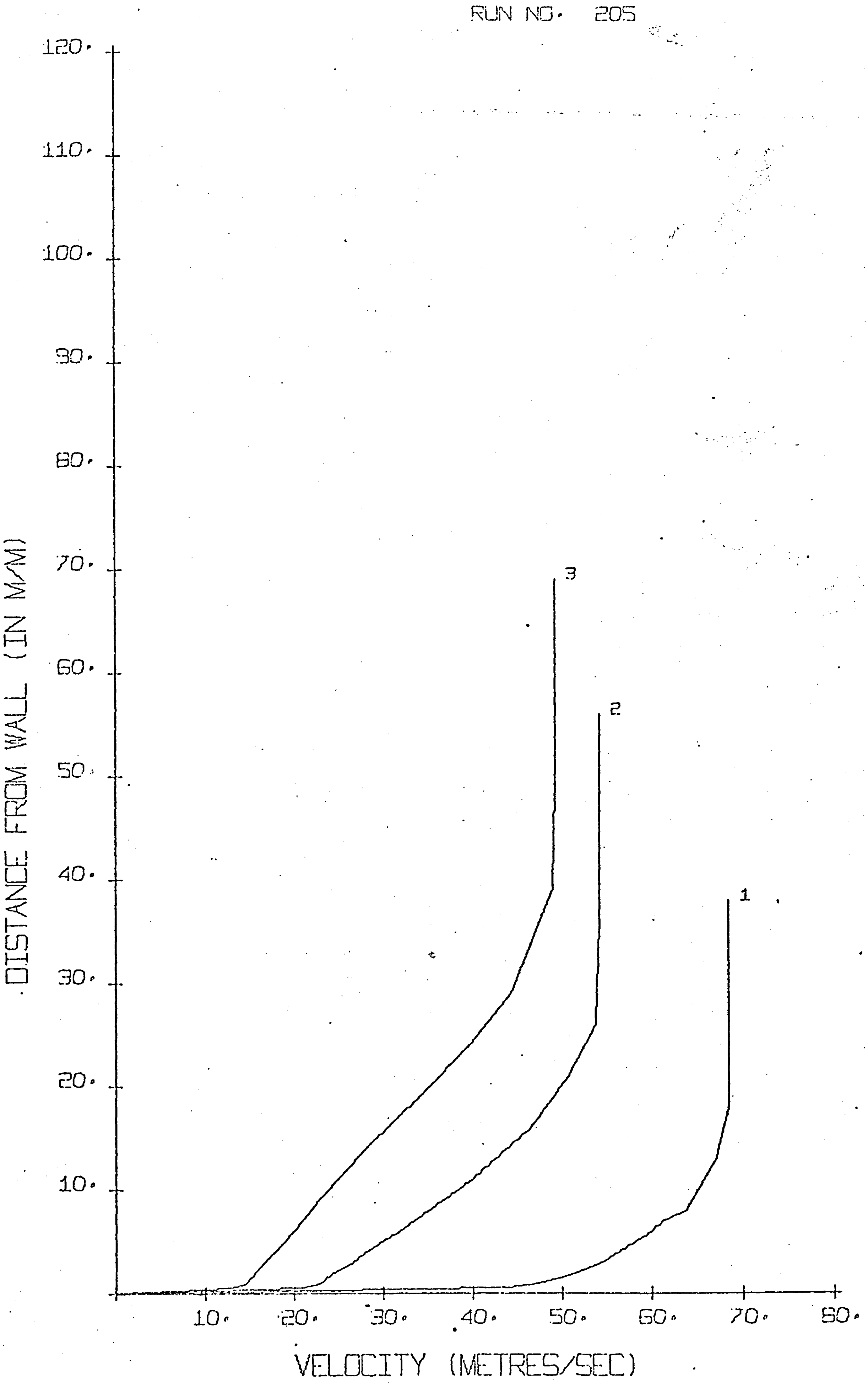

RUN NO. 205
DISTANCE FROM WALL (IN M/M)
VELOCITY (METRES/SEC)
120.
110.
100.
90.
80.
70.
60.
50.
40.
30.
20.
10.
10.
20.
30.
40.
50.
60.
70.
80.
1
2
3

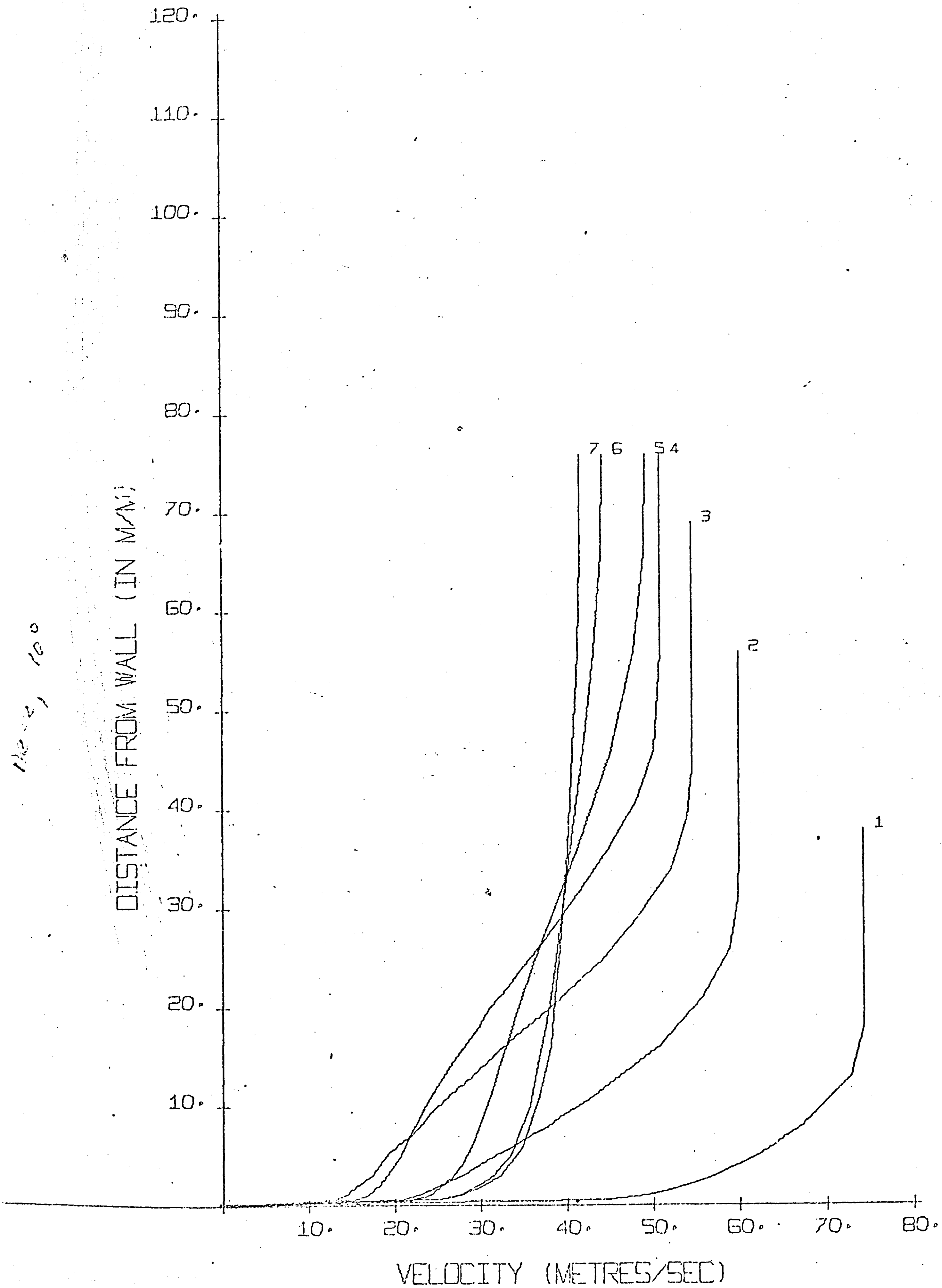

DISTANCE FROM WALL (IN M/M)
120.
110.
100.
90.
80.
70.
60.
50.
40.
30.
20.
10.
10.
20.
30.
40.
50.
60.
70.
80.
7
6
5
4
3
2
1
VELOCITY (METRES/SEC)

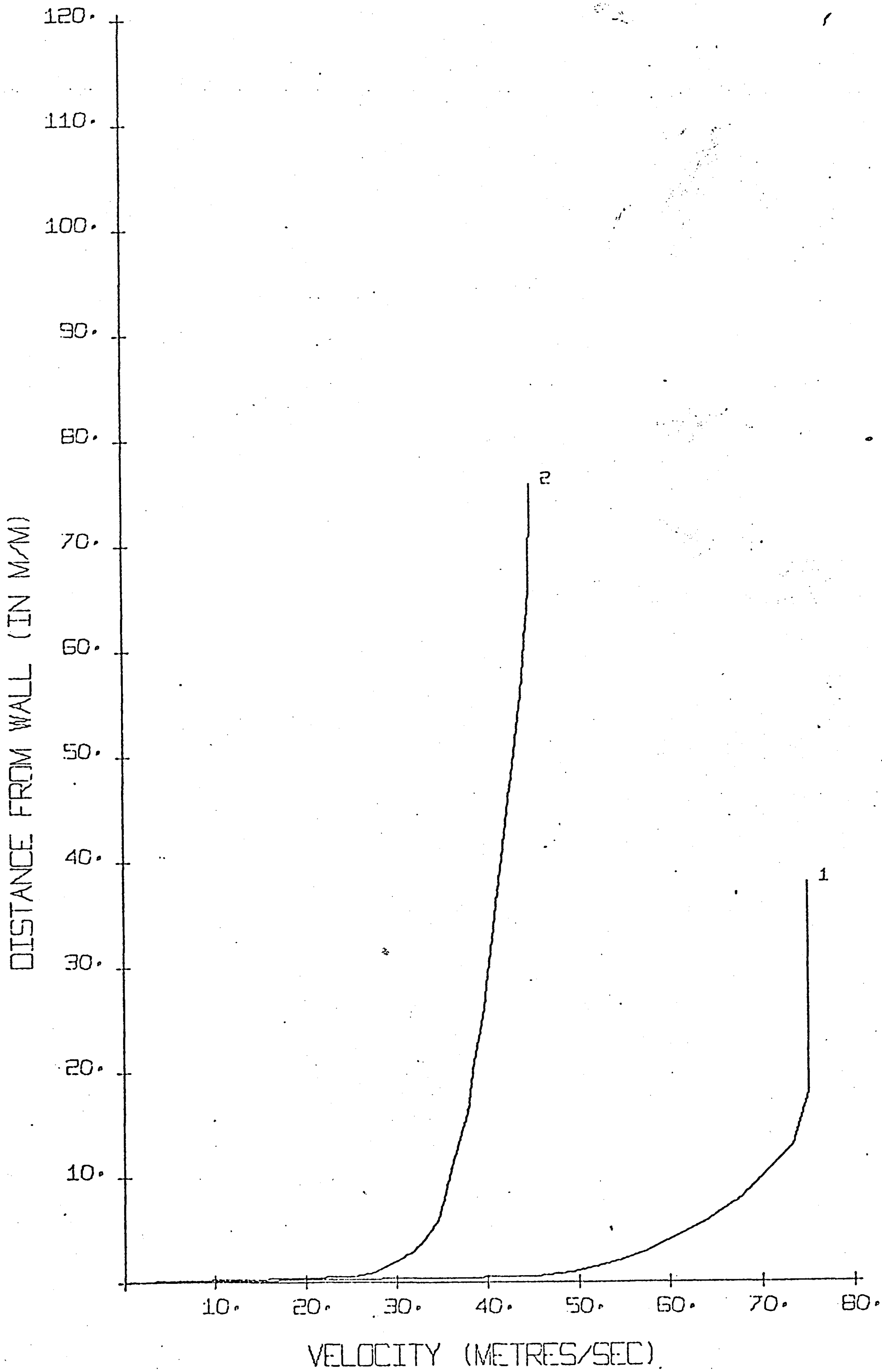
120.
110.
100.
90.
80.
70.
60.
50.
40.
30.
20.
10.
DISTANCE FROM WALL (IN M/M)
2
1
10.
20.
30.
40.
50.
60.
70.
80.
VELOCITY (METRES/SEC)

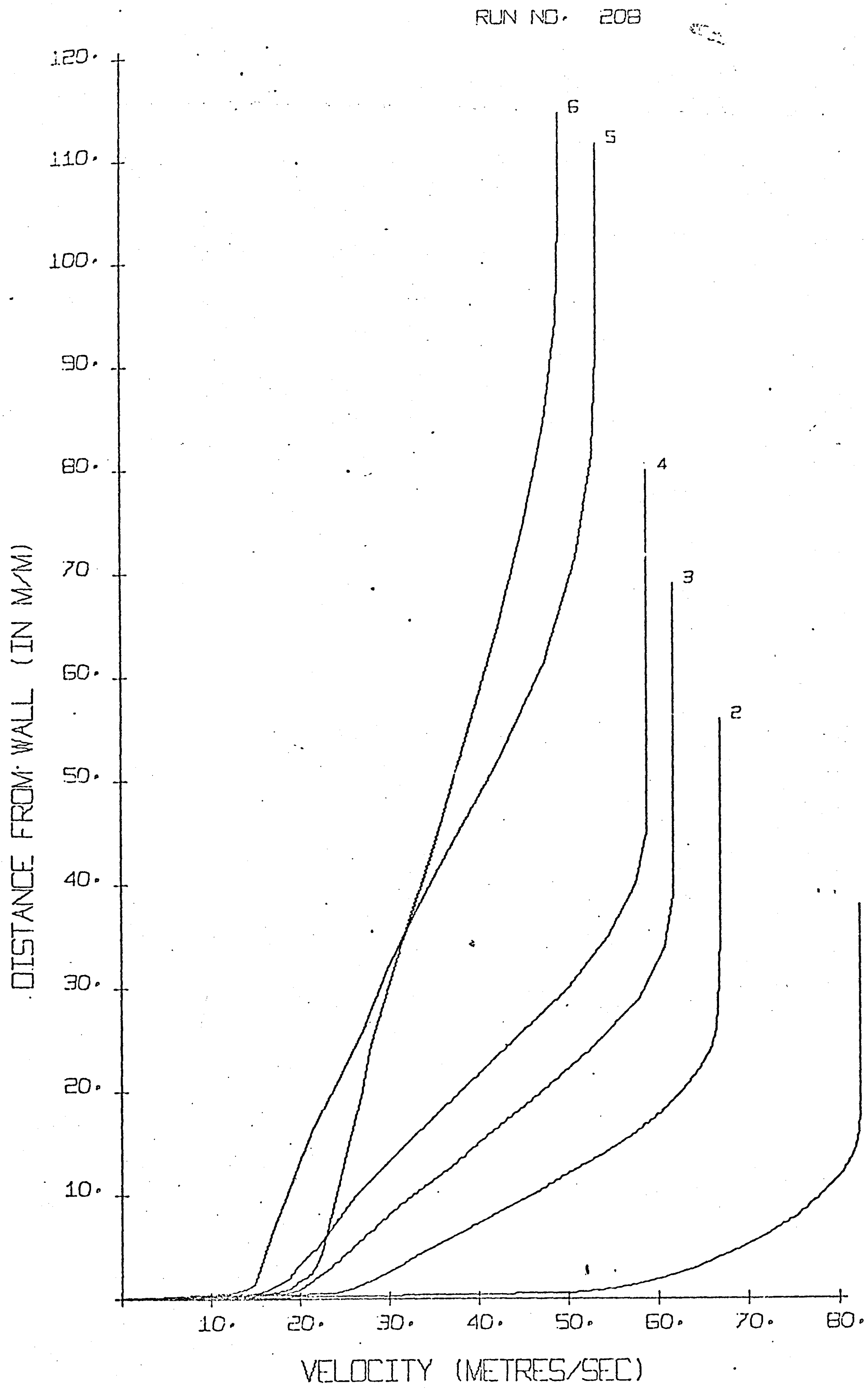

RUN NO. 208
120.
110.
100.
90.
80.
70
60.
50.
40.
30.
20.
10.
DISTANCE FROM WALL (IN M/M)
1
2
3
4
5
6
10.
20.
30.
40.
50.
60.
70.
80.
VELOCITY (METRES/SEC)

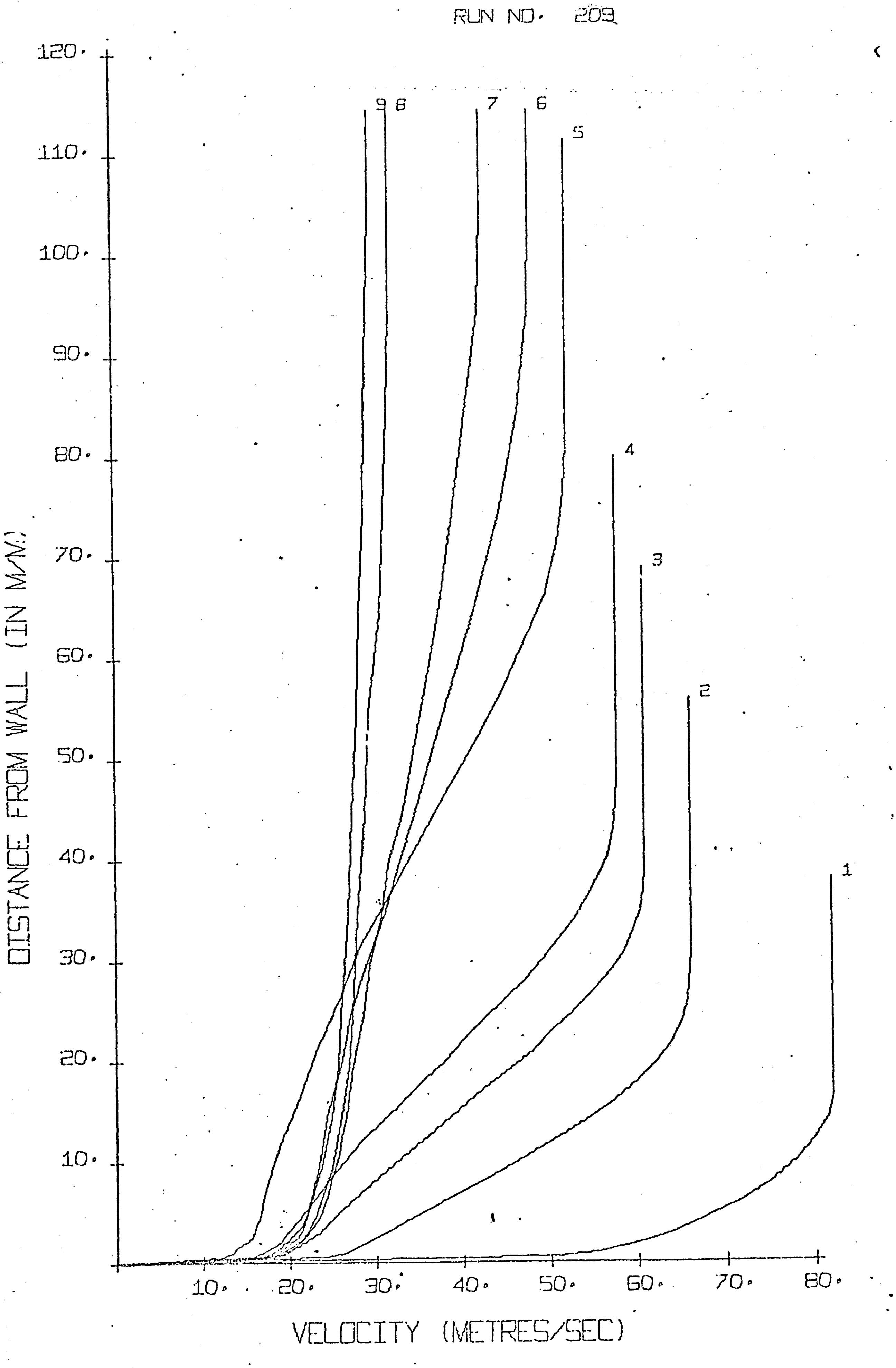
RUN NO. 209
DISTANCE FROM WALL (IN M/M)
VELOCITY (METRES/SEC)
120.
110.
100.
90.
80.
70.
60.
50.
40.
30.
20.
10.
10.
20.
30.
40.
50.
60.
70.
80.
1
2
3
4
5
6
7
8
9

RUN NO. 210

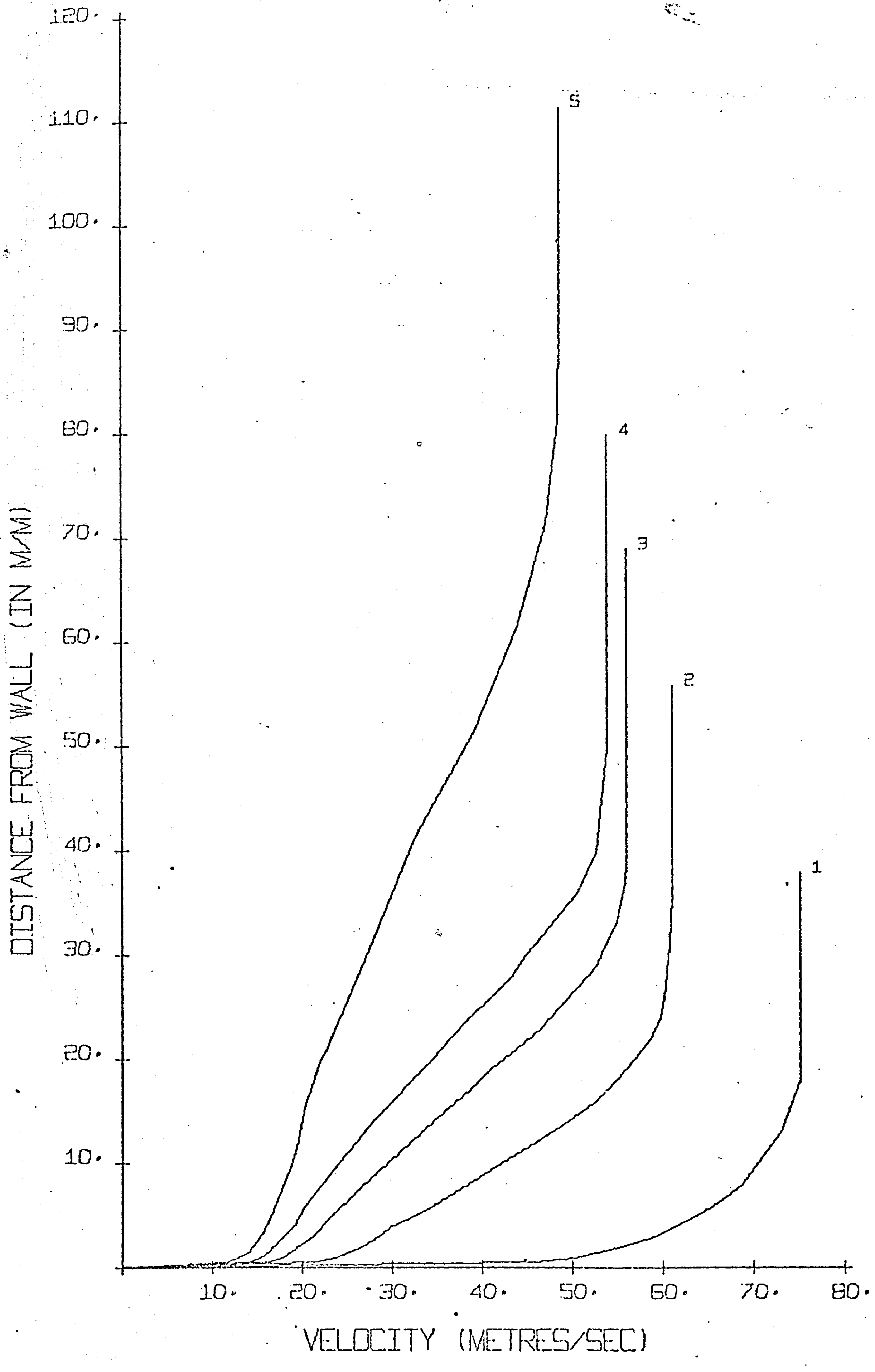

120.
110.
100.
90.
80.
70.
60.
50.
40.
30.
20.
10.
DISTANCE FROM WALL (IN M/M)
5
4
3
2
1
10.
20.
30.
40.
50.
60.
70.
80.
VELOCITY (METRES/SEC)

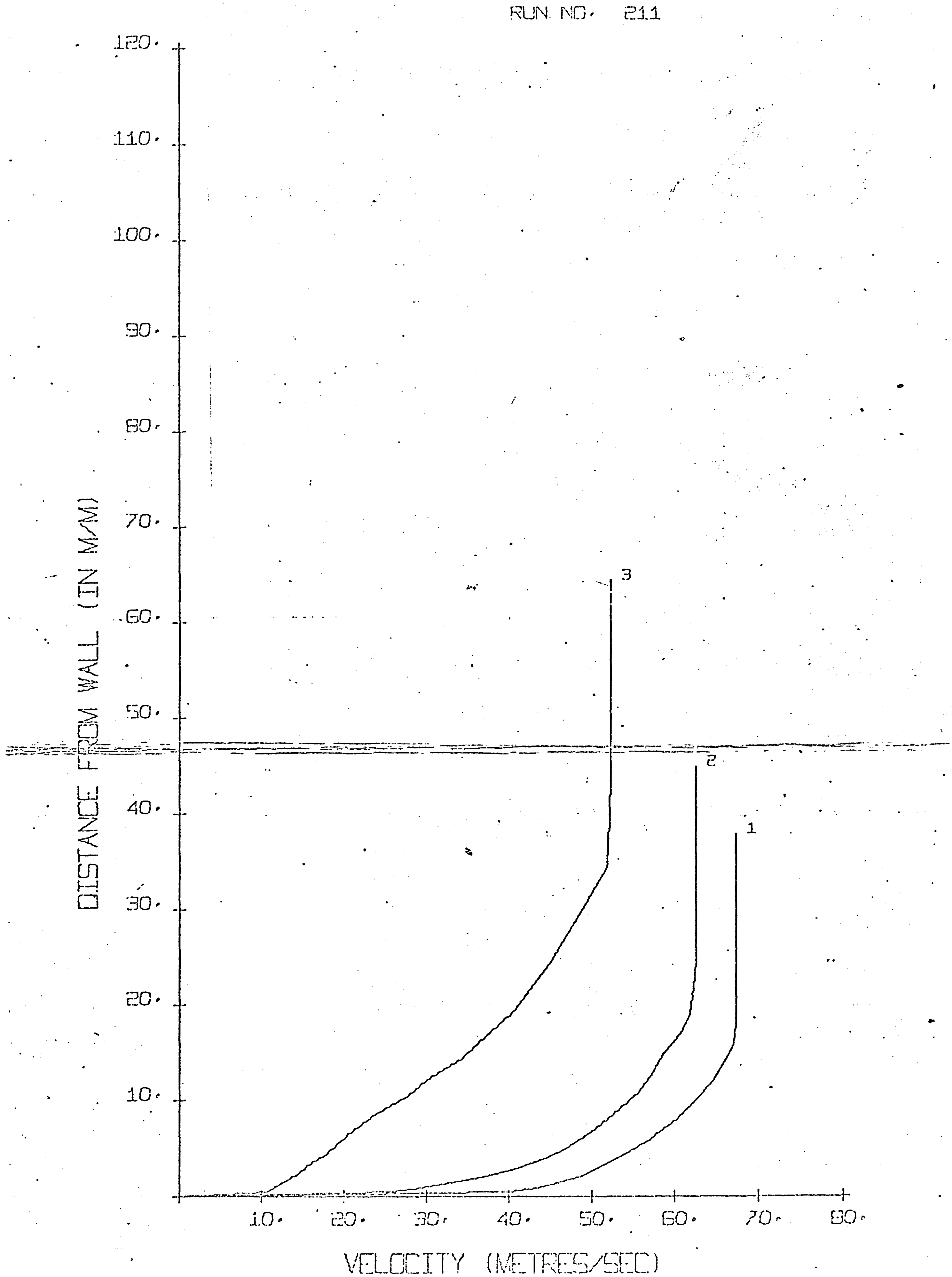
RUN. NO. 211
DISTANCE FROM WALL (IN M/M)
VELOCITY (METRES/SEC)
120.
110.
100.
90.
80.
70.
60.
50.
40.
30.
20.
10.
10.
20.
30.
40.
50.
60.
70.
80.
1
2
3

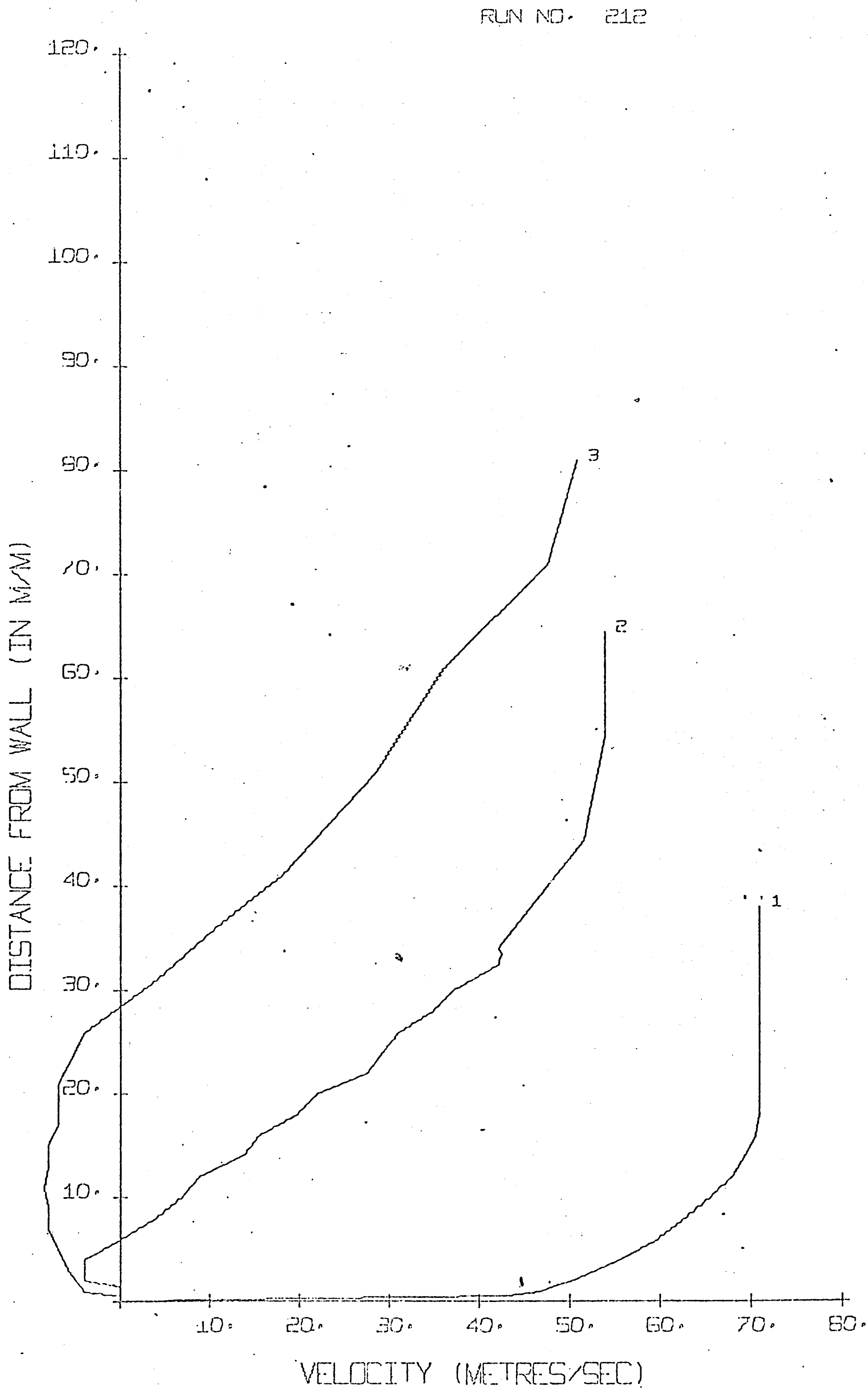

RUN NO. 212
120.
110.
100.
90.
80.
70.
60.
50.
40.
30.
20.
10.
DISTANCE FROM WALL (IN M/M)
3
2
1
10.
20.
30.
40.
50.
60.
70.
80.
VELOCITY (METRES/SEC)

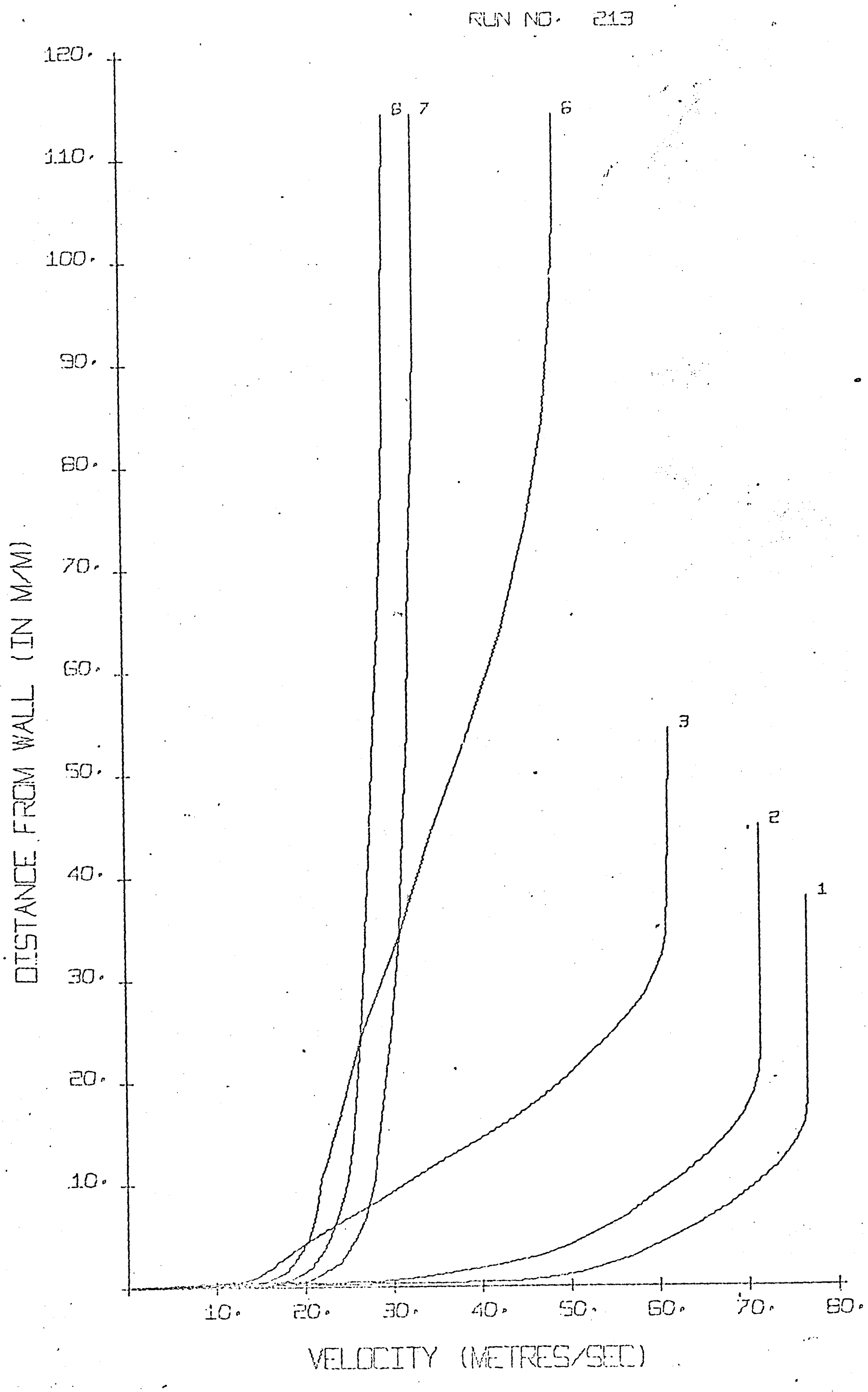

RUN NO. 213
120.
110.
100.
90.
80.
70.
60.
50.
40.
30.
20.
10.
DISTANCE FROM WALL (IN M/M)
8
7
6
3
2
1
10.
20.
30.
40.
50.
60.
70.
80.
VELOCITY (METRES/SEC)

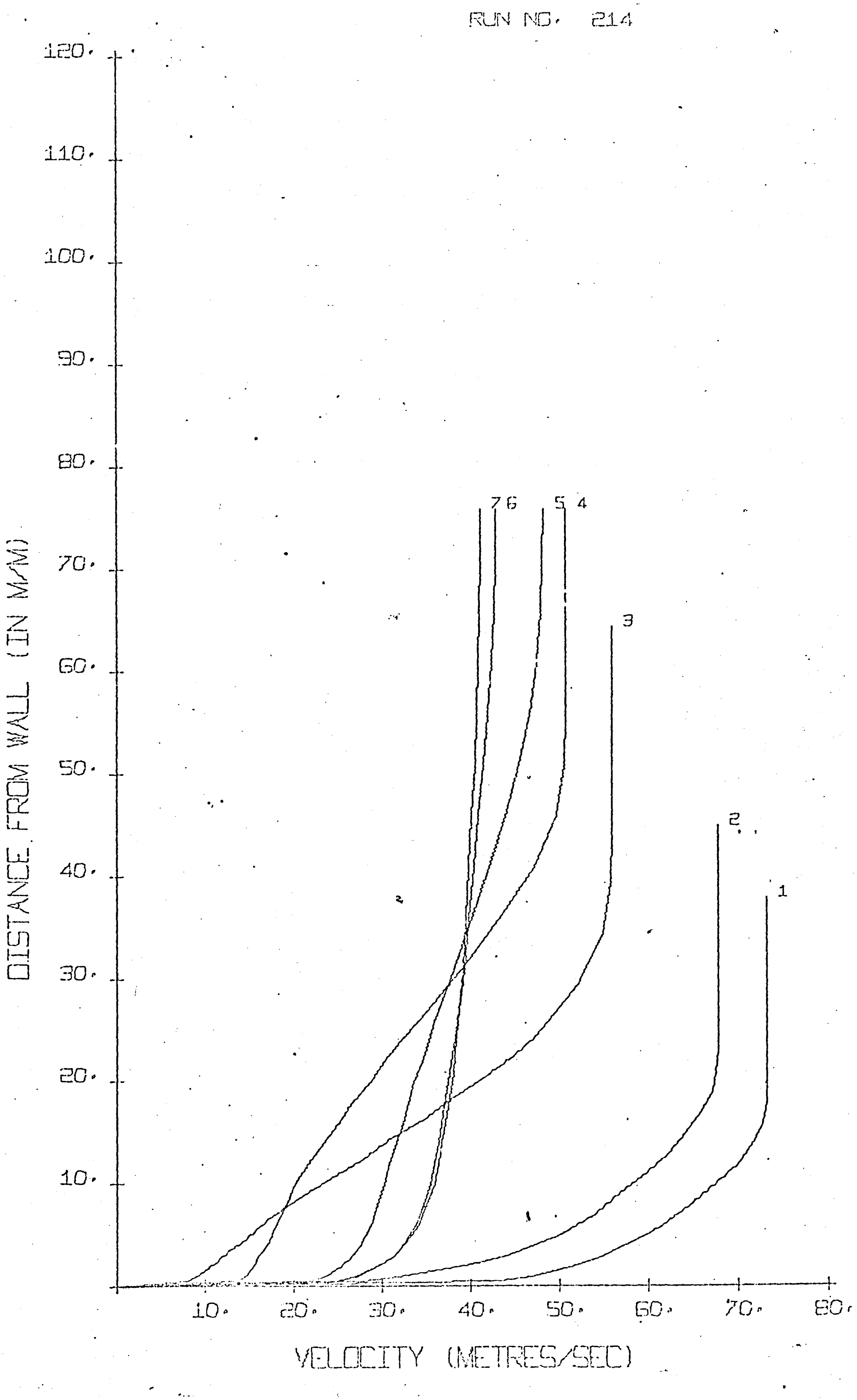

RUN NO. 214
120.
110.
100.
90.
80.
70.
60.
50.
40.
30.
20.
10.
DISTANCE FROM WALL (IN M/M)
7 6
5 4
3
2
1
10.
20.
30.
40.
50.
60.
70.
80.
VELOCITY (METRES/SEC)

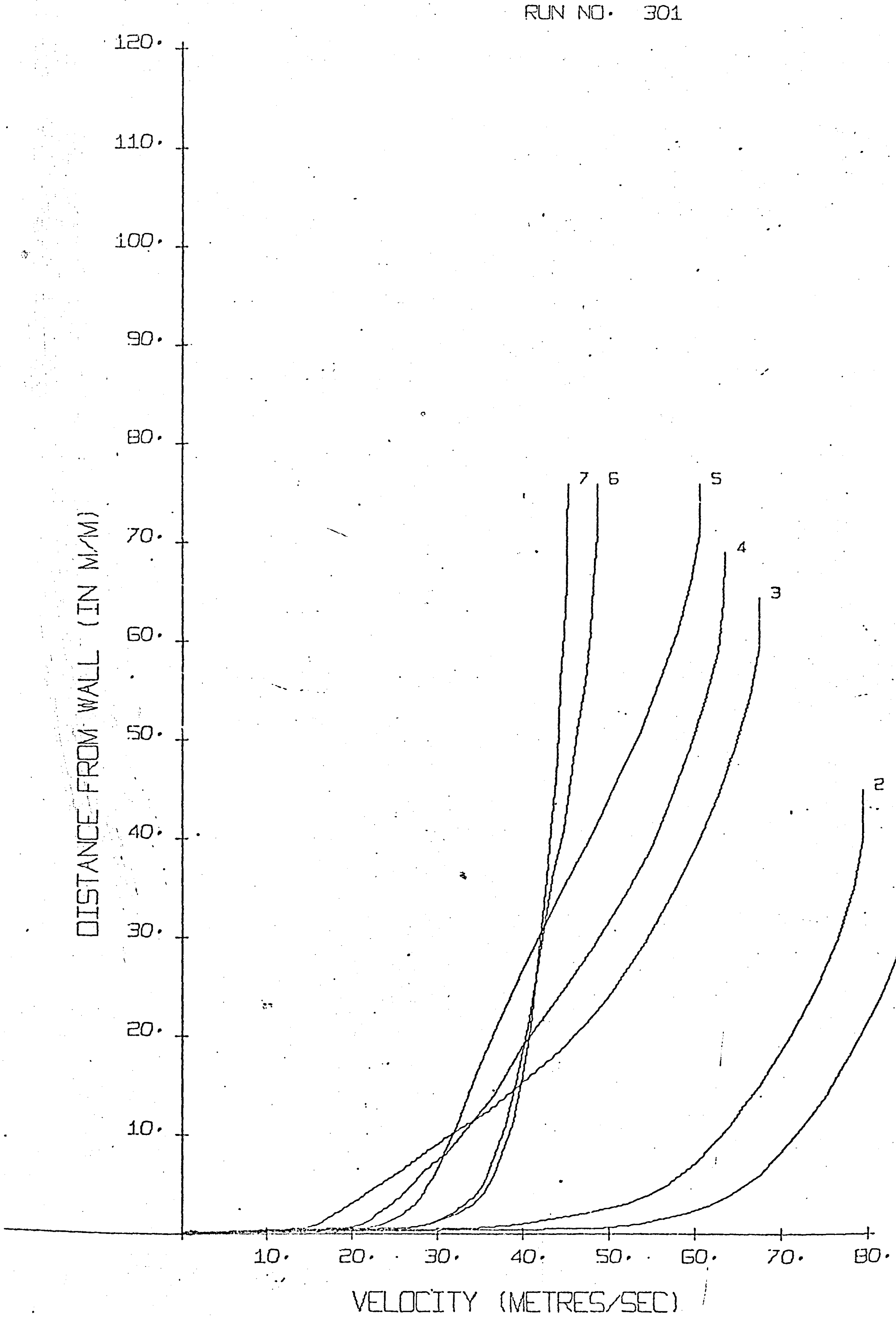

RUN NO. 301
120.
110.
100.
90.
80.
70.
60.
50.
40.
30.
20.
10.
DISTANCE FROM WALL (IN M/M)
10.
20.
30.
40.
50.
60.
70.
80.
VELOCITY (METRES/SEC)
7
6
5
4
3
2
1

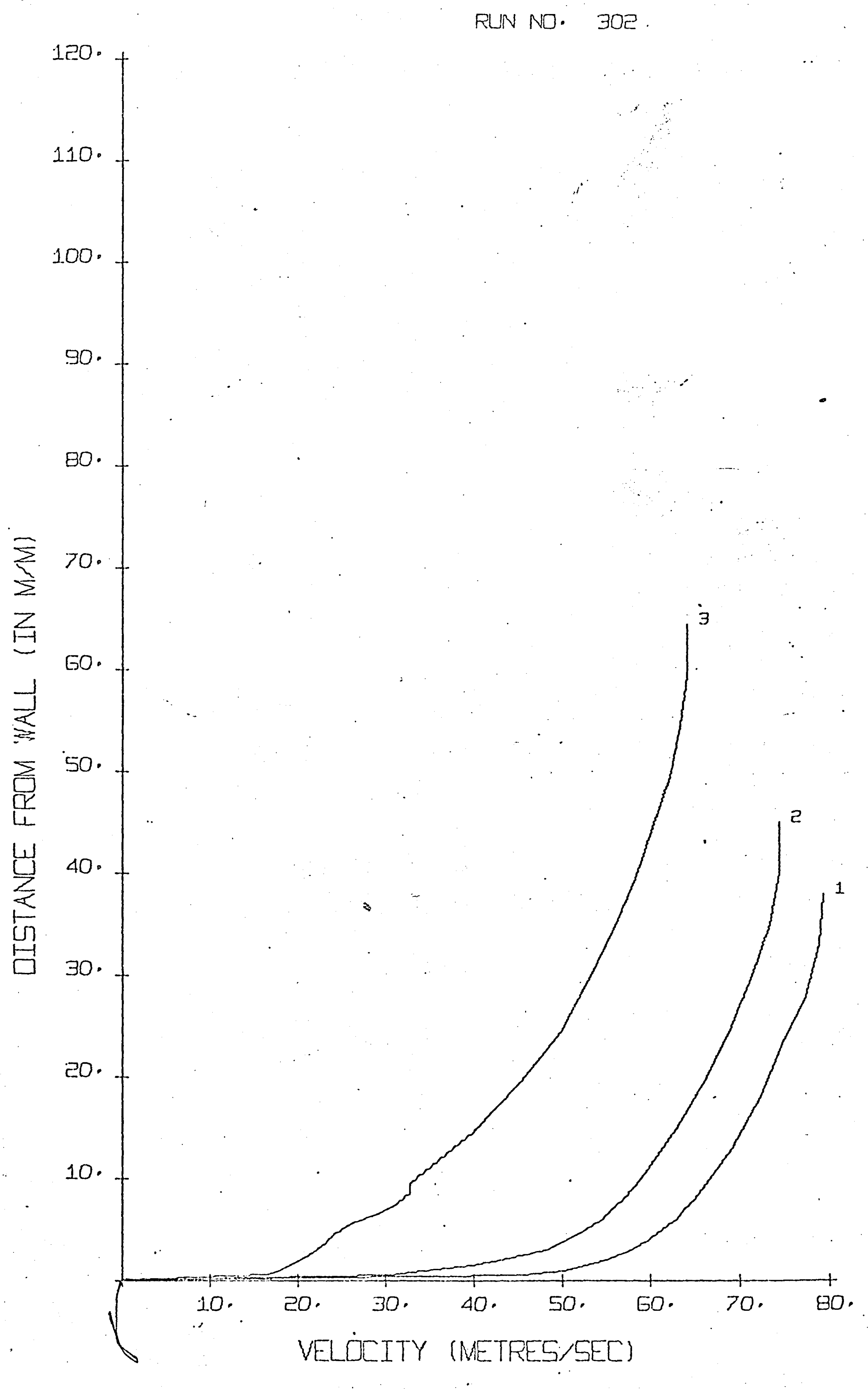
RUN NO. 302
DISTANCE FROM WALL (IN M/M)
120.
110.
100.
90.
80.
70.
60.
50.
40.
30.
20.
10.
10.
20.
30.
40.
50.
60.
70.
80.
VELOCITY (METRES/SEC)
3
2
1

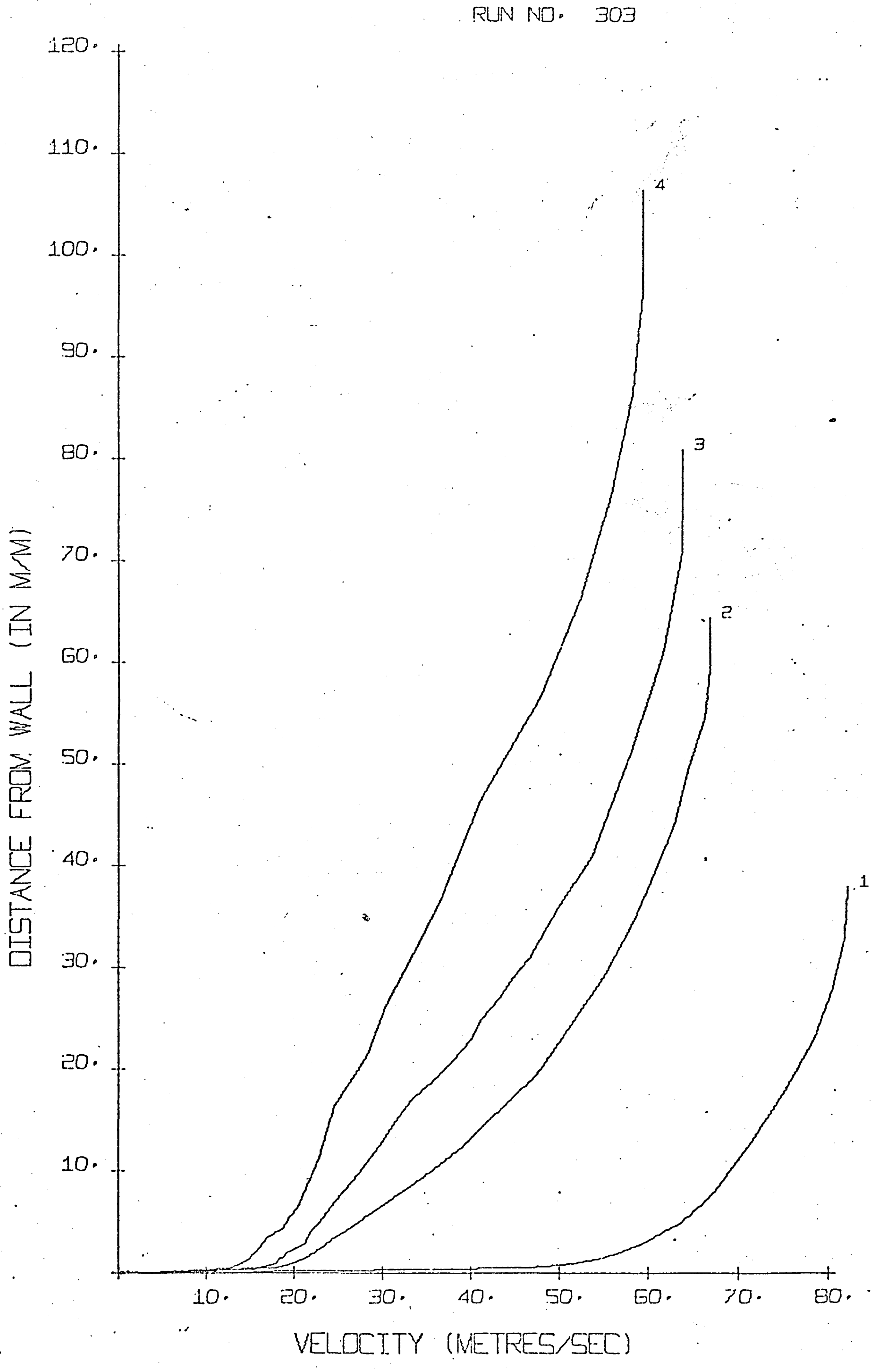

RUN NO. 303
DISTANCE FROM WALL (IN M/M)
VELOCITY (METRES/SEC)
120.
110.
100.
90.
80.
70.
60.
50.
40.
30.
20.
10.
10.
20.
30.
40.
50.
60.
70.
80.
1
2
3
4

RUN NO.. 304

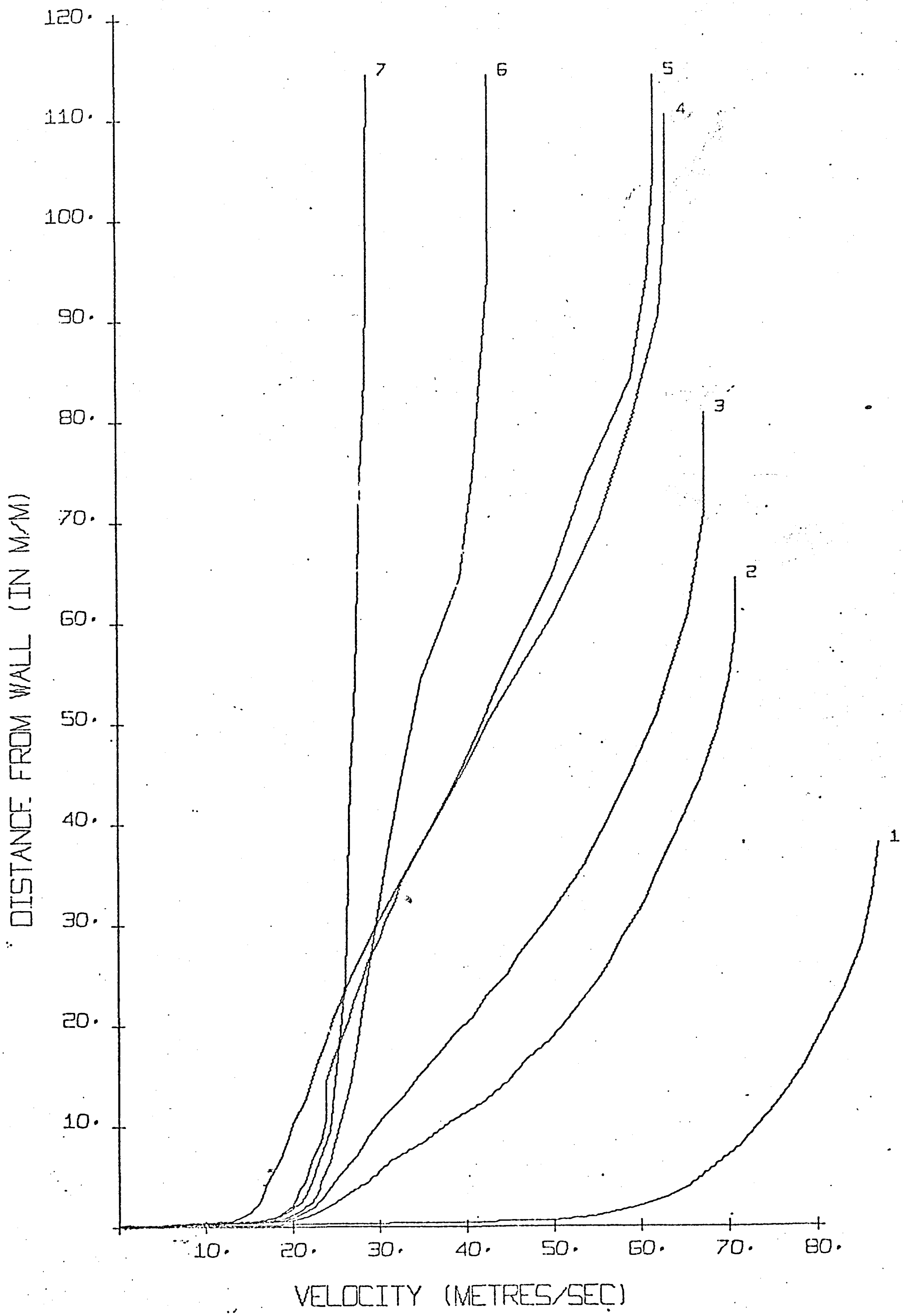

120.
110.
100.
90.
80.
70.
60.
50.
40.
30.
20.
10.
DISTANCE FROM WALL (IN M/M)
10.
20.
30.
40.
50.
60.
70.
80.
VELOCITY (METRES/SEC)
1
2
3
4
5
6
7

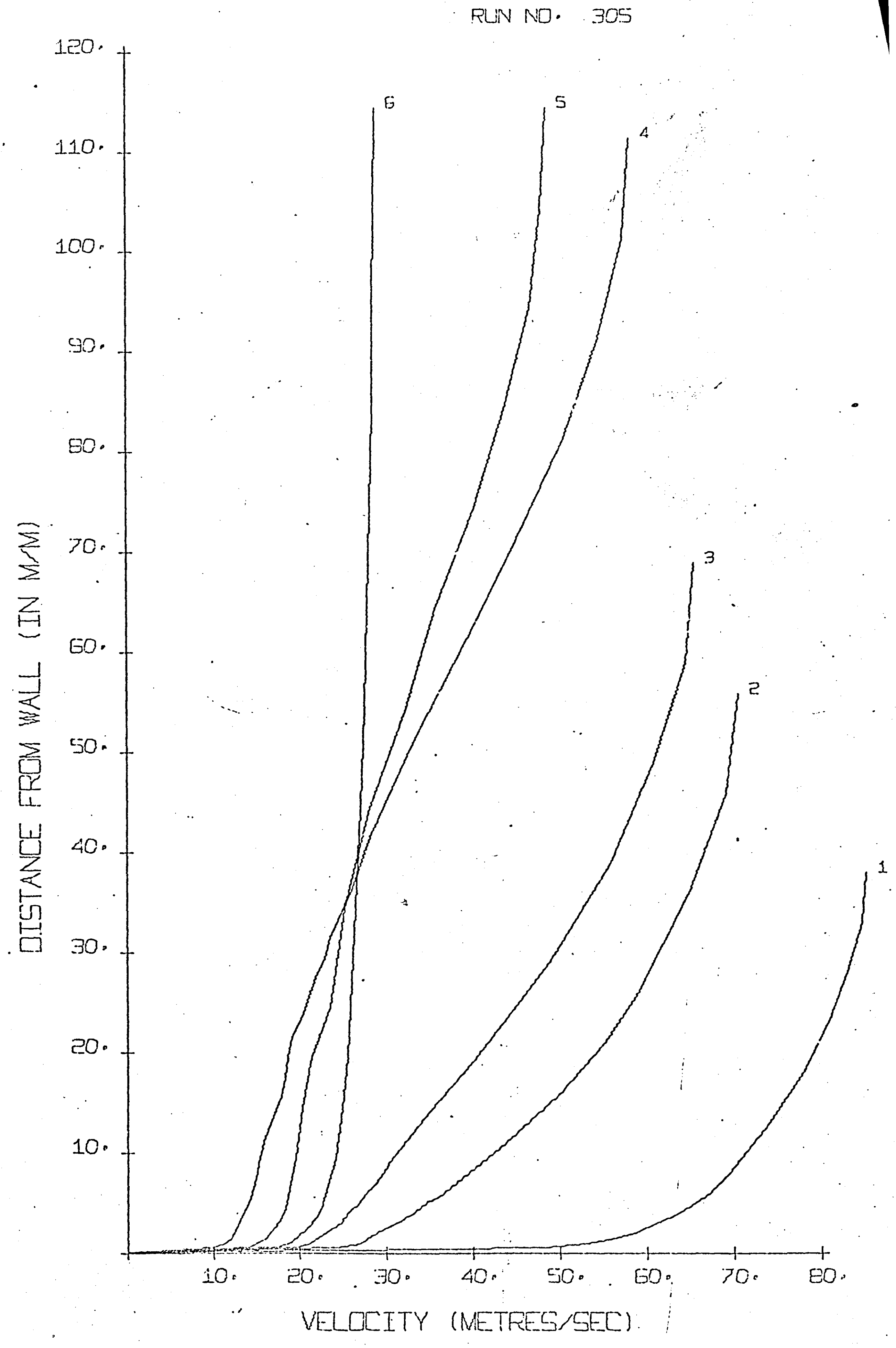
RUN NO. 305
DISTANCE FROM WALL (IN M/M)
VELOCITY (METRES/SEC)
120.
110.
100.
90.
80.
70.
60.
50.
40.
30.
20.
10.
10.
20.
30.
40.
50.
60.
70.
80.
1
2
3
4
5
6

RUN NO. 306

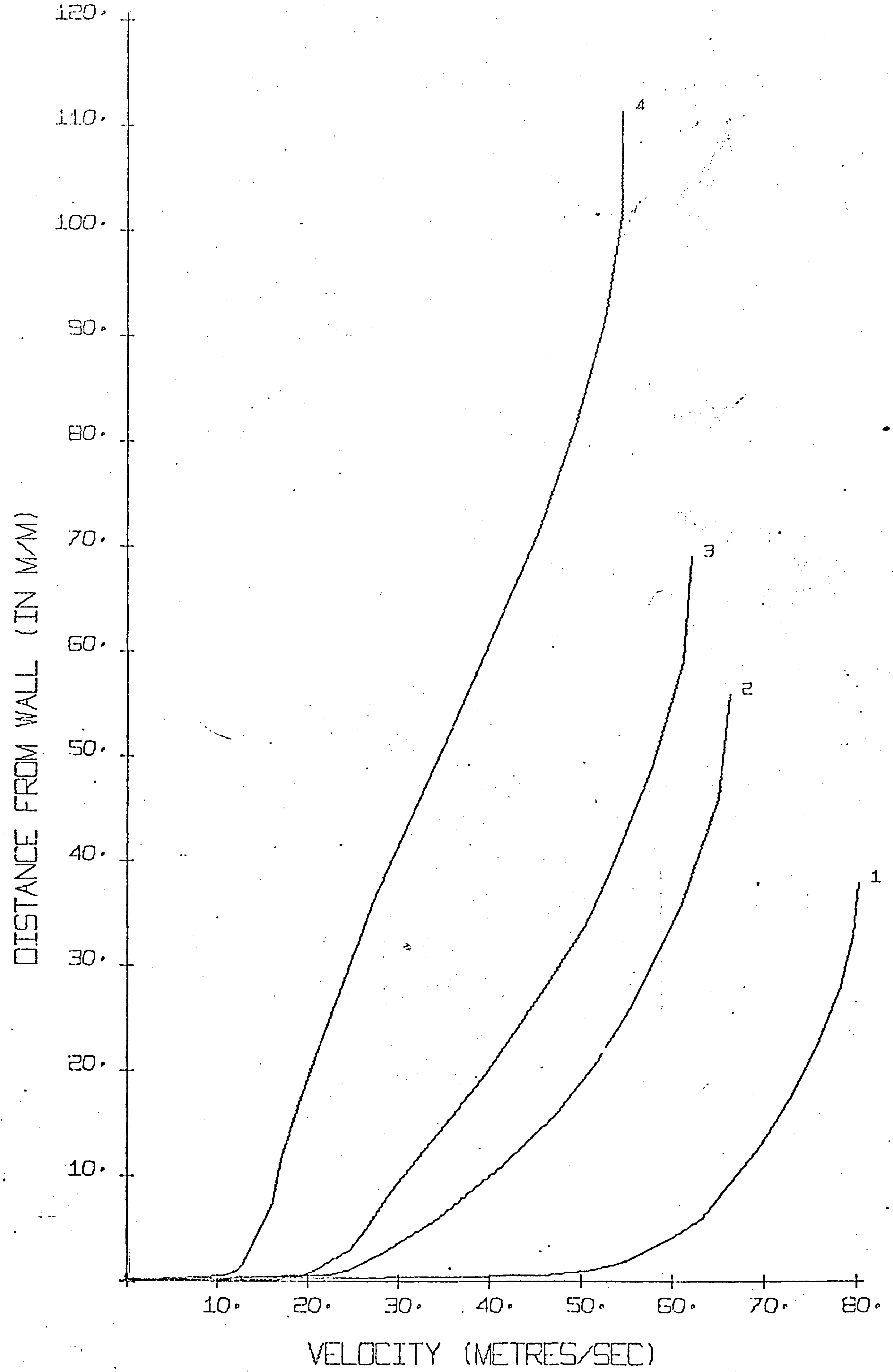

Intek

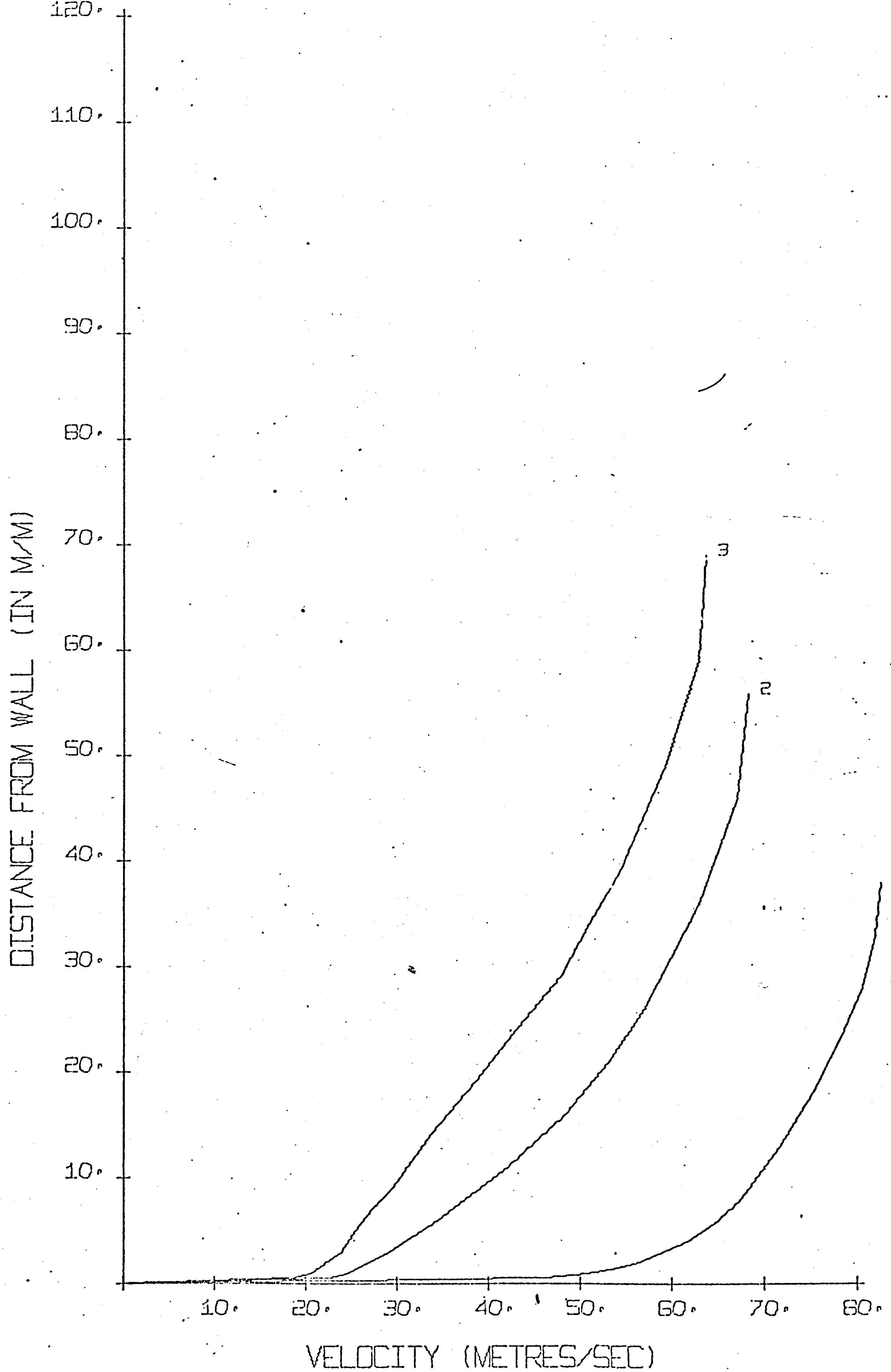
DISTANCE FROM WALL (IN M/M)
120.
110.
100.
90.
80.
70.
60.
50.
40.
30.
20.
10.
10.
20.
30.
40.
50.
60.
70.
80.
VELOCITY (METRES/SEC)
1
2
3

RUN NO. 308

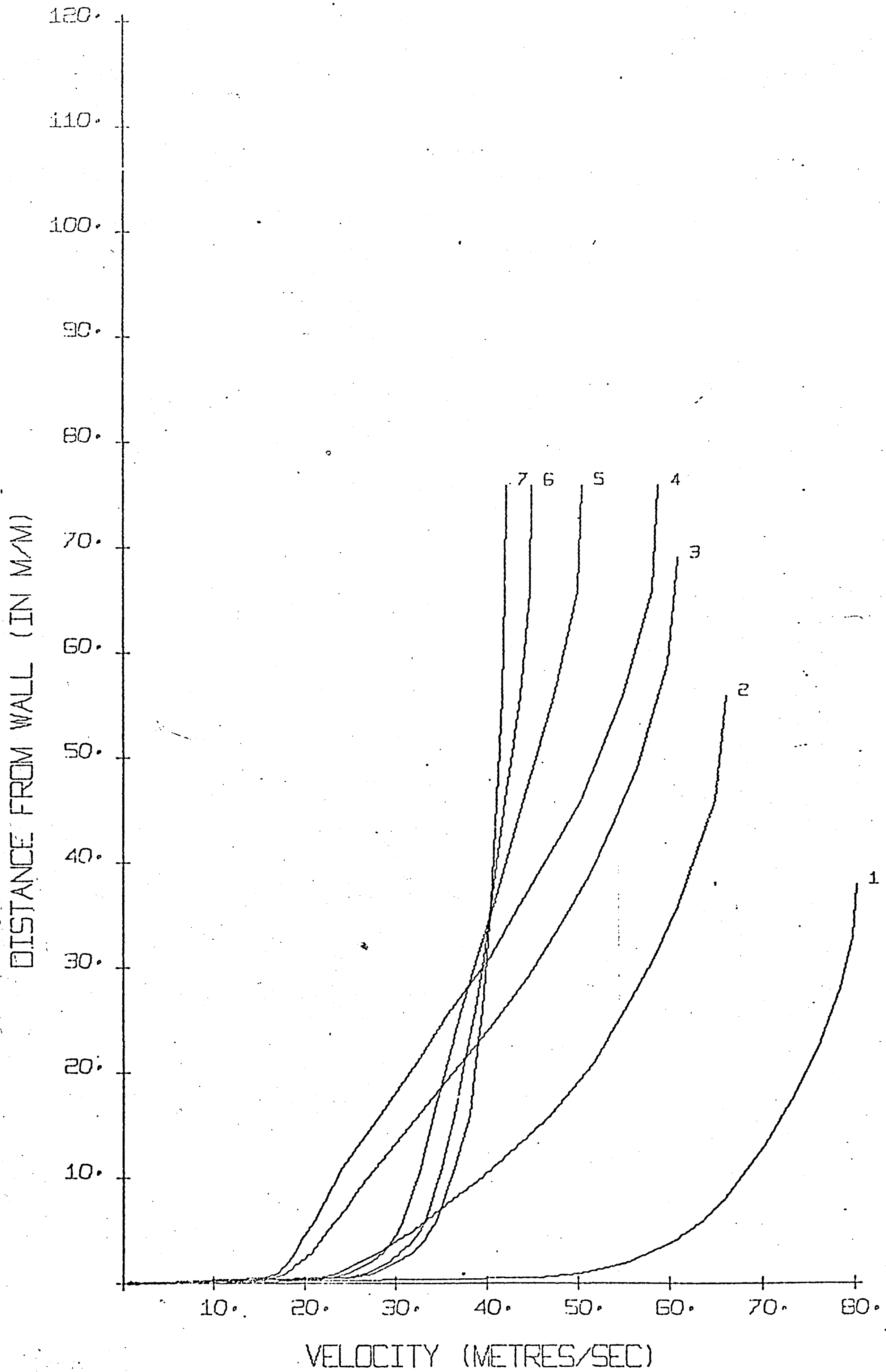

6/73 RCP/305/1C

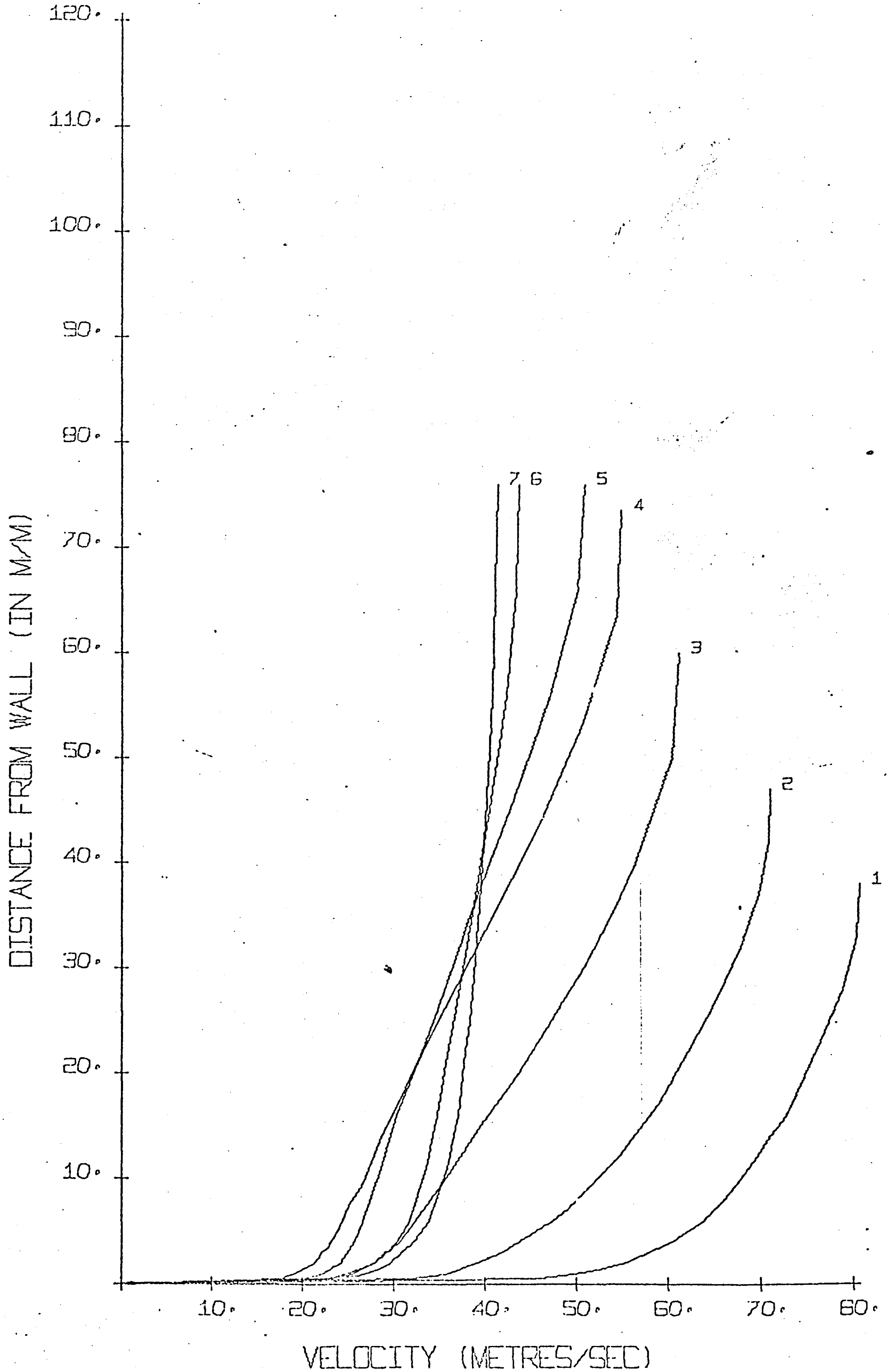

DISTANCE FROM WALL (IN M/M)
120.
110.
100.
90.
80.
70.
60.
50.
40.
30.
20.
10.
10.
20.
30.
40.
50.
60.
70.
80.
VELOCITY (METRES/SEC)
7
6
5
4
3
2
1

RUN NO. 310

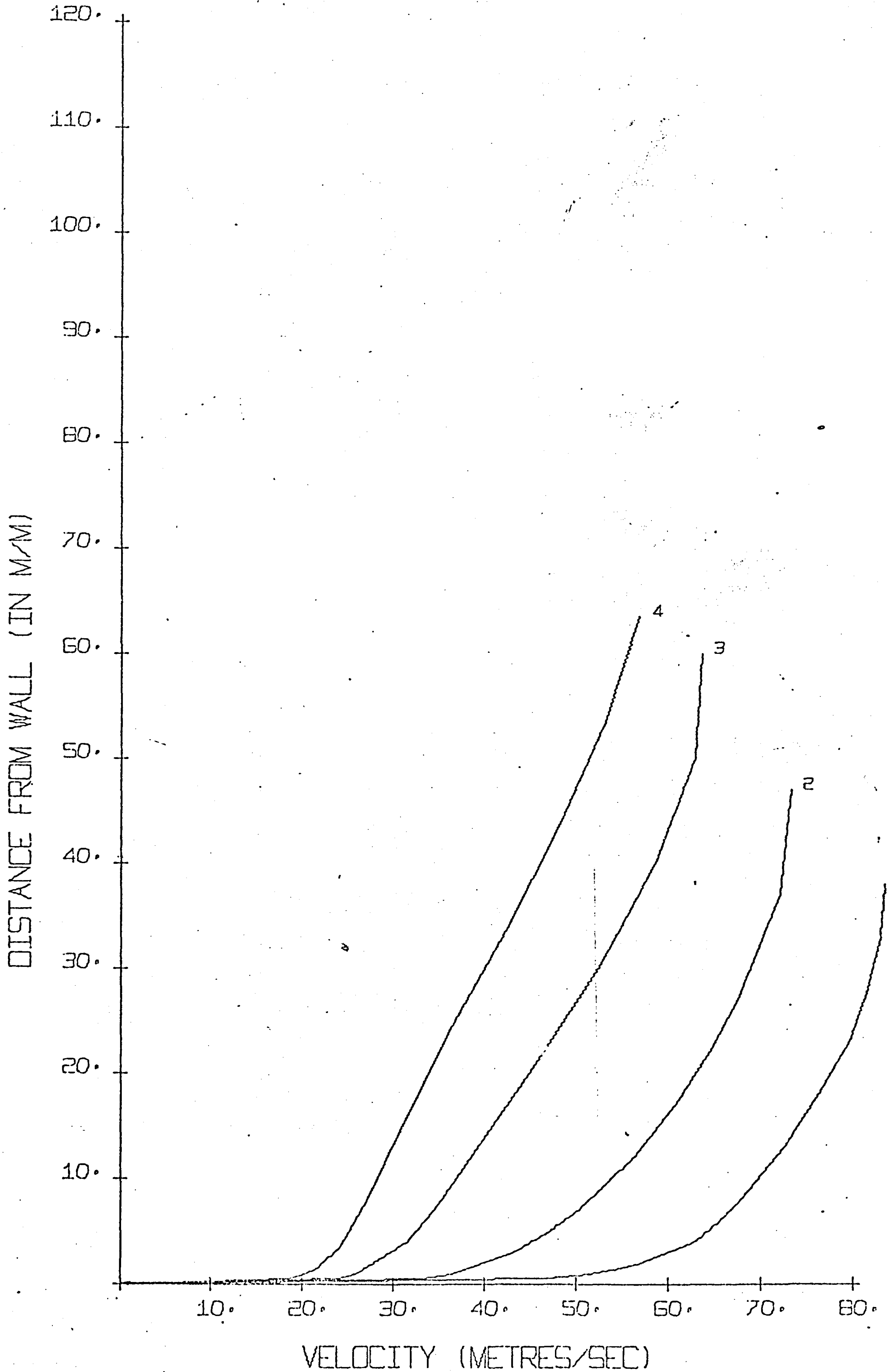
120.
110.
100.
90.
80.
70.
60.
50.
40.
30.
20.
10.
DISTANCE FROM WALL (IN M/M)
4
3
2
10.
20.
30.
40.
50.
60.
70.
80.
VELOCITY (METRES/SEC)

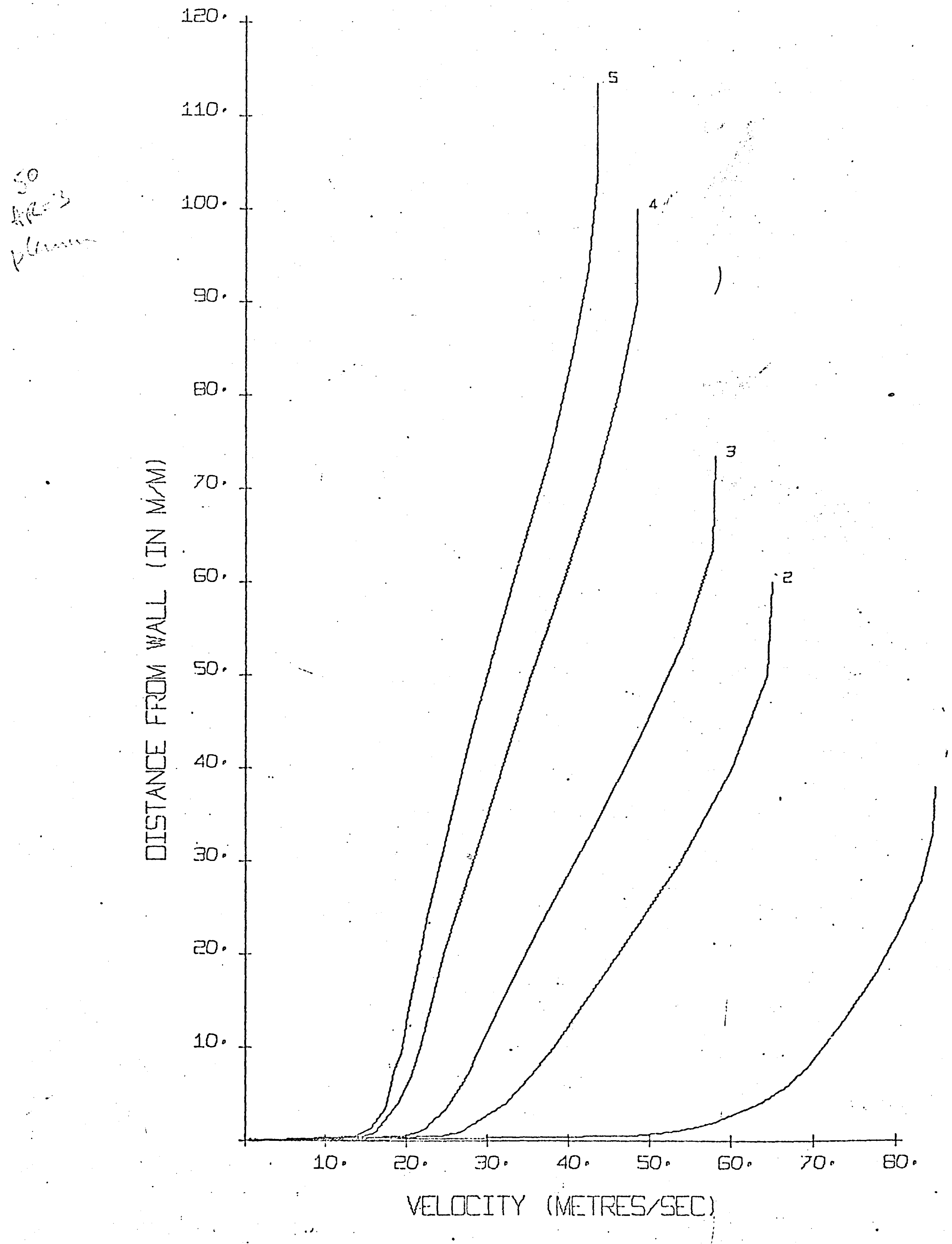

6/73 RCP/305/1004 400

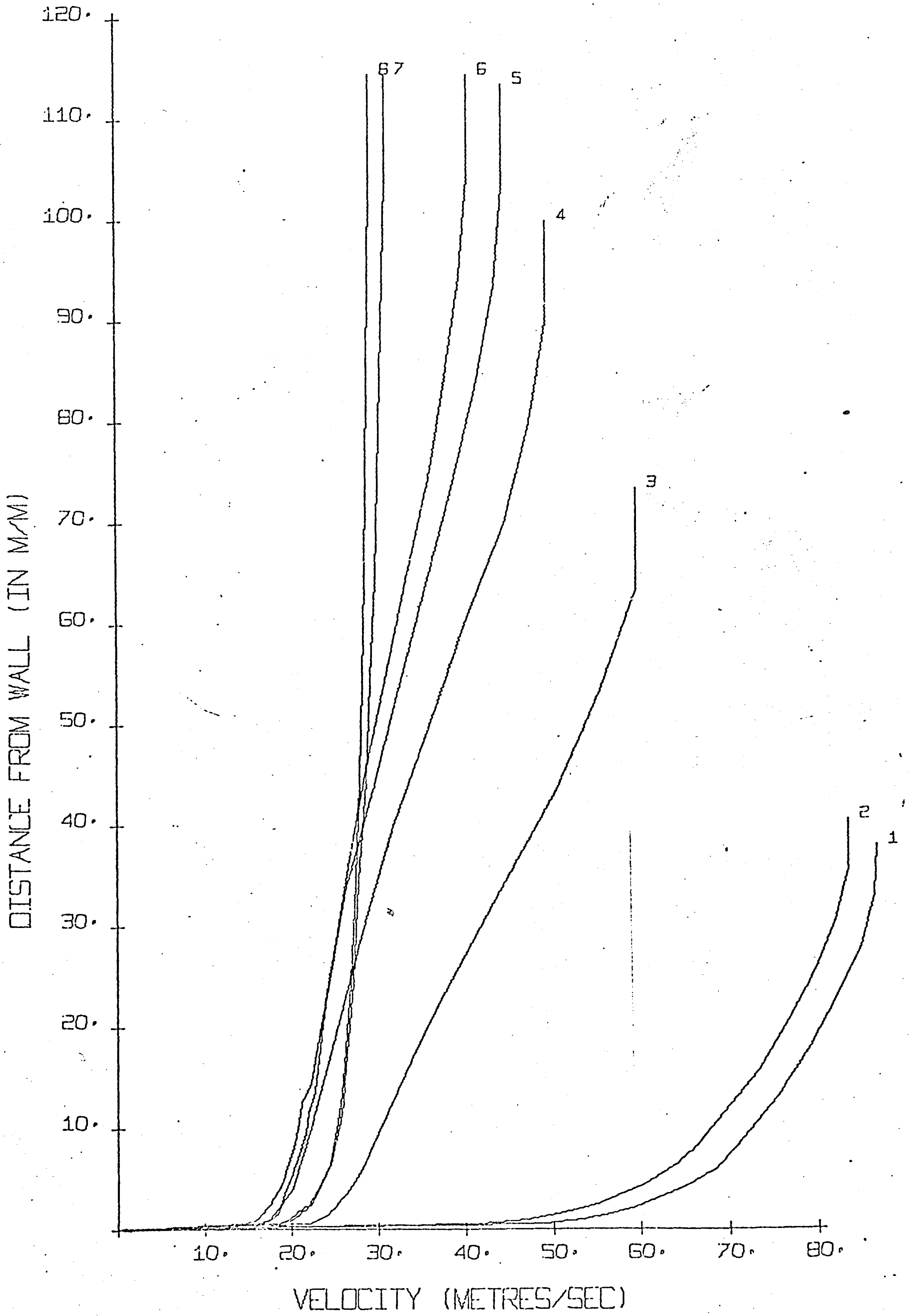

DISTANCE FROM WALL (IN M/M)
VELOCITY (METRES/SEC)
120.
110.
100.
90.
80.
70.
60.
50.
40.
30.
20.
10.
10.
20.
30.
40.
50.
60.
70.
80.
8
7
6
5
4
3
2
1

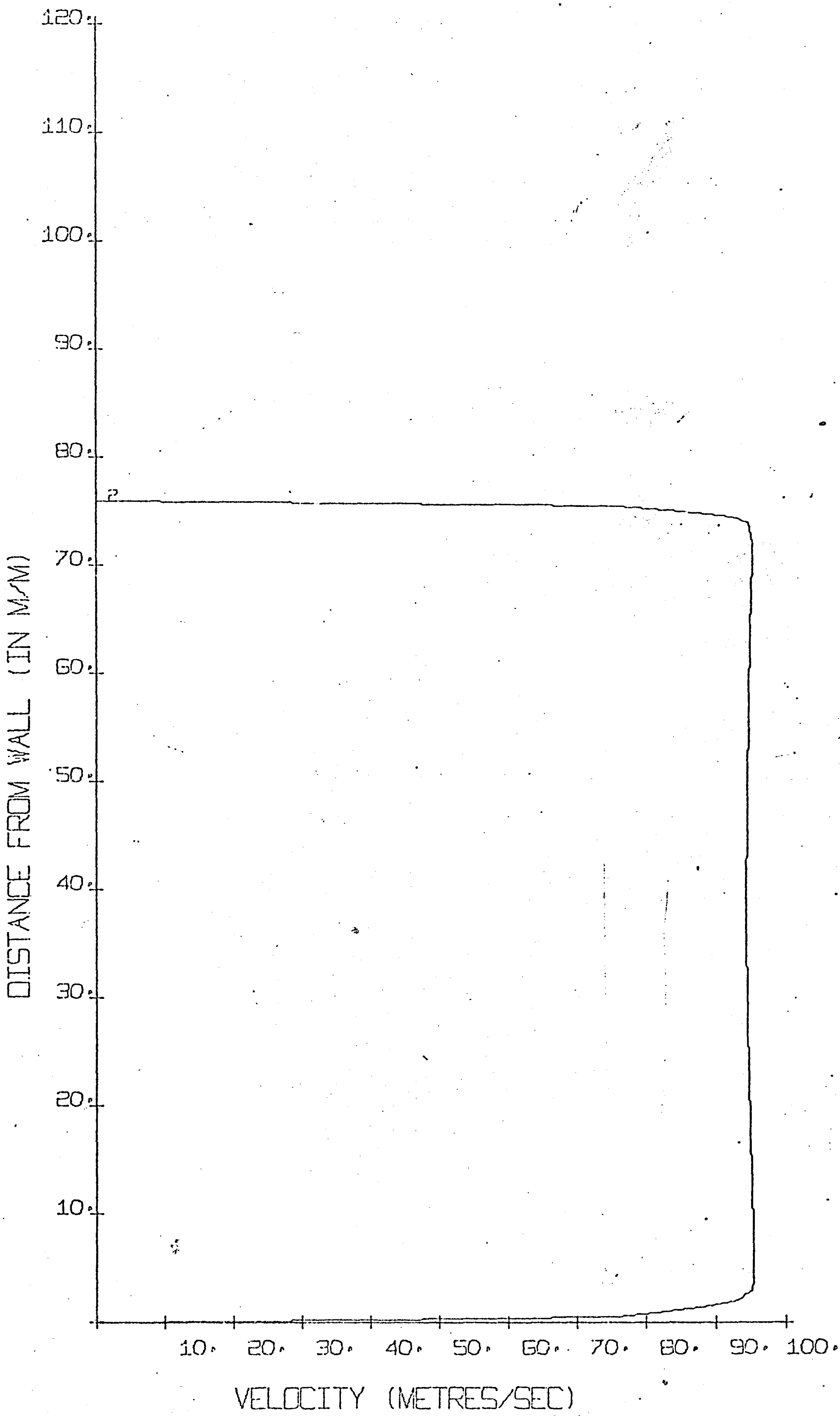
120.
110.
100.
90.
80.
70.
60.
50.
40.
30.
20.
10.
DISTANCE FROM WALL (IN M/M)
10. 20. 30. 40. 50. 60. 70. 80. 90. 100.
VELOCITY (METRES/SEC)

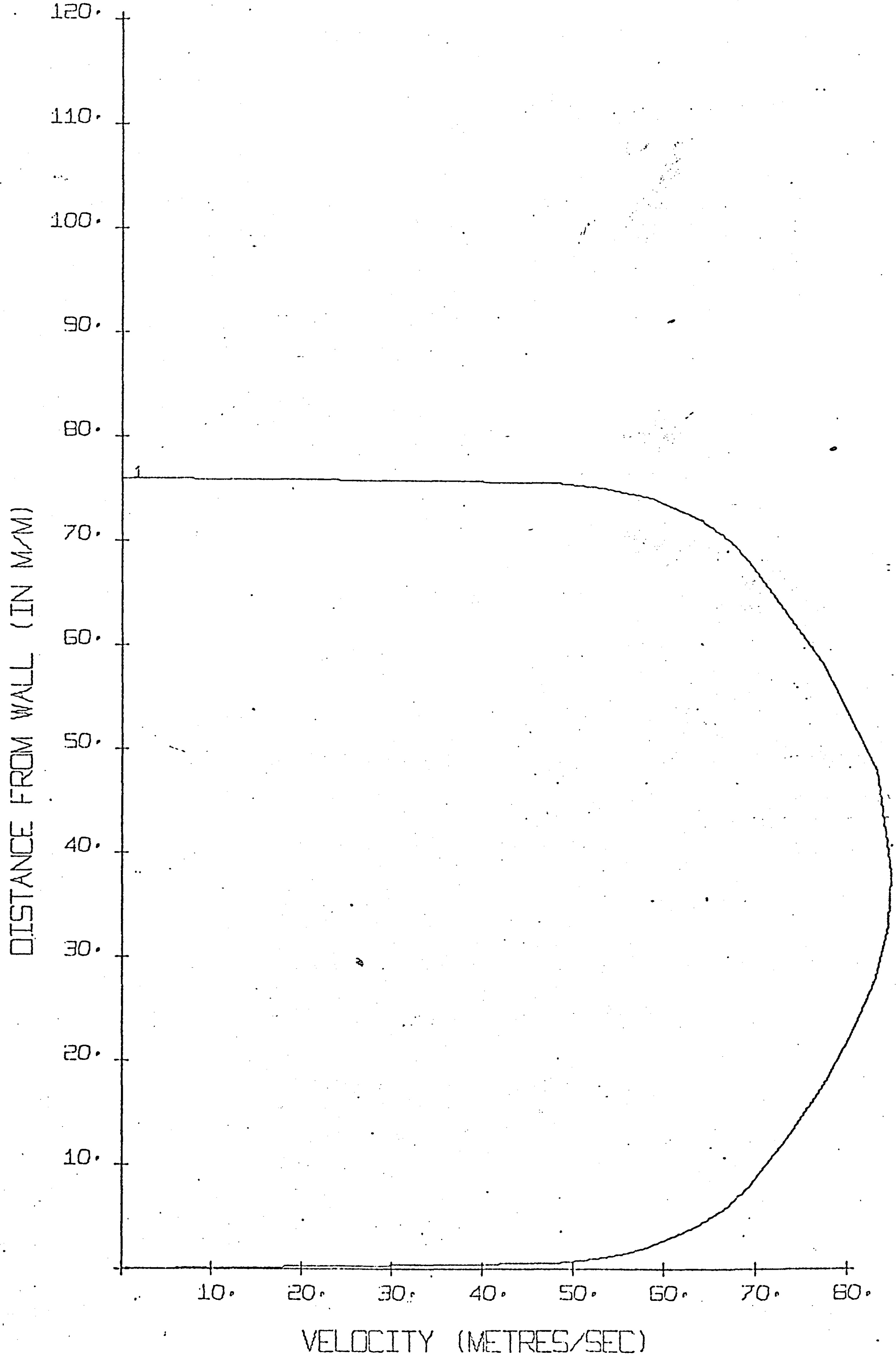
120
110
100
90
80
70
60
50
40
30
20
10
DISTANCE FROM WALL (IN M/M)
1
10
20
30
40
50
60
70
80
VELOCITY (METRES/SEC)

Intek

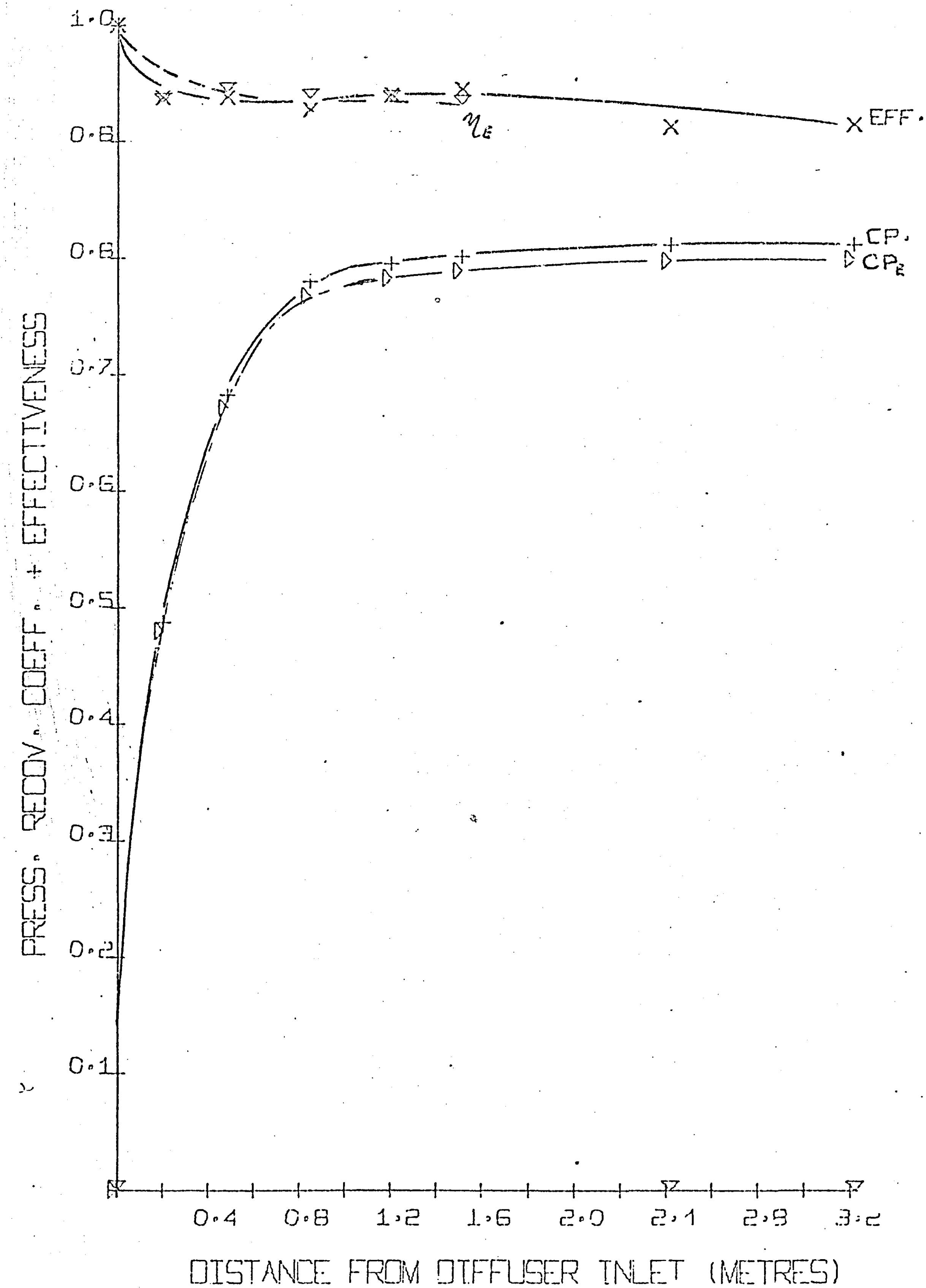

1·0
0·9
0·8
0·7
0·6
0·5
0·4
0·3
0·2
0·1
PRESS. RECOV. COEFF. + EFFECTIVENESS
EFF.
η_E
CP.
CP_E
0·4
0·8
1·2
1·6
2·0
2·4
2·8
3·2
DISTANCE FROM DIFFUSER INLET (METRES)

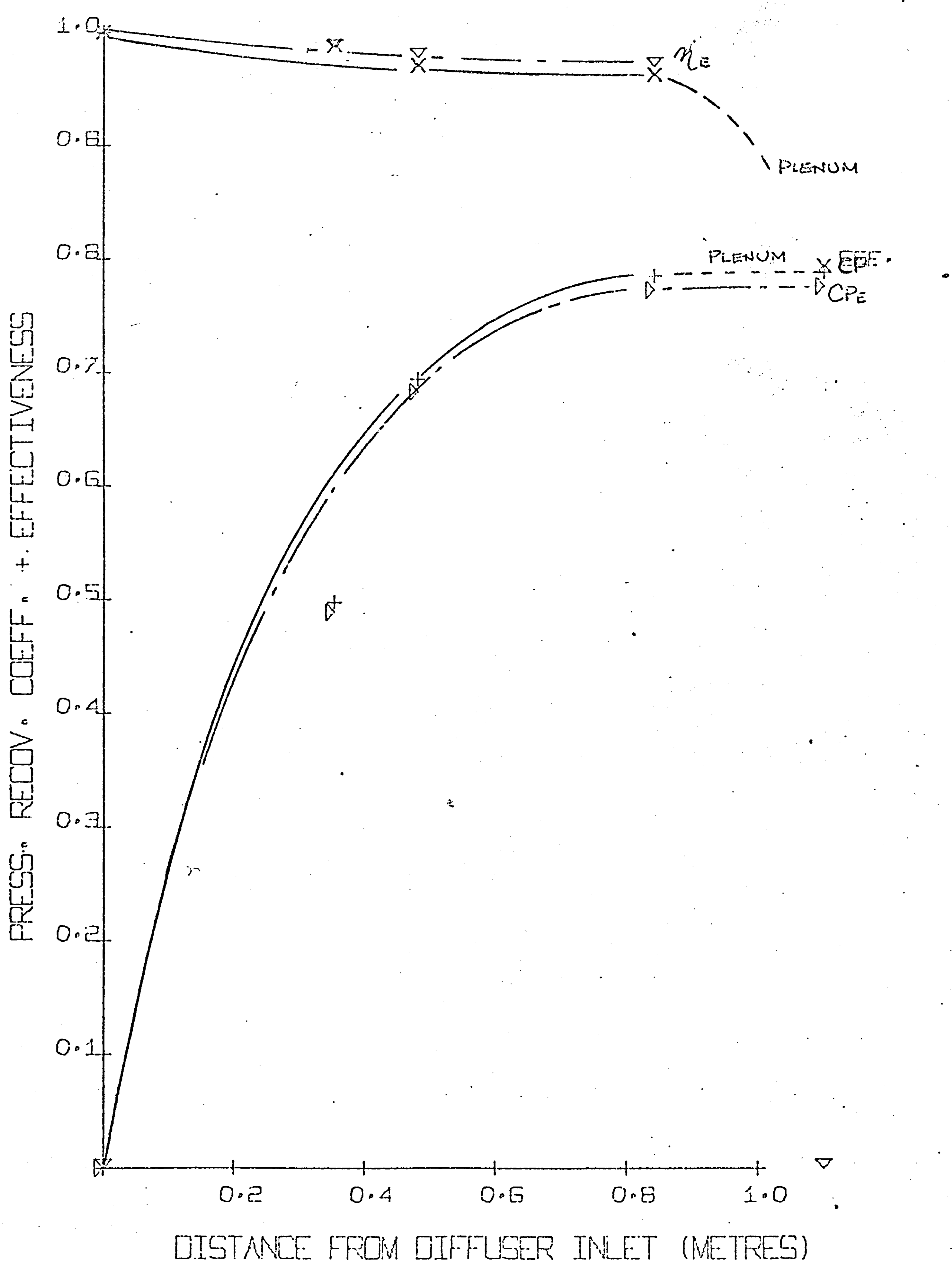

1·0
0·9
0·8
0·7
0·6
0·5
0·4
0·3
0·2
0·1
0·2
0·4
0·6
0·8
1·0
PRESS. RECOV. COEFF. + EFFECTIVENESS
DISTANCE FROM DIFFUSER INLET (METRES)
η_E
PLENUM
PLENUM
EPF.
CP_E

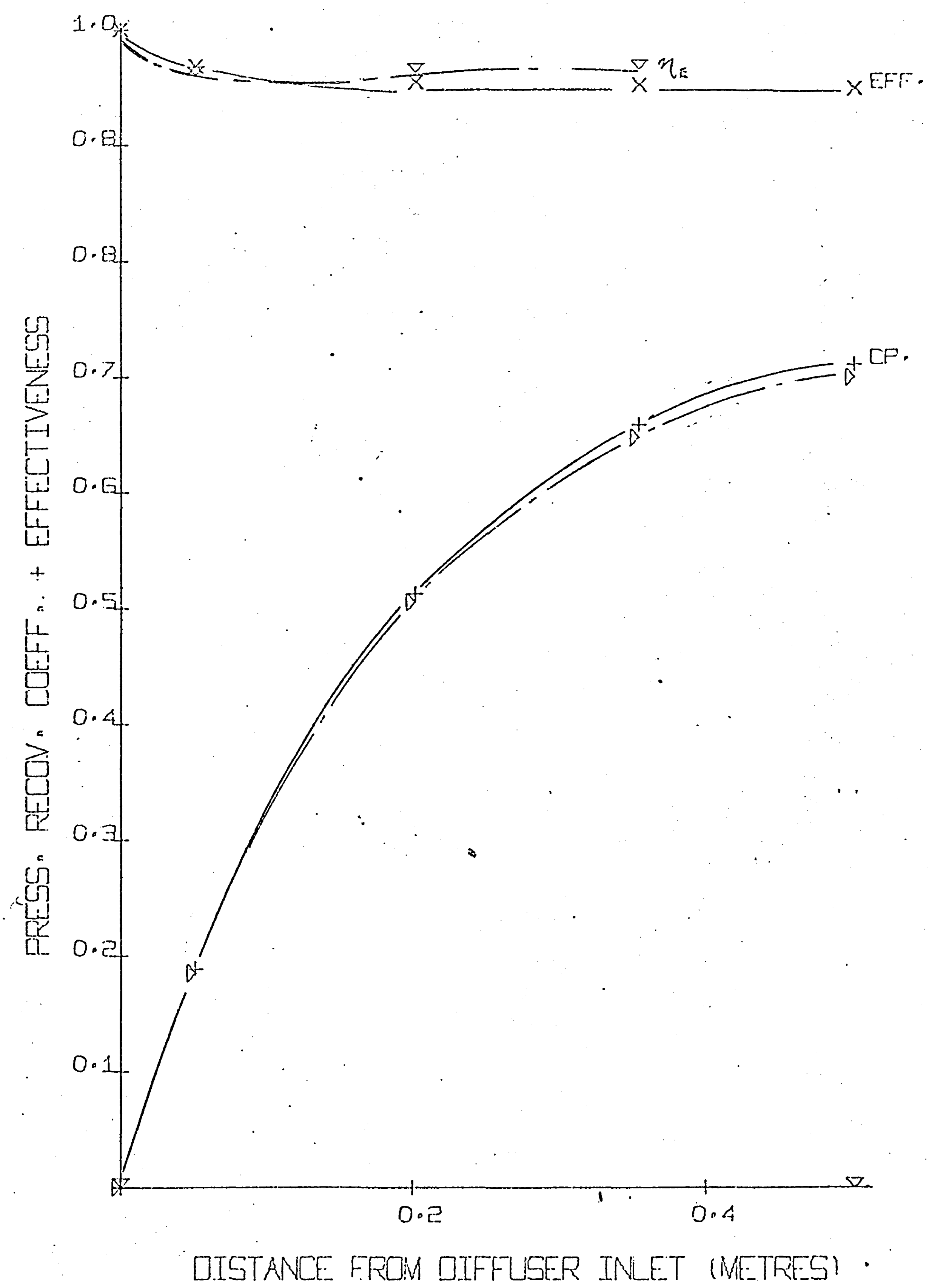

1·0
0·8
0·8
0·7
0·6
0·5
0·4
0·3
0·2
0·1
0·2
0·4
η_E
EFF.
CP.
PRESS. RECOV. COEFF. + EFFECTIVENESS
DISTANCE FROM DIFFUSER INLET (METRES)

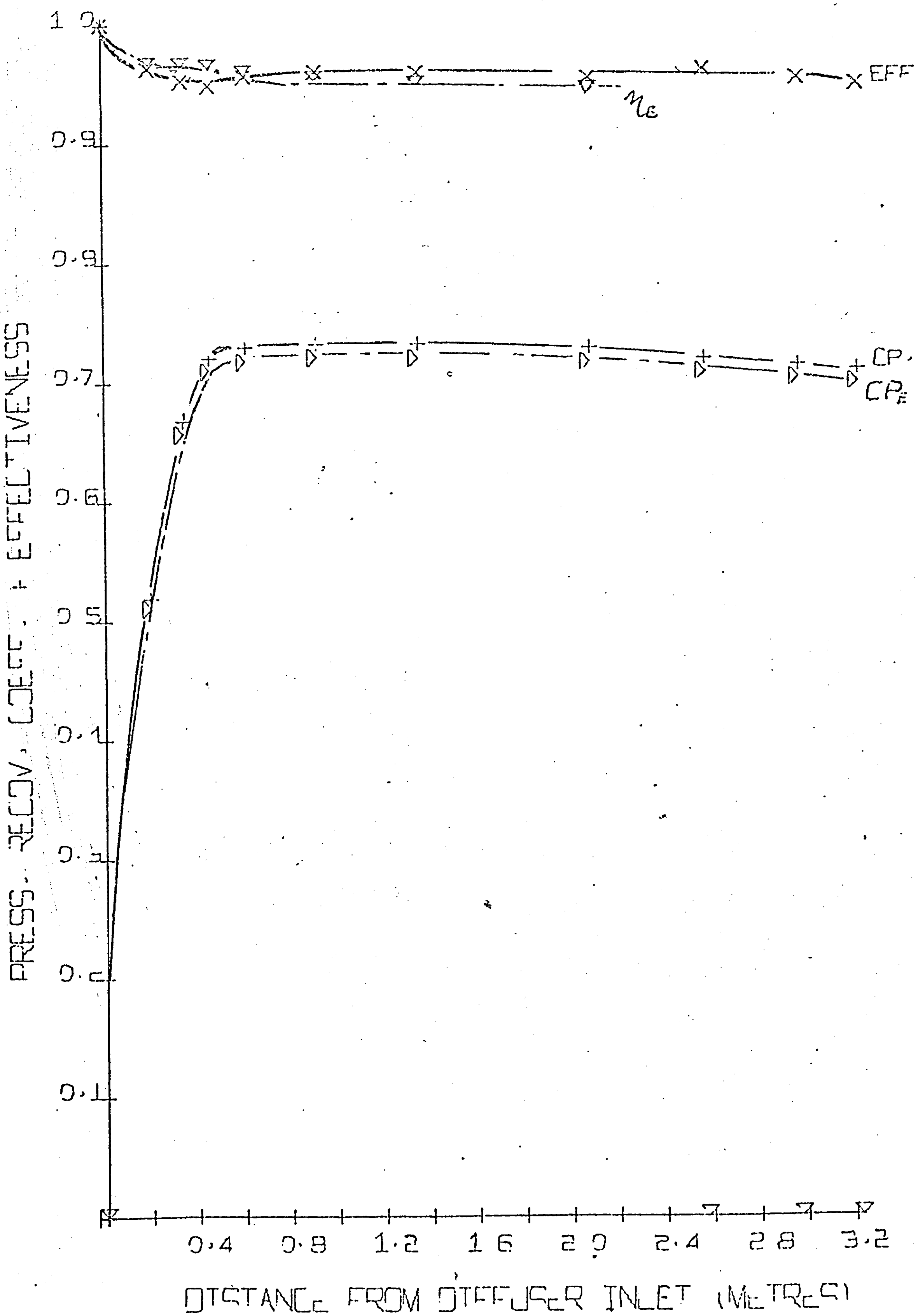

PRESS. RECOV. COEFF. + EFFECTIVENESS
DISTANCE FROM DIFFUSER INLET (METRES)
EFF.
η_E
CP.
CP_E
1.0
0.9
0.9
0.7
0.6
0.5
0.4
0.1
0.4
0.8
1.2
1.6
2.0
2.4
2.8
3.2

RUN NO. 105

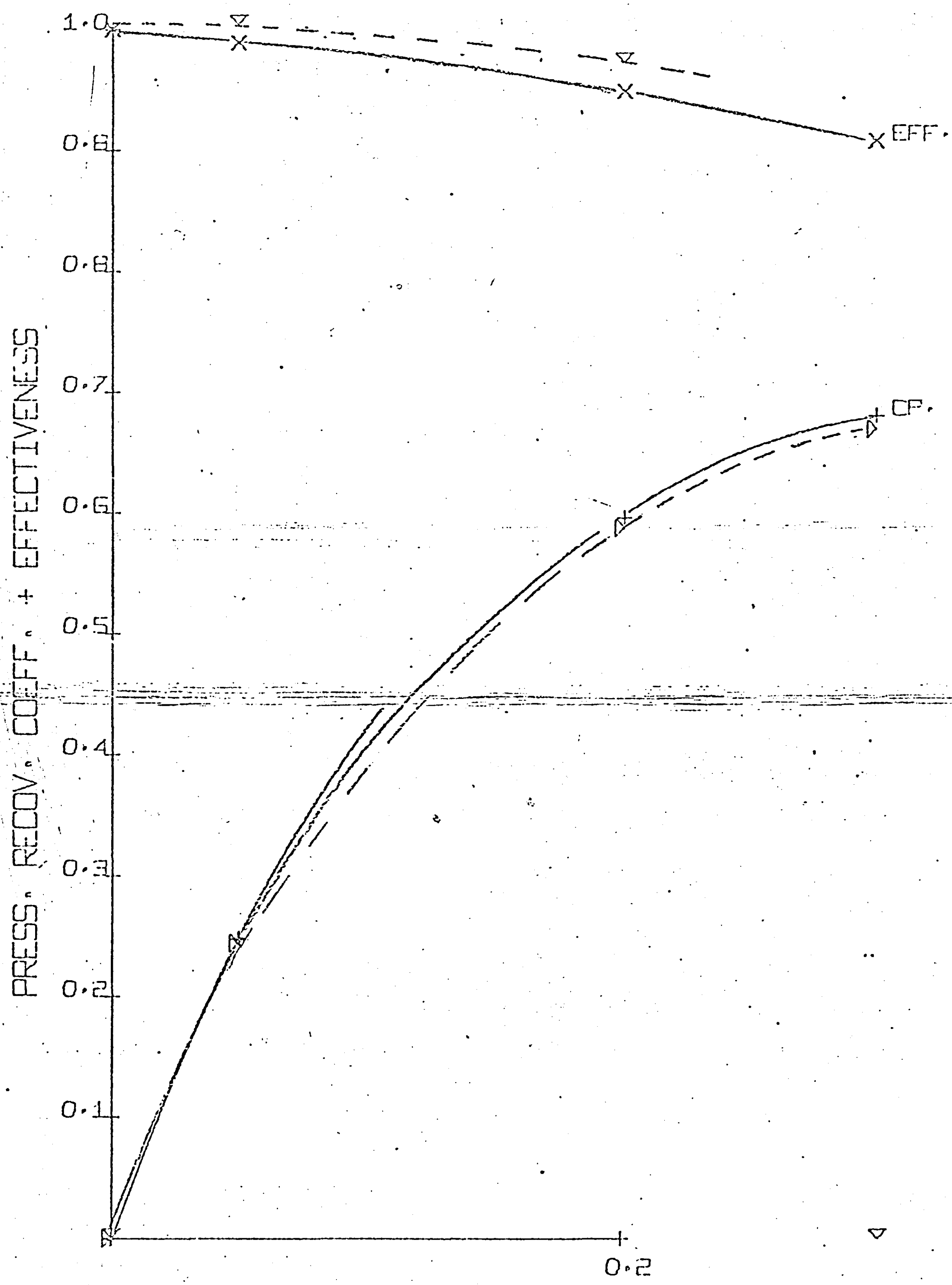

1.0
0.9
0.8
0.7
0.6
0.5
0.4
0.3
0.2
0.1
EFF.
CP.
PRESS. RECOV. COEFF. + EFFECTIVENESS
0.2
DISTANCE FROM DIFFUSER INLET (METRES)

RUN NO. 106

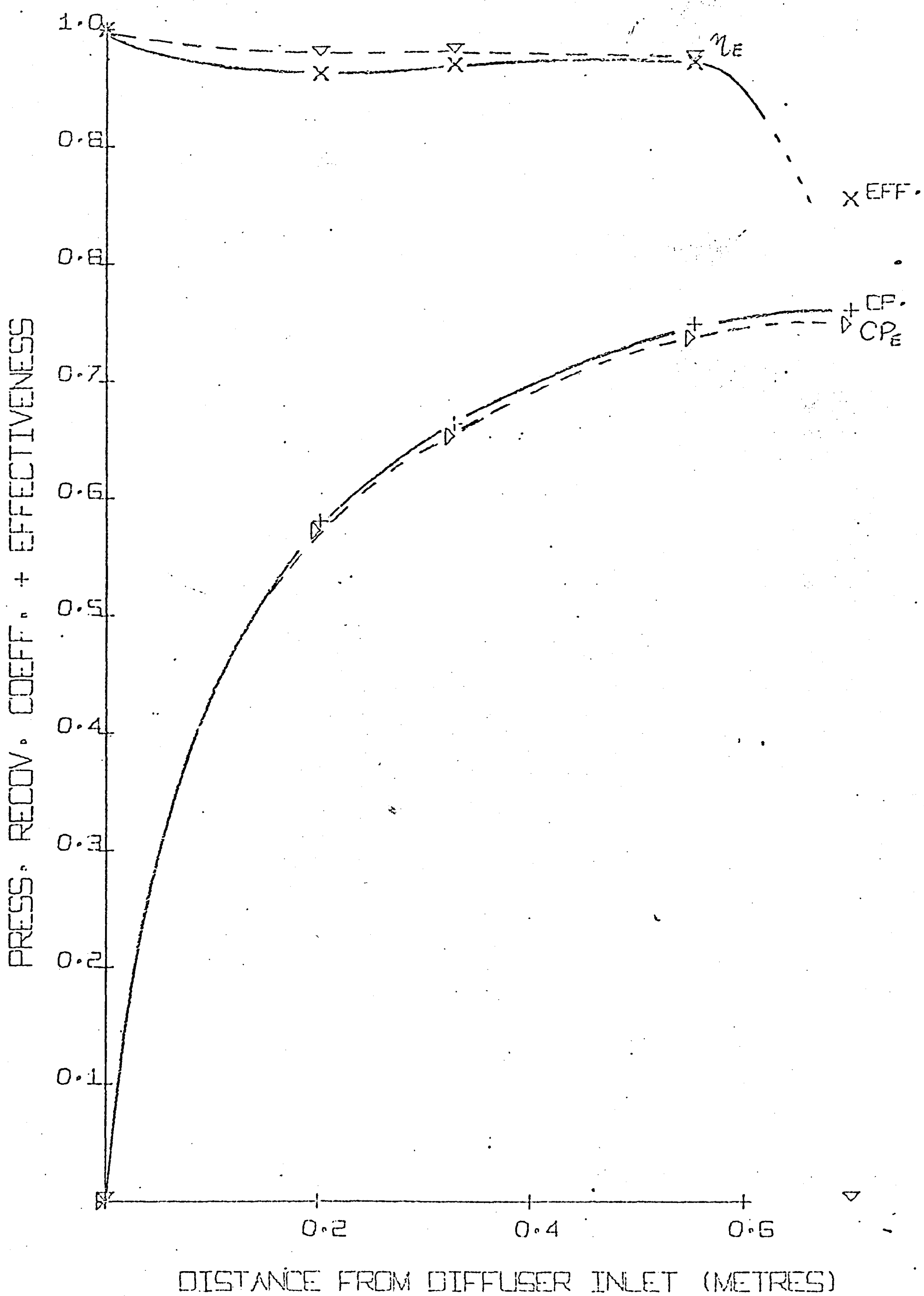

1·0
0·8
0·8
0·7
0·6
0·5
0·4
0·3
0·2
0·1
0·2
0·4
0·6
η_E
EFF.
CP.
CP_E
PRESS. RECOV. COEFF. + EFFECTIVENESS
DISTANCE FROM DIFFUSER INLET (METRES)

RUN NO. 107

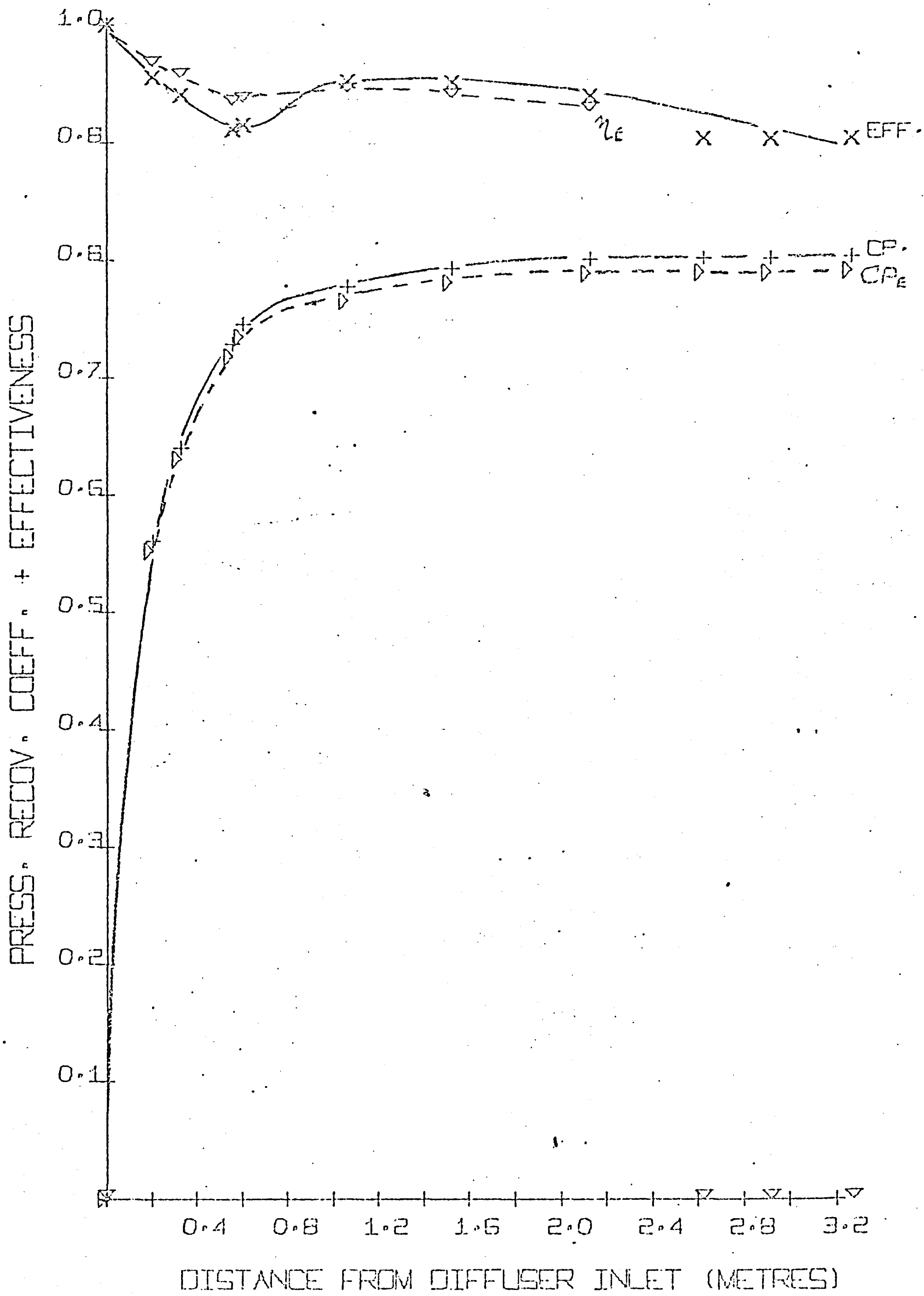
1.0
0.9
0.8
0.7
0.6
0.5
0.4
0.3
0.2
0.1
0.4
0.8
1.2
1.6
2.0
2.4
2.8
3.2
EFF.
η_E
CP.
CP_E
PRESS. RECOV. COEFF. + EFFECTIVENESS
DISTANCE FROM DIFFUSER INLET (METRES)

RUN NO. 108

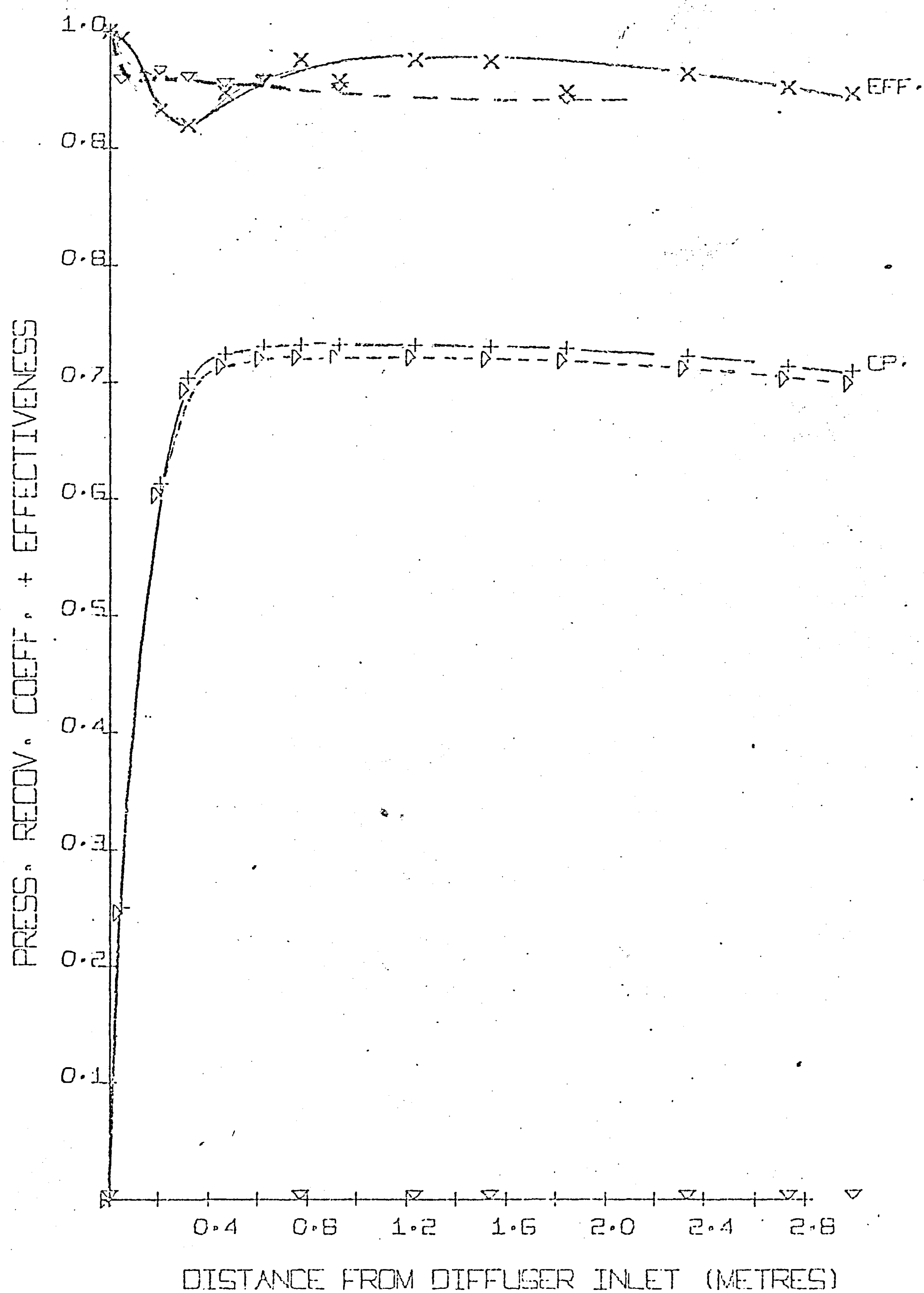

Intek

2/1004 400

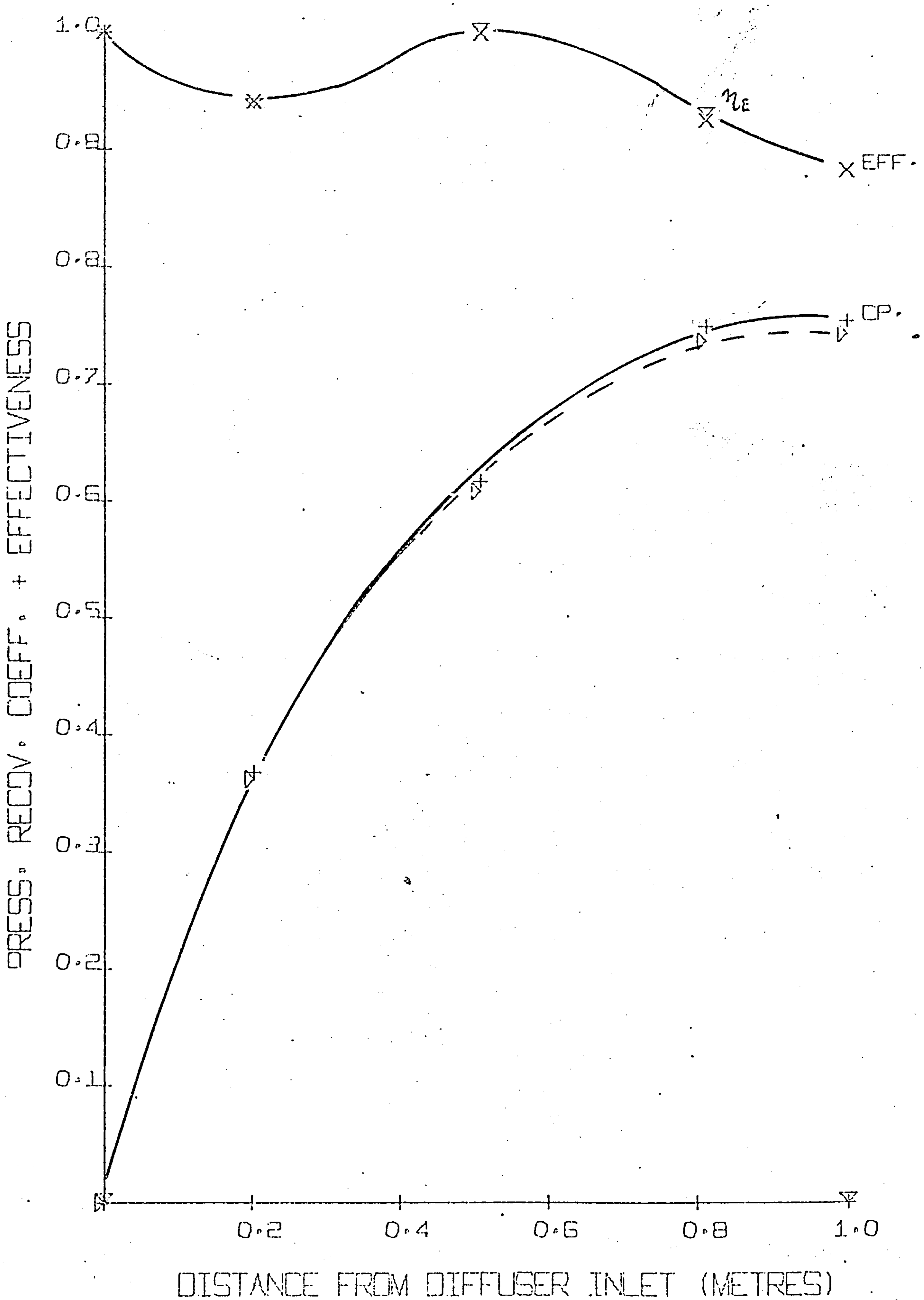
PRESS. RECOV. COEFF. + EFFECTIVENESS
1.0
0.8
0.8
0.7
0.6
0.5
0.4
0.3
0.2
0.1
0.2
0.4
0.6
0.8
1.0
DISTANCE FROM DIFFUSER INLET (METRES)
EFF.
CP.
η_E

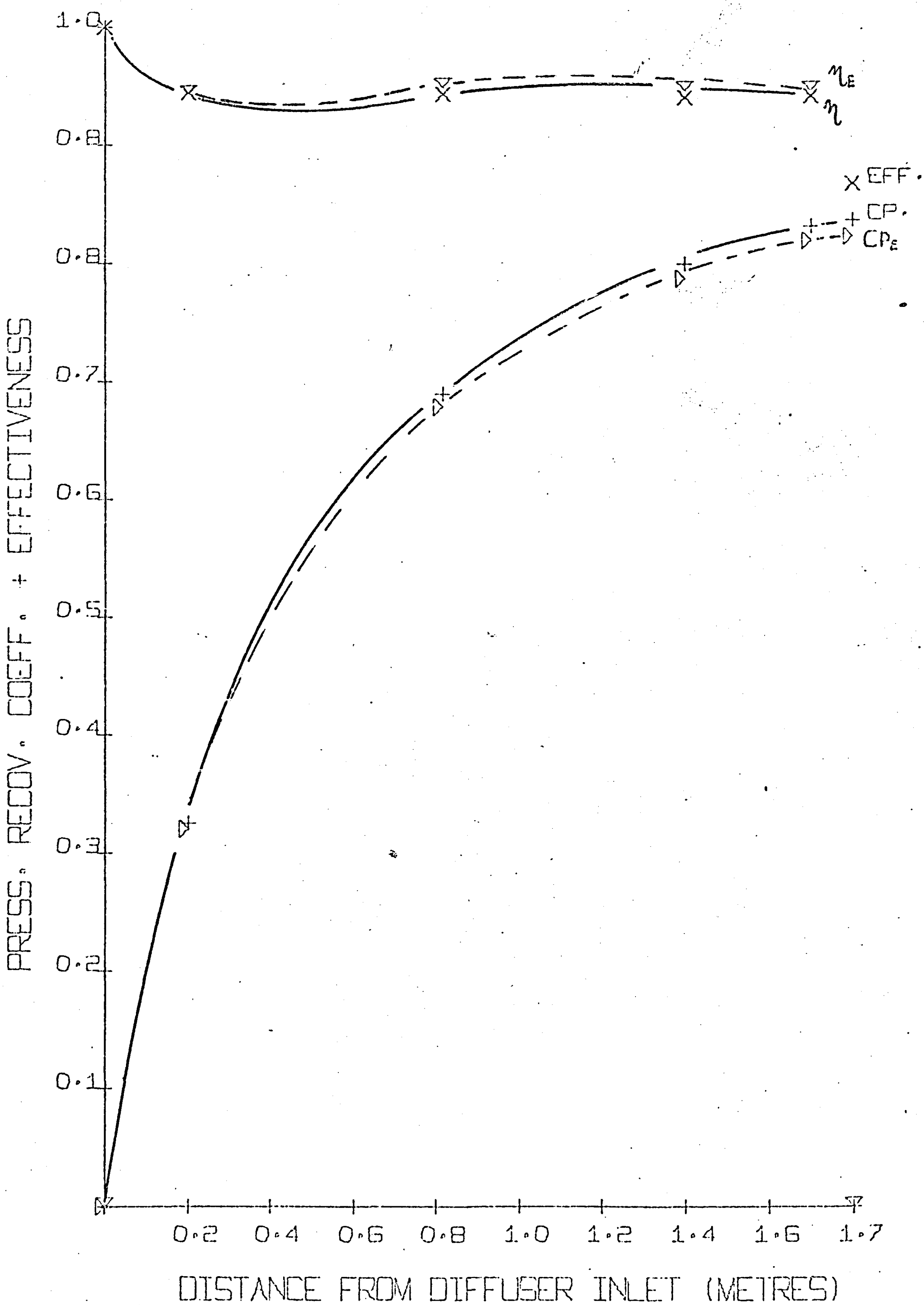

PRESS. RECOV. COEFF. + EFFECTIVENESS
1·0
0·8
0·8
0·7
0·6
0·5
0·4
0·3
0·2
0·1
0·2
0·4
0·6
0·8
1·0
1·2
1·4
1·6
1·7
DISTANCE FROM DIFFUSER INLET (METRES)
X EFF.
+ CP.
CPE

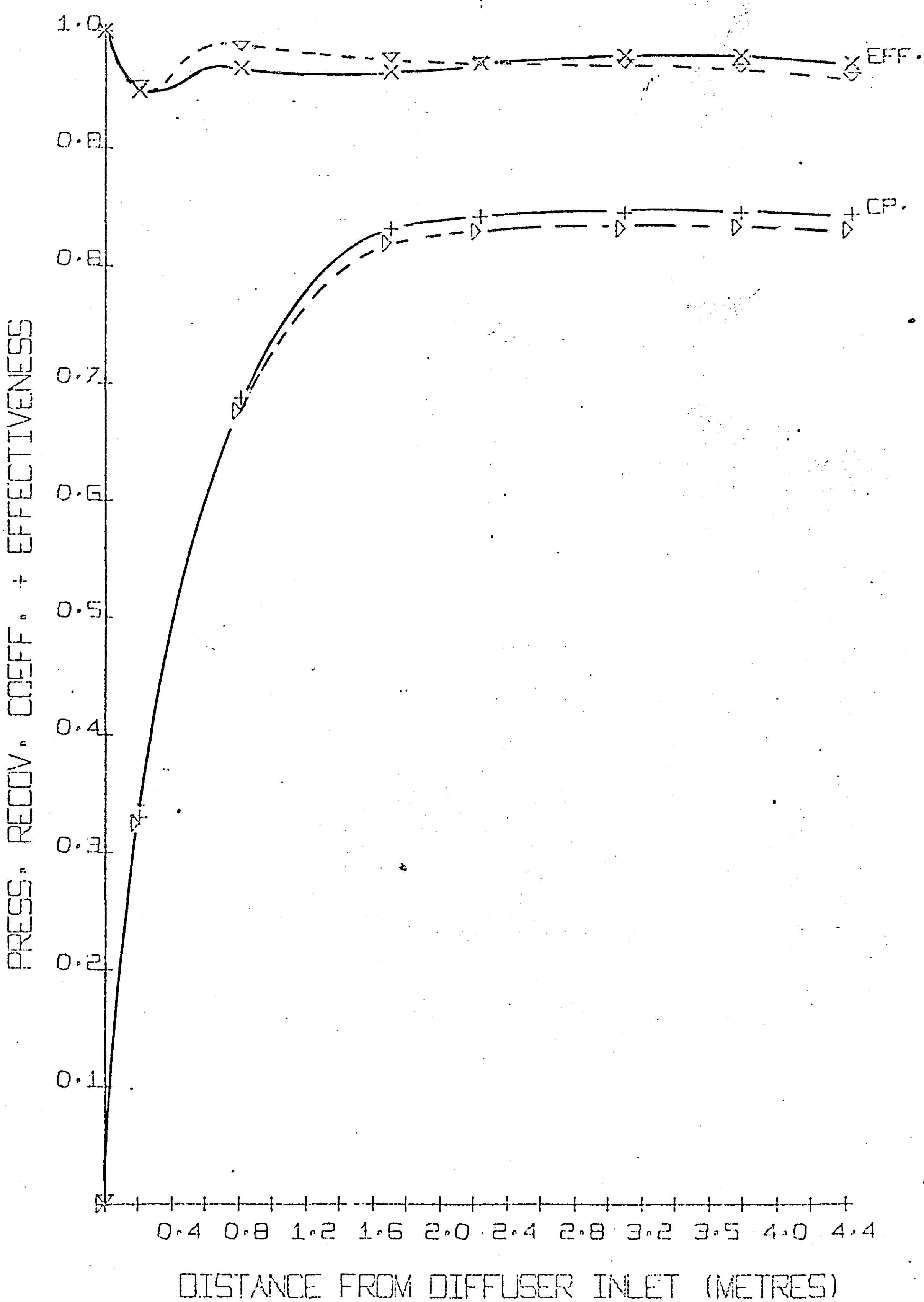

PRESS. RECOV. COEFF. + EFFECTIVENESS
1·0
0·9
0·8
0·7
0·6
0·5
0·4
0·3
0·2
0·1
0·4 0·8 1·2 1·6 2·0 2·4 2·8 3·2 3·5 4·0 4·4
DISTANCE FROM DIFFUSER INLET (METRES)
EFF.
CP.

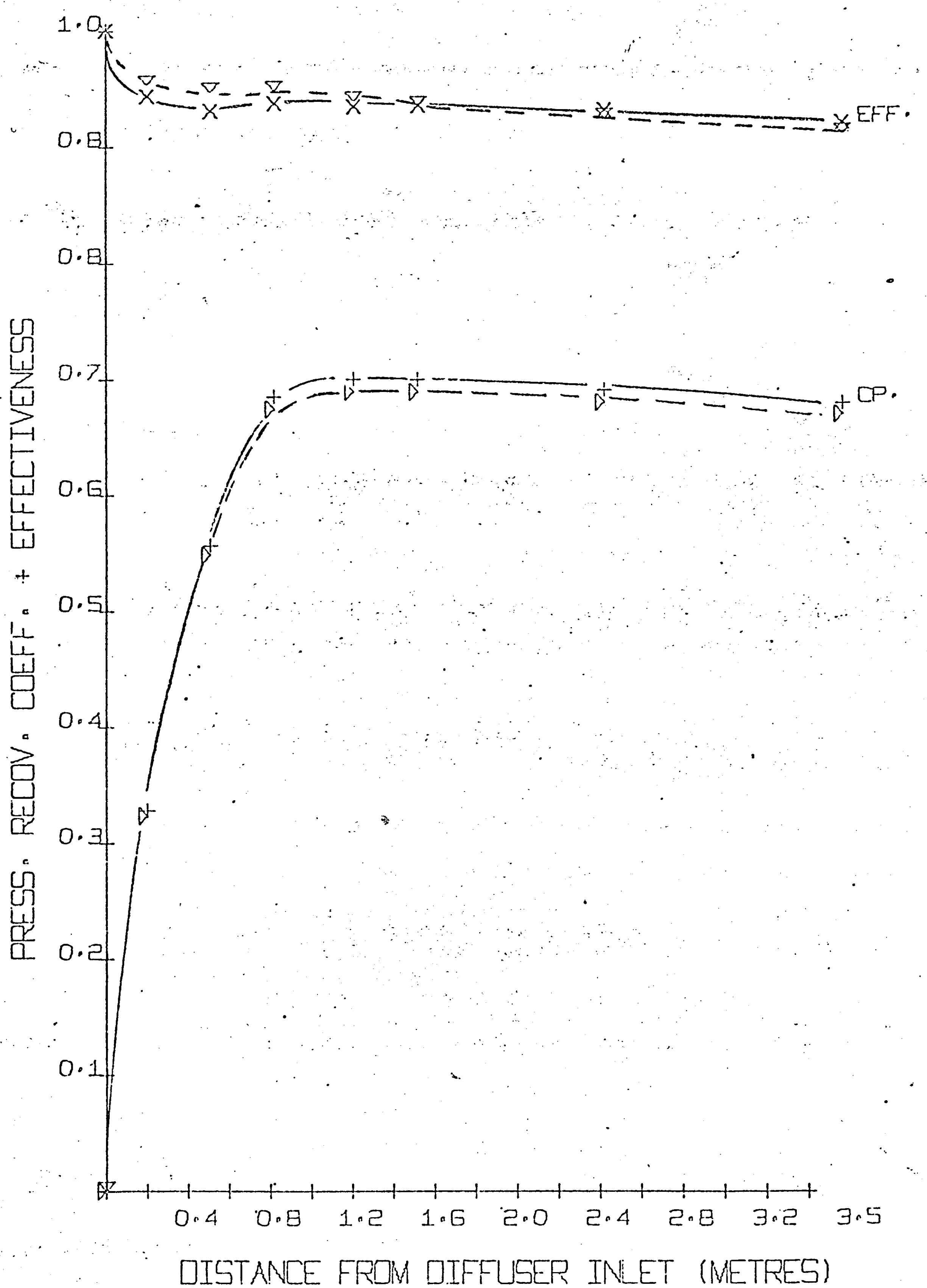

1·0
0·8
0·8
0·7
0·6
0·5
0·4
0·3
0·2
0·1
EFF.
CP.
0·4
0·8
1·2
1·6
2·0
2·4
2·8
3·2
3·5
PRESS. RECOV. COEFF. + EFFECTIVENESS
DISTANCE FROM DIFFUSER INLET (METRES)

RUN NO. 201

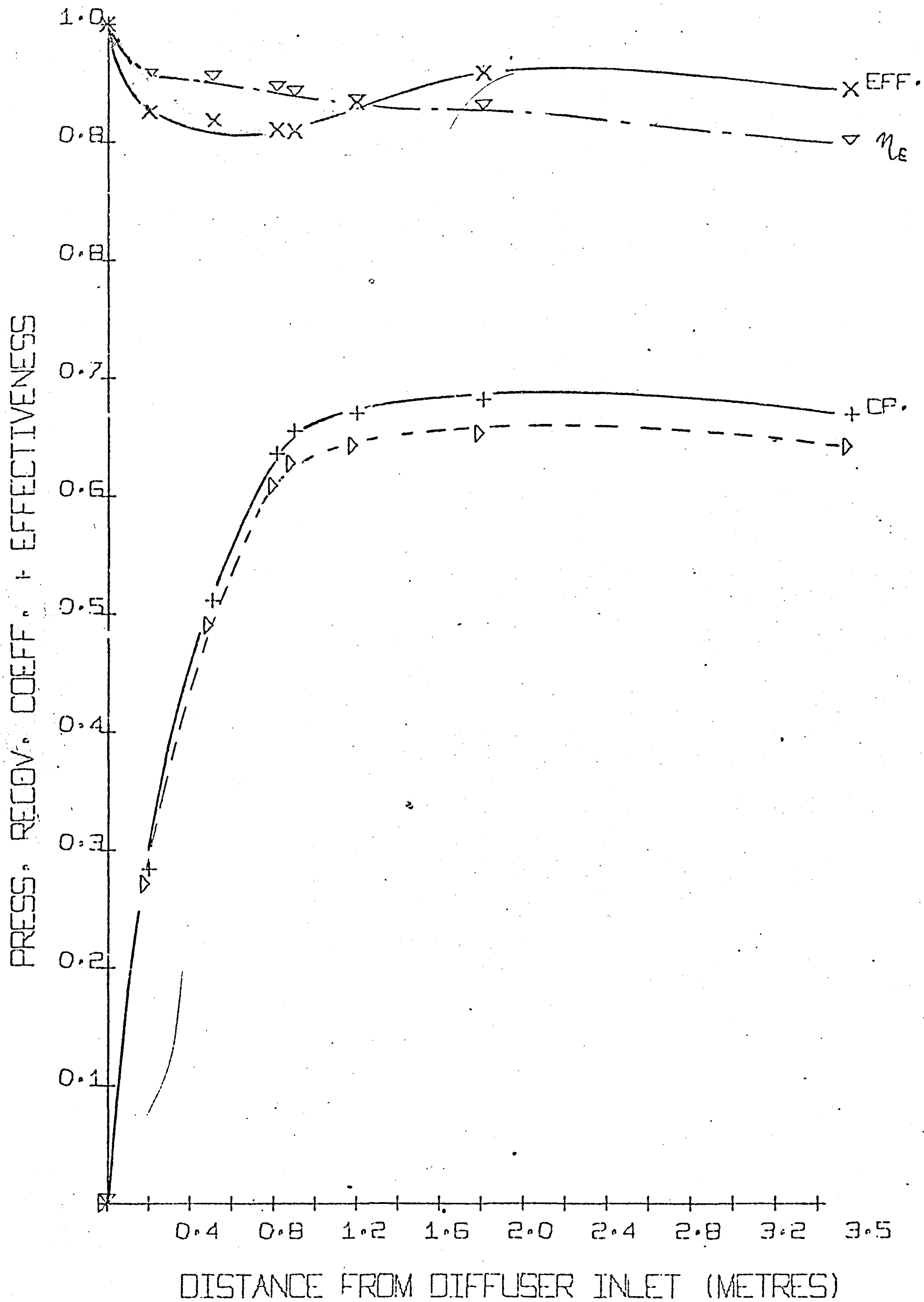

1.0
0.8
0.8
0.7
0.6
0.5
0.4
0.3
0.2
0.1
EFF.
η_E
CP.
PRESS. RECOV. COEFF. + EFFECTIVENESS
0.4
0.8
1.2
1.6
2.0
2.4
2.8
3.2
3.5
DISTANCE FROM DIFFUSER INLET (METRES)

RUN NO. 202

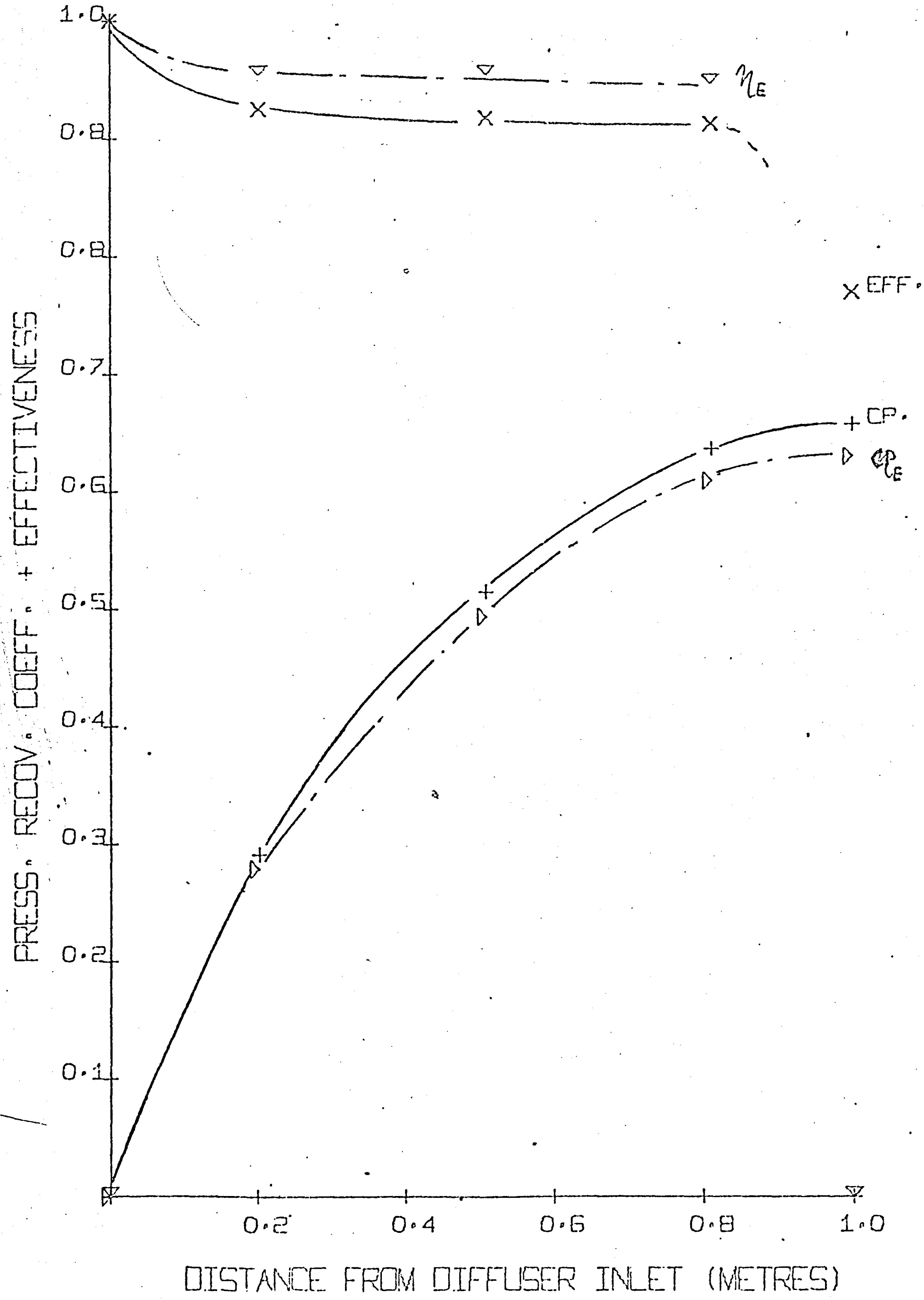
1.0
0.8
0.8
0.7
0.6
0.5
0.4
0.3
0.2
0.1
PRESS. RECOV. COEFF. + EFFECTIVENESS
η_E
EFF.
CP.
CP_E
0.2
0.4
0.6
0.8
1.0
DISTANCE FROM DIFFUSER INLET (METRES)

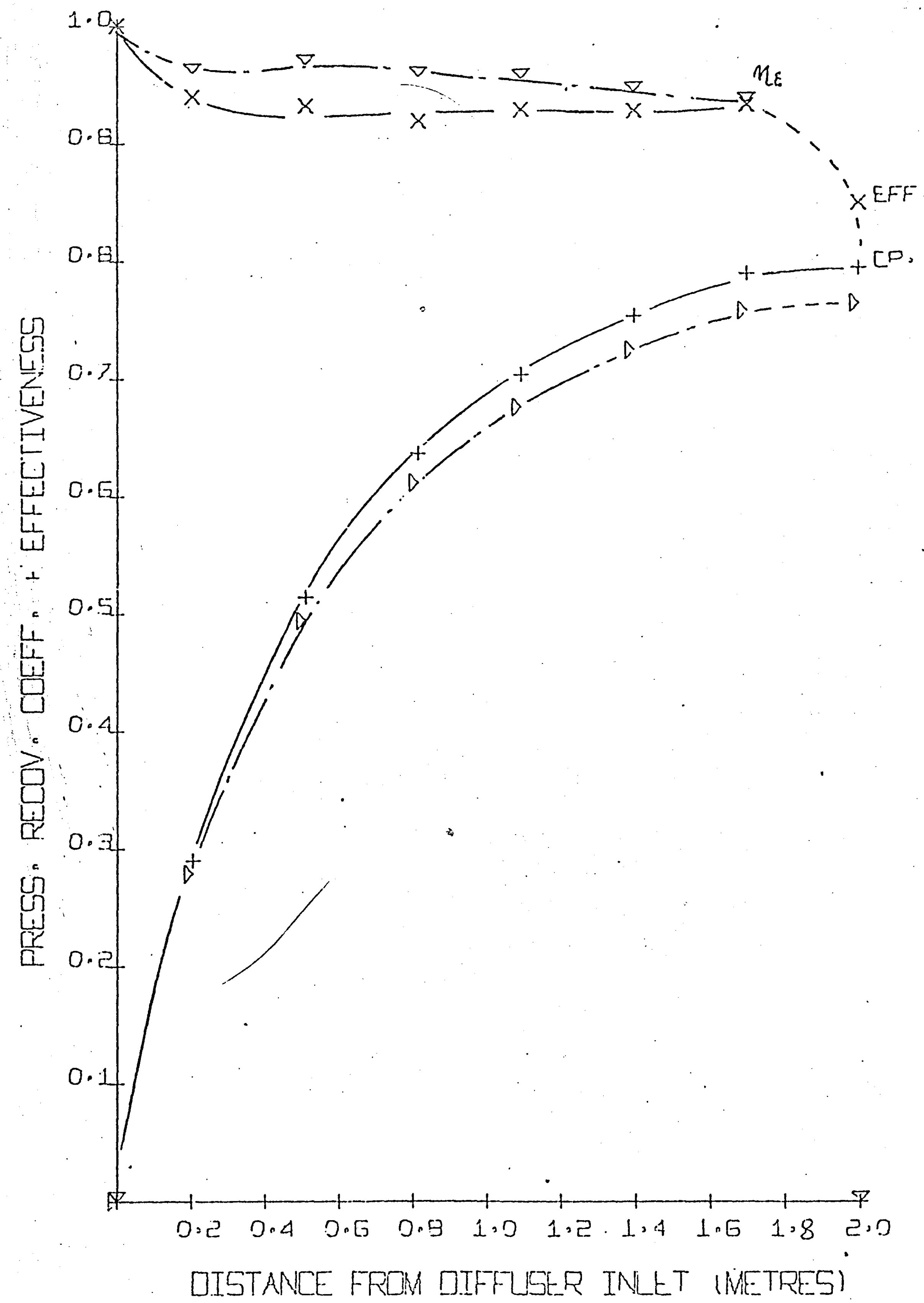
1·0
0·9
0·8
0·7
0·6
0·5
0·4
0·3
0·2
0·1
0·2
0·4
0·6
0·8
1·0
1·2
1·4
1·6
1·8
2·0
η_E
EFF.
CP.
PRESS. RECOV. COEFF. + EFFECTIVENESS
DISTANCE FROM DIFFUSER INLET (METRES)

RUN NO. 204

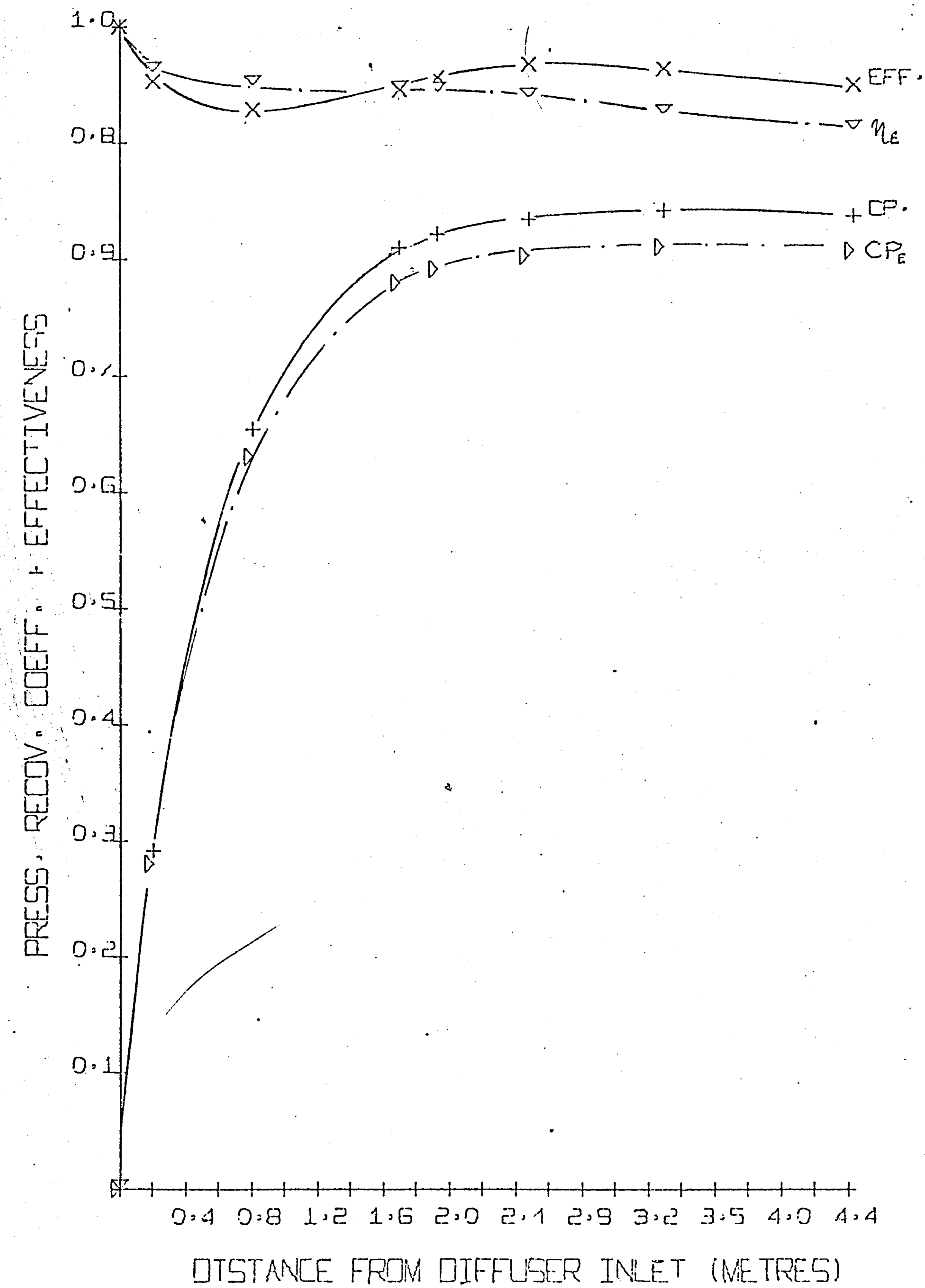

1.0
0.8
0.9
0.7
0.6
0.5
0.4
0.3
0.2
0.1
EFF.
η_E
CP.
CP_E
PRESS. RECOV. COEFF. + EFFECTIVENESS
0.4 0.8 1.2 1.6 2.0 2.1 2.9 3.2 3.5 4.0 4.4
DISTANCE FROM DIFFUSER INLET (METRES)

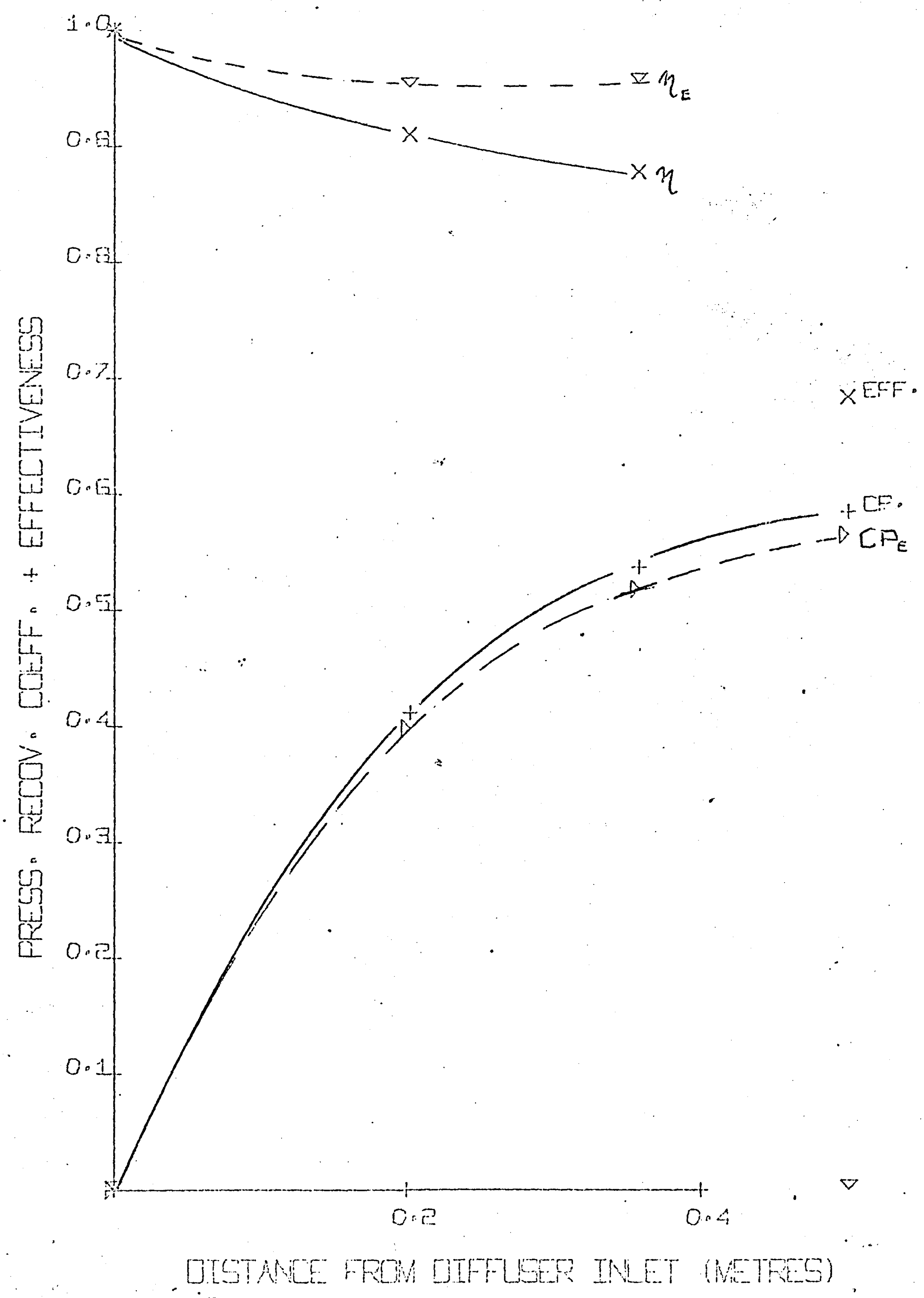
1·0
0·9
0·8
0·7
0·6
0·5
0·4
0·3
0·2
0·1
0·2
0·4
PRESS. RECOV. COEFF. + EFFECTIVENESS
DISTANCE FROM DIFFUSER INLET (METRES)
η_E
η
EFF.
CP.
CP_E

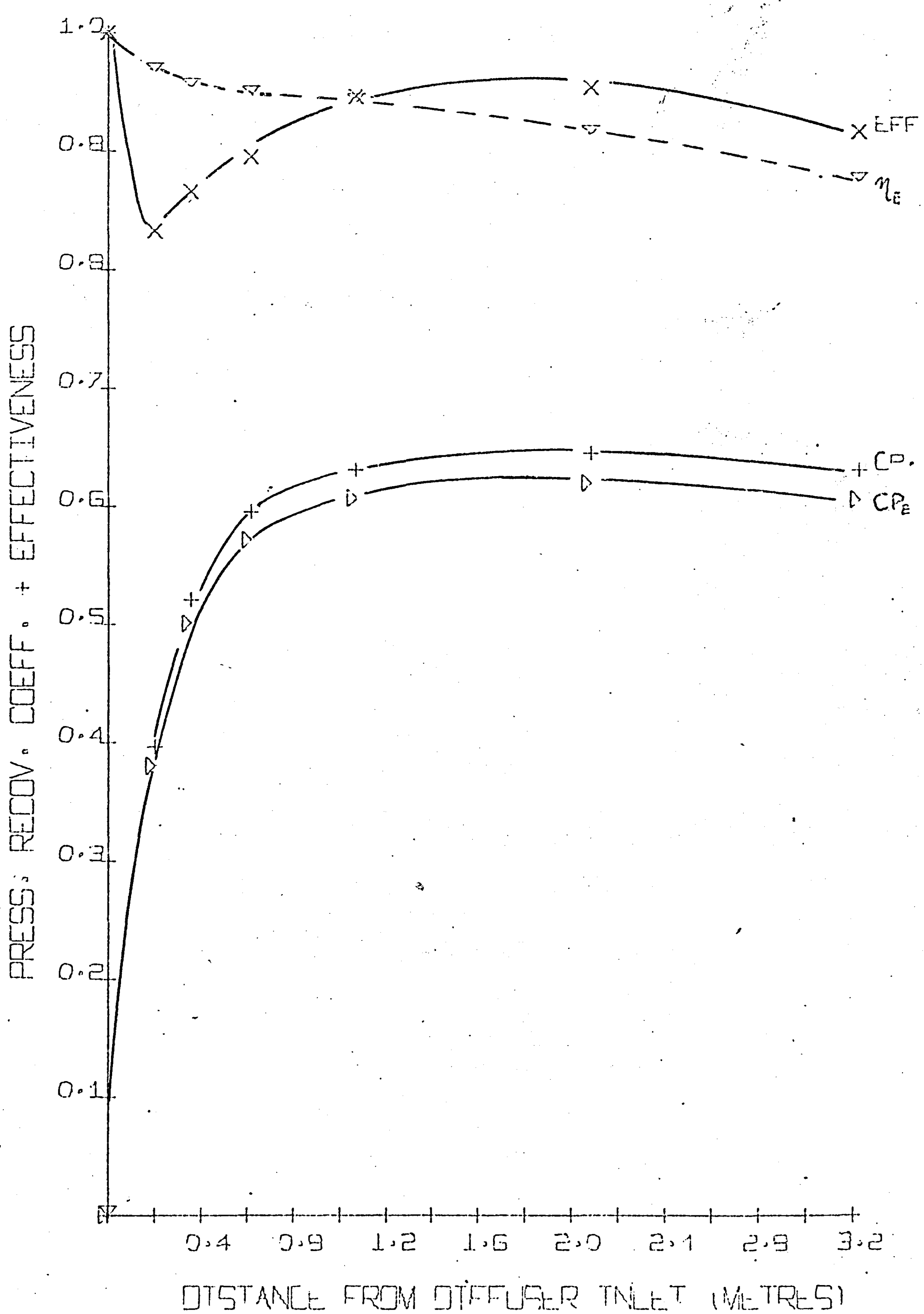

1·0
0·9
0·8
0·7
0·6
0·5
0·4
0·3
0·2
0·1
EFF
η_E
CP.
CP_E
PRESS. RECOV. COEFF. + EFFECTIVENESS
0·4
0·8
1·2
1·6
2·0
2·4
2·8
3·2
DISTANCE FROM DIFFUSER INLET (METRES)

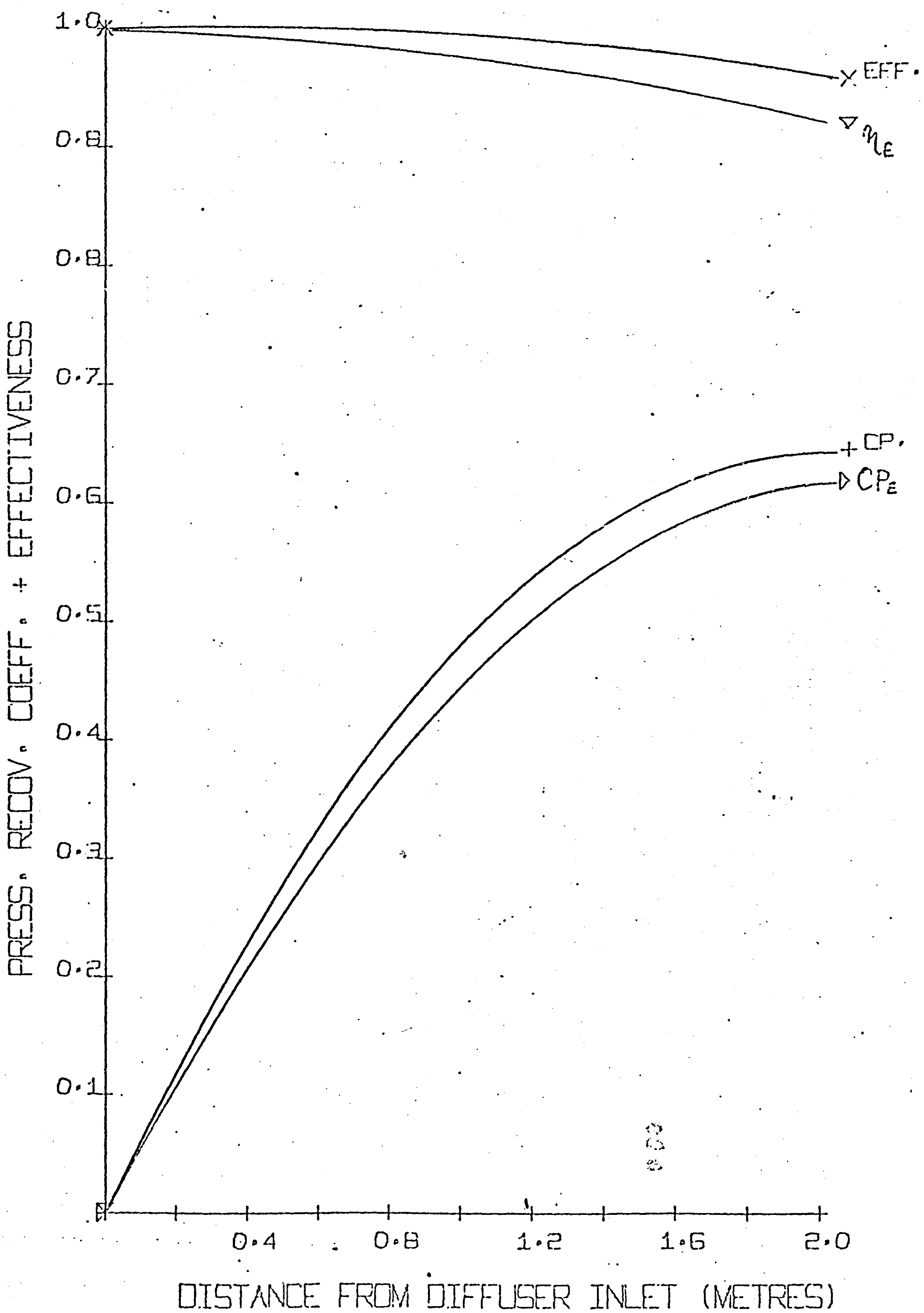
PRESS. RECOV. COEFF. + EFFECTIVENESS
1.0
0.8
0.8
0.7
0.6
0.5
0.4
0.3
0.2
0.1
0.4
0.8
1.2
1.6
2.0
DISTANCE FROM DIFFUSER INLET (METRES)
EFF.
η_E
CP.
CP_E

RUN NO. 208

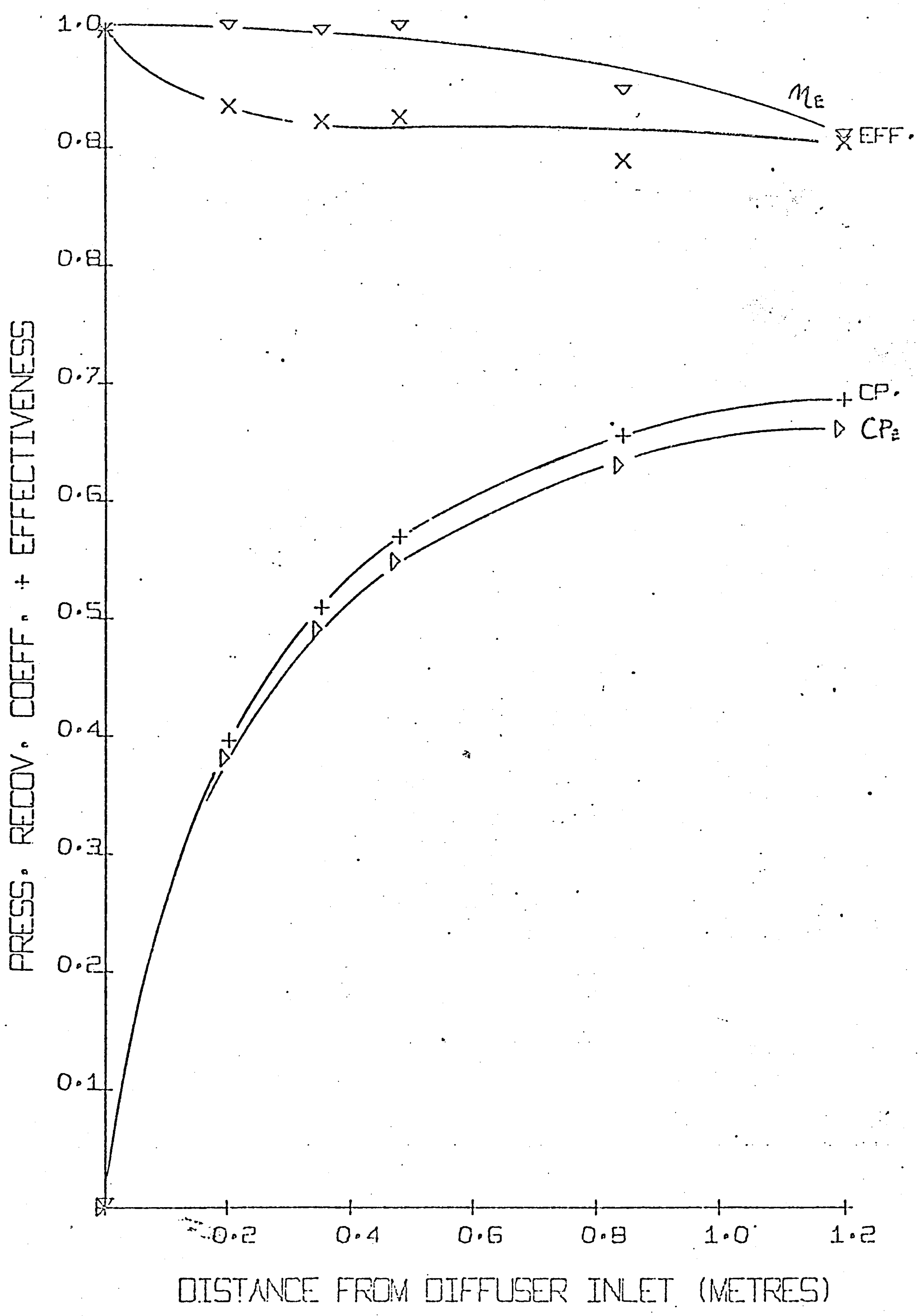

1.0
0.8
0.8
0.7
0.6
0.5
0.4
0.3
0.2
0.1
0.2
0.4
0.6
0.8
1.0
1.2
η_E
EFF.
CP.
CP_E
PRESS. RECOV. COEFF. + EFFECTIVENESS
DISTANCE FROM DIFFUSER INLET (METRES)

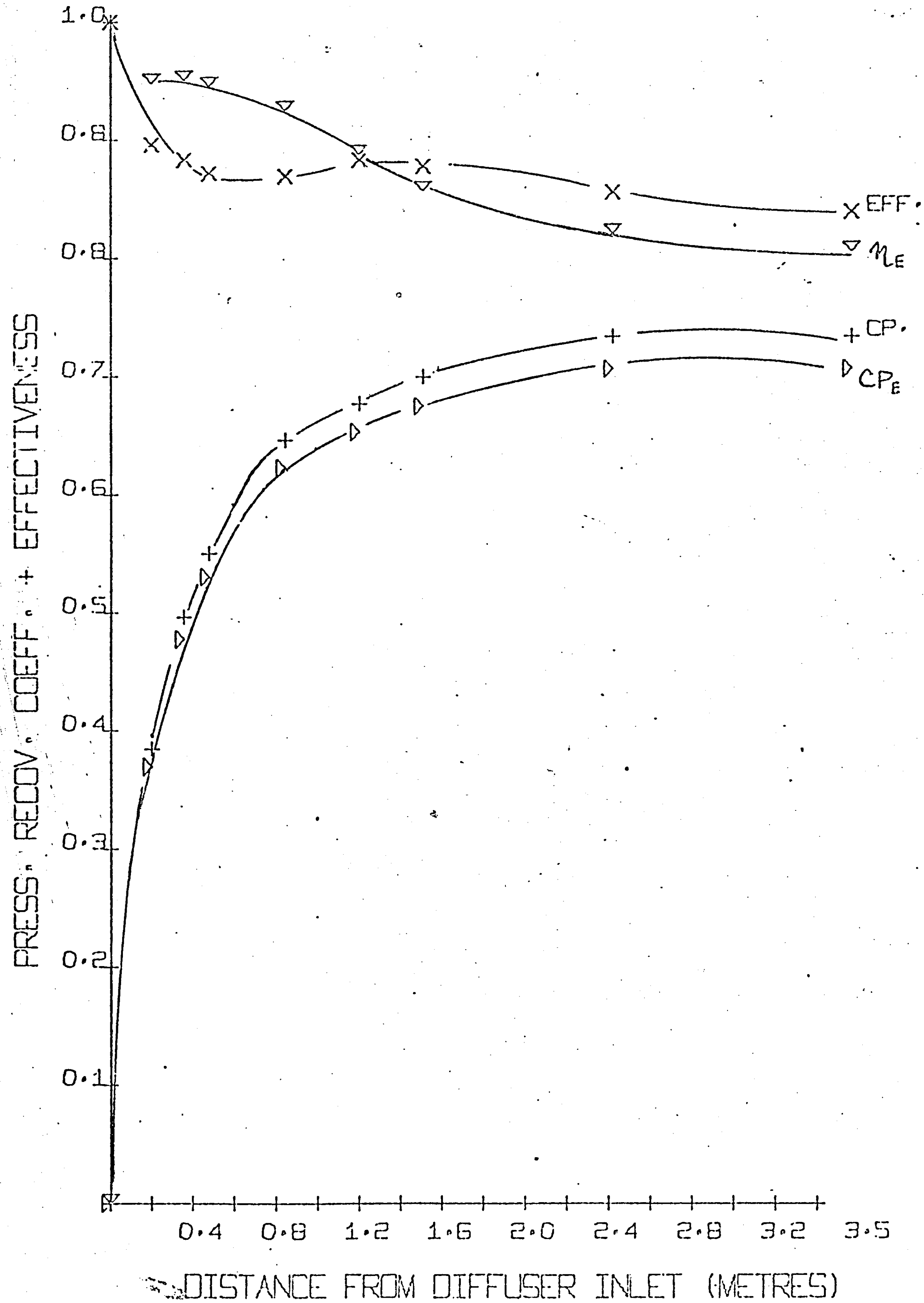

PRESS. RECOV. COEFF. + EFFECTIVENESS
1.0
0.9
0.8
0.7
0.6
0.5
0.4
0.3
0.2
0.1
0.4
0.8
1.2
1.6
2.0
2.4
2.8
3.2
3.5
DISTANCE FROM DIFFUSER INLET (METRES)
EFF.
η_E
CP.
CP_E

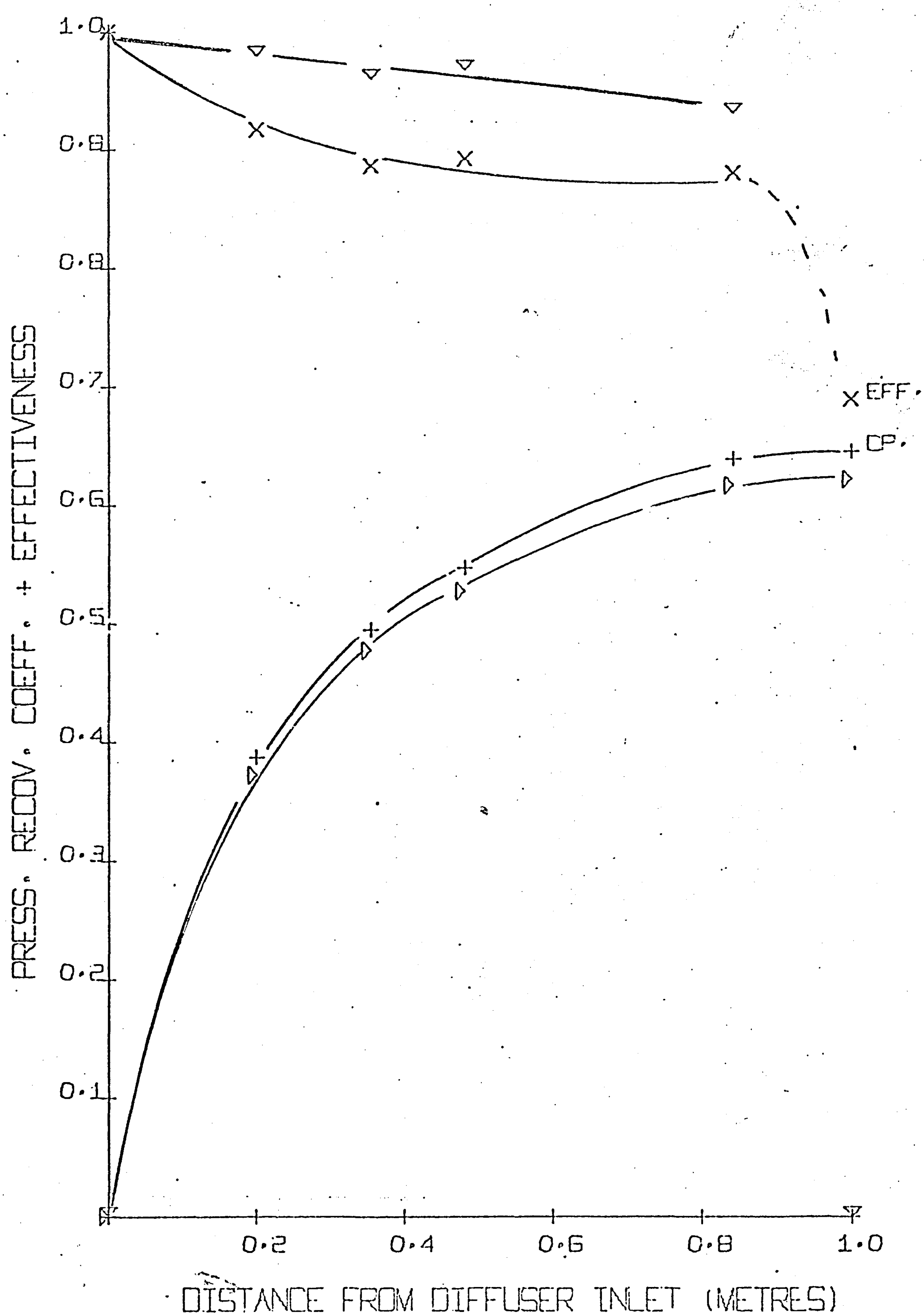

PRESS. RECOV. COEFF. + EFFECTIVENESS
1·0
0·8
0·8
0·7
0·6
0·5
0·4
0·3
0·2
0·1
EFF.
CP.
0·2
0·4
0·6
0·8
1·0
DISTANCE FROM DIFFUSER INLET (METRES)

RUN NO. 212

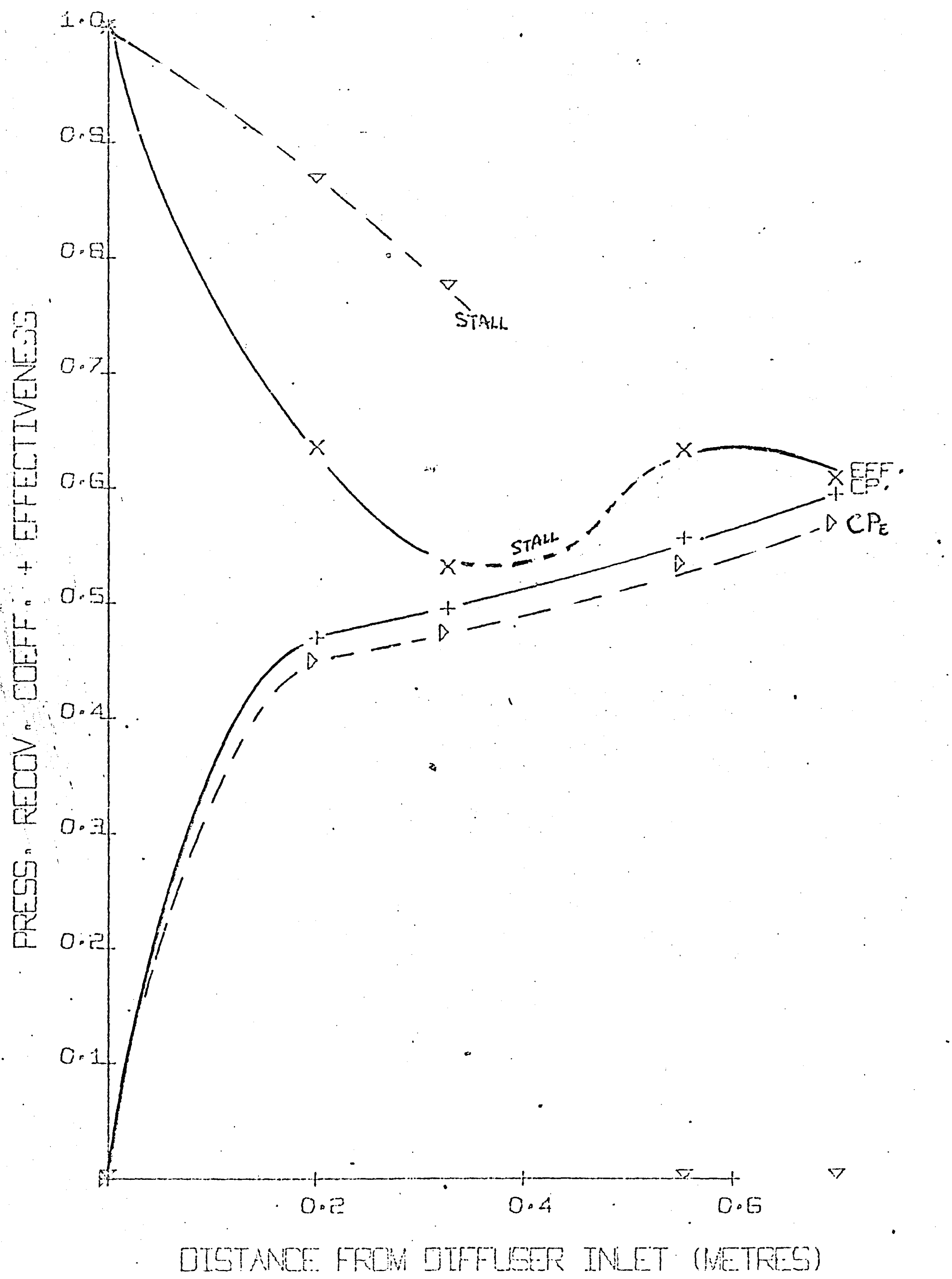

1.0
0.9
0.8
0.7
0.6
0.5
0.4
0.3
0.2
0.1
0.2
0.4
0.6
STALL
STALL
EFF.
CP.
CPE
PRESS. RECOV. COEFF. + EFFECTIVENESS
DISTANCE FROM DIFFUSER INLET (METRES)

RUN NO. 213

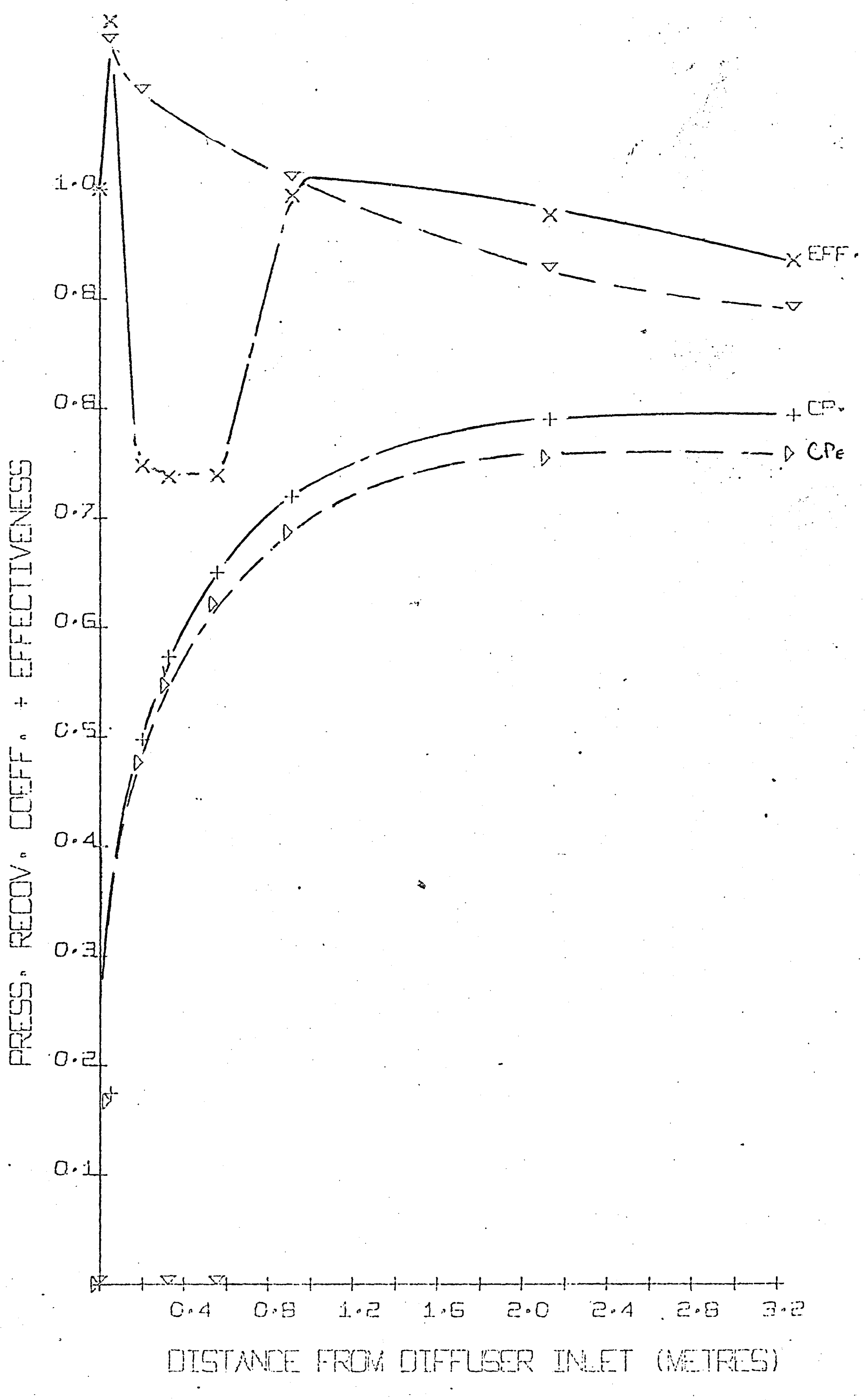

1.0
0.9
0.8
0.7
0.6
0.5
0.4
0.3
0.2
0.1
0.4
0.8
1.2
1.6
2.0
2.4
2.8
3.2
EFF.
CP.
CPE
PRESS. RECOV. COEFF. + EFFECTIVENESS
DISTANCE FROM DIFFUSER INLET (METRES)

RUN NO. 214

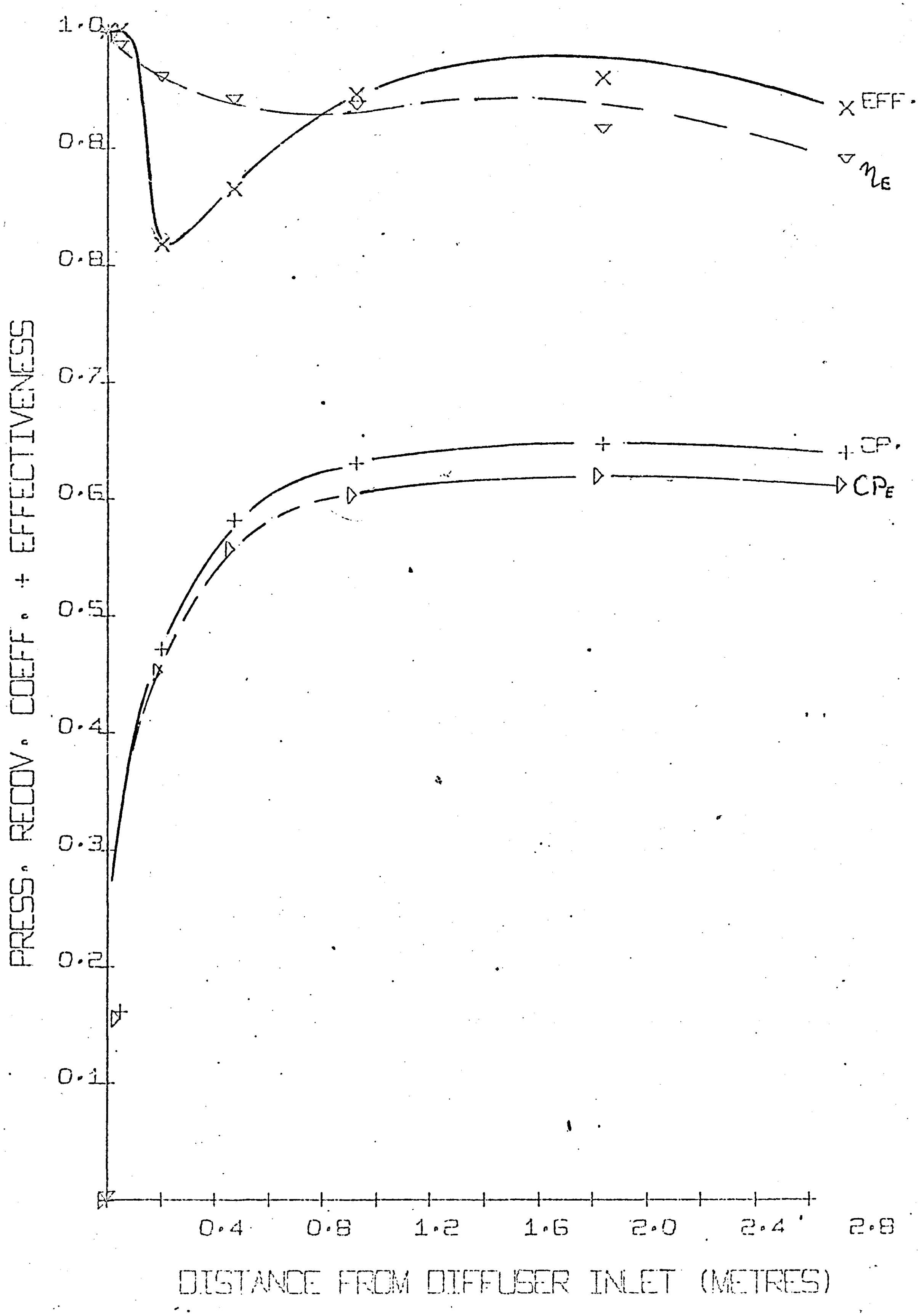

1.0
0.8
0.8
0.7
0.6
0.5
0.4
0.3
0.2
0.1
EFF.
η_E
CP.
CP_E
0.4
0.8
1.2
1.6
2.0
2.4
2.8
PRESS. RECOV. COEFF. + EFFECTIVENESS
DISTANCE FROM DIFFUSER INLET (METRES)

RUN NO. 301

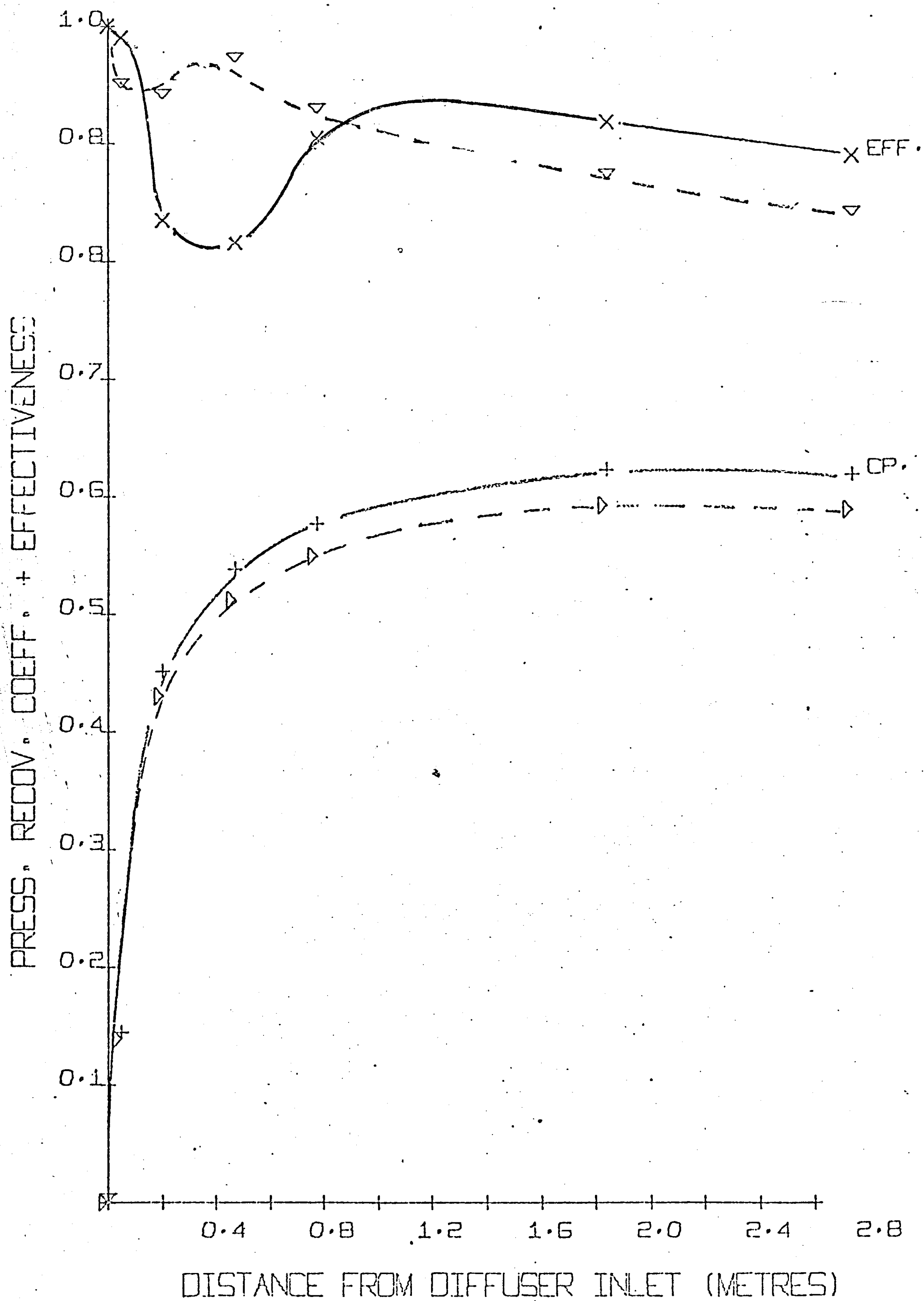

1·0
0·8
0·8
0·7
0·6
0·5
0·4
0·3
0·2
0·1
EFF.
CP.
0·4
0·8
1·2
1·6
2·0
2·4
2·8
PRESS. RECOV. COEFF. + EFFECTIVENESS
DISTANCE FROM DIFFUSER INLET (METRES)

RUN NO. 302

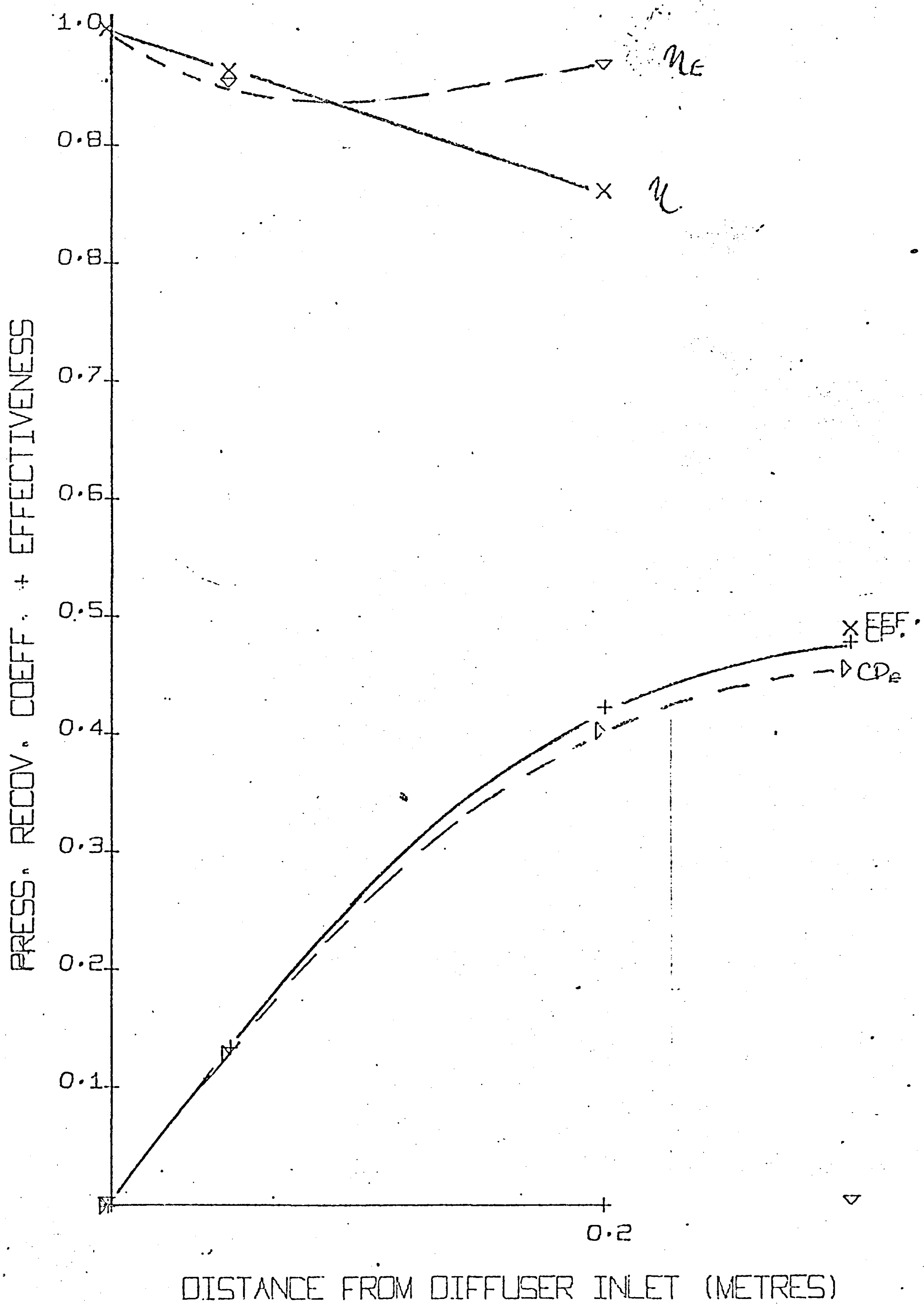

1.0
0.8
0.8
0.7
0.6
0.5
0.4
0.3
0.2
0.1
0.2
η_E
η
EFF.
CP.
CP_E
PRESS. RECOV. COEFF. + EFFECTIVENESS
DISTANCE FROM DIFFUSER INLET (METRES)

RUN NO. 303

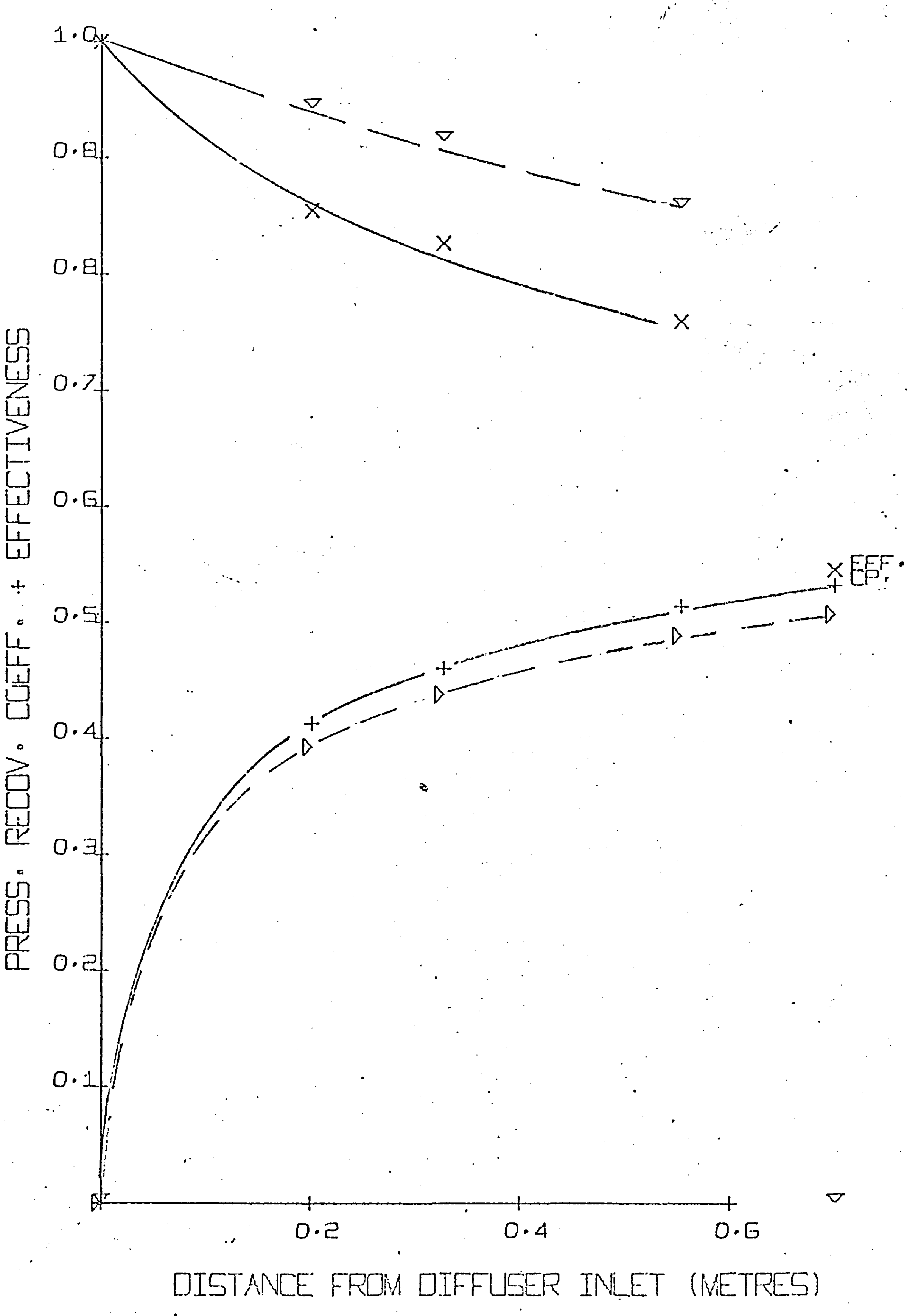
1.0
0.9
0.8
0.7
0.6
0.5
0.4
0.3
0.2
0.1
0.2
0.4
0.6
EFF.
CP.
PRESS. RECOV. COEFF. + EFFECTIVENESS
DISTANCE FROM DIFFUSER INLET (METRES)

RUN NO. 304

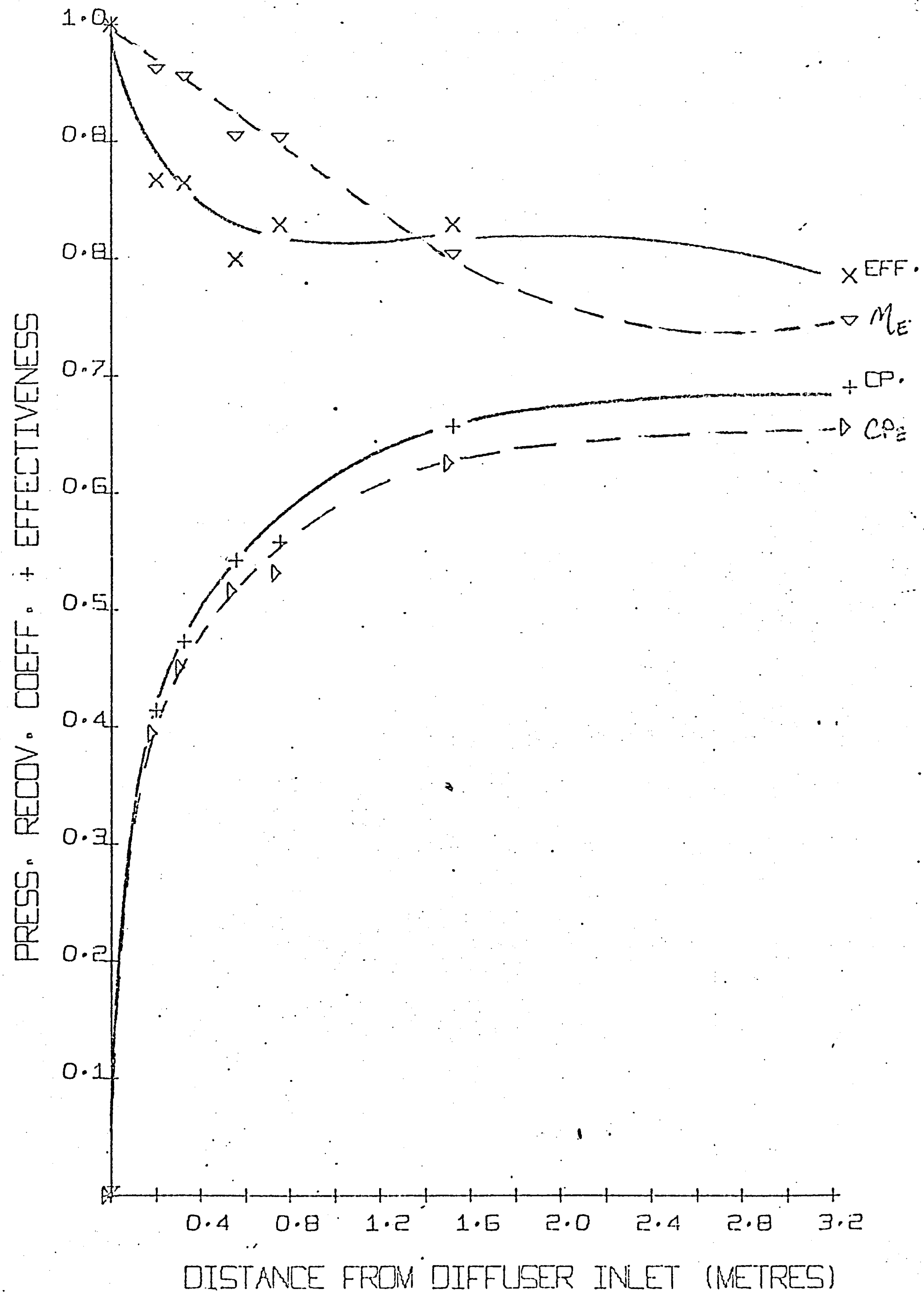
1.0
0.9
0.8
0.7
0.6
0.5
0.4
0.3
0.2
0.1
0.4
0.8
1.2
1.6
2.0
2.4
2.8
3.2
EFF.
M_E
CP.
CP_E
PRESS. RECOV. COEFF. + EFFECTIVENESS
DISTANCE FROM DIFFUSER INLET (METRES)

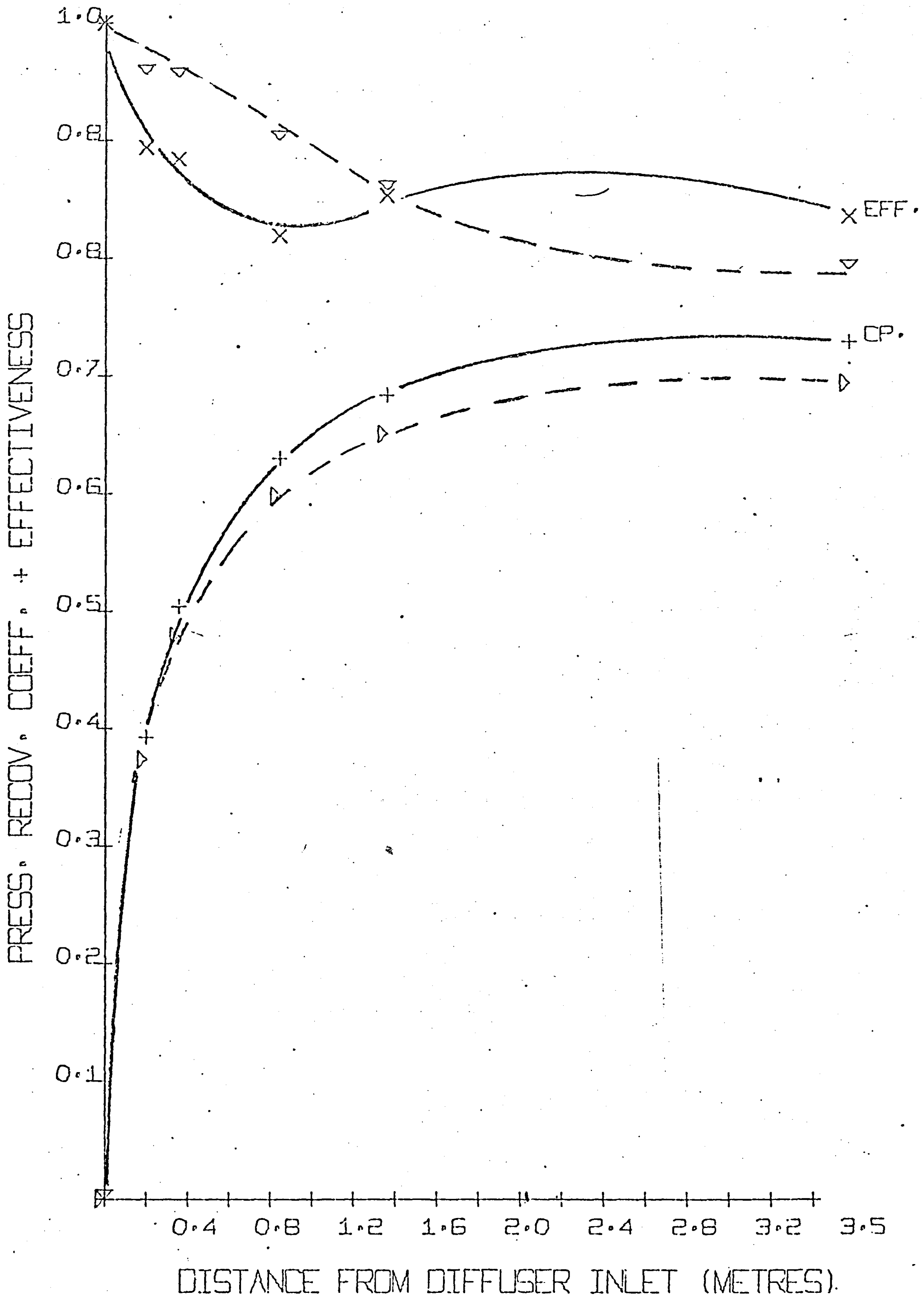
1·0
0·8
0·8
0·7
0·6
0·5
0·4
0·3
0·2
0·1
PRESS. RECOV. COEFF. + EFFECTIVENESS
EFF.
CP.
0·4
0·8
1·2
1·6
2·0
2·4
2·8
3·2
3·5
DISTANCE FROM DIFFUSER INLET (METRES).

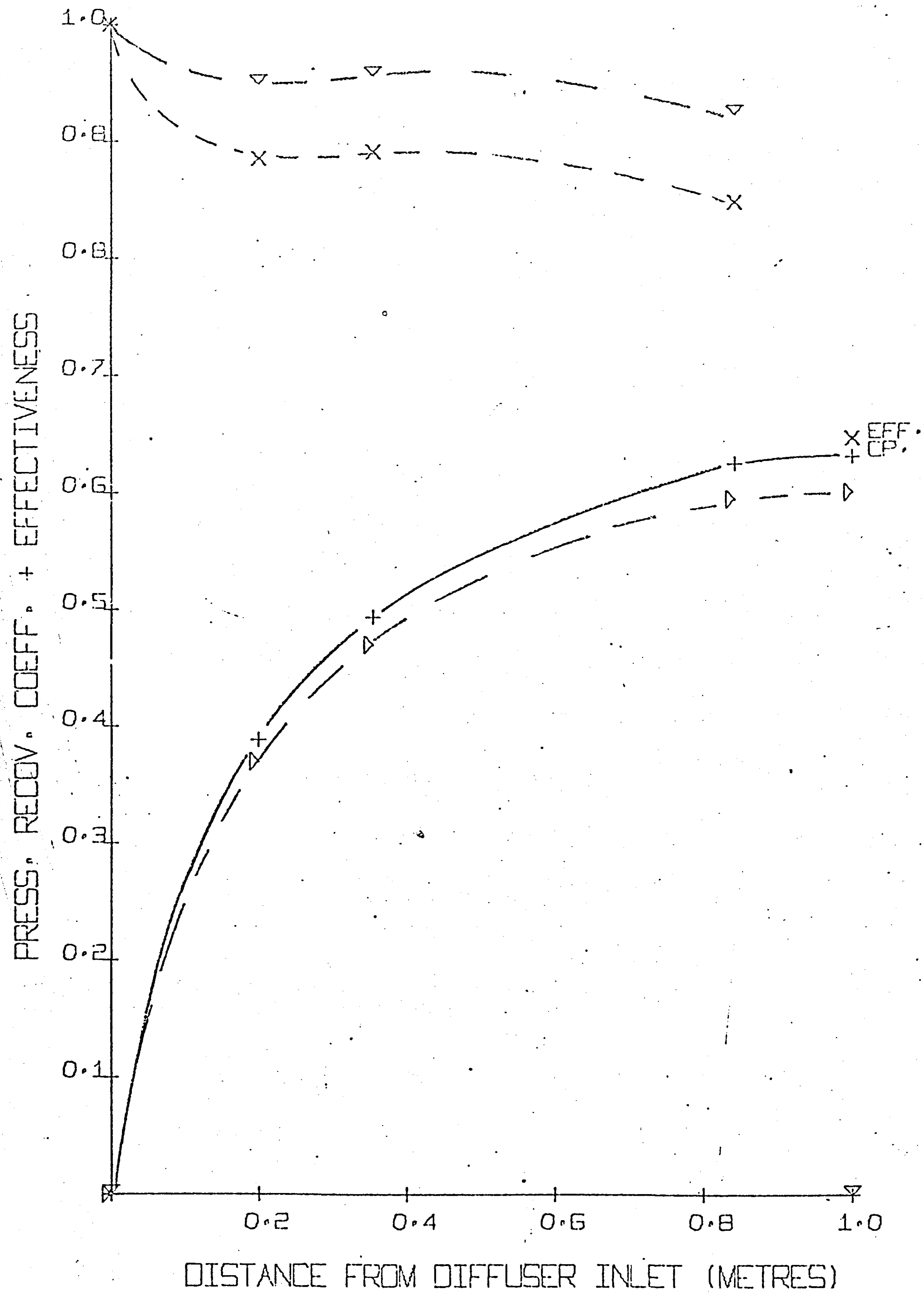

PRESS. RECOV. COEFF. + EFFECTIVENESS
DISTANCE FROM DIFFUSER INLET (METRES)
EFF.
CP.
1.0
0.9
0.8
0.7
0.6
0.5
0.4
0.3
0.2
0.1
0.2
0.4
0.6
0.8
1.0

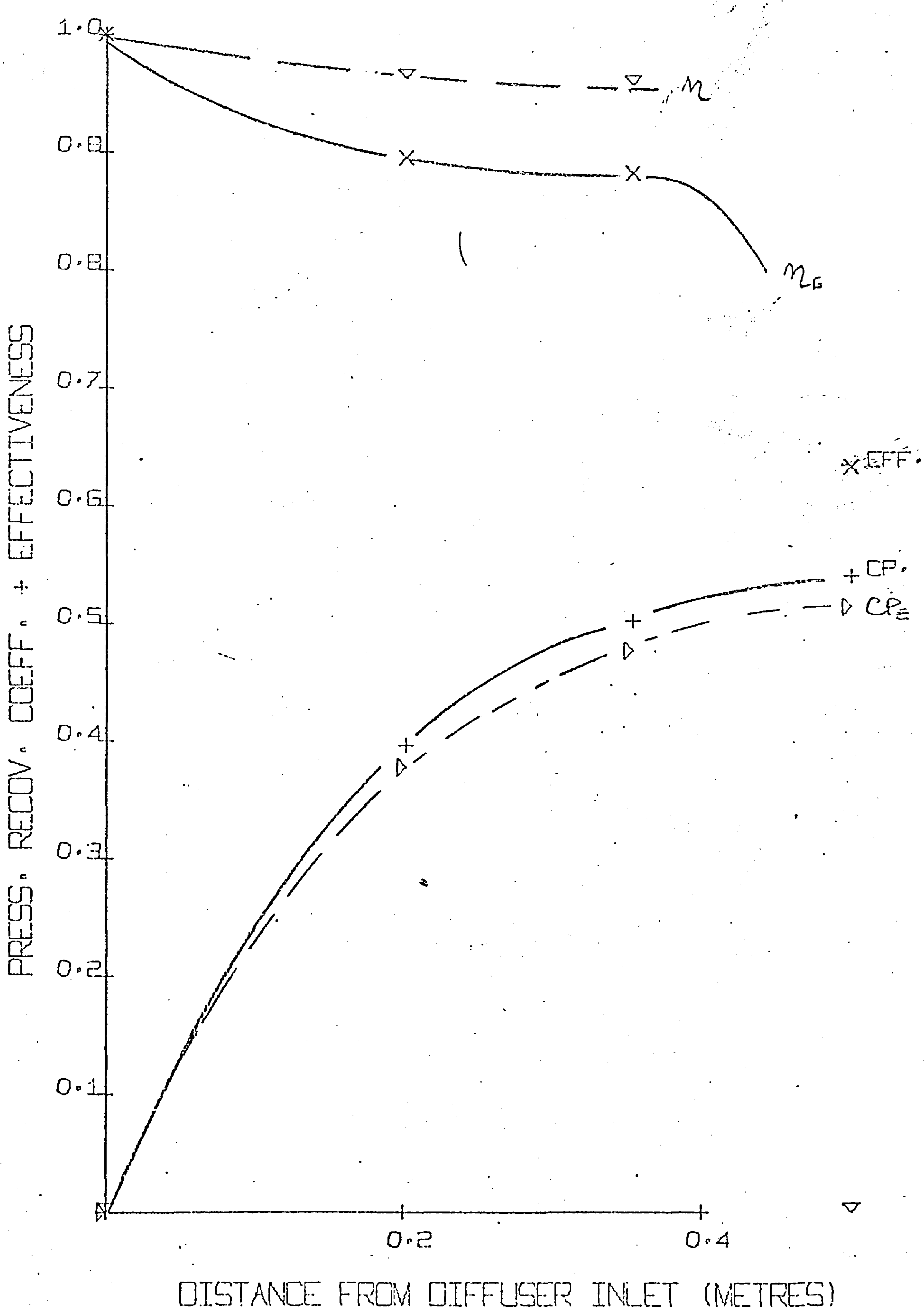

1·0
0·8
0·8
0·7
0·6
0·5
0·4
0·3
0·2
0·1
0·2
0·4
PRESS. RECOV. COEFF. + EFFECTIVENESS
DISTANCE FROM DIFFUSER INLET (METRES)
η
η_E
EFF.
CP.
CP_E

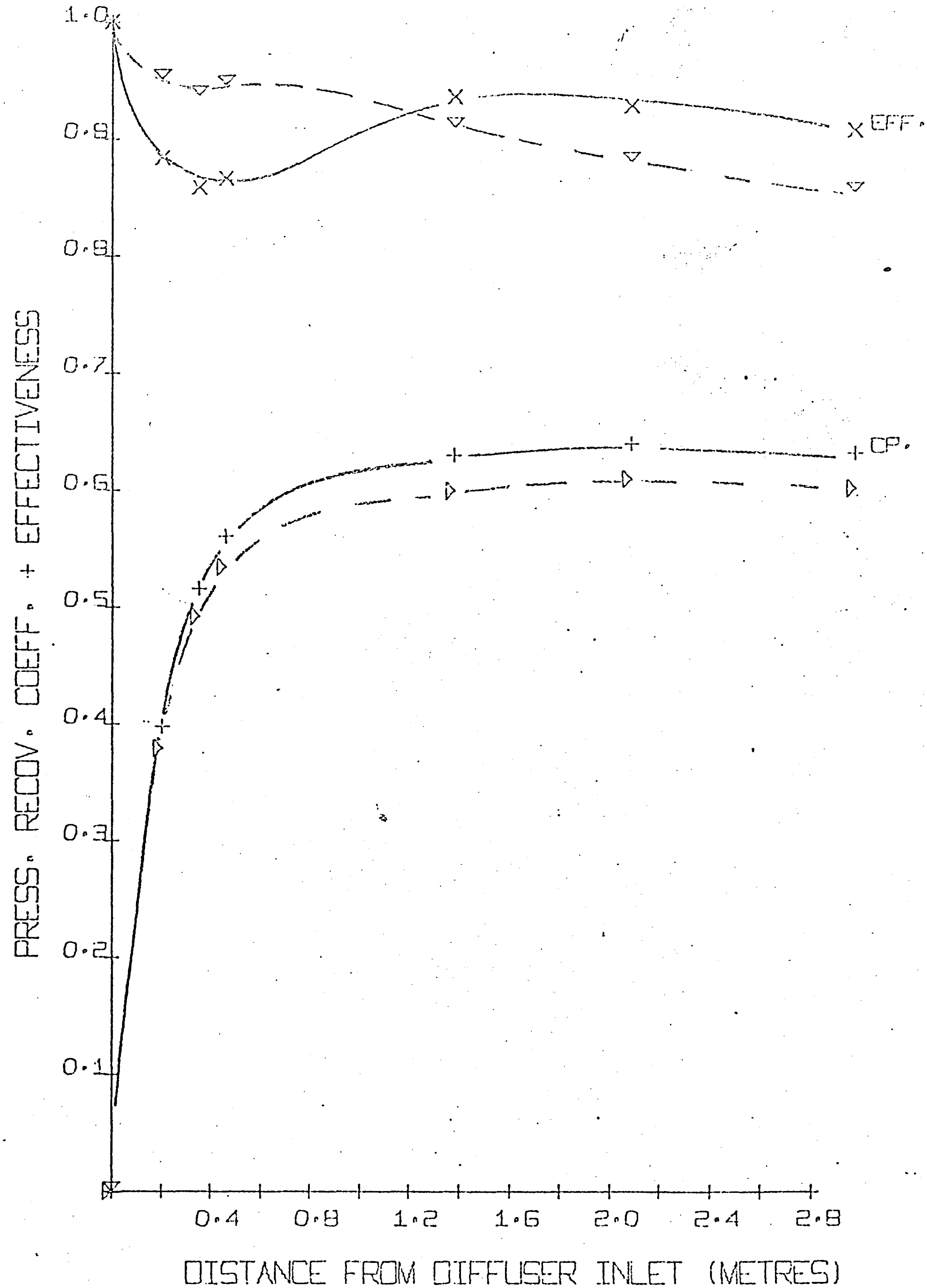

1·0
0·9
0·8
0·7
0·6
0·5
0·4
0·3
0·2
0·1
EFF.
CP.
PRESS. RECOV. COEFF. + EFFECTIVENESS
0·4
0·8
1·2
1·6
2·0
2·4
2·8
DISTANCE FROM DIFFUSER INLET (METRES)

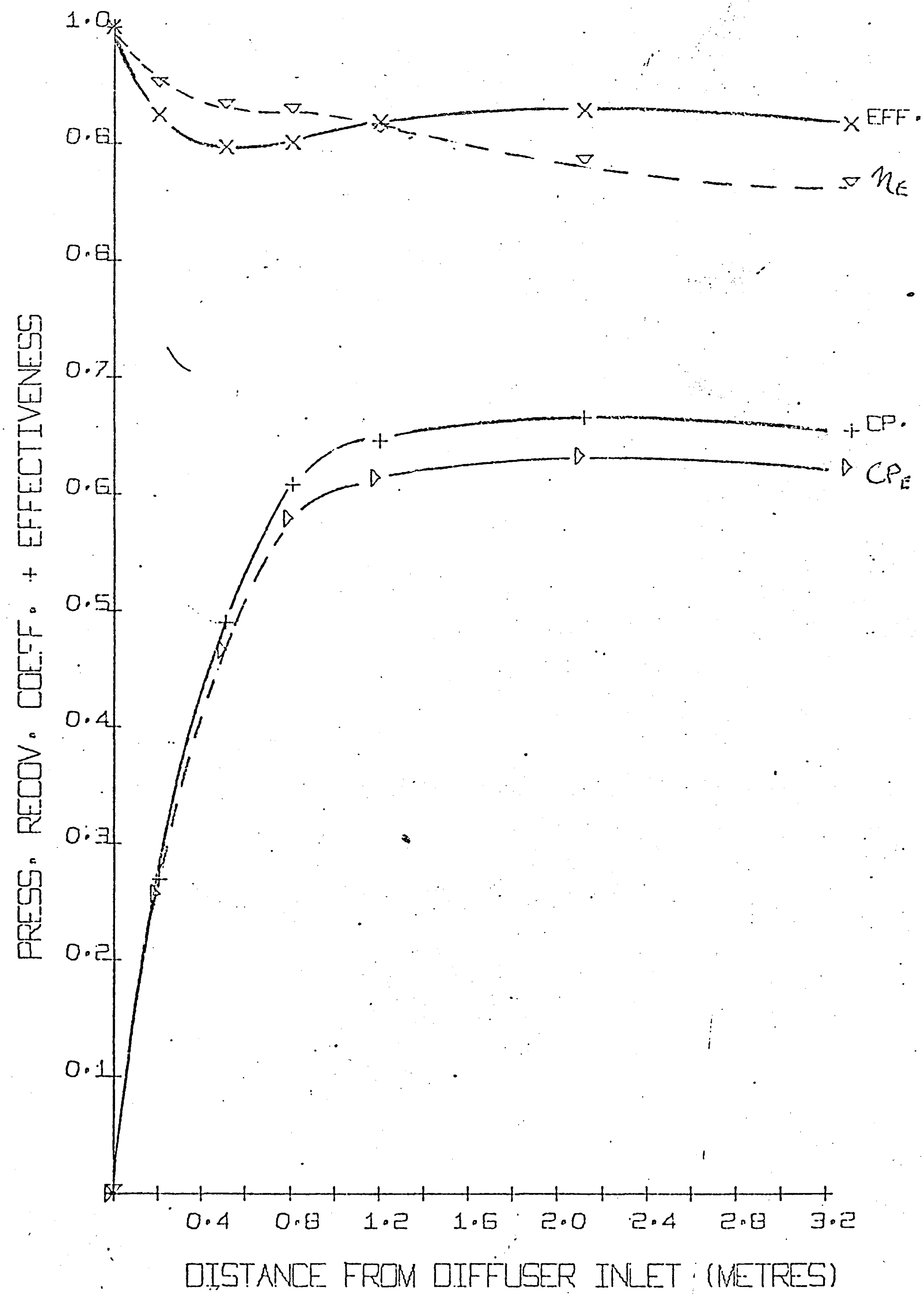

1·0
0·9
0·8
0·7
0·6
0·5
0·4
0·3
0·2
0·1
PRESS. RECOV. COEFF. + EFFECTIVENESS
EFF.
η_E
CP.
CP_E
0·4
0·8
1·2
1·6
2·0
2·4
2·8
3·2
DISTANCE FROM DIFFUSER INLET (METRES)

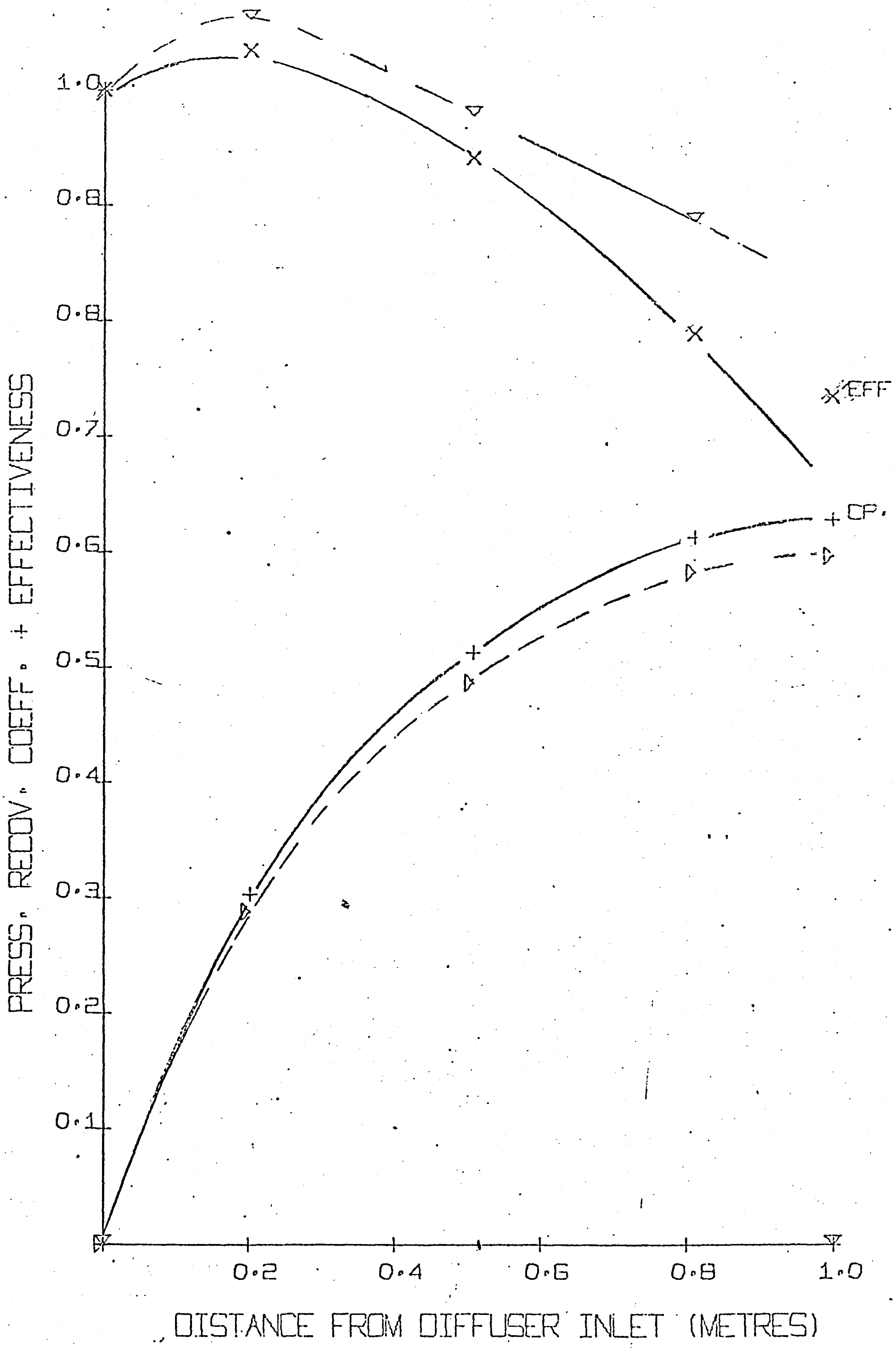
PRESS. RECOV. COEFF. + EFFECTIVENESS
1·0
0·8
0·8
0·7
0·6
0·5
0·4
0·3
0·2
0·1
0·2
0·4
0·6
0·8
1·0
EFF
CP.
DISTANCE FROM DIFFUSER INLET (METRES)

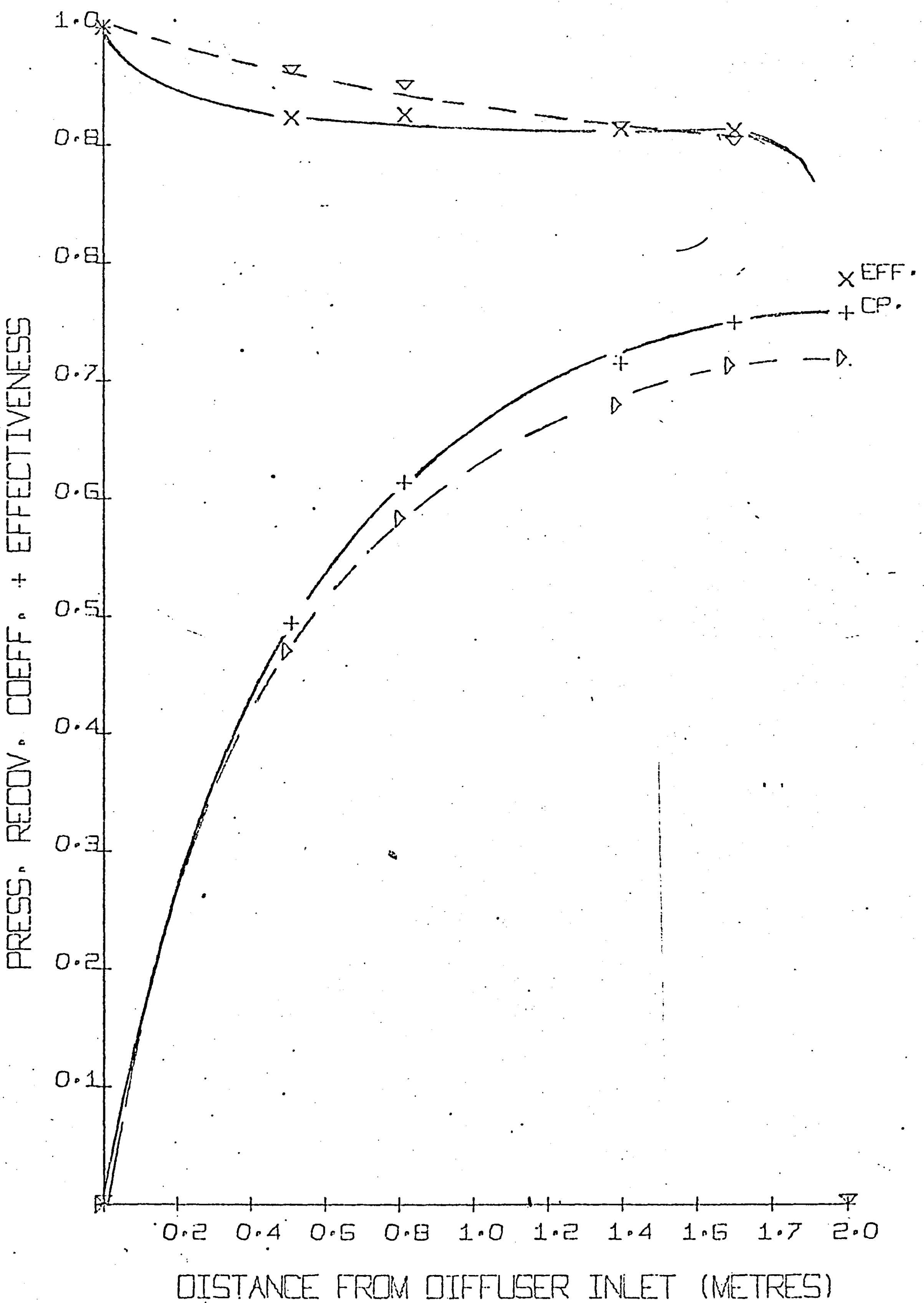
PRESS. RECOV. COEFF. + EFFECTIVENESS
1·0
0·8
0·8
0·7
0·6
0·5
0·4
0·3
0·2
0·1
0·2
0·4
0·6
0·8
1·0
1·2
1·4
1·6
1·7
2·0
DISTANCE FROM DIFFUSER INLET (METRES)
EFF.
CP.

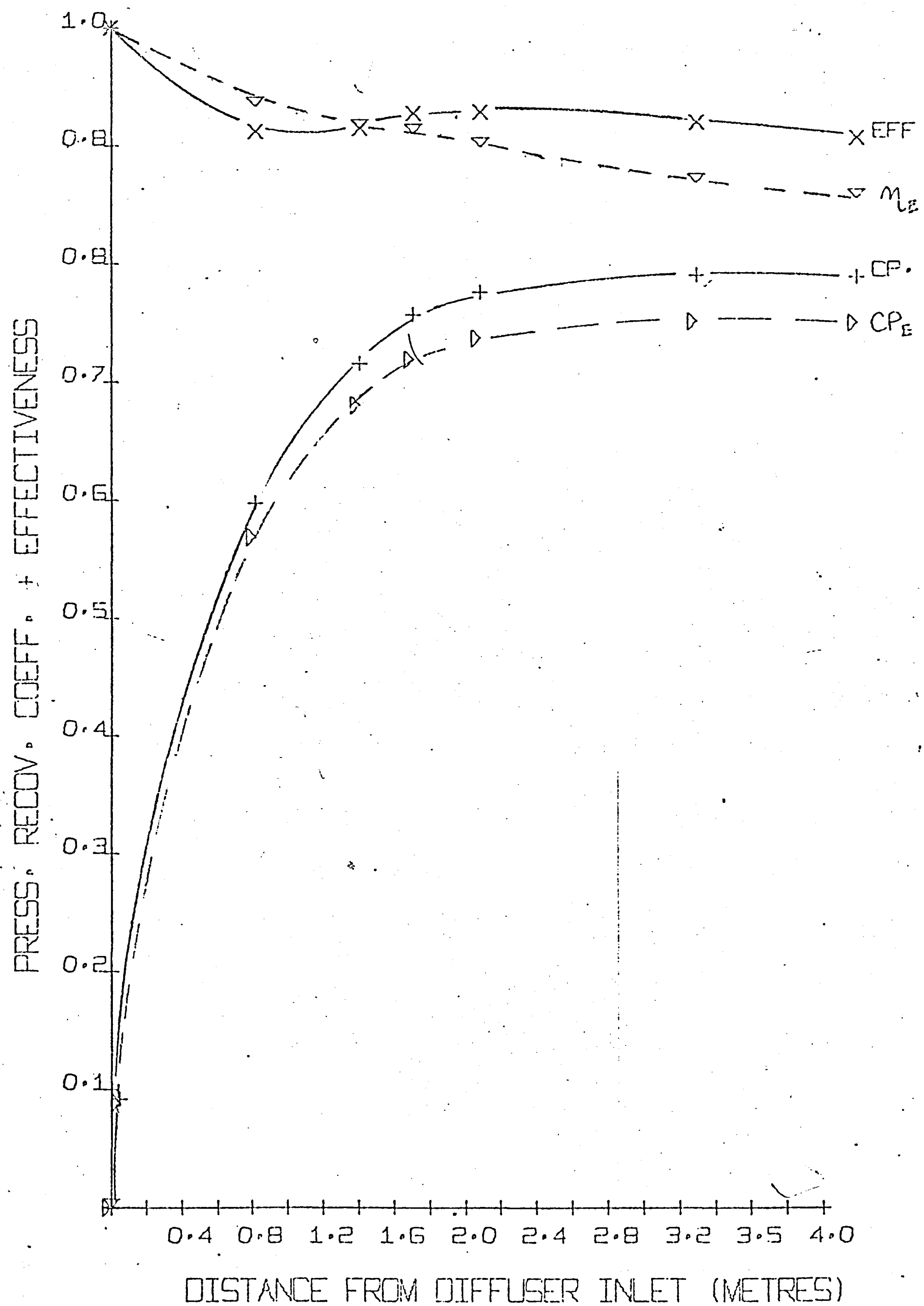

1·0
0·8
0·8
0·7
0·6
0·5
0·4
0·3
0·2
0·1
EFF
η_{LE}
CP·
CP_E
PRESS. RECOV. COEFF. + EFFECTIVENESS
0·4 0·8 1·2 1·6 2·0 2·4 2·8 3·2 3·5 4·0
DISTANCE FROM DIFFUSER INLET (METRES)

7.1 ANALYSIS OF LIKELY ERRORS IN THE EXPERIMENTAL RESULTS.

The analysis used in this work is the method of KLINE and McLINTOCH[23] on the "Uncertainties of single sample experiments". This analysis attempts to estimate the probability of the result to be between certain limits.

7.1.1 The Uncertainty of the Velocity Values Obtained from the Pitot Probe.

$$V = \sqrt{\frac{\Delta p \times R \times T}{Pa}} \qquad \text{----------(7.1)}$$

where Δp is the dynamic pressure from the pitot and Pa is the atmospheric pressure.

The pitot was found to be relatively insensitive to small angles of yaw $< 5^{\circ}$ and therefore any error from a slight yaw has been ignored in this analysis.

The major area of error in the Δp value occurs in the readings taken near the wall, for a thin boundary layer $d\Delta p/dy$ is very large and therefore the uncertainty in Δp ($W\Delta p$) is large. A variation in y of as little as 0.5 mm could yield a variation of the order of 50mm of water. The probable uncertainty for the wall readings is in the region of $\pm$ 3 mm of water (for a 50;1 certainty, estimated from tests on pitot positioning). Therefore the maximum uncertainty in velocity occurs near the wall (since all the other parameters remain constant across the section). Thus it can be estimated that the readings of dynamic pressure of the streamline 0.5mm out from the wall are generally of the order of 100 $\pm$ 3mm water.

Therefore if it is assumed that the probability of these readings being within $\pm$ 3mm of water is of a similar order to the certainty than the "certainty" of the velocity (w vel) is :-

$$w\,vel = \left[\left(\frac{\partial v}{\partial \Delta p} W\Delta p\right)^2 + \left(\frac{\partial v}{\partial T} W_T\right)^2 + \left(\frac{\partial v}{\partial P_a} W P_a\right)^2\right]^{1/2}$$

which gives:-

$$w\,vel = \left[\frac{1}{4}\,\frac{2RT}{(\Delta p)\,pa}\,(w\,\Delta p)^2 + \frac{\frac{1}{4}\cdot 2(\Delta p)RT(wpa)^2}{Pa\,Ta} + \frac{1}{4}\,2(\Delta p)R\,(wT)^2\right] \qquad \text{----(7.2)}$$

Dividing by velocity to non-dimensionalise eg. (7.2) becomes:-

$$\frac{w\ vel}{vel} = \left[\left(\frac{\frac{1}{2}(w\Delta p)}{\Delta p}\right)^2 + \left(\frac{1}{2}\frac{(wpa)}{pa}\right)^2 + \left(\frac{\frac{1}{2}(wt)}{Ta}\right)^2\right]^{1/2} \qquad \text{-------(7.3)}$$

For values of $p = 100 \pm 3$
$T = 300 \pm 0.5$
$pa = 760 \pm 0.1$

$$\frac{w\ vel}{vel} = \left[\left(\frac{1x3}{2x100}\right)^2 + \left(\frac{1}{2}x\frac{0.1}{760}\right)^2 + \left(\frac{1}{2}x\frac{0.5}{300}\right)^2\right]^{\frac{1}{2}}$$

$$= \frac{wvel}{vel} = 1.5\%$$

This value of uncertainty reduces at the centreline to $\frac{w\ vel}{vel} = 0.2\%$ due to

the much higher certainty of the Δ p value.

Therefore the uncertainty of the mean velocity

$$\frac{w\bar{u}}{\bar{u}} = \frac{1}{n}\sum_{1}^{n}(u_a-u)^2 = 0.5\%$$

7.1.2 The Uncertainty in the Cp Value.

By a similar method the uncertainty of the Cp value be determined.

$$Cp = \Delta p/\tfrac{1}{2}\rho\bar{u}_1{}^2 = \frac{\Delta pRT}{\frac{1}{2}p_a\bar{u}_1{}^2}$$

therefore:-

$$wCp = \left[\left(\frac{\partial Cp.w\Delta p}{\partial p}\right)^2 + \left(\frac{\partial Cp.wT}{\partial T}\right)^2 + \left(\frac{\partial Cp.wp_a}{\partial p_a}\right)^2 + \left(\frac{\partial Cp}{\partial \bar{u}_1}.w\bar{u}_1\right)^2\right]^{\frac{1}{2}}$$

which gives

$$wCp = \left[\left(\frac{RT}{\frac{1}{2}p_a{}^2.\bar{u}_1{}^2}.w\Delta p\right)^2 + \left(\frac{\Delta pR.wT}{\frac{1}{2}p_a\bar{u}_1^2}\right) + \left(\frac{-\Delta pRT.wp_a}{\frac{1}{2}p_a{}^2\bar{u}_1^2}\right) + \left(\frac{-2\Delta pRT.w\bar{u}_1}{\frac{1}{2}p_a\bar{u}_1{}^3}\right)\right]^{\frac{1}{2}}$$

dividing by Cp to non-dimensionalise

$$\frac{wCp}{Cp} = \left[\left(\frac{w\Delta p}{\Delta p}\right)^2 + \left(\frac{wT}{T}\right)^2 + \left(\frac{wp_a}{p_a}\right)^2 + \left(\frac{2.w\bar{u}_1}{\bar{u}_1}\right)^2\right]^{\frac{1}{2}}$$

Taking typical values:-

$\bar{u}_1 = 70 \pm 0.35$, $\Delta p = 200 \pm 0.5$, $Ta = 300 \pm 0.5$ $pa = 760 \pm 0.1$

we obtain an uncertainty for Cp of

$$\frac{wCp}{Cp} = \left[\left(\frac{0.5}{200}\right)^2 + \left(\frac{0.5}{300}\right)^2 + \left(\frac{0.1}{760}\right)^2 + \left(\frac{2\ x\ 035}{70}\right)^2\right]^{\frac{1}{2}}$$

$= 1.04\% \simeq \underline{1.0\%}$

The main error in this is the value of $\varpi\bar{u}_1$ which if halved would reduce the error to the region of 0.5%.

The likely maximum errors in the experimental results can be summarised as follows:-

$u = \pm 0.2$ to 1.5% depending on the y value.

$\bar{u}_1 = \pm 0.5\%$

$\bar{u}_2 = \pm 0.2\%$

$Cp = \pm 1.0\%$

$\tau = \pm 1.5\%$

$\delta^* = \pm 0.5\%$

$\theta = \pm 0.25\%$.

It must however be noted that these values are for normal cases, however at the limit of flow stability these values of error will be greatly increased.

7.2 Errors in the Data Reduction Method.

The use of the Simpson's rule subroutine for integration of the boundary layer parameters could incur some error due to the large value of du/dy near the wall. This is shown for the axisymetric rig in figure 77.

It can be seen that a simple $1/7$ th power law approximates to the general from of the profile (i.e $\frac{u}{u_o} = \left(\frac{r}{R}\right)^{1/n}$ where n = 7, in actual fact n = 8 gives a closer approximation). From the $1/7$th power law profile it can be shown that as the spacing betwe-n the readings, especially near the wall, reduce then the accuracy of the calculated boundary layer parameters will increase. ('H' is shown for the $1/7$ power law profile against the number of readings taken in figure 78.). However, it was not possible to traverse closer to the wall than 0.5mm, therefore dictating the minimum step distance. It can be shown that for a $1/7$ power law profile the value obtained for 'H' using the Simpson's rule subroutine is 1.411 as against an actual value of 1.365 from the expression,

$$H = \frac{\delta^*}{\theta} = \frac{1 - \left(2n^2/(2n+1)(n+1)\right)^{1/2}}{1 - \left(1 - 3n^2/(2n+1)(n+1)(n+2)\right)^{1/2}}$$

Therefore for n = 7, H = 1.365.

which is + 3%. Which is a fairly large discrepancy and is larger than the

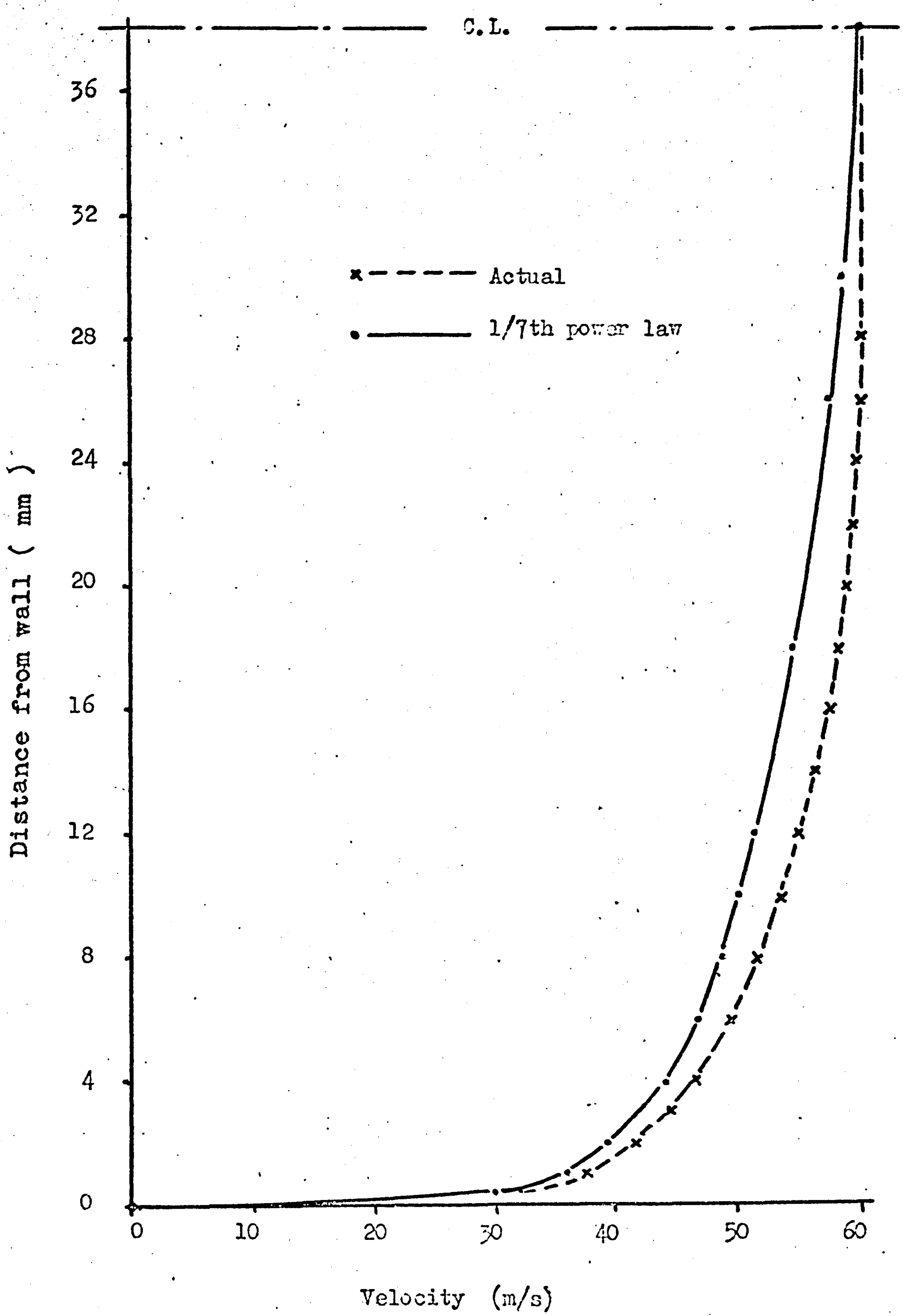
C.L.
36
32
28
24
20
16
12
8
4
0
Actual
1/7th power law
Distance from wall (mm)
0
10
20
30
40
50
60
Velocity (m/s)

FIGURE . . 77

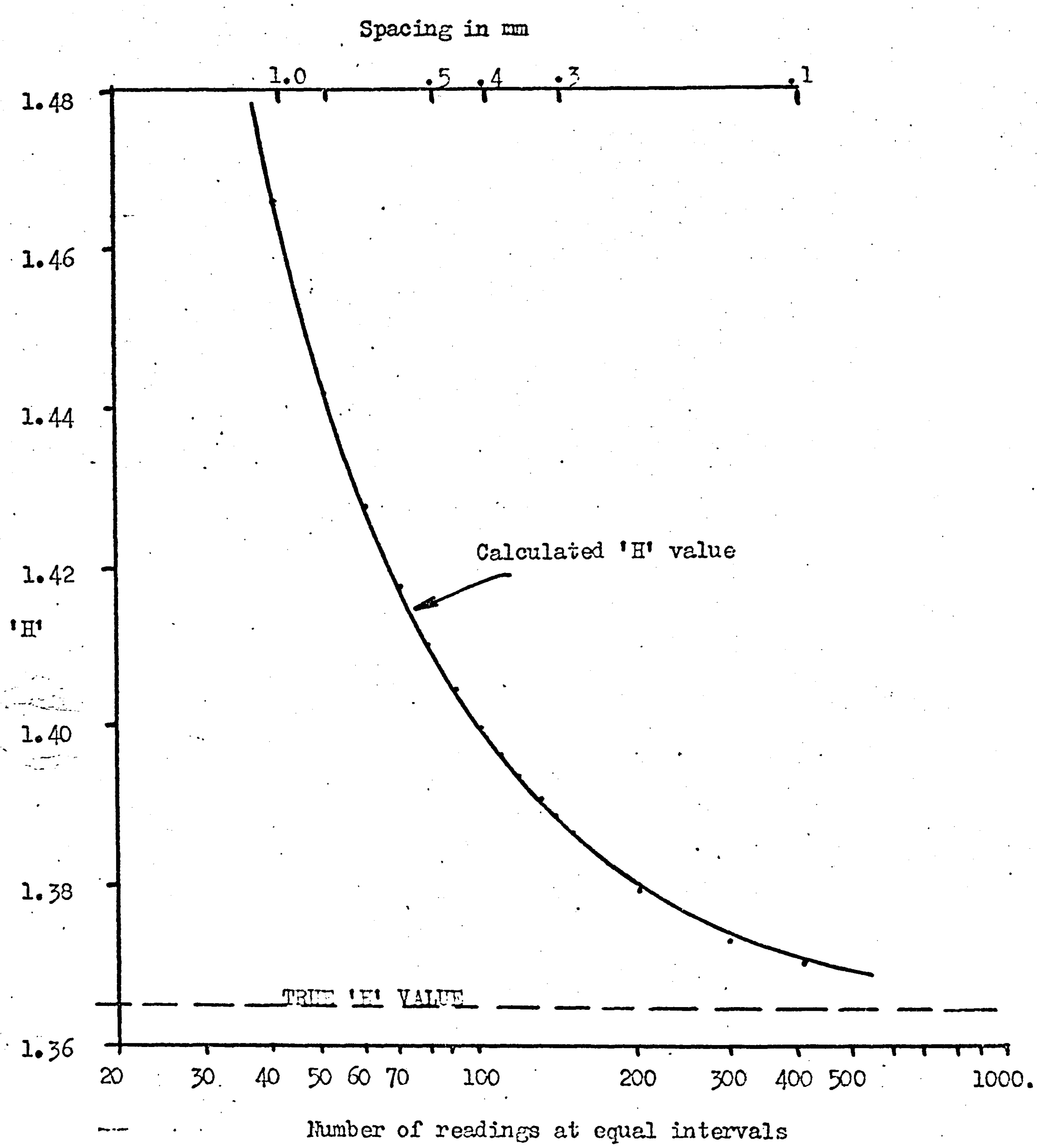

Spacing in mm
1.0
.5
.4
.3
.1
1.48
1.46
1.44
1.42
'H'
1.40
1.38
1.36
Calculated 'H' value
TRUE 'H' VALUE
20
30
40
50
60
70
100
200
300
400
500
1000.
Number of readings at equal intervals

FIGURE....78

error incurred by the uncertainty of the accuracy of the experimental results. The error on the actual profile can be expected to be of a similar order, however in the diffuser where the profile is distorted the error will be much less marked since it is the large du/dy value which causes the problem, however the thin inlet boundary layer profile has an even higher du/dy value, therefore the error can be expected to be at a maximum here due to the inability of a Simpson's rule subroutine (based on a quadratic function between the experimental points), to accurately integrate very rapid changes in velocity as experienced near the wall. This error at the inlet plane can be expected to be always greater than 3% on H for all inlet boundary layer conditions and of a similar order for the displacement thickness and momentum thickness.

APPENDIX 8.

DERIVATION OF FORMULAE AND BOUNDARY LAYER DEFINITIONS.

8.1 Displacement Thickness (δ^*).

The displacement thickness is defined as the distance the duct wall must be displaced in order that the actual flow rate would be the same for an ideal flow at the velocity outside the boundary layer. (uo).

Mass flow $\dot{m} = \int_0^{W/2} \rho u dw$ ------------------ (8.1)

also by definition $\dot{m} = \rho_o u_o (w/2 - \delta^*)$ --------------(8.2)

equating (8.1) and (8.2)

$$w/2 - \delta^* = \int_0^{W/2} (\rho u/\rho_o u_o) dw$$

Therefore : $\delta^* = \int_0^{W/2} (1 - \rho u/\rho_o u_o) dw$ ---------(8.3)

8.1 Momentum Thickness (θ).

Momentum thickness (θ) is defined as the distance to the duct wall must be moved such that the momentum flux deficit through this distance θ at the free stream velocity will be the same of the deficit of momentum flux in the boundary layer from an ideal flow.

The momentum in the boundary layer :

$$= \int_0^{W/2} u^2 \rho \, dw \quad \text{----------------------(8.4)}$$

Therefore the deficit from an ideal flow :

$$= \int_0^{W/2} u \rho (u_o - u) dw \quad \text{-----------------(8.5)}$$

By definition $\theta u_o^2 \rho_o = \int_0^{W/2} \rho u (u_o - u) dw$

Therefore $\theta = \int_0^{W/2} \frac{\rho u}{\rho_o u_o} \left\{ 1 - \frac{u}{u_o} \right\} dw$ ----(8.6)

8.3 The Momentum Integral Equation for Two-Dimensional, Compressible Flow.

Considering the element shown in figure 79.

Mass entering CA = $\int_0^{W1} \rho u dw = \dot{m}$ -------------(8.7)

Mass leaving DF = $\int_0^{W2} \rho_2 u_2 dw = \dot{m} + \Delta \dot{m}$ -------------(8.8)

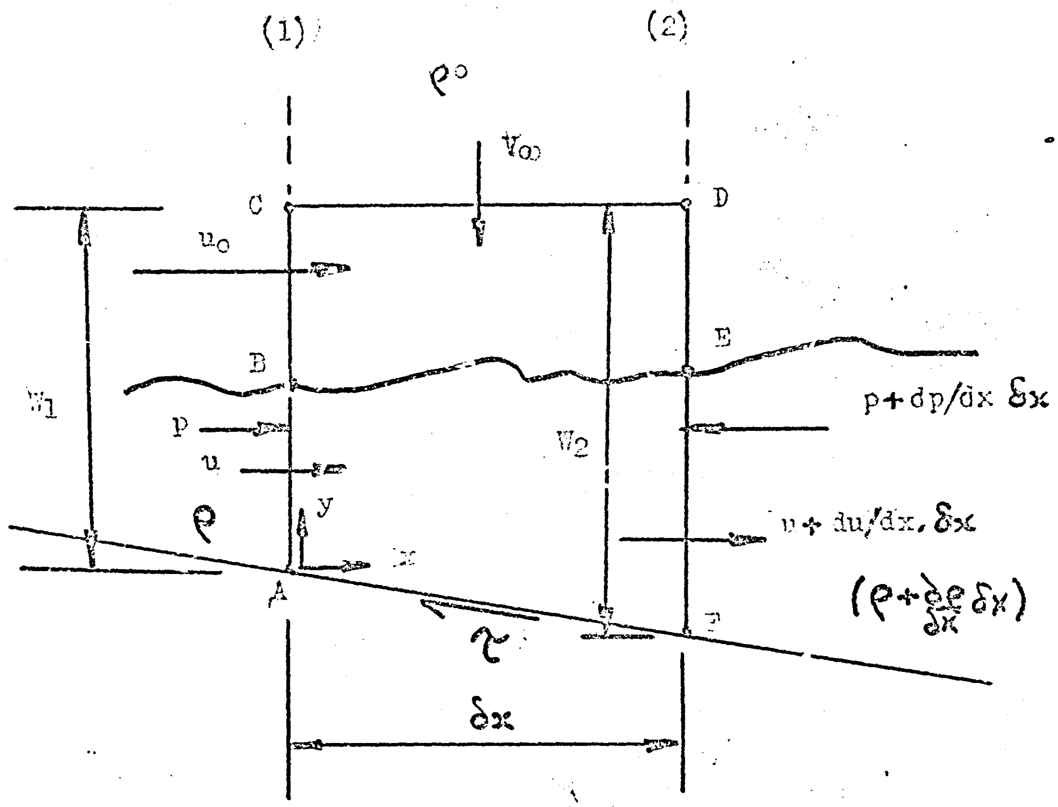

FIGURE......79

Since:

$$\rho_2 = \rho + \frac{\partial \rho}{\partial x}\delta, \quad u_2 = u + \frac{\partial u}{\partial x}\delta x\ , \quad w_2 = w_1 + \frac{\partial w}{\partial x}\delta x . \frac{1}{2}$$

$$\int_0^{w_2} \rho_2 u_2 dw = \int_0^{w_1} \rho u dw + \frac{d}{dx}\left\{\int_0^{w_1} \rho u dw\right\}\delta x + \int_{w_1}^{w_1+\frac{1}{2}\frac{\partial w}{\partial x}\delta x} \rho u dw + \frac{d}{dx}\left\{\int_{w_1}^{w_1+\frac{1}{2}\frac{\partial w}{\partial x}\delta x} \rho u dw\right\}\delta x + \text{2nd order terms} \quad \text{-----}(8.9)$$

Hence net flow through surfaces CA and DF out of element ;

$$= \int_{w_1}^{w_1+\frac{1}{2}\frac{\partial w}{\partial x}\delta x} \rho u dw + \frac{d}{dx}\left\{\int_{w_1}^{w_1+\frac{1}{2}\frac{\partial w}{\partial x}\delta x} \rho u dw\right\}\delta x + \frac{d}{dx}\left\{\int_0^{w_1} \rho u dw\right\}\delta x \quad \text{----------------}(8.10)$$

Mass flow through face CD :

$$= \int_{(1)}^{(2)} \rho_o v_o dx$$

Where suffix 'o' denotes values outside the boundary layer

Therefore from continuity ;

$$\int_1^2 \rho_o v_o dx = -\left\{\int_{w_1}^{w_1+\frac{1}{2}\frac{\partial w}{\partial x}\delta x} \rho u dw + \frac{d}{dx}\left\{\int_0^{w_1} \rho u dw\right\}\delta x + \frac{d}{dx}\left\{\int_{w_1}^{w_1+\frac{1}{2}\frac{\partial w}{\partial x}\delta x} \rho u dw\right\}\delta x\right\} + \text{2nd order terms} \quad \text{------}(8.11)$$

For the balance of the rate of change of momentum in the x direction and the applied force in the x direction.

In the x direction the rate of momentum transport through AC ;

$$= \int_0^{w_1} \rho u^2 dw$$

Through DF ;

$$= \int_0^{w_2} \rho_2 u_2 dw$$

$$= \int_0^{w_1} \rho u^2 dw + \frac{d}{dx}\left\{\int_0^{w_1} \rho u^2 dw\right\}\delta x + \int_{w_1}^{w_1+\frac{\partial w}{\partial x}\frac{1}{2}\delta x} \rho u^2 dw + \frac{d}{dx}\left\{\int_0^{w_1+\frac{1}{2}\frac{\partial w}{\partial x}\delta x} \rho u^2 dw\right\}\delta x + \text{2nd order terms}$$

Therefore increase in momentum over the length δx ;

$$= \int_{w_1}^{w_1+\frac{1}{2}\frac{\partial w}{\partial x}\delta x} \rho u^2 dw + \frac{d}{dx}\left\{\int_0^{w_1} \rho u^2 dw\right\}\delta x + \frac{d}{dx}\left\{\int_{w_1}^{w_1+\frac{1}{2}\frac{\partial w}{\partial x}\delta x} \rho u^2 dw\right\}\delta x + \text{2nd order terms} \quad \text{---}(8.12)$$

At the limit of δx terms of $1/2\ \frac{\delta w}{\delta x}\delta x$ will equal the values at the wall. Therefore the increase in momentum in the x direction over the length δx ;

$$= \frac{d}{dx}\left\{\int_0^{w_1} \rho u^2 dw\right\}\delta x + \text{2nd order terms} \quad \text{----------------}(8.13)$$

The momentum flux through CD in the x direction ;

$$= u_o \int_1^2 \rho_o v_o dx$$

$$= -u_o\left\{\int_{w_1}^{w_1+\frac{1}{2}\frac{\partial w}{\partial x}\delta x} \rho u dw + \frac{d}{dx}\left\{\int_0^{w_1} \rho u dw\right\}\delta x - \frac{d}{dx}\left\{\int_{w_1}^{w_1+\frac{1}{2}\frac{\partial w}{\partial x}\delta x} \rho u dw\right\}\delta x\right\} + \text{2nd order terms}$$

$$= -u_o\left(\frac{d}{dx}\left(\int_0^{w_1} \rho u dw\right)\delta x\right) + \text{2nd order terms} \quad \text{----------}(8.14)$$

Pressure force on surface CA ;

$$= pw_1$$

$$\text{on DE} = -\left(p+\frac{\partial p}{\partial x}\delta x\right)\left(w_1+\frac{\partial w}{\partial x}\delta x.\tfrac{1}{2}\right) + \text{2nd order terms}$$

Therefore net force in x direction ;

$$= -w_1\frac{\partial p}{\partial x}\delta x - \frac{p}{2}\frac{\partial w}{\partial x}\delta x + \text{2nd order terms} \quad \text{------------(8.15)}$$

Pressure force in x direction from the wall assumed that over element

mean pressure ;

$$= p+\tfrac{1}{2}\frac{\partial p}{\partial x}\delta x$$

Therefore pressure force from wall ;

$$= \left(-w_1+\left(w_1+\tfrac{1}{2}\frac{\partial w}{\partial x}\delta x\right)\right)\left(p+\tfrac{1}{2}\frac{\partial p}{\partial x}\delta x\right)$$

$$= \tfrac{1}{2}\frac{\partial w}{\partial x}\delta x p + \text{2nd order terms} \quad \text{----------------------(8.16)}$$

Therefore net pressure force in x direction ;

$$= -w_1\frac{\partial p}{\partial x}\delta x \quad \text{--------------------------(8.17)}$$

Force due to friction at wall ;

$$= -\tau_w\delta x\cos\phi/2 \;/\; \cos\phi/2 = \tau_w\delta x \quad \text{------------(8.18)}$$

Therefore since momentum change in x direction = force in x direction

$$\frac{d}{dx}\left\{\int_0^{w_1}\rho u^2 dw\right\}\delta x - u_0\frac{d}{dx}\left\{\int_0^{w_1}\rho u\, dw\right\}\delta x = -\frac{\partial p}{\partial x}\delta x w_1 - \tau_w\delta x + \text{2nd order terms}$$

$$\text{--------------(8.19)}$$

dividing by δx and letting δx tend to 0. ;

$$\frac{d}{dx}\left\{\int_0^{w_1}\rho u^2 dw\right\} - u_0\frac{d}{dx}\left\{\int_0^{w_1}\rho u dw\right\} = \rho_0 u_0 w_1\frac{du_0}{dx} - \tau_w \quad \text{-----(8.20)}$$

Where $\frac{\partial p}{\partial x}$ has been eliminated by the bernouli equation ;

$$u_0\frac{du_0}{dx} = -\frac{1}{\rho_0}\frac{dp}{dx}$$

Since $w_1 = w/2$, Equation (8.20) can be expressed as ;

$$\tau_w = \rho_0 u_0\frac{w}{2}\frac{du_0}{dx} - \frac{d}{dx}\left\{\int_0^{w/2}\rho u^2 dw\right\} + u_0\frac{d}{dx}\left\{\int_0^{w/2}\rho u dw\right\} \quad \text{--------(8.21)}$$

$$\text{Since } \delta^* = \int_0^{w/2}\left(1-\frac{\rho u}{\rho_0 u_0}\right)dw$$

$$\text{and } \theta = \int_0^{w/2}\frac{\rho u}{\rho_0 u_0}\left(1-\frac{u}{u_0}\right)dw$$

With some rearrangement equation (8.21) becomes ;

$$\frac{\tau_w}{\rho_0 u_0^2} = \frac{d\theta}{dx} + \theta\left(\frac{1}{u_0}\frac{du_0}{dx}\left\{(H+2)\right\} + \frac{1}{\rho_0}\frac{d\rho_0}{dx} + \frac{1}{w}\frac{dw}{dx}\right)$$

8.4 Entrainment Function

Figure 80 shows the flow element in consideration, where $\dot{m}$ = mass flow in the boundary layer at the section under consideration.

Thus mass flow per unit breadth ;

$$\dot{m} = \int_0^\delta \rho u \, dw$$

$$= \rho_o u_o \left\{ \int_0^\delta dw - \int_0^\delta \left(1 - \frac{\rho u}{\rho_o u_o}\right) dw \right\} \text{ ---------------(8.23)}$$

now $$\delta^* = \int_0^\delta \left(1 - \frac{\rho u}{\rho_o u_o}\right) \text{ --------------------------------(8.24)}$$

Therefore substituting in (8.23) becomes ;

$$\dot{m} = \rho_o u_o (\delta - \delta^*)$$

differentiating with respect to x ;

$$\frac{d\dot{m}}{dx} = \frac{d}{dx}\left\{ \rho_o u_o (\delta - \delta^*) \right\}$$

substituting H1 for $(\delta - \delta^*)/\theta$

$$\frac{d}{dx} \rho_o u_o (\delta - \delta^*) = f(H1, \delta - \delta^*, \rho_o u_o)$$

which can be expressed in the non-dimensional form;

$$\frac{1}{\rho_o u_o} \cdot \frac{d}{dx}\left\{ \rho_o u_o (\delta - \delta^*) \right\} = F(H1)$$

Where F = Heads entrainment function.

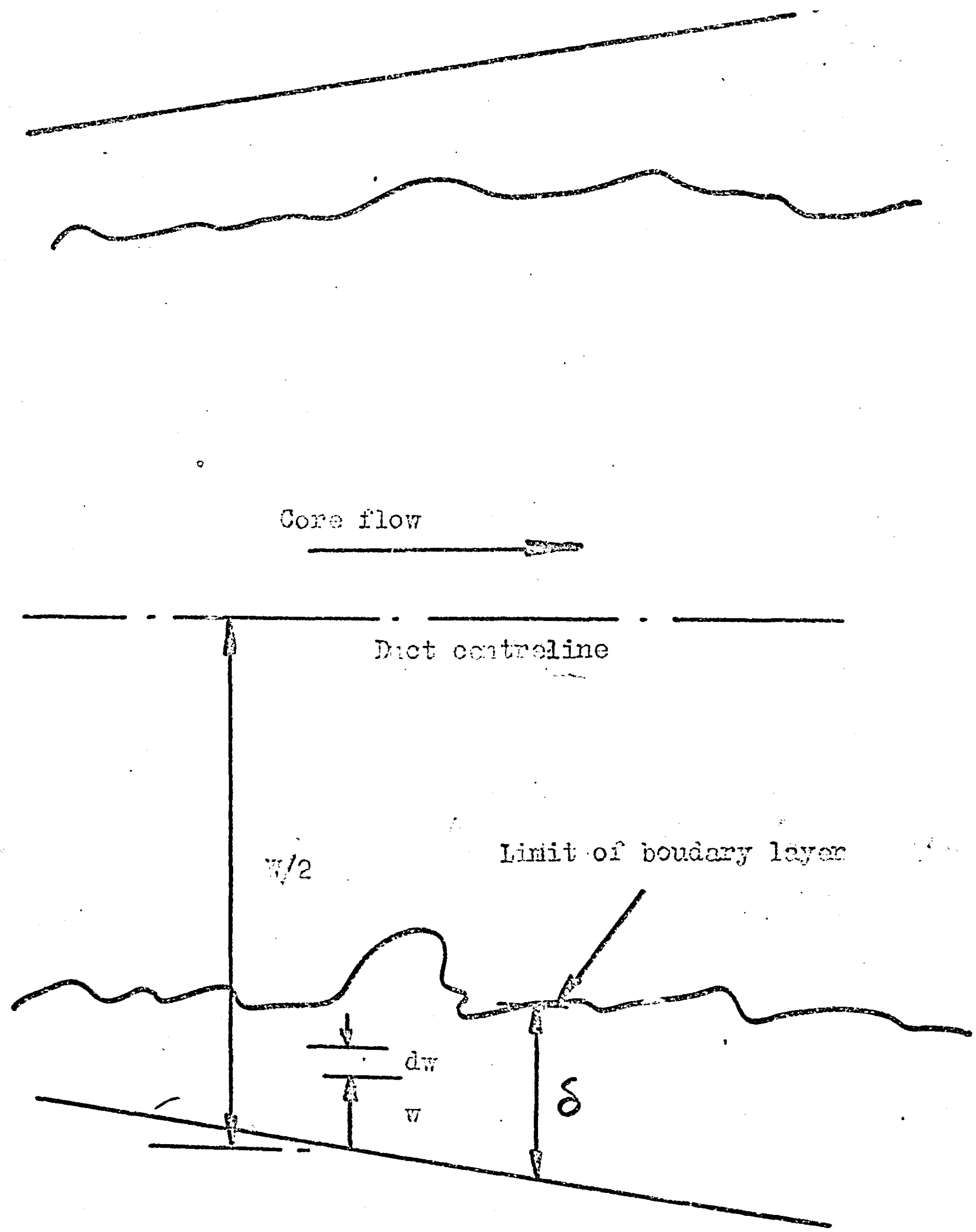

FIGURE.....80